

AD-A068 757

IIT RESEARCH INST ANNAPOLIS MD

F/G 17/2.1

WIDEBAND FDM/FM MICROWAVE RADIO RELAY PERFORMANCE DEGRADATION I--ETC(U)

APR 79 A A HERNANDEZ

F19628-78-C-0006

UNCLASSIFIED

ESD-TR-79-100

NL

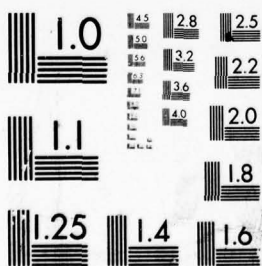
1 OF 5
AD
A068 757



1 P 1 E D

1 OF 5

AD
A068757



MICROCOPY RESOLUTION TEST CHART
NATIONAL BUREAU OF STANDARDS-1963-A

ESD-TR-79-100

LEVEL II

12

**WIDEBAND FDM/FM MICROWAVE
RADIO RELAY PERFORMANCE
DEGRADATION INVESTIGATION**

Arecio A. Hernandez
of

[IIT Research Institute]

Under Contract to

DEPARTMENT OF DEFENSE

Electromagnetic Compatibility Analysis Center
Annapolis, Maryland 21402



April 1979

FINAL REPORT

Approved for public release; distribution unlimited.

DDC

RECEIVED
MAY 21 1979
D

DDC FILE COPY

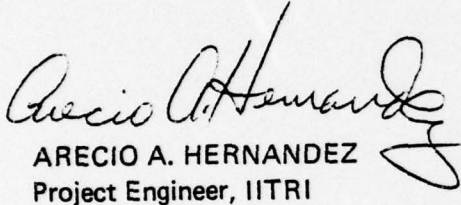
AD A068757

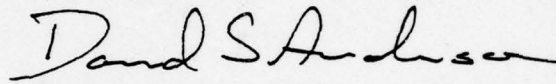
20 05 18 068


ESD-TR-79-100

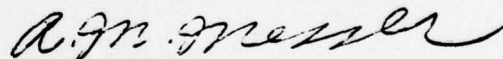
This report was prepared by the IIT Research Institute under Contract F-19628-78-C-0006 with the Electronic Systems Division of the Air Force Systems Command for the technical operation of the DoD Electromagnetic Compatibility Analysis Center, Annapolis, Maryland.

This report has been reviewed and is approved for publication.


ARECIO A. HERNANDEZ
Project Engineer, IITRI


DAVID S. ANDERSON
Assistant Director
Contractor Operations


THOMAS A. ANDERSON
Colonel, USAF
Director


A. M. MESSER
Chief, Plans & Resource Management
Office

SECURITY CLASSIFICATION OF THIS PAGE (When Data Entered)

DD FORM 1473
1 JAN 73

EDITION OF 1 NOV 65 IS OBSOLETE

i/ii

UNCLASSIFIED

SECURITY CLASSIFICATION OF THIS PAGE (When Data Entered)

NOT
Preceding Page BLANK - FILMED

ESD-TR-79-100

PREFACE

The Electromagnetic Compatibility Analysis Center (ECAC) is a Department of Defense facility, established to provide advice and assistance on electromagnetic compatibility matters to the Secretary of Defense, the Joint Chiefs of Staff, the military departments and other DoD components. The center, located at North Severn, Annapolis, Maryland 21402, is under the policy control of the Assistant Secretary of Defense for Communication, Command, Control, and Intelligence and the Chairman, Joint Chiefs of Staff, or their designees, who jointly provide policy guidance, assign projects, and establish priorities. ECAC functions under the executive direction of the Secretary of the Air Force and the management and technical direction of the Center are provided by military and civil service personnel. The technical operations function is provided through an Air Force-sponsored contract with the IIT Research Institute (IITRI).

This report was prepared as part of AF Project 649E under Contract F-19628-78-C-0006 by the staff of the IIT Research Institute at the Department of Defense Electromagnetic Compatibility Analysis Center.

To the extent possible, all abbreviations and symbols used in this report are taken from American Standard Y10.19 (1967) "Units Used in Electrical Science and Electrical Engineering" issued by the USA Standards Institute.

Users of this report are invited to submit comments that would be useful in revising or adding to this material to the Director, ECAC, North Severn, Annapolis, Maryland 21402, Attention XM.

ACCESSION for	
DTIC	White Section <input checked="" type="checkbox"/>
DDC	Buff Section <input type="checkbox"/>
UNANNOUNCED	<input type="checkbox"/>
JUSTIFICATION.....	
BY.....	
DISTRIBUTION/AVAILABILITY CODES	
Dist.	AVAIL. and/or SPECIAL
A	

PRECEDING PAGE BLANK - NOT FILMED

ESD-TR-79-100

EXECUTIVE SUMMARY

A general investigation of the performance degradation in FDM/FM systems when exposed to various types of interference signals was made through a combined use of detailed measurements and analyses. The interference signals used in the investigation were: Gaussian noise, CW, FM, FDM/FM, pulsed (chirped and nonchirped), spread-spectrum and ECM type (i.e., barrage noise, swept-spot noise, etc.).

The general investigation resulted in two general methods for evaluating the performance degradation effects produced by these interference signals in FDM/FM systems. The first method involves a computer model for time-waveform simulation of FDM/FM receivers that provides theoretical solutions for a wide range of interference and receiver parameters. The theoretical details of the computer model, including the user-oriented documentation and model validation were reported earlier in ECAC-UM-78-018.

The second method, described in this report, uses a combination of measured data and engineering trends covering a reasonably complete range of receiver and interference parameters. The measurement methodology used is also documented. In addition, information on FDM/FM systems (i.e., modulation characteristics, baseband noise loading techniques, emission spectrum synthesis techniques, etc.) has been included in this report to facilitate performing performance degradation analyses for FDM/FM systems.

Preceding Page BLANK - NOT FILMED

TABLE OF CONTENTS (Continued)

<u>Subsection</u>	<u>Page</u>
SECTION 3 (Continued)	
Residual Carrier Power	32
RF Bandwidth Calculations	32
SUMMARY OF TYPICAL FDM/FM PARAMETERS	33
POWER SPECTRUM OF FDM/FM SIGNALS	33
Small RMS Modulation Index ($m \leq 0.3$)	37
Large RMS Modulation Index ($m \geq 1.5$)	38
Intermediate Values of RMS Modulation Index ($0.3 \leq m \leq 1.5$)	38
Computer Approximations of the FDM/FM Spectra	38
Empirically Derived FDM/FM Spectrum Curves	41
Summary of FDM/FM Power Spectrum Synthesis Techniques	42
SECTION 4	
SYSTEM NOISE PERFORMANCE	
GENERAL	45
THERMAL NOISE	45
INTERMODULATION NOISE	48
MULTIPLEX SYSTEM NOISE	49
INTERFERENCE NOISE	49
DETERMINATION OF SYSTEM NOISE	50
Gaussian Noise Transfer Function	50
Accounting for Emphasis in FM Systems	55
CHANNEL OUTPUT NOISE WEIGHTING	57
(S/N) AND NPR	58
COMPARISONS BETWEEN MEASURED AND CALCULATED NOISE PERFORMANCE	59

TABLE OF CONTENTS

<u>Subsection</u>	<u>Page</u>
GLOSSARY OF TERMS	xxix

SECTION 1

INTRODUCTION

BACKGROUND	1
OBJECTIVES	2
APPROACH	2

SECTION 2

DESCRIPTION OF MEASUREMENTS

WIDEBAND FDM/FM MICROWAVE SYSTEM DESCRIPTION	5
NOISE POWER RATIO MEASUREMENTS	6
White Noise Testing Theory	6
Composite Speech and Data Loading	13
NPR Measurement Procedure	13
SYSTEM PARAMETER MEASUREMENTS	17
Transmitter Measurements	17
Receiver Measurements	19
PERFORMANCE DEGRADATION MEASUREMENTS	20
MEASUREMENT SETUP AND PROCEDURES	21
AUDIO OUTPUT PERFORMANCE MEASURES	23
RECEIVER TRANSFER FUNCTIONS	24

SECTION 3

FDM/FM PARAMETERS AND EMISSION SPECTRUM

DEFINITION OF USEFUL PARAMETERS	25
Test Tone Deviation Per Channel	25
Overall RMS Deviation of the FDM/FM Signal	28
Peak Deviation of the FDM/FM Signal	29
RMS Modulation Index	30

TABLE OF CONTENTS (Continued)

<u>Subsection</u>	<u>Page</u>
SECTION 5	
ECM (NOISE JAMMING) INTERFERENCE	
GENERAL	65
BARRAGE AND SPOT NOISE INTERFERENCE	65
Noise Generation	65
Barrage and Spot Noise Processing Gain	66
Comparisons Between Measured and Calculated Transfer Functions	71
Off-Tuning Effects	77
AFC Effects	81
AMPLITUDE MODULATED BARRAGE NOISE INTERFERENCE	82
Time Domain Representation	87
Average Power of Amplitude-Modulated Barrage Noise	88
Amplitude-Modulated Barrage Noise Processing Gain	89
PULSE-MODULATED BARRAGE NOISE INTERFERENCE	90
Average Power of Pulsed Modulated Barrage Noise	90
Pulse-Modulated Barrage Noise Interference Processing Gain	93
Off-Tuning Effects	93
SWEPT-SPOT NOISE INTERFERENCE	95
Receiver Response to Swept-Spot Noise Interference	95
Swept-Spot Noise Processing Gain	100
SECTION 6	
NOISE-MODULATED FM AND CW INTERFERENCE	
NOISE-MODULATED FM AND CW INTERFERENCE TRANSFER FUNCTIONS	109
Noise-Modulated FM Interference ($m \leq 0.3$)	110
Noise-Modulated FM Interference ($m \geq 0.3$)	114

TABLE OF CONTENTS (Continued)

<u>Subsection</u>	<u>Page</u>
SECTION 6 (Continued)	
CW Interference ($m \leq 0.3$)	115
CW Interference ($m \geq 0.3$)	116
COMPARISONS BETWEEN MEASURED AND CALCULATED DATA	116
Low Desired Signal Level - AGC Effects	126
AFC Effects	138
SECTION 7	
PULSED RADAR INTERFERENCE	
MEASUREMENT DESCRIPTION AND RESULTS	142
ACCOUNTING FOR THE MODULATION CHARACTERISTICS OF OTHER	
FDM/FM SYSTEMS	178
General	178
Determining the Thermal Noise Processing Gain	180
OTHER TECHNICAL CONSIDERATIONS	181
SECTION 8	
SPREAD-SPECTRUM INTERFERENCE TO FDM/FM SYSTEMS	
GENERAL	191
SPREAD-SPECTRUM SIGNALS	191
Direct Sequence	191
Frequency Hopping	192
MEASUREMENT DESCRIPTION AND RESULTS FOR DIRECT-SEQUENCE	
SPREAD-SPECTRUM (DSSS) INTERFERENCE	192
DSSS Signal Generation and Characteristics	192
Measurement Results	193
MEASUREMENT DESCRIPTION AND RESULTS FOR FREQUENCY-HOPPING	
SPREAD-SPECTRUM (FHSS) INTERFERENCE	197
FHSS Signal Generation and Characteristics	197
Measurement Results	211

TABLE OF CONTENTS (Continued)

<u>Subsection</u>	<u>Page</u>
-------------------	-------------

SECTION 9

SUMMARY OF RESULTS	245
--------------------	-----

LIST OF ILLUSTRATIONS

Figure

1	Block diagram of the GTE Lenkurt 778A2 transmitter assembly	7
2	Block diagram of the GTE Lenkurt 778A2 receiver assembly	8
3	46A2 carrier multiplex 600-channel modulation plan	9
4	Principle of white noise testing	10
5	Required baseband noise power levels as a function of nominal channel capacity	12
6	Baseband noise power ratio measurement block diagram	14
7	Performance degradation measurement setup	22
8	Variation of peak-to-RMS ratio of a multiplex signal with the number of active channels	31
9	Relative FDM/FM power spectra ($0.2 \leq m \leq 1.5$)	42
10	Comparisons between measured and calculated spectrum of 600-channel FDM/FM	44
11	FDM/FM noise transfer function model	51
12	Thermal noise transfer function for a low test channel (340-344 kHz)	60
13	Thermal noise transfer function for a middle test channel (1244-1248 kHz)	61
14	Thermal noise transfer function for a high test channel (2432-2436 kHz)	62
15	200-MHz barrage noise frequency domain emission spectrum	67

TABLE OF CONTENTS (Continued)

LIST OF ILLUSTRATIONS (Continued)

<u>Figure</u>		<u>Page</u>
16	10-MHz spot noise frequency domain emission spectrum	68
17	5-MHz spot noise frequency domain emission spectrum	69
18	250-kHz spot noise frequency domain emission spectrum	70
19	Transfer function for 200-MHz barrage noise interference; low test channel (340-344 kHz)	72
20	Transfer function for 200-MHz barrage noise interference; high test channel (2432-2436 kHz)	73
21	Transfer function for 10-MHz spot noise interference; low test channel (340-344 kHz)	74
22	Transfer function for 5-MHz spot noise interference; low test channel (340-344 kHz)	75
23	Transfer function for 250-kHz spot noise interference; low test channel (340-344 kHz)	76
24	Off-tuning rejection to 250-kHz spot noise interference; low test channel (340-344 kHz)	78
25	Off-tuning rejection to 5-MHz spot noise interference; low test channel (340-344 kHz)	79
26	Off-tuning rejection to 10-MHz spot noise interference; low test channel (340-344 kHz)	80
27	IF output frequency domain photograph showing 600-channel FDM/FM signal and 250-kHz spot noise interference, [AFC on; $(C/I)_{IF\ OUT} = -0.2\ dB$]	83
28	IF output frequency domain photograph showing 600-channel FDM/FM signal and 250-kHz spot noise interference, [AFC on; $(C/I)_{IF\ OUT} = -5\ dB$]	84

TABLE OF CONTENTS (Continued)

LIST OF ILLUSTRATIONS (Continued)

<u>Figure</u>		<u>Page</u>
29	IF output frequency domain photograph showing 600-channel FDM/FM signal and 250-kHz spot noise interference, [AFC off; (C/I) _{IF OUT} = - 5 dB]	85
30	200-MHz amplitude-modulated barrage noise frequency domain emission spectrum showing 100-Hz modulation waveform	86
31	Transfer function for 200-MHz amplitude-modulated barrage noise interference; low test channel (340-344 kHz)	90
32	Pulse-modulated barrage noise interference frequency domain emission spectrum	92
33	Transfer function for pulse-modulated barrage noise interference; low test channel (340-344 kHz)	94
34	Swept-spot noise frequency domain emission spectrum, no sweep (A), and sweep on (B)	96
35	Swept-spot noise frequency (A) and time (B) domain representation	97
36	Transfer function for 20-MHz swept-spot noise interference; low test channel (340-344 kHz)	102
37	Transfer function for CW-swept interference; high test channel (2432-2436 kHz)	103
38	Transfer function for 5-MHz swept-spot noise interference; high test channel (2432-2436 kHz)	104
39	Transfer function for 10-MHz swept-spot noise interference; high test channel (2432-2436 kHz)	105
40	Transfer function for 20-MHz swept-spot noise interference; high test channel (2432-2436 kHz)	106
41	Transfer function for 50-MHz swept-spot noise interference; high test channel (2432-2436 kHz)	107

TABLE OF CONTENTS (Continued)

LIST OF ILLUSTRATIONS (Continued)

<u>Figure</u>		<u>Page</u>
42	Transfer function for identical 600-channel on-tune FDM/FM interference; low test channel (340-344 kHz)	117
43	Transfer function for identical 600-channel on-tune FDM/FM interference; middle test channel (1244-1248 kHz)	118
44	Transfer function for identical 600-channel on-tune FDM/FM interference; high test channel (2432-2436 kHz)	119
45	Transfer function for on-tune 12-channel FDM/FM interference; low test channel (340-344 kHz) . . .	120
46	Transfer function for on-tune 12-channel FDM/FM interference; middle test channel (1244-1248 kHz)	121
47	Transfer function for on-tune 12-channel FDM/FM interference; high test channel (2432-2436 kHz) .	122
48	Transfer function for on-tune CW interference; low test channel (340-344 kHz)	123
49	Transfer function for on-tune CW interference; middle test channel (1244-1248 kHz)	124
50	Transfer function for on-tune CW interference; high test channel (2432-2436 kHz)	125
51	Transfer function for on-tune single channel narrowband FM interference; low channel (340-344 kHz)	127
52	Off-frequency rejection to an identical 600-channel FDM/FM interfering signal; low test channel (340-344 kHz)	128

TABLE OF CONTENTS (Continued)

LIST OF ILLUSTRATIONS (Continued)

<u>Figure</u>		<u>Page</u>
53	Off-frequency rejection to an identical 600-channel FDM/FM interfering signal; middle test channel (1244-1248 kHz)	129
54	Off-frequency rejection to an identical 600-channel FDM/FM interfering signal; high test channel (2432-2436 kHz)	130
55	Off-frequency rejection to a 12-channel FDM/FM interfering signal; low test channel (340-344 kHz)	131
56	Off-frequency rejection to a 12-channel FDM/FM interfering signal; middle test channel (1244-1248 kHz)	132
57	Off-frequency rejection to a 12-channel FDM/FM interfering signal; high test channel (2432-2436 kHz)	133
58	Off-frequency rejection to a CW interfering signal; low test channel (340-344 kHz)	134
59	Off-frequency rejection to a CW interfering signal; middle test channel (1244-1248 kHz)	135
60	Off-frequency rejection to a CW interfering signal; high test channel (2432-2436 kHz)	136
61	Off-frequency rejection to a single channel narrowband FM interfering signal; low test channel (340-344 kHz)	137
62	AFC effects for CW interference, photographs (a) and (b) taken at IF auxiliary output; (C/I) _{IF OUT} = - 2 dB; spectrum analyzer bandwidth = 100 kHz; scanwidth = 1 MHz/division; center frequency = 70 kHz	139

TABLE OF CONTENTS (Continued)

LIST OF ILLUSTRATIONS (Continued)

<u>Figure</u>		<u>Page</u>
63	Measured interference noise power in a low base-band channel (340-344 kHz) for cochannel, non-chirped, pulse interference; PRF = 10 pps	143
64	Measured interference noise power in a low base-band channel (340-344 kHz) for cochannel, non-chirped, pulse interference; PRF = 40 pps	144
65	Measured interference noise power in a low base-band channel (340-344 kHz) for cochannel, non-chirped, pulse interference; PRF = 50 pps	145
66	Measured interference noise power in a low base-band channel (340-344 kHz) for cochannel, non-chirped, pulse interference; PRF = 80 pps	146
67	Measured interference noise power in a low base-band channel (340-344 kHz) for cochannel, non-chirped, pulse interference; PRF = 160 pps	147
68	Measured interference noise power in a low base-band channel (340-344 kHz) for cochannel, non-chirped, pulse interference; PRF = 300 pps	148
69	Measured interference noise power in a low base-band channel (340-344 kHz) for cochannel, non-chirped, pulse interference; PRF = 400 pps	149
70	Measured interference noise power in a low base-band channel (340-344 kHz) for cochannel, non-chirped, pulse interference; PRF = 500 pps	150
71	Measured interference noise power in a low base-band channel (340-344 kHz) for cochannel, non-chirped, pulse interference; PRF = 1000 pps	151

TABLE OF CONTENTS (Continued)

LIST OF ILLUSTRATIONS (Continued)

<u>Figure</u>		<u>Page</u>
72	Measured interference noise power in a low baseband channel (340-344 kHz) for cochannel, nonchirped, pulse interference; PRF = 3000 pps . . .	152
73	Measured interference noise power in a low baseband channel (340-344 kHz) for cochannel, nonchirped, pulse interference; PRF = 5000 pps . . .	153
74	Measured interference noise power in a low baseband channel (340-344 kHz) for cochannel, nonchirped, pulse interference; PRF = 15,000 pps . .	154
75	Measured interference noise power in a middle baseband channel (1244-1248 kHz) for cochannel, nonchirped, pulse interference; PRF = 80 pps . .	155
76	Measured interference noise power in a middle baseband channel (1244-1248 kHz) for cochannel, nonchirped, pulse interference; PRF = 400 pps . .	156
77	Measured interference noise power in a middle baseband channel (1244-1248 kHz) for cochannel, nonchirped, pulse interference; PRF = 500 pps . .	157
78	Measured interference noise power in a high baseband channel (2432-2436 kHz) for cochannel, nonchirped, pulse interference; PRF = 80 pps	158
79	Measured interference noise power in a high baseband channel (2432-2436 kHz) for cochannel, nonchirped, pulse interference; PRF = 400 pps . . .	159
80	Measured interference noise power in a high baseband channel (2432-2436 kHz) for cochannel, nonchirped, pulse interference; PRF = 500 pps . . .	160

TABLE OF CONTENTS (Continued)

LIST OF ILLUSTRATIONS (Continued)

<u>Figure</u>		<u>Page</u>
81	Measured interference noise power in a high base-band channel (2432-2436 kHz) for cochannel, non-chirped, pulse interference; PRF = 5000 pps	161
82	Measured interference noise power in a high base-band channel (2432-2436 kHz) for cochannel, non-chirped, pulse interference, PRF = 15,000 pps . . .	162
83	Measured interference noise power in a low base-band channel (340-344 kHz) for cochannel, chirped, pulse interference; PRF = 80 pps	163
84	Measured interference noise power in a low base-band channel (340-344 kHz) for cochannel, chirped, pulse interference; PRF = 300 pps	164
85	Measured interference noise power in a low base-band channel (340-344 kHz) for cochannel, chirped, pulse interference; PRF = 400 pps	165
86	Measured interference noise power in a low base-band channel (340-344 kHz) for cochannel, chirped, pulse interference; PRF = 1000 pps	166
87	Measured interference noise power in a low base-band channel (340-344 kHz) for cochannel, chirped, pulse interference; PRF = 3000 pps	167
88	Measured interference noise power in a low base-band channel (340-344 kHz) for cochannel ($\Delta f = 0$) and off-tuned ($\Delta f > 0$), nonchirped, pulse interference; PW = 1 μ s, PRF = 500 pps	168
89	Measured interference noise power in a low base-band channel (340-344 kHz) for cochannel ($\Delta f = 0$) and off-tuned ($\Delta f > 0$), nonchirped, pulse interference; PW = 1 μ s, PRF = 5000 pps	169

TABLE OF CONTENTS (Continued)

LIST OF ILLUSTRATIONS (Continued)

<u>Figure</u>		<u>Page</u>
90	Measured interference noise power in a high baseband channel (2432-2436 kHz) for cochannel ($\Delta f = 0$) and off-tuned ($\Delta f > 0$) nonchirped, pulse interference; PW = 1 μ s, PRF = 5000 pps	170
91	Required C/I power ratio for a low channel (340-344 kHz) S/N output of 52 dB as a function of frequency off-tuning; PW = 10 μ s, PRF = 400 pps .	171
92	Required C/I power ratio for a high channel (2432-2436 kHz) S/N output of 53 dB as a function of frequency off-tuning; PW = 10 μ s, PRF = 400 pps .	172
93	Required C/I power ratio for a low channel (340-344 kHz) S/N output of 52 dB as a function of frequency off-tuning; PW = 100 μ s, PRF = 400 pps .	173
94	Required C/I power ratio for a high channel (2432-2436 kHz) S/N output of 53 dB as a function of frequency off-tuning; PW = 100 μ s, PRF = 400 pps .	174
95	Required C/I power ratio for a low channel (340-344 kHz) S/N output of 55 dB as a function of frequency off-tuning; PW = 400 μ s, PRF = 400 pps .	175
96	Required C/I power ratio for a low channel (340-344 kHz) S/N output of 53 dB as a function of frequency off-tuning; PW = 1000 μ s, PRF = 160 pps .	176
97	Envelope and transfer functions of the observed interference noise power in a low baseband channel (340-344 kHz) for cochannel, nonchirped, pulse interference and duty cycle of approximately -18 dB	179

TABLE OF CONTENTS (Continued)

LIST OF ILLUSTRATIONS (Continued)

<u>Figure</u>		<u>Page</u>
98	Comparisons between measured and calculated interference noise power in a low baseband channel (340-344 kHz) for cochannel, nonchirped, pulse interference; PRF = 500 pps	182
99	Comparisons between measured and calculated interference noise power in a high baseband channel (2432-2436 kHz) for cochannel, nonchirped, pulse interference; PRF = 500 pps	183
100	Comparisons between measured and calculated interference noise power in a low baseband channel (340-344 kHz) for cochannel, nonchirped, pulse interference; PRF = 15,000 pps	184
101	Comparisons between measured and calculated interference noise power in a high baseband channel (2432-2436 kHz) for cochannel, nonchirped, pulse interference; PRF = 15,000 pps	185
102	Comparisons between measured and calculated interference noise power in a middle baseband channel (1244-1248 kHz) for cochannel, nonchirped, pulse interference; PRF = 80 pps	186
103	Comparisons between measured and calculated interference noise power in a middle baseband channel (1244-1248 kHz) for cochannel, nonchirped, pulse interference; PRF = 400 pps	187
104	Comparisons between measured and calculated interference noise power in a low baseband channel (340-344 kHz) for cochannel, nonchirped, pulse interference; PRF = 40 pps	188

TABLE OF CONTENTS (Continued)

LIST OF ILLUSTRATIONS (Continued)

<u>Figure</u>		<u>Page</u>
105	Comparisons between measured and calculated interference noise power in a low baseband channel (340-344 kHz) for cochannel, nonchirped, pulse interference; PRF = 160 pps	189
106	BPSK DS interference generator	193
107	DSSS signal, 180° biphas-modulated by a 125-kbps code	194
108	DSSS signal, 180° biphas-modulated by a 2.5 Mbps code	195
109	DSSS signal, 180° biphas-modulated by a 5-Mbps code	196
110	Transfer function for on-tune DSSS interference 180° biphas-modulated by a 125-kbps code; low test channel (340-344 kHz)	198
111	Transfer function for on-tune DSSS interference 180° biphas-modulated by a 2.5-Mbps code; low test channel (340-344 kHz)	199
112	Transfer function for on-tune DSSS interference 180° biphas-modulated by a 5-Mbps code; low test channel (340-344 kHz)	200
113	Transfer function for on-tune DSSS interference 180° biphas-modulated by a 125 kbps code; high test channel (2432-2436 kHz)	201
114	Transfer function for on-tune DSSS interference 180° biphas-modulated by a 2.5-Mbps code; high test channel (2432-2436 kHz)	202
115	Transfer function for on-tune DSSS interference 180° biphas-modulated by a 5-Mbps code; high test channel (2432-2436 kHz)	203

TABLE OF CONTENTS (Continued)

LIST OF ILLUSTRATIONS (Continued)

<u>Figure</u>		<u>Page</u>
116	Off-frequency rejection to DSSS interference 180° biphase-modulated by a 125-kbps code; low test channel (340-344 kHz)	204
117	Off-frequency rejection to DSSS interference 180° biphase-modulated by a 2.5-Mbps code; low test channel (340-344 kHz)	205
118	Off-frequency rejection to DSSS interference 180° biphase-modulated by a 5-Mbps code; low test channel (340-344 kHz)	206
119	Off-frequency rejection to DSSS interference 180° biphase-modulated by a 125-kbps code; high test channel (2432-2436 kHz)	207
120	Off-frequency rejection to DSSS interference 180° biphase-modulated by a 2.5 Mbps code; high test channel (2432-2436 kHz)	208
121	Off-frequency rejection to DSSS interference 180° biphase-modulated by a 5-Mbps code; high test channel (2432-2436 kHz)	209
122	BPSK frequency-hopping interference generator . .	210
123	FHSS signal, 180° biphase-modulated by a 19.2- kbps code	212
124	FHSS signal, 180° biphase-modulated by a 250- kbps code	213
125	FHSS signal, 180° biphase-modulated by a 5-Mbps code	214
126	FHSS signal, 180° biphase-modulated by a 10-Mbps code	215

TABLE OF CONTENTS (Continued)

LIST OF ILLUSTRATIONS (Continued)

<u>Figure</u>		<u>Page</u>
127	Measured interference noise power in a low base-band channel (340-344 kHz) for BPSK FHSS interference; dwell time = 0.1 μ s, inband average hop rate = 10,000 hps	217
128	Measured interference noise power in a low base-band channel (340-344 kHz) for BPSK FHSS interference; dwell time = 0.2 μ s, inband average hop rate = 10,000 hps	218
129	Measured interference noise power in a low base-band channel (340-344 kHz) for BPSK FHSS interference; dwell time = 1 μ s, inband average hop rate = 10,000 hps	219
130	Measured interference noise power in a low base-band channel (340-344 kHz) for BPSK FHSS interference; dwell time = 4.0 μ s, inband average hop rate = 10,000 hps	220
131	Measured interference noise power in a low base-band channel (340-344 kHz) for BPSK FHSS interference; dwell time = 0.1 μ s, inband average hop rate = 1000 hps	221
132	Measured interference noise power in a low base-band channel (340-344 kHz) for BPSK FHSS interference; dwell time = 0.2 μ s, inband average hop rate = 1000 hps	222
133	Measured interference noise power in a low base-band channel (340-344 kHz) for BPSK FHSS interference; dwell time = 1 μ s, inband average hop rate = 1000 hps	223

TABLE OF CONTENTS (Continued)

LIST OF ILLUSTRATIONS (Continued)

<u>Figure</u>		<u>Page</u>
134	Measured interference noise power in a low base-band channel (340-344 kHz) for BPSK FHSS interference; dwell time = 4 μ s, inband average hop rate = 1000 hps	224
135	Measured interference noise power in a low base-band channel (340-344 kHz) for BPSK FHSS interference; dwell time = 100 μ s, inband average hop rate = 1000 hps	225
136	Measured interference noise power in a low base-band channel (340-344 kHz) for BPSK FHSS interference; dwell time = 300 μ s, inband average hop rate = 1000 hps	226
137	Measured interference noise power in a low base-band channel (340-344 kHz) for BPSK FHSS interference; dwell time = 1000 μ s, inband average hop rate = 400 hps	227
138	Measured interference noise power in a low base-band channel (340-344 kHz) for BPSK FHSS interference; dwell time = 0.1 μ s, inband average hop rate = 100 hps	228
139	Measured interference noise power in a low base-band channel (340-344 kHz) for BPSK FHSS interference; dwell time = 0.2 μ s, inband average hop rate = 100 hps	229
140	Measured interference noise power in a low base-band channel (340-344 kHz) for BPSK FHSS interference; dwell time = 4 μ s, inband average hop rate = 100 hps	230

TABLE OF CONTENTS (Continued)

LIST OF ILLUSTRATIONS (Continued)

<u>Figure</u>		<u>Page</u>
141	Measured interference noise power in a low base-band channel (340-344 kHz) for BPSK FHSS interference; dwell time = 1 μ s, inband average hop rate = 100 hps	231
142	Measured interference noise power in a low base-band channel (340-344 kHz) for BPSK FHSS interference; dwell time = 100 μ s, inband average hop rate = 100 hps	232
143	Measured interference noise power in a low base-band channel (340-344 kHz) for BPSK FHSS interference; dwell time = 300 μ s, inband average hop rate = 100 hps	233
144	Measured interference noise power in a low base-band channel (340-344 kHz) for BPSK FHSS interference; dwell time = 1000 μ s, inband average hop rate = 100 hps	234
145	Measured interference noise power in a low base-band channel (340-344 kHz) for BPSK FHSS interference; dwell time = 0.2 μ s, inband average hop rate = 10 hps	235
146	Measured interference noise power in a low base-band channel (340-344 kHz) for BPSK FHSS interference; dwell time = 1 μ s, inband average hop rate = 10 hps	236
147	Measured interference noise power in a low base-band channel (340-344 kHz) for BPSK FHSS interference; dwell time = 4 μ s, inband average hop rate = 10 hps	237

TABLE OF CONTENTS (Continued)

LIST OF ILLUSTRATIONS (Continued)

<u>Figure</u>		<u>Page</u>
148	Measured interference noise power in a low base-band channel (340-344 kHz) for BPSK FHSS interference; dwell time = 100 μ s, inband average hop rate = 10 hps	238
149	Measured interference noise power in a low base-band channel (340-344 kHz) for BPSK FHSS interference; dwell time = 1000 μ s, inband average hop rate = 10 hps	239
150	Measured interference noise power in a high base-band channel (2432-2436 kHz) for BPSK FHSS interference; dwell time = 300 μ s, inband average hop rate = 10 hps	240
151	Measured interference noise power in a high base-band channel (2432-2436 kHz) for BPSK FHSS interference; dwell time = 100 μ s, inband average hop rate = 10 hps	241
152	Measured interference noise power in a high base-band channel (2432-2436 kHz) for BPSK FHSS interference; dwell time = 100 μ s, inband average hop rate = 100 hps	242
153	Measured interference noise power in a high base-band channel (2432-2436 kHz) for BPSK FHSS interference; dwell time = 100 μ s, inband average hop rate = 1000 hps	243

TABLE OF CONTENTS (Continued)

LIST OF TABLES

<u>Table</u>		<u>Page</u>
1	RECOMMENDED AND MEASURED NOISE PERFORMANCE (ONE-HOP 600-CHANNEL 78A2 SYSTEM)	18
2	RECOMMENDED AND MEASURED NOISE PERFORMANCE (ONE-HOP 1200-CHANNEL 78A2 SYSTEM)	18
3	PARAMETERS OF CCIR AND DCA FDM/FM SYSTEMS	26
4	ACTIVITY COEFFICIENTS	30
5	PARAMETERS OF GTE LENKURT FDM/FM SYSTEMS	34
6	INTELSAT IV TRANSMISSION PARAMETERS (STANDARD AND EXPANDED).	35
7	SUMMARY OF FDM/FM NOISE-POWER SPECTRUM SYNTHESIS METHODS	43
8	SUMMARY OF MEASURED FDM/FM SYSTEM PARAMETERS	63
9	COMPARISON OF MEASURED AND THEORETICAL BARRAGE AND SPOT NOISE PROCESSING GAIN	77

LIST OF APPENDIXES

<u>Appendix</u>		
A	PARAMETER MEASUREMENT DATA	249
B	RECEIVER PERFORMANCE	303
C	SPECTRAL CHARACTERISTICS OF PREEMPHASIZED FDM/FM SIGNALS	321
	REFERENCES	361

ESD-TR-79-100

GLOSSARY OF TERMS

ADCS	=	Automatic Data Collection System
AFC	=	Automatic frequency control
AGC	=	Automatic gain control
AI	=	Articulation index
AM	=	Amplitude modulation
AS	=	Articulation score
B	=	Noise bandwidth, in Hz, approximately equal to the receiver IF bandwidth
BPSK	=	Binary-phase shift keying
B_{RF}	=	Necessary RF bandwidth
$B_{\Delta f}$	=	Off-tuning factor, in dB
C	=	Average power of the desired FDM/FM carrier, in dBm
c	=	RF input FDM/FM carrier, in watts
CCIR	=	International Radio Consultative Committee
CCITT	=	International Telephone and Telegraph Consultative Committee
C/I	=	RF input carrier-to-average interference power ratio, in dB
C/\hat{I}	=	RF input carrier-to-peak interference power ratio, in dB
(c/n)	=	RF input carrier-to-effective thermal noise power ratio, where the thermal noise is calculated in the predetection bandwidth
CW	=	Continuous wave
dBm0	=	dBm at a point of zero relative level
dBrnc	=	Reference noise C-message-weighted, in dB
dBrnc0	=	dBrnc at a point of zero relative level

GLOSSARY (Continued)

DCA	=	Defense Communications Agency
D_{peak}	=	Peak deviation of the multiplexed signal, in Hz
d_{peak}	=	Peak deviation of a channel for a signal of test tone level, in Hz
D_{rms}	=	RMS deviation of the multiplexed signal, in Hz
D'_{rms}	=	Total RMS deviation of an interfering FDM/FM signal, in Hz
d_{rms}	=	RMS deviation of a channel for a signal of test tone level, in Hz
DS	=	Direct-sequence
DSSS	=	Direct-sequence spread-spectrum
E	=	Preemphasis factor, in dB
ECM	=	Electronic countermeasures
f	=	Frequency relative to the FDM/FM carrier frequency, in Hz
F_{ch}	=	Center frequency occupied by the test channel in the baseband, in Hz
FDM/FM	=	Frequency-division-multiplex/frequency-modulation
F_g	=	Receiver noise figure, in dB
f_g	=	Receiver noise factor
FH	=	Frequency-hopping
F_H	=	Highest baseband modulating frequency, in Hz
F'_H	=	Highest modulating frequency of an interfering FDM/FM signal, in Hz
f_H	=	Upper 3-dB cutoff frequency of the standard FDM audio channel, normally 3400 Hz, in Hz

GLOSSARY (Continued)

FHSS	=	Frequency-hopping spread-spectrum
F_L	=	Lowest baseband modulating frequency, in Hz
F'_L	=	Lowest modulating frequency of an interfering FDM/FM signal, in Hz
f_L	=	Lower 3-dB cutoff frequency of the standard FDM audio channel, normally 300 Hz, in Hz
FM	=	Frequency modulation
f_m	=	Noise factor associated with the mth stage
f_o	=	Carrier frequency of an interfering signal
FSVM	=	Frequency selective voltmeter
I	=	Average power of the interfering signal, in dBm
\hat{I}	=	Peak power of the interfering signal, in dBm
IF	=	Intermediate frequency
INTELSAT	=	International Telecommunications Satellite Consortium
k	=	Boltzmann's constant = 1.38×10^{-23} joules per Kelvin
LOS	=	Line-of-sight
m	=	RMS modulation index of the FDM/FM signal
m'	=	RMS modulation index of an interfering FDM/FM signal
MINIT	=	Minimum interference threshold
n	=	Noise power, in watts
n_a	=	Number of active FDM channels
N_B	=	Barrage or spot noise 3-dB bandwidth, in Hz
NBFM	=	Narrowband frequency modulation
n_d	=	RF input effective thermal noise power density, in watts/Hz

GLOSSARY (Continued)

NPR	= Noise power ratio
(NPR) _{CS}	= Noise power ratio due to the continuous portions of the desired and interfering FDM/FM spectra
(NPR) _{DC}	= Noise power ratio due to the residual carrier of the FDM/FM desired signal
(NPR) _{IC}	= Noise power ratio due to the residual carrier of the FDM/FM interfering signal on the desired signal
N_t	= Total number of FDM baseband channels
P	= Maximum average power of an ECM noise interference signal, in watts
P_{BAM}	= Average power of an AM barrage noise signal, in watts
PB50	= Phonetically balanced 50-word list
P_{ch}	= Per-channel noise-loading power, in dBm0
P_d	= Power density of a barrage noise signal, in watts/Hz
PG	= Processing gain
PG_{BAM}	= FDM/FM receiver processing gain to barrage amplitude-modulated noise interference, in dB
PG_{BSN}	= FDM/FM receiver processing gain for barrage and spot noise interference, in dB
PG_{CW}	= FDM/FM receiver processing gain for a CW interfering signal, in dB
PG_{FM}	= FDM/FM receiver processing gain for an FM interfering signal, in dB
PG_{GN}	= FDM/FM receiver processing gain for Gaussian noise interference, in dB
PG_{PBN}	= FDM/FM receiver processing gain for a pulse-modulated barrage noise signal, in dB

GLOSSARY (Continued)

- $P_{G_{SPN}}$ = FDM/FM receiver processing gain for a swept-spot noise signal, in dB
- P_m = Baseband mean white-noise-loading power, in dBm0
- PN = Pseudonoise
- P_{PBN} = Average power of a pulse-modulated barrage noise signal, in watts
- P_{RC} = Residual carrier power as a fraction of the total carrier power, in dB
- PRF = Pulse repetition frequency, in pps
- PW = Pulsewidth
- p_{Wp} = Psophometric-weighted noise power, in picowatts
- p_{WOp} = p_{Wp} at a point of zero relative level
- $P(x)$ = Noise-power density spectrum of the FDM/FM signal as a fraction of the carrier power, in Hz^{-1}
- R_c = Chirp rate
- RF = Radio frequency
- RMS = Root mean square
- $R_x(0)$ = Average power in a phase-modulating baseband signal
- SINAD = When no interference is added to the receiver, it represents the ratio of the audio output signal plus noise plus distortion to noise plus distortion, $(S + N + D)/(N + D)$. When interference is added to the receiver, it represents the ratio of the signal plus noise plus distortion plus interference to noise plus distortion plus interference, $(S + N + D + I)/(N + D + I)$
- S/N = Audio output (test channel) test tone-to-noise power ratio, in dB
- (s/n) = Channel output test tone-to-noise power ratio

GLOSSARY (Continued)

SR	=	Sweep rate of a swept-spot noise signal, in sweeps/second
SS	=	Spread-spectrum
S_T	=	Sweep time of swept-spot noise interference, in seconds
S_W	=	Sweep width of swept-spot noise interference, in Hz
$S_x(f)$	=	Power spectral density of the phase-modulating baseband signal
$S_x^*(f)$	=	Power spectral density of the frequency-modulating baseband signal
T_A	=	Antenna effective noise temperature, in Kelvin
T_{FM}	=	FM improvement threshold, in dBm
TLP	=	Transmission level point
T_m	=	Noise temperature (referred to its input) of the mth stage, in Kelvin
T_S	=	System noise temperature, in Kelvin
TTL	=	Test tone level, in dB
TV	=	Television
TWS	=	Time waveform simulation
UPL	=	Upper performance level
VIAS	=	Voice intelligibility analysis set
WF	=	Weighting factor, in dB
x	=	f/F_H
x_1	=	F_L/F_H
$Y(x)$	=	Power spectrum of the FDM/FM signal relative to the carrier power, in dB

GLOSSARY (Continued)

- Δf = Frequency difference between the desired FDM/FM carrier frequency and the interference signal carrier frequency, in Hz
- σ = Standard deviation (RMS voltage) of the Gaussian distribution
- $\sigma_x(f)$ = Normalized power spectral density of a phase-modulating signal
- $\sigma_x^*(f)$ = Normalized power spectral density of the frequency-modulating signal
- $\sigma_{y_o}(f)$ = Normalized lowpass equivalent power spectral density of a phase-modulated signal
- τ_{eff} = Effective transient width at IF output of FDM/FM receiver produced by a swept-spot noise interference signal, in seconds

SECTION 1

INTRODUCTION

BACKGROUND

The Electromagnetic Compatibility Analysis Center (ECAC) is engaged in a continuing effort to develop theoretical and/or empirical models of the performance of certain types of communication systems when subjected to various types of interference. The communication systems of interest include:

1. Amplitude modulation (AM)
 - a. Voice
 - b. Analog
 - c. Digital
2. Television (TV)
3. Angle modulation
 - a. Voice (narrowband and wideband)
 - b. Analog
 - c. Digital
4. Frequency division multiplex - FM (FDM/FM)
 - a. Voice
 - b. Analog
 - c. Digital.

The performance degradation effects of pulsed interference to amplitude modulation (AM), television (TV) and narrowband FM (NBFM) receivers were previously reported.^{1,2,3}

¹Hatch, W., Hinkle, R., and Mayher, R., *Analysis of Pulsed Interference to Amplitude Modulated Receivers*, ESD-TR-70-207, ECAC, Annapolis, MD, December 1970.

²Conklin, S., *Analysis of Pulsed Interference to Television Receivers*, ESD-TR-75-079, ECAC, Annapolis, MD, October 1974.

³Hernandez, A., *Investigation of Pulsed Interference to Narrowband FM Receivers*, ESD-TR-75-023, ECAC, Annapolis, MD, January 1976.

The investigation reported herein is part of the ECAC effort to formulate methods to analyze the performance degradation effects produced by various types of interfering signals on FDM/FM radio relay systems.

OBJECTIVES

The overall objective of the FDM/FM Wideband Radio Relay Degradation investigation was to develop a capability for predicting the performance of FDM/FM systems operating in the presence of interference. The specific objectives were:

1. To develop and validate a computerized model for determining the manner in which various types of interference signals affect the performance of narrowband and wideband FDM/FM radio relay communication systems
2. To obtain, through measurements and analyses, the system transfer functions that describe the performance of FDM/FM systems as a function of the RF input desired signal plus interference plus noise conditions
3. To compile information on FDM/FM systems (i.e., modulation characteristics, baseband noise-loading techniques, emission spectrum synthesis techniques, etc.) to facilitate performing degradation analyses for FDM/FM systems.

APPROACH

The FDM/FM investigation was divided into two different but simultaneous efforts, one involving a detailed measurements program and the other entailing the development of a computerized FDM/FM receiver simulation model. The measurements program, which was conducted at the U.S. Army Electronic Proving Ground (USAEPG), Fort Huachuca, Arizona, was divided into two major phases. Phase I

consisted of MIL-STD-449(D)⁴ parameter measurements which were made to obtain the receiver and transmitter characteristics (i.e., dynamic range, IF selectivity, etc.) of both a 600-channel and a 1200-channel FDM/FM microwave system.^a Phase II consisted of performance degradation measurements which were made to evaluate the degradation effects of various types of interference signals (i.e., pulse, FDM/FM, noise, etc.) on the performance of a 600-channel FDM/FM microwave system. The Phase I and Phase II measurements were conducted on a GTE Lenkurt 78A2 microwave radio with 46A2 carrier multiplex equipment.

The development of the FDM/FM receiver model involved the extension of ECAC's computerized time waveform simulation (TWS) methods to the problem of simulating the FDM/FM receiver system and the desired and undesired signals. The FDM/FM TWS model that was developed as part of this effort represents a tool for determining the manner in which various types of interference signals affect the performance of FDM/FM radio relay communication systems.

The data from the measurements program was analyzed and the results were used to develop receiver performance transfer functions. These transfer functions, in turn, were compared with predicted transfer function data from the FDM/FM TWS model for the purpose of validating the FDM/FM TWS model. The theoretical details of the FDM/FM TWS model (Objective 1), including the model validation, were documented in a separate report.⁵

⁴Military Standard, *Radio Frequency Spectrum, Measurements of*, MIL-STD-449(D), February 1973.

^aSome of the measurement methodologies developed during the FDM/FM measurements are currently being used to update MIL-STD-449(D).

⁵Hernandez, A. A., Lewis, C. E., *A Model for Time Waveform Simulation of FDM/FM Receivers*, ECAC-UM-78-018, ECAC, Annapolis, MD, November 1978.

The results of the efforts performed in meeting the second and third objectives, including the measurement procedures, are documented in the various sections and appendixes of this report.

SECTION 2

DESCRIPTION OF MEASUREMENTS

An extensive measurements program was conducted in support of the FDM/FM radio relay performance degradation investigation. These measurements were made to acquire the system parameter data and the performance degradation data necessary for developing the receiver transfer functions.

The measurements program was divided into two major phases. Phase I consisted of MIL-STD-449(D) (Reference 4) closed system receiver and transmitter parameter measurements conducted on both a 600-channel and a 1200-channel FDM/FM system. Phase II consisted of detailed closed system performance degradation tests conducted on a 600-channel FDM/FM system. Noise power ratio (NPR) measurements were made prior to commencing the Phase I testing to confirm that the FDM/FM systems were operating within manufacturer specifications.

WIDEBAND FDM/FM MICROWAVE SYSTEM DESCRIPTION

Two systems were tested during the Phase I and Phase II measurements. One system consisted of a GTE Lenkurt 78A2 FDM/FM microwave radio with 46A2 carrier multiplex equipment configured for 600-channel operation. The other system consisted of a GTE Lenkurt 78A2 FDM/FM microwave radio configured for 1200-channel operation.

The 78A2 microwave radio is an all-solid-state FDM/FM system operating in the 5.925- to 6.425-GHz telephone common carrier frequency band. All measurements involving the 600-channel system were conducted on a tuned frequency of 6382.6 MHz. The 1200-channel system was operated on a tuned frequency of 5982.3-MHz. The

microwave radio system is comprised of a 778A2 microwave radio assembly and a 758B baseband assembly. The block diagrams⁶ of the 778A2 microwave radio transmitter and receiver assemblies are illustrated in Figures 1 and 2, respectively.

The GTE Lenkurt 46A2 Carrier Multiplex is a fully transistorized, single-sideband, suppressed-carrier system employing a modulation plan which is compatible with other systems meeting the International Telephone and Telegraph Consultative Committee (CCITT) recommendations. The modulation plan of the 600-channel 46A2 carrier multiplex used in the measurements is illustrated in Figure 3.

NOISE POWER RATIO MEASUREMENTS

NPR measurements were conducted on both the 600-channel and the 1200-channel FDM/FM systems prior to commencing the Phase 1 testing to determine both the idle (intrinsic) noise level and the idle plus intermodulation (IM) noise level of these two FDM/FM microwave systems. The measured noise levels were compared with the manufacturer's recommended noise levels to determine if the system under test met the recommended noise performance criteria. The NPR measurement technique will be discussed next.

White Noise Testing Theory

The NPR is a common unit of noise testing and is defined by Tant⁷ as the decibel ratio of the noise level in a measuring channel with the baseband fully noise-loaded to the level in that channel with all of the baseband noise-loaded except the measuring channel. The NPR measurement technique is illustrated in Figure 4.

⁶All *Solid-State Microwave Radio*; GTE Lenkurt, 78A2, Issue Two, August 1971.

⁷Tant, M. J., *Multichannel Communication Systems and White Noise Testing*, Marconi Instruments, New Jersey, July 1974.

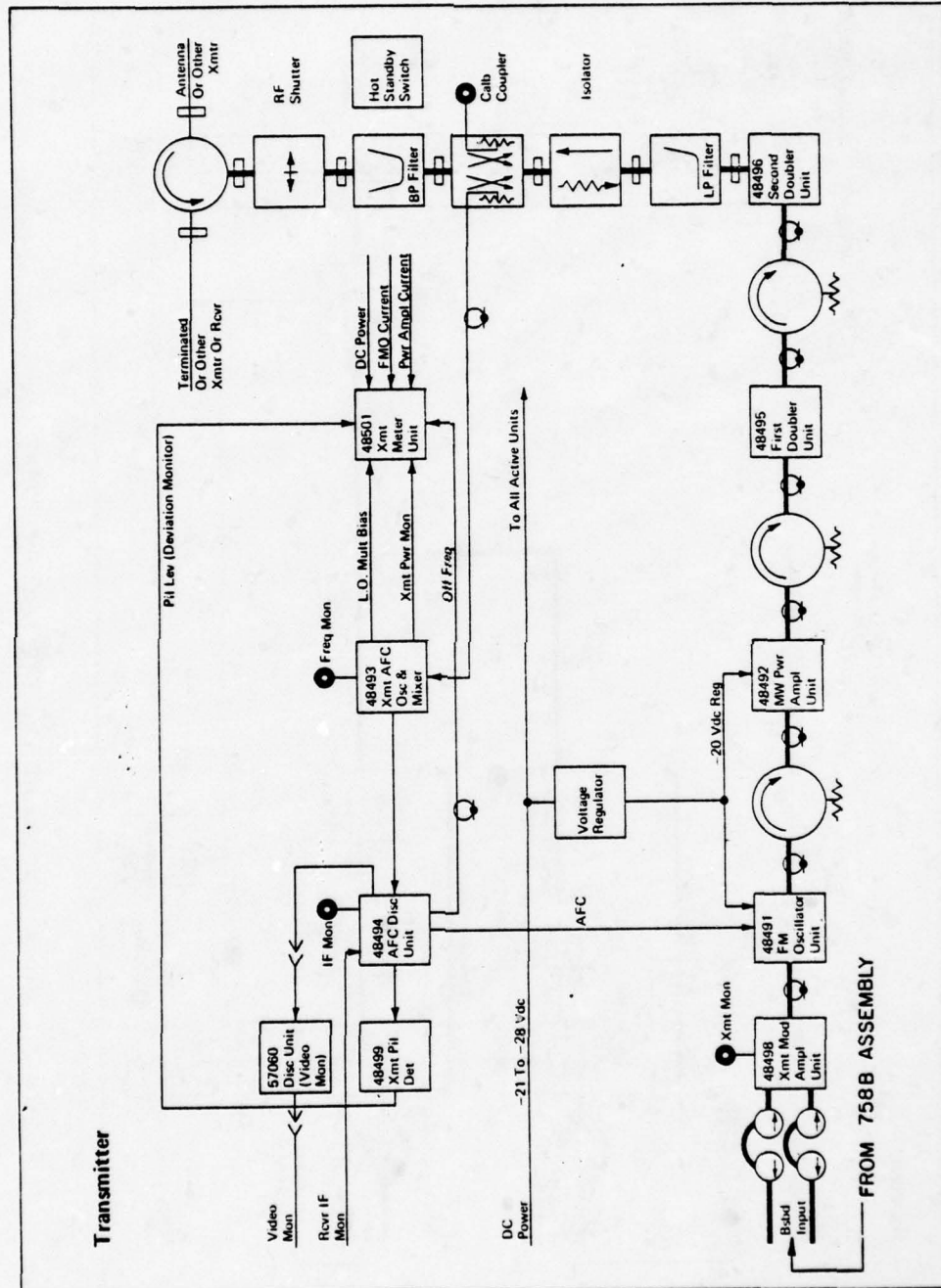


Figure 1. Block diagram of the GTE Lenkurt 778A2 transmitter assembly.

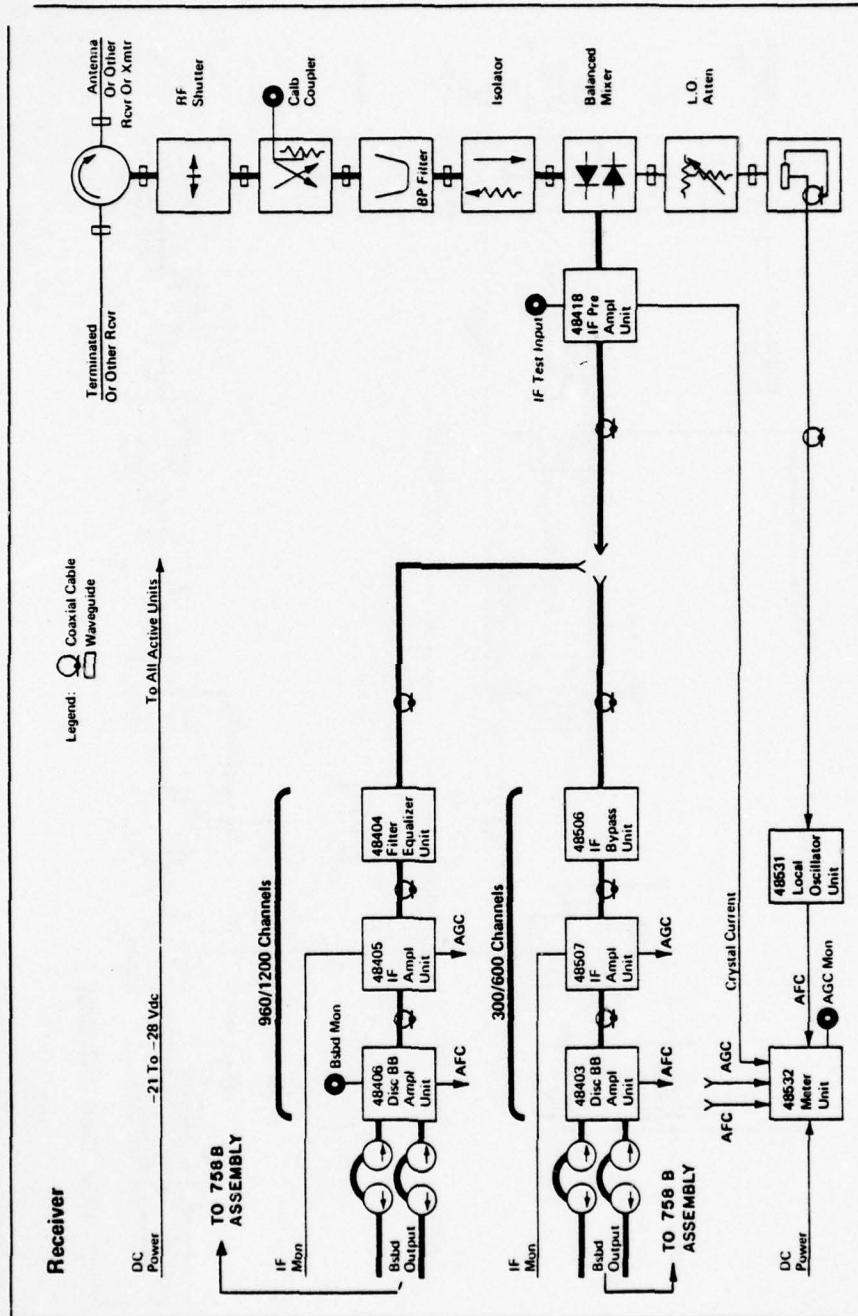


Figure 2. Block diagram of the GTE Lenkurt 778A2 receiver assembly.

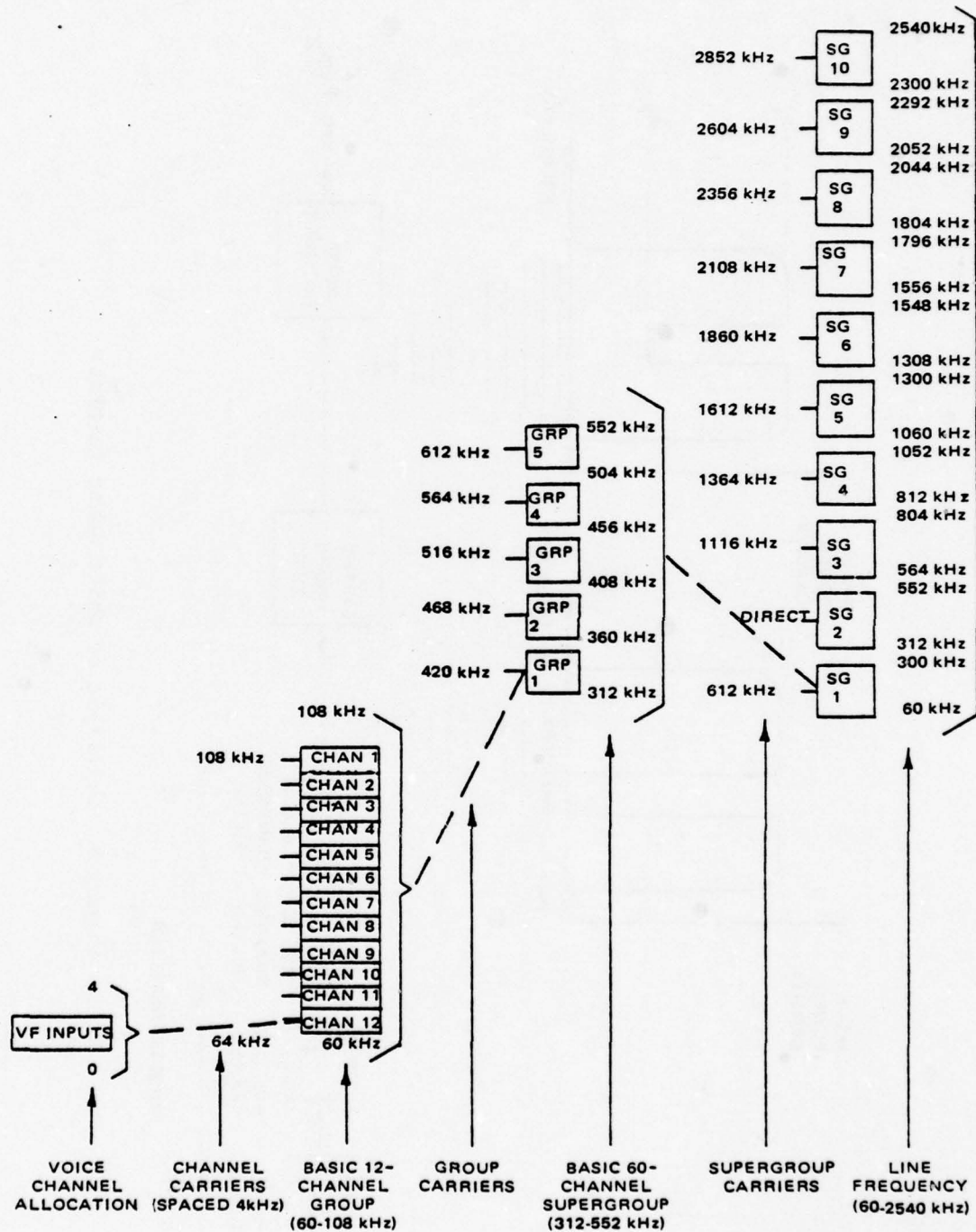


Figure 3. 46A2 carrier multiplex 600-channel modulation plan.

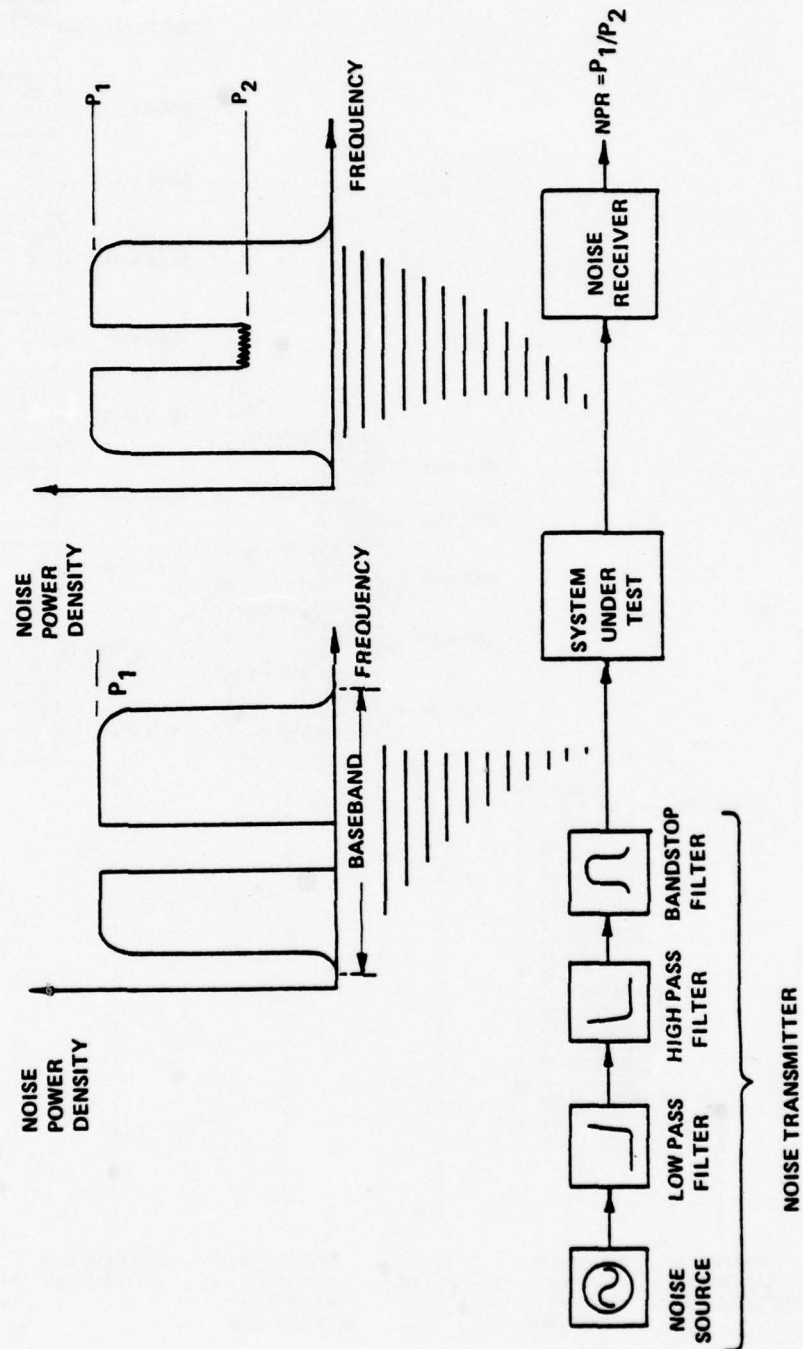


Figure 4. Principle of white noise testing.

The noise power density required to load the FDM/FM system baseband for white noise testing is related to both the nominal channel capacity and the type of information being represented. Figure 5 illustrates the power, in dBmO, required to noise-load (simulate) the FDM baseband as a function of system channel capacity for both speech and data information (Reference 7).

The mean white noise power level needed to simulate speech or data loading for 99% of the busy hour and a given system channel capacity can also be derived from the following equations:

Speech loading, $N_t < 240$ channels

$$P_{ch} = -1 - 6 \log N_t \quad (1)$$

Speech loading, $N_t \geq 240$ channels

$$P_m = -15 + 10 \log N_t \quad (2)$$

Speech loading, $12 < N_t < 240$ channels

$$P_m = -1 + 4 \log N_t \quad (3)$$

Data loading, $N_t > 12$ channels

$$P_m = -10 + 10 \log N_t \quad (4)$$

where

P_{ch} = per-channel noise-loading power, in dBmO

P_m = baseband mean white-noise-loading power,
in dBmO

N_t = number of channels.

Equations 1 through 4 are the internationally agreed equivalent noise-loading levels and are quoted by CCIR, CCITT, DCA, INTELSAT, etc. A slightly different loading formula which was established by the Bell Systems is given by:

Speech loading, $N_t \geq 240$ channels

$$P_m = -16 + 10 \log N_t, \text{ in dBmO} \quad (5)$$

This equation represents 1 dB lighter loading than Equation 2, and reflects a reduction in talker volumes from previous values.

The Defense Communications Agency (DCA) is currently specifying that "it shall be a design objective that all multichannel communication equipment" (for U.S. military systems) "be designed for 100% digital data loading." This type of loading, which is given by Equation 4, allows essentially unrestricted use of data.

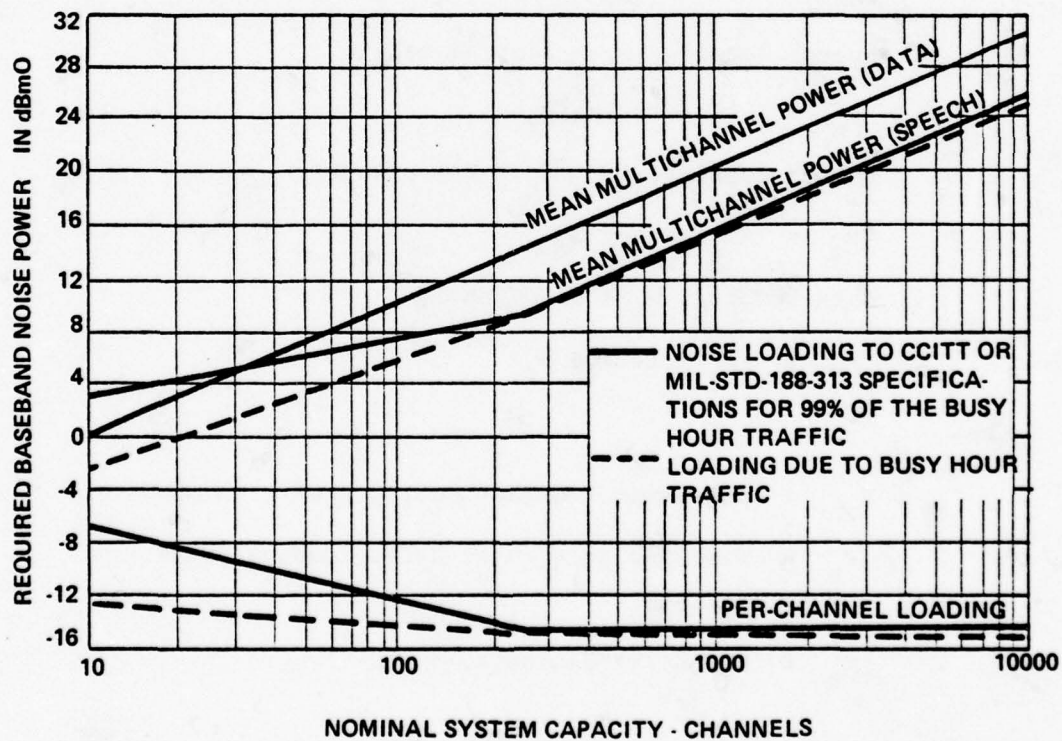


Figure 5. Required baseband noise power levels as a function of nominal channel capacity.

Composite Speech and Data Loading

For those cases in which a system is carrying relatively large numbers of data and speech channels simultaneously, the equivalent noise loading becomes more complex. In this case, it is customary to calculate separately the equivalent RMS loading for the data and speech channels and then to sum the two on a power basis to obtain the composite white-noise-loading power.

NPR Measurement Procedure

The test setup used in the NPR measurements is shown in Figure 6. The following procedure was used to perform these measurements.

600-Channel System

1. The 78A2 Lenkurt system was configured for a 600-channel capacity and operated on a radio frequency (RF) of 6382.6 MHz. This system was set up and aligned in accordance with Lenkurt procedures.
2. The measurement configuration as shown in Figure 6 was set up for NPR measurements. The test tone level (TTL) at both the transmitter baseband input and the receiver baseband output was -25.0 dB.
3. The noise transmitter was set up with a 60-kHz high pass, a 2660-kHz low pass, a 70-kHz band stop and a 2438-kHz band stop filter. The noise receiver had a 70-kHz bandpass and a 2438-kHz bandpass filter.

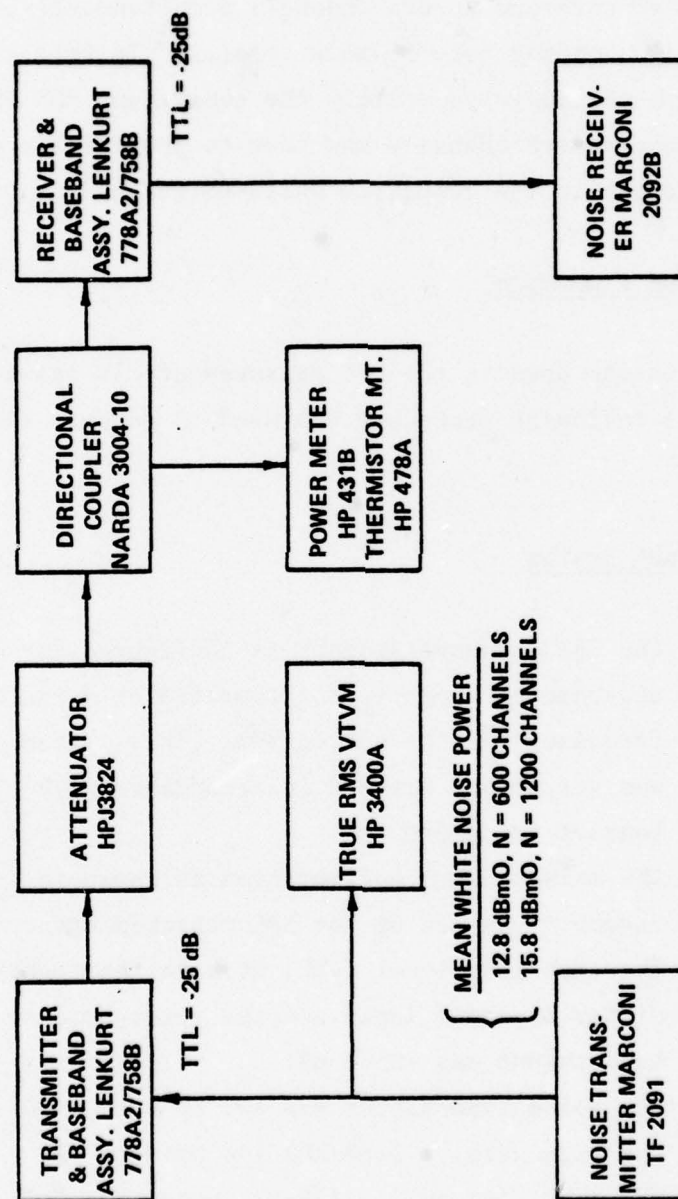


Figure 6. Baseband noise power ratio measurement block diagram.

4. The output of the noise transmitter was adjusted for a 12.8-dBm0 level with the high pass and low pass filters inserted. The RF input level to the 778A2 receiver was set at -36 dBm.
5. The 70-kHz bandpass filter in the noise receiver was inserted and a 0 dB reference level established on the noise receiver. The 70-kHz band stop filter was inserted in the noise transmitter and the attenuators on the noise receiver adjusted to reestablish the reference level. The change in attenuation from the reference level represented the idle-noise plus intermodulation-noise NPR. The input to the transmitter baseband was removed and replaced with a 75-ohm termination. The attenuators on the noise receiver were adjusted to reestablish the reference level. The change in attenuation from the reference level represented the idle-noise NPR. The above measurements were repeated using the 2438-kHz band stop and bandpass filters in the noise transmitter and noise receiver, respectively.

1200-Channel System

1. The 78A2 Lenkurt system was configured for 1200-channel capacity and operated on a radio frequency of 5982.3 MHz. This system was set up and aligned in accordance with Lenkurt procedures.

2. Same as Step 2 in 600-channel system.
3. The noise transmitter was set up with a 60-kHz high pass filter, a 5600-kHz low pass filter, a 70-kHz, 534 kHz, 1248-kHz, 2438-kHz and a 5340-kHz bandstop filter. The noise receiver had a 70-kHz, 534-kHz, 1248-kHz, 2438-kHz and a 5340-kHz bandpass filter.
4. The output of the noise transmitter was adjusted for a 15.8-dBm0 level with the high pass and low pass filters inserted. The RF input level to the 778A2 receiver was set at -30 dBm.
5. Same as Step 5 in 600-channel system except that the measurements were repeated using the 534-kHz, 1248-kHz, 2438-kHz and 5340-kHz band stop and bandpass filters.

After measuring the NPR's for both systems, corresponding values of C-message-weighted noise and psophometric-weighted noise were calculated using the following equations:

$$\text{dBrncO} = 71.7 - \text{NPR}, N_t \geq 240 \text{ channels} \quad (6)$$

where

dBrncO = C-message-weighted noise referenced to a zero dBm0 test point, in dB

NPR = Noise power ratio, in dB

$$\text{dBrncO} = 10 \log \text{pWOp} \quad (7)$$

where

pWOp = psophometric-weighted noise referenced to a zero dBm0 test point, in picowatts.

The conversions given by Equation 6 are within 0.3 dB for conventional loading and channel capacity greater than or equal to 240 channels.

The measured and calculated noise performance levels for both the 600-channel and 1200-channel systems are presented in TABLES 1 and 2, respectively. Also shown in these tables are the noise performance levels recommended by GTE Lenkurt.⁸ The results shown in TABLE 1 and TABLE 2 indicate that the noise performance levels of the systems tested were better than the manufacturer's recommended noise performance levels.

The NPR measurements were followed by MIL-STD-449(D) parameter measurements on both systems. These measurements are discussed next.

SYSTEM PARAMETER MEASUREMENTS

MIL-STD-449(D) (Reference 4) transmitter and receiver parameter measurements were made to obtain the characteristics (i.e., RF selectivity, IF selectivity, dynamic range, modulator bandwidth, etc.) of both the 600-channel and the 1200-channel FDM/FM microwave systems.

Transmitter Measurements

The following transmitter characteristics were measured:

1. Modulator bandwidth
2. Modulation characteristics
3. Power output

⁸"GTE Lenkurt 78A2/B2 Solid State Microwave System (System Noise Measurements)," *GTE Practices*, Section 394-781-681, Issue Two, January 1975.

TABLE 1
RECOMMENDED AND MEASURED NOISE PERFORMANCE
(ONE-HOP 600-CHANNEL 78A2 SYSTEM)

	Number Channels	Rcv RF Input Level (dBm)	Test Slot f (kHz) ^a								Idle Noise (1 Hop Only)			Idle Noise + I M (1 Hop Only)		
			70	534	1248	1722	2438	3886	5340	dBrnc0	NPR	pWOp	dBrnc0	NPR	pWOp	
Recommended	600	-36	X		X		X			18	54	63	21	51	126	
Measured (worst slot)	600	-36	X				X			17.2	54.5	52.5	19.2	52.5	83.2	

^a X = recommended and measured test slots.

TABLE 2
RECOMMENDED AND MEASURED NOISE PERFORMANCE
(ONE-HOP 1200-CHANNEL 78A2 SYSTEM)

	Number Channels	Rcv RF Input Level (dBm)	Test Slot f (kHz) ^a								Idle Noise (1 Hop Only)			Idle Noise + I M (1 Hop Only)		
			70	534	1248	1722	2438	3886	5340	dBrnc0	NPR	pWOp	dBrnc0	NPR	pWOp	
Recommended	1200	-30		X				X	X	20	52	100	23	49	200	
Measured (worst slot)	1200	-30	X	X	X		X		X	16.7	55	46.7	21.7	50	147.9	

^a X = recommended and measured test slots.

4. Carrier frequency stability
5. Conducted emission spectrum characteristics (narrow bandwidth)
6. Conducted emission spectrum characteristics (wide bandwidth)
7. Intermodulation.

Receiver Measurements

The following receiver characteristics were measured:

1. Sensitivity
2. Dynamic range
3. Audio selectivity
4. RF and IF selectivity
5. Conducted spurious responses
6. Intermodulation
7. Oscillator emission
8. Adjacent signal interference
9. Discriminator bandwidth.

The test setup and procedures used to perform these measurements together with the measured data are documented in Volume 1 of ECAC's Wideband FDM/FM Measurements Handbook.⁹ The results of the transmitter and receiver parameter measurements (i.e., selectivity plots, emission spectrum photographs, etc.) are documented in APPENDIX A.

⁹Hernandez, A., *Lenkurt Wideband FDM/FM Measurements Handbook (Volume 1)*, ECAC-HDBK-77-041-1, ECAC, Annapolis, MD, September 1977. NOTE: This is original data as received from test agency and only one copy of this data exists.

PERFORMANCE DEGRADATION MEASUREMENTS

Detailed performance degradation measurements were made to evaluate the degradation effects of various types of interfering signals on the performance of the 600-channel Lenkurt 78A2/46A2 FDM/FM system.

The following interfering signals were used in this investigation:

1. Noise
2. CW
3. FM
4. FDM/FM
5. Pulsed (chirped and nonchirped)
6. Spread-spectrum
 - a. Direct-sequence
 - b. Frequency-hopping
7. ECM (jamming)
 - a. Barrage and spot noise
 - b. AM barrage noise
 - c. Swept-spot noise
 - d. Pulse-modulated barrage noise.

The performance degradation measurements setup, generalized measurement procedure and channel output performance measures will be described in the remainder of this section. The measured data are documented in Volumes 2 through 8 of ECAC's Wideband FDM/FM Measurements Handbook.¹⁰

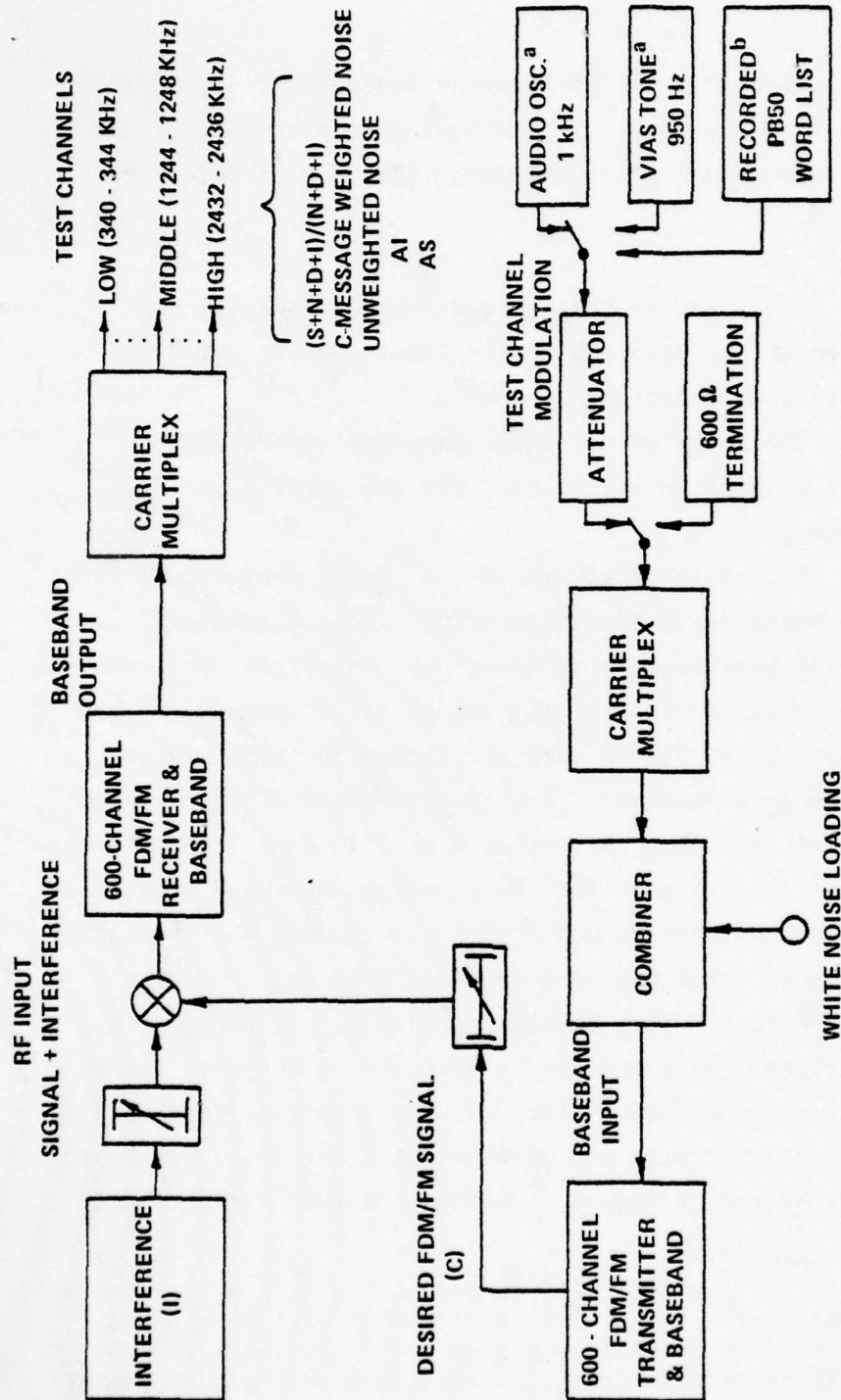
¹⁰Hernandez, A., *Lenkurt Wideband FDM/FM Measurements Handbook (Volumes 2 through 8)*, ECAC-HDBK-77-041-2 through ECAC-HDBK-77-041-8, ECAC, Annapolis, MD, May 1978. NOTE: This is original data as received from test agency and only one copy of this data exists.

MEASUREMENT SETUP AND PROCEDURES

A block diagram of the performance degradation measurement setup is shown in Figure 7. The following is a summary of the generalized measurement procedure used with each of the interfering signals:

1. The power of the desired FDM/FM signal at the receiver RF input was adjusted to the level specified for use with the particular interference source.
2. The interfering signal parameters were adjusted to one of the combinations specified for the particular interference source.
3. The articulation index (AI) upper performance level (UPL) was measured (with the interfering signal turned off) using the 950 Hz VIAS test tone to modulate the transmitter test channel.
4. With the interfering signal still turned off, the channel output $(S+N+D)/(N+D)^a$ and the channel output C-message-weighted noise were measured. For the $(S+N+D)/(N+D)$ measurements, the 950 Hz VIAS test tone was replaced by a 1000 Hz low distortion (≤ 0.1 percent) test tone. For the C-message-weighted noise measurements, the test channel modulation was removed and the multiplex test channel input was terminated in 600 ohms.
5. With the test channel modulation turned off, the interfering signal was turned on at a low RF input power level. The interfering signal power level (I) was then increased until a just noticeable increase in audio output noise level was heard independently by two listeners. The desired FDM/FM signal and

^aThroughout this report C/I will be used to specify RF input levels, and S/N, $(S+N+D)/(N+D)$ and $(S+N+D+I)/(N+D+I)$ will be used to specify baseband or channel output levels. The $(S+N+D)/(N+D)$ and $(S+N+D+I)/(N+D+I)$ power ratios are often referred to as the channel output SINAD.



^aAUDIO OSCILLATOR AND VOICE INTELLIGIBILITY ANALYSIS SET TONE LEVELS ADJUSTED TO -31 dBm AT MULTIPLEXER INPUT.

^bPEAK LEVEL OF WORD LIST TAPE ADJUSTED TO -24 dBm AT MULTIPLEXER INPUT.

Figure 7. Performance degradation measurement setup.

the interfering signal RF input power levels were then recorded for each listener. The average of the two levels was recorded as the minimum interference threshold (MINIT) for that particular interferer.

6. Measurements of AI, $(S+N+D+I)/(N+D+I)$ and C-message-weighted noise were made for the RF input power ratio (C/I) corresponding to the MINIT (Step 5). Articulation score (AS) measurements were also made for the on-tune, continuous-type interfering signals.

7. The interfering signal power level was increased until a 3 dB decrease in the channel output $(S+N+D+I)/(N+D+I)$ was obtained. The measurements outlined in Step 6 were repeated for the new RF input (C/I) power ratio.

8. Step 7 was repeated for a full range of RF input C/I power ratios to obtain the complete power transfer characteristics of the system.

9. Steps 1 through 8 were repeated for the remaining interfering and desired signal parameter combinations specified for use with the particular interfering signal.

10. Steps 1 through 9 were repeated for the remaining interfering signals.

The performance degradation measurements outlined in Steps 1 through 10 were conducted at a low, middle and high test channel. The low test channel was located in supergroup 2, group carrier 1 (340-344 kHz), the middle test channel in supergroup 5, group carrier 2 (1244-1248 kHz) and the high test channel in supergroup 10, group carrier 3 (2432-2436 kHz).

AUDIO OUTPUT PERFORMANCE MEASURES

AI, AS, C-message-weighted noise, and SINAD were the audio output measures used to evaluate the performance of the 600-channel FDM/FM system. The theoretical details of these audio output performance measures are included herein as part of APPENDIX B.

RECEIVER TRANSFER FUNCTIONS

The measured channel output performance data were used to develop two types of receiver transfer functions. One type of transfer function relates the various types of channel output performance measures to each other (i.e., AS vs. AI and AI vs. channel output test tone-to-noise power ratio). The empirically developed AS vs. AI and AI vs. S/N transfer functions are included herein as part of APPENDIX B.

The other type of transfer function relates the channel output performance (i.e., weighted noise, test tone-to-noise power ratio, etc.) to the RF input carrier-to-interference power ratio. The input/output transfer functions that were derived for the various types of interference signals used in the measurements are presented in the remaining sections of this report. Various parameters and techniques used to develop the receiver transfer functions are discussed next.

SECTION 3

FDM/FM PARAMETERS AND EMISSION SPECTRUM

DEFINITION OF USEFUL PARAMETERS

A number of FDM/FM parameters are often needed when performing degradation analyses for FDM/FM systems. While some of these parameters are often included in the equipment specifications, others are not, and therefore have to be calculated from the available information. The parameters for various capacity FDM/FM systems as specified by the CCIR and DCA¹¹ are given in TABLE 3. Methods for calculating these parameters will be discussed next.

Test Tone Deviation Per Channel

As a point of departure it is worth noting that the equipment manufacturer almost always specifies the RMS deviation that will be developed in the radio equipment by a 0-dBm test tone at a point of zero relative level. For systems with no emphasis, the specified per-channel deviation will be constant throughout the baseband. For systems with emphasis, however, the specified per-channel RMS deviation is not constant, with the specified deviation occurring only at the baseband frequency which corresponds to the crossover point between the preemphasis and deemphasis transfer functions ($0.608 F_H$ for CCIR emphasis where F_H is the maximum baseband frequency.) This is discussed further in Section 4.

The per-channel peak deviation for a signal of test tone level can be calculated from the per channel RMS deviation as:

¹¹ *Military Communication System Technical Standards, MIL-STD-188 Series.*

TABLE 3
PARAMETERS OF CCIR AND DCA FDM/FM SYSTEMS
(Page 1 of 2)

Number Channels N_t	Baseband (kHz)	d_{rms} (kHz) ^a	D_{rms} (kHz) ^b	m^c	P_{RC} (dB) ^d	B_{RF} (kHz) (12 dB Peak Factor) ^e	User Group
12	12-60	90	132	2.2	Negligible	1176.0	TERRESTRIAL CARRIERS
	60-108		132	1.22	-11.6	1272.0	
24	12-108	25	58.9	0.55	-11.6	687.2	
60	12-252	50	101.0	0.40	-14.7	1312.0	
	60-300	100	202.0	0.67	-9.8	2216.0	
		200	404.1	1.35	-40.0	3832.8	
120	12-552	50	116.1	0.21	-8.8	2032.8	
	60-552	100	232.3	0.42	-7.1	2962.4	
		200	464.6	0.84	-28.2	4820.8	
300	60-1300	200	615.9	0.47	-21.0	7527.2	
	64-1296	200	615.9	0.48	-20	7519.2	
600	60-2540	200	871.2	0.34	-21.6	12,049.6	
	64-2660		871.2	0.33	-19.6	12,289.6	
960	60-4028	200	1103.6	0.27	-22.2	16,884.8	
1260	60-5564	140	884.7	0.16	-10.7	18,205.6	
	60-5636	200	1263.8	0.22	-20.5	21,382.4	
1800	316-3204	140	1056.6	0.13	-1.9	24,860.8	
2700	312-12,388	140	1293.6	0.10	-1.9	35,124.8	
	316-12,388	140	1293.6	0.10	-1.9	35,124.8	

TABLE 3

(Page 2 of 2)

Number Channels N_t	Baseband (kHz)	d_{rms} (kHz) ^a	D_{rms} (kHz) ^b	m^c	P_{RC} (dB) ^d	B_{RF} (kHz) (12 dB Peak Factor) ^e	User Group
3	12-24	73	81.1	3.38	NEGLECTIBLE	696.8	SATELLITE CARRIERS
6	12-36	84	107.1	2.98		928.8	
9	12-48	91	125.9	2.62		1103.2	
12	12-60	90	131.9	2.2		1176	
24	12-108	125	210.4	1.95		1899.2	
36	12-156	160	292	1.87		2648	
48	12-204	182	351.9	1.73		3223.2	
72	12-300	232	486.3	1.62		4490.4	

^a d_{rms} = Per-channel RMS deviation for a signal of test tone level.

^b D_{rms} = FDM/FM signal RMS deviation.

^c m = FDM/FM signal RMS modulation index.

^d P_{RC} = Residual carrier power relative to full carrier power.

^e B_{RF} = Necessary RF bandwidth.

$$d_{\text{peak}} = \sqrt{2} d_{\text{rms}} \quad (8)$$

where

d_{peak} = Peak deviation of the channel for a signal of test tone level, in Hz

d_{rms} = RMS deviation of the channel for a signal of test tone level, in Hz.

It should be noted that the mean level deviation developed under speech and data loading conditions on each channel is dependent on the channel loading (Equations 1 through 5). For example, with CCIR loading, the mean level deviation developed under speech conditions on each channel of carriers with a capacity of 240 channels or greater is 15 dB below the RMS per-channel deviation.

Overall RMS Deviation of the FDM/FM Signal

The mean level deviation of all the baseband channels are added in power to produce an overall deviation whose RMS value is given by:

$$D_{\text{rms}} = d_{\text{rms}} \left[10^{P_m/20} \right] \quad (9)$$

where

D_{rms} = Overall RMS deviation, in Hz

d_{rms} = RMS deviation of the channel for a signal of test tone level, in Hz

P_m = Mean white noise power (Equations 2 through 5), in dBmO.

Peak Deviation of the FDM/FM Signal

The peak-to-RMS ratio (peak factor) of the multiplex signal is a function of several factors, including:

1. The peak-to-RMS ratio of the information in each channel
2. The variation in the information mean power levels
3. The number of active channels, since all channels will rarely be heavily loaded at the same time.

Detailed investigations conducted by Holbrook and Dixon (of Bell Laboratories in 1939)¹² into the amplitude distribution of single channel and multi-channel basebands have resulted in the activity coefficients shown in TABLE 4. The peak factor is then related to the number of active channels according to Figure 8. A peak factor of 12 dB is often used with systems of the fixed terrestrial service and is quoted by the CCIR. The FCC, however, has established a peak factor of 11.5 dB for multichannel loading of 12 channels and over on FM radio systems of the fixed terrestrial service. A peak factor of 10 dB is currently used for earth station systems (for all channel capacities) of the fixed satellite service.

From this information the peak deviation of the multiplexed signal can be calculated as:

$$D_{\text{peak}} = D_{\text{rms}} 10^{(\text{peak factor})/20} \quad (10)$$

where

$$D_{\text{peak}} = \begin{array}{l} \text{Peak deviation of the multiplexed signal,} \\ \text{in Hz} \end{array}$$

¹²Holbrook, B. D., and Dixon, J. T., "Load Rating Theory for Multi-Channel Amplifiers," *Bell System Tech. J.*, Volume 18 (October 1939), pp. 624-644.

D_{rms} = RMS deviation of the multiplexed
signal, in Hz

peak factor = Peak-to-RMS ratio of the multiplexed
signal, in dB.

TABLE 4
ACTIVITY COEFFICIENTS

Nominal System Capacity N_t	Number of Active Channels n_a	Activity Coefficient n_a/N_t
12	7	0.583
24	11	0.458
36	15	0.417
60	23	0.383
120	41	0.342
240	76	0.317
300	93	0.310
600	175	0.292
900	256	0.284
960	272	0.283
1200	335	0.279
1260	351	0.279
1800	493	0.274
2700	728	0.270

RMS Modulation Index

The RMS modulation index of the multiplexed signal is given
by:

$$m = D_{rms}/F_H \quad (11)$$

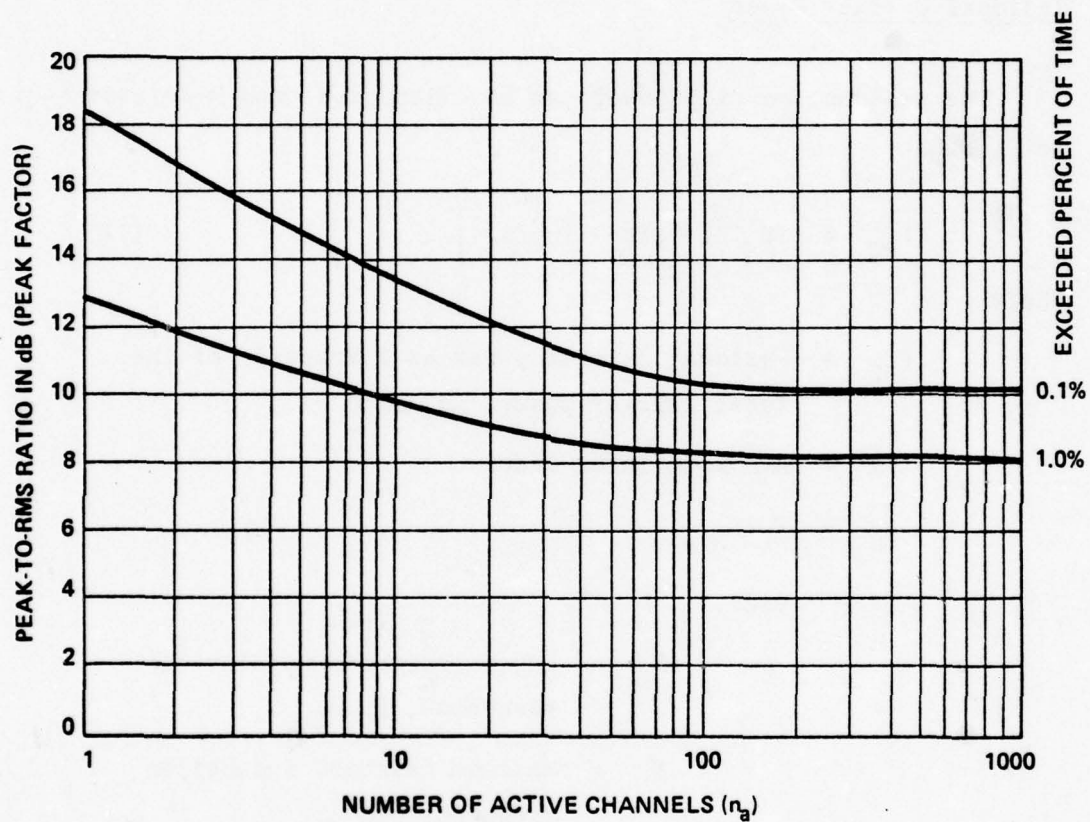


Figure 8. Variation of peak-to-RMS ratio of a multiplex signal with the number of active channels.

where

m = Multiplexed signal RMS modulation index

F_H = Maximum baseband frequency, in Hz.

Residual Carrier Power

The residual carrier power can be calculated from Middleton¹³ as:

$$P_{RC} = 10 \log \left[\exp - (m^2/x_1) \right] \quad (12)$$

where

P_{RC} = Residual carrier power as a fraction of the total carrier power, in dB

m = RMS modulation index

$x_1 = F_L/F_H$

where

F_L = Lowest baseband modulation frequency, in Hz

F_H = Maximum baseband modulation frequency, in Hz.

RF Bandwidth Calculations

The necessary RF bandwidth of the multiplexed signal can be calculated from the peak deviation with the following approximation:

¹³Middleton, D., "The Distribution of Energy in Randomly Modulated Waves," *Philosophical Magazine*, 42, 1951, p. 689.

$$B_{RF} = 2 D_{peak} + 2F_H \quad (13)$$

where

B_{RF} = The necessary RF bandwidth of the FDM/FM signal, in Hz

D_{peak} = Peak deviation of the multiplexed signal in Hz.

SUMMARY OF TYPICAL FDM/FM PARAMETERS

The parameters for various capacity GTE Lenkurt FDM/FM systems of the type widely used by the fixed terrestrial service are listed in TABLE 5. For the case of the fixed satellite service, the Intelsat IV transmission parameters are tabulated in TABLE 6. The parameters given in TABLES 3, 5 and 6 are representative of the extremes that will be found when performing degradation analyses for FDM/FM systems.

POWER SPECTRUM OF FDM/FM SIGNALS

The power spectral characteristics of FDM/FM signals have been investigated by other authors¹⁴⁻²⁰ and measurements have

¹⁴Ferris, C. C., "Spectral Characteristics of FDM/FM Signals," *IEEE Trans. Commun. Technol.*, Vol. COM-16, April 1968, pp. 233-238.

¹⁵Medhurst, R. G., "RF Bandwidth of Frequency-Division Multiplex Systems Using Frequency Modulation," *Proc. IRE*, Vol. 44, No. 2, February 1956.

¹⁶Medhurst, R. G., "RF Spectra and Interfering Carrier Distortion in FM Trunk Radio Systems with Low Modulation Ratios," *IRE Trans. On Communication Systems*, Vol. CS-9, No. 2, June 1961.

¹⁷Stewart, J., "The Power Spectrum of a Carrier Frequency Modulated by Noise," *Proc. IRE*, Vol. 42, October 1954.

¹⁸Middleton, D., *An Introduction to Statistical Communication Theory*, New York, McGraw Hill, 1960.

TABLE 5
PARAMETERS OF GTE LENKURT FDM/FM SYSTEMS

Service ^a	Band (Glz)	Number Channels N _t	Test Tone RMS Dev/ Ch. (klz)	D _{peak} (klz) (11.5 dB Peak Factor)	F _H (klz)	Continuity Pilot (Mhz)	Emission Designator
CC	2.11-2.2	132	130	1155	552	.607 1.499	3414F9
CC	2.11-2.2	252	65	690	1052	1.499	3484F9
IND	2.11-2.2	24	40	252	108	---	720F9
IND	1.85-1.99	300	200	2320	1300	1.499	7240F9
IND	1.85-1.99	420	140	1905	1800	3.200	7410F9
IND	6.575-6.875 12.2-12.7	420	200	2720	1800	3.200	9040F9
IND	6.575-6.875	600	140	2300	2660	3.200	9920F9
IND	12.2-12.7	600	200	3280	2660	3.200	11880F9
IND	12.2-12.7	960	200	4120	4200	4.715 6.199	16640F9
IND	12.2-12.7	1200	140	3250	5772	6.199 8.500	18044F9
CC	5.925-6.425 10.7-11.7	600	200	3280	3084	3.200 4.715	12728F9
CC	5.925-6.425 10.7-11.7	960	200	4120	4200	4.715 6.199	16640F9
CC	5.925-6.425 10.7-11.7 3.7-4.2	1200	140	3250	5772	6.199 8.500	18044F9
CC	5.925-6.425 10.7-11.7 3.7-4.2	1500	100	2600	6988	8.500	19176F9
CC	5.925-6.425 10.7-11.7	1800	140	3990	8524	9.023	25028F9

^a CC = Common carrier service.
IND = Industrial service.

TABLE 6
INTELSAT IV TRANSMISSION PARAMETERS
(STANDARD AND EXPANDED)

	Number Channels N_t	F_H (kHz)	B_{RF} (kHz) (10 dB Peak Factor)	d_{rms} (kHz)	D_{rms} (kHz)
GLOBAL BEAM	24 (STD)	108.0	2.00	164	275
	36 (EXP)	156.0	2.25	168	307
	60 (EXP)	252.0	2.25	136	276
	60 (STD)	252.0	4.00	270	546
	72 (EXP)	300.0	4.50	294	616
	96 (EXP)	408.0	4.50	263	584
	132 (EXP)	552.0	4.40	223	529
	96 (STD)	408.0	5.90	360	799
	132 (EXP)	552.0	6.75	376	891
	192 (EXP)	804.0	6.40	397	758
	132 (STD)	552.0	7.50	430	1020
	192 (EXP)	804.0	9.00	457	1167
	252 (EXP)	1052.0	8.50	358	1009
	252 (STD)	1052.0	12.40	577	1627
	312 (EXP)	1300.0	13.50	546	1716
	432 (EXP)	1796.0	15.75	517	1919
	432 (EXP)	1796.0	18.0	616	2276
	432 (STD)	1796.0	20.7	729	2688
	972 (STD)	4028.0	36.0	802	4417
	1092 (EXP)	4892.0	36.0	701	4118
SPOT BEAM	60 (STD)	252.0	2.25	136	276
	72 (EXP)	300.0	2.25	125	261
	132 (STD)	552.0	4.40	223	529
	192 (EXP)	804.0	4.50	180	459
	192 (STD)	804.0	6.40	297	758
	252 (EXP)	1052.0	6.75	260	733
	252 (STD)	1052.0	8.50	358	1009
	312 (EXP)	1300.0	9.00	320	1005
	432 (STD)	1796.0	13.00	401	1479
	612 (STD)	2540.0	17.8	454	1996
	792 (EXP)	3284.0	18.0	356	1784
	792 (STD)	3284.0	22.4	499	2494
	972 (EXP)	4028.0	22.5	410	2274
	1872 (STD)	8120.0	36.0	419	3181

also been reported.^{21,22} The usual treatment in these investigations has been to model the multiplexed signal as an ideally band-limited Gaussian noise signal. The bounded continuous spectrum may then be approximated for small values of RMS modulation index (≤ 0.3) by the first few terms of an infinite series; for large values of RMS modulation index (≥ 1.5), the probability density function of the baseband may be used to approximate the continuous and unbounded spectrum of Gaussian form.

For intermediate RMS modulation index coefficients, two different approaches have generally been followed. One approach consists of generating computer approximations of the FDM/FM spectra by utilizing Abramson's²³ expansion of the RF spectrum in convolution terms of the baseband spectrum (retaining convolution terms out to approximately the tenth order). The other approach (believed by some authors to be the most reliable) is to derive the power spectra from measurements.

This section summarizes the approximate formulas for sufficiently small and for very large values of RMS modulation

¹⁹Hamer, R., "Radio-Frequency Interference in Multichannel Telephony FM Radio Systems," *Inst., Elec. Eng.*, Paper 3326E, January 1961, pp. 75-89.

²⁰Cherry, E. C., and Rivlin, R. S., "Non-Linear Distortion, With Particular Reference to the Theory of Frequency Modulated Waves", *Philosophical Magazine*, 32, 1941, p. 265.

²¹Hamer, R., and Acton, R. A., "Power Spectrum of a Carrier Modulated in Phase or Frequency by White Noise," *Electronic and Radio Engineer*, Vol. 34, 1957, p. 246.

²²Pontano, B. A., Fuenzalida, J. C., and Chitre, Nand Kishore, M., "Interference into Angle-Modulated Systems Carrying Multichannel Telephony Signals," *IEEE Trans. On Communication*, Vol. COM-21, No. 6, June 1973.

²³Abramson, N., "Bandwidth and Spectra of Phase-and-Frequency-Modulated Waves," *IEEE Trans. on Communication Systems*, Vol. CS-11, No. 4, December 1963.

coefficients. For intermediate values of RMS modulation coefficients, the results of both the theoretical and empirical approach are summarized.

Small RMS Modulation Index ($m \leq 0.3$)

The continuous spectrum for non-preemphasized basebands and RMS modulation indices less than approximately 0.3 is given by (Reference 20):

$$Y(x) = 10 \log [F_H P(x)] = 10 \log \left[\frac{m^2}{2x^2(1 - x_1)} \right]$$

for $x_1 \leq |x| \leq 1$ and $m^2/x_1 < 1$ (14)

where

$$Y(x) = 10 \log [F_H P(x)] = \text{Power spectrum relative to carrier power, in dB}$$

$$F_H = \text{Maximum modulation frequency of multiplex signal, in Hz}$$

$$P(x) = \text{Noise-power density of the spectrum as a fraction of the carrier power, in Hz}^{-1}$$

$$m = \text{Multiplex signal RMS modulation index}$$

$$x = f/F_H$$

where

$$f = \text{frequency relative to the carrier frequency, in Hz}$$

$$x_1 = F_L / F_H$$

where

F_L = minimum modulation frequency of
multiplex signal, in Hz.

The residual carrier which corresponds to the carrier component of the spectrum for a single modulating tone is given by Equation 12.

As indicated, Equation 14 is valid only for that part of the spectrum which lies within the frequency limits defined by plus and minus $f = F_H$. Measurements reported by CCIR²⁴ and additional measurements made by this author (APPENDIX C) have demonstrated that the spectra beyond these limits decay almost linearly with x' , where $x' = x(1/\sqrt{2} m)$. Therefore, the slopes of the spectra were determined from the plots in Reference 24 and APPENDIX C and used to derive an empirical formula which may be used to approximate the spectrum beyond the limits of Equation 14. Thus, beyond $|x| = 1$:

$$Y(x) = 10 \log \left[\frac{m^2}{2(1 - x_1)} \right] - \left[\left(\frac{10}{\sqrt{2} m} \right) (|x| - 1) \right]$$

for $|x| \geq 1$. (15)

For preemphasized basebands and small values of RMS modulation index, the spectrum takes some form between those observed for frequency modulation and phase modulation. Generalized spectrum plots for a CCIR preemphasized baseband and small values of RMS modulation index are shown in Figure C-1 of APPENDIX C.

²⁴*Spectra and Bandwidth of Frequency-Modulated Emissions*, CCIR Report No. 419, XIIth Plenary Assembly, New Delhi, 1970.

Large RMS Modulation Index ($m \geq 1.5$)

For larger values of the RMS modulation index, the spectrum envelope may be derived from (Reference 17 and 19):

$$Y(x) = 10 \log[F_H P(x)] = 10 \log \left[\frac{1}{\sqrt{2\pi} m} \exp - (x^2/2 m^2) \right]. \quad (16)$$

For large values of RMS modulation index ($m \geq 2$), the residual carrier becomes negligible and the spectrum follows the Gaussian function whether or not preemphasis is used.

Intermediate Values of RMS Modulation Index ($0.3 \leq m \leq 1.5$)

The results of two different approaches will be summarized here. These are, the theoretical approach, which may be used to generate computer approximations of the spectra, and the empirical approach, which was used by Hamer (References 19 and 21) and this author (APPENDIX C) to generate generalized spectrum curves.

Computer Approximations of the FDM/FM Spectra

It is of interest to present here the theoretical FDM/FM power spectrum equation given by Ferris (Reference 14) which is valid for small and intermediate values of RMS modulation coefficients. The form of the spectrum is given as:

$$\sigma_{y_o}(f) = \sum_{n=0}^{\infty} \exp \left[-R_x(0) \right] \frac{[R_x(0)]^n}{n!} \left[\sigma_x(f) \right]^* \left[\sigma_x(f) \right] \quad (17)$$

where

$\sigma_{y_o}(f)$ = Normalized low-pass equivalent power spectral density of a phase-modulated signal

$R_x(0)$ = Average power in the phase-modulating baseband signal

$\sigma_x(f)$ = Normalized power spectral density of the phase-modulating signal

$[\sigma_x(f)]^n$ = N-fold convolution ($n > 1$).

The normalized low-pass equivalent power spectral density of a frequency-modulated signal can also be calculated from Equation 17 if the phase-modulating parameters are written in terms of the frequency-modulation parameters, which are given in Reference 14.

Thus, for FM:

$$R_x(0) = \int_{-\infty}^{\infty} S_x(f) df = \int \frac{S_x^*(f) df}{4\pi f^2} \quad (18)$$

and

$$\sigma_x(f) = \frac{\sigma_x^*(f)}{f^2} \quad (19)$$

where

$S_x(f)$ = Power spectral density of the phase-modulating baseband signal

$S_x^*(f)$ = Power spectral density of the frequency-modulating baseband signal

$\sigma_x^*(f)$ = Normalized power spectral density of the frequency-modulating signal

f = frequency relative to the carrier frequency.

The FDM/FM spectra can be calculated using Equations 17, 18 and 19 by performing the convolution, weighting, and summation of the weighted convolutions on a computer. It should be pointed out that Equations 17 through 19 were summarized here only to acquaint the reader with Ferris' method, and therefore the reader is directed to References 14 and 23 for all the mathematical details of this approach.

Empirically Derived FDM/FM Spectrum Curves

The generalized curves published by Hamer (Reference 19) may be used to obtain the FDM/FM spectrum for non-preemphasized basebands and intermediate values of RMS modulation indices, Figure 9. These curves were obtained from the measurements reported by Hamer and Acton (Reference 21). Similarly, the generalized curves shown in Figure C-2 of APPENDIX C may be used to obtain the FDM/FM spectrum for CCIR preemphasized basebands and intermediate values of RMS modulation indices. The ordinate in Figure 9 and in Figure C-2 gives the actual power spectrum relative to the carrier power as a function of normalized frequency relative to the mean carrier frequency.

In some cases, it is desired to normalize the power density of the spectrum to the power density at the mean carrier frequency ($x = 0$). For non-preemphasized basebands, the power density at $x = 0$ can be read directly from Figure 9, or it can be approximated by Equation 16 when $m \geq 0.5$ with x set to zero. When $m < 0.5$, the approximation given by Stewart can be used with x set to zero. That is:

$$Y(x) = 10 \log[F_H P(x)] = 10 \log \left[\frac{2m^2}{\pi^2 m^4 + 4x^2} \right]. \quad (20)$$

Equation 20 also gives the unbounded continuous spectrum when $m \leq 0.2$ and $m^2/x_1 \gg 1$ (i.e., when $F_L = 0$).

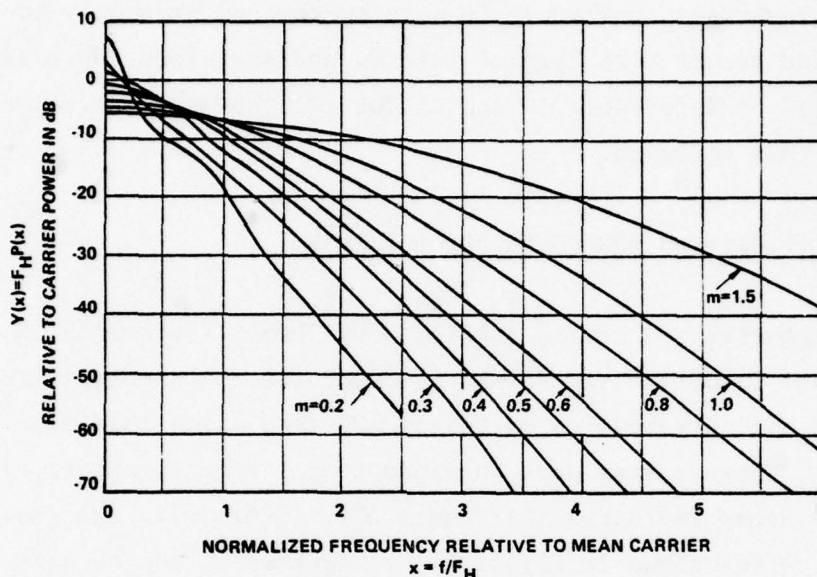


Figure 9. Relative FDM/FM power spectra ($0.2 \leq m \leq 1.5$).

For CCIR preemphasized basebands, the power density at $x = 0$ can be read directly from Figures C-1 and C-2, or it can be approximated by Equation 16 when $m \geq 1$.

Summary of FDM/FM Power Spectrum Synthesis Techniques

The various equations and methods which may be used to synthesize the power spectrum of an FDM/FM signal are summarized in TABLE 7. The measured power spectrum for a 600-channel FDM/FM signal is shown compared with the theoretically calculated spectrum^a and with the empirically calculated spectrum in Figure 10.

^aThe theoretical spectrum was synthesized using the computerized form of Equations 17, 18 and 19 programmed by Madison (1976, ECAC).

TABLE 7
SUMMARY OF FDM/FM NOISE-POWER SPECTRUM SYNTHESIS METHODS

RMS Modulation Index	Spectrum Synthesis Method	Residual Carrier	Remarks
$m < 0.3$	Equations 14 and 15 (no preemphasis) Figure C-1 (CCIR preemphasis)	Residual carrier present and given by Equation 12	The smaller the m^2/x_1 ratio, the more closely the spectrum approaches the form of Equations 14 and 15 and of Figure C-1
$0.3 \leq m \leq 1.5$	Figure 9 (No preemphasis) Figure C-2 (CCIR preemphasis) Equations 17, 18 and 19 (with or without preemphasis)	Residual carrier present and given by Equation 12 Residual carrier present and given by Equation 12	The greater the m^2/x_1 ratio, the more closely the spectrum approaches the form shown in Figures 9 and C-2 This method was also programmed by Madison (1976, ECAC)
$m > 1.5$	Equation 16 (with or without preemphasis)	Small residual carrier given by Equation 12 for $1.5 \leq m \leq 2$. For $m > 2$ the residual carrier is negligible	Spectrum is of Gaussian form

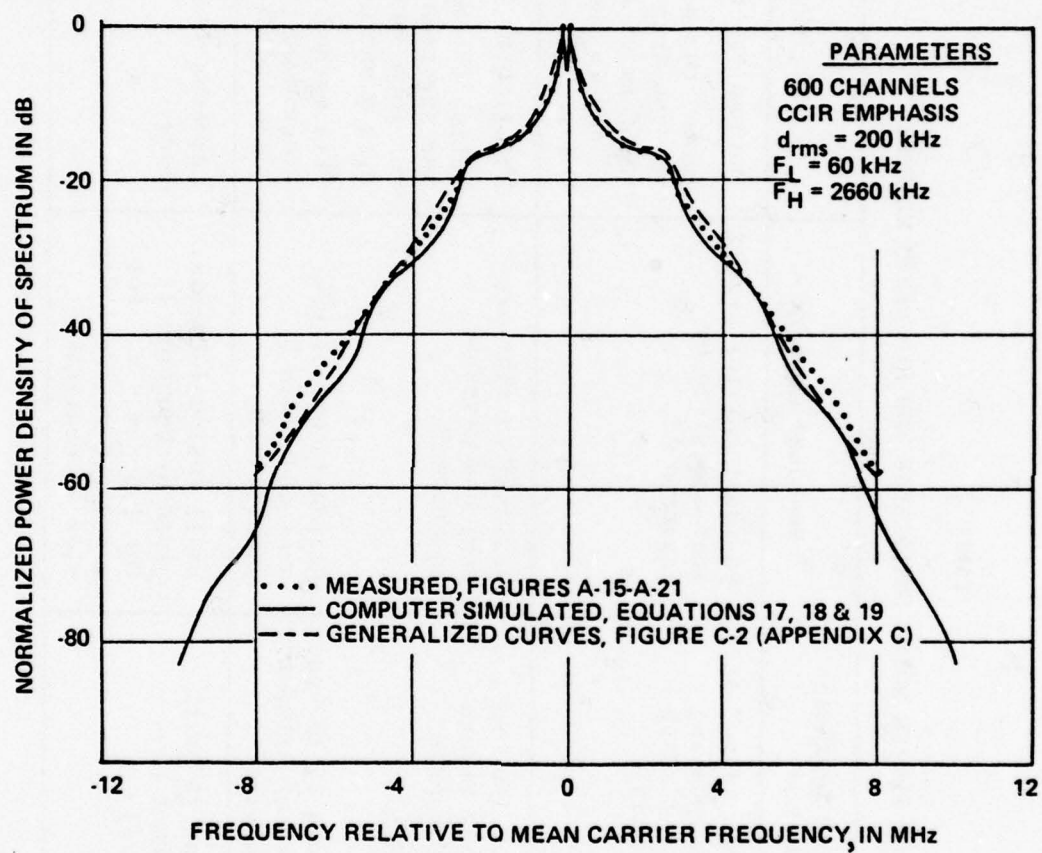


Figure 10. Comparisons between measured and calculated spectrum of 600-channel FDM/FM.

SECTION 4
SYSTEM NOISE PERFORMANCE

GENERAL

The total noise in any baseband channel is composed of noise contributions of several types, including: thermal, intermodulation, multiplex equipment and interference. These noise sources are discussed next.

THERMAL NOISE

Thermal noise contributions are of two general types, resistance noise and intrinsic noise. The resistance noise is generated in the antenna resistance and in the front-end circuits of the receiver. This noise is amplified within the receiver along with the RF carrier and, as a result of the FM process, the noise at the output of the receiver will vary inversely with the RF carrier input level.

The effective antenna resistance noise power at the input of a receiver can be calculated using the system noise temperature or using the antenna noise temperature and the noise figure associated with the receiver. For earth station receivers, the system noise temperature (T_S) is usually specified by the figure of merit (G/T_S) for that terminal, where G is the antenna gain. The noise power is then calculated as:

$$n = kT_S B \quad (21)$$

where

n = Noise power, in watts

k = Boltzmann's constant = 1.38×10^{-23} joules
per Kelvin

B = Noise bandwidth, in Hz, approximately equal to the IF bandwidth

T_S = System noise temperature, in Kelvin.

In the case of terrestrial microwave receivers, the antenna noise temperature is generally assumed to be 290 Kelvin. Equation 21 is modified to calculate the noise power as shown in Equation 22:

$$N = -114 + 10 \log B + F_g \quad (22)$$

where

N = Noise power for 290 Kelvin system noise temperature, in dBm

B = IF bandwidth, in MHz

F_g = Receiver noise figure, in dB.

In the case of earth station receivers, the actual system noise temperature has to be used in Equation 21. The system noise temperature can be computed from:²⁵

$$T_S = \sigma_t(T_A) + T_O(1 - \sigma_t) + T_1 + \sum_{m=2}^M \frac{T_m}{g_{m-1}} \quad (23)$$

where

T_S = System noise temperature, in Kelvin

σ_t = Transmission line coefficient ($1/L_1$, where L_1 is the waveguide loss between antenna output flange and receiver input flange)

T_A = Antenna effective noise temperature, in Kelvin

²⁵Reference Data for Satellite Communications Earth Stations, ITT Space Communications, Inc., Ramsey, NJ, Revised June 1973.

T_o = Physical temperature of the transmission line
(usually 290 Kelvin), in Kelvin

T_1 = Equivalent noise temperature of parametric
amplifier, in Kelvin

T_m = The noise temperature of the succeeding m^{th}
stage

g_{m-1} = The gain preceding the m^{th} stage.

The noise temperature, T_m , of a device (referred to the input port) may be expressed in terms of its noise factor, f_m , by means of the following relationship:

$$T_m = (f_m - 1)T_o \quad (24)$$

where

T_m = Noise temperature (referred to its input) of
the m^{th} stage

f_m = Noise factor associated with the m^{th} stage.

The equivalent noise power given by Equation 21 is often called the "detection threshold" when no other sources of noise (interference) are present at the receiver input. However, in an FM microwave system, this threshold does not represent a usable signal level. The true working threshold, often called the "threshold of FM improvement," occurs when the effective power of the signal is approximately 10 dB higher than the effective power of the noise. At this point, the peaks of the signal begin to exceed the peaks of the noise and FM quieting begins. The FM improvement threshold (T_{FM}) can be calculated as:

$$T_{FM} = 10 + 10 \log (kT_s B) \quad (25)$$

where

$$T_{FM} = \text{FM improvement threshold, in dBm.}$$

For RF input signals (C) higher than T_{FM} , the thermal noise in the baseband will decrease 1 dB for each 1 dB increase in RF input level.

The second type of thermal noise contribution, namely, the "intrinsic" or "idle" noise is that noise developed in the electronic circuitry of the transmitter and in the late stages of the receiver. This type of noise is independent of receiver RF input level and is the limiting noise performance level which could be measured between terminals under conditions of no modulating signal and a very strong RF input signal level. The intrinsic noise level for a particular system can be determined from the manufacturer's specifications, or from actual measurements. The measured and recommended levels of intrinsic noise for both the 600- and 1200-channel systems used in the measurements are given in TABLES 1 and 2 (Section 2).

INTERMODULATION NOISE

This type of noise consists of spurious signals created whenever the complex modulating signal passes through any kind of phase or amplitude nonlinearity. Statistically, this noise is very similar to the thermal noise and is present only when the system is being modulated, increasing as the loading increases.

The intermodulation noise for a given system can be obtained from the manufacturer's specifications, or from actual measurements.

The measured and recommended levels of intermodulation plus intrinsic noise for both the 600-and 1200-channel systems used in the measurements are also given in TABLES 1 and 2 (Section 2).

MULTIPLEX SYSTEM NOISE

The amount of noise contributed by the multiplex system under loaded conditions is a characteristic of the equipment and remains relatively fixed for a given load and equipment configuration. Typical values of multiplex noise (600- to 1260-channel LOS system with normal load) range between 21 dBrnc0 and 28 dBrnc0.²⁶

The total multiplex noise is composed of noise contributions from several subsystems including: channel bank, group bank, supergroup bank, mastergroup bank and line amplifiers. These noise contributions can be determined from the manufacturer's specifications. Reference 26 provides information on the subject of multiplex noise and gives maximum noise levels for the various subsystems integrating the GTE Lenkurt 46A carrier system.

The noise contributed by the GTE Lenkurt 46A2 multiplex system during the performance degradation measurements was approximately 16.5 dBrnc0.

INTERFERENCE NOISE

The noise sources that have been described thus far have a significant effect on the overall microwave system design. These noise sources, with the exception of atmospheric and some forms

²⁶GTE Lenkurt 46A Carrier System Engineering Considerations, GTE Lenkurt Incorporated, San Carlos, CA, Issue 2, June 1971.

of man-made noise (which are believed to be negligible at microwave frequencies), would represent the major sources of noise to a microwave system if such a system was operated alone in the environment. However, the huge proliferation, in recent years, of terrestrial microwave systems, radars, earth stations, etc., have resulted in another source of noise^a in the form of interfering signals. These interfering signals affect the performance of FDM/FM systems by increasing the overall level of noise at the baseband channels and by degrading the FM threshold (T_{FM}).

DETERMINATION OF SYSTEM NOISE

The total noise present at the receiver input is combined with the carrier oscillations when receiving a useful signal, ($C > T_{FM}$), to produce a spectrum of interference at the receiver output. It is advantageous at this point to develop an expression (transfer function) that will allow one to calculate the output noise, in any baseband channel, in terms of the RF input desired signal plus interference plus noise conditions. The various parameters to be considered in the complete transfer function are illustrated by the noise model shown in Figure 11.

Gaussian Noise Transfer Function

The relationship between the channel output test tone-to-noise power ratio, s/n , and the RF input carrier power-to-effective thermal noise power density ratio, c/n_d , for $C > T_{FM}$, can be derived from Fagot and Magne²⁷ as:

^aThe term "noise" is also used here to describe unwanted signals appearing at the receiver baseband output.

²⁷Fagot, J., and Magne, P., *Frequency Modulation Theory*, Pergamon Press, The MacMillan Company, New York, 1961.

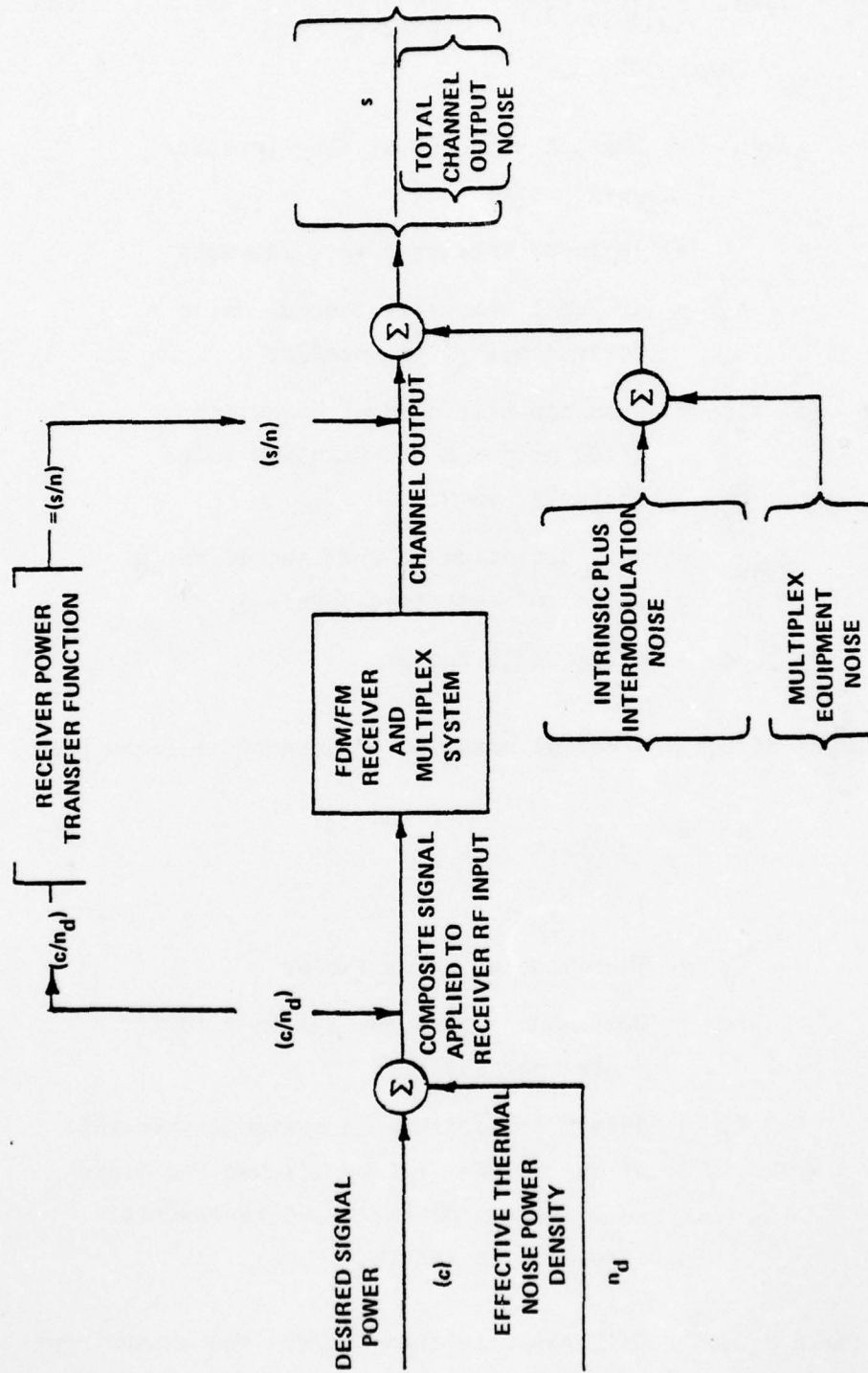


Figure 11. FDM/FM noise transfer function model.

$$(s/n) = \left[\left(\frac{c}{n_d} \right) \left(\frac{1}{2(f_H - f_L)} \right) \right] \left[\frac{d_{\text{peak}}}{F_{\text{ch}}} \right]^2 [e] \quad (26)$$

where

(s/n) = Channel output test tone-to-noise power ratio

c = RF input carrier power, in watts

n_d = RF input effective thermal noise power density, in watts/Hz

$(f_H - f_L)$ = Demultiplexer channel bandwidth (3100 Hz for a standard FDM voice channel), in Hz

d_{peak} = Peak deviation of the channel for a signal of test tone level, in Hz

e = Preemphasis factor.

The RF input effective thermal noise power density is given by:

$$n_d = f_g k T_S \quad (27)$$

where

f_g = The receiver noise factor

k = Boltzmann's constant = 1.38×10^{-23} joules per Kelvin

T_S = System temperature (a system temperature of 290 Kelvin will be assumed for microwave systems of the fixed terrestrial service), in Kelvin.

Another useful relationship is that between the channel output test tone-to-noise power ratio, s/n , and the RF input carrier-

to-effective thermal noise power ratio, c/n . The RF input effective thermal noise power is assumed to be contained in the IF 3-dB bandwidth, B_{IF} . This relationship can be derived from Equation 26 by multiplying and dividing the right-hand side of Equation 26 by B_{IF} and by setting the product, $n_d B_{IF}$, equal to the RF input effective thermal noise power ($n = n_d B_{IF}$). This gives:

$$(s/n) = (c/n) \left[\frac{B_{IF}}{(f_H - f_L)} \right] \left[\frac{d_{rms}}{F_{ch}} \right]^2 [e] \quad (28)$$

where

c/n = The RF input carrier-to-effective thermal noise power ratio (where the thermal noise is calculated in the IF bandwidth)

B_{IF} = 3-dB IF bandwidth, in Hz

$d_{rms} = \frac{d_{peak}}{\sqrt{2}}$ = RMS deviation of the channel for a signal of test tone level, in Hz

and all other terms are as previously described in Equation 26.

For the case in which it is desired to express the channel output test tone-to-noise power ratio (Equations 26 and 28) in dB we have for Equation 26:

$$(S/N) = C - 67.92 - 10 \log n_d + 20 \log(d_{peak}/F_{ch}) + E \quad (29)$$

and for Equation 28:

$$(S/N) = (C/N) + 10 \log(B_{IF}/3100) + 20 \log(d_{rms}/F_{ch}) + E \quad (30)$$

where

(S/N) = Channel output test tone-to-noise power ratio, in dB

(C/N) = RF input carrier-to-effective thermal noise power ratio (where the thermal noise is calculated in the IF bandwidth), in dB

C = RF input carrier power, in dBm

E = Preemphasis factor, in dB

and all other terms are as previously described.

For the case of microwave systems of the fixed terrestrial service, for which the system noise temperature is assumed to be 290 Kelvin, Equation 30 reduces to:

$$(S/N) = C + 136.1 - F_g + 20 \log(d_{\text{peak}}/F_{\text{ch}}) + E \quad (31)$$

where

F_g = Receiver noise figure, in dB

and all other terms are as previously described.

A term which is often found in the FDM/FM literature is the system's processing gain, PG, which is defined as:

$$PG = \begin{cases} (S/N) - (C/N) \\ (S/N) - (C/I) \end{cases} \quad (32)$$

For white Gaussian noise, the system's processing gain can be written immediately from Equation 30 as:

$$PG_{GN} = 10 \log(B_{IF}/3100) + 20 \log(d_{rms}/F_{ch}) + E \quad (33)$$

where

PG_{GN} = Gaussian noise processing gain for FDM/FM,
in dB

and all other terms are as previously described.

Equations 26, 28 through 31, and 33 represent various forms of the noise transfer function for FDM/FM systems. It should be pointed out that the "S" and "s" terms in (S/N) and (s/n), respectively, represent a standard zero dBm test tone at a zero relative level. Similarly, the terms "N" and "n" represent unweighted (flat) noise in a 3100-Hz bandwidth. The effects of preemphasis, E, as well as the effects of other common types of noise weightings will be discussed next.

Accounting for Emphasis in FM Systems

In FDM/FM systems without emphasis the channel peak deviation, d_{peak} , has a constant value regardless of the baseband frequency occupied by the channel. Also for these systems ($E = 0$), Equations 29 through 31 and 33 show that the noise will be worst in the high channels increasing at a rate of 20 dB per decade.

The use of emphasis networks in FM systems results in a more even distribution of noise across the baseband. However, even with emphasis, the noise is higher in the higher frequency channels. For CCIR-recommended emphasis, the specified deviation occurs at the $0.608 F_H$ crossover point of the preemphasis and deemphasis transfer functions, where F_H is the highest

baseband frequency.^{28,29} Channels near the lower end of the baseband will have deviations approximately 4 dB lower than the reference deviation, while the top channel will have a deviation 4 dB higher than the reference deviation.

The increase or reduction in deviation, for channels at baseband frequencies other than $0.608 F_H$, can be accounted for in Equations 29 through 31 and 33 by adding to these equations the amount of preemphasis (E) for the channel under consideration.

For CCIR preemphasis the dB value to be added is given by:

$$E = 5 - 10 \log \left\{ 1 + \frac{6.90}{1 + \frac{5.25}{\left[\frac{5F_H}{4F_{ch}} - \frac{4F_{ch}}{5F_H} \right]^2}} \right\} \quad (34)$$

where

E = Preemphasis value to be added to Equations 29, 30, 31 and 33, in dB

F_H = Maximum baseband frequency, in Hz

F_{ch} = Baseband frequency at the center of any channel, in Hz.

²⁸MIL-STD-188-313, *Subsystem Design and Engineering Standards and Equipment Technical Design Standards for Long-Haul Communications Transversing Microwave LOS Radio and Tropospheric Scatter Radio*, 19 December 1973.

²⁹"Preemphasis Characteristics for Frequency-Modulation Systems," *CCIR Recommendation 275-2*, CCIR XIIth Plenary Assembly, Volume IV, Part 1, New Delhi, 1970.

CHANNEL OUTPUT NOISE WEIGHTING

When the channel output noise is white or nearly white, the effect of weighting is simply to reduce the noise level by a fixed and predictable amount. The relationship between unweighted (flat) noise and weighted noise for the more common types of noise weighting is as follows:

$$\text{Psophometric-weighted noise} = \text{flat noise} - 2.5 \text{ dB} \quad (35)$$

$$\text{FlA-weighted noise} = \text{flat noise} - 3 \text{ dB} \quad (36)$$

$$\text{C-message-weighted noise} = \text{flat noise} - 1.5 \text{ dB} \quad (37)$$

where the flat noise is contained in the audio range from 300 to 3400 Hz.

The various units commonly used to express the channel output noise are related as follows (see APPENDIX B):

$$\text{dBm0} = \text{dBmOp} + 2.5 \quad (38)$$

$$\text{dBm0} = \text{dBrnc0} - 88.5 \quad (39)$$

$$\text{dBm0} = \text{dBa0} - 82 \quad (40)$$

where

dBm0 = Noise power referenced to the zero transmission level point. The zero transmission level point (o TLP) is taken as 0 dBm

dBmOp = Psophometric-weighted noise power referenced to 0 TLP

dBrnc0 = dB above reference noise, C-message-weighted, relative to 0 TLP. Reference noise is equivalent to a 1000-Hz tone at -90 dBm.

dBa0 = dB above reference noise, FlA-weighted, relative to 0 TLP. Reference noise is equivalent to a 1000-Hz tone at -85 dBm.

An approximate relationship between these units which is commonly accepted is:

$$\text{dBrnc0} = \text{dBa0} + 6 = \text{dBm0p} + 90. \quad (41)$$

(S/N) AND NPR

The test tone-to-noise power ratio in a 3.1-kHz voice channel is related to the noise in that channel expressed in dBm0 as follows:

$$\text{S/N (unweighted)} = -\text{dBm0}. \quad (42)$$

Similarly, from Equations 39 and 40:

$$\text{S/N (unweighted)} = 88.5 - \text{dBrnc0} \quad (43)$$

$$\text{S/N (unweighted)} = 82 - \text{dBa0}. \quad (44)$$

Other useful relationships from Equations 35, 36 and 37 are:

$$\text{S/N (psophometric)} = \text{S/N (unweighted)} + 2.5 \text{ dB} \quad (45)$$

$$S/N \text{ (C-message)} = S/N \text{ (unweighted)} + 1.5 \text{ dB} \quad (46)$$

$$S/N \text{ (F1A)} = S/N \text{ (unweighted)} + 3 \text{ dB.} \quad (47)$$

The unweighted^a test tone-to-noise ratio in a 3.1-kHz channel is related to the noise power ratio (NPR) by (see Section 2):

$$\begin{aligned} (S/N) &= \text{NPR} + 6 \log N_t + 2.1, \\ N_t &< 240 \text{ channels} \end{aligned} \quad (48)$$

$$\begin{aligned} (S/N) &= \text{NPR} + 16.3, \\ N_t &\geq 240 \text{ channels.} \end{aligned} \quad (49)$$

The various relationships presented here (Equations 35 through 49) are used to convert the noise performance of a system from values in one unit to values in any of the other commonly accepted units.

COMPARISONS BETWEEN MEASURED AND CALCULATED NOISE PERFORMANCE

One test conducted on the 600-channel system was designed to obtain the thermal noise transfer function of the system. This was accomplished by measuring the channel output C-message-weighted noise as a function of the carrier level at the receiver RF input (see Figures 12, 13 and 14).

Figures 12, 13 and 14 show comparisons between the measured thermal noise transfer function data and the theoretically calculated transfer functions. The results of these comparisons indicate that the measured processing gains agree closely with the calculated 30.1-dB, 21.1-dB and 20.1-dB processing gains for the low, middle and high test channels, respectively. The FDM/FM system parameters used in the calculations are summarized in TABLE 8. These were also the parameters of the system tested.

^aUnweighted noise is generally not labeled. That is, the "N" term in S/N is understood to represent unweighted noise in a 3.1-kHz voice channel.

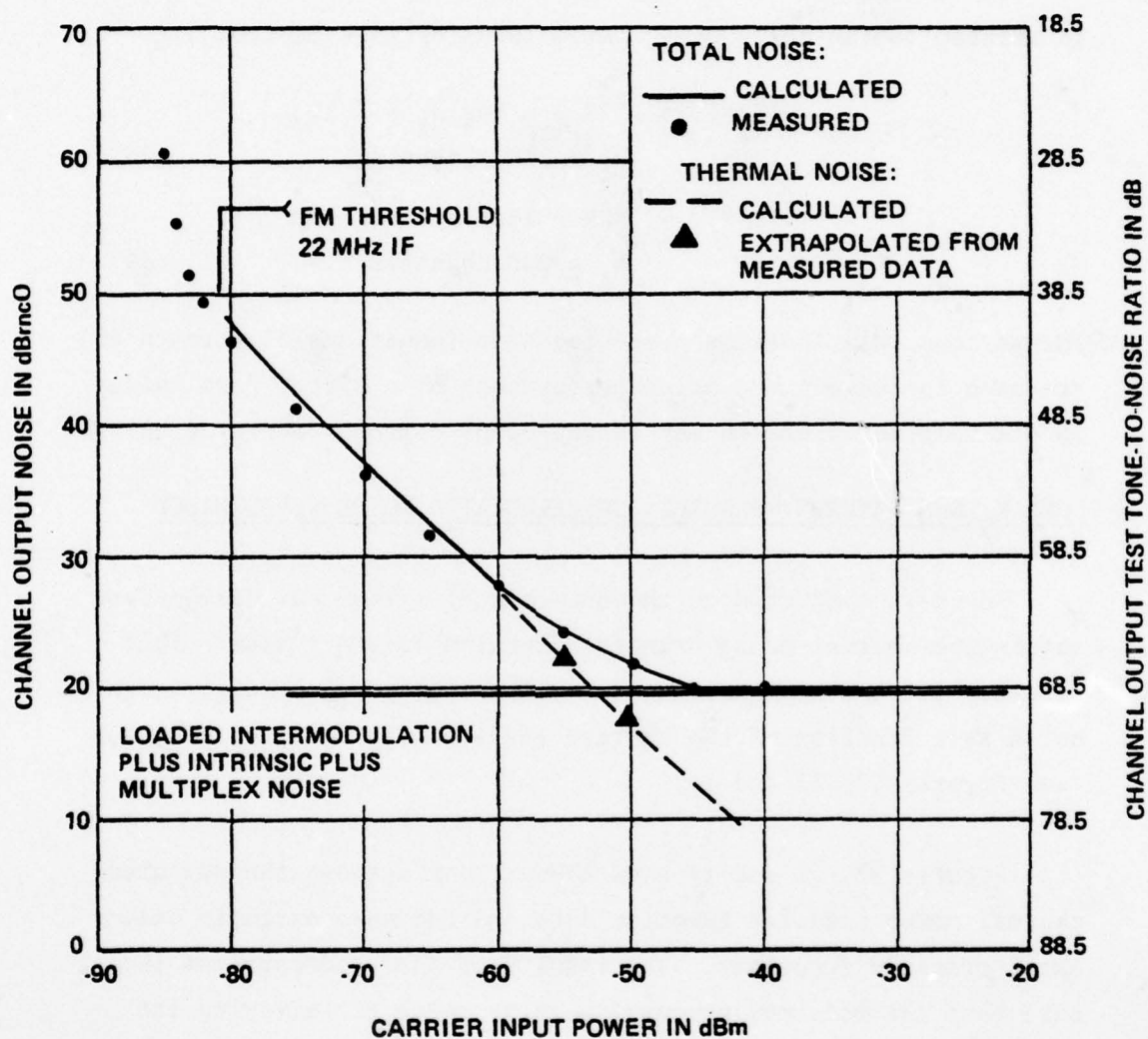


Figure 12. Thermal noise transfer function for a low test channel (340-344 kHz).

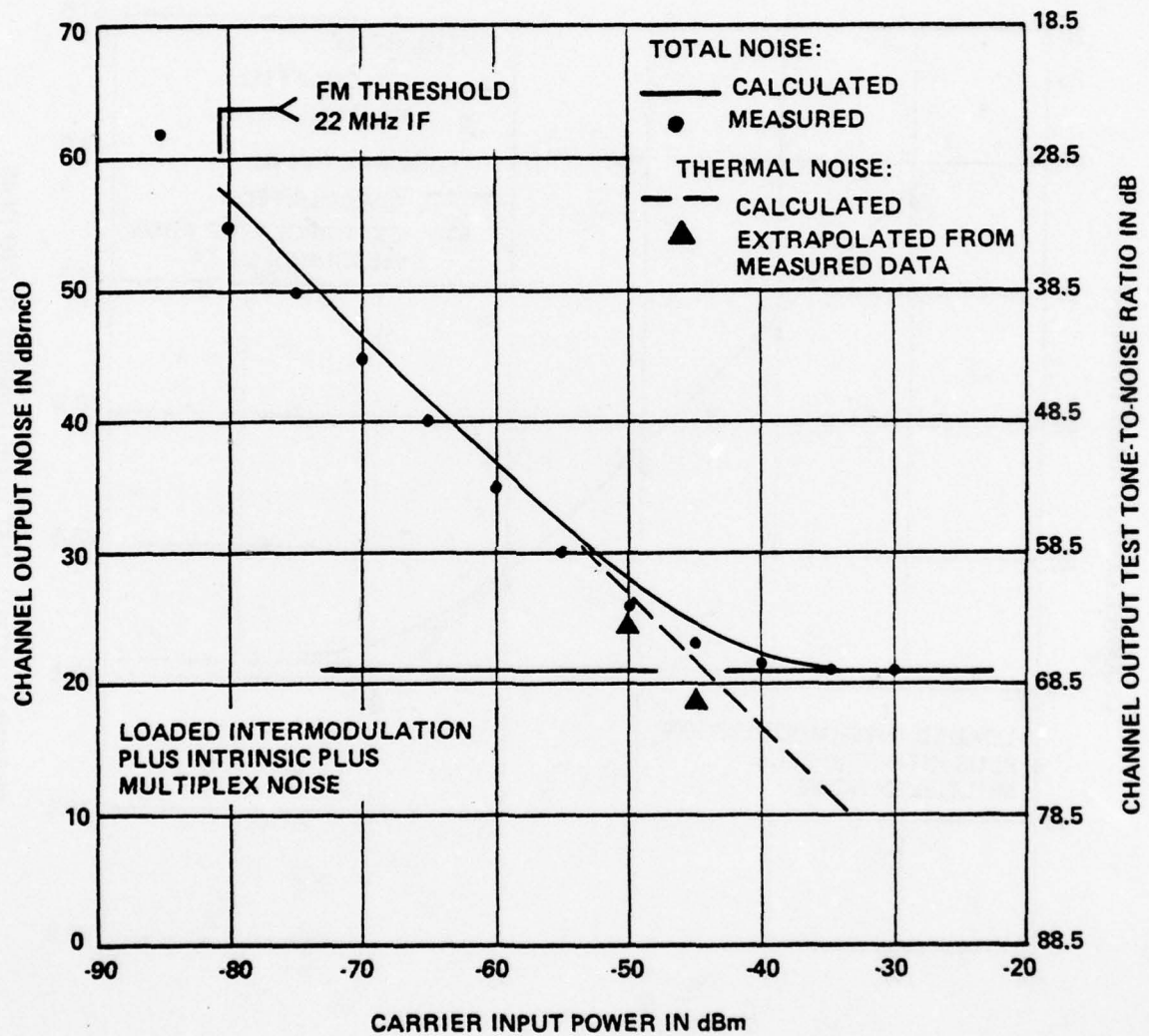


Figure 13. Thermal noise transfer function for a middle test channel (1244-1248 kHz).

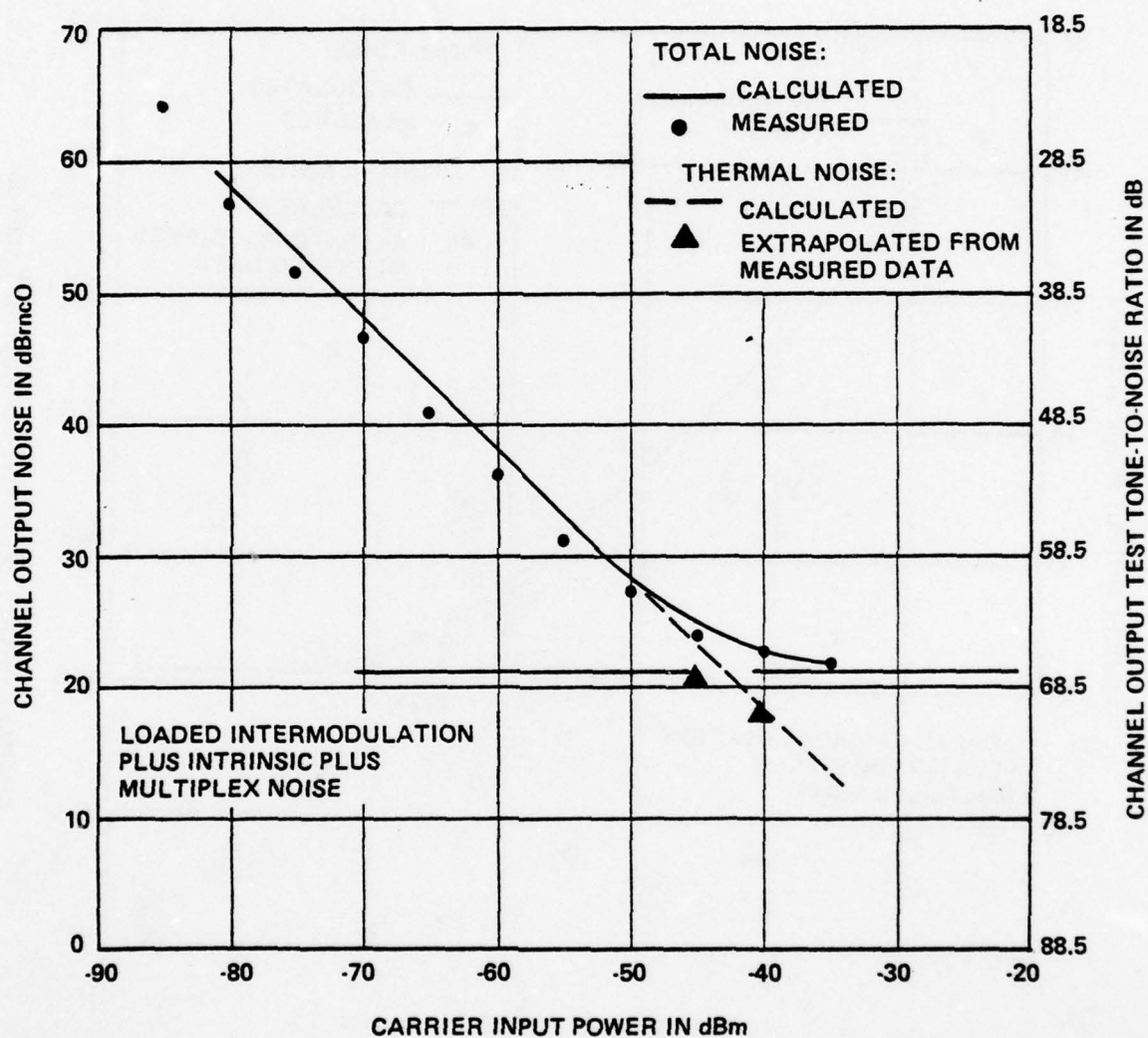


Figure 14. Thermal noise transfer function for a high test channel (2432-2436 kHz).

TABLE 8

SUMMARY OF MEASURED FDM/FM SYSTEM PARAMETERS

Parameter Type	Measured FDM/FM System Parameters
System capacity	600 channels
IF 3-dB bandwidth	22 MHz
IF selectivity	Three-stage LC bandpass filter
Baseband range	60-2660 kHz
Emphasis	CCIR
RMS frequency deviation per channel	200 kHz
Noise loading	12.8 dBm0
Equivalent noise-loaded RMS frequency deviation	872 kHz
Peak deviation for a 12-dB peak factor	3480 kHz
Noise figure	10 dB

AD-A068 757

IIT RESEARCH INST ANNAPOLIS MD

F/G 17/2.1

WIDEBAND FDM/FM MICROWAVE RADIO RELAY PERFORMANCE DEGRADATION I--ETC(U)

APR 79 A A HERNANDEZ

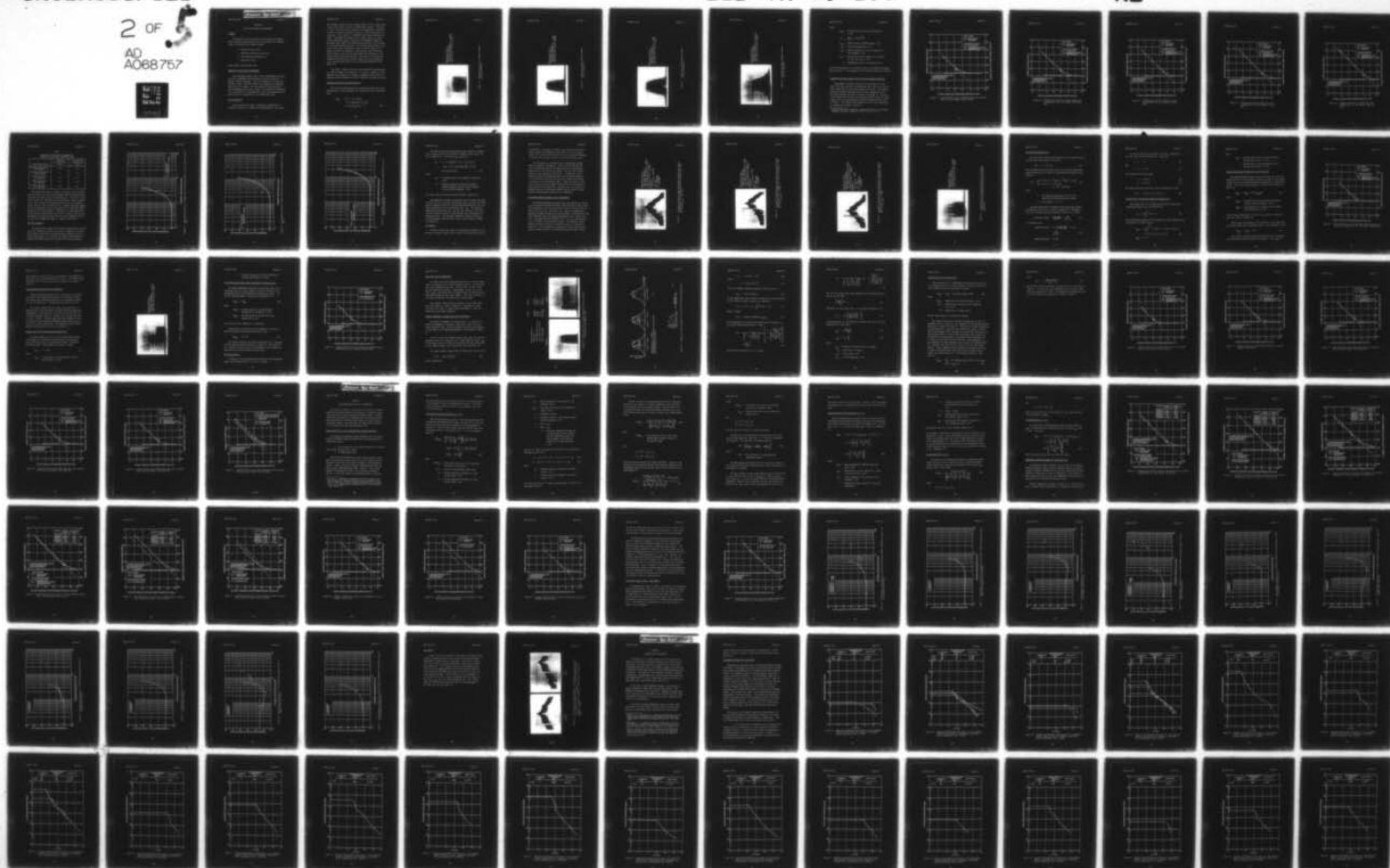
F19628-78-C-0006

UNCLASSIFIED

ESD-TR-79-100

NL

2 OF 5
AD
A068757



875

SECTION 5

ECM (NOISE JAMMING) INTERFERENCE

GENERAL

The objective of this test was to investigate the FDM/FM power transfer characteristics for the following four different types of simulated noise jamming signals:

1. Barrage and spot noise
2. Amplitude-modulated barrage noise
3. Pulse-modulated barrage noise
4. Swept-spot noise.

These signals are described next.

BARRAGE AND SPOT NOISE INTERFERENCE

The interfering signal used in these measurements consisted of a flat, bandwidth-limited spectrum of noise centered at a specific carrier frequency. The four bandwidths of noise used, 200 MHz, 10 MHz, 5 MHz and 250 kHz, were generated by frequency-modulation of a carrier. For the purpose of this discussion, noise bandwidths wider than or equal to the receiver IF bandwidth will be referred to as barrage noise, while noise bandwidths narrower than the IF bandwidth will be termed spot noise.

Noise Generation

Since modulation voltage is essentially proportional to frequency deviation in a quasi-static approximation, the carrier

was frequency-modulated with a random signal having a uniform amplitude distribution to obtain a uniform power density. This signal (for the 200 MHz noise bandwidth) was generated by connecting a 50-kHz triangular waveform, which had a uniform amplitude distribution, to the input of a broadband non-coherent sampling voltmeter. The sample-hold output of this meter, which is a statistically equivalent signal consisting of noncoherent samples of the meter input signal, was amplified and applied to the FM input of a microwave sweep oscillator. The spectral power density variation of the noise interference signal at the RF output of the sweep oscillator was measured by the Automatic Data Collection System (ADCS), which for this measurement was essentially a computer-controlled spectrum analyzer. The result of the ADCS measurements confirmed that the noise signal was quite rectangular, with a uniform power density over the specified bandwidth (see Figure 15).

The 10-MHz, 5-MHz and 250-kHz noise bandwidths were generated in a similar manner (see Figures 16, 17 and 18). However, a noise generator and clipping (2 σ clipping) arrangement rather than the sampling voltmeter method was used to modulate the sweep oscillator.

Barrage and Spot Noise Processing Gain

The on-tune processing gain for barrage and spot noise interference when $C > T_{FM}$ was empirically derived and can be calculated from:

$$\begin{aligned}
 PG_{BSN} = & -30.91 + 10 \log(f_{s1}) \\
 & + 10 \log \left[\exp(F_{ch}^2 / 2f_{s1}^2) \right] \\
 & + 20 \log (d_{rms} / F_{ch}) + E
 \end{aligned} \tag{50}$$

Spectrum Analyzer:
Bandwidth 100 kHz
Scan Width Per Division 50 MHz
Scan Time Per Division 2 s



Figure 15. 200-MHz barrage noise frequency domain emission spectrum.

Spectrum Analyzer:
Bandwidth 100 kHz
Scan Width Per Division 5 MHz
Scan Time Per Division 50 ms

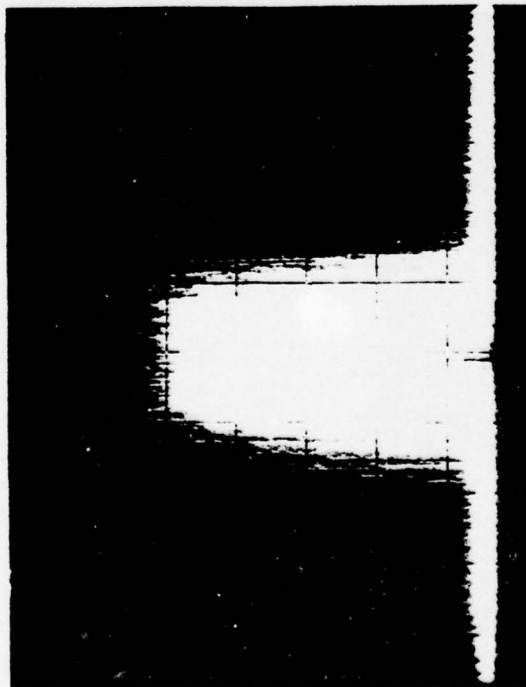


Figure 16. 10-MHz spot noise frequency domain emission spectrum.

Spectrum Analyzer:
Bandwidth 100 kHz
Scan Width Per Division 2 MHz
Scan Time Per Division 0.1 s

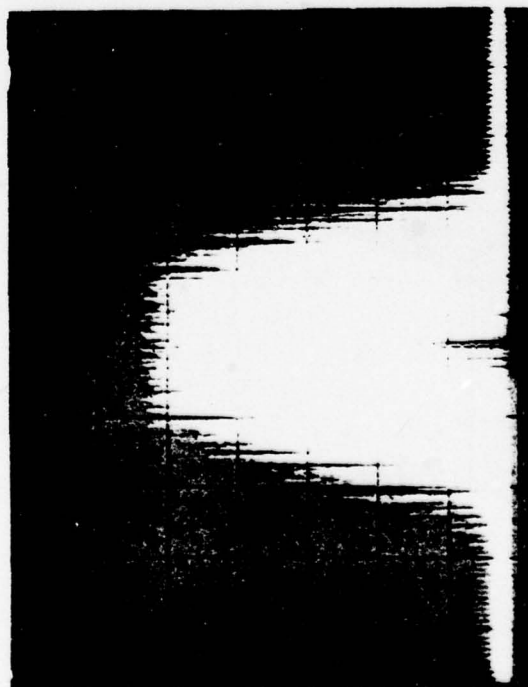


Figure 17. 5-MHz spot noise frequency domain emission spectrum.

Spectrum Analyzer:
Bandwidth 30 kHz
Scan Width Per Division 100 kHz
Scan Time Per Division 0.2 s

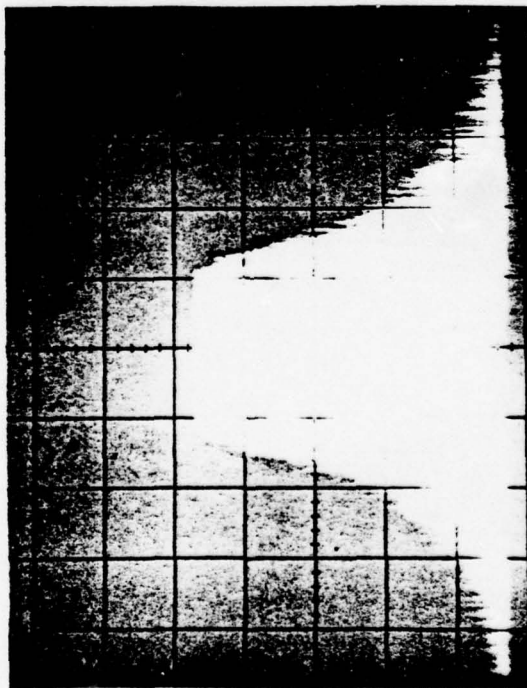


Figure 18. 250-kHz spot noise frequency domain emission spectrum.

where

PG_{BSN} = Barrage and spot noise processing gain,
in dB

$$f_{sl} = \left[D_{rms}^2 + (N_B/2)^2 \right]^{1/2}$$

D_{rms} = RMS deviation of FDM/FM signal, in Hz

N_B = Noise 3-dB bandwidth, in Hz

F_{ch} = Center frequency of the test channel in
the baseband, in Hz

d_{rms} = RMS deviation of the channel for a signal
of test tone level, in Hz

E = Preemphasis factor, in dB (Equation 34).

The form of Equation 50 is similar to the on-tune FDM/FM processing gain equation.³⁰ This equation will be further discussed in Section 6.

Comparisons Between Measured and Calculated Transfer Functions

Measurements of channel output noise were made for a wide range of RF input carrier-to-interference power ratios with the RF input FDM/FM carrier level held constant at -36 dBm. The transfer functions obtained from these data are shown compared with the calculated transfer functions in Figures 19 through 23. The measured barrage noise and spot noise processing gain values are shown compared with the corresponding calculated processing gain values in TABLE 9. The FDM/FM system parameters used in the calculations are summarized in TABLE 8, Section 4.

³⁰International Radio Consultative Committee (CCIR), XIIth Plenary Assembly, New Delhi, Volume IV, Part 2, 1970, p. 203.

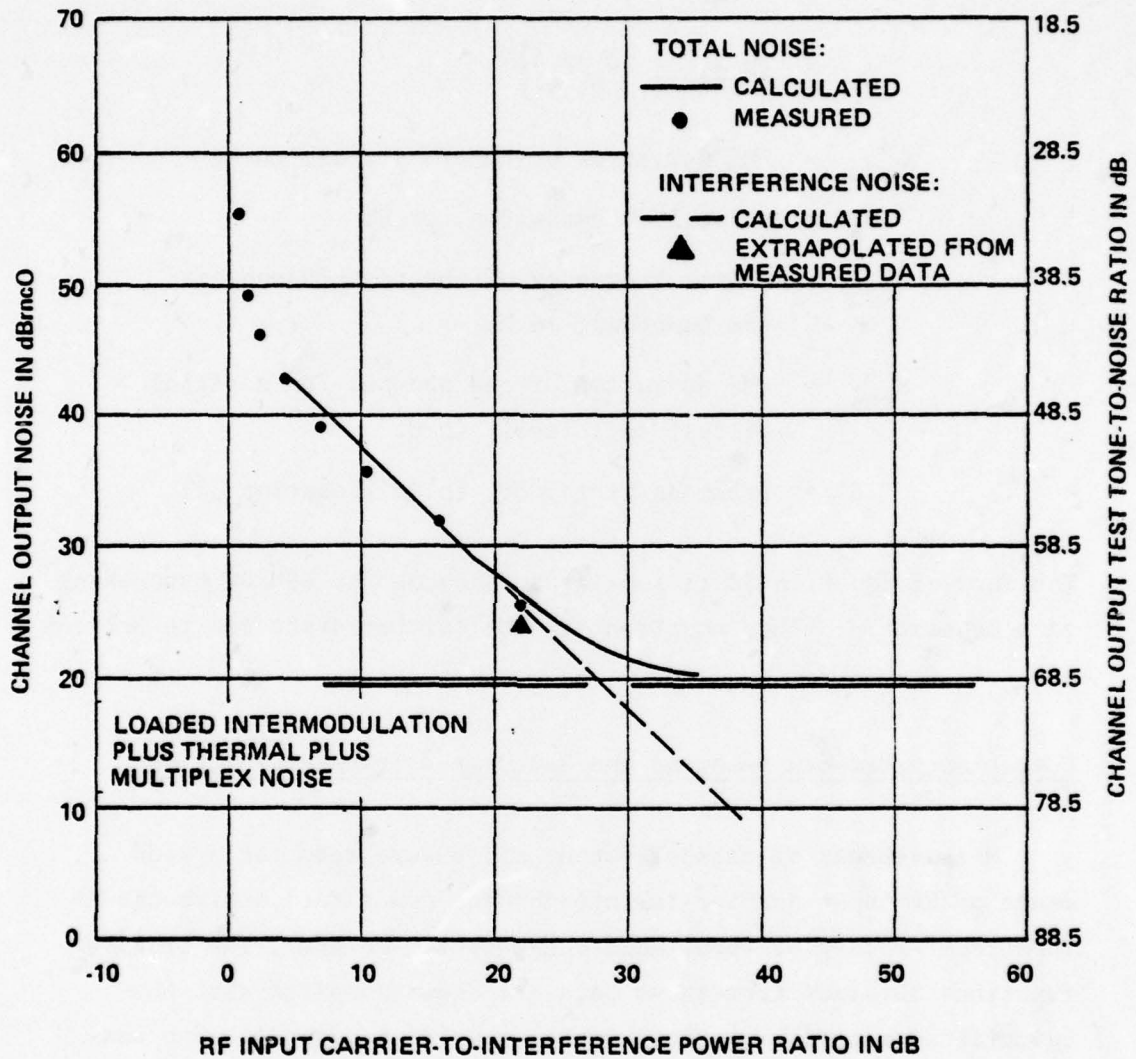


Figure 19. Transfer function for 200-MHz barrage noise interference; low test channel (340-344 kHz).

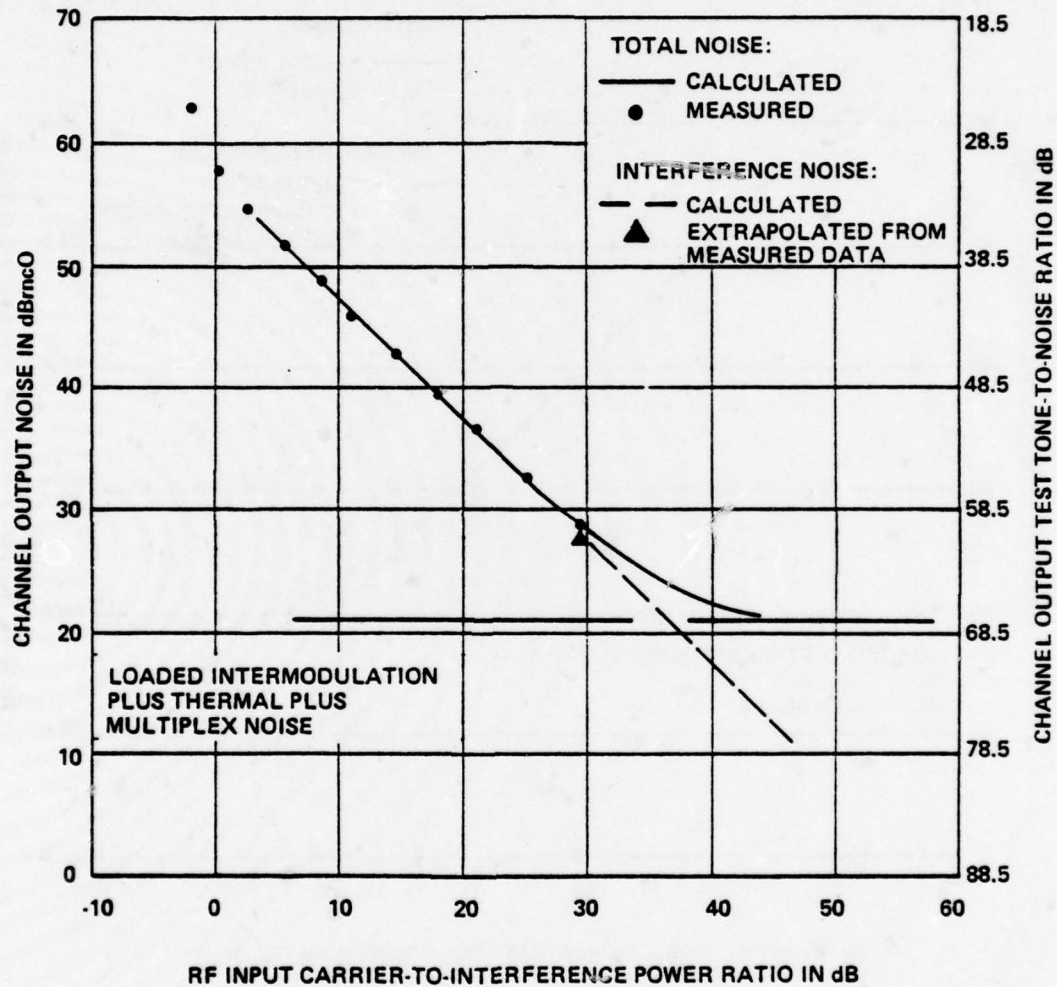


Figure 20. Transfer function for 200-MHz barrage noise interference; high test channel (2432-2436 kHz).

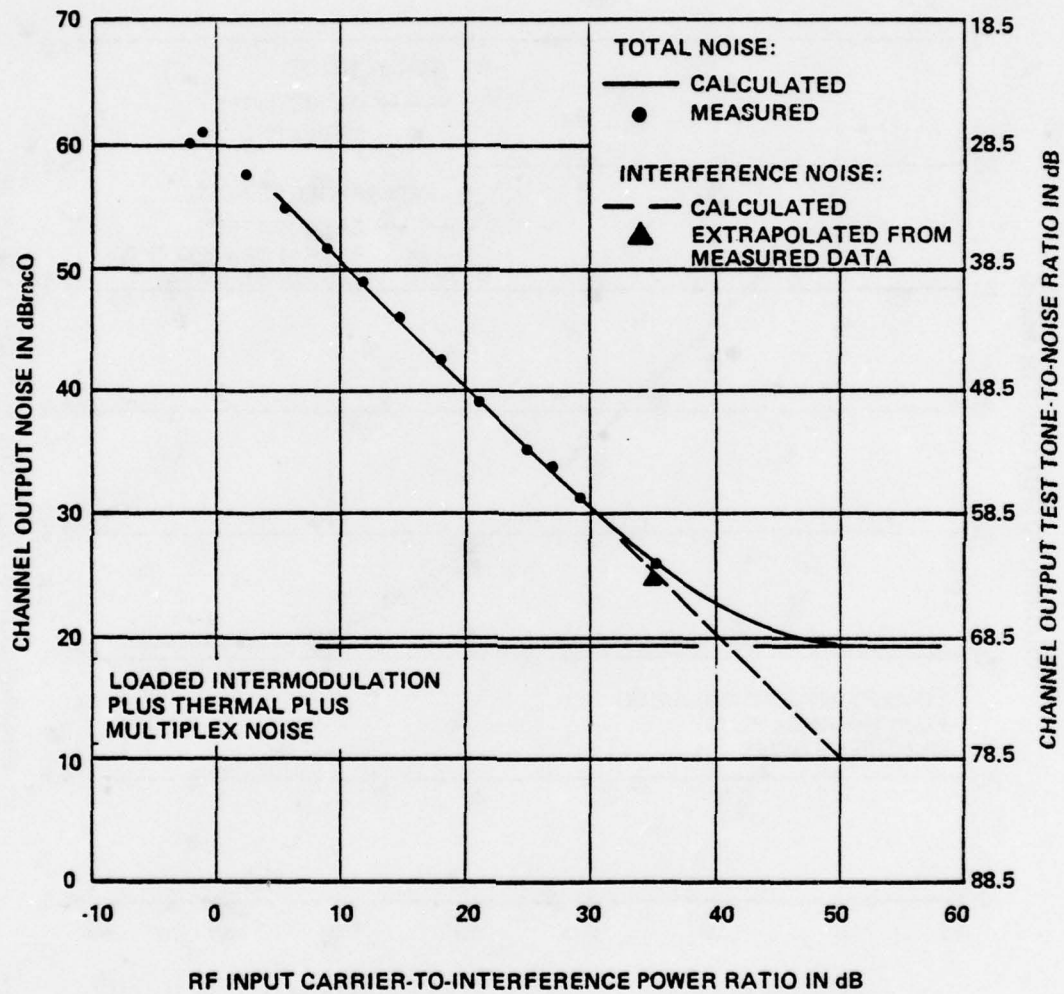


Figure 21. Transfer function for 10-MHz spot noise interference; low test channel (340-344 kHz).

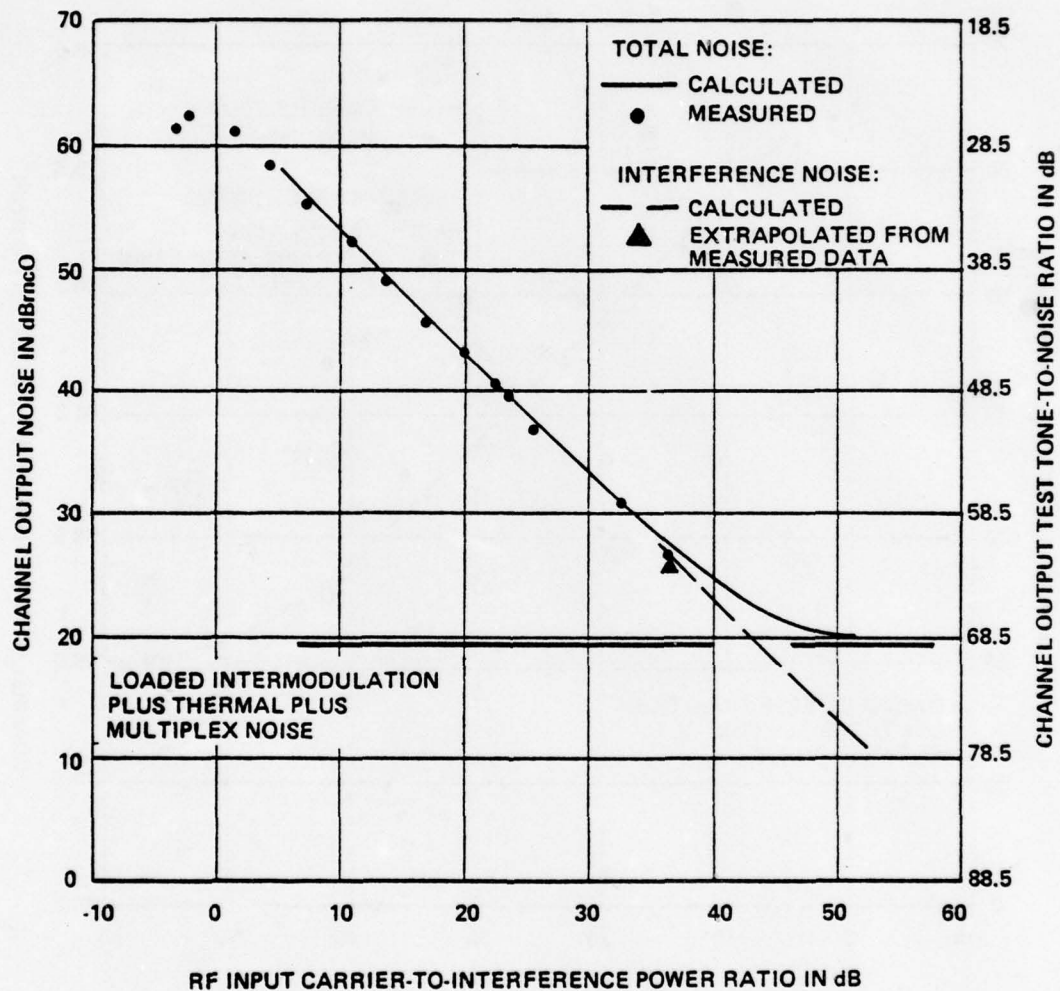


Figure 22. Transfer function for 5-MHz spot noise interference; low test channel (340-344 kHz).

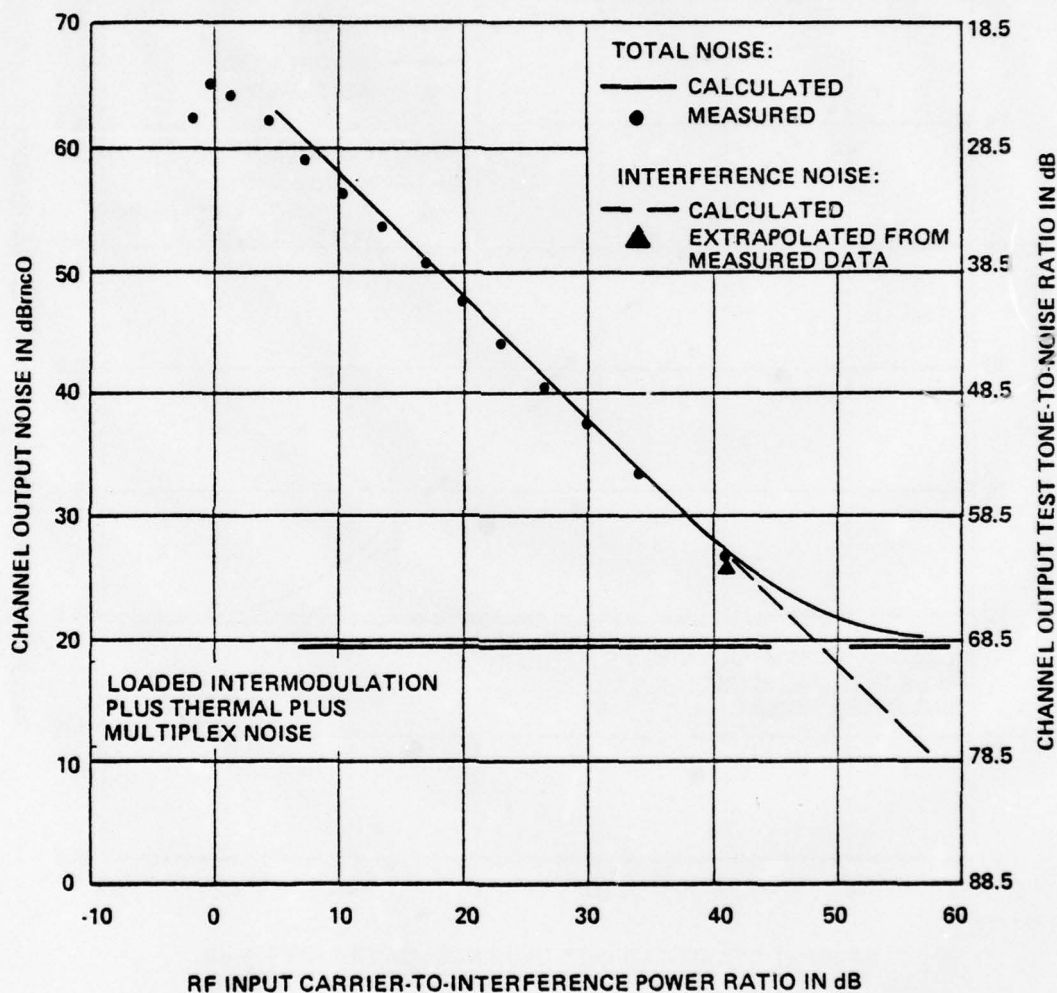


Figure 23. Transfer function for 250-MHz spot noise interference; low test channel (340-344 kHz).

TABLE 9

COMPARISON OF MEASURED AND THEORETICAL
BARRAGE AND SPOT NOISE PROCESSING GAIN

Interfering Signal	Measured Processing Gain (dB)	Calculated Processing Gain (dB)
200-MHz Barrage Noise (Low Channel)	40.7	40.7
200-MHz Barrage Noise (High Channel)	31	30.7
10-MHz Spot Noise (Low Channel)	27.5	27.7
5-MHz Spot Noise (Low Channel)	25.4	24.9
250-kHz Spot Noise (Low Channel)	21.6	20.4

The comparisons shown in Figures 19 through 23 and in TABLE 9 indicate that in all cases close agreement exists between the measured and calculated values of processing gain. The plots in Figures 21 through 23 show that the processing gain remained constant for RF input carrier-to-interference power ratios up to approximately zero dB. This was due to the 2σ clipping introduced during the noise generation process which resulted in a very small peak-to-RMS ratio for these signals. Therefore, the nonlinearities in processing gain which normally occur for C/I ratios lower than approximately 10 dB did not occur and the system remained linear until the noise interference began to capture the receiver.

Off-Tuning Effects

The measured and theoretical off-tuning characteristics of the spot noise interfering signals are shown in Figures 24, 25 and 26. These figures show plots of processing gain, relative to the on-tune processing gain, as a function of frequency separation (Δf) between the FDM/FM carrier and the spot noise center frequency.

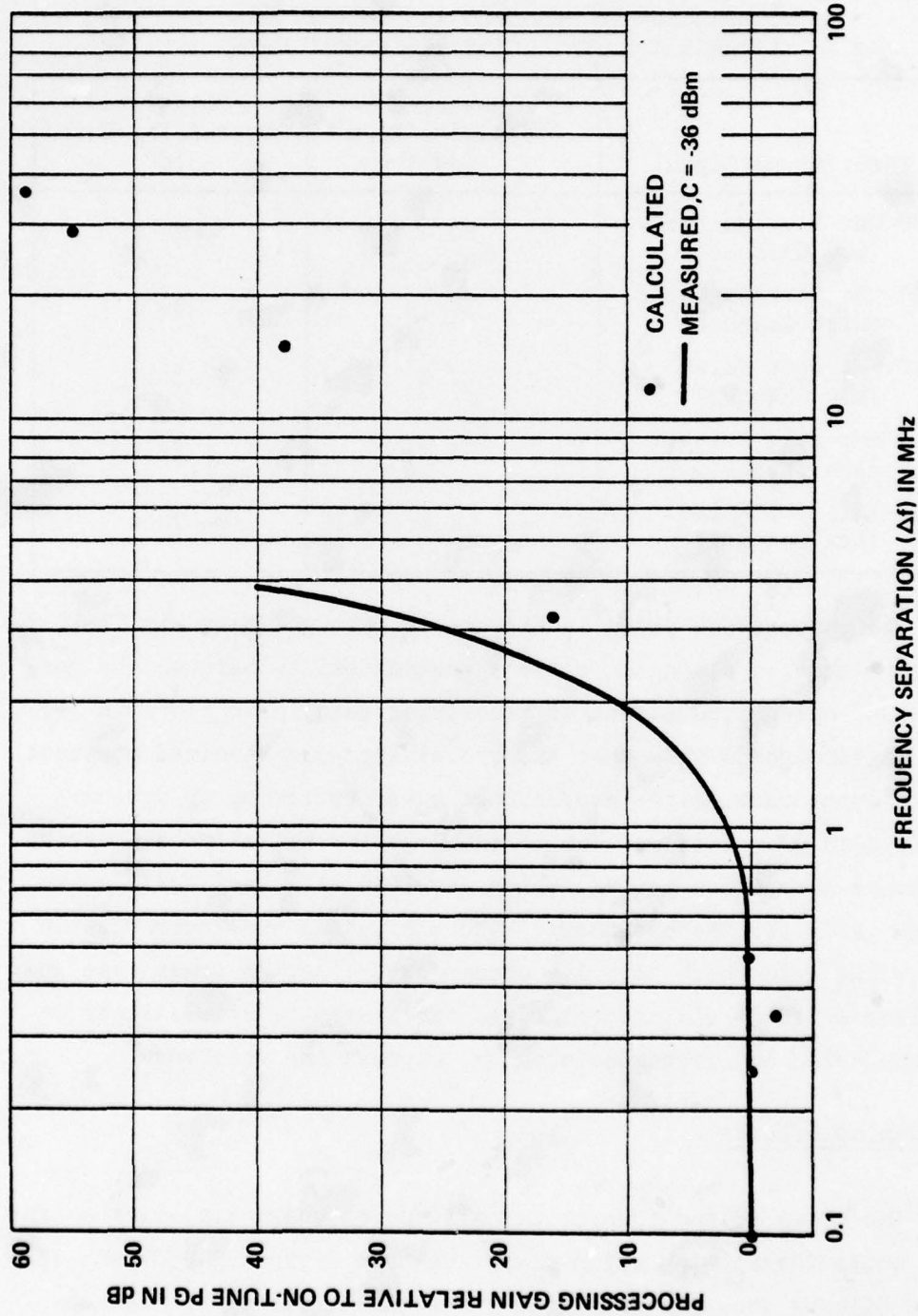


Figure 24. Off-tuning rejection to 250-MHz spot noise interference; low test channel (340-344 kHz).

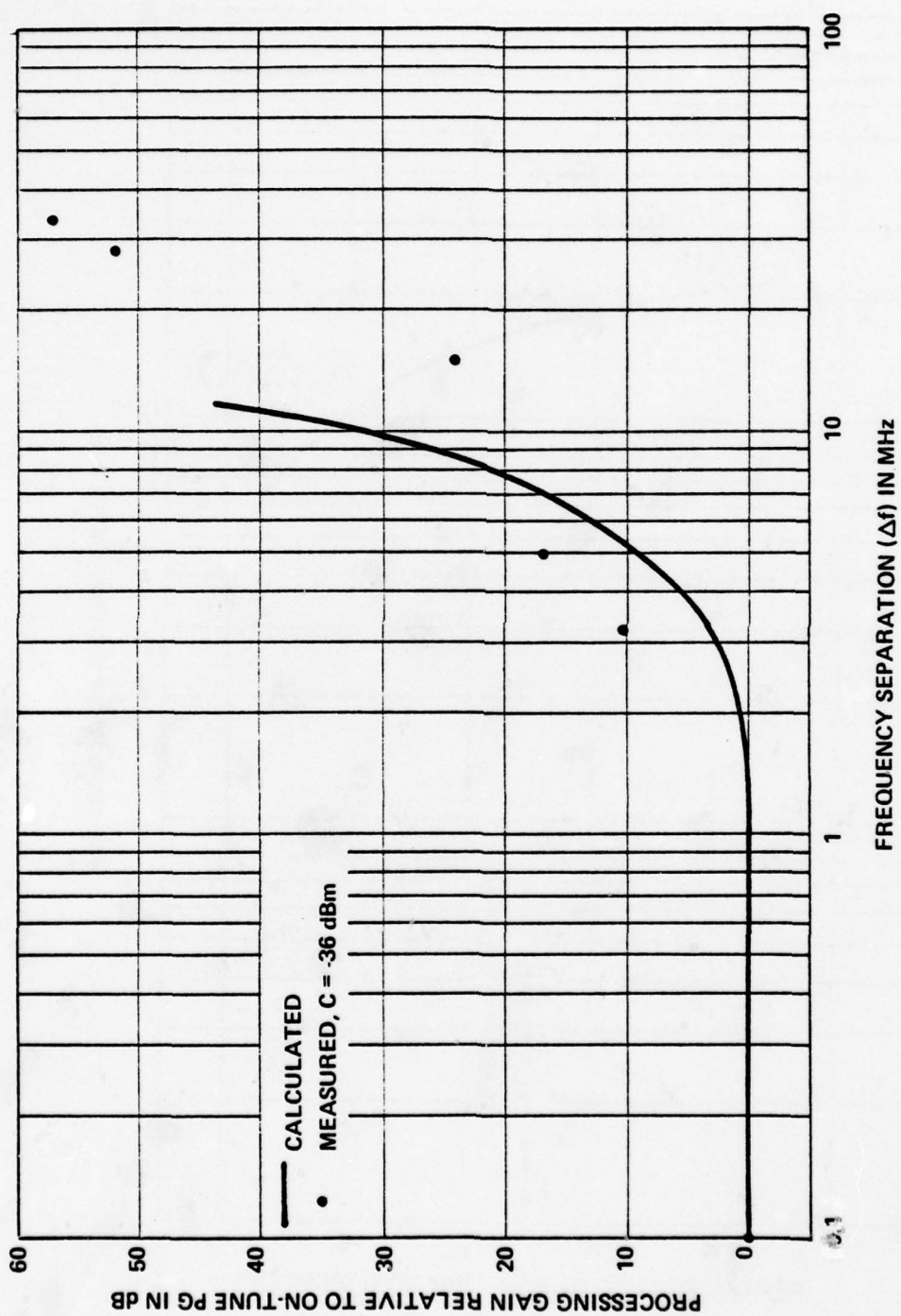


Figure 25. Off-tuning rejection to 5-MHz spot noise interference; low test channel (340-344 kHz).

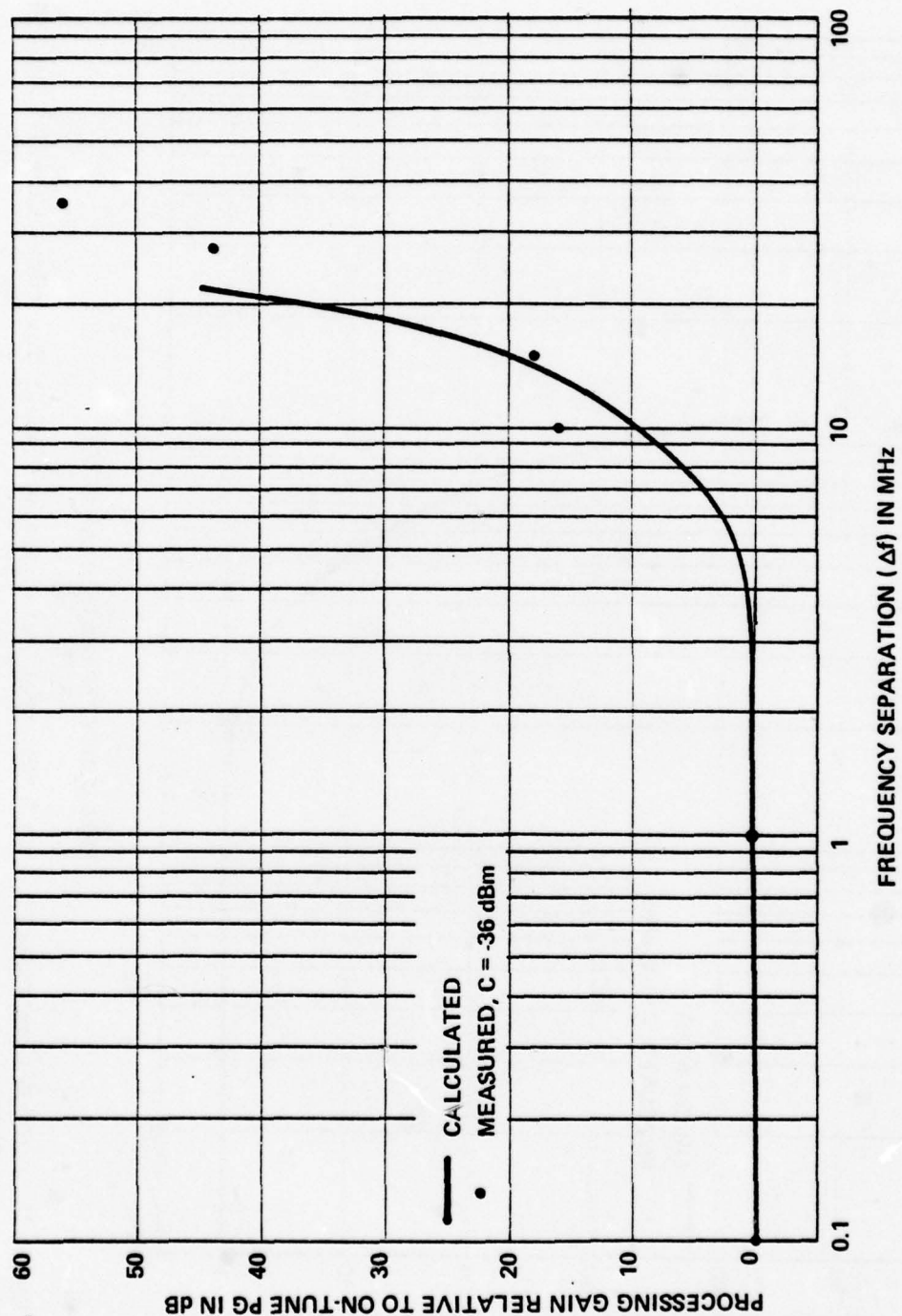


Figure 26. Off-tuning rejection to 10-MHz spot noise interference, low test channel (340-344 kHz).

The theoretical off-tuned processing gain values were empirically derived and can be calculated by adding a factor, $B_{\Delta f}$, (in dB) to Equation 50. The factor $B_{\Delta f}$ is given by:

$$B_{\Delta f} = 3 - 10 \log \left[\exp - [(\Delta f - F_{ch})^2 / 2f_{s1}^2] + \exp - [(\Delta f + F_{ch})^2 / 2f_{s1}^2] \right] - 10 \log \exp [(F_{ch})^2 / 2f_{s1}^2] \quad (51)$$

where

$B_{\Delta f}$ = Off-tuning factor to be added to Equation 50, in dB

Δf = Frequency separation between the FDM/FM carrier frequency and the center frequency of the noise interference, in Hz

all other terms have been previously defined in Equation 50.

The comparisons between the measured and calculated off-tuning rejection for the spot noise interfering signals indicate that Equation 51 adequately predicts the off-tuning characteristics for frequency separations up to approximately $|F_H + N_B|$. For frequency separations greater than $|F_H + N_B|$ but less than $B_{IF}/2$, the calculated off-tuning rejection is much greater than the measured off-tuning rejection. For frequency separations greater than $B_{IF}/2$, the off-frequency rejection due to the IF filter should be added to Equation 51.

AFC Effects

A number of tests were made to investigate the effects of the Automatic Frequency Control (AFC) circuits on off-tuned spot noise

interference. The results of these tests indicate that for IF output carrier-to-interference power ratios less than approximately 0 dB, the AFC action shifts the local oscillator frequency and causes the receiver to lock on to the interfering signal.

The AFC action is illustrated by the photograph sequence shown in Figures 27 through 29. Figure 27 shows 250-kHz spot noise interference with an IF output carrier-to-interference power ratio of -0.2 dB and the AFC-ON. For this case, the AFC action is just starting to take place. In Figure 28, the IF output carrier-to-interference power ratio has been decreased to -5 dB (AFC-ON); here the AFC action has caused the receiver to lock on to the interfering signal. Figure 29 depicts a situation similar to the one shown in Figure 28 with the exception that the AFC is now turned off. For this case, the receiver remained locked on to the desired FDM/FM signal as the IF output carrier-to-interference power ratio was decreased.

AMPLITUDE MODULATED BARRAGE NOISE INTERFERENCE

The amplitude-modulated barrage noise interference was similar to the previously described 200 MHz barrage FM-noise signal, except that the power of the total emission was varied 20 dB in level at a 100-Hz sine wave rate. Basically, this signal was generated by passing a 200-MHz barrage noise signal through a traveling wave tube (TWT) amplifier which was amplitude-modulated with a 100-Hz sine wave. The amplitude and DC offset of the sine wave were adjusted so as to obtain a 20-dB modulation depth. The frequency domain emission spectrum, showing the modulation depth, is depicted in Figure 30. This photograph was obtained by varying the spectrum analyzer sweep time until the modulation waveform became visible.

Spectrum Analyzer:
 Bandwidth 100 kHz
 Scan Width Per Division 2 MHz
 Scan Time Per Division 1 s
 Center Frequency 70 MHz
 Conditions:
 (C/I) IF OUT -0.2 dB
 AFC On
 Δf 3.255 MHz
 C -36 dBm

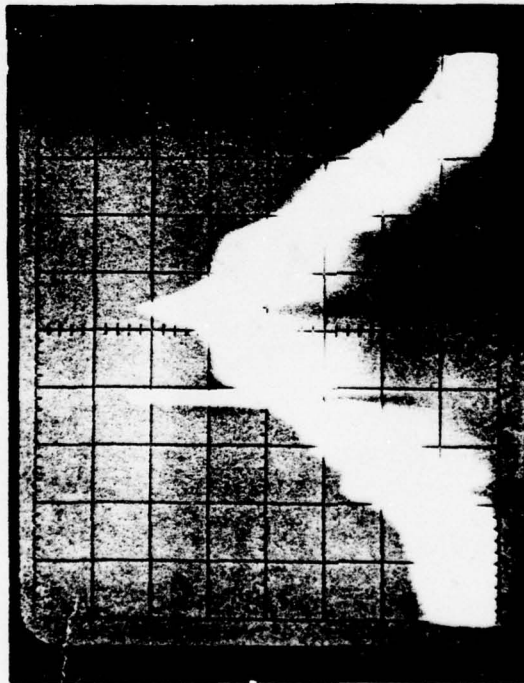


Figure 27. IF output frequency domain photograph showing 600-channel FDM/FM signal and 250-kHz spot noise interference, (AFC on; (C/I) IF OUT = -0.2 dB).

Spectrum Analyzer:
 Bandwidth 100 kHz
 Scan Width Per Division 2 MHz
 Scan Time Per Division 1 s
 Center Frequency 70 MHz
 Conditions:
 (C/I) IF OUT -5 dB
 AFC On
 Δf 3.255 MHz
 C -36 dBm



Figure 28. IF output frequency domain photograph showing 600-channel FDM/FM signal and 250-kHz spot noise interference, (AFC on; (C/I) IF OUT = -5 dB).



Spectrum Analyzer:
 Bandwidth 100 kHz
 Scan Width Per Division 2 MHz
 Scan Time Per Division 2 s
 Center Frequency 70 MHz
 Conditions:
 (C/I) IF OUT -5 dB
 AFC Off
 Δf 3.255 MHz
 C -36 dBm

Figure 29. IF output frequency domain photograph showing 600-channel FDM/FM signal and 250-kHz spot noise interference, (AFC off; (C/I) IF OUT = -5 dB).

Spectrum Analyzer:
Bandwidth 300 kHz
Scan Width Per Division 50 MHz
Scan Time Per Division 10 ms

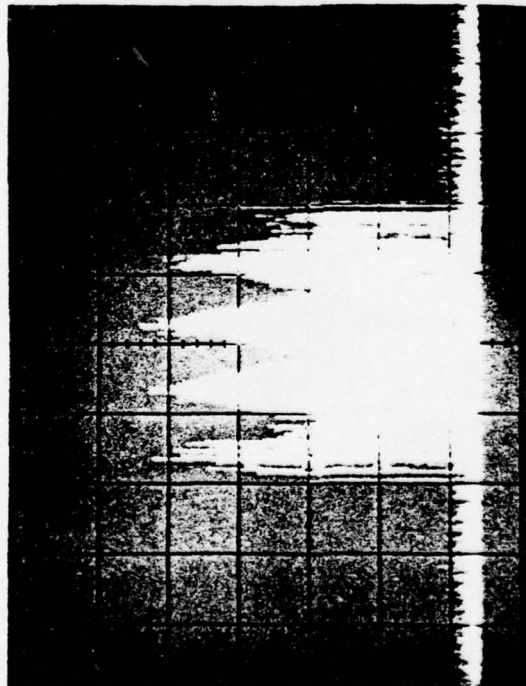


Figure 30. 200-MHz amplitude-modulated barrage noise frequency domain emission spectrum showing 100-Hz modulation waveform.

Time Domain Representation

The time domain waveform representation of the amplitude modulated barrage noise signal has the form:

$$V(t) = A + B \sin \omega t \quad (52)$$

with the amplitude and DC offset levels of the 100-Hz modulating signal adjusted so as to meet the 20-dB modulation depth criteria given by:

$$V(t) = \begin{cases} A + B \sin \omega t = \sqrt{P} & \text{when } t = \frac{n^2 + 1}{2} (0.0025) \\ A + B \sin \omega t = 0.1 \sqrt{P} & \text{when} \\ & t = (2n + 1)(0.0025) \end{cases} \quad (53)$$

where

P = The maximum average power level of the modulated 200-MHz barrage noise signal

n = Odd integer, 1, 3, 5, 7, ...

The modulation depth is defined by the maximum and minimum instantaneous values of $V(t)$ given by Equation 53. Therefore, with $V(t)$ varying sinusoidally between \sqrt{P} and $0.1 \sqrt{P}$, we have:

$$\text{modulation depth} = \frac{V(t)_{\max}}{V(t)_{\min}} = \frac{\sqrt{P}}{0.1 \sqrt{P}} \quad (54)$$

or expressed in dB

$$\begin{aligned} \text{modulation depth} &= 20 \log \frac{V(t)_{\max}}{V(t)_{\min}} = 20 \log \\ &\frac{\sqrt{P}}{0.1 \sqrt{P}} \end{aligned} \quad (55)$$

$$\text{modulation depth} = 20 \text{ dB.}$$

We can now evaluate the constants, A and B, in Equation 52 over the limits given by Equation 53. This gives:

$$A + B = \sqrt{P} \quad (56)$$

and

$$A - B = 0.1 \sqrt{P}. \quad (57)$$

Then solving for A and B yields:

$$A = 0.55 \sqrt{P} \quad (58)$$

$$B = 0.45 \sqrt{P} \quad (59)$$

and substituting the values for A and B in Equation 52 gives:

$$V(t) = 0.55 \sqrt{P} + 0.45 \sqrt{P} \sin \omega t. \quad (60)$$

Average Power of Amplitude-Modulated Barrage Noise

The average power of the amplitude-modulated barrage noise interfering signal can be calculated from:

$$P_{av} = \frac{1}{T} \int_0^T V^2(t) dt \quad (61)$$

Then substituting Equation 60 into Equation 61 and integrating over one period [$T = (1/100)$] gives:

$$\begin{aligned} P_{BAM} &= 100 \int_0^{0.01} [(0.55)^2 P + (0.45)^2 P \sin^2 \omega t \\ &\quad + (0.55)(0.45) P \sin \omega t] dt \\ P_{BAM} &= 0.4 P \end{aligned} \quad (62)$$

where

P_{BAM} = Average power of the amplitude-modulated
barrage noise signal, in watts

P = Maximum power of the amplitude-modulated
barrage noise signal, in watts.

Amplitude-Modulated Barrage Noise Processing Gain

The FDM/FM degradation data analyzed indicates that the interference noise in a voice channel is directly related to the maximum average power of the amplitude-modulated barrage noise interfering signal. The on-tune processing gain is then given by Equations 50 and 62 as:

$$PG_{BAM} = PG_{BSN} + 10 \log(P_{BAM}/P) \quad (63)$$

where

PG_{BAM} = Processing gain of the amplitude-modulated
barrage noise interference, in dB

PG_{BSN} = Processing gain for barrage noise interference,
Equation 50, in dB.

For off-tuned interference, the factor, $B_{\Delta f}$, given by Equation 51 should be added to Equation 63.

Substituting into Equation 63 the parameters of the amplitude-modulated barrage noise interference used in the measurements yields:

$$PG_{BAM} = PG_{BSN} - 3.98. \quad (64)$$

The transfer function calculated from Equation 64 is compared with the measured transfer function in Figure 31. The result of

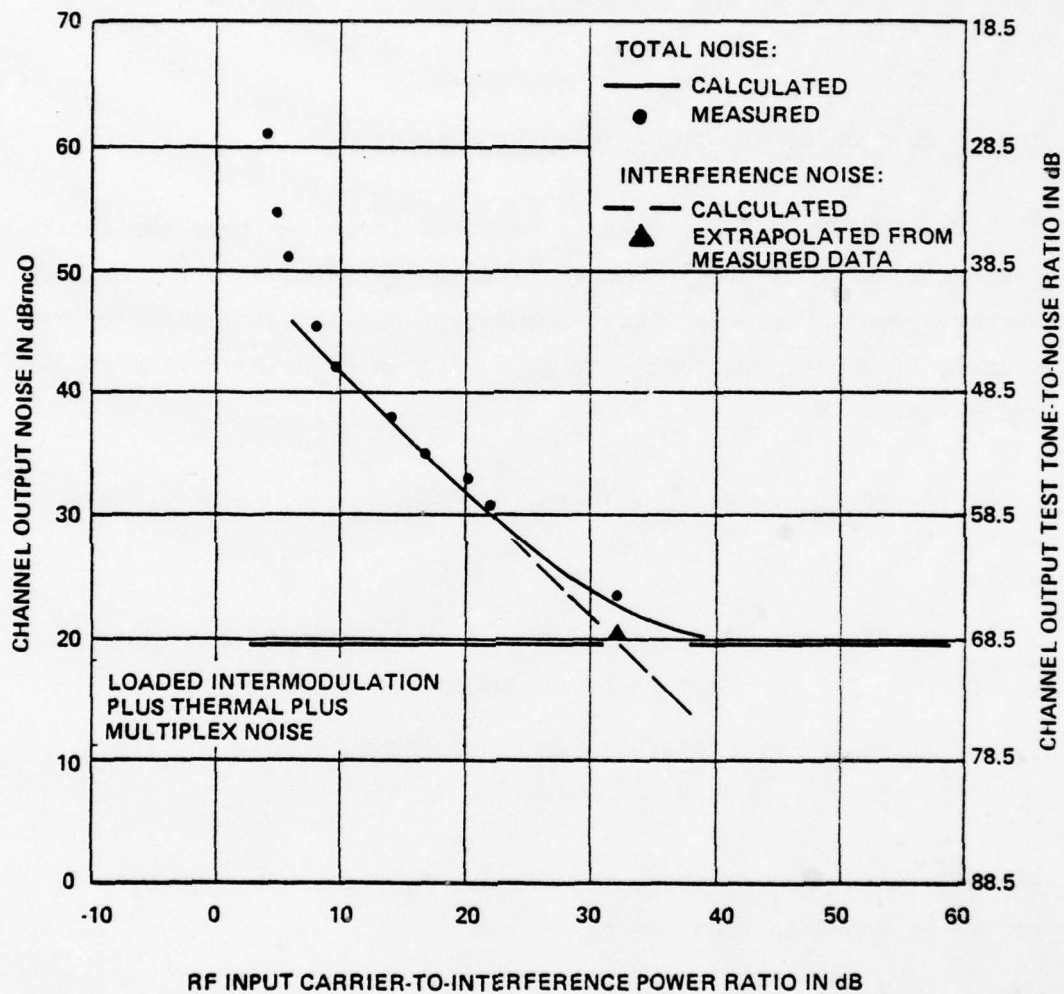


Figure 31. Transfer function for 200-MHz amplitude-modulated bar-rage noise interference; low test channel (340-344 kHz).

this comparison indicates that close agreement exists between the measured and calculated processing gain values. The FDM/FM system parameters used in the calculations are summarized in TABLE 8, Section 4.

PULSE-MODULATED BARRAGE NOISE INTERFERENCE

The pulse-modulated barrage noise interference consisted of two 100-MHz wide barrage noise signals with contiguous spectra whose levels were amplitude-modulated in a complementary manner by a 100-Hz square wave. The amplitude variation was 20 dB.

The 100-MHz barrage FM-noise signals were generated in a manner similar to the previously described 200-MHz barrage noise interference, except that one of the sweep oscillators was set to produce emissions from $f_0 - 100$ MHz to f_0 , and the other from f_0 to $f_0 + 100$ MHz. The two signals were then coupled to a signal combiner which alternately amplitude-modulated each signal 20 dB with a 100-Hz square wave. The frequency domain emission spectrum characteristics are shown in Figure 32.

Average Power of Pulsed Modulated Barrage Noise

The power density in each of the two 100-MHz wide barrage noise signals is alternately varying between P_d watts/Hz and $(P_d/100)$ watts/Hz (for a 20-dB modulation depth). Therefore, the average power of the 200-MHz wide signal is simply:

$$P_{\text{PBN}} = P + P/100 \quad (65)$$

where

$$P_{\text{PBN}} = \text{Average power of pulse-modulated barrage noise signal, in watts}$$

Spectrum Analyzer:
Bandwidth 300 kHz
Scan Width Per Division 50 MHz
Scan Time Per Division 0.2 s

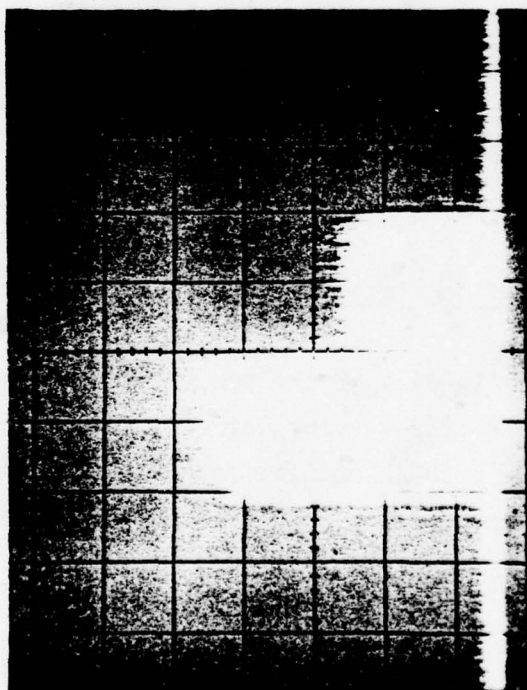


Figure 32. Pulse-modulated barrage noise interference frequency domain emission spectrum.

P = Maximum average power of pulse-modulated
barrage noise signal, in watts.

Pulse-Modulated Barrage Noise Interference Processing Gain

The FDM/FM degradation data analyzed indicates that the interference noise in a voice channel is directly related to the average power of the pulse-modulated barrage noise signal. The on-tune processing gain is then given by Equation 50 as:

$$PG_{PBN} = PG_{BSN} \quad (66)$$

where

PG_{PBN} = Processing gain of pulsed-modulated
barrage noise interference, in dB

PG_{BSN} = Processing gain of barrage spot noise,
Equation 50, in dB.

For off-tuned cases, Equation 51 is applicable.

Substituting into Equation 66 the parameters of the pulse modulated barrage noise interfering signal yields:

$$PG_{PBN} = 40.6 \text{ dB.} \quad (67)$$

The transfer function calculated from Equation 67 is compared with the measured transfer function in Figure 33. The results of this comparison indicates that close agreement exists between the measured and calculated processing gain values.

Off-Tuning Effects

No anomalies in processing gain were found as the interfering signal was off-tuned from $\Delta f = 0$ to $\Delta f = +100$ MHz.

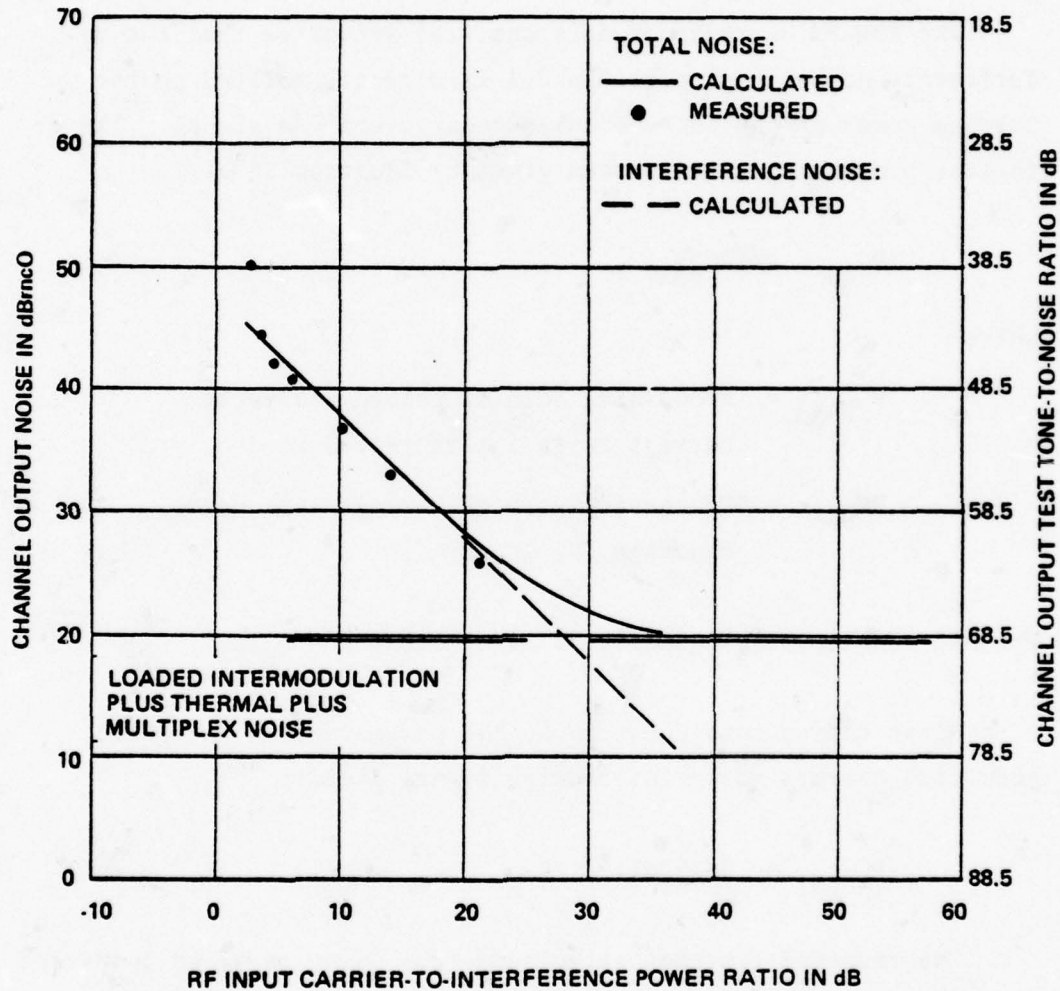


Figure 33. Transfer function for pulse-modulated barrage noise interference; low test channel (340-344 kHz).

SWEPT-SPOT NOISE INTERFERENCE

The swept-spot noise interference consisted of a noise signal swept in frequency with a 100-Hz sawtooth waveform. The following spot noise bandwidths were used: 5 MHz, 10 MHz, 20 MHz, 50 MHz and CW (unmodulated carrier). These signals, except for the CW swept signal, were generated in a manner similar to the previously described barrage and spot noise signals. The center frequency of the swept interference was swept over a 100-MHz range.

The frequency domain emission spectrum of the 20-MHz swept-spot noise signal is shown in Figure 34. Photograph (A) shows the spot noise signal (no sweep) while Photograph (B) shows the swept-spot noise signal (sweep on).

Receiver Response to Swept-Spot Noise Interference

The receiver response to the swept signals is a function of a number of parameters, including: sweep time, sweep width, and sweep repetition rate. The relationships between these parameters, as they apply to the FDM/FM measurements, are presented in Figure 35.

It can be shown that sweeping these signals past the receiver passband results in a transient, $y(t)$, whose effective width, τ_{eff} , at the output of the IF filter can be derived from the convolution of the sweeping signal, $f(t)$, and the IF filter response, $h(t)$.

The sweep frequency signal shown in Figure 34(B) has the form:

$$f(t) = \exp j\pi(S_W/S_T)t^2 \quad (68)$$

which transforms to:

	PHOTO A	PHOTO B
Spectrum Analyzer:		
Bandwidth	<u>100 kHz</u>	<u>100 kHz</u>
Scan Width Per Division	<u>10 MHz</u>	<u>20 MHz</u>
Scan Time Per Division	<u>0.2 s</u>	<u>0.2 s</u>
Noise Bandwidth	<u>No sweep</u>	<u>Sweep on</u>

PHOTO A

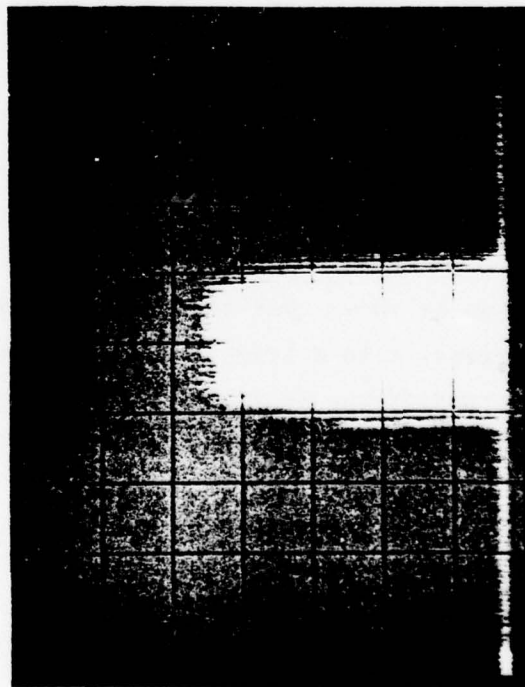


PHOTO B

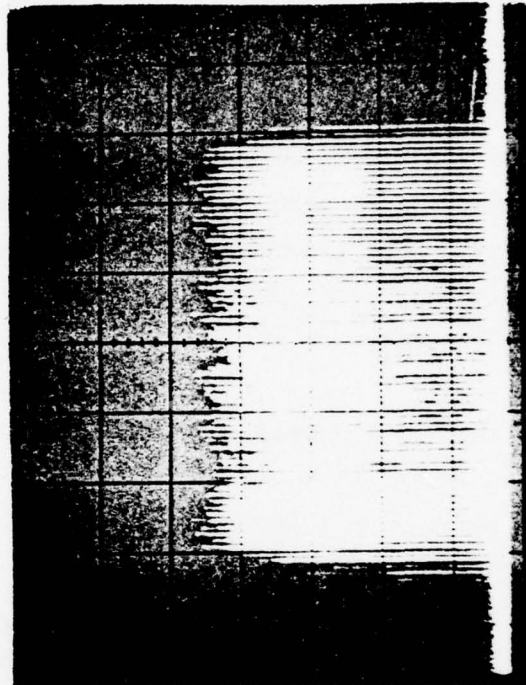
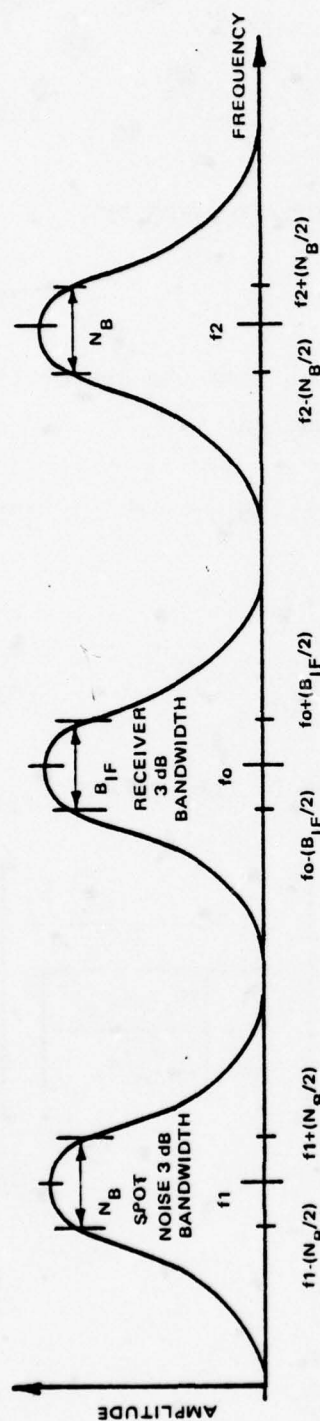
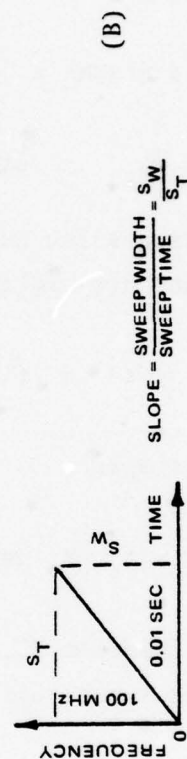


Figure 34. Swept-spot noise frequency domain emission spectrum, no sweep (A), and sweep on (B).



(A)

SWEEP WIDTH = $S_W = f_2 - f_1 = 100 \text{ MHz}$
 NOISE BANDWIDTH = $N_B = \text{CW}, 5 \text{ MHz}, 10 \text{ MHz}, 20 \text{ MHz AND } 50 \text{ MHz}$
 RECEIVER BANDWIDTH = $B_{IF} = 22 \text{ MHz}$



(B)

Figure 35. Swept-spot noise frequency (A) and time (B) domain representation.

$$F_{(\omega)} = \tau \sqrt{2\pi} \exp - \frac{1}{2}(\tau\omega)^2 \quad (69)$$

where

$$\tau = [(jS_T)/(2\pi S_W)]^{\frac{1}{2}}. \quad (70)$$

Now, if we assume a Gaussian response, which is given by:

$$H_{(\omega)} = \exp -\frac{1}{2}(\omega/\pi B_{IF})^2 \quad (71)$$

we can compute the output transient response from the convolution of $f(t)$ and $h(t)$ which is given by the equation:

$$y(t) = f(t) * h(t) = \int_{-\infty}^{\infty} f(\tau)h(t - \tau)d\tau \quad (72)$$

which is simply:

$$y(t) = \text{Inverse transform } F_{(\omega)}H_{(\omega)} \quad (73)$$

and from Equation 73, the inverse transform of the product $F_{(\omega)}H_{(\omega)}$ after substituting back for τ gives:

$$y(t) = \frac{1}{\left[1 - j \frac{2\pi S_W}{S_T(\pi B_{IF})^2}\right]^{\frac{1}{2}}} \exp \left[- \frac{1 - j \frac{(\pi B_{IF})^2 S_T}{2\pi S_W}}{1 + \left[\frac{S_T(\pi B_{IF})^2}{2\pi S_W}\right]^2} \right] \frac{(\pi B_{IF}t)^2}{2} \quad (74)$$

from which the envelope of $y(t)$ is simply:

$$y(t) = \frac{1}{\left[1 + \left[\frac{2\pi S_W}{S_T(\pi B_{IF})^2}\right]^2\right]^{\frac{1}{4}}} \exp - \frac{\frac{(\pi B_{IF}t)^2}{2}}{1 + \left[\frac{S_T(\pi B_{IF})^2}{2\pi S_W}\right]^2} \quad (75)$$

Now, for slow sweep rates, which represent the situation being analyzed, we have that:

$$\frac{(\pi B_{IF})^2 S_T}{2\pi S_W} \gg 1. \quad (76)$$

Therefore, for slow sweep rates, we can simplify Equation 75 to:

$$y(t) = \exp \left[-\frac{1}{2} \left[\frac{2\pi S_W}{\pi B_{IF} S_T} \right]^2 t^2 \right] \quad (77)$$

and from Equation 77, the effective transient width can be written immediately by noting that:

$$\tau_{eff} = 2 \frac{\pi B_{IF} S_T}{2\pi S_W} \quad (78)$$

$$\tau_{eff} = B_{IF} \frac{S_T}{S_W} \quad (79)$$

where

τ_{eff} = Effective transient width, in seconds

S_T = Sweep time, in seconds

S_W = Sweep width, in Hz

B_{IF} = IF 3-dB bandwidth, in Hz.

Swept-Spot Noise Processing Gain

The swept-spot noise interference data analyzed indicate that the interference noise in a voice channel is related to the transient response width and sweep rate as follows:

$$PG_{SPN} = PG_{GN} - 20 \log[(B_{IF} S_T/S_W) (SR)] \quad (80)$$

where

PG_{SPN} = Swept-spot noise processing gain, in dB

PG_{GN} = Gaussian noise processing gain (Equation 33), in dB

SR = Sweep rate, in sweeps/second

and the other terms are as previously defined.

The transfer functions calculated from Equation 80, for the parameters shown in Figure 35, are compared with the measured transfer functions in Figures 36 through 41. The results of these comparisons (using Equation 80), except for the 50-MHz noise signal, indicate that close agreement exists between the measured and calculated processing gain values. For the 50-MHz swept-spot noise signal, the calculated PG was approximately 3 dB higher than the measured PG. It should be noted that for the 50-MHz spot noise bandwidth, the spot bandwidth-to-swept bandwidth ratio is equal to 50 MHz/100 MHz = 0.5. However, this ratio was less than 0.2 for the other swept signals. Closer agreement can be obtained if an additional factor is added to Equation 80 for those cases where the above ratio is greater than approximately 0.3. The modified equation is then given by:

$$PG_{SPN} = PG_{GN} - 20 \log[(B_{IF} S_T/S_W) (SR)] + 10 \log S_{NR},$$

for $0 < S_{NR} < 0.7$ (81)

where

$$S_{NR} = 1 - \left(\frac{\text{spot width}}{S_W} \right). \quad (82)$$

The transfer function calculated from Equation 81 is also shown in Figure 41. For this case, good agreement exists between the measured and calculated PG values. The FDM/FM system parameters used in the calculations are summarized in TABLE 8, Section 4.

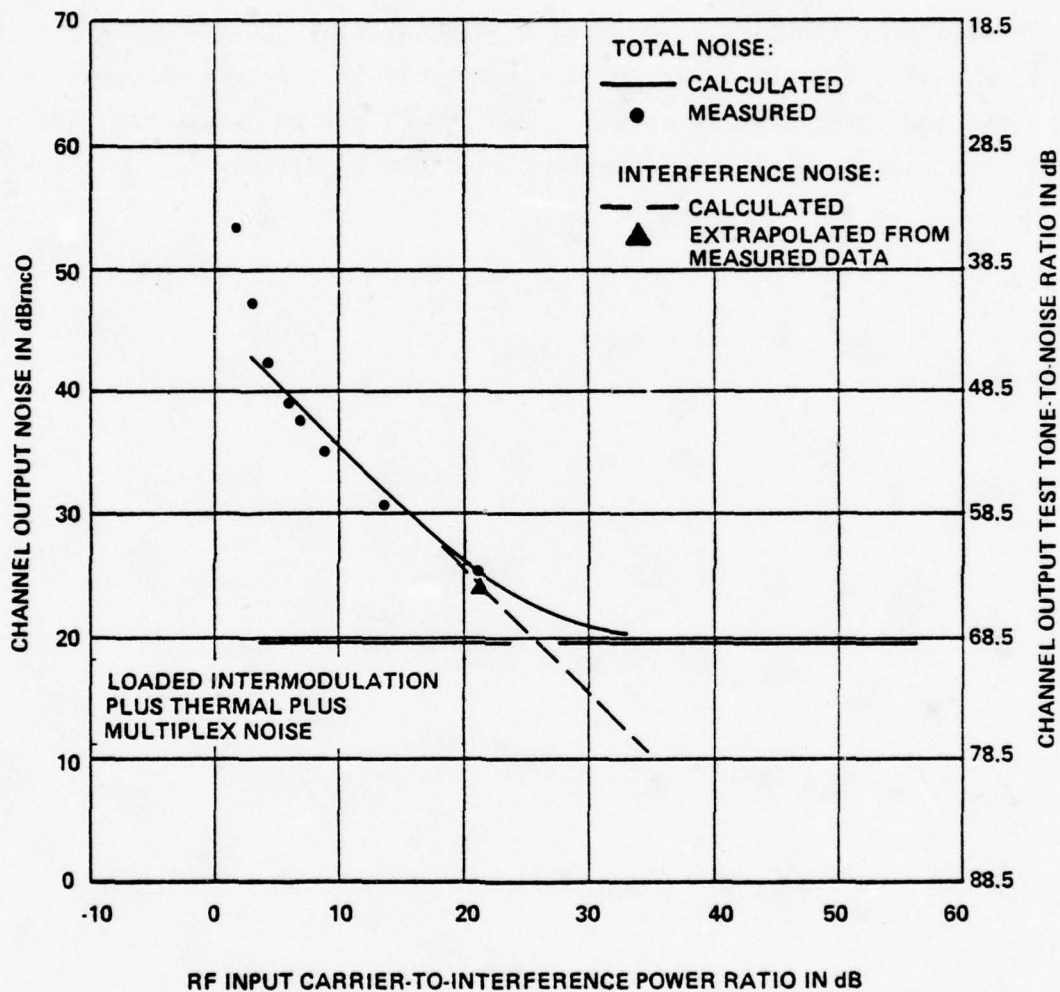


Figure 36. Transfer function for 20-MHz swept-spot noise interference; low test channel (340-344 kHz).

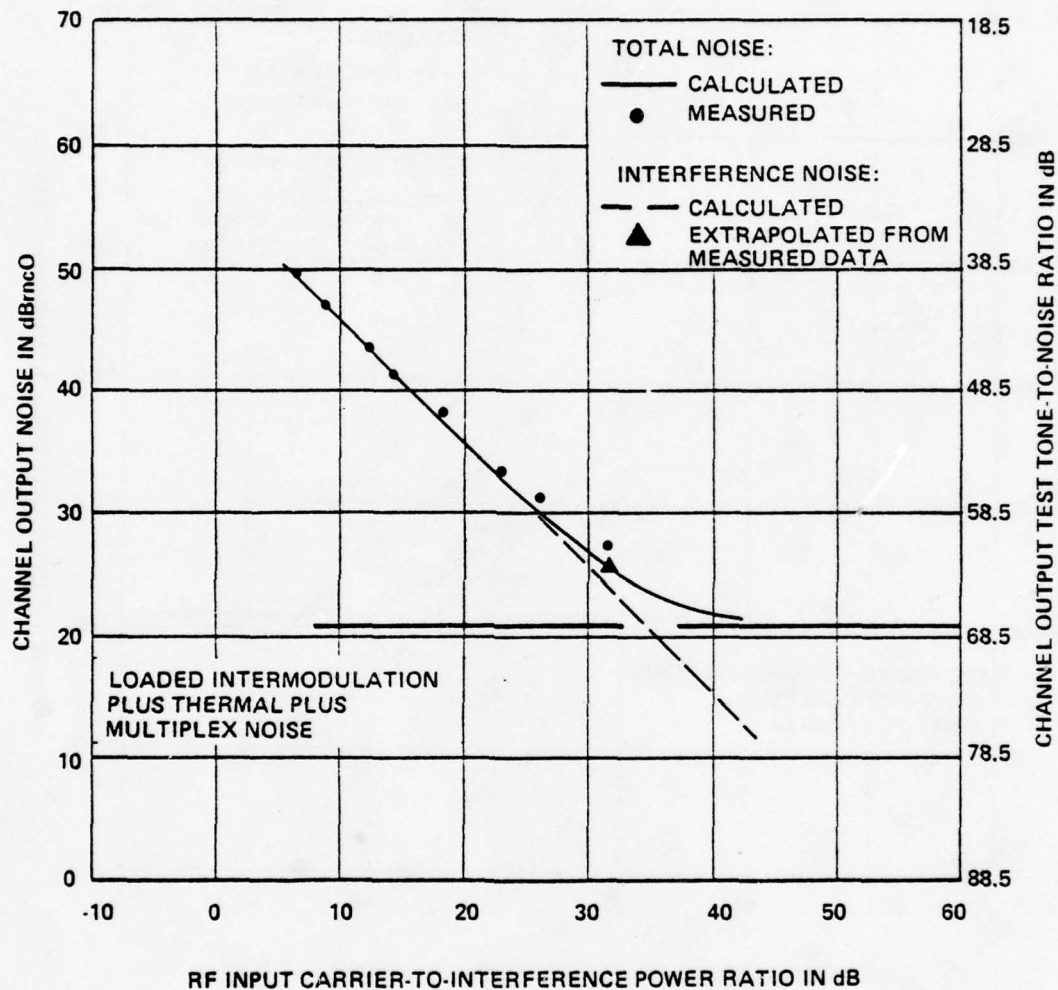


Figure 37. Transfer function for CW-swept interference; low test channel (340-344 kHz).

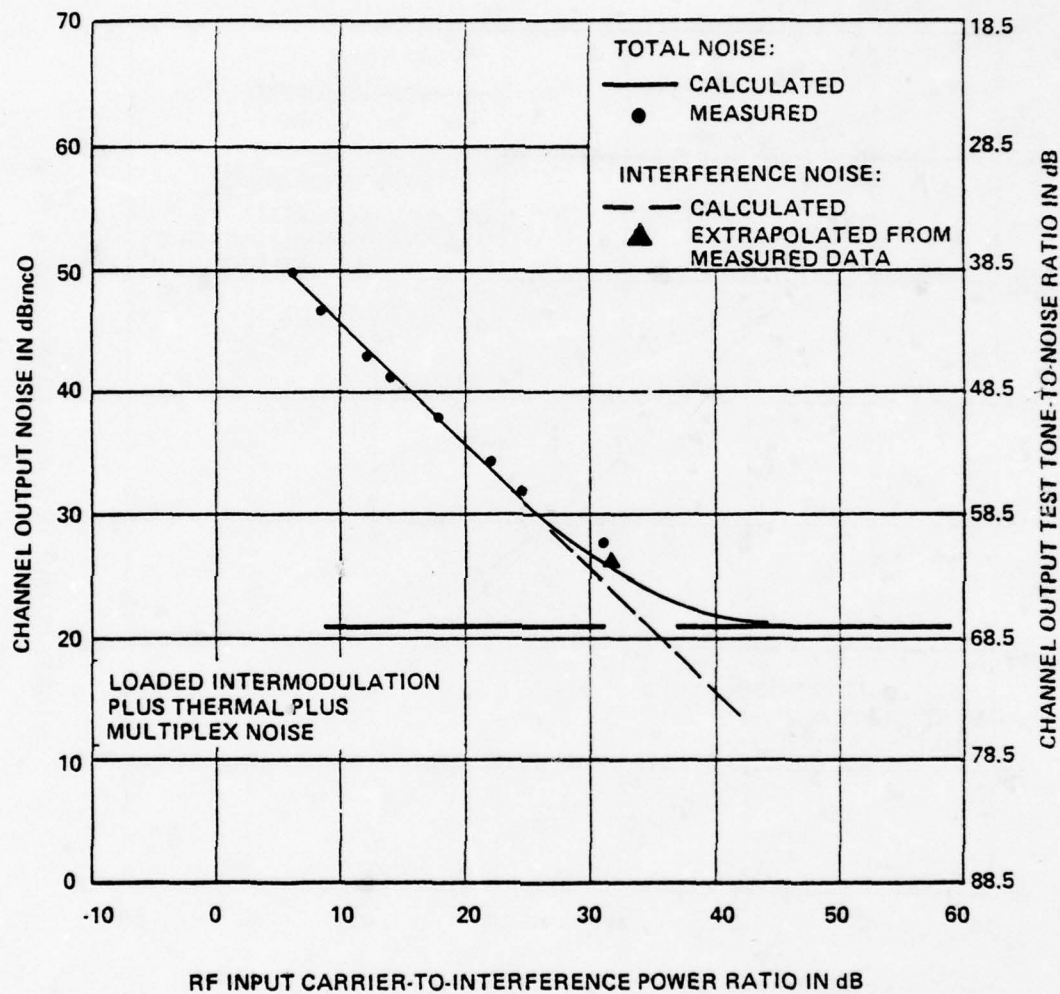


Figure 38. Transfer function for 5-MHz swept-spot noise interference; high test channel (2432-2436 kHz).

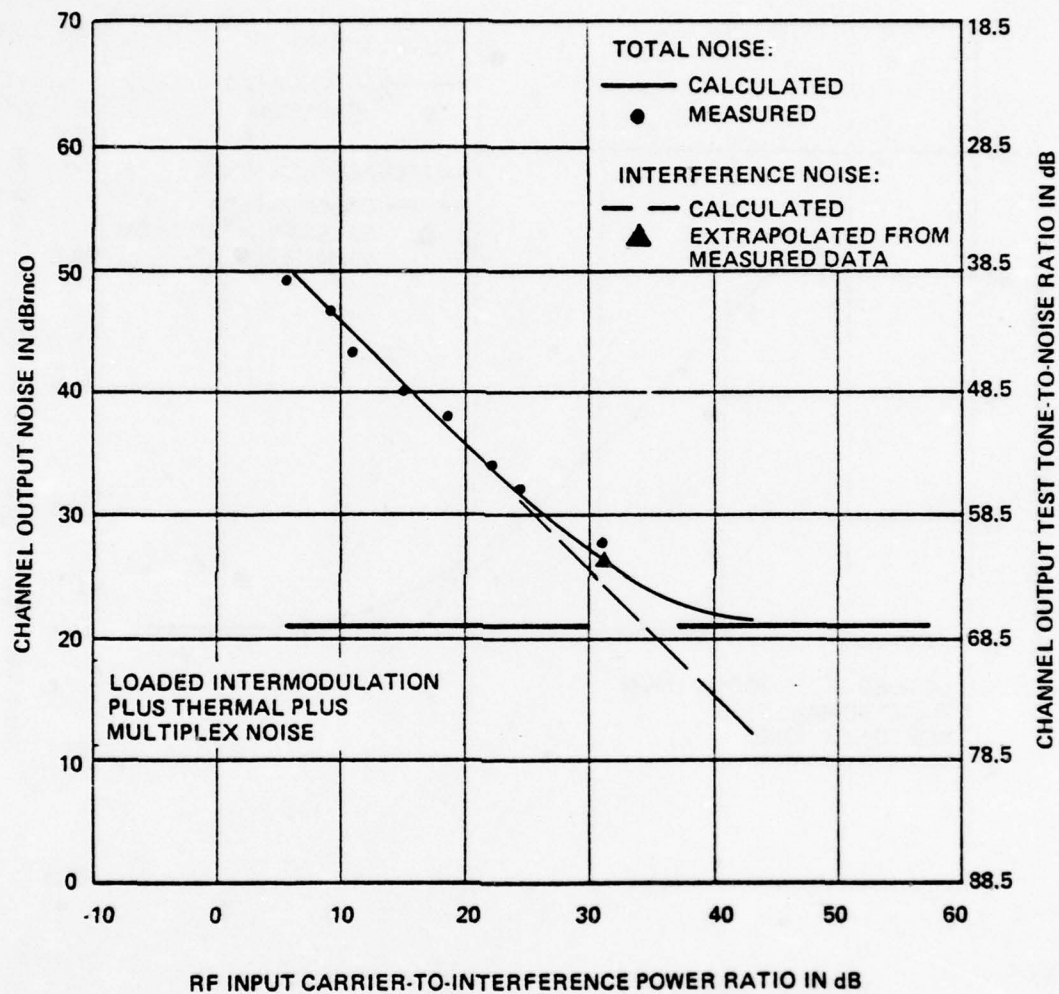


Figure 39. Transfer function for 10-MHz swept-spot noise interference; high test channel (2432-2436 kHz).

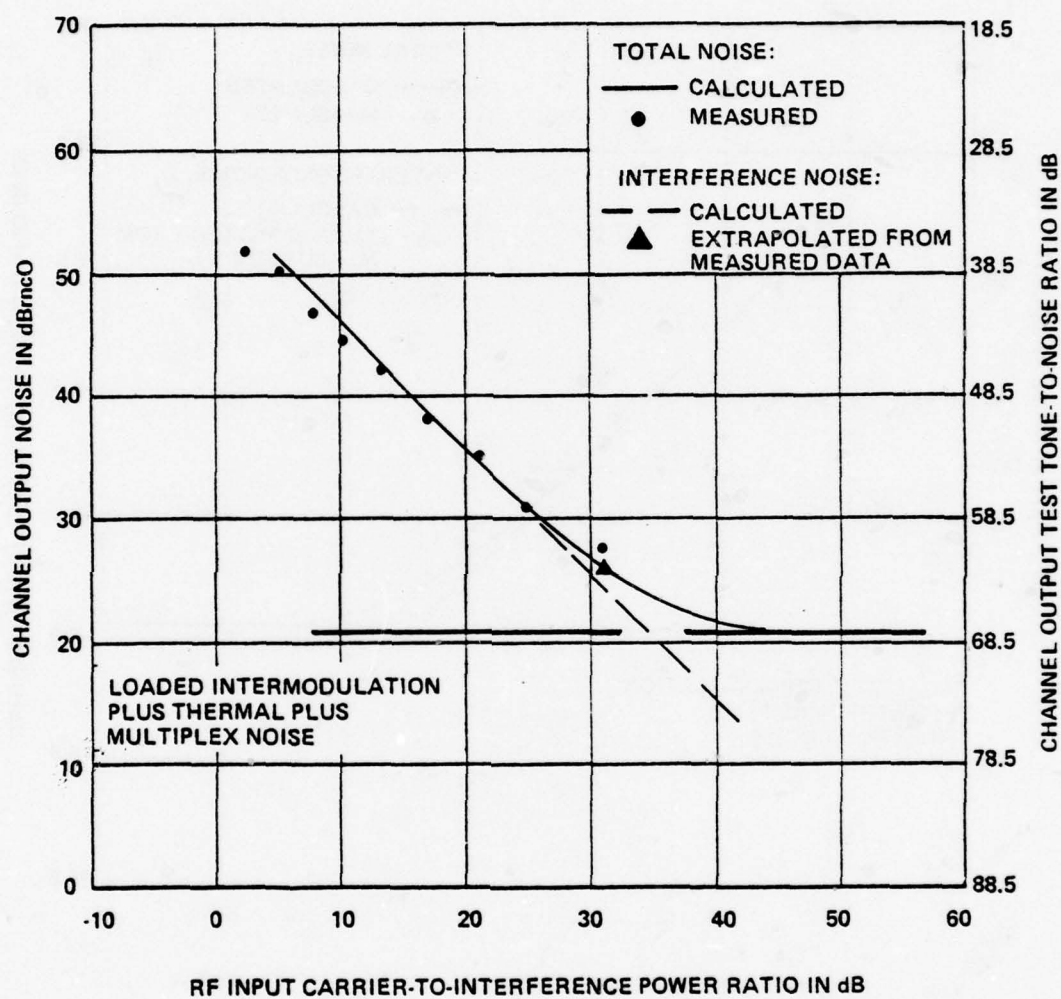


Figure 40. Transfer function for 20-MHz swept-spot noise interference; high test channel (2432-2436 kHz).

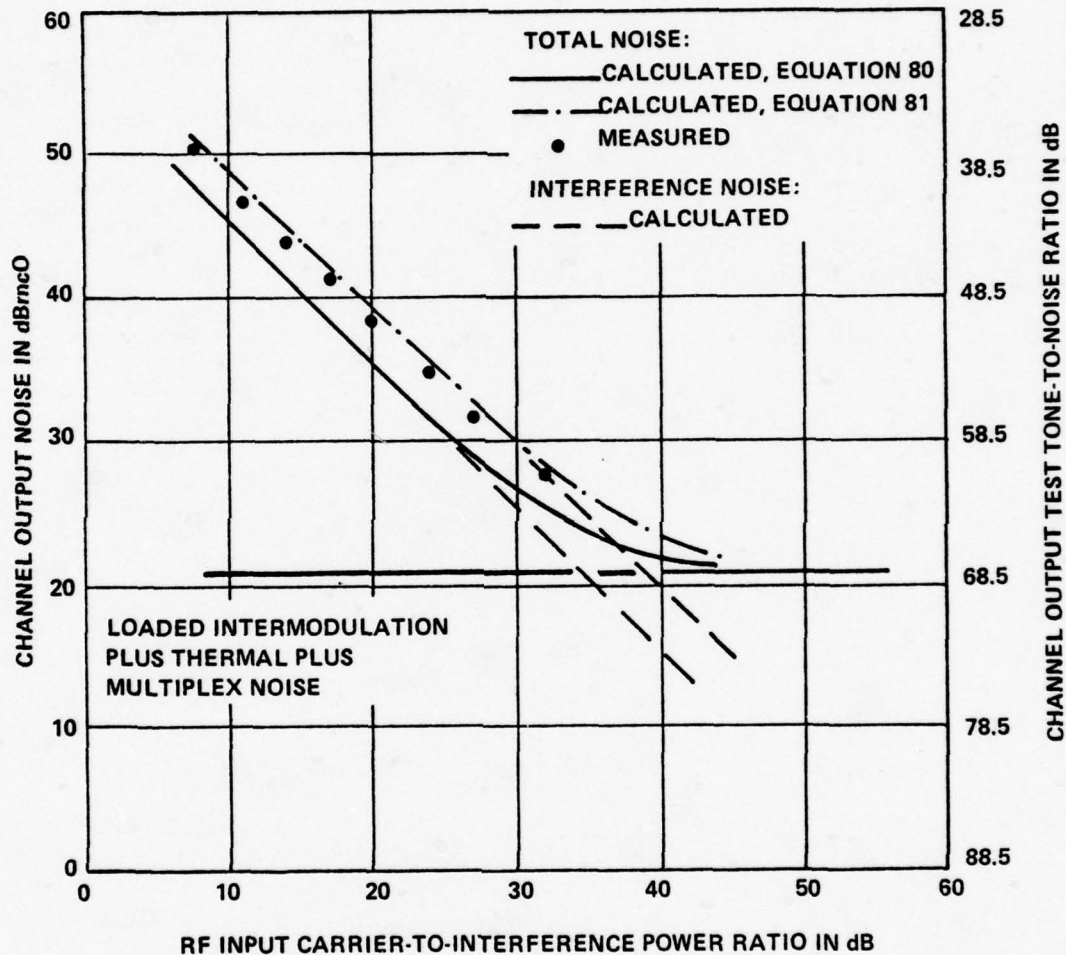


Figure 41. Transfer function for 50-MHz swept-spot noise interference; high test channel (2432-2436 kHz).

SECTION 6

NOISE-MODULATED FM AND CW INTERFERENCE

This section contains a discussion of the effects of noise-modulated FM and unmodulated CW interference in frequency-modulated systems carrying multichannel telephony signals. Various techniques and equations are presented for analyzing the performance degradation to FDM/FM systems produced by these types of interfering signals, and comparisons are made between theoretically calculated and measured performance data.

NOISE-MODULATED FM AND CW INTERFERENCE TRANSFER FUNCTIONS

The equations developed by Hamer (Reference 19) were used to obtain the FDM/FM transfer functions for the following types of interfering signals:

1. An FM signal with the baseband modeled as an ideally band-limited Gaussian noise signal
2. An unmodulated signal.

Hamer derived the FDM/FM noise power ratio equations (from which the test tone-to-noise power ratio can be readily derived, Equations 48 and 49) for two specific ranges of RMS modulation indices. Namely, very small values of RMS modulation index and large values of RMS modulation index. However, a more recent parametric examination of Hamer's NPR equations performed by Harold J.Y. Ng of the Office of Telecommunications³¹ indicates

³¹Ng, H.J.Y., *A Parametric Examination of the Processing Gain Relationship of a Frequency Division Multiplex Receiver Subject to Frequency Division Modulation Interference*, OT Report TN-76-1, U.S. Department of Commerce/Office of Telecommunications, March 1976.

that these equations can be used to predict the processing gain for intermediate values of RMS modulation indices. These equations and their range of validity will be treated in the following subsections.

Noise-Modulated FM Interference ($m \leq 0.3$)

When the RMS modulation indices of both the desired and the interfering noise-modulated FM signals are small (≤ 0.3), the normalized continuous noise power spectra can be approximated by Equation 14. For this case, Hamer shows that the NPR due to the continuous portions of the spectra (for $c \gg i$) can be approximated by:

$$\begin{aligned}
 (\text{NPR})_{\text{CS}} = & \left[\frac{32(c/i)(F_H' - F_L')e}{F_{\text{ch}}^2 D_{\text{rms}}^2} \right] \left\{ \frac{1}{x^3} \left[\log \left| \frac{f+x}{f-x} \right| \right. \right. \\
 & - \frac{x}{f+x} - \frac{x}{f-x} \Big] + \frac{1}{y^3} \left[\log \left| \frac{f+y}{f-y} \right| \right. \\
 & \left. \left. - \frac{y}{f+y} - \frac{y}{f-y} \right] \right\}^{-1} \quad (83)
 \end{aligned}$$

where

$(\text{NPR})_{\text{CS}}$ = Noise power ratio due to the continuous portions of the spectra

(c/i) = Carrier-to-interference power ratio

F_H' = Maximum modulation frequency of interfering signal, in Hz

F_L' = Minimum modulation frequency of interfering signal, in Hz

F_{ch} = Center frequency of the channel in the baseband, in Hz

D'_{rms} = Total RMS deviation of the interfering signal, in Hz

e = Preemphasis factor

f = Frequency relative to the desired signal carrier frequency, in Hz

$x = \frac{1}{2}(\Delta f - F_{ch})$

$y = \frac{1}{2}(\Delta f + F_{ch})$

Δf = frequency separation between the desired signal carrier frequency and the interfering signal carrier frequency (only positive values of Δf being considered), in Hz.

With the "x" terms in Equation 83 evaluated over the following overlapping limits of f:

$$(-x - F_H) \text{ to } (-x - F_L); (-x + F_L) \text{ to } (-x + F_H) \quad (84)$$

$$(x - F'_H) \text{ to } (x - F'_L); (x + F'_L) \text{ to } (x + F'_H) \quad (85)$$

where

F_H = Maximum modulation frequency of desired signal, in Hz

F_L = Minimum modulation frequency of desired signal, in Hz

and similarly for the "y" terms by replacing the "x" with "y" in Equations 84 and 85.

The NPR, and thus the processing gain due to the continuous portions of the spectra, is further degraded by the interaction of the spectra with the residual carriers. The NPR due to the interaction between the interfering signal residual carrier and the continuous spectrum of the desired signal can be approximated from:

$$(NPR)_{IC} = \frac{[4F_H^2 (c/i) e / F_{ch}^2] \exp(D_{rms}^2 / F_L' F_H')}{\left[\left(\frac{F_H}{\Delta f - F_{ch}} \right)^2 + \left(\frac{F_H}{\Delta f + F_{ch}} \right)^2 \right]} \quad (86)$$

where

$(NPR)_{IC}$ = Noise power ratio due to the interfering signal residual carrier on the desired signal

and

$$F_L \leq |\Delta f - F_{ch}| \leq F_H$$

$$F_L \leq (\Delta f + F_{ch}) \leq F_H$$

with only positive values of Δf being considered. Similarly, the NPR due to the interaction between the continuous spectrum of the interfering signal and the desired signal residual carrier can be approximated by:

$$(NPR)_{DC} = \frac{\frac{[4F_H^2 D_{rms}^2 (c/i) e (F_H' - F_L')]}{[F_{ch} D_{rms} (F_H - F_L)]} \exp[D_{rms} / F_H F_L]}{\left(\frac{F_H}{\Delta f - F_{ch}} \right)^2 + \left(\frac{F_H}{\Delta f + F_{ch}} \right)^2} \quad (87)$$

where

$(\text{NPR})_{\text{DC}}$ = Noise power ratio due to the residual carrier of the desired signal

D_{rms} = Total RMS deviation of the interfering signal, in Hz

and

$$F_L \leq |\Delta f - F_{\text{ch}}| \leq F_H$$

$$F_L \leq (\Delta f + F_{\text{ch}}) \leq F_H$$

with only positive values of Δf being considered.

The NPR due to noise-modulated interference for very small values of RMS modulation index and $c \gg i$ is given by Equations 83, 86 and 87. The total NPR is therefore given by:

$$\text{NPR} = \left\{ \frac{1}{(\text{NPR})_{\text{CS}}} + \frac{1}{(\text{NPR})_{\text{IC}}} + \frac{1}{(\text{NPR})_{\text{DC}}} \right\}^{-1} \quad (88)$$

where

NPR = Total NPR due to a noise-modulated interfering signal.

The NPR computed from Equation 88 can be used in conjunction with Equations 48 and 49 to obtain the test tone-to-noise ratio in the channel of interest.

The small modulation index approximation given by Equation 88 is only valid for small values of $(mD_{\text{rms}})/F_L$, namely $(mD_{\text{rms}})F_L < 1$ and $(m'D'_{\text{rms}})/F'_L < 1$, where the primes indicate interfering signal parameters. When the above conditions are met, the residual carriers will be large, and for this case Equations 86 and 87 will

contribute the most to the total NPR. Generally, the contribution from Equation 83 is negligible when both of these ratios are very small.

Noise-Modulated FM Interference ($m \geq 0.3$)

When the RMS modulation indices of both the desired and the interfering noise-modulated FM signals are large, the normalized noise power spectra can be calculated from Equation 16. For this case, with $c \gg i$, the FM processing gain is given by (Reference 30):

$$\begin{aligned}
 PG_{FM} = & -27.91 + 20 \log(d_{rms}/F_{ch}) + 10 \log f_s + E \\
 & - 10 \log \left\{ \exp \left[- \frac{(\Delta f - F_{ch})^2}{2f_s^2} \right] \right. \\
 & \left. + \exp \left[- \frac{(\Delta f + F_{ch})^2}{2f_s^2} \right] \right\} \quad (89)
 \end{aligned}$$

where

- PG_{FM} = Noise-modulated FM (FDM/FM) processing gain, in dB
- d_{rms} = RMS deviation of the channel for a signal of test tone level, in Hz
- F_{ch} = Center frequency of the channel in the baseband, in Hz
- E = Preemphasis factor (Equation 34 for CCIR preemphasis)

Δf = Frequency separation between the wanted and interfering carrier frequencies, in Hz

$$f_s = [D_{rms}^2 + D'_{rms}{}^2]^{1/2}$$

D_{rms} = Multichannel RMS frequency deviation of the desired signal, in Hz

D'_{rms} = Multichannel RMS frequency deviation of the interfering signal, in Hz

which agrees with the results of Hamer (Reference 19).

The parametric examination of Equations 88 and 89 (Reference 13) is significant in that it shows that Equation 89 can be used to approximate the processing gain for values of RMS modulation indices as low as approximately 0.3. The extent of the inaccuracies caused by using the Gaussian noise approximation with intermediate values of RMS modulation index ($0.3 \leq m \leq 1.5$) were illustrated by Pontano, et al., (Reference 22).

CW Interference ($m \leq 0.3$)

The NPR due to the interaction between an unmodulated interfering carrier and the continuous portion of the desired FDM/FM signal spectrum can be derived from Equation 86 by setting D'_{rms} equal to zero. This yields:

$$(NPR)_{CW} = \frac{[4F_H^2(c/i)e/F_{ch}^2]}{\left[\left(\frac{F_H}{\Delta f - F_{ch}} \right)^2 + \left(\frac{F_H}{\Delta f + F_{ch}} \right)^2 \right]} \quad (90)$$

where

$$F_L \leq |\Delta f - F_{ch}| \leq F_H$$

and

$$F_L \leq (\Delta f + F_{ch}) \leq F_H.$$

Only positive values of Δf are considered. This equation agrees with the results of Hamer.

CW Interference ($m \geq 0.3$)

For high values of RMS modulation index Equation 89 may be used to approximate the CW processing gain by setting D'_{rms} equal to zero. This gives:

$$\begin{aligned} PG_{CW} = & -27.91 + 20 \log(d_{rms}/F_{ch}) + 10 \log D_{rms} + E \\ & - 10 \log \left\{ \exp \left[- \frac{(\Delta f - F_{ch})^2}{2D_{rms}^2} \right] \right. \\ & \left. + \exp \left[- \frac{(\Delta f + F_{ch})^2}{2D_{rms}^2} \right] \right\} \end{aligned} \quad (91)$$

which once again agrees with the results of Hamer.

COMPARISONS BETWEEN MEASURED AND CALCULATED DATA

The measured transfer functions for an identical 600-channel FDM/FM interfering signal are shown compared with the calculated transfer functions (Equation 89) for the low, middle and high test channels in Figures 42, 43 and 44, respectively. The results of these comparisons indicate that good agreement exists between the measured and calculated processing gain values.

Similar comparisons are shown in Figures 45, 46 and 47 for on-tune 12 channel FDM/FM interference; in Figures 48, 49 and 50 for

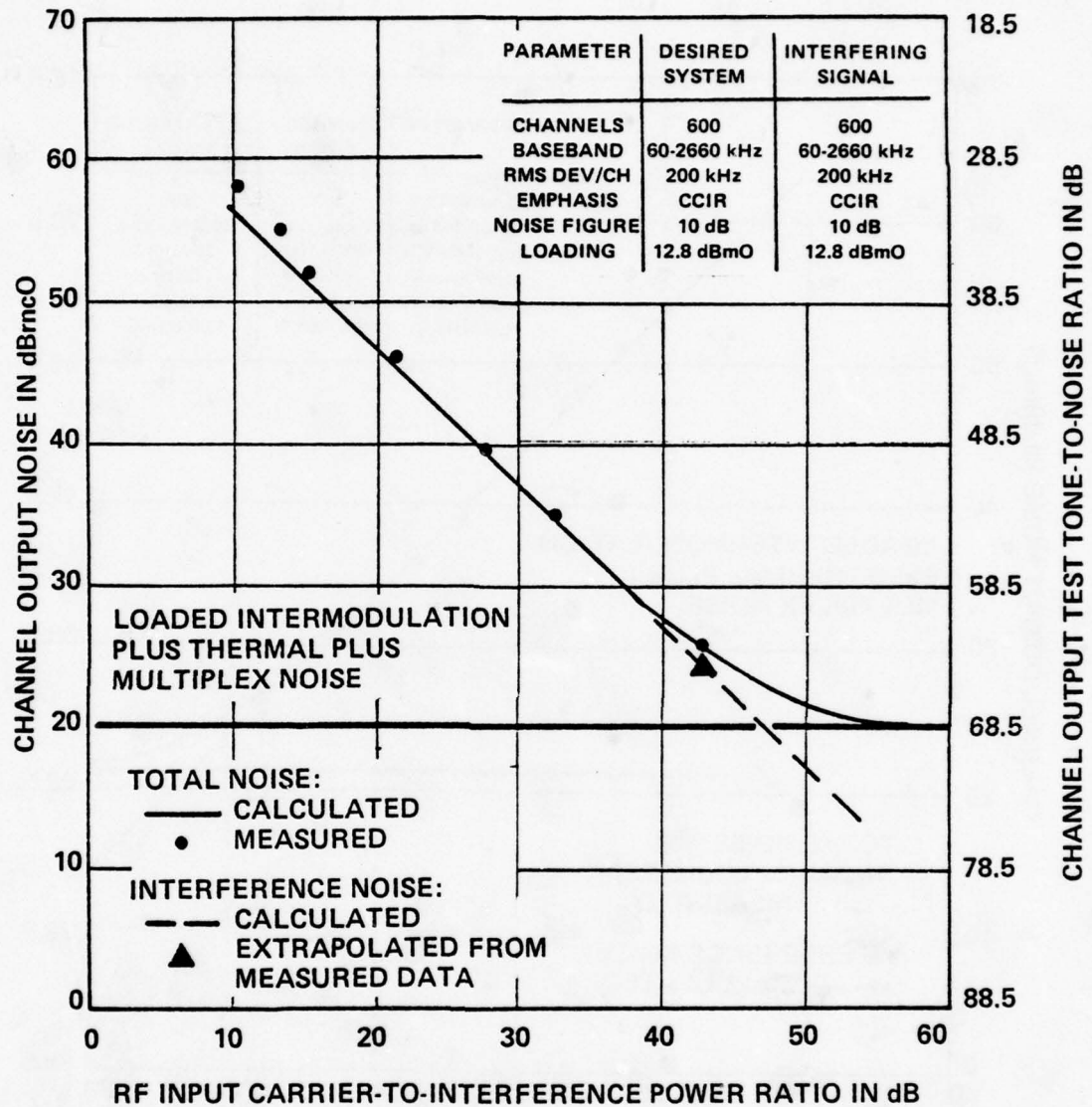


Figure 42. Transfer function for identical 600-channel on-tune FDM/FM interference; low test channel (340-344 kHz).

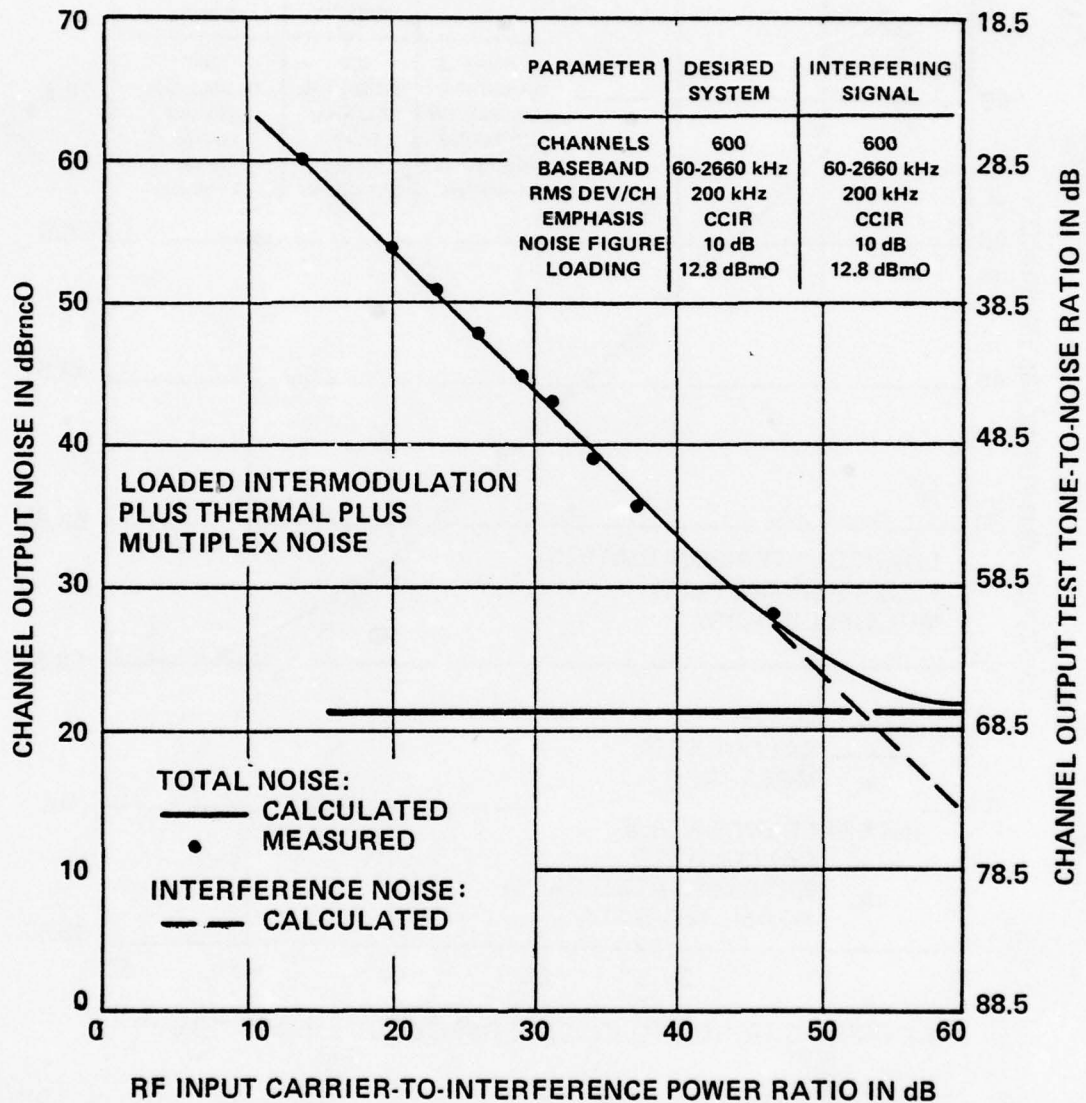


Figure 43. Transfer function for identical 600-channel on-tune FDM/FM interference; middle test channel (1244-1248 kHz).

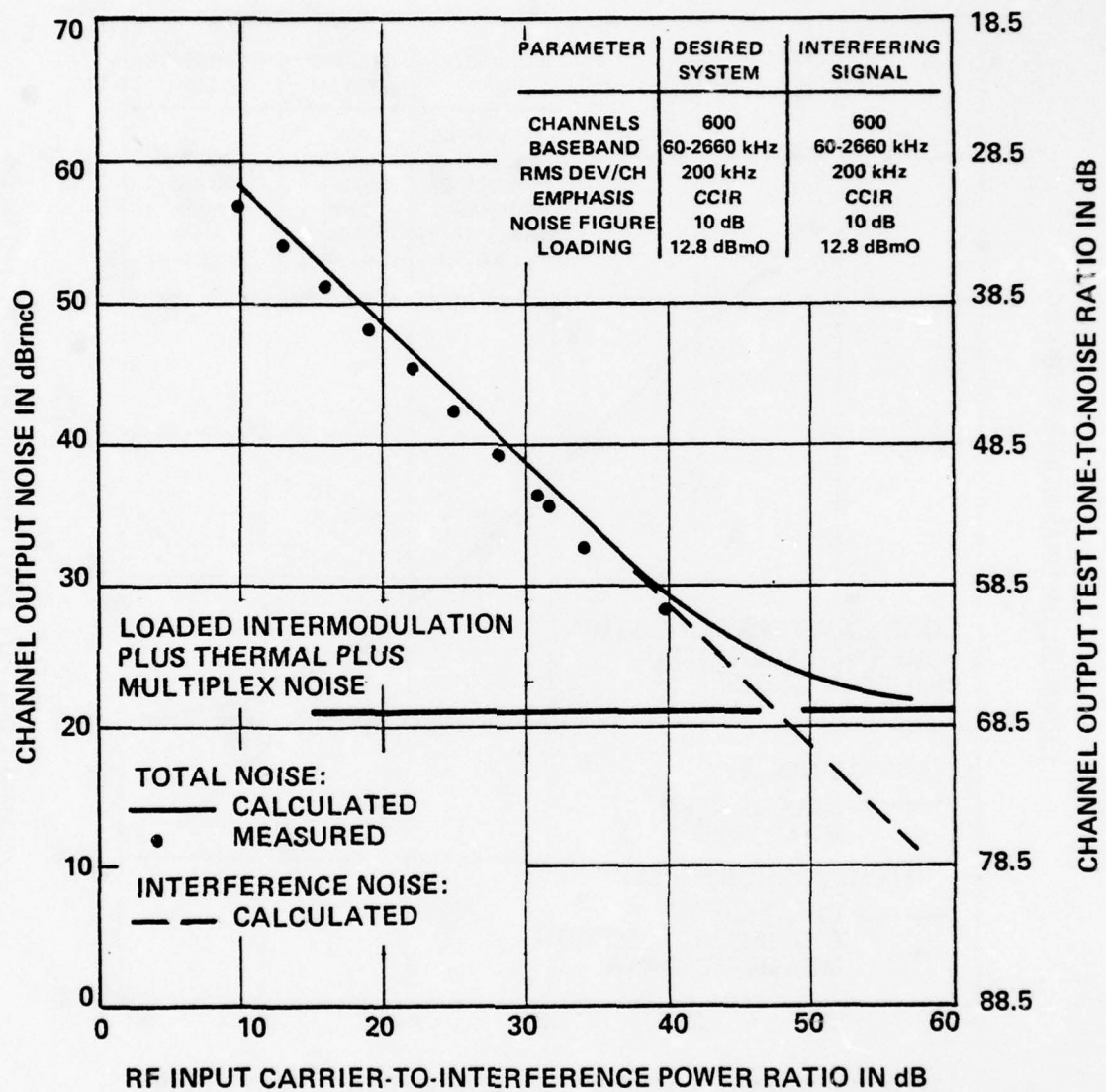


Figure 44. Transfer function for identical 600-channel on-tune FDM/FM interference; high test channel (2432-2436 kHz).

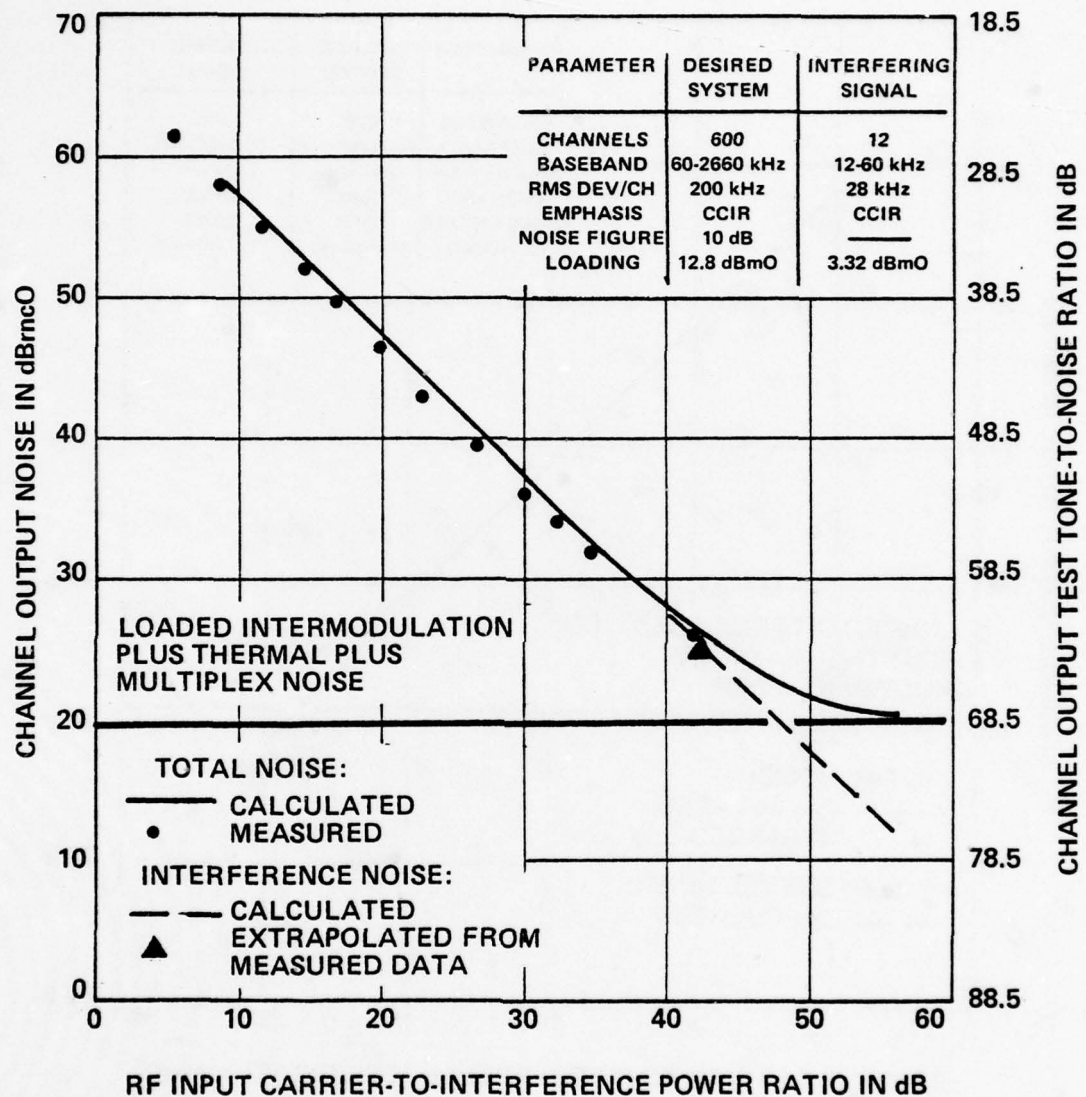


Figure 45. Transfer function for on-tune 12-channel FDM/FM interference; low test channel (340-344 kHz).

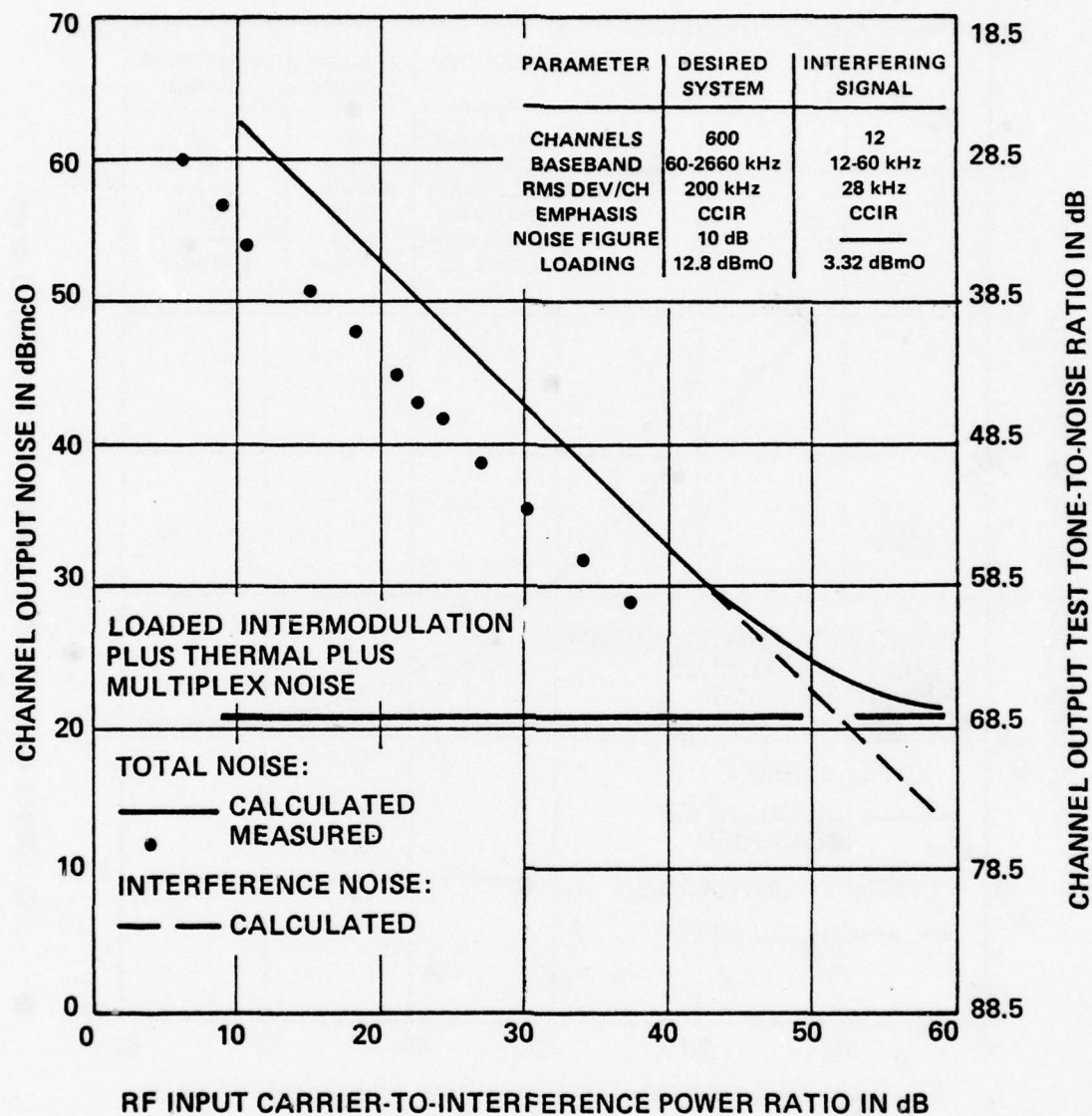


Figure 46. Transfer function for on-tune 12-channel FDM/FM interference; middle test channel (1244-1248 kHz).

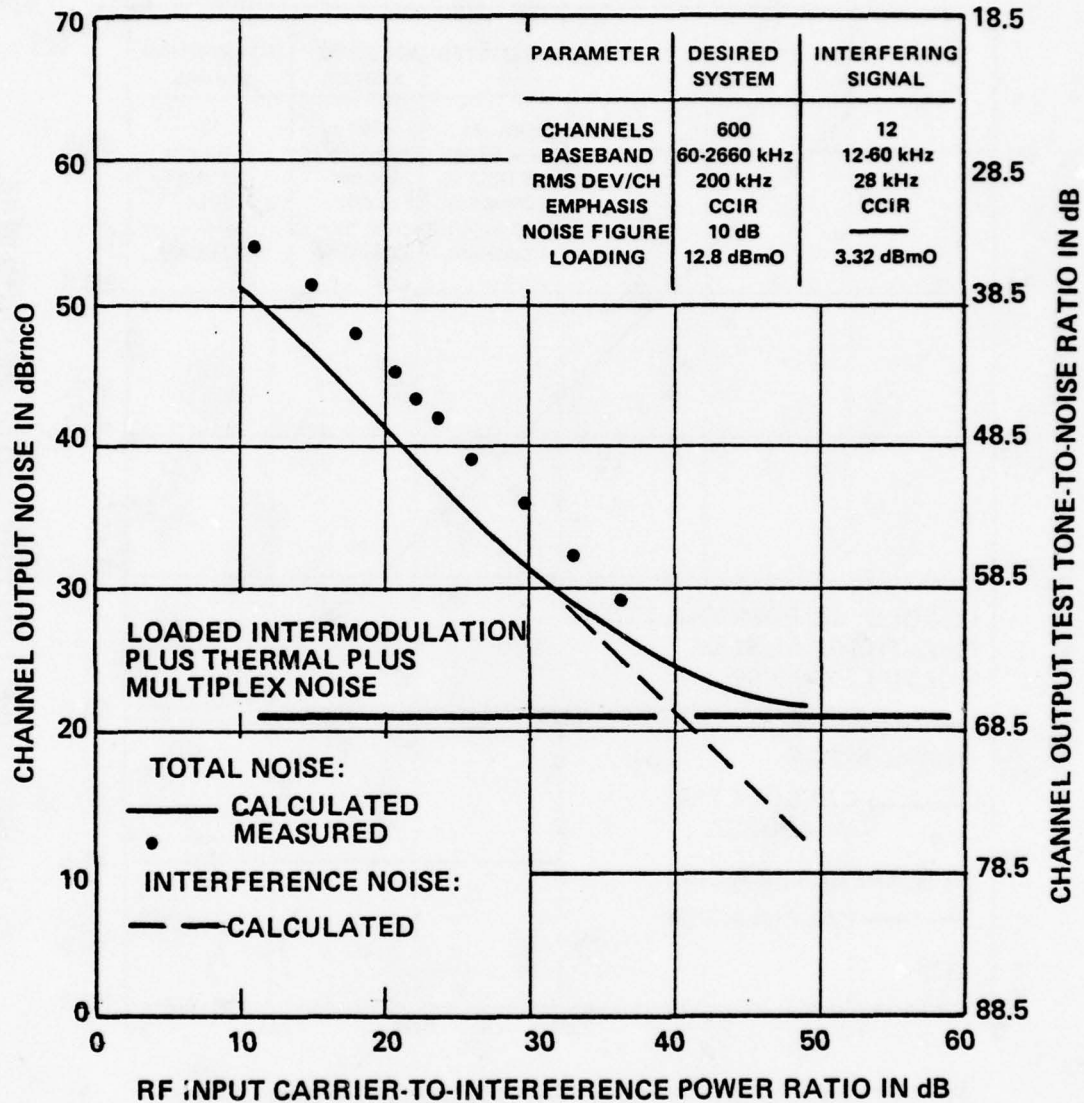


Figure 47. Transfer function for on-tune 12-channel FDM/FM interference; high test channel (2432-2436 kHz).

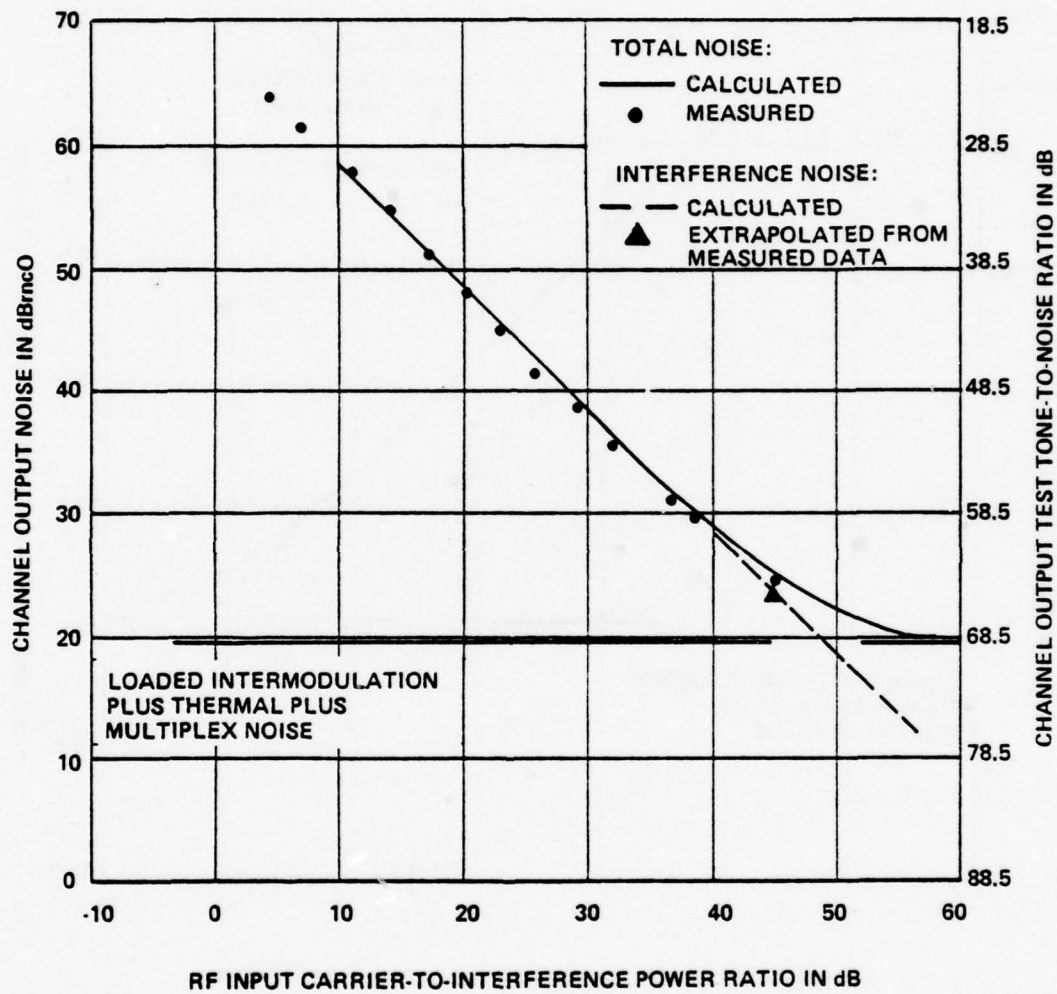


Figure 48. Transfer function for on-tune CW interference; low test channel (340-344 kHz).

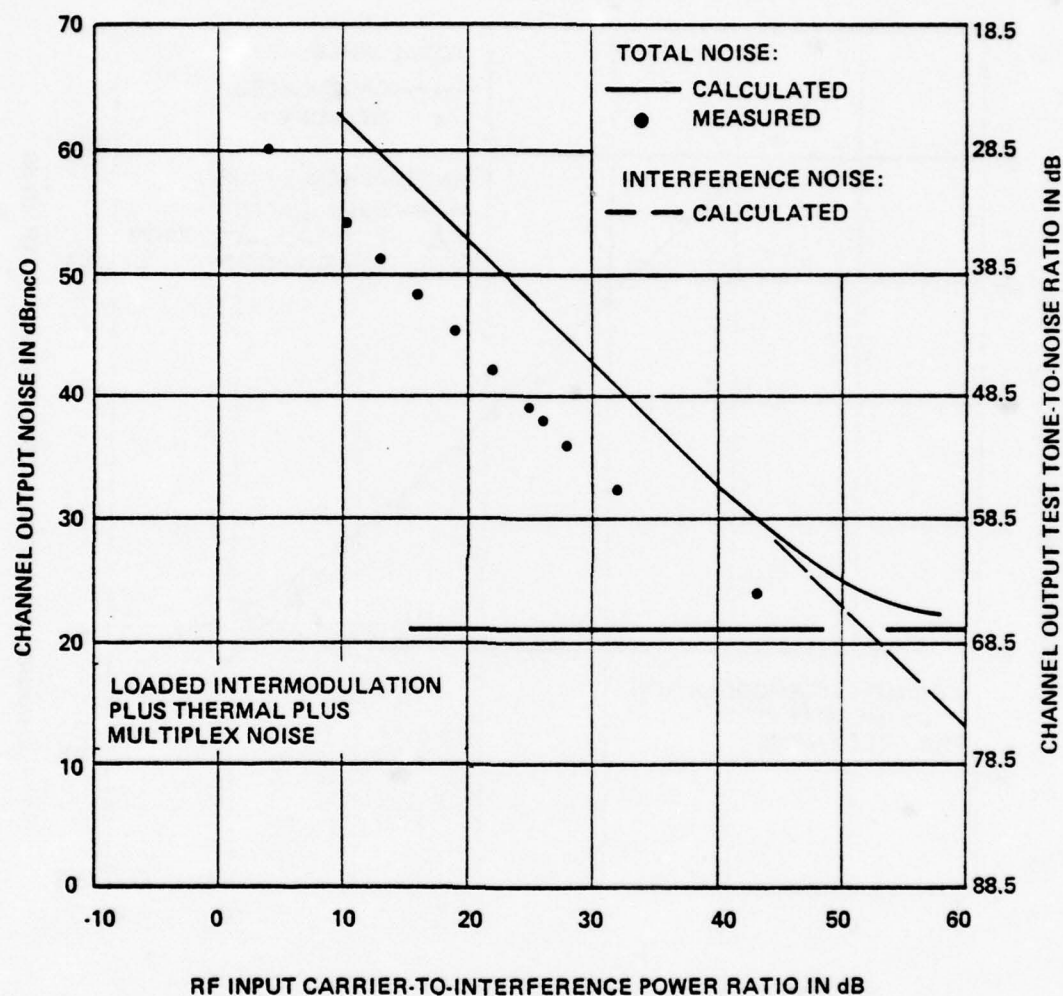


Figure 49. Transfer function for on-tune CW interference; middle test channel (1244-1248 kHz).

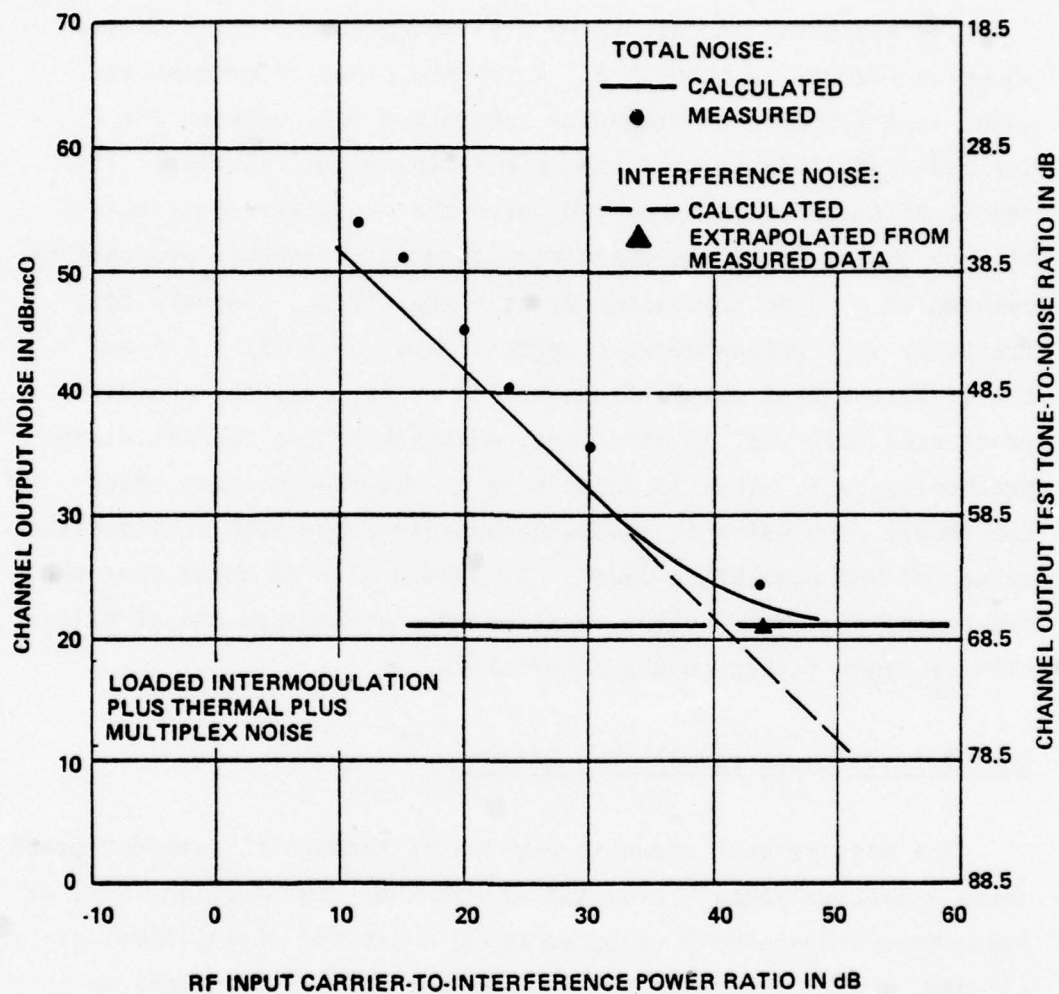


Figure 50. Transfer function for on-tune CW interference; high test channel (2432-2436 kHz).

on-tune CW interference; and in Figure 51 (low test channel) for on-tune single channel narrowband FM interference. In all cases, good agreement exists between the measured and calculated data.

The measured and calculated off-tuning characteristics are shown in Figures 52 through 61, which are plots of processing gain, as a function of frequency separation (Δf) between the desired signal carrier and the interfering signal carrier. The result of these comparisons indicates that good agreement exists between the measured and calculated data for frequency separations between $\Delta f = 0$ and approximately $\Delta f = (F_H + F'_H)$. However, for frequency separations between approximately $\Delta f = (F_H + F'_H)$ and the IF filter 3-dB cutoff frequency ($\Delta f = \pm B_{IF}/2$), the measured processing gain was, in all cases, much lower than the calculated processing gain. This is indicative of the inaccuracies which can result from using the Gaussian approximation with intermediate values of RMS modulation index. It should also be noted that the off-tuning factors in these equations do not include the IF filter off-frequency rejection characteristics.

Low Desired Signal Level - AGC Effects

The measurements shown in Figures 42 through 61 were performed using a desired signal level (C) of -36 dBm. In addition, some of those measurements were repeated using a desired signal level of -76 dBm, and in all cases the results were almost identical to those obtained with the -36 dBm desired signal level. The only discrepancies encountered were for Δf 's greater than approximately F_H Hz. The receiver AGC characteristics are shown plotted in Figure A-38 of APPENDIX A.

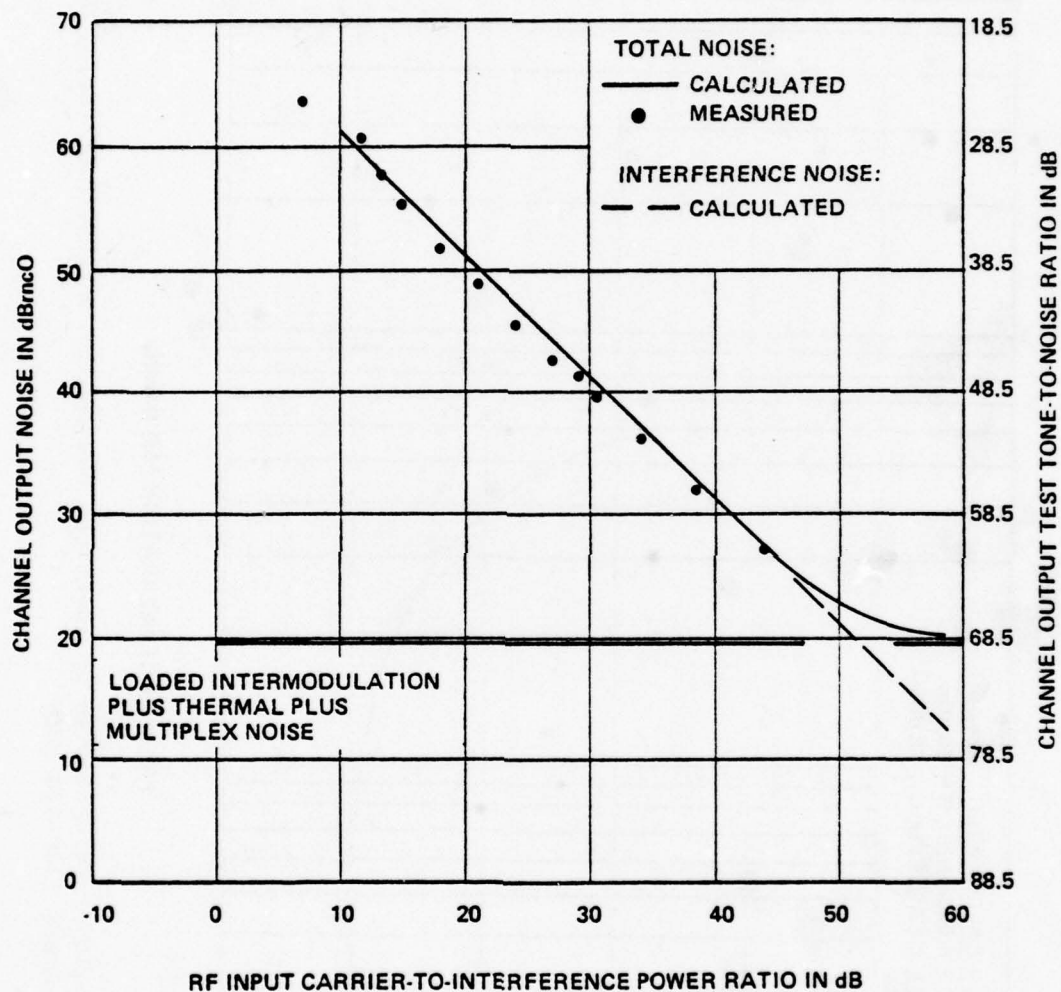


Figure 51. Transfer function for on-tune single channel narrowband FM interference; low test channel (340-344 kHz).

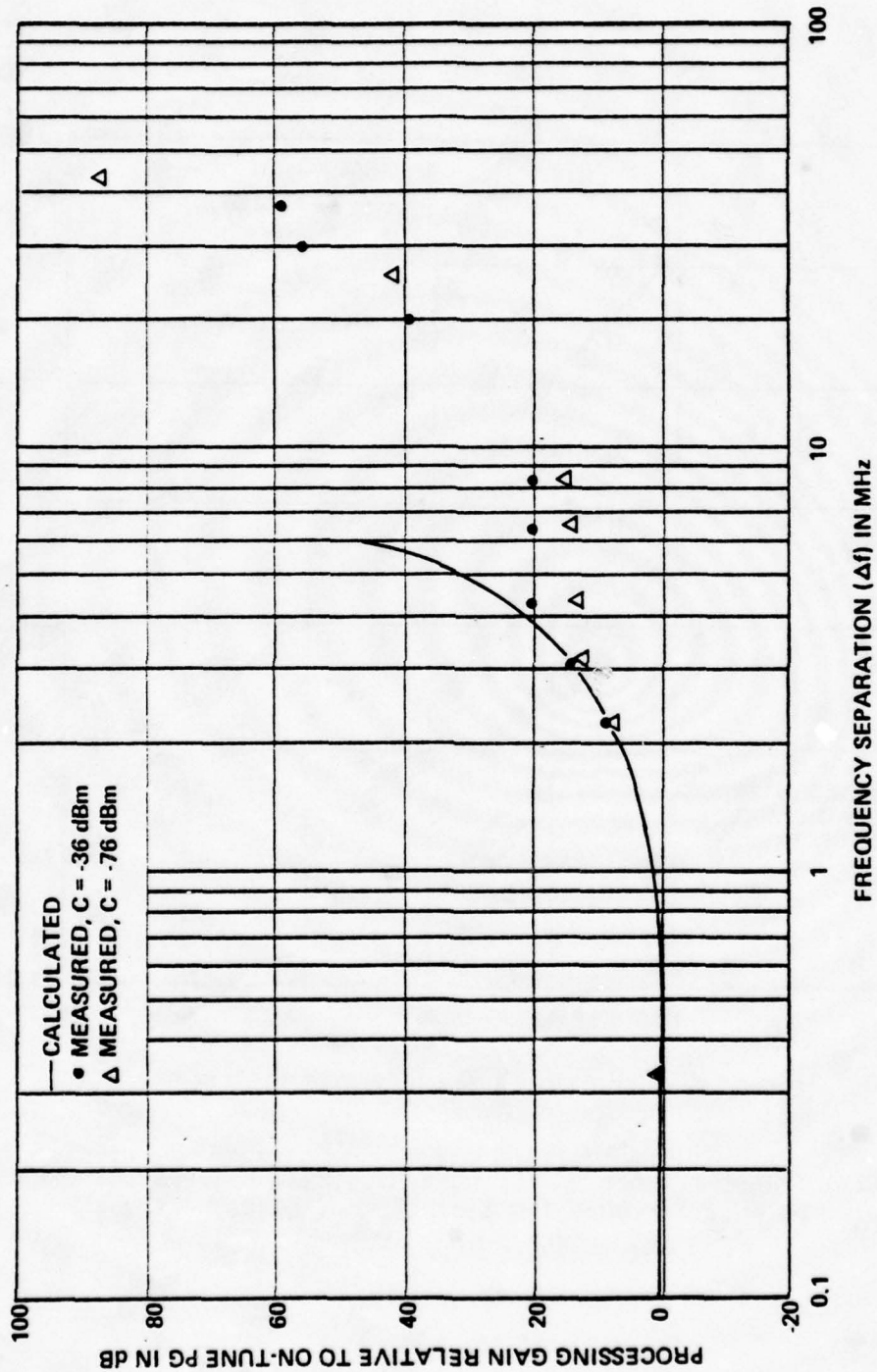


Figure 52. Off-frequency rejection to an identical 600-channel FDM/FM interfering signal; low test channel (340-344 kHz).

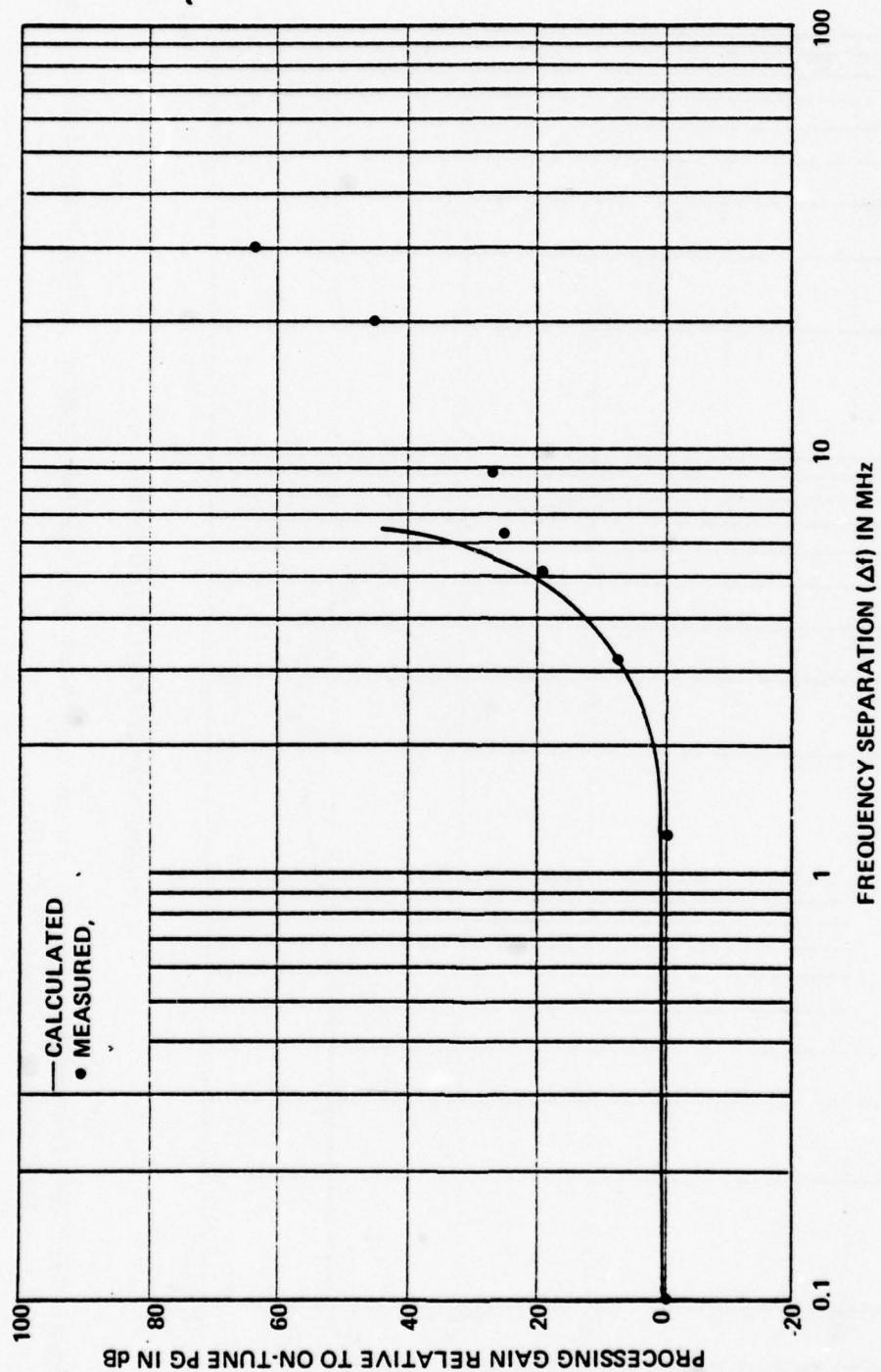


Figure 53. Off-frequency rejection to an identical 600-channel FDM/FM interfering signal; middle test channel (1244-1248 kHz).

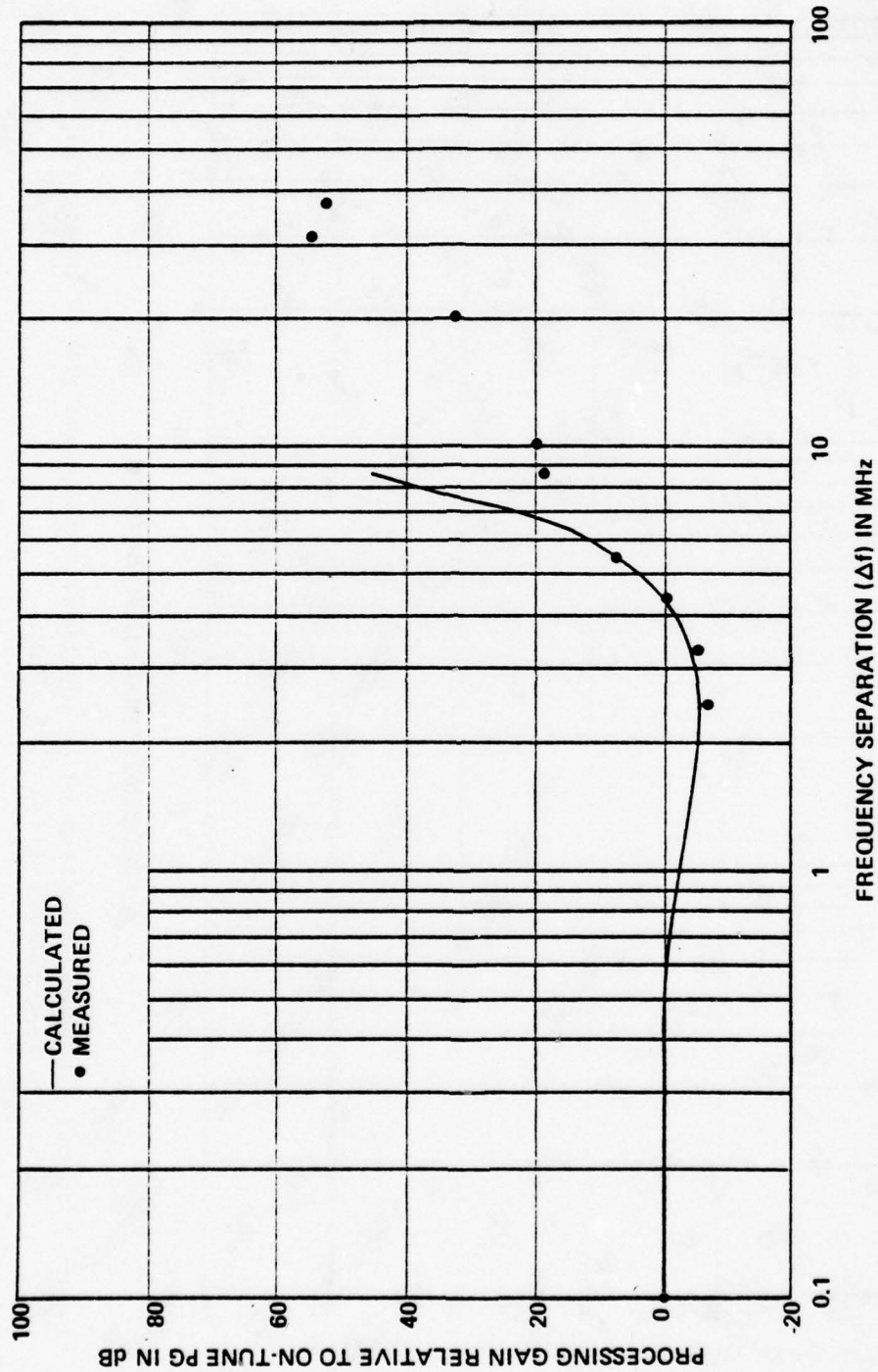


Figure 54. Off-frequency rejection to an identical 600-channel FDM/FM interfering signal; high test channel (2432-2436 kHz).

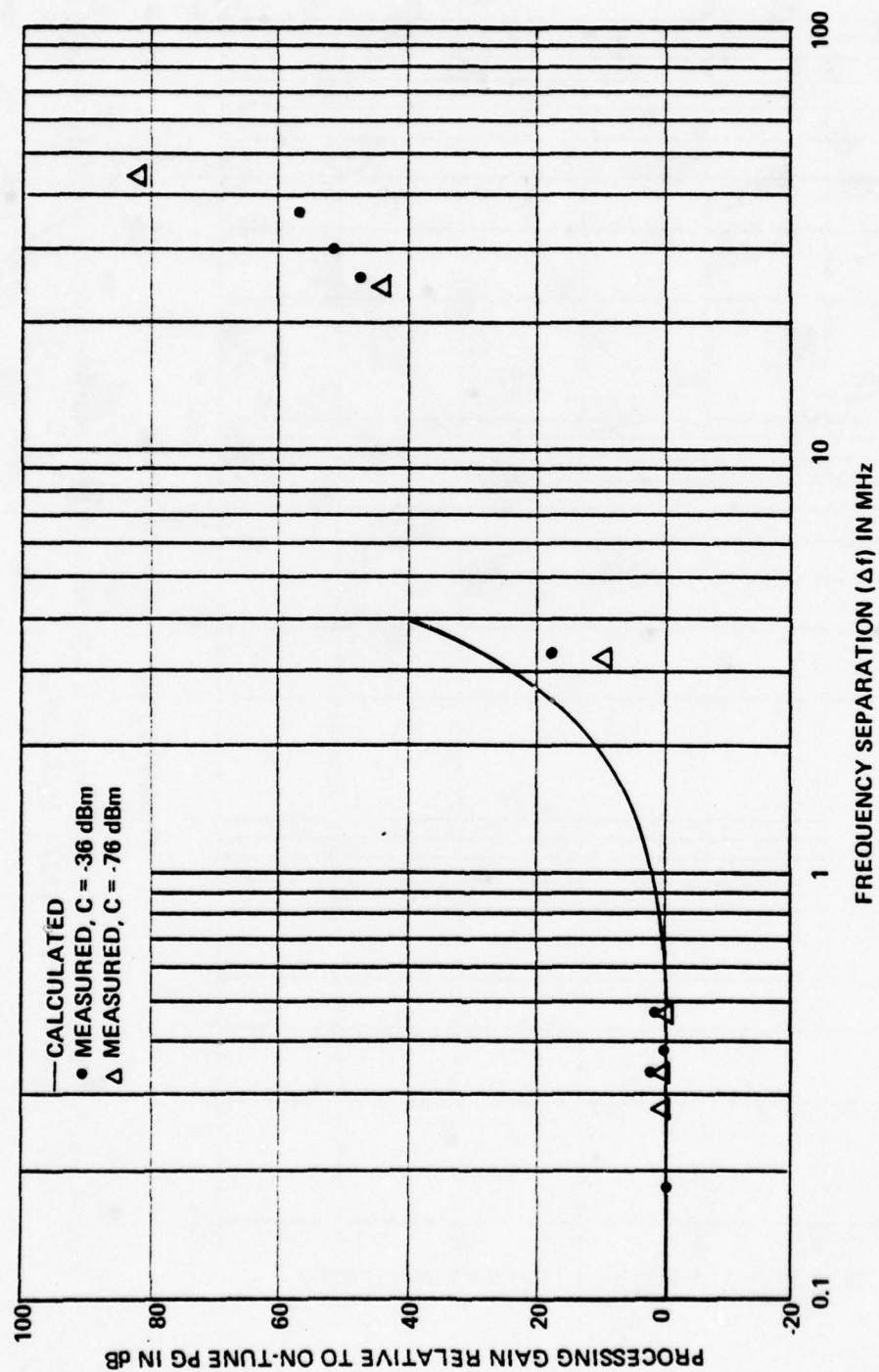


Figure 55. Off-frequency rejection to a 12-channel FDM/FM interfering signal; low test channel (340-344 kHz).

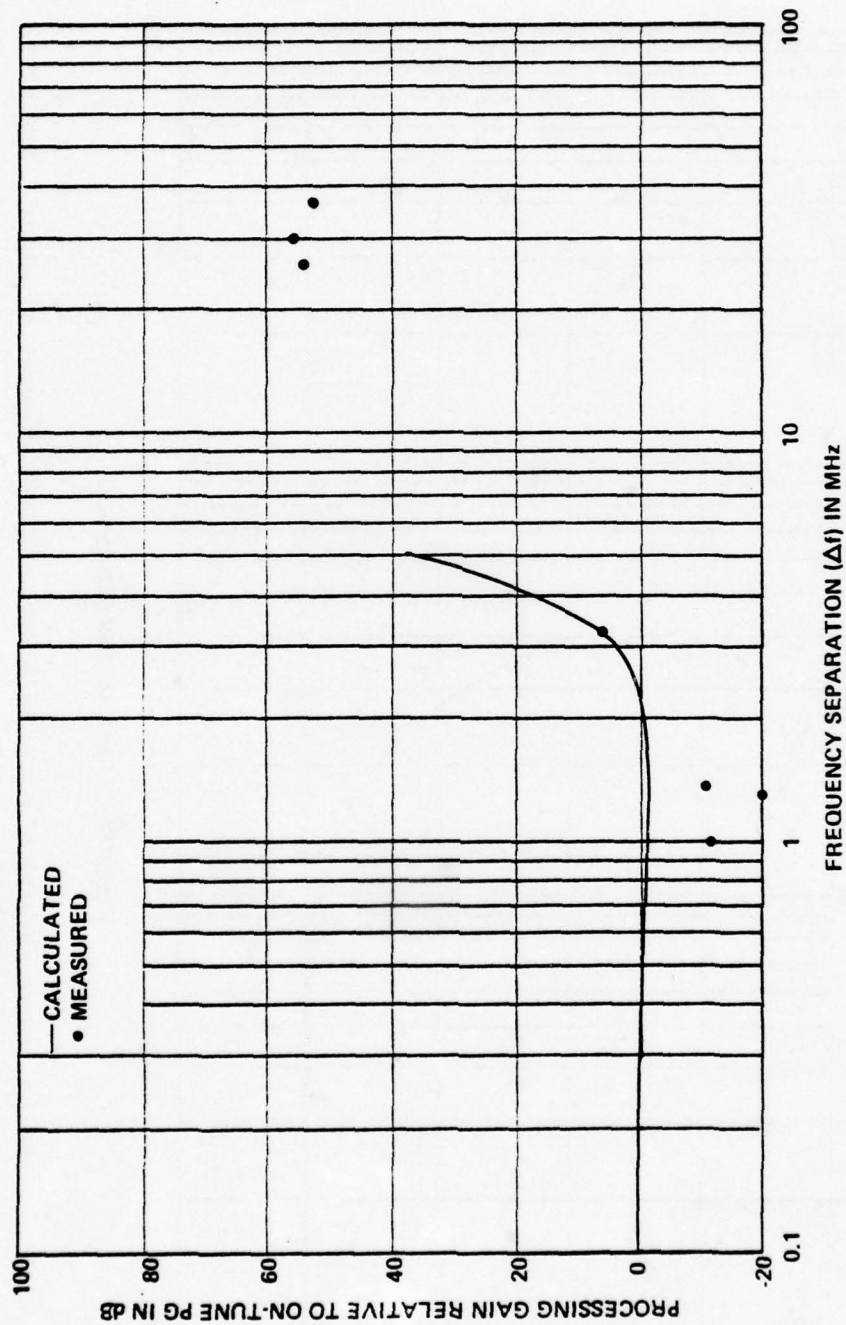


Figure 56. Off-frequency rejection to a 12-channel FDM/FM interfering signal; middle test channel (1244-1248 kHz).

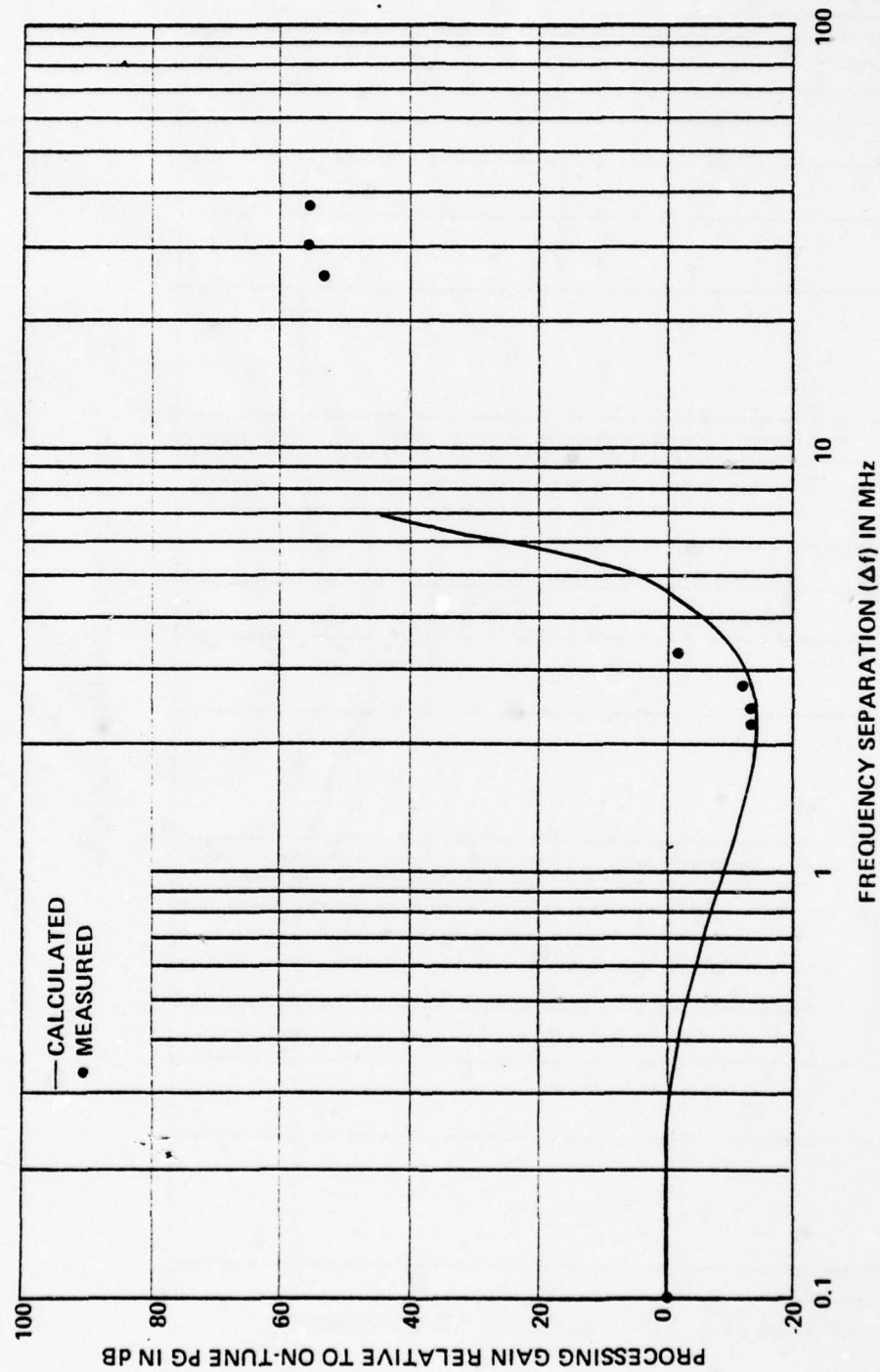


Figure 57. Off-frequency rejection to a 12-channel FDM/FM interfering signal; high test channel (2432-2436 kHz).

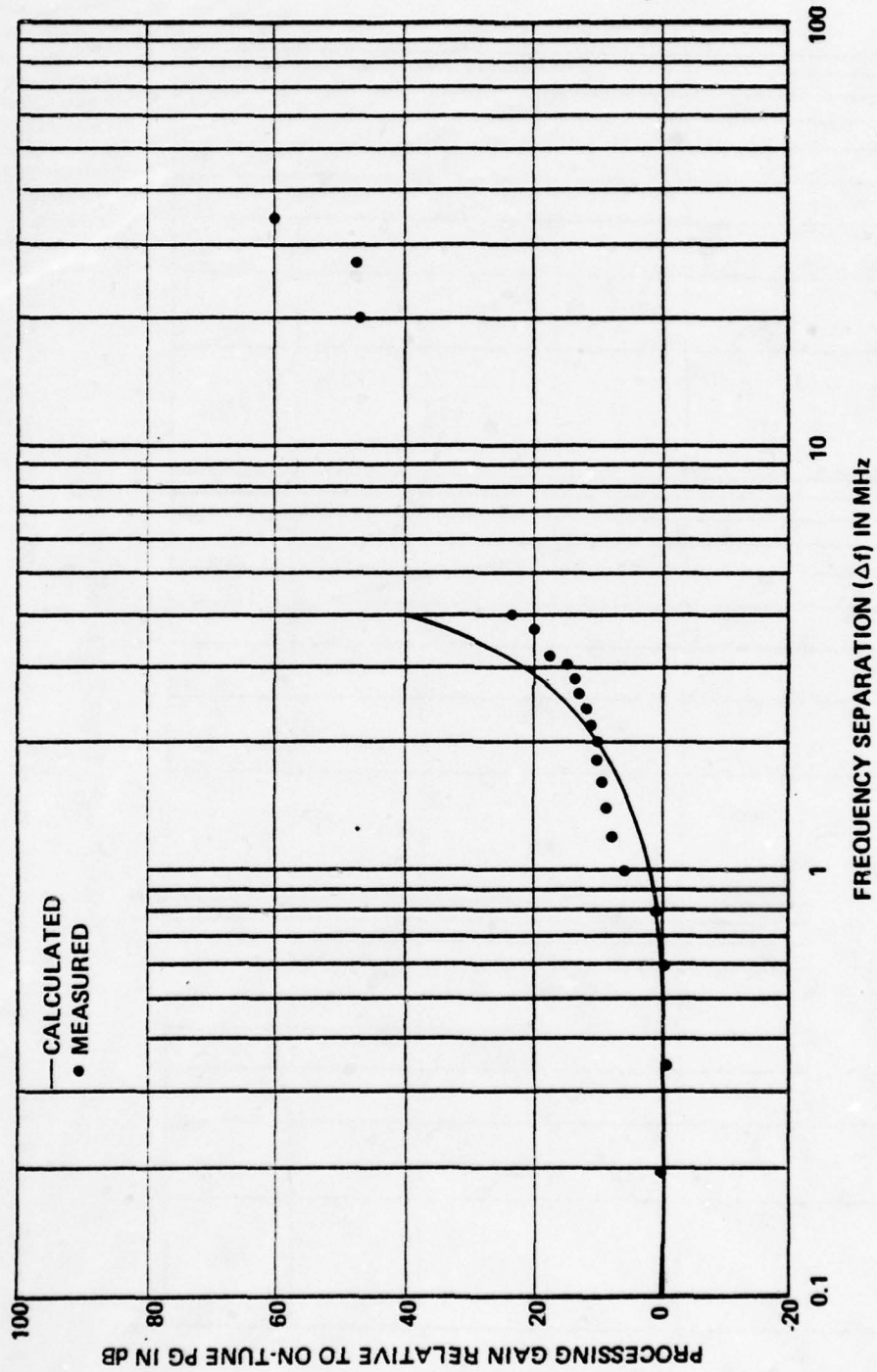


Figure 58. Off-frequency rejection to a CW interfering signal; low test channel (340-344 kHz).

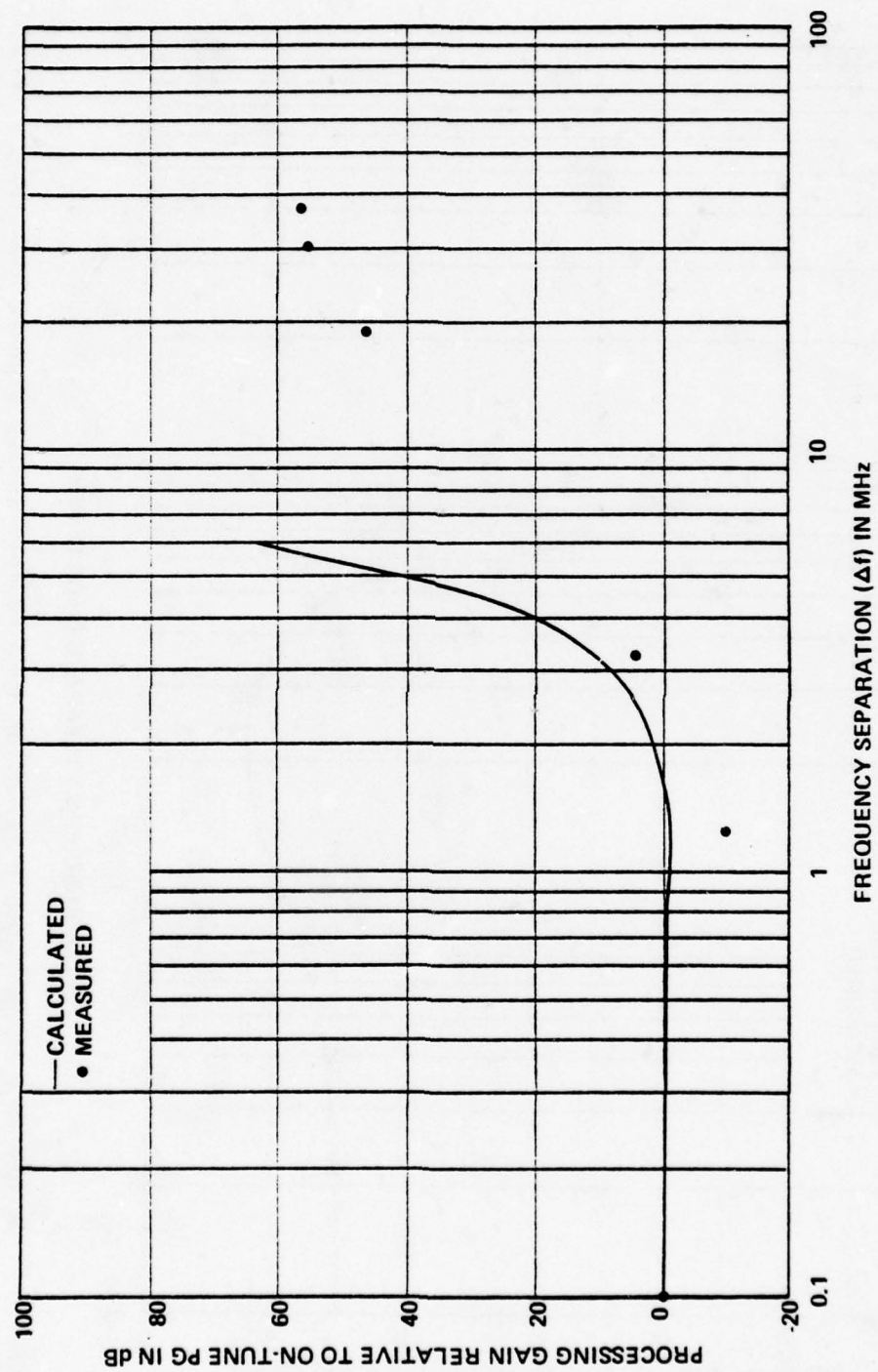


Figure 59. Off-frequency rejection to a CW interfering signal; middle test channel (1244-1248 kHz).

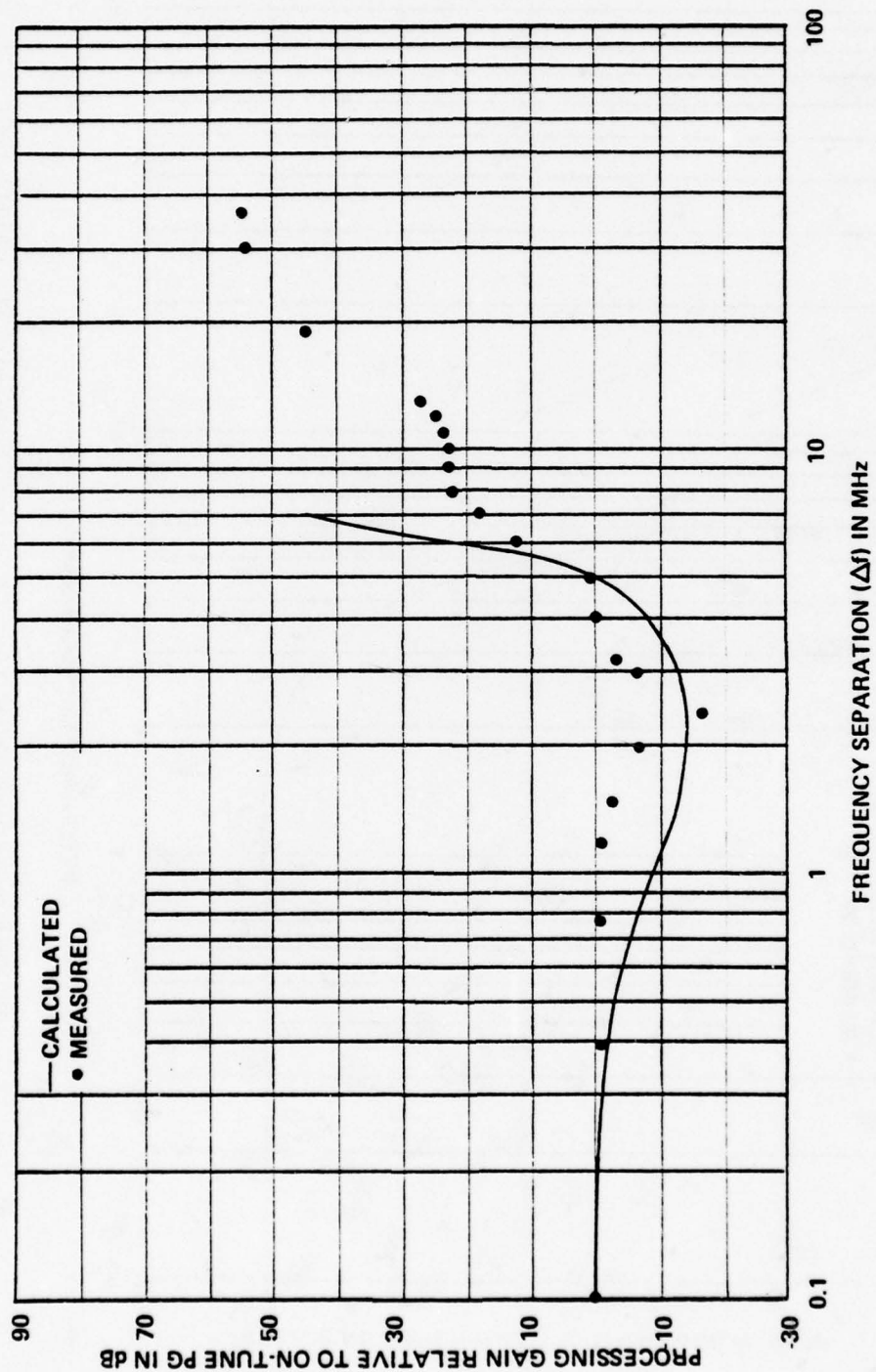


Figure 60. Off-frequency rejection to a CW interfering signal; high test channel (2432-2436 kHz).

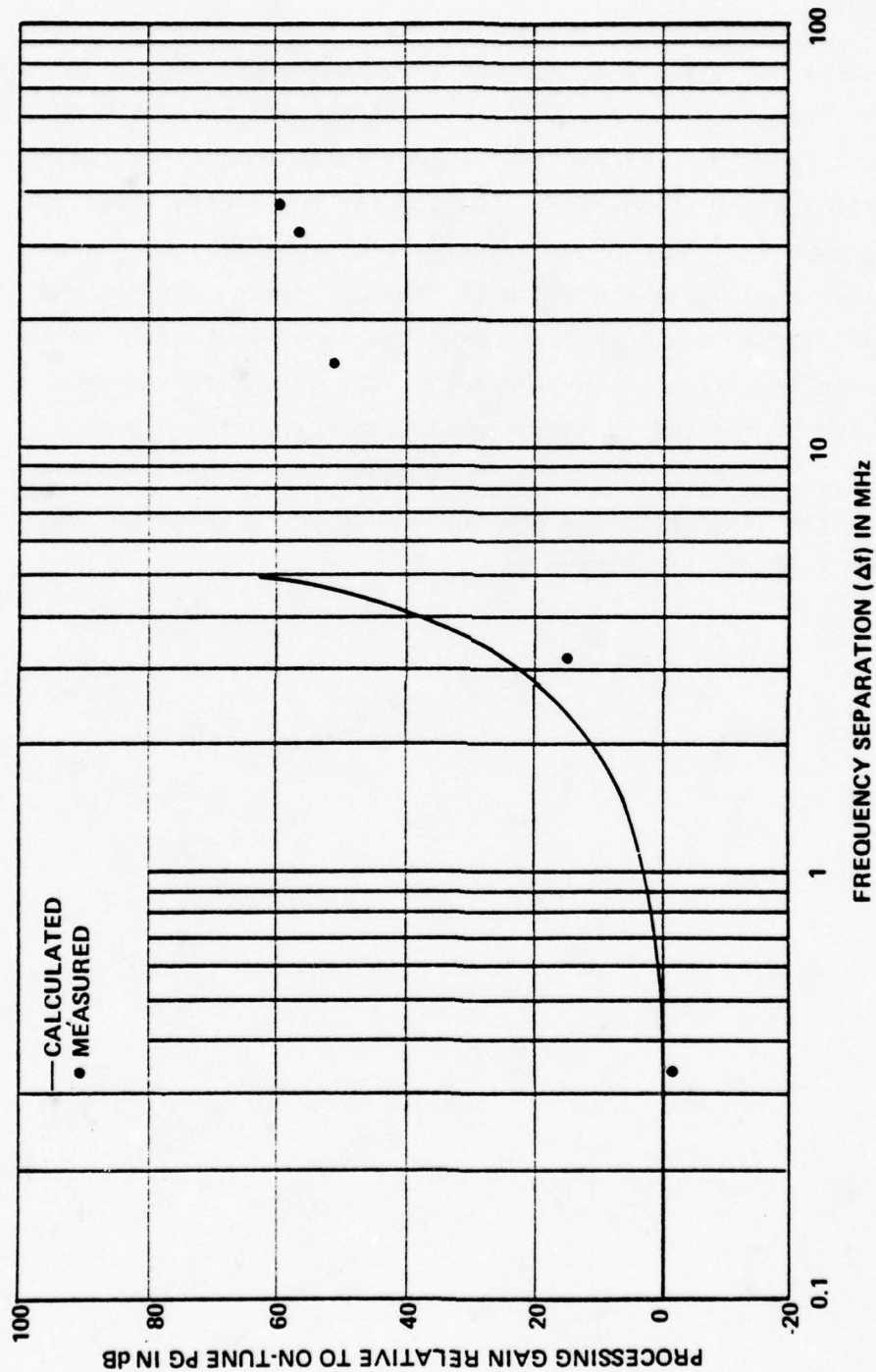


Figure 61. Off-frequency rejection to a single channel narrowband FM interfering signal; low test channel (340-344 kHz).

AFC Effects

A number of tests were made to investigate the effects of the Automatic Frequency Control (AFC) circuits on off-tuned FDM/FM, Narrowband FM (NBFM) and CW interference. The results of these tests were similar to the ones obtained for spot noise interference (Section 5). For IF output carrier-to-interference power ratios less than approximately 0 dB, the AFC action shifted the local oscillator frequency and caused the receiver to lock on to the interfering signal. The AFC action for CW interference is illustrated by the two IF output photographs shown in Figure 62. The $(C/I)_{\text{IF OUT}}$ level for these photographs was -2 dB. Photograph (a) was taken with the AFC turned off and photograph (b) was taken with the AFC turned on.

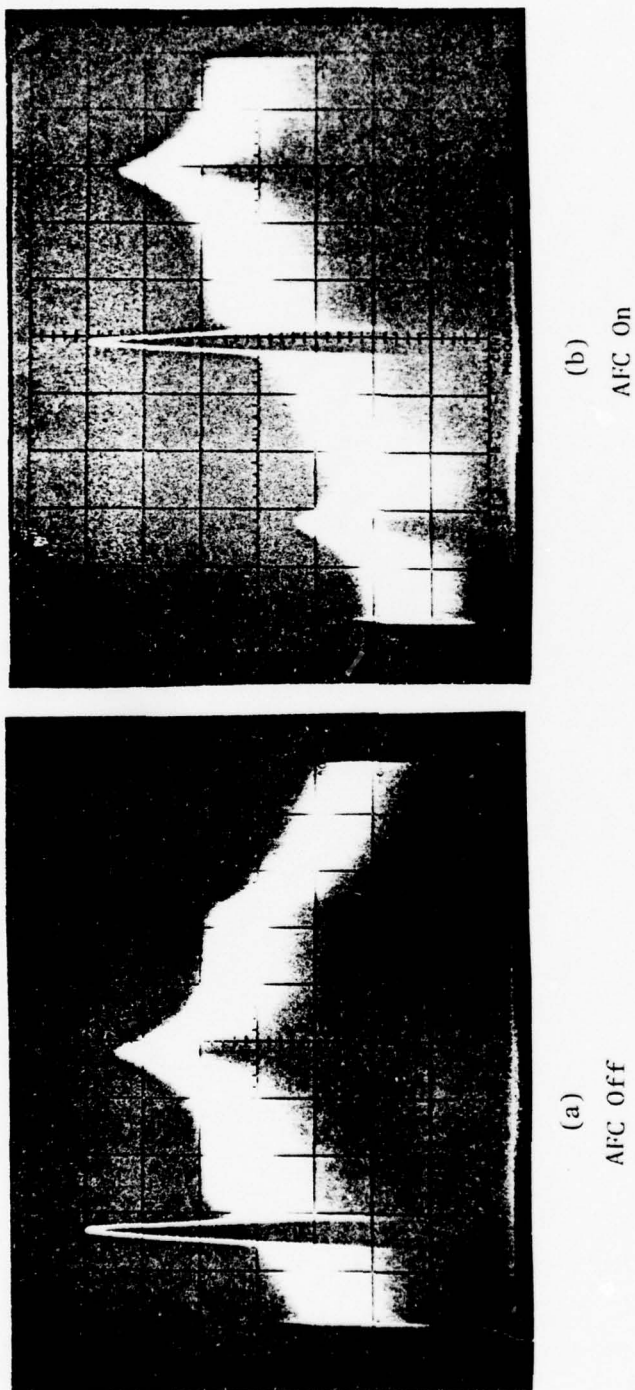


Figure 62. AFC effects for CW interference. Photographs (a) and (b) taken at IF auxiliary output; $(C/I)_{IF\ OUT} = -2\ dB$; spectrum analyzer bandwidth = 100 kHz; scanwidth = 1 MHz/division; center frequency = 70 kHz.

SECTION 7

PULSED RADAR INTERFERENCE

The degradation in FDM/FM communication systems when exposed to pulsed radar interference depends upon several factors, including: the radar modulation characteristics, the carrier-to-interference power ratio, the frequency separation between the desired and interfering carriers, and the FDM/FM modulation characteristics. The concept of two degradation regions of FDM/FM communication systems subjected to pulsed radar interference has been demonstrated^{32,33} and is based upon the desired carrier-to-peak radar pulse interference power ratio (C/\hat{I}).

In the quasi-linear degradation region, desired carrier power is generally larger than the peak radar power.^a The baseband interference noise spectrum is computed as proportional to the convolution of the desired carrier spectrum and the radar interference RF spectrum. In any given channel, degradation decreases with increasing C/\hat{I} .

In the quasi-constant degradation region, the peak radar pulse power is always greater than the desired carrier power. During the interference pulse, demodulation of the desired

³²Wachs, M. R., and Arroyo, B., *Technical Consideration of Frequency Sharing Between Satellite Communications and Radar*, International Conference on Communications (ICC '78), IEEE, 1978.

³³Hernandez, A. A., *Effects of Pulse Interference on FDM/FM Multichannel Telephony Transmissions of the Fixed Satellite Service*, ECAC-CR-78-075, ECAC, Annapolis, MD, August 1978.

^aThis is generally the case for on-tune pulse interference. However, as indicated in Reference 33, for off-tuned interference the quasi-linear region can extend into negative power ratios of C/\hat{I} .

carrier ceases and the radar captures the demodulator. Consequently, further increases in radar power do not increase base-band noise.

MEASUREMENT DESCRIPTION AND RESULTS

Measured data obtained during the FDM/FM measurement program were used to investigate the manner in which pulse radar interference affects the performance of an FDM/FM multichannel telephony system. The telephony signal was the 600-channel carrier previously discussed in Section 2. The interference signal was represented by a pulse train with variable pulsewidth (1-1000 μ s), variable repetition frequency (10-15,000 pps), variable frequency relative to the tuned frequency of the telephony system (Δf), variable frequency shift during the "ON" time of the pulse (chirping), and variable power relative to that of the telephony signal. The rise and fall times of the interference pulses were approximately 0.025 microseconds. The desired and interference signals were added ahead of the waveguide circulator (RF input) of the telephony receiver. The noise performance of the telephony system was measured at the output of a low (340-344 kHz), middle (1234-1238 kHz), and high (2432-2436 kHz) multiplexer channel.

The results of the channel output noise measurements, for on-tune and off-tuned pulse interference conditions, are shown in Figures 63 through 87 and 88 through 96, respectively. From these measurements the following conclusions can be drawn:

1. For on-tune pulse interference, the envelope of the maximum observed interference in a voice channel of an FDM/FM telephony carrier is a function of the carrier-to-average pulse interference power, C/I , and of the duty cycle, δ , where I is the average power of the pulsed interference in the desired-signal necessary predetection bandwidth.

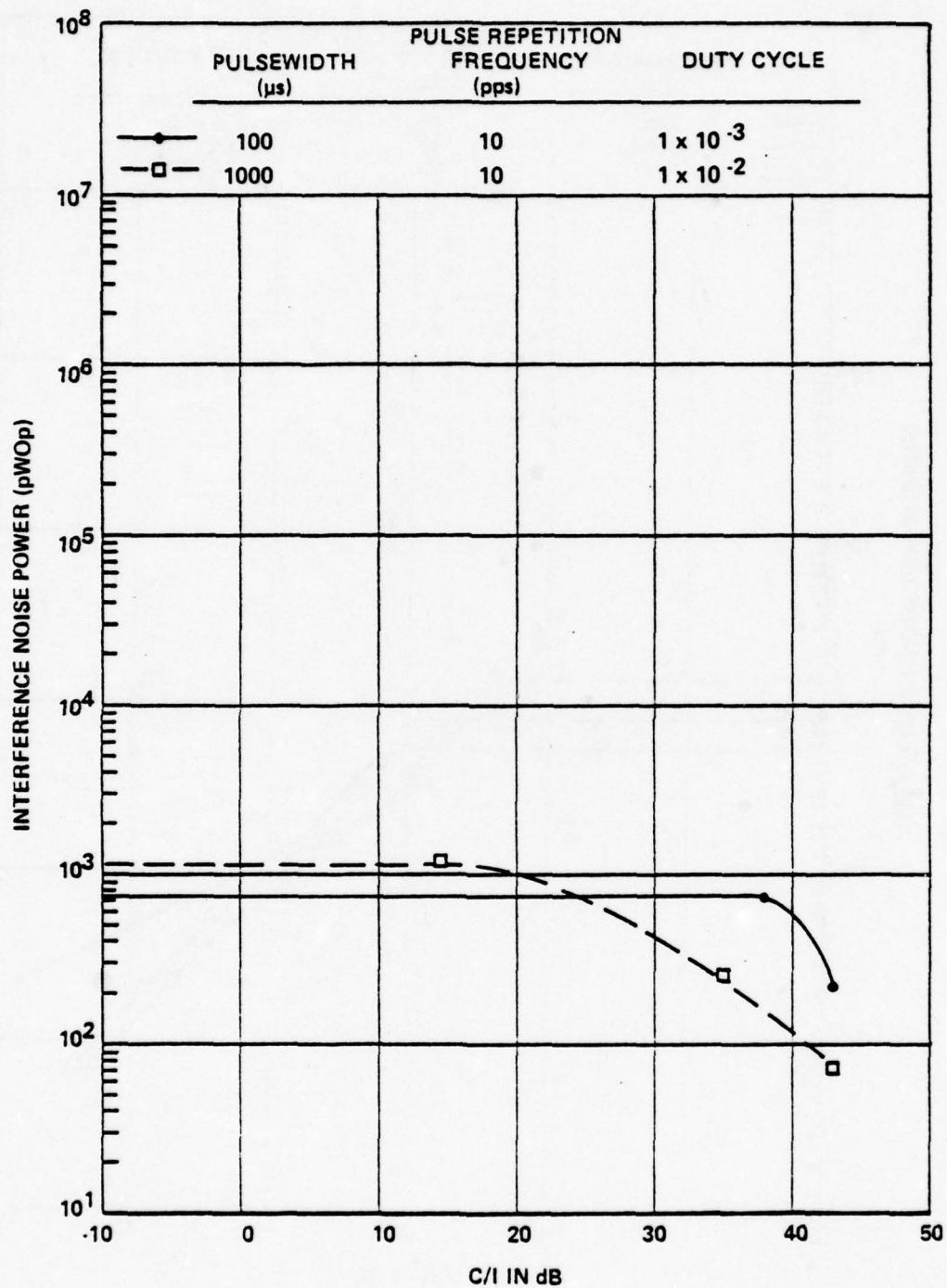


Figure 63. Measured interference noise power in a low baseband channel (340-344 kHz) for cochannel, nonchirped, pulse interference; PRF = 10 pps.

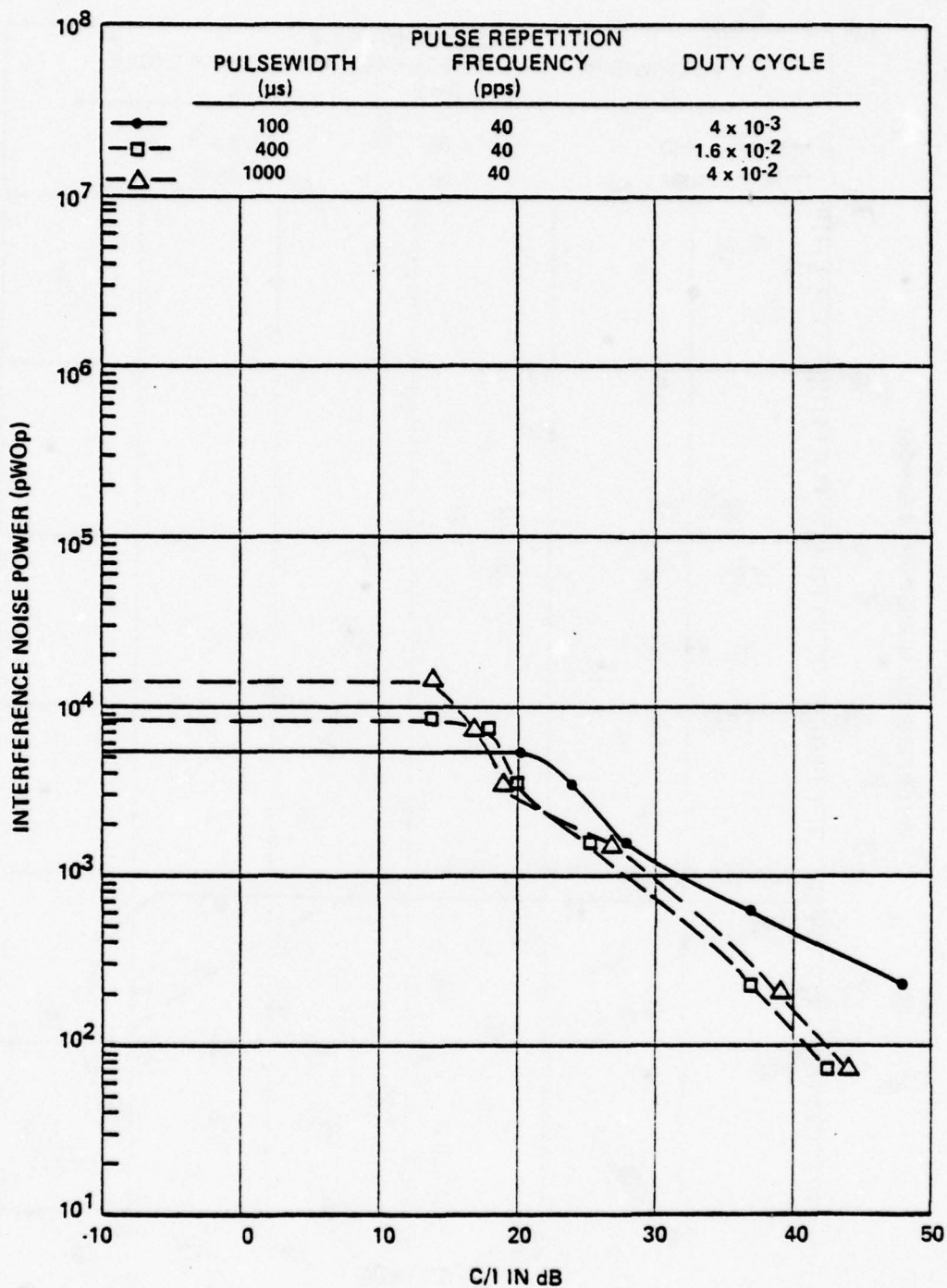


Figure 64. Measured interference noise power in a low baseband channel (340-344 kHz) for cochannel, nonchirped, pulse interference; PRF = 40 pps.

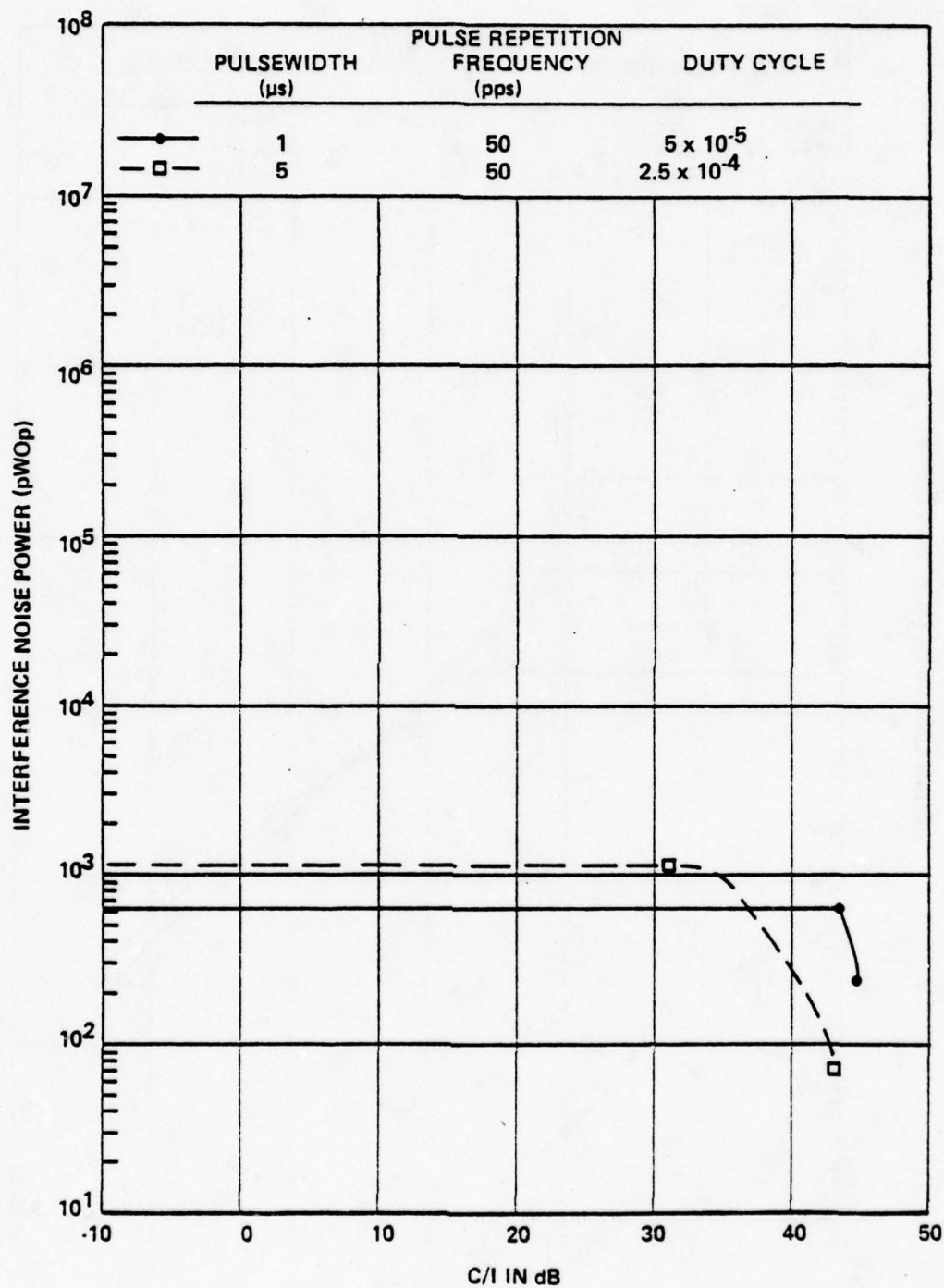


Figure 65. Measured interference noise power in a low baseband channel (340-344 kHz) for cochannel, nonchirped, pulse interference; PRF = 50 pps.

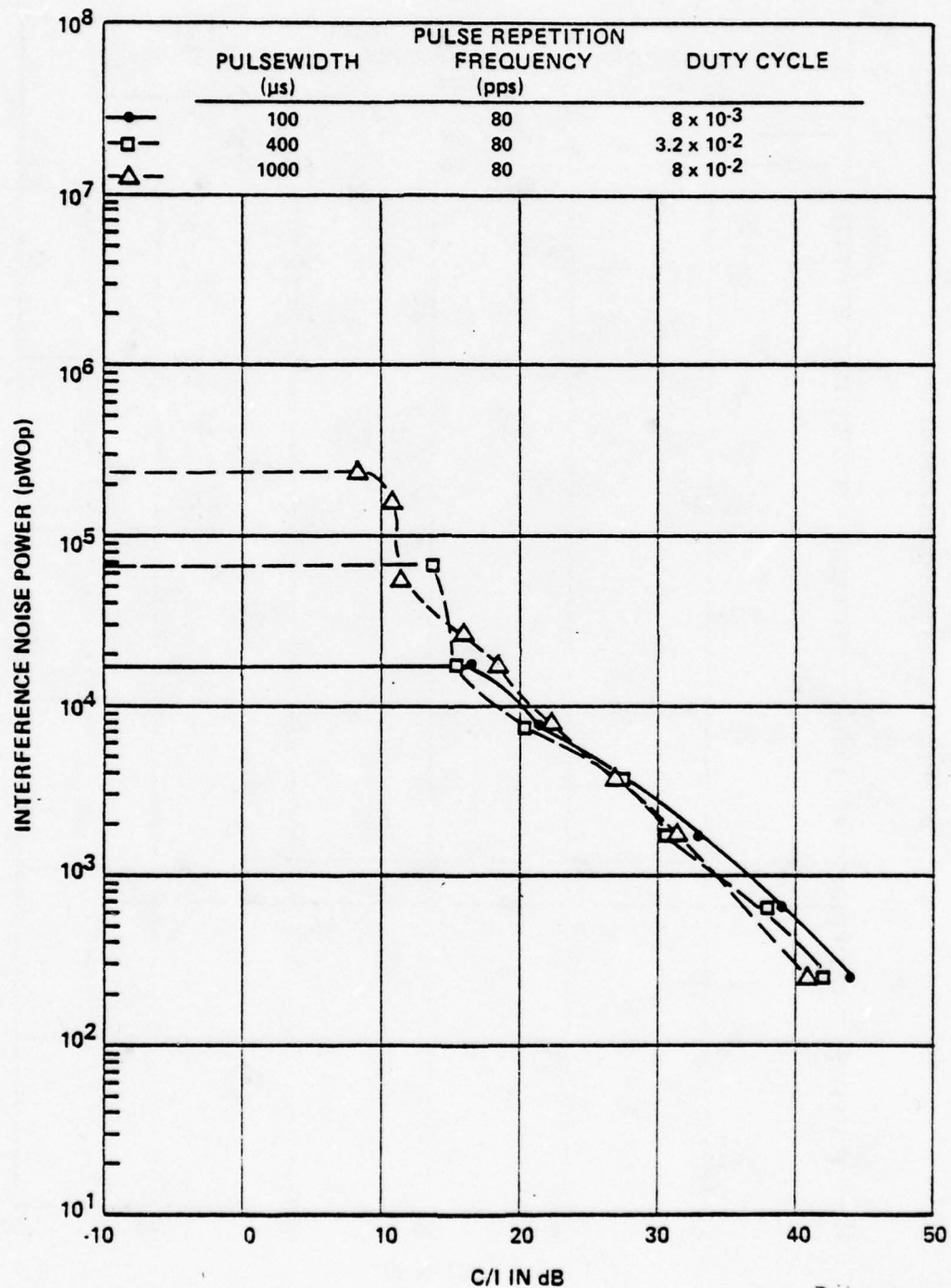


Figure 66. Measured interference noise power in a low baseband channel (340-344 kHz) for cochannel, nonchirped, pulse interference; PRF = 80 pps.

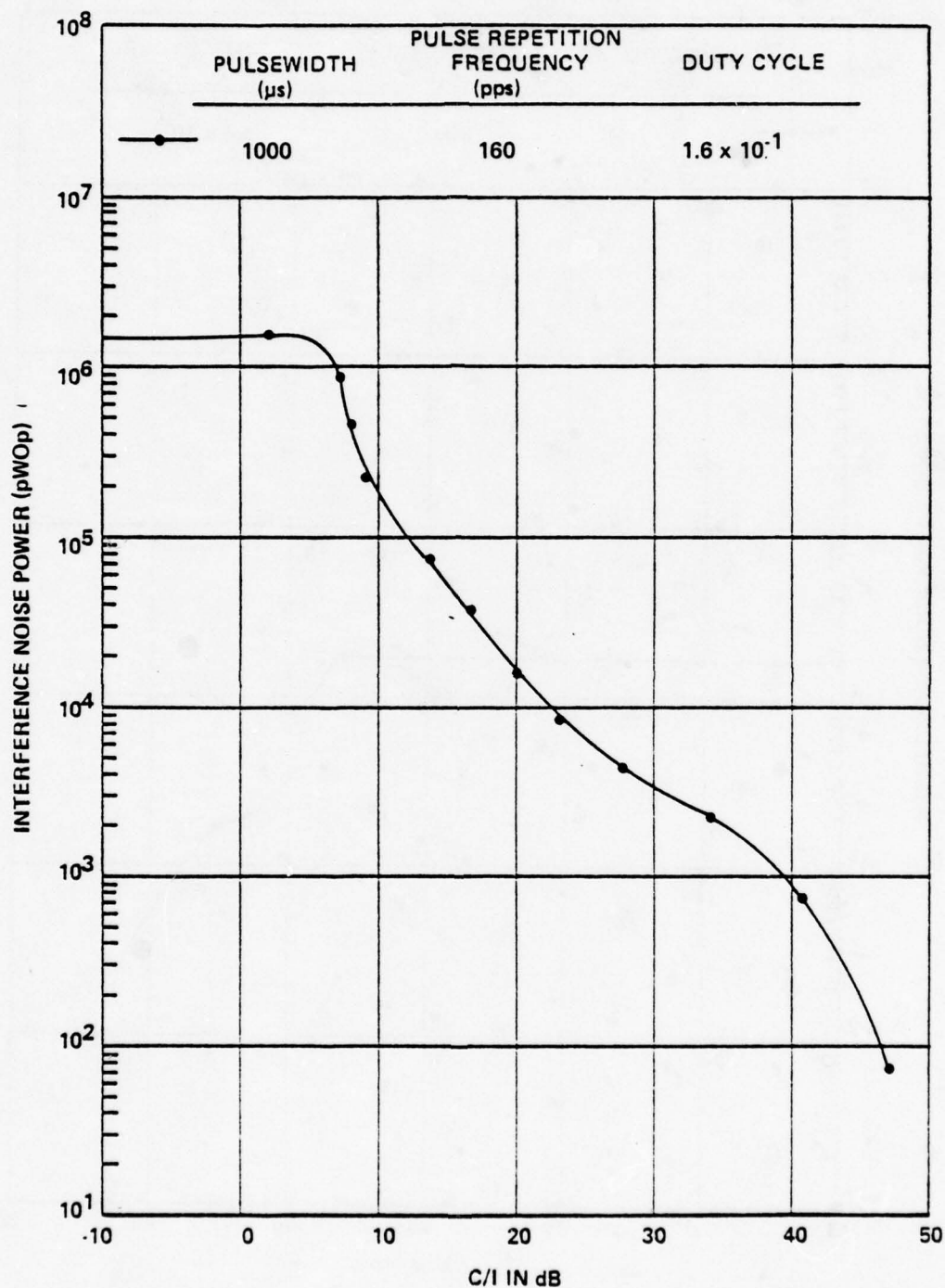


Figure 67. Measured interference noise power in a low baseband channel (340-344 kHz) for cochannel, nonchirped, pulse interference; PRF = 160 pps.

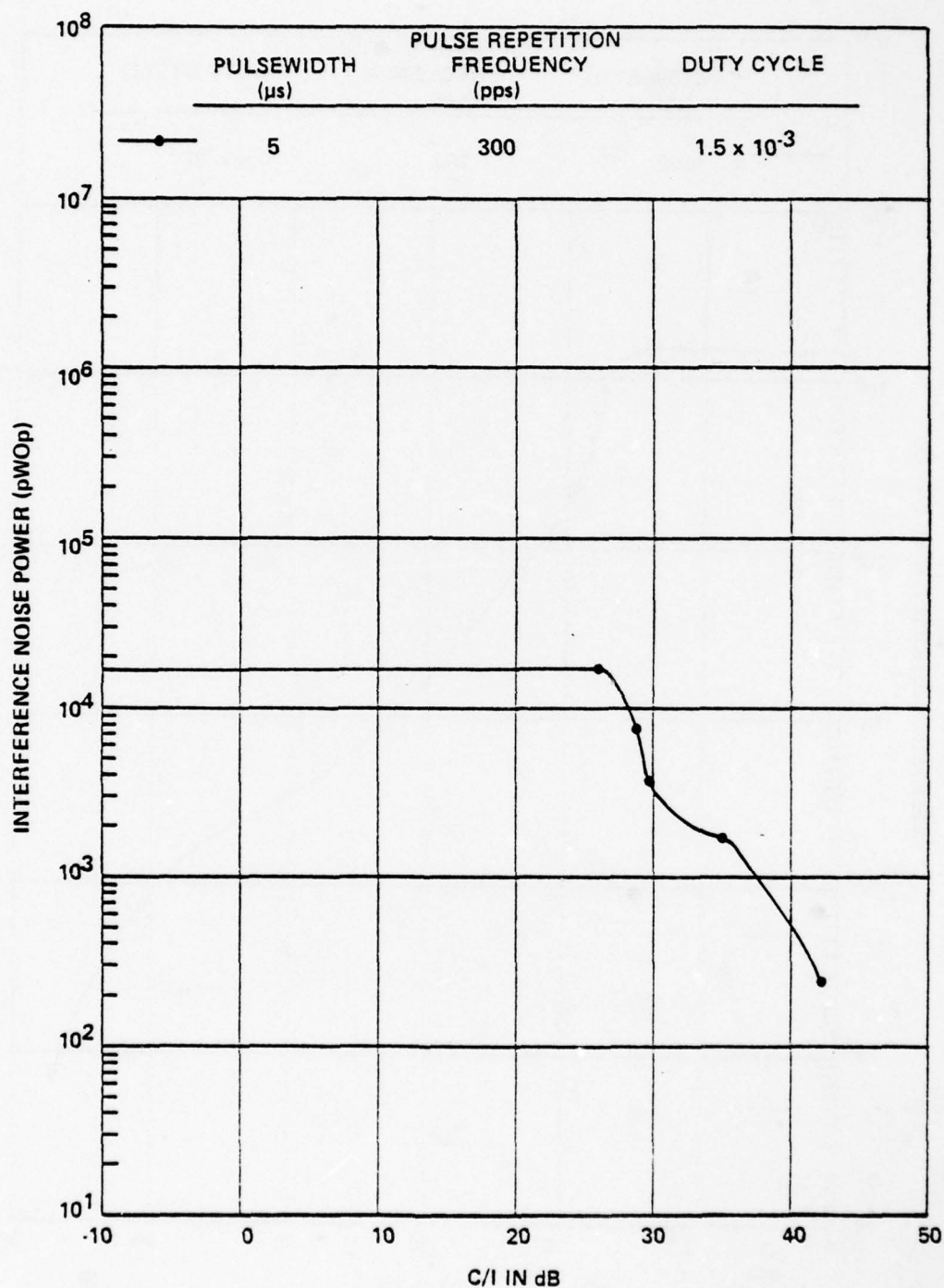


Figure 68. Measured interference noise power in a low baseband channel (340-344 kHz) for cochannel, nonchirped, pulse interference; PRF = 300 pps.

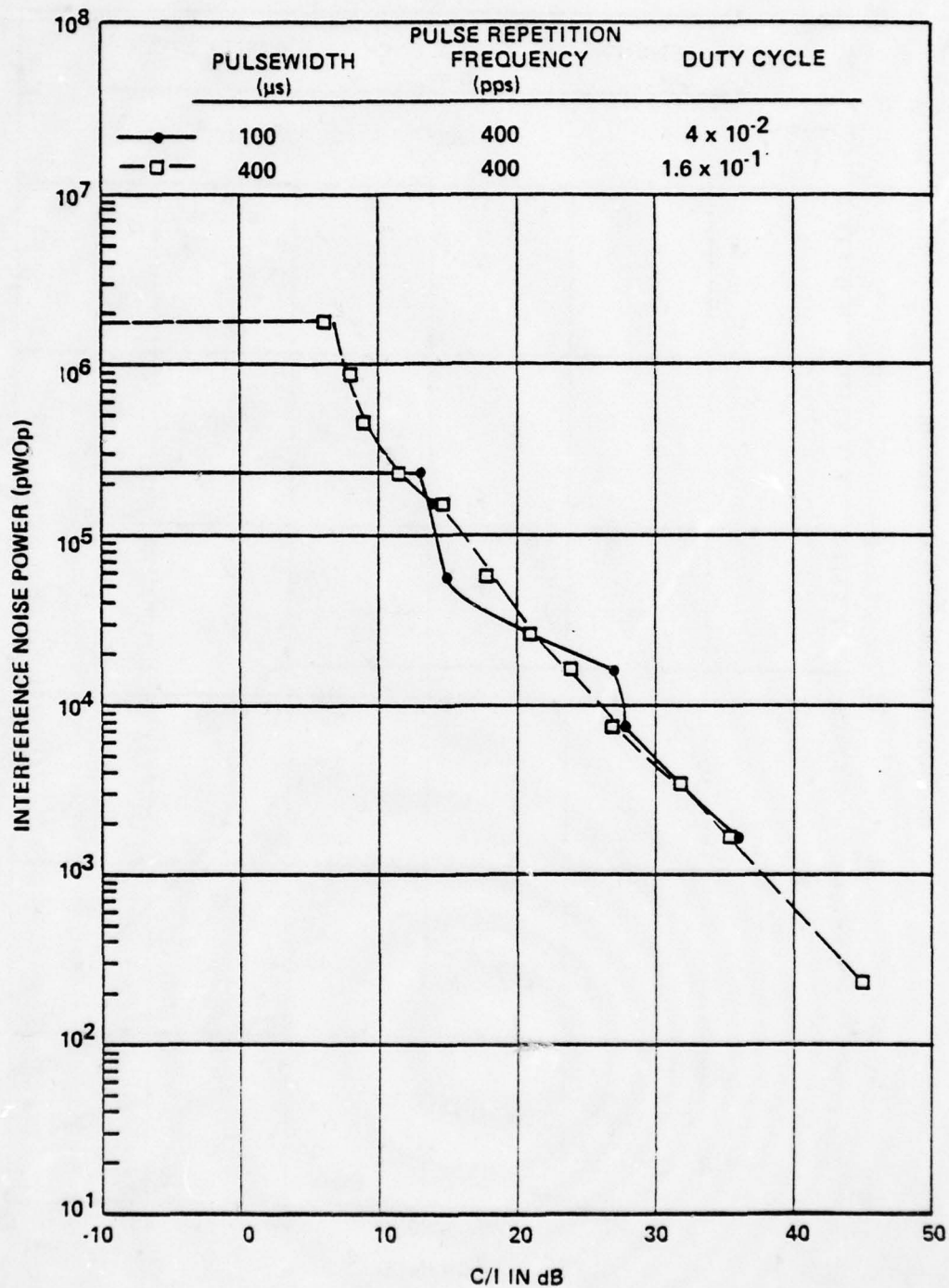


Figure 69. Measured interference noise power in a low baseband channel (340-344 kHz) for cochannel, nonchirped, pulse interference; PRF = 400 pps.

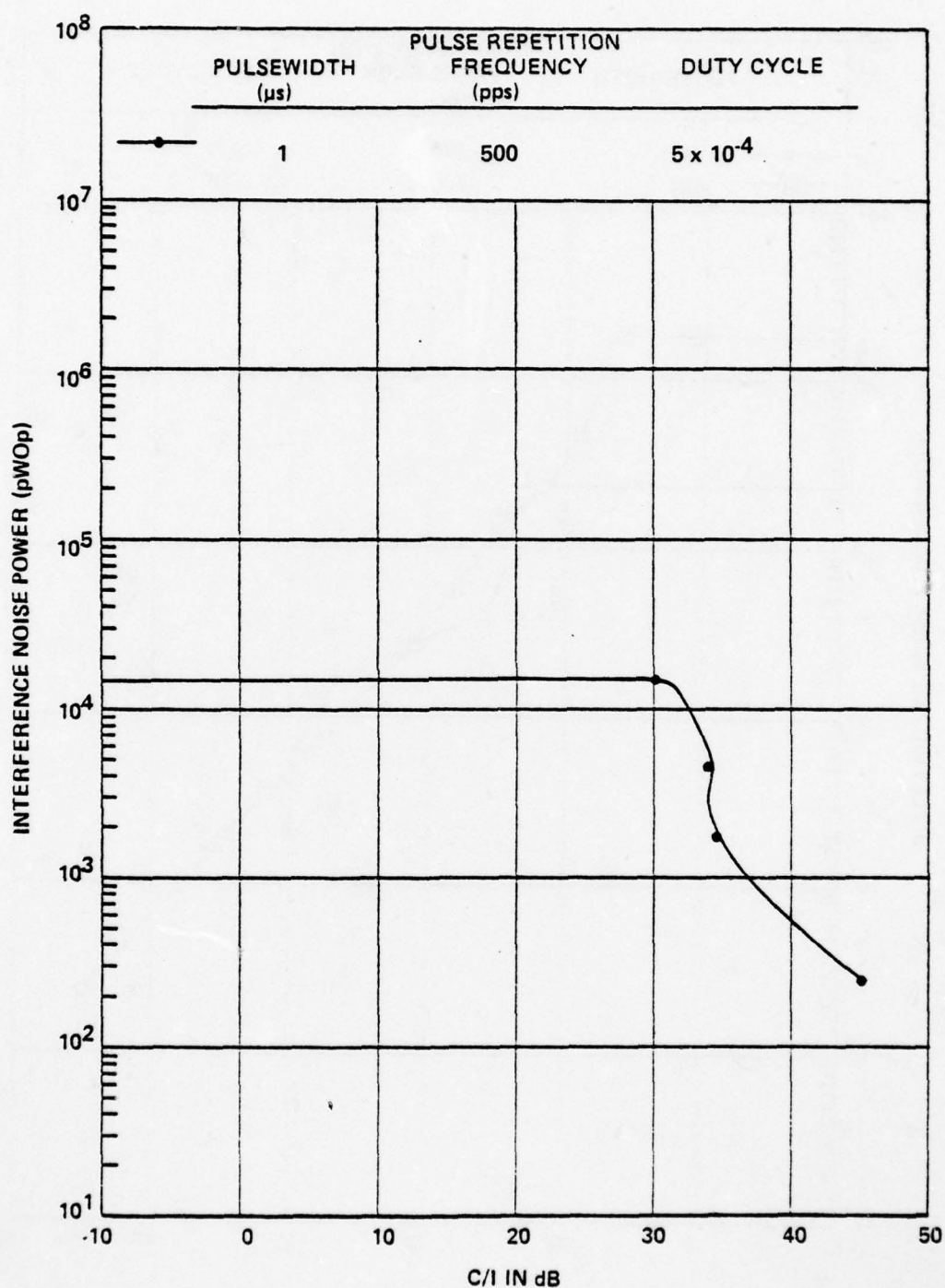


Figure 70. Measured interference noise power in a low baseband channel (340-344 kHz) for cochannel, nonchirped, pulse interference; PRF = 500 pps.

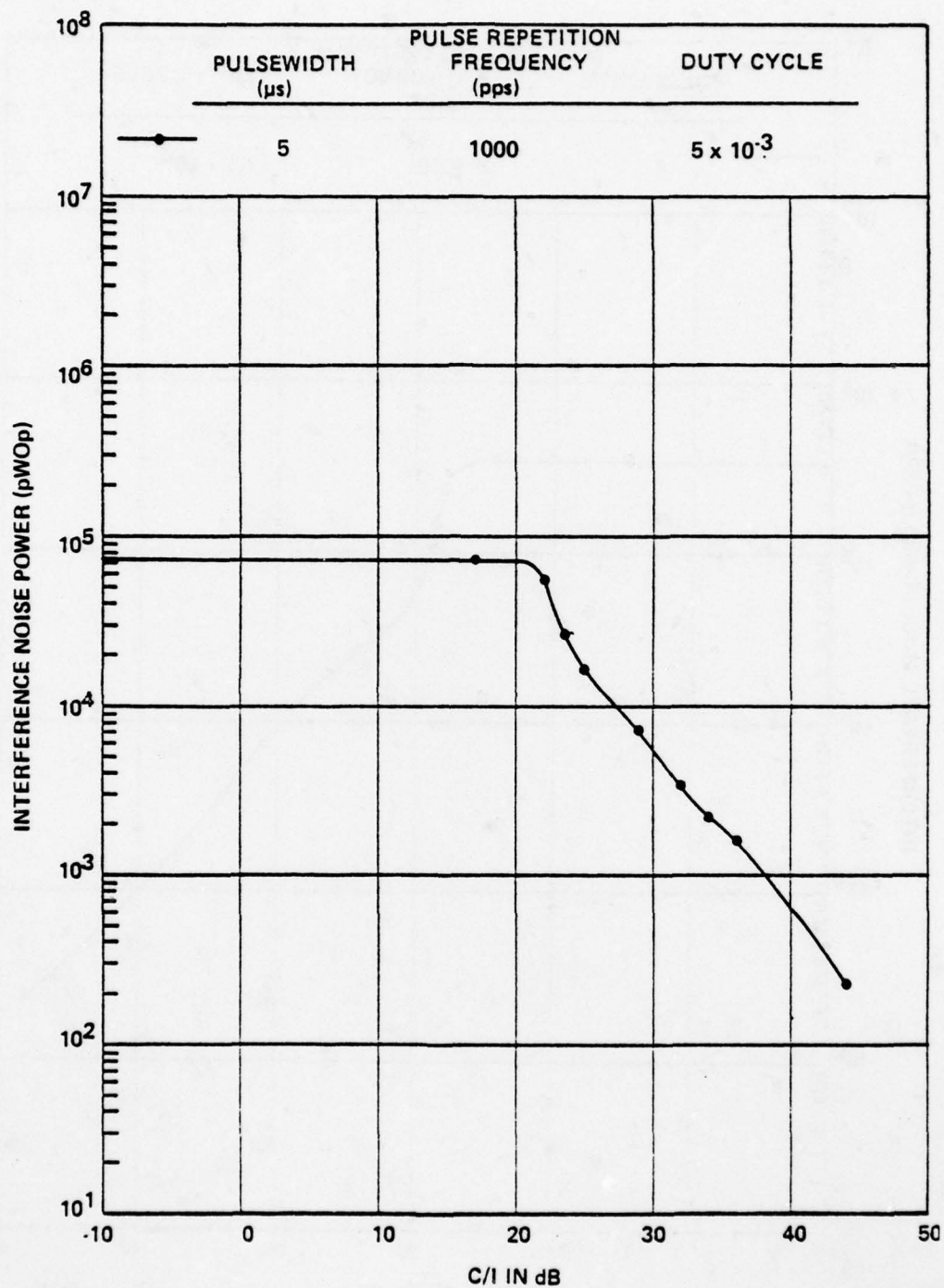


Figure 71. Measured interference noise power in a low baseband channel (340-344 kHz) for cochannel, nonchirped, pulse interference; PRF = 1000 pps.

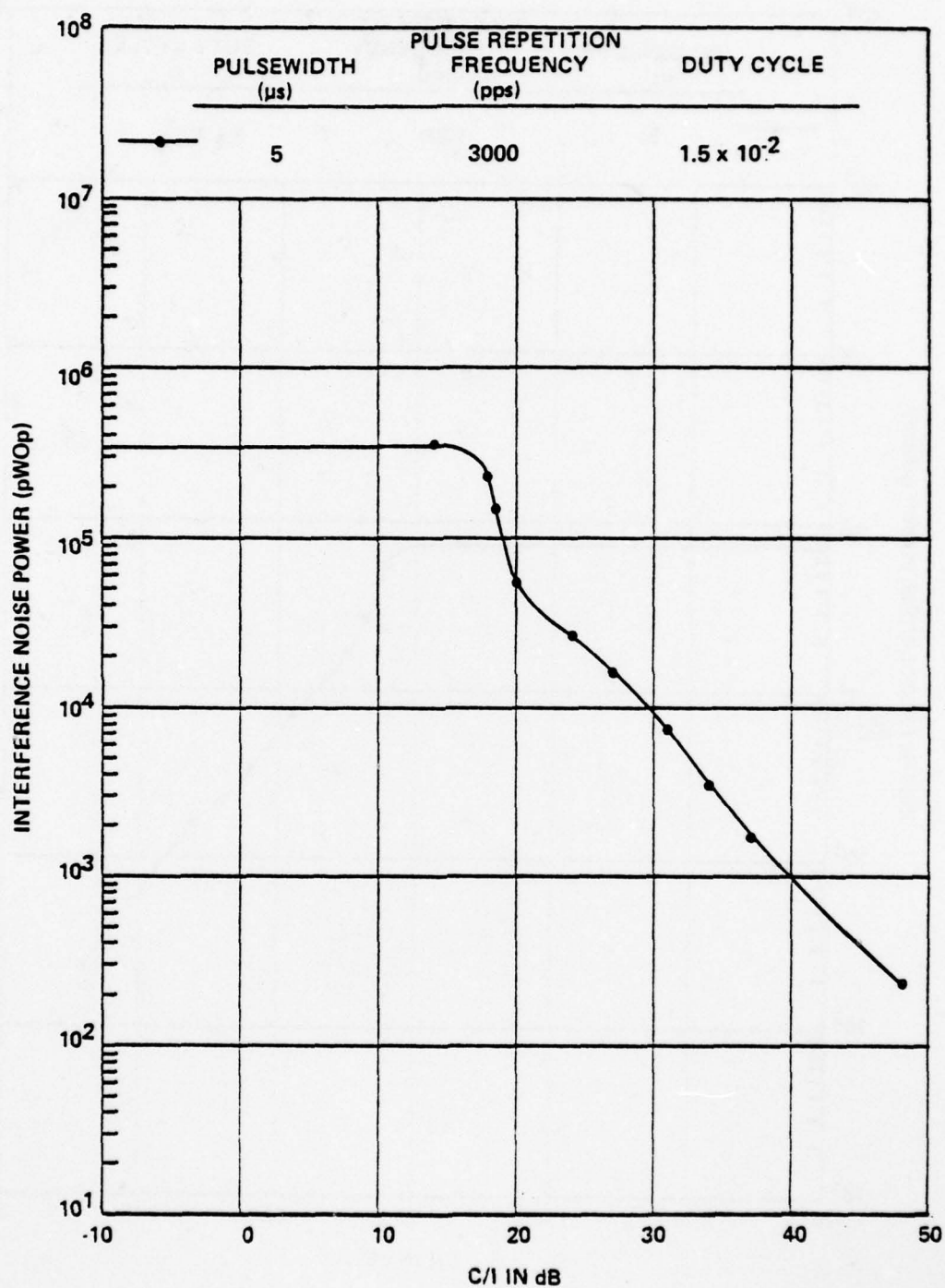


Figure 72. Measured interference noise power in a low baseband channel (340-344 kHz) for cochannel, nonchirped, pulse interference; PRF = 3000 pps.

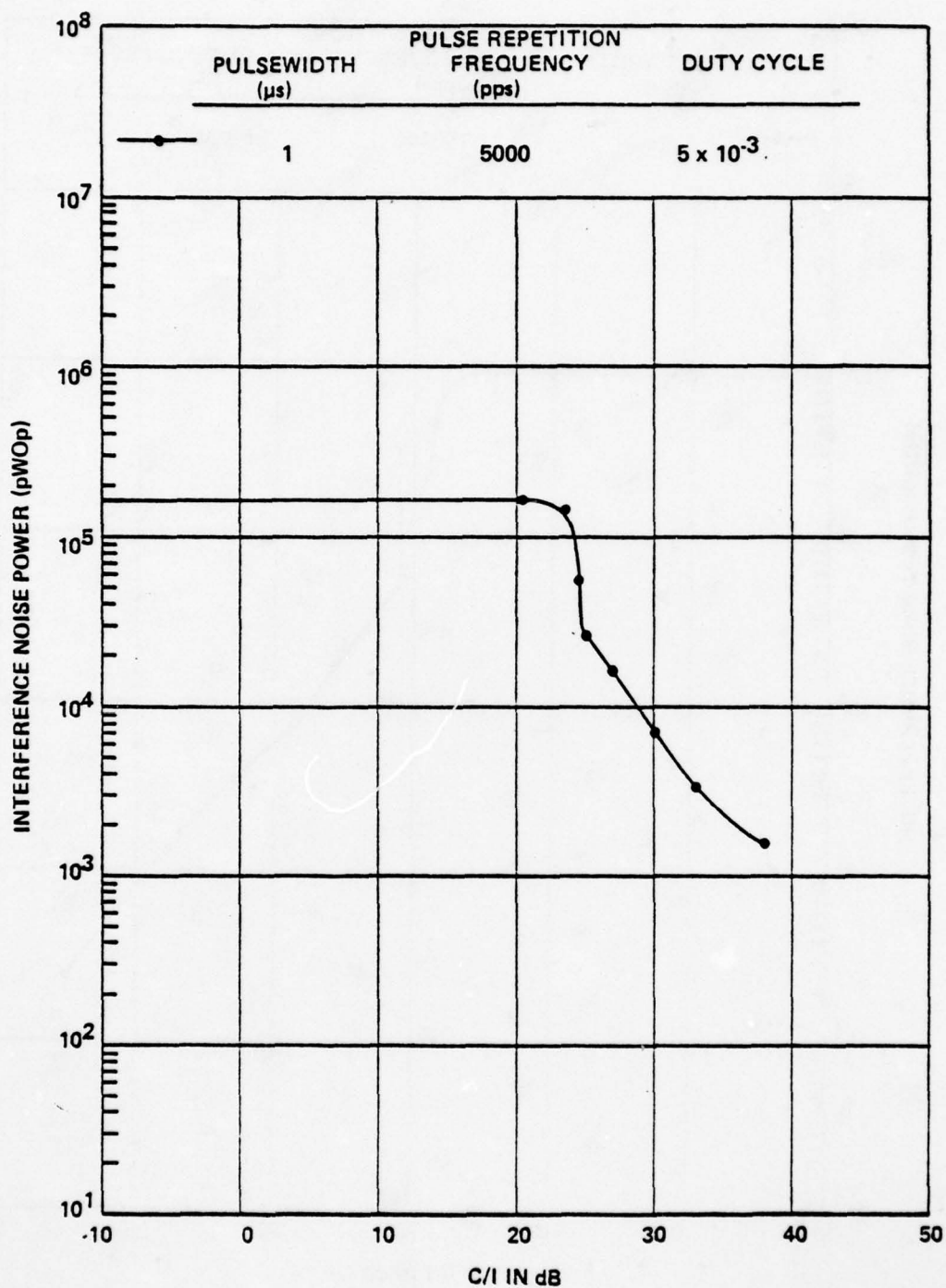


Figure 73. Measured interference noise power in a low baseband channel (340-344 kHz) for cochannel, nonchirped, pulse interference; PRF = 5000 pps.

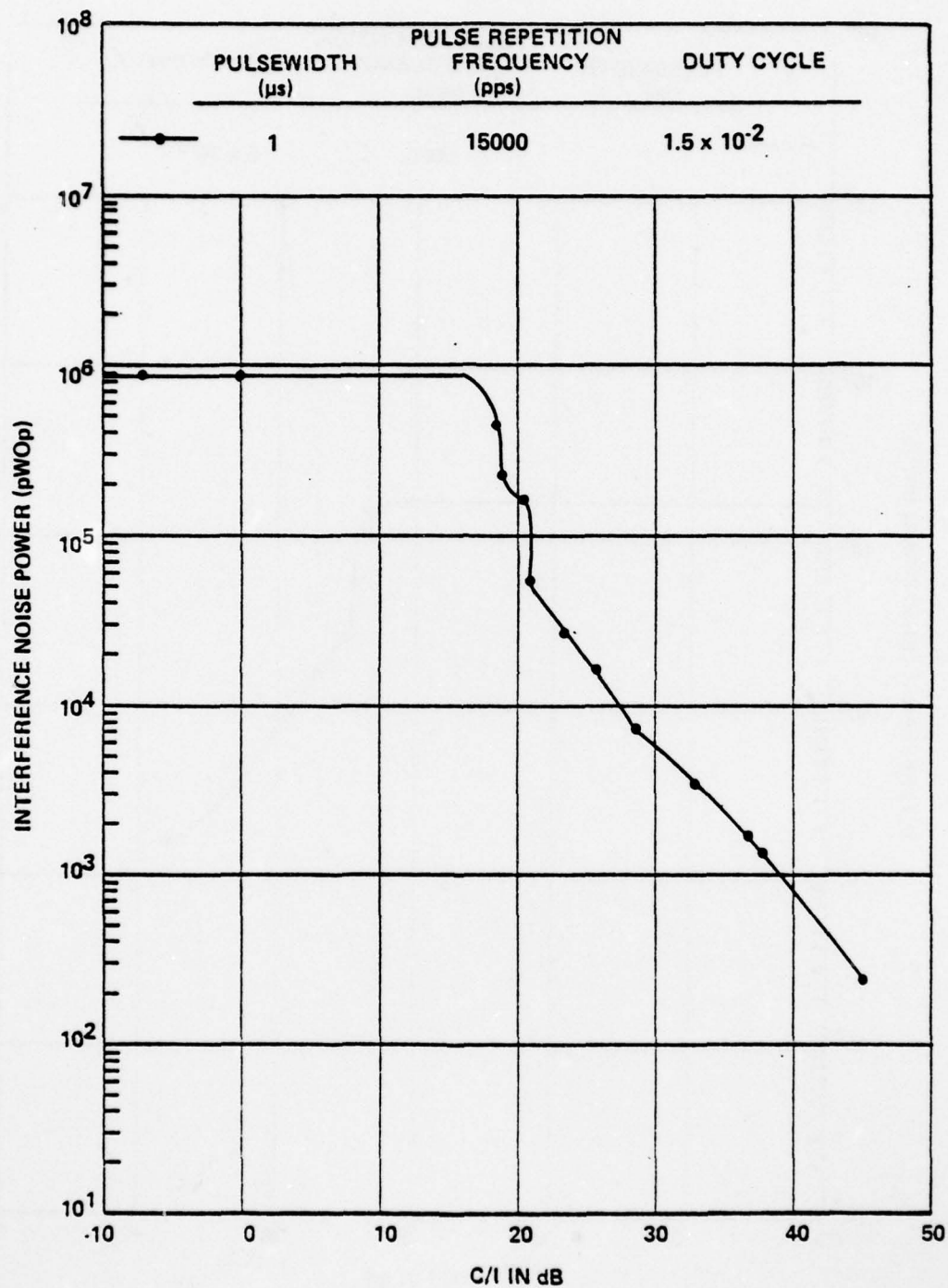


Figure 74. Measured interference noise power in a low baseband channel (340-344 kHz) for cochannel, nonchirped, pulse interference; PRF = 15,000 pps.

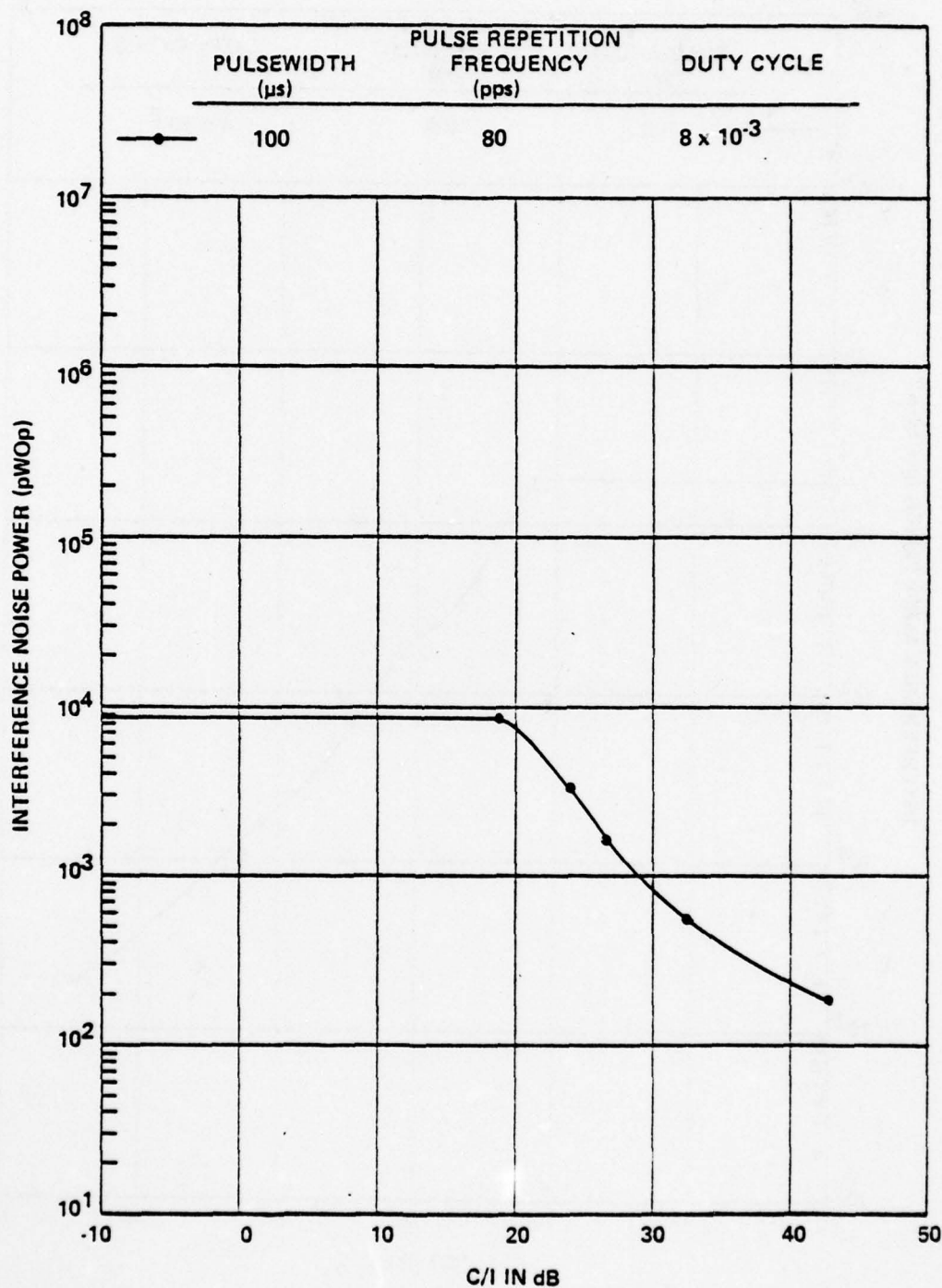


Figure 75. Measured interference noise power in a middle base-band channel (1244-1248 kHz) for cochannel, non-chirped, pulse interference; PRF = 80 pps.

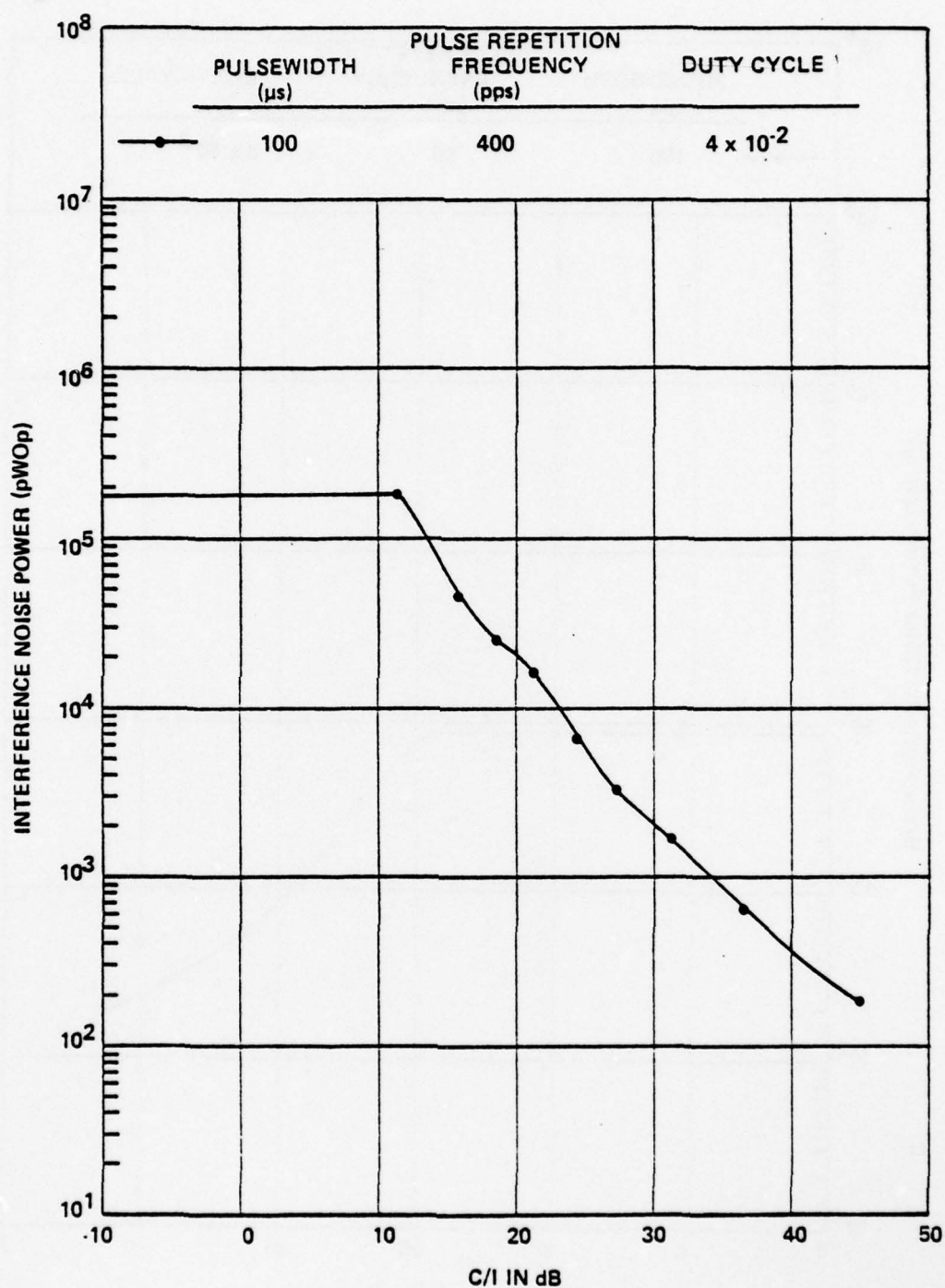


Figure 76. Measured interference noise power in a middle base-band channel (1244-1248 kHz) for cochannel, non-chirped, pulse interference; PRF = 400 pps.

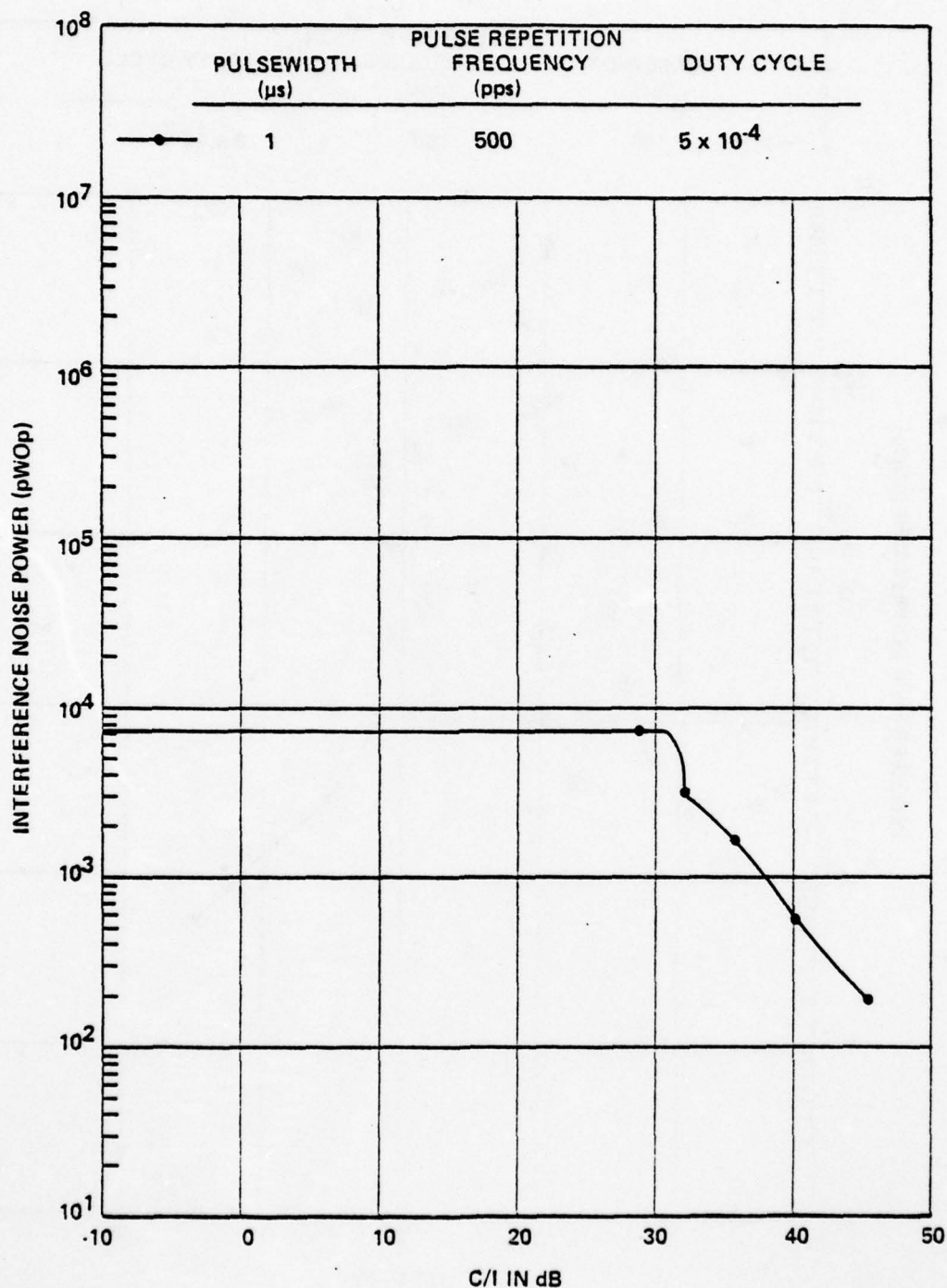


Figure 77. Measured interference noise power in a middle base-band channel (1244-1248 kHz) for cochannel, non-chirped, pulse interference; PRF = 500 pps.

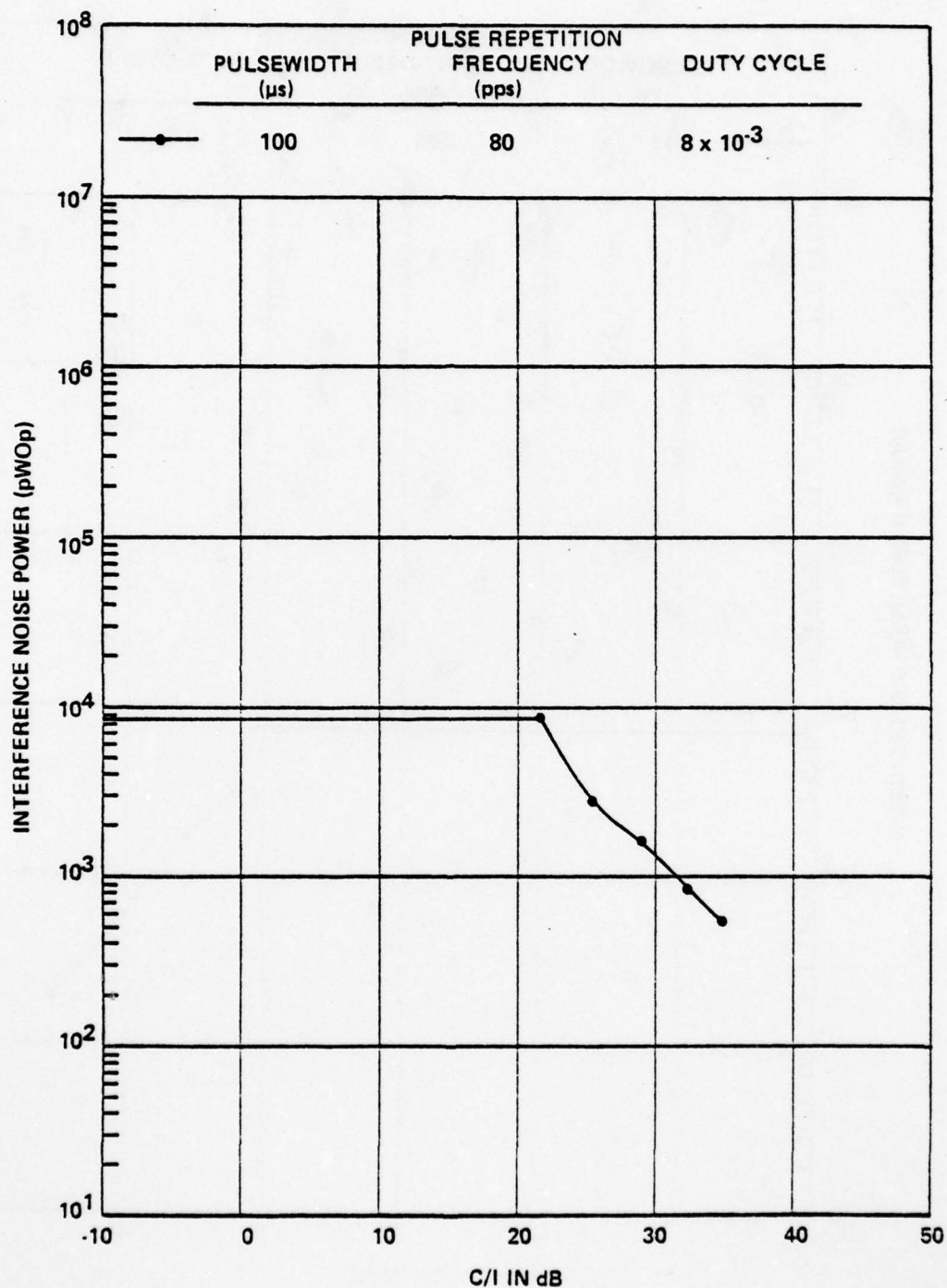


Figure 78. Measured interference noise power in a high baseband channel (2432-2436 kHz) for cochannel, nonchirped, pulse interference; PRF = 80 pps.

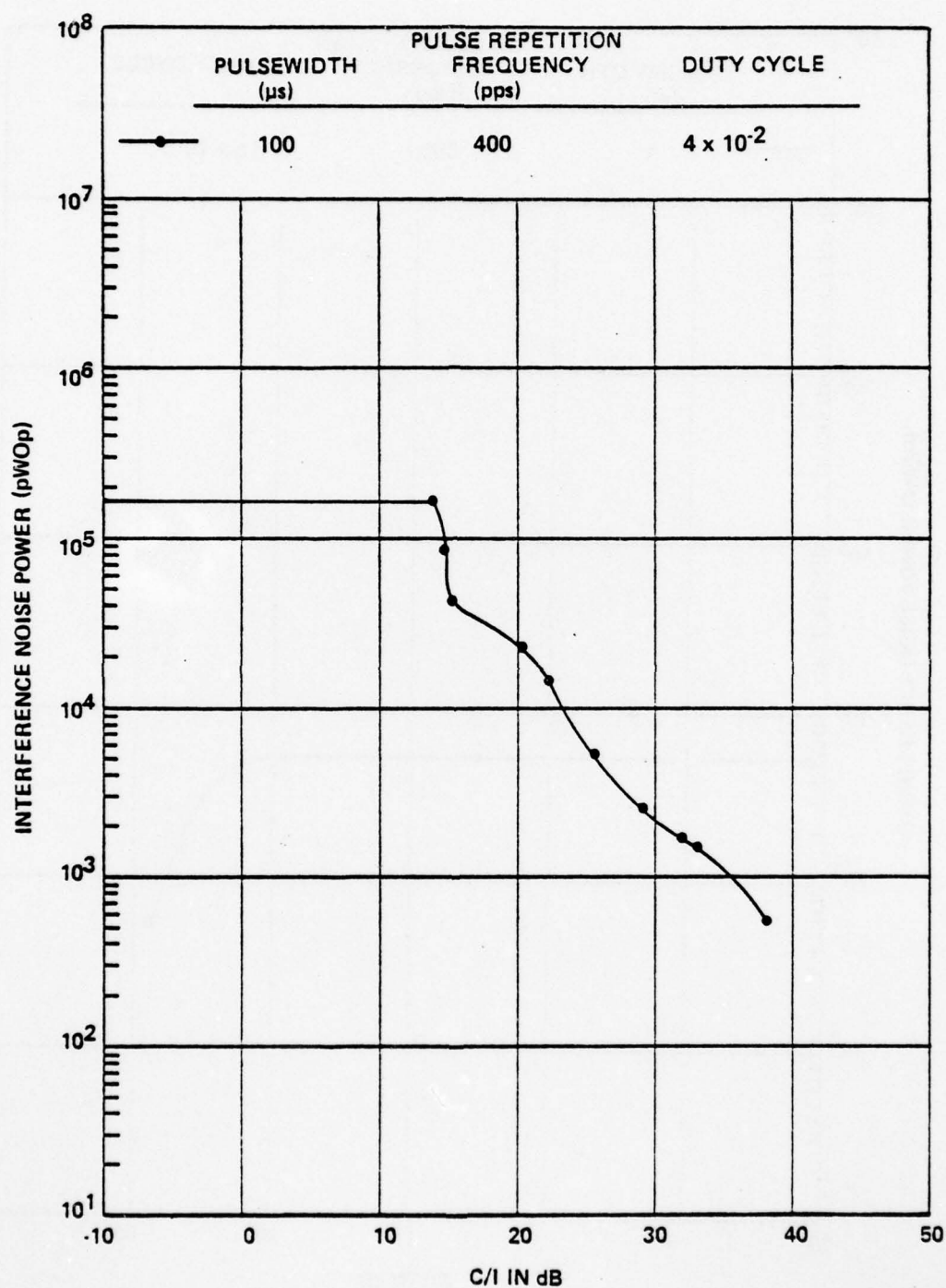


Figure 79. Measured interference noise power in a high baseband channel (2432-2436 kHz) for cochannel, nonchirped, pulse interference; PRF = 400 pps.

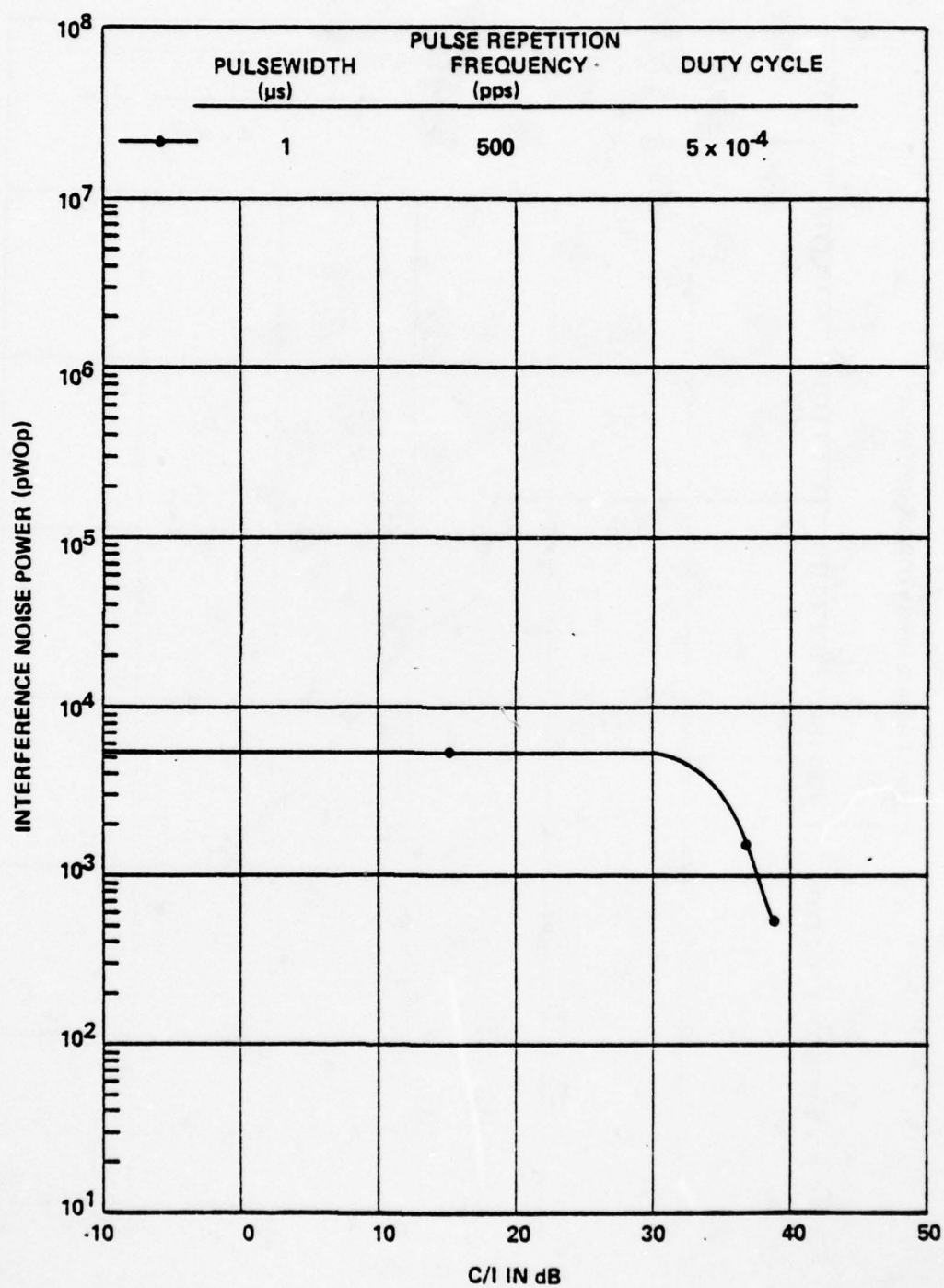


Figure 80. Measured interference noise power in a high baseband channel (2432-2436 kHz) for cochannel, nonchirped, pulse interference; PRF = 500 pps.

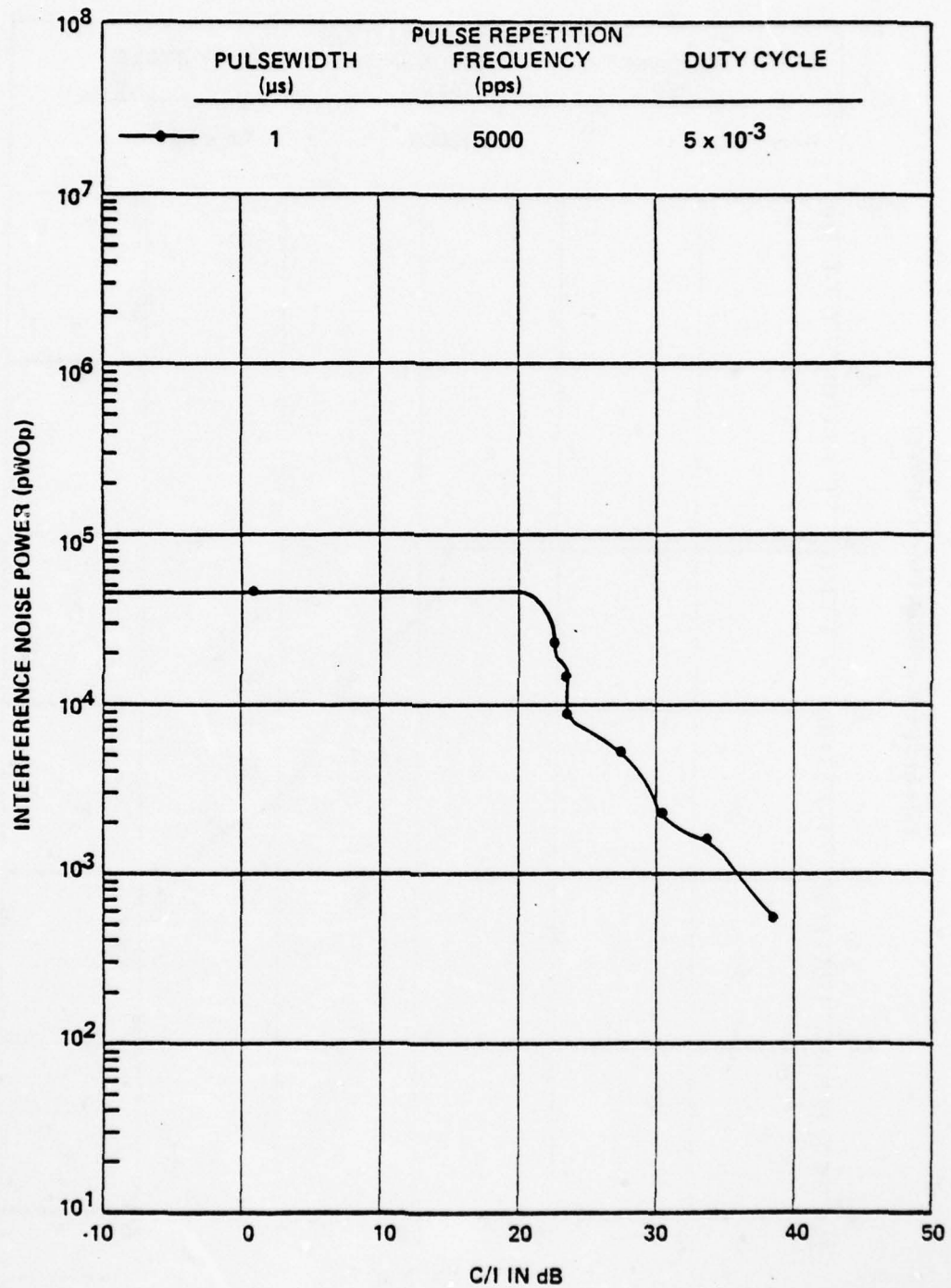


Figure 81. Measured interference noise power in a high baseband channel (2432-2436 kHz) for cochannel, nonchirped, pulse interference; PRF = 5000 pps.

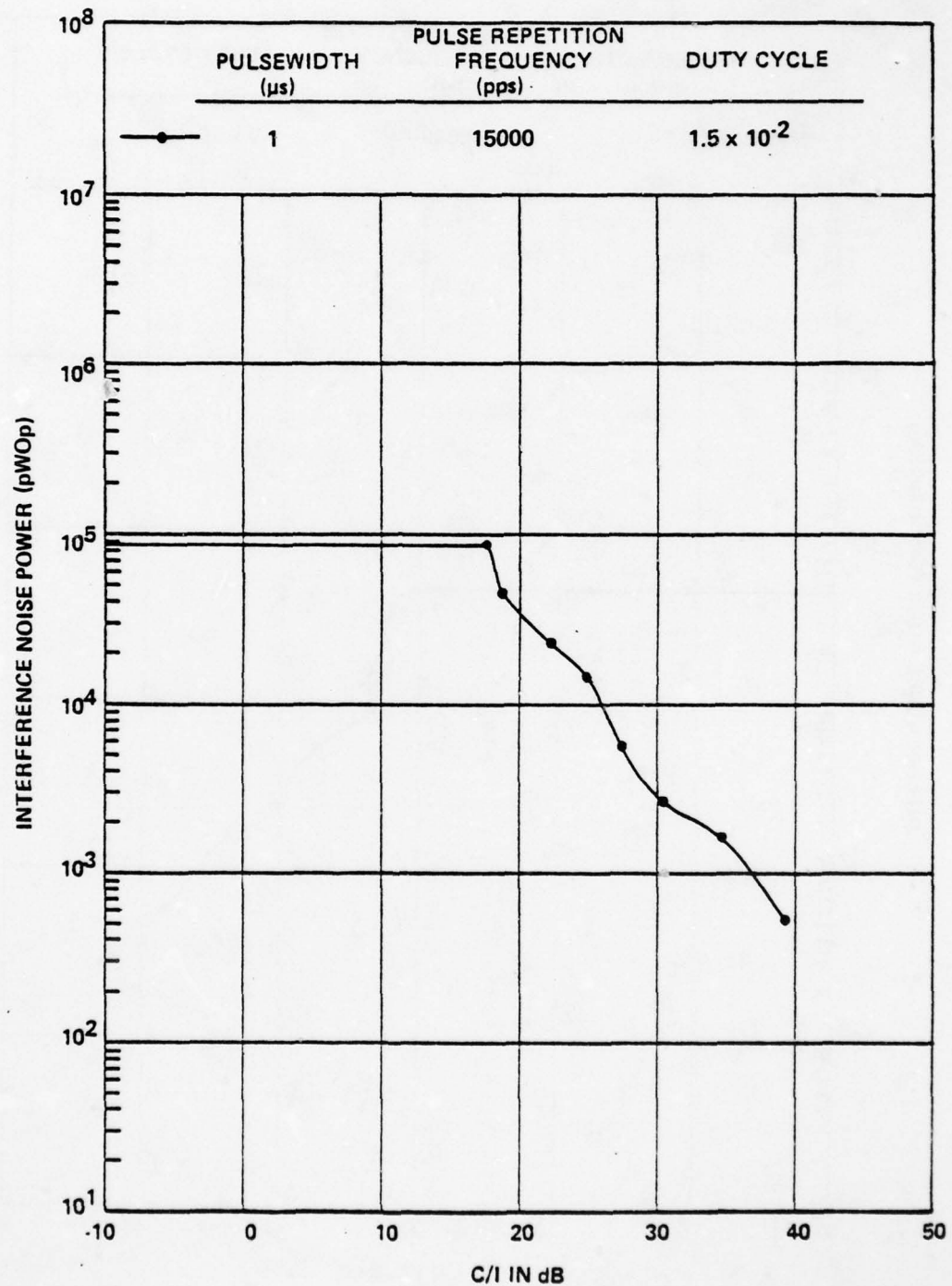


Figure 82. Measured interference noise power in a high baseband channel (2432-2436 kHz) for cochannel, nonchirped, pulse interference; PRF = 15,000 pps.

AD-A068 757

IIT RESEARCH INST ANNAPOLIS MD

F/G 17/2.1

WIDEBAND FDM/FM MICROWAVE RADIO RELAY PERFORMANCE DEGRADATION I--ETC(U)

APR 79 A A HERNANDEZ

F19628-78-C-0006

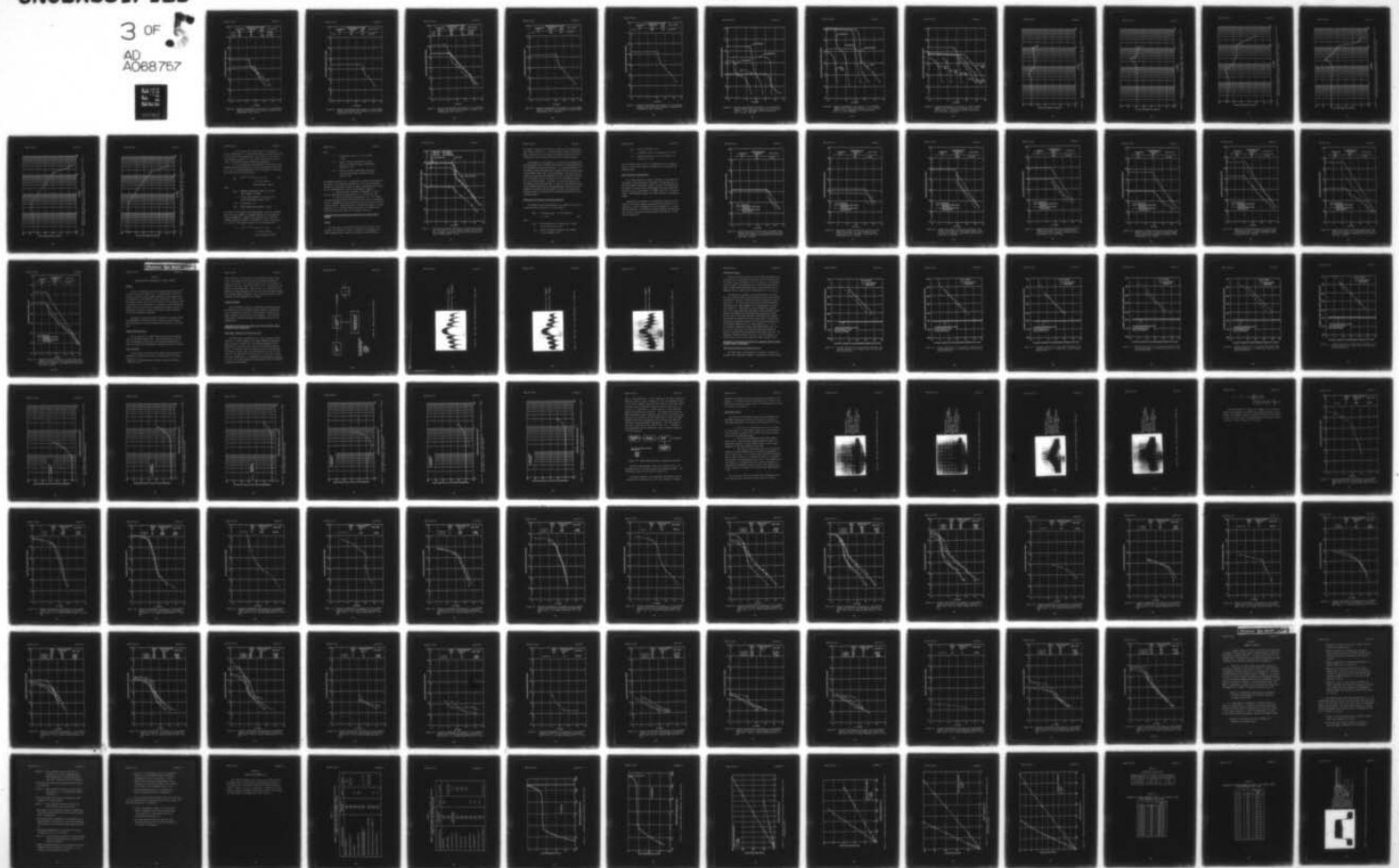
UNCLASSIFIED

ESD-TR-79-100

NL

3 OF 5

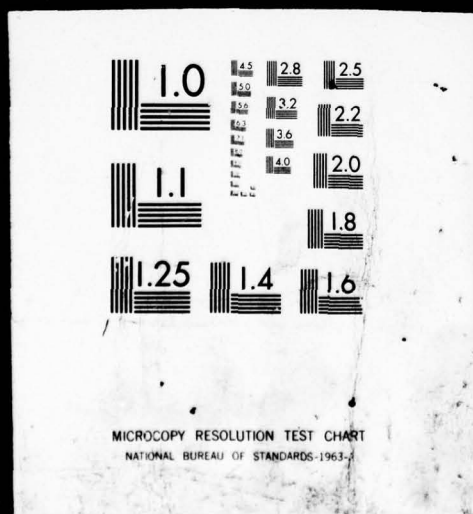
AD
A068757



1 F 1 E D

3 OF 5

AD
A068757



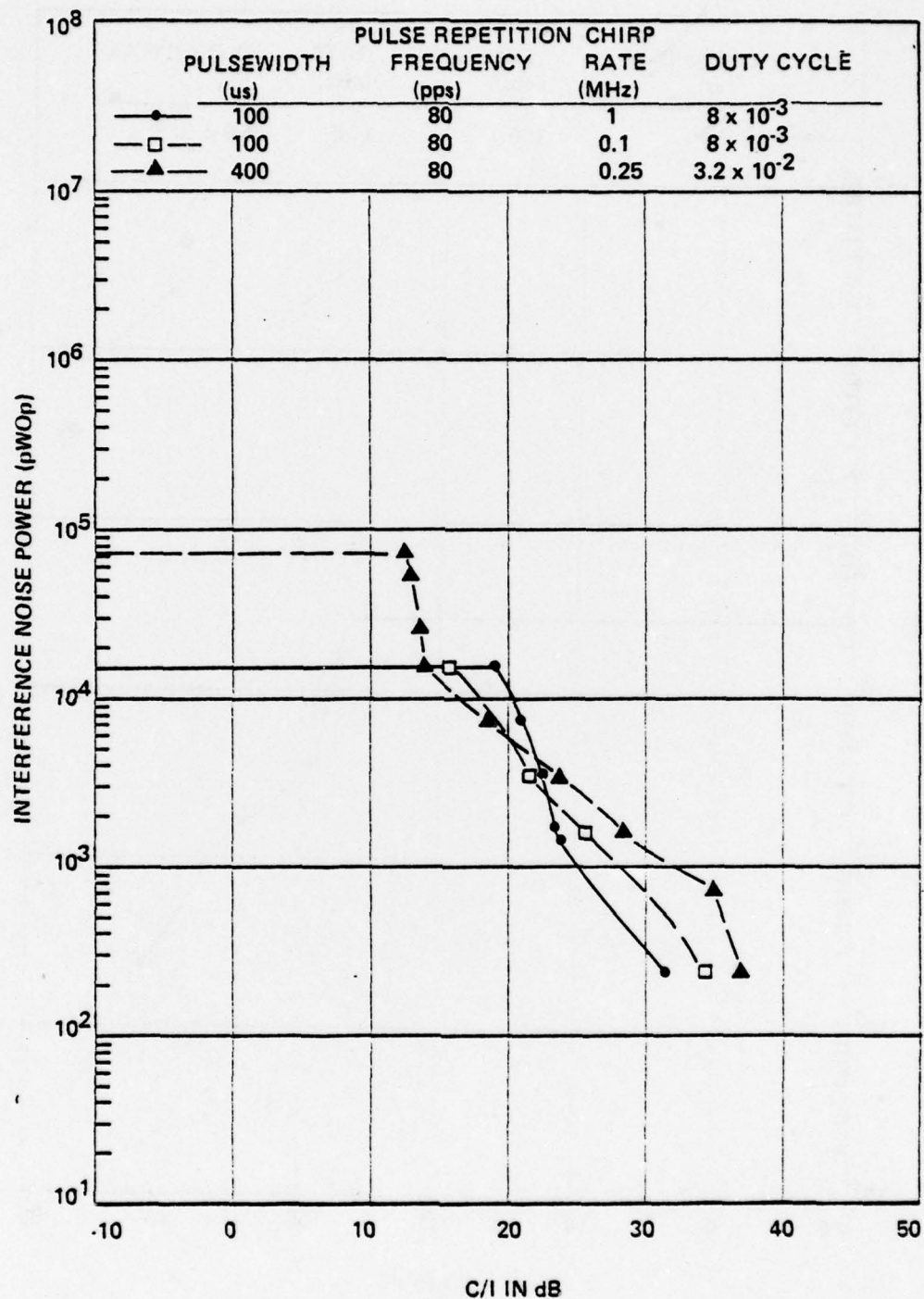


Figure 83. Measured interference noise power in a low baseband channel (340-344 kHz) for cochannel, chirped, pulse interference; PRF = 80 pps.

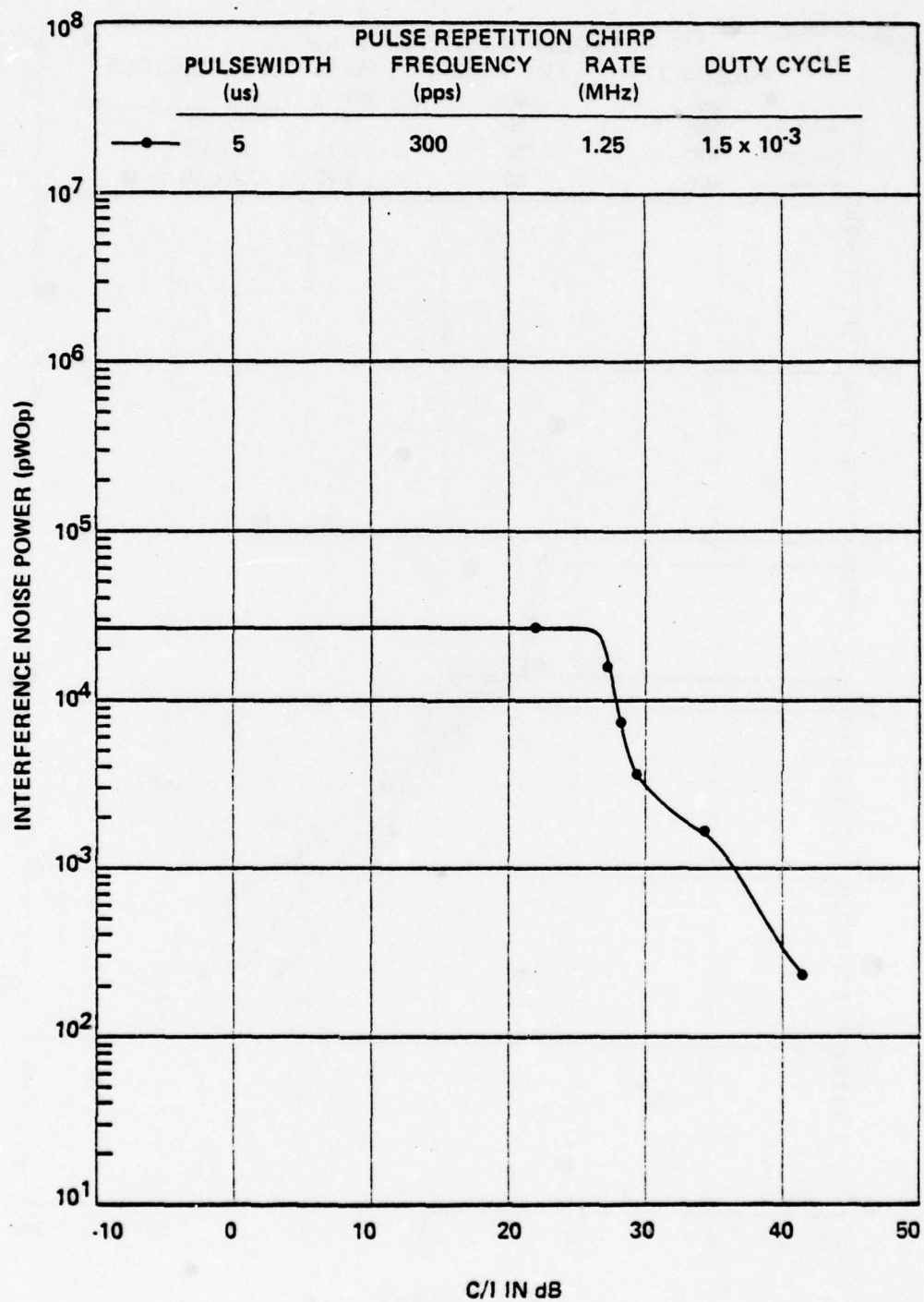


Figure 84. Measured interference noise power in a low baseband channel (340-344 kHz) for cochannel, chirped, pulse interference; PRF = 300 pps.

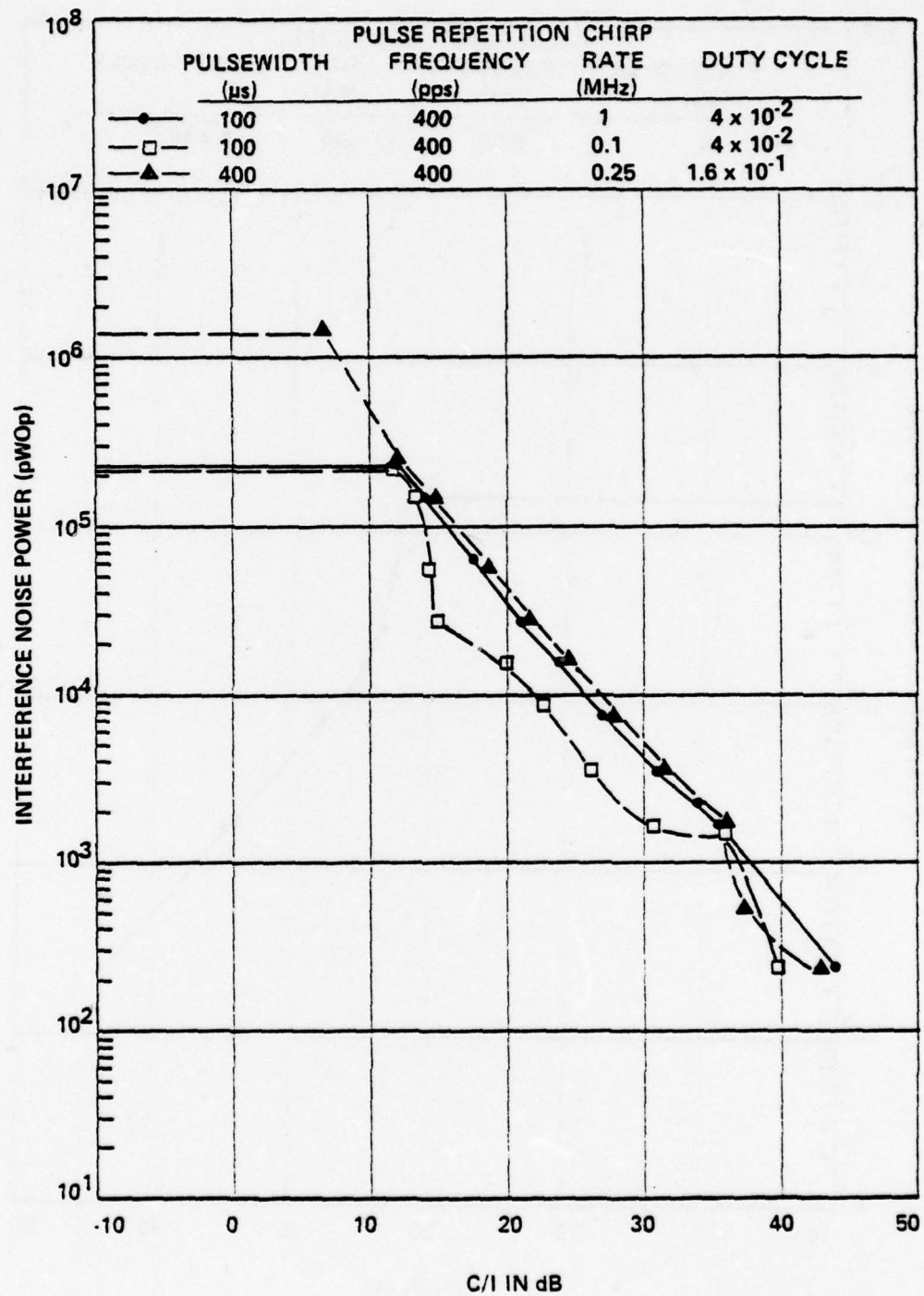


Figure 85. Measured interference noise power in a low baseband channel (340-344 kHz) for cochannel, chirped, pulse interference; PRF = 400 pps.

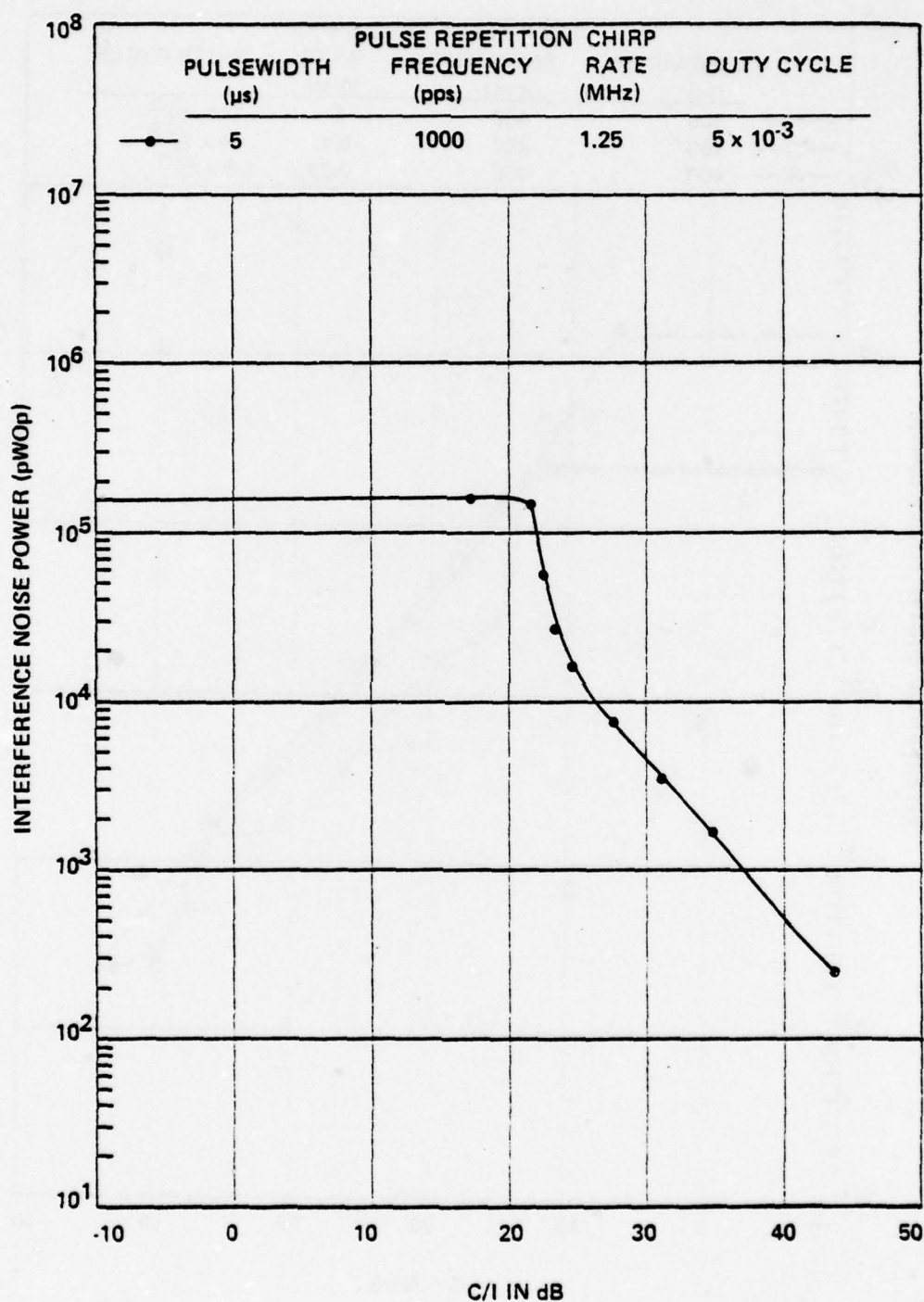


Figure 86. Measured interference noise power in a low baseband channel (340-344 kHz) for cochannel, chirped, pulse interference; PRF = 1000 pps.

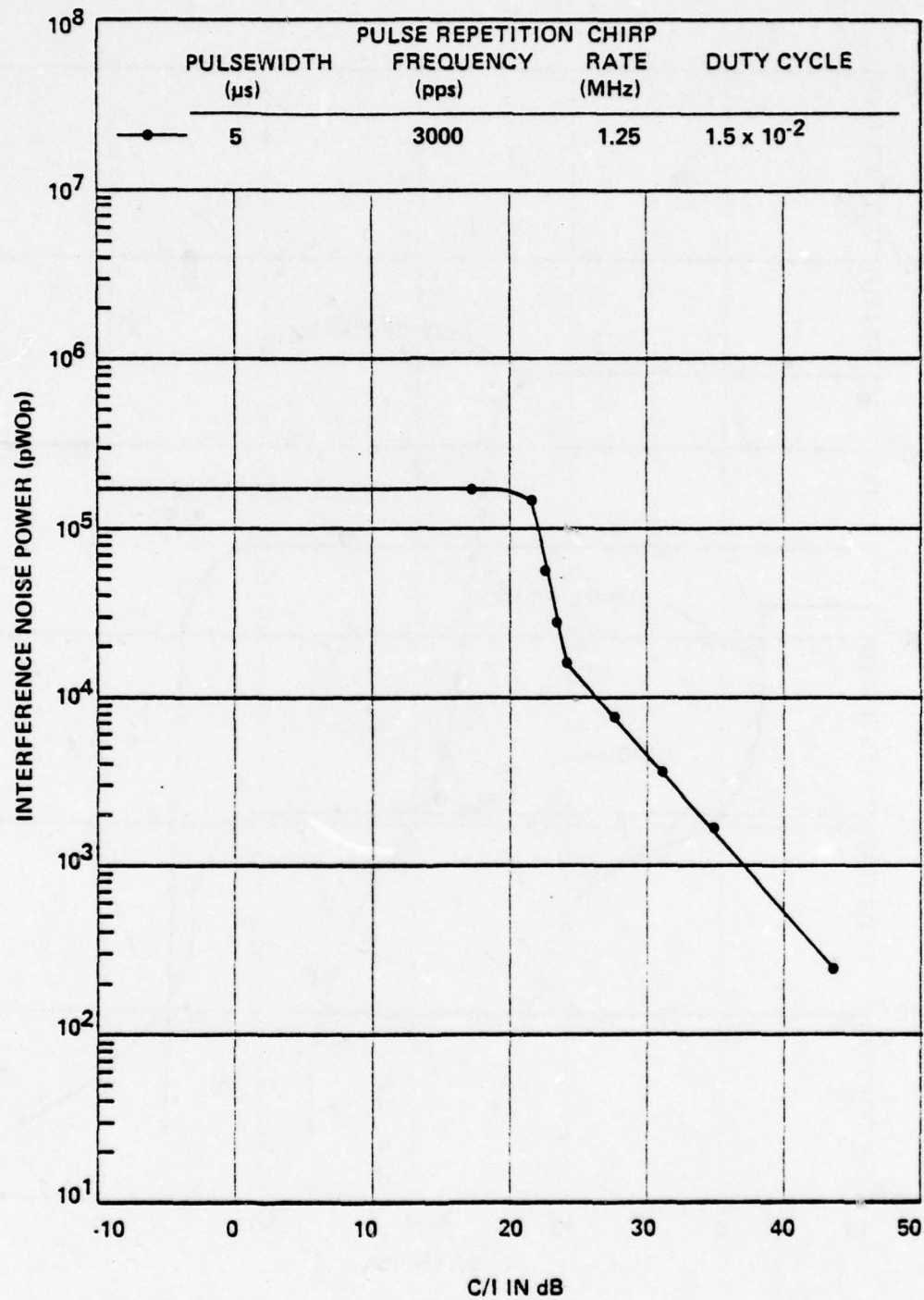


Figure 87. Measured interference noise power in a low baseband channel (340-344 kHz) for cochannel, chirped, pulse interference; PRF = 3000 pps.

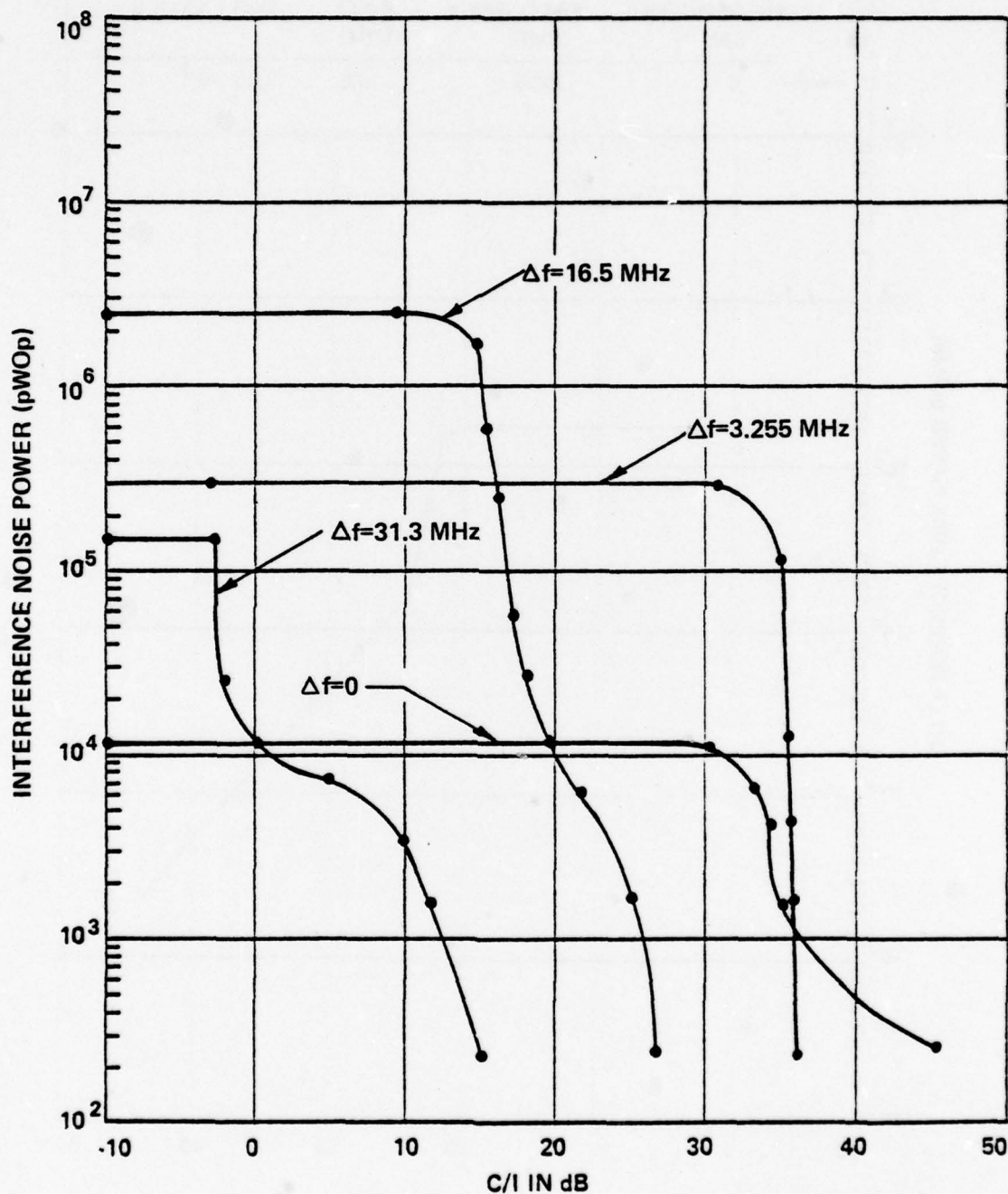


Figure 88. Measured interference noise power in a low baseband channel (340-344 kHz) for cochannel ($\Delta f = 0$) and off-tuned ($\Delta f > 0$), nonchirped, pulse interference, PW = 1 μ s, PRF = 500 pps.

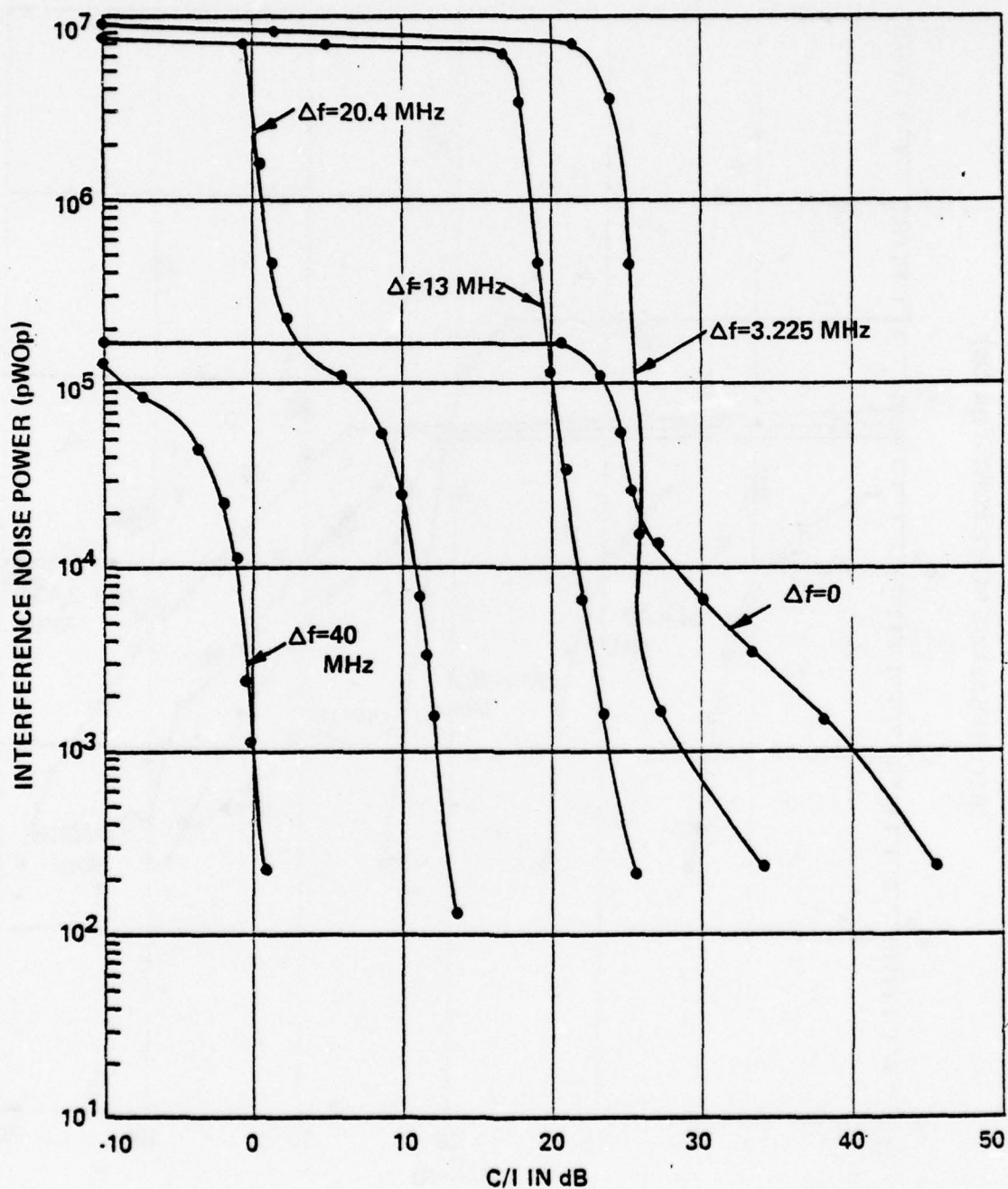


Figure 89. Measured interference noise power in a low baseband channel (340-344 kHz) for cochannel ($\Delta f = 0$) and off-tuned ($\Delta f > 0$), nonchirped, pulse interference; PW = 1 μ s, PRF = 5000 pps.

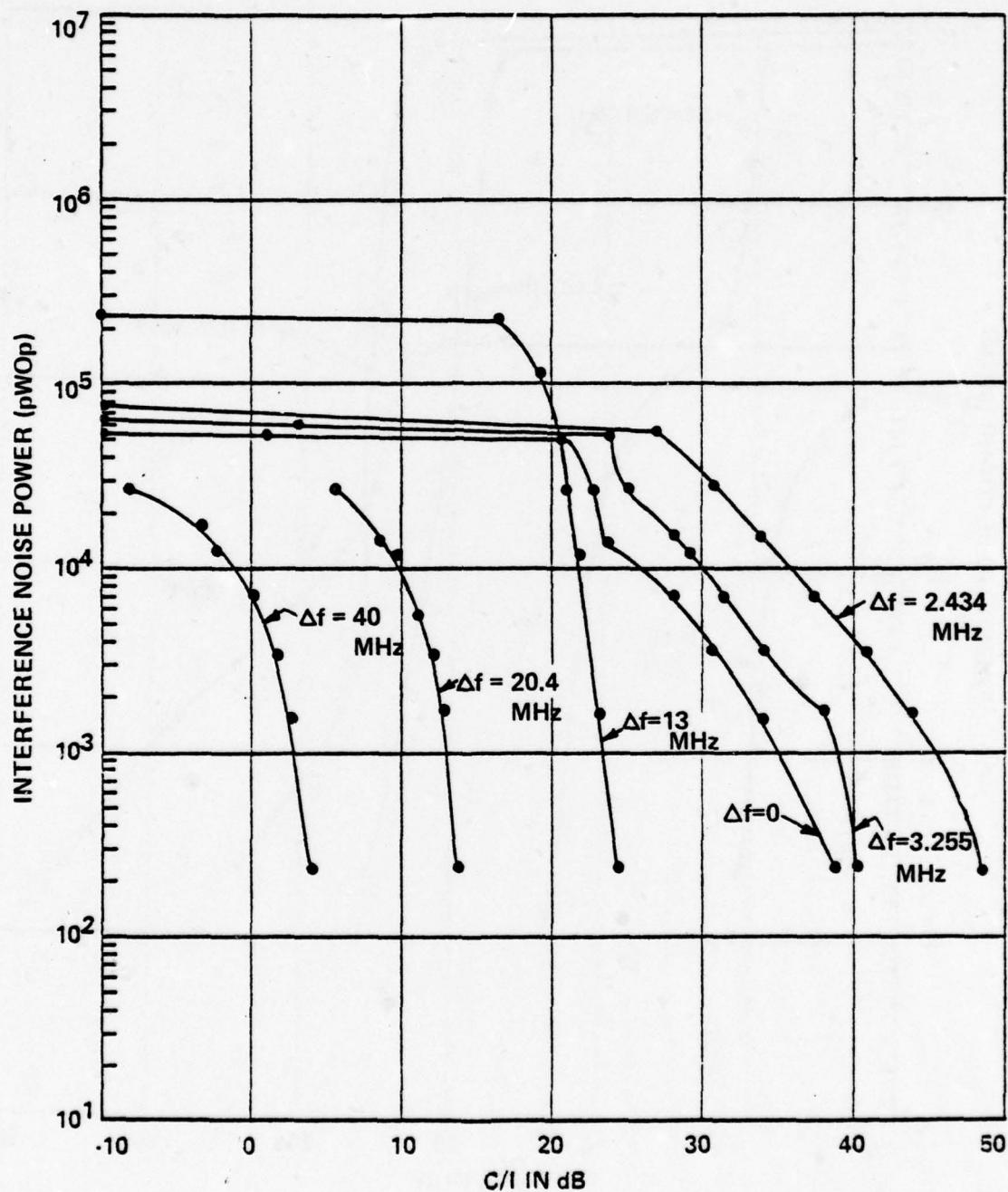


Figure 90. Measured interference noise power in a high baseband channel (2432-2436 kHz) for cochannel ($\Delta f = 0$) and off-tuned ($\Delta f > 0$) nonchirped, pulse interference; PW = 1 μ s, PRF = 5000 pps.

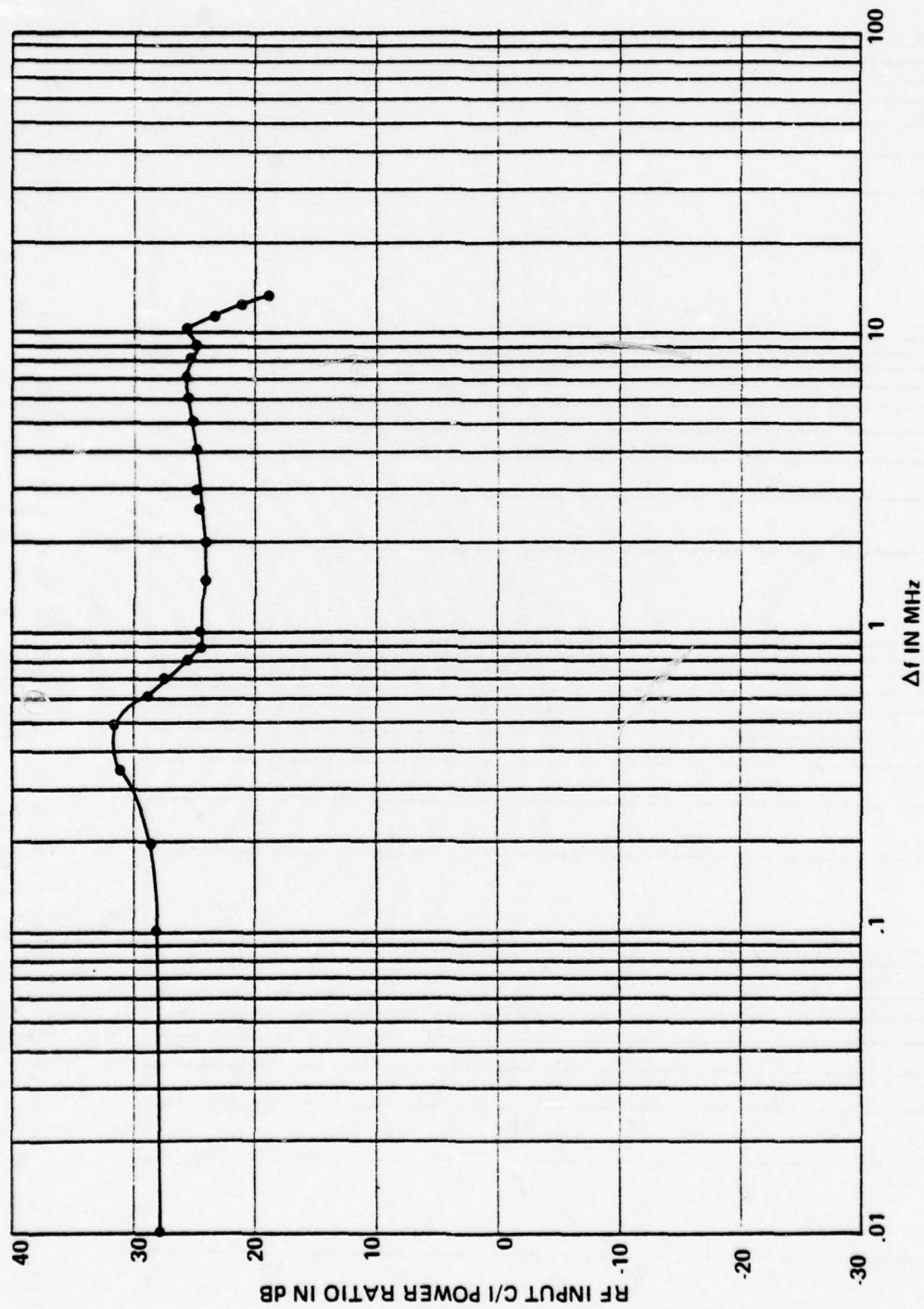


Figure 91. Required C/I power ratio for a low channel (340-344 kHz) S/N output of 52 dB as a function of frequency off-tuning; PW = 10 μ s, PRF = 400 pps.

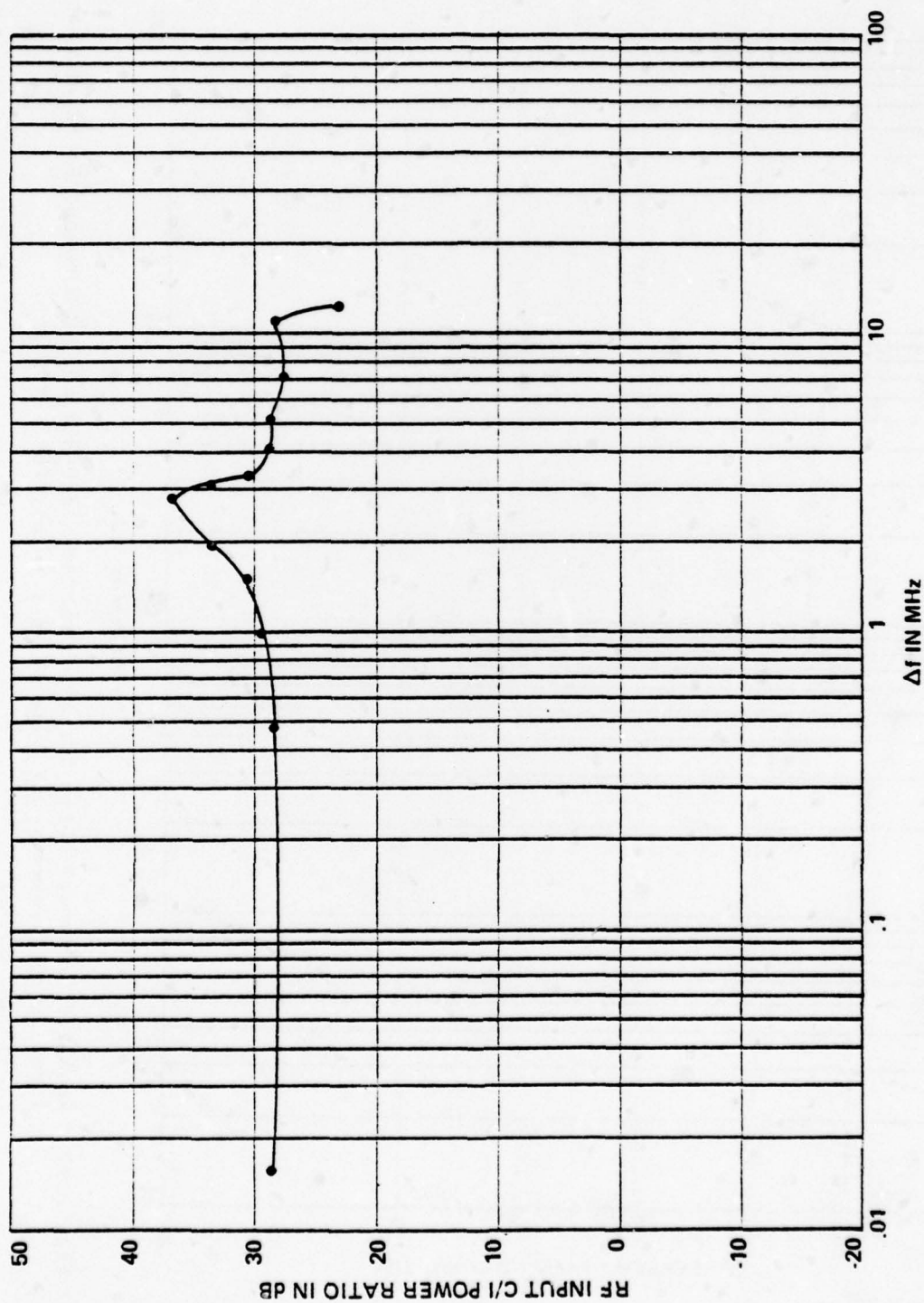


Figure 92. Required C/I power ratio for a high channel (2432-2436 kHz) S/N output of 53 dB as a function of frequency off-tuning; PW = 10 μ s, PRF = 400 pps.

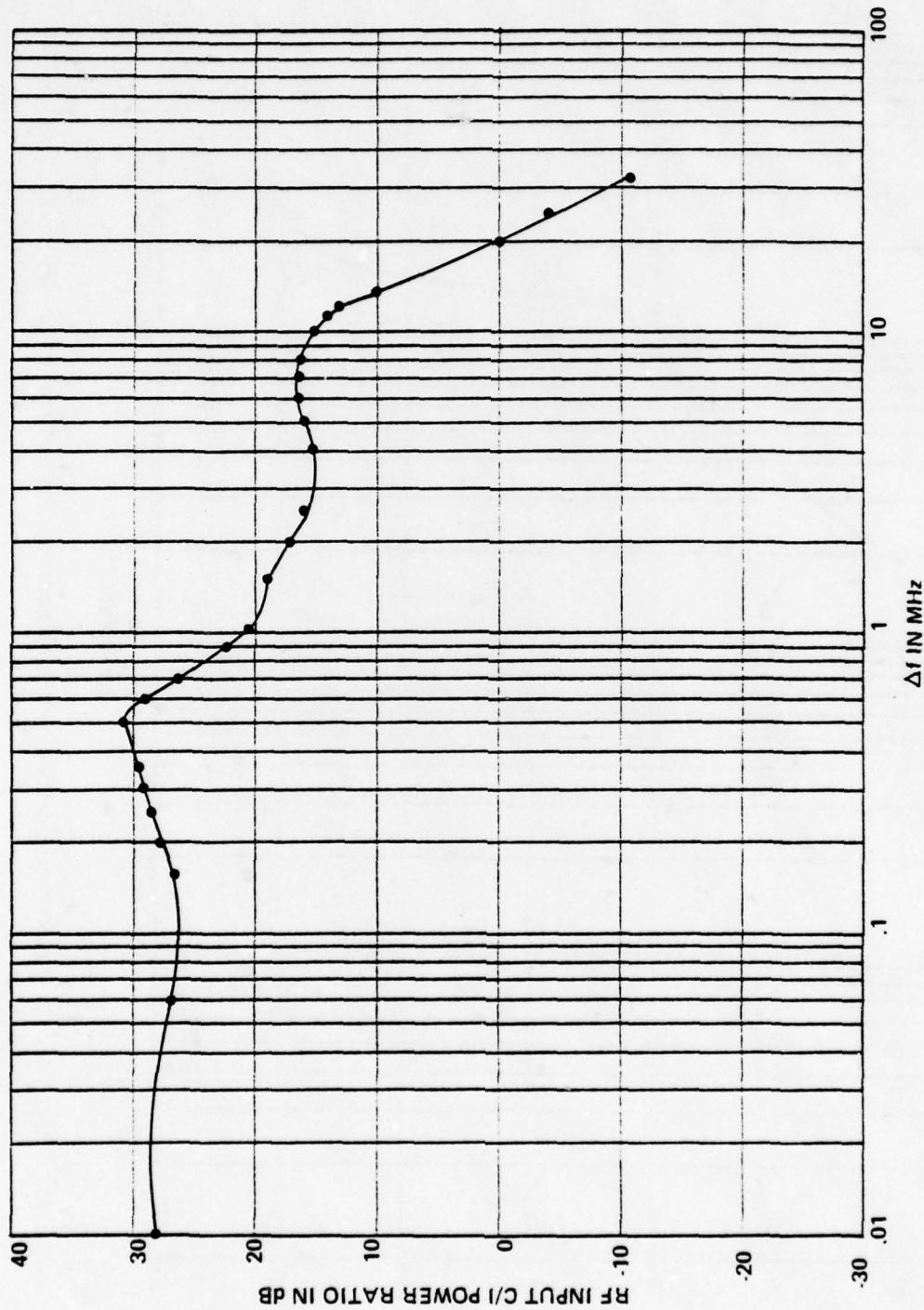


Figure 93. Required C/I power ratio for a low channel (340-344 kHz) S/N output of 52 dB as a function of frequency off-tuning; PW = 100 μ s, PRF = 400 pps.

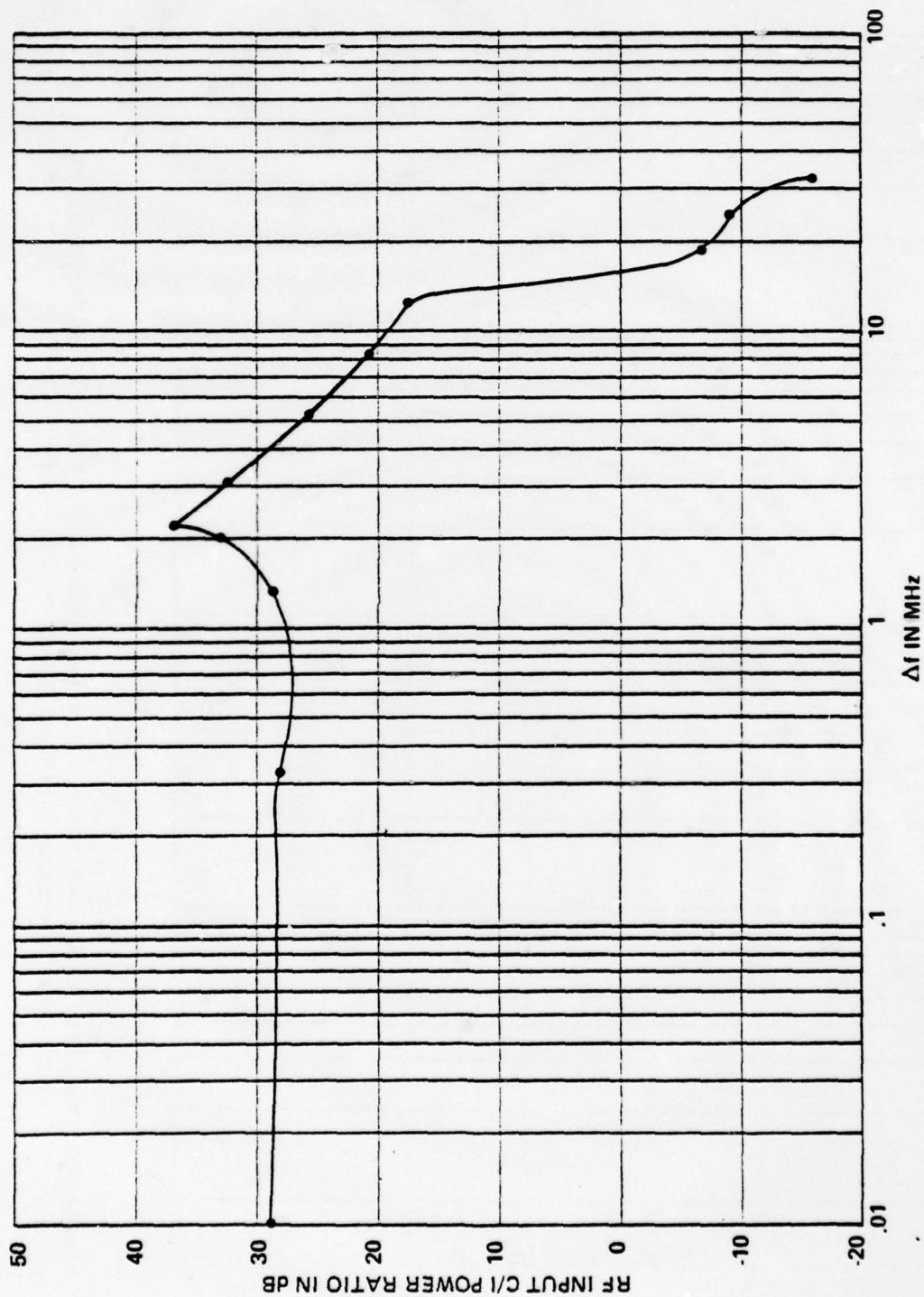


Figure 94. Required C/I power ratio for a high channel (2432-2436 kHz) S/N output of 53 dB as a function of frequency off-tuning; $PW = 100 \mu s$, $PRF = 400$ pps.

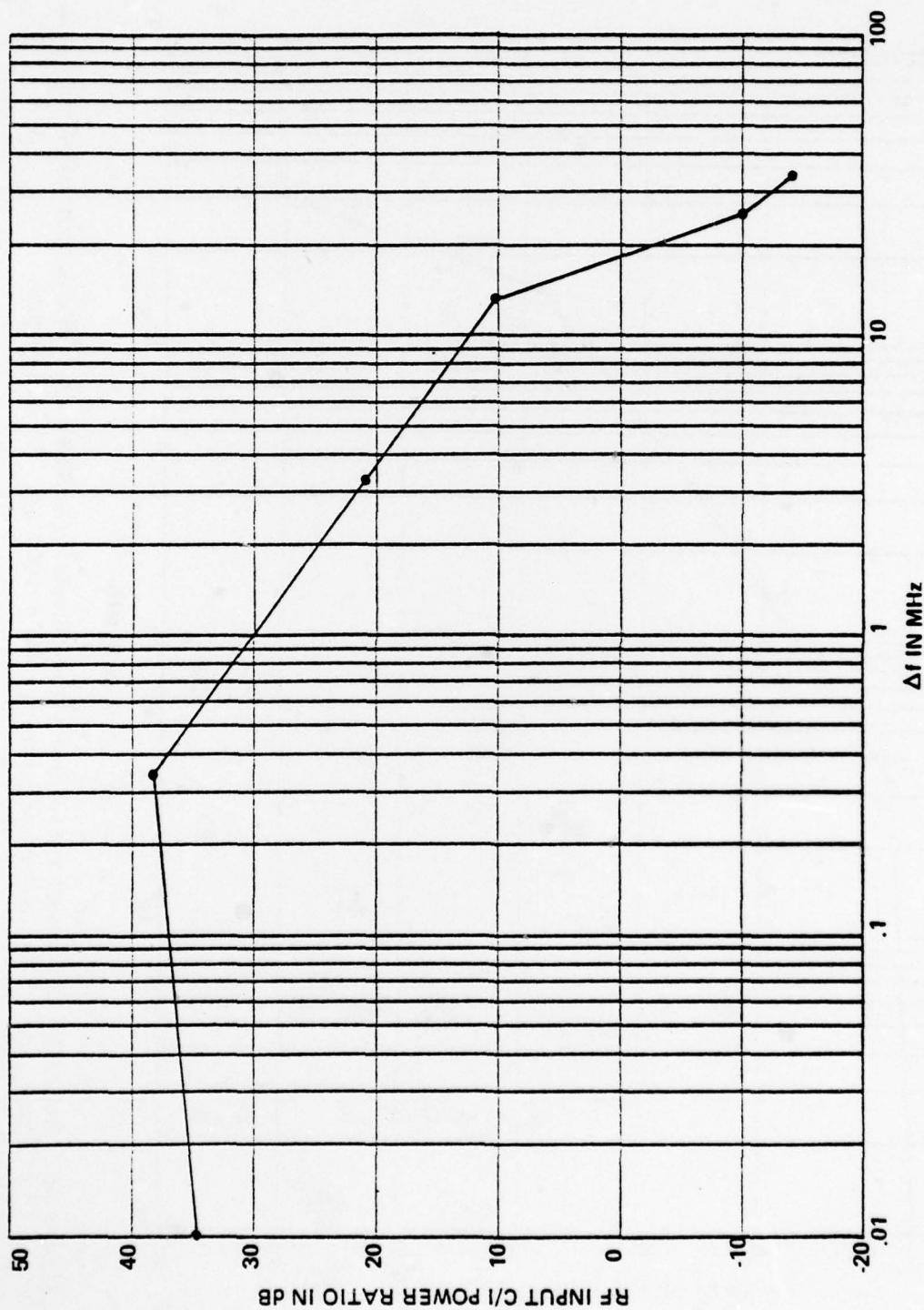


Figure 95. Required C/I power ratio for a low channel (340-344 kHz) S/N output of 55 dB as a function of frequency off-tuning; PW = 400 μ s, PRF = 400 pps.

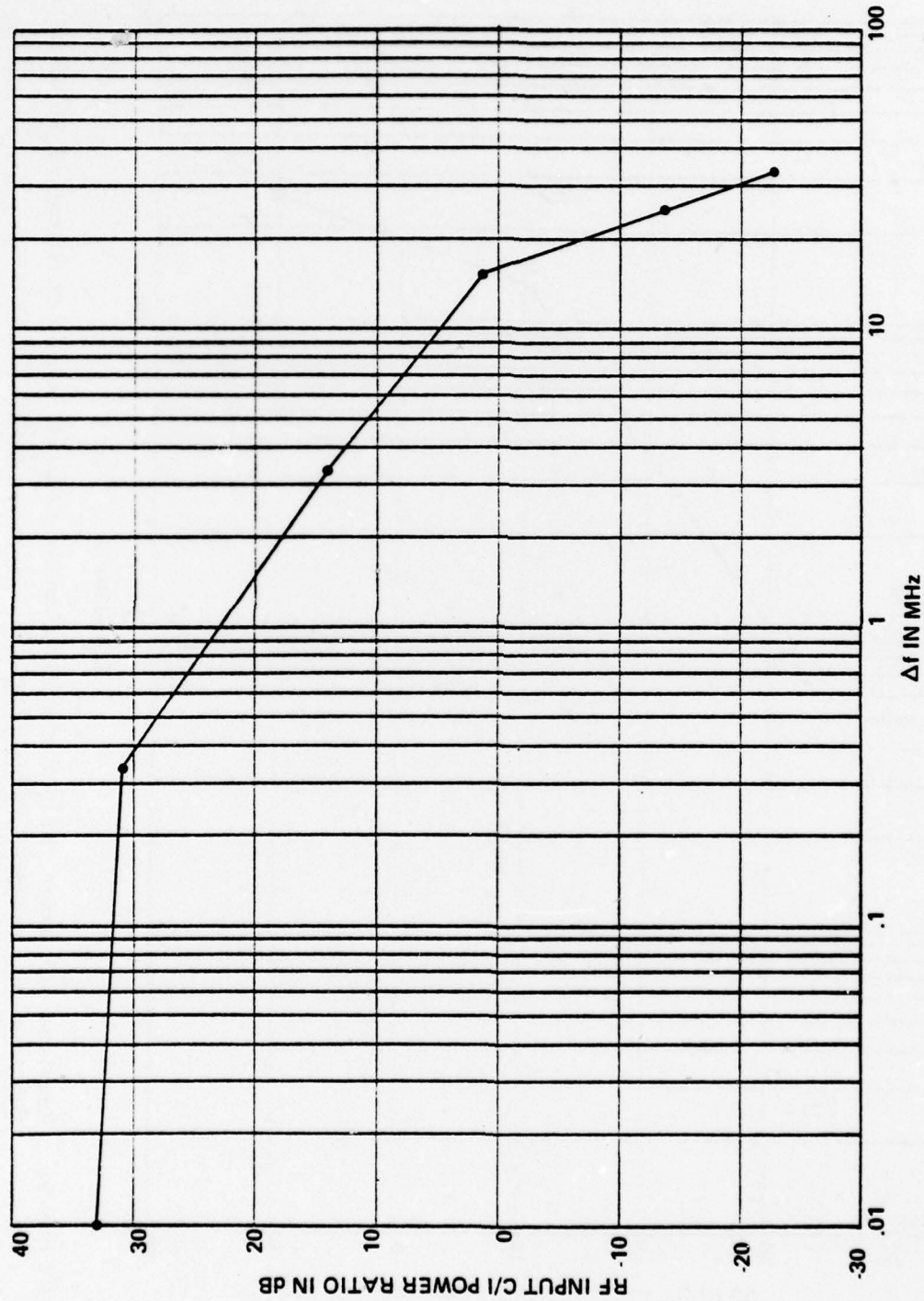


Figure 96. Required C/I power ratio for a low channel (340-344 kHz) S/N output of 53 dB as a function of frequency off-tuning; PW = 1000 μ s, PRF = 160 pps.

2. For on-tune pulse interference, the maximum observed interference in a voice channel remains constant for values of C/\hat{I} smaller than approximately -2 dB, where \hat{I} is the pulsed interference peak power (i.e., the RMS power during the pulse on time) in the desired-signal predetection bandwidth.

3. For on-tune pulse interference, the envelope of the maximum observed interference in the worst performing voice channel (i.e., for these measurements, the low channel) of a 600-channel carrier can be calculated from:

$$N_{\max} = 10^{(66 + \delta)/8}, \text{ for } C/\hat{I} \leq -2 \text{ dB}, \quad (92)$$

$$1 \mu\text{s} \leq \text{PW} \leq 1000 \mu\text{s},$$

and 600-channel carrier

where

N_{\max} = Maximum interference power in the worst voice channel, in pWOp

δ = $10 \log [(PW) (PRF) 10^{-6}]$ = duty cycle of pulse interference signal, in dB

PW = Pulsewidth, in μs

PRF = Pulse repetition frequency, in pps.

For values of C/\hat{I} greater than approximately -2 dB, the interference in a voice channel is a complex function of the pulse and receiver parameters. However, the envelope of all the noise transfer functions (Figures 63 through 87) is only a function of C/I , and for a 600-channel carrier can be calculated from:

$$N = 10^{(64 - C/I)/8}, \text{ for } C/\hat{I} > -2 \text{ dB} \quad (93)$$

$$1 \mu\text{s} \leq \text{PW} \leq 1000 \mu\text{s},$$

and 600-channel carrier

where

N = Interference power in a voice channel,
in pWOp

C/I = carrier-to-pulse interference average
power in the desired-signal predetection
bandwidth, in dB

C/\hat{I} = Carrier-to-pulse interference peak power
in the desired-signal predetection band-
width, in dB.

The complete envelope (i.e., the envelope calculated from Equations 92 and 93) of the observed interference in the worst performing channel of a 600-channel carrier for pulse interference with a duty cycle of approximately -18 dB is illustrated in Figure 97.

4. The conclusions outlined in Paragraphs 1, 2 and 3 are also applicable to chirped pulses (i.e., pulses with FM).

5. For off-tuned pulse interference (i.e., for offsets in center frequency between the desired carrier and the interfering carrier), degradation may be greater than the levels given in Equations 92 and 93. Note further that, for moderate offsets in center frequency ($\Delta f = 3.255$ MHz, Figures 88 and 89), the higher noise levels may occur for values of C/\hat{I} greater than zero.

ACCOUNTING FOR THE MODULATION CHARACTERISTICS OF OTHER FDM/FM SYSTEMS

General

The data shown in Figures 63 through 96 can be used in conjunction with Equations 92 and 93 to predict the degradation in FDM/FM communications systems whose modulation characteristics

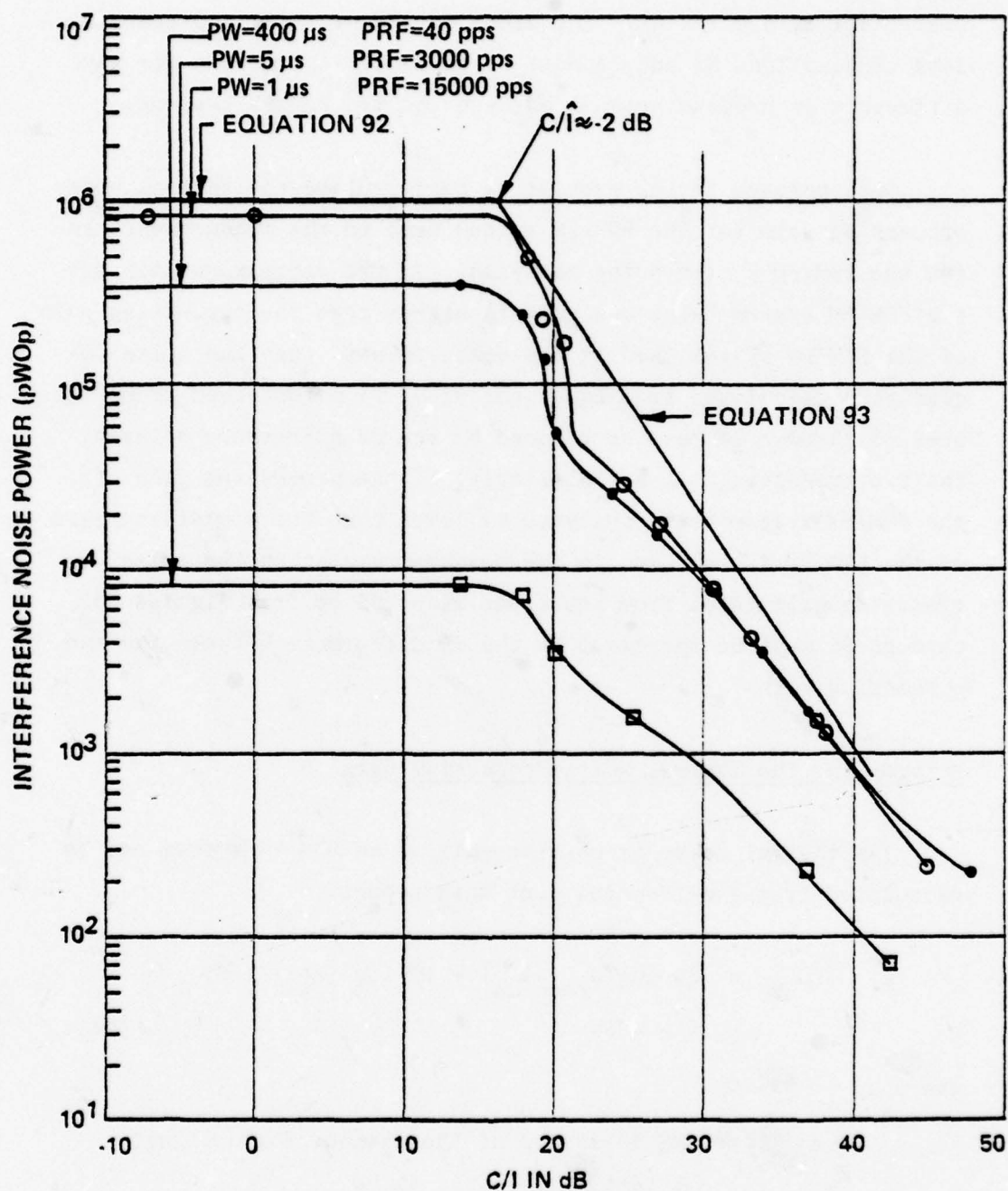


Figure 97. Envelope and transfer functions of the observed interference noise power in a low baseband channel (340-344 kHz) for co-channel, nonchirped, pulse interference and duty cycle of approximately -18 dB.

and channel capacities are similar to those of the system tested (see TABLE 8, Section 4). For other FDM/FM systems, the measured data or Equations 92 and 93 must be corrected to account for any difference in processing gain between the two FDM/FM systems.

One approach to the problem is to calculate the thermal noise processing gain for the FDM/FM system used in the measurements and for the FDM/FM system being analyzed. If the processing gain of the FDM/FM system being analyzed is higher than the processing gain of the FDM/FM system used in the measurements, then the noise degradation calculated from Equations 92 or 93 or obtained from Figures 63 through 96 must be reduced by the dB difference between the two processing gains. Similarly, if the processing gain of the FDM/FM system being analyzed is lower than the processing gain of the FDM/FM system used in the measurements, then the noise degradation calculated from Equations 92 or 93 or from Figures 63 through 96 must be increased by the dB difference between the two processing gains.

Determining the Thermal Noise Processing Gain

The thermal noise processing gain of an FDM/FM system can be calculated from (see Section 4 of this report):

$$\begin{aligned} PG_{GN} = & 20 \log(d_{rms}/F_{ch}) + 10 \log(B_{IF}/3100) \\ & + E + WF \end{aligned} \quad (94)$$

where

d_{rms} = RMS deviation of the channel for a signal of test tone level, in Hz

F_{ch} = Center frequency occupied by the channel in the baseband, in Hz

B_{IF} = 3-dB IF bandwidth, in Hz

E = Preemphasis factor (see Equation 34), in dB

WF = Weighting network factor (see Equations 35, 36 and 37), in dB.

For the FDM/FM system tested, the parameters given in TABLE 8, Section 4 can be used directly in Equation 94 to calculate the reference PG_{GN} .

OTHER TECHNICAL CONSIDERATIONS

In a recent analysis of radar interference with FDM/FM communications, Wachs and Arroyo (Reference 32) suggested that in the quasi-linear interference region, the radar interference may be treated as an equivalent average power FM carrier whose RMS deviation (D_{rms}) corresponds to $1/\sqrt{2\pi PW}$, where PW is the pulsewidth. This treatment assumes the radar spectrum to be Gaussian-shaped.

Following this treatment, the interference noise was calculated for the system tested using Equations 89 (Section 6), 32 (Section 4), and B-3 (APPENDIX B) for pulsewidths of 1, 100 and 1000 microseconds. The results are shown compared with measured data and with the envelope method (Equations 92 and 93) in Figures 98 through 105.

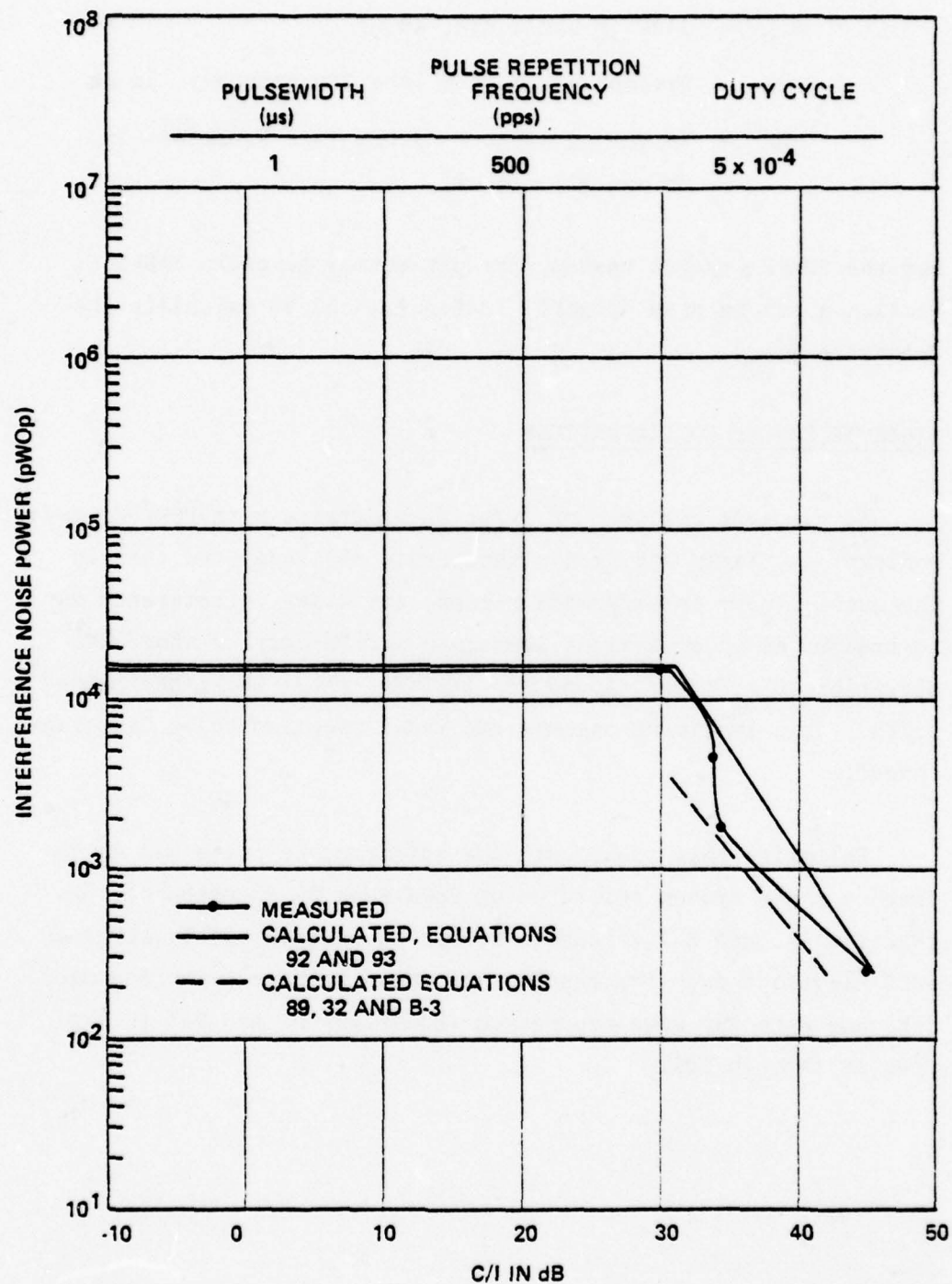


Figure 98. Comparisons between measured and calculated interference noise power in a low baseband channel (340-344 kHz) for cochannel, nonchirped, pulse interference; PRF = 500 pps.

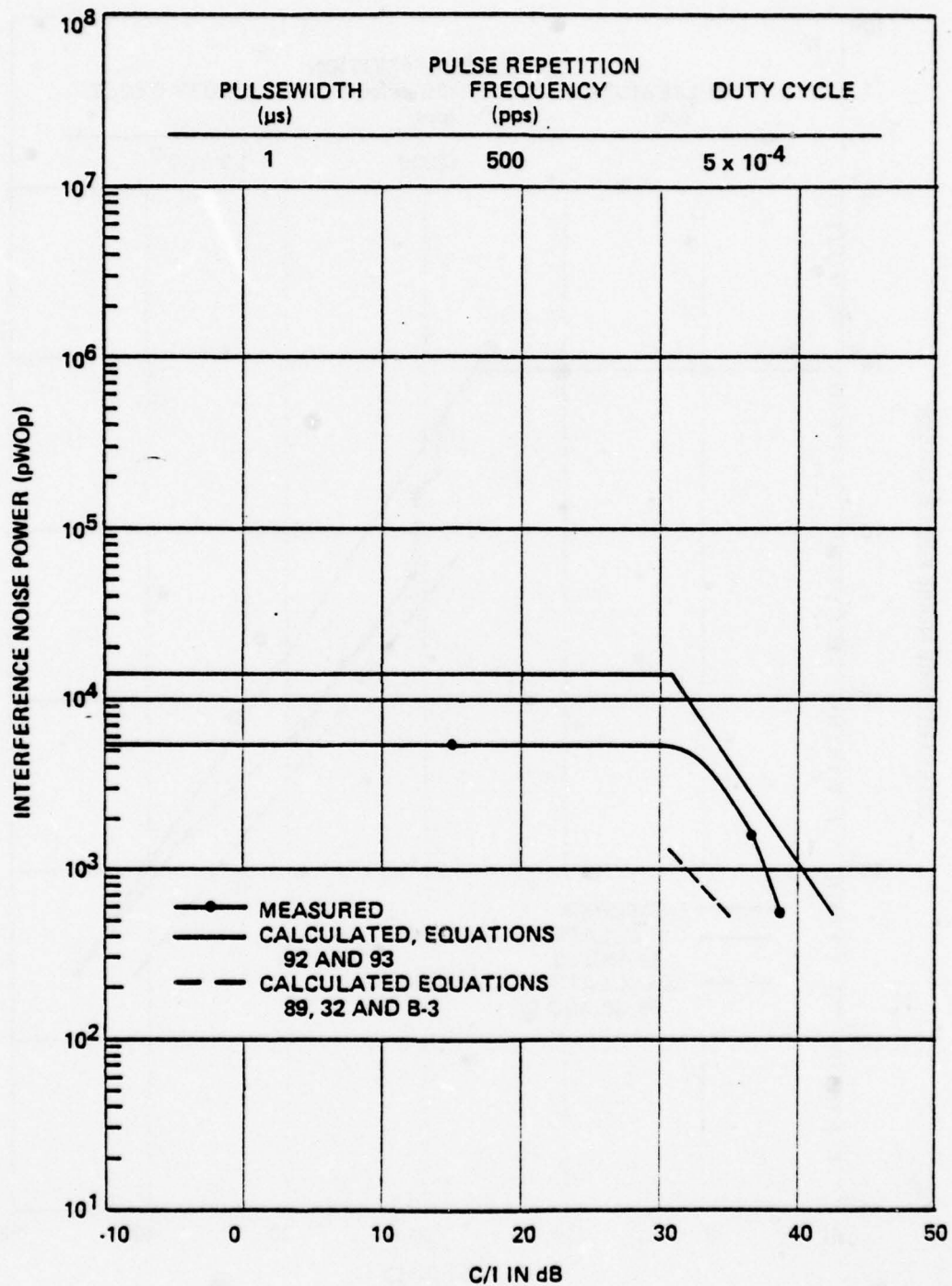


Figure 99. Comparisons between measured and calculated interference noise power in a high baseband channel (2432-2436 kHz) for cochannel, nonchirped, pulse interference; PRF = 500 pps.

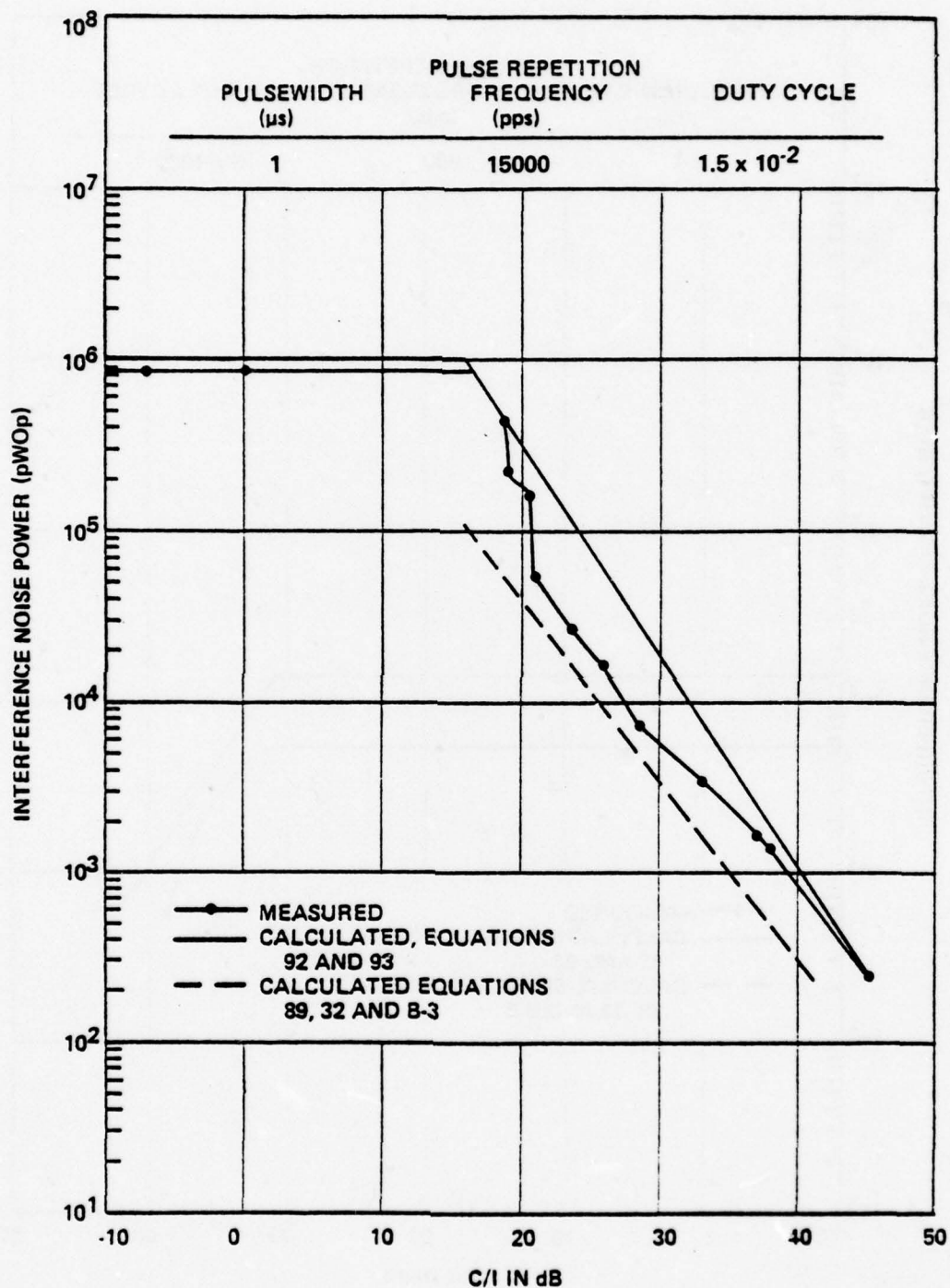


Figure 100. Comparisons between measured and calculated interference noise power in a low baseband channel (340-344 kHz) for cochannel, nonchirped, pulse interference; PRF = 15,000 pps.

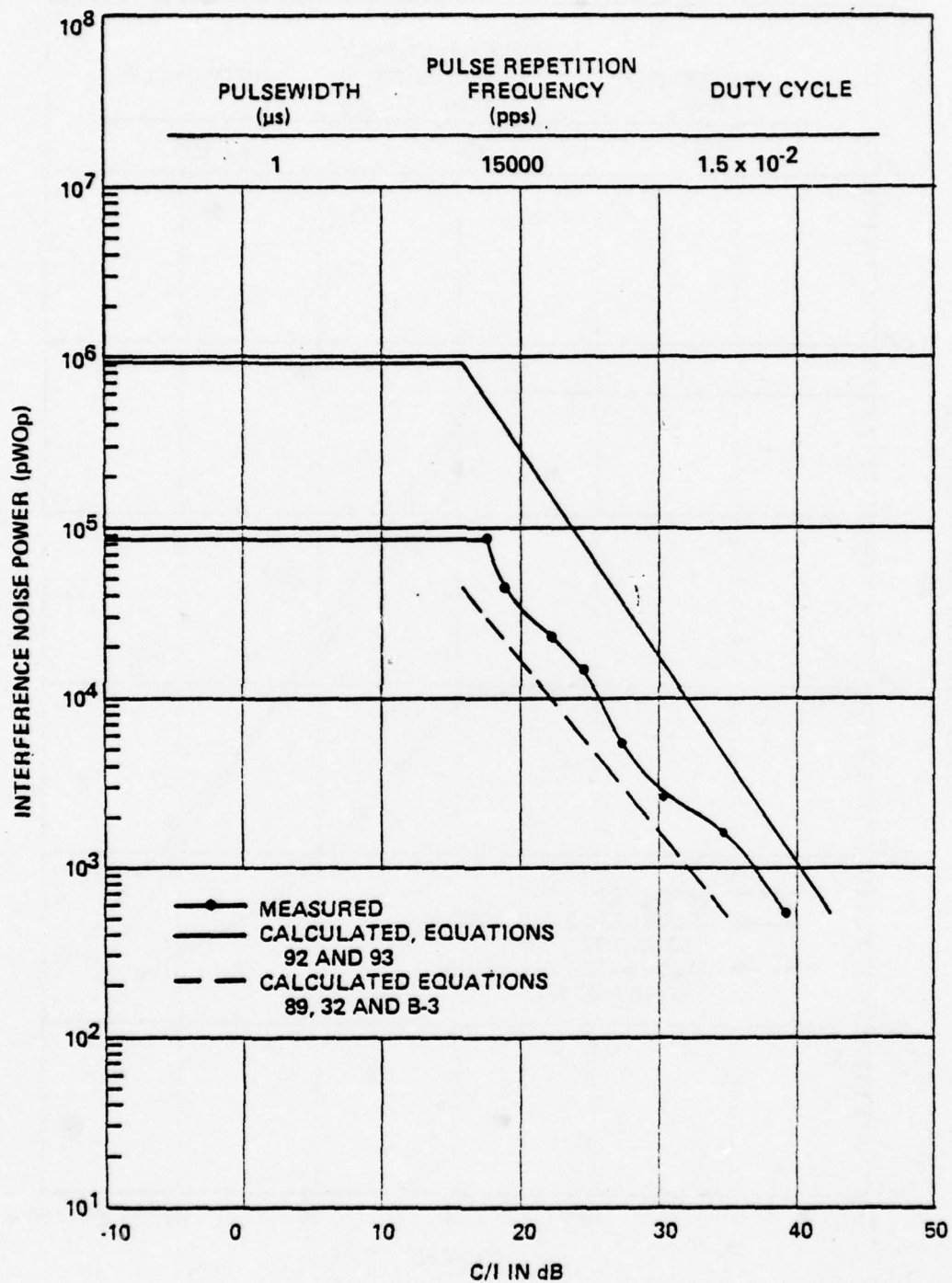


Figure 101. Comparisons between measured and calculated interference noise power in a high baseband channel (2432-2436 kHz) for cochannel, nonchirped, pulse interference; PRF = 15,000 pps.

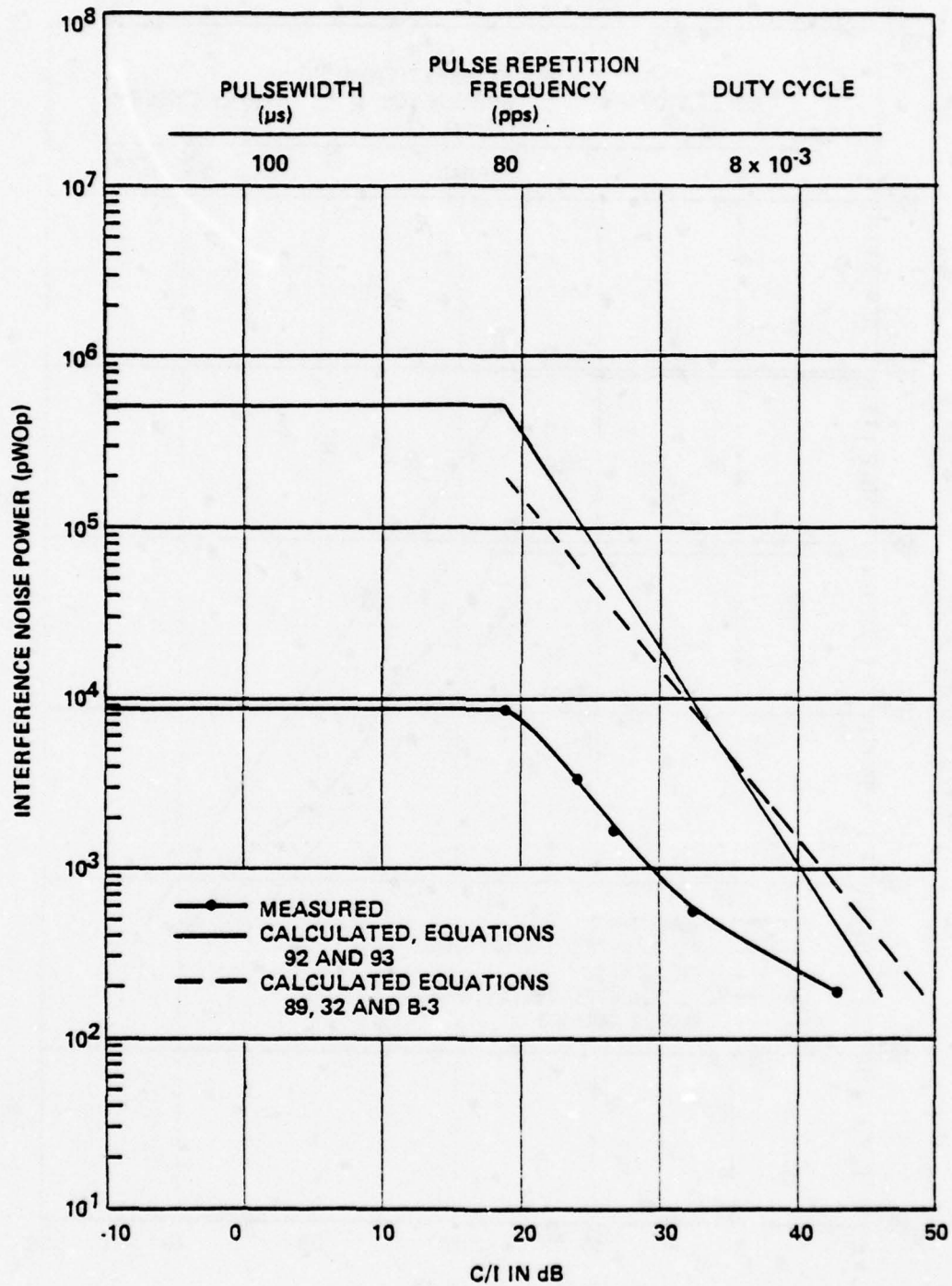


Figure 102. Comparisons between measured and calculated interference noise power in a middle baseband channel (1244-1248 kHz) for cochannel, nonchirped, pulse interference; PRF = 80 pps.

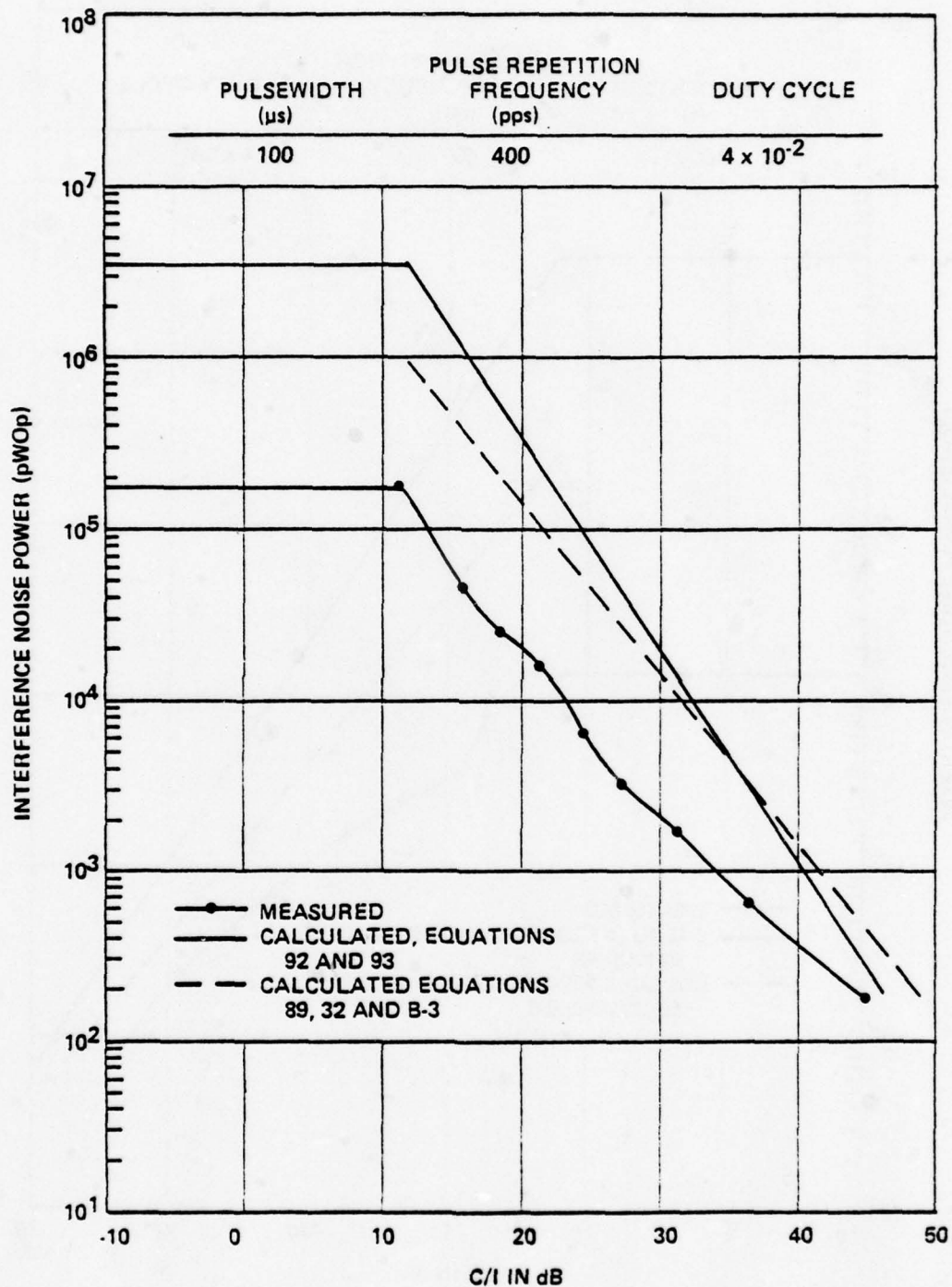


Figure 103. Comparisons between measured and calculated interference noise power in a middle baseband channel (1244-1248 kHz) for cochannel, nonchirped, pulse interference; PRF = 400 pps.

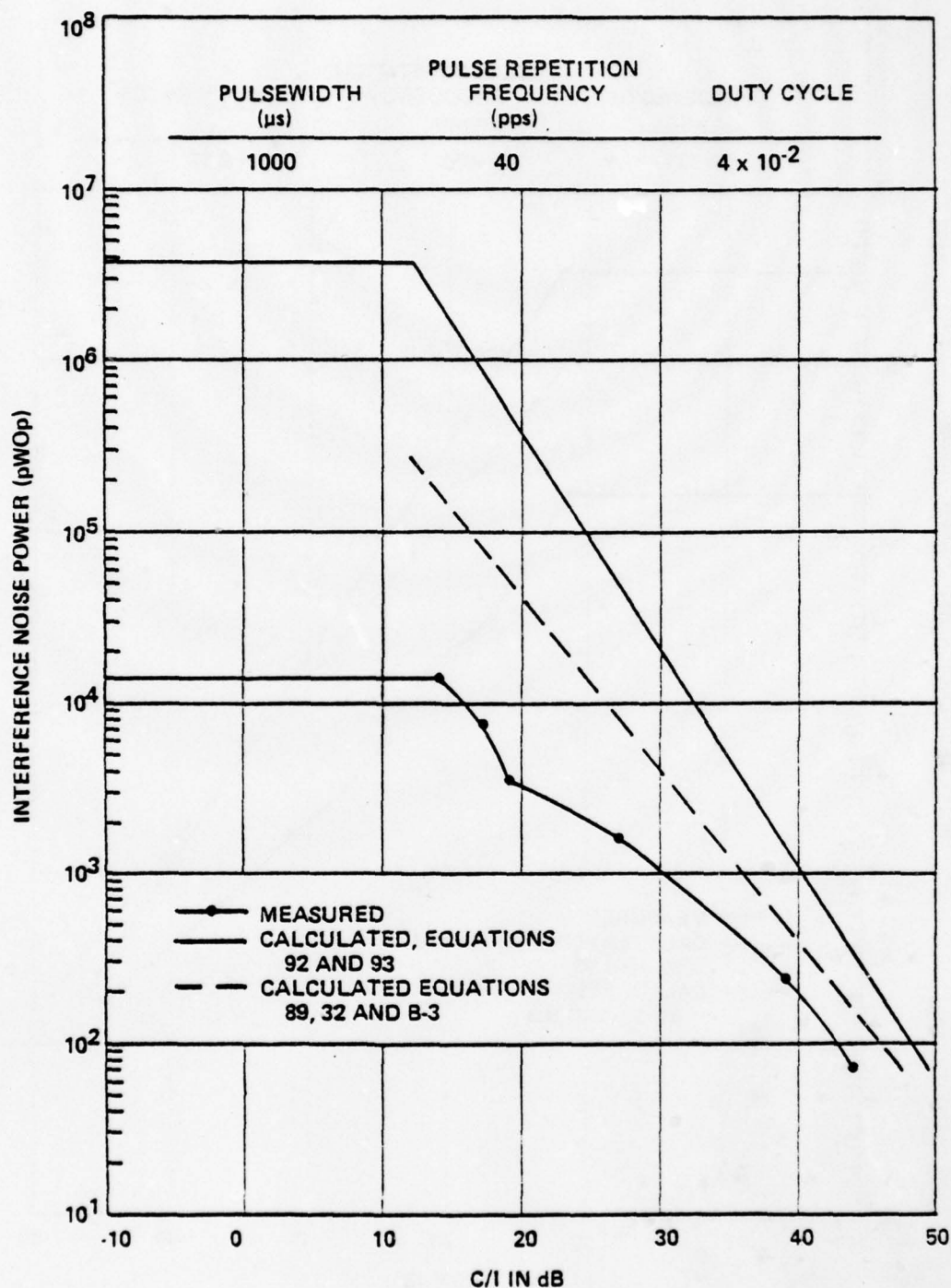


Figure 104. Comparisons between measured and calculated interference noise power in a low baseband channel (340-344 kHz) for cochannel, nonchirped, pulse interference; PRF = 40 pps.

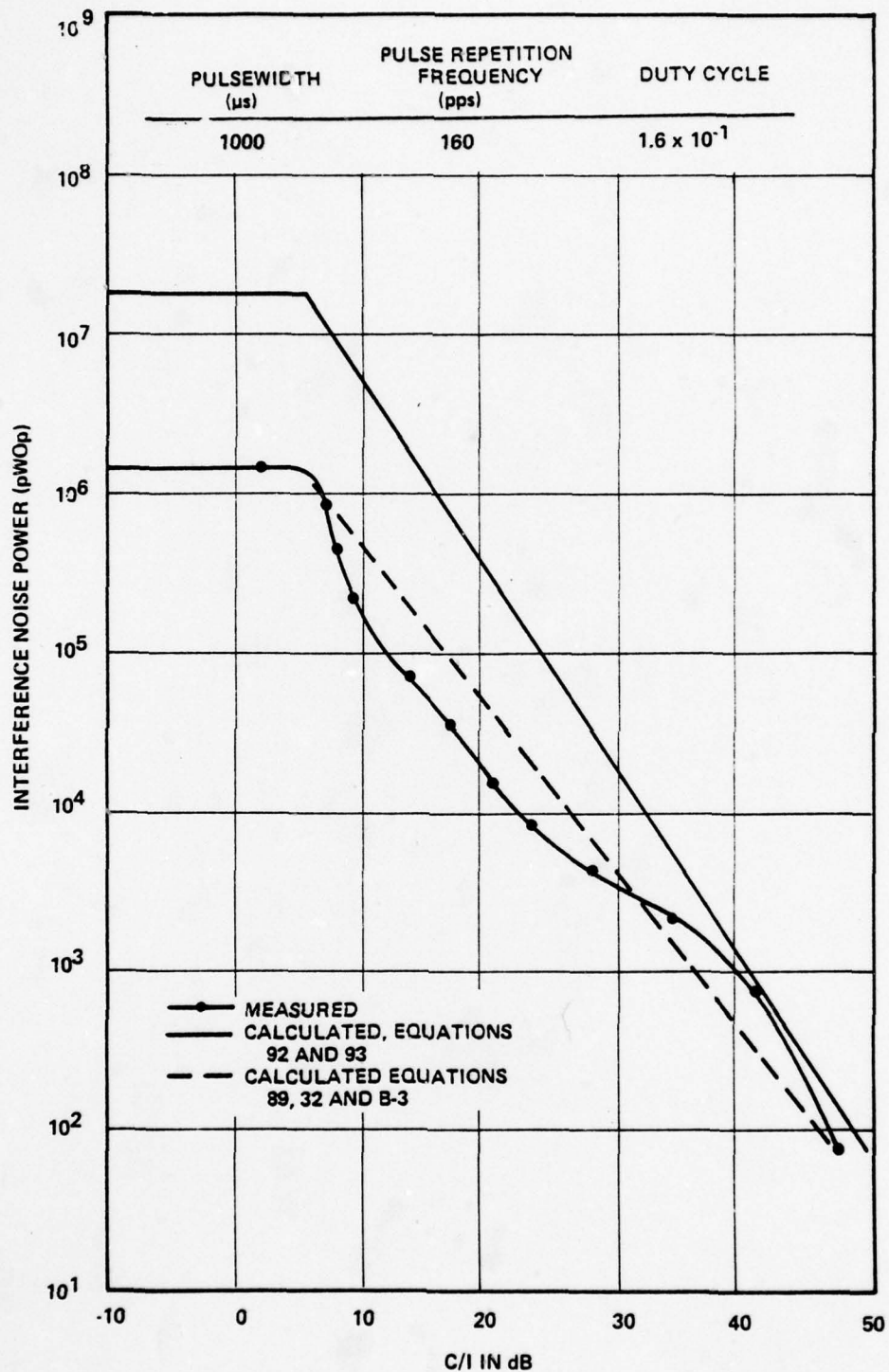


Figure 105. Comparisons between measured and calculated interference noise power in a low baseband channel (340-344 kHz) for cochannel, nonchirped, pulse interference; PRF = 160 pps.

SECTION 8

SPREAD-SPECTRUM INTERFERENCE TO FDM/FM SYSTEMS

GENERAL

A class of communication systems termed spread spectrum (SS) has been evolving in recent years. One characteristic of an SS system is that the emitted signal bandwidth is much greater than the bandwidth of the information being transmitted. Thus, one of the primary reasons for the current interest in SS systems is that they should be less susceptible to interference than conventional systems since the ability of a communication system to resist interference is directly related to the emitted signal bandwidth for a given information bandwidth.

The manner in which two types of undesired SS signals affect the performance of FDM/FM systems is analyzed in this section. The characteristics of the two undesired SS signals are discussed next.

SPREAD-SPECTRUM SIGNALS

The two undesired SS signals analyzed were direct-sequence (DS) and frequency-hopping (FH). Brief descriptions of the DS and FH techniques are given here with detailed descriptions of these and additional SS modulation techniques available in Dixon.³⁴

Direct Sequence

The DS method of generating the wideband signal consists of appropriately combining the digital baseband data with a high-

³⁴Dixon, R. C., *Spread Spectrum Systems*, John Wiley and Sons, New York, 1976.

speed (relative to the data rate of the baseband desired signal) binary code sequence and then using the resulting sequence to modulate a carrier. The signaling speed of the code sequence is termed the chip rate, while the term bit rate is reserved for the speed of the baseband data. Theoretically, any suitable form of amplitude or angle modulation may be used, with some form of phase-shift keying commonly employed. Direct sequence systems are also sometimes called pseudonoise (PN) systems.

Frequency Hopping

The FH technique consists of generating the broad spectrum by hopping the carrier frequency among a number of frequencies over a wide band at some rate, with the specific order of frequency selection controlled by a code sequence. The SS system requirements determine the number of frequencies used and the hopping rate.

MEASUREMENT DESCRIPTION AND RESULTS FOR DIRECT-SEQUENCE SPREAD-SPECTRUM (DSSS) INTERFERENCE

DSSS Signal Generation and Characteristics

The DSSS signal was generated by a direct sequence biphase modulator. A block diagram of the DSSS interference generator setup is shown in Figure 106. The mainlobe bandwidth of the DSSS signal is twice the clock rate of the modulating code sequence. The measured spectral characteristics of the BPSK DSSS interference signals used in the measurements are shown in Figures 107, 108 and 109 for code rates (R_c) of 125 Kb/s, 2.5 Mb/s and 5 Mb/s respectively. As expected, the DS modulation produces a $[(\sin x)/x]^2$ power spectrum with approximately 90% of the power contained in the mainlobe.

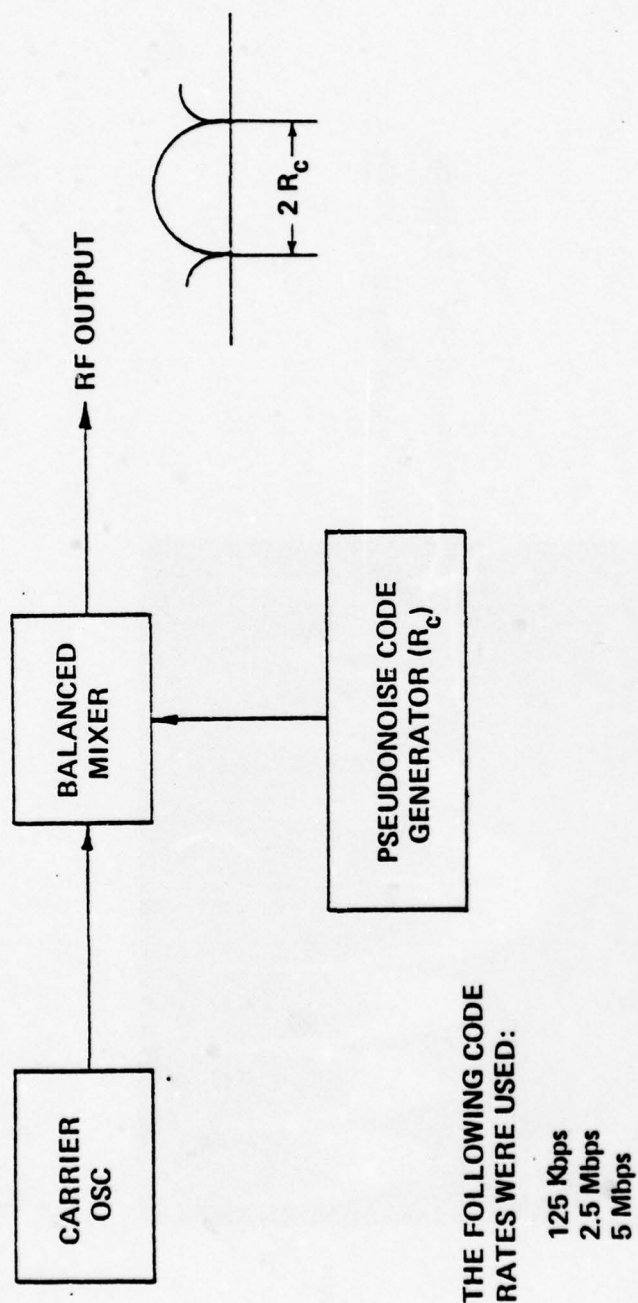


Figure 106. BPSK DS interference generator.

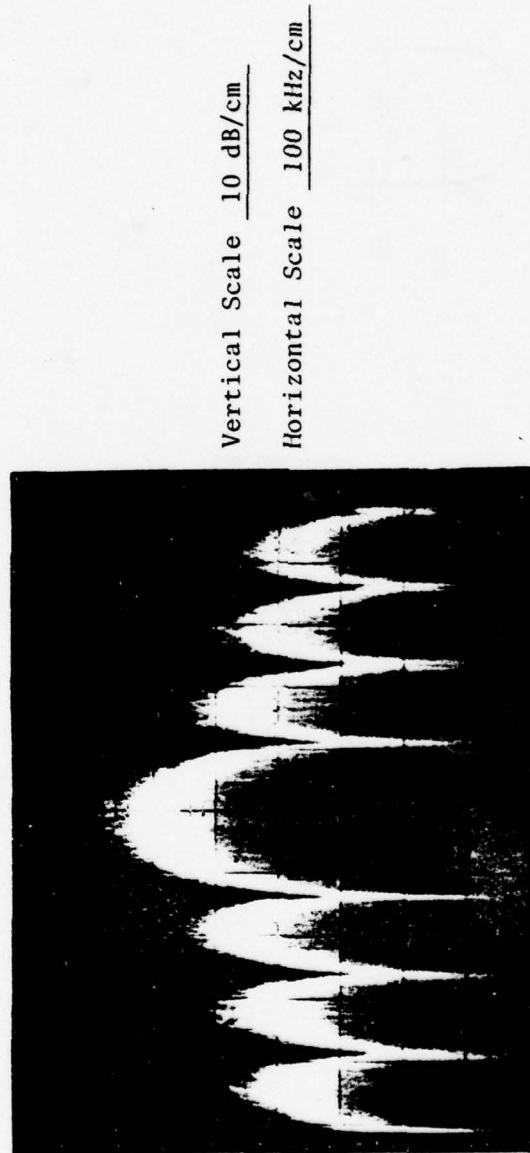


Figure 107. DSSS signal, 180° biphase-modulated by a 125-kbps code.

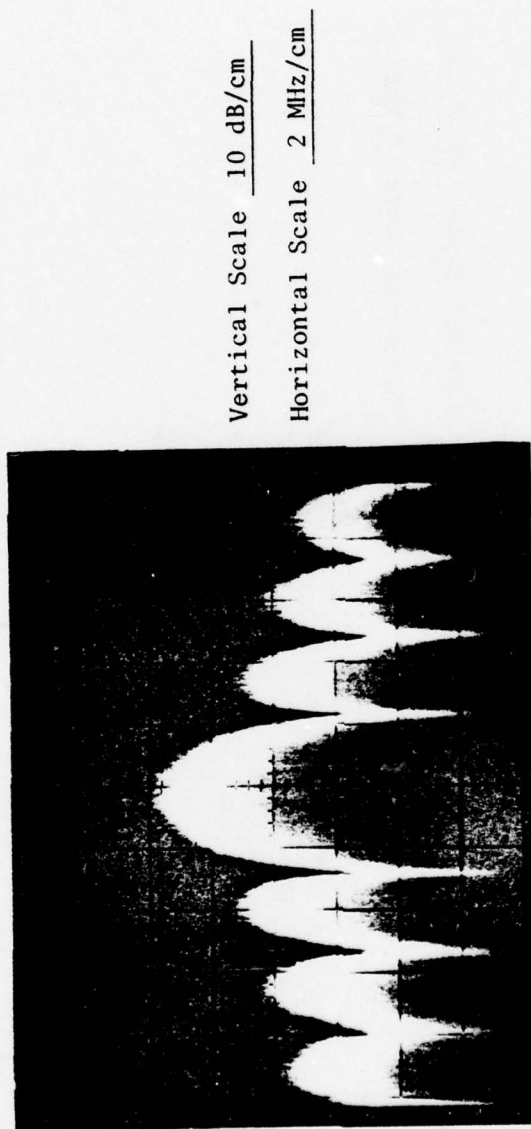


Figure 108. DSSS signal, 180° biphase-modulated by a 2.5-Mbps code.

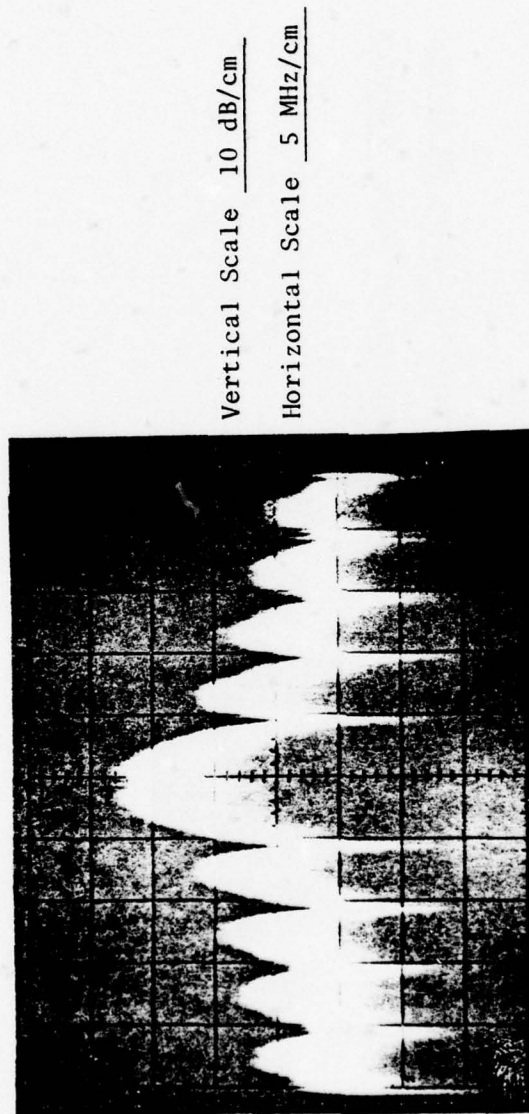


Figure 109. DSSS signal, 180° biphase-modulated by a 5-Mbps code.

Measurement Results

The data analyzed indicates that the DSSS interference can be treated as an equivalent average power FM carrier whose RMS deviation (D'_{rms}) corresponds to $1.6 R_c$, where R_c is the modulating code rate. The processing gain of FDM/FM systems when exposed to BPSK DSSS interference can be calculated from the FM equations given in Section 6 by substituting $1.6 R_c$ for D'_{rms} .

Following this treatment, the processing gain, and from this the S/N power ratio, were calculated for the system tested (see TABLE 8, Section 4) using Equations 89 (Section 6) and 32 (Section 4). The results for on-tune and off-tuned BPSK DSSS interference are shown compared with measured data in Figures 110 through 121. The results of these comparisons indicate that, for on-tune BPSK DSSS interference, good agreement exists between the measured and calculated processing gains values. For the case of off-tuned BPSK DSSS interference, the comparisons between the measured and calculated results indicate that Equation 89 adequately predicts the off-tuning characteristics for frequency separations up to approximately $F_H + (1.6 R_c)$. For frequency separations greater than approximately $F_H + (1.6 R_c)$ but less than $B_{\text{IF}}/2$, the calculated off-tuning rejection tends to be greater than the measured off-tuning rejection. For frequency separation greater than $B_{\text{IF}}/2$, the off-frequency rejection due to the IF filter should be added to Equation 89.

MEASUREMENT DESCRIPTION AND RESULTS FOR FREQUENCY-HOPPING SPREAD-SPECTRUM (FHSS) INTERFERENCEFHSS Signal Generation and Characteristics

The FHSS signal was generated by a frequency synthesizer/balanced mixer combination capable of responding to coded outputs

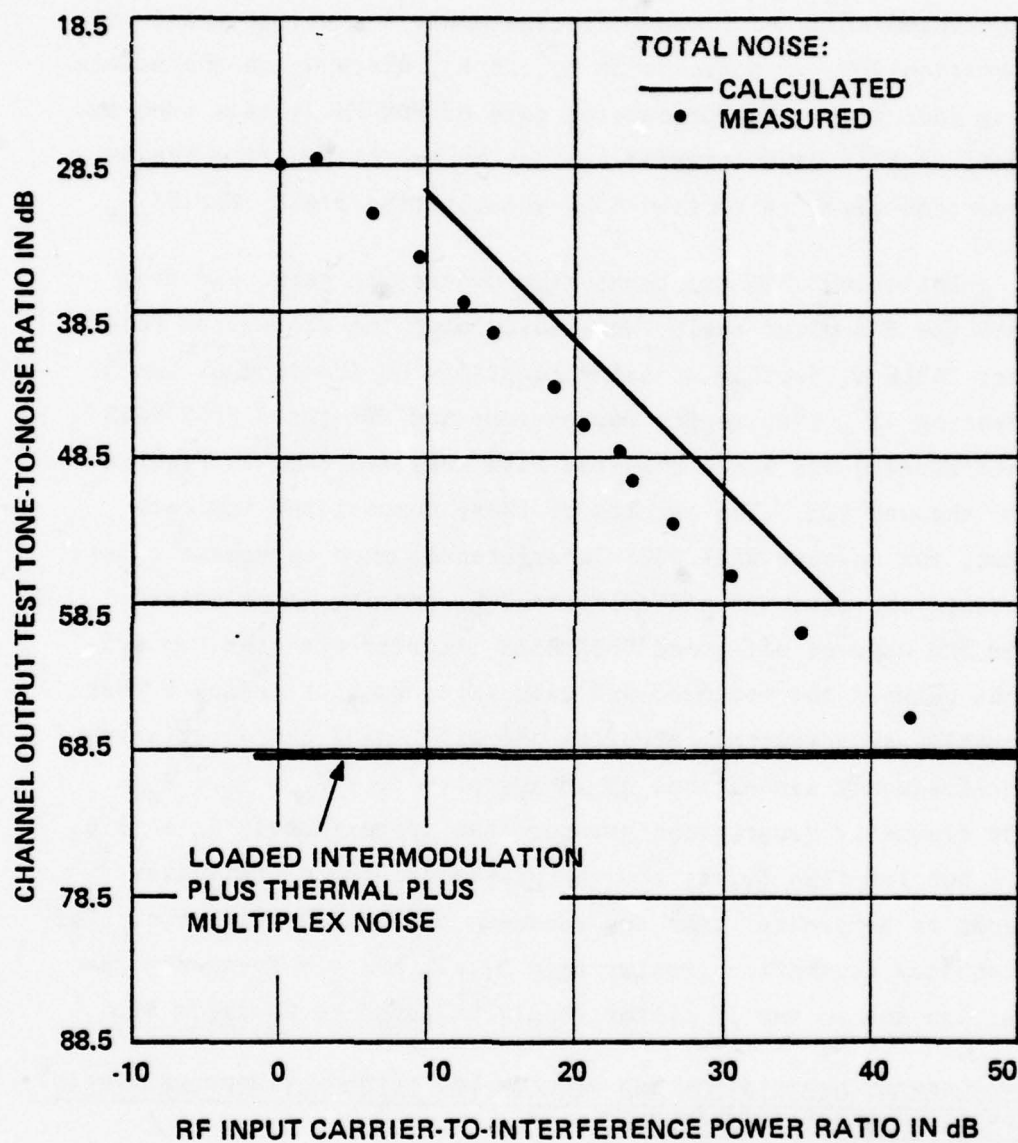


Figure 110. Transfer function for on-tune DSSS interference 180° biphase-modulated by a 125-kbps code; low test channel (340-344 kHz).

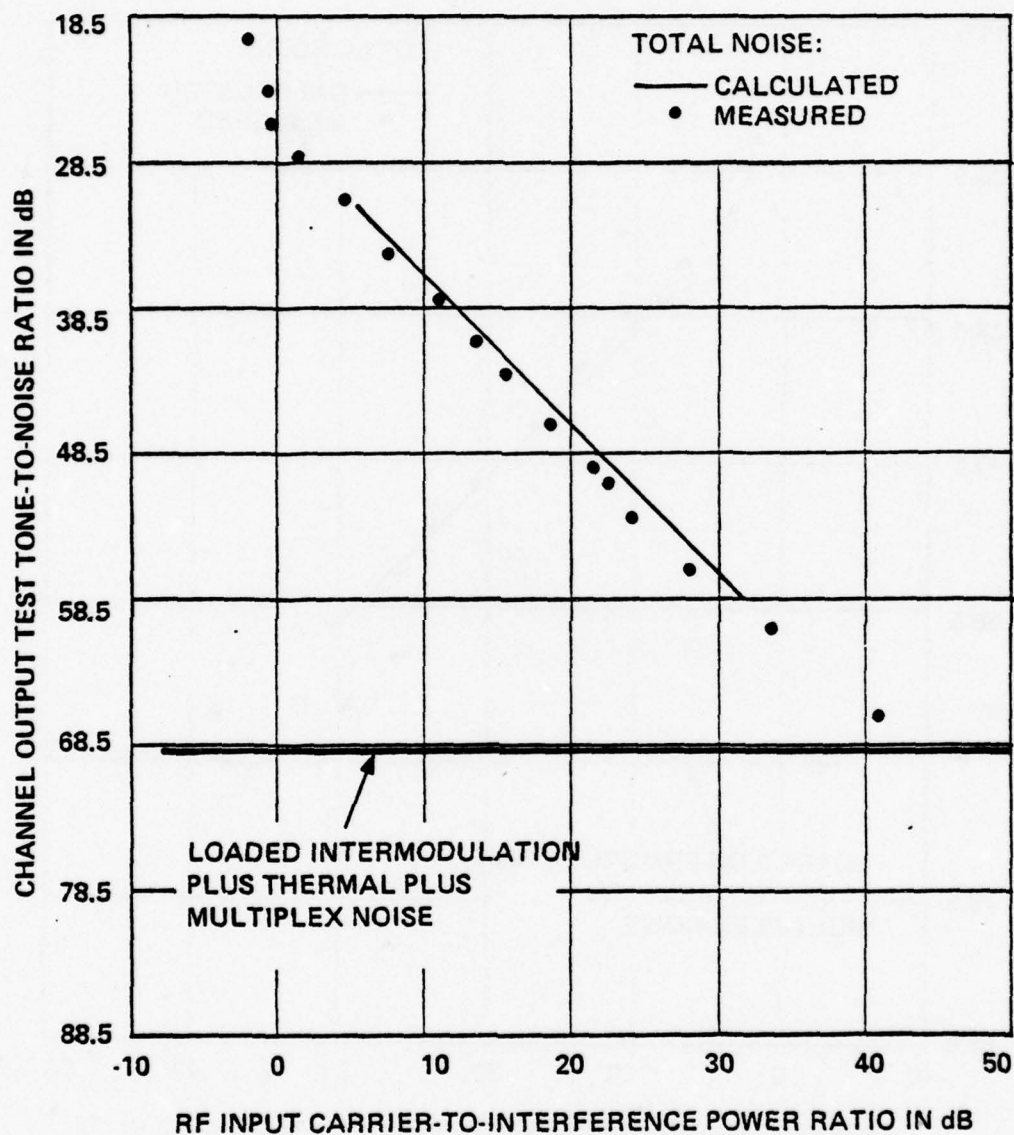


Figure 111. Transfer function for on-tune DSSS interference 180° biphase-modulated by a 2.5-Mbps code; low test channel (340-344 kHz).

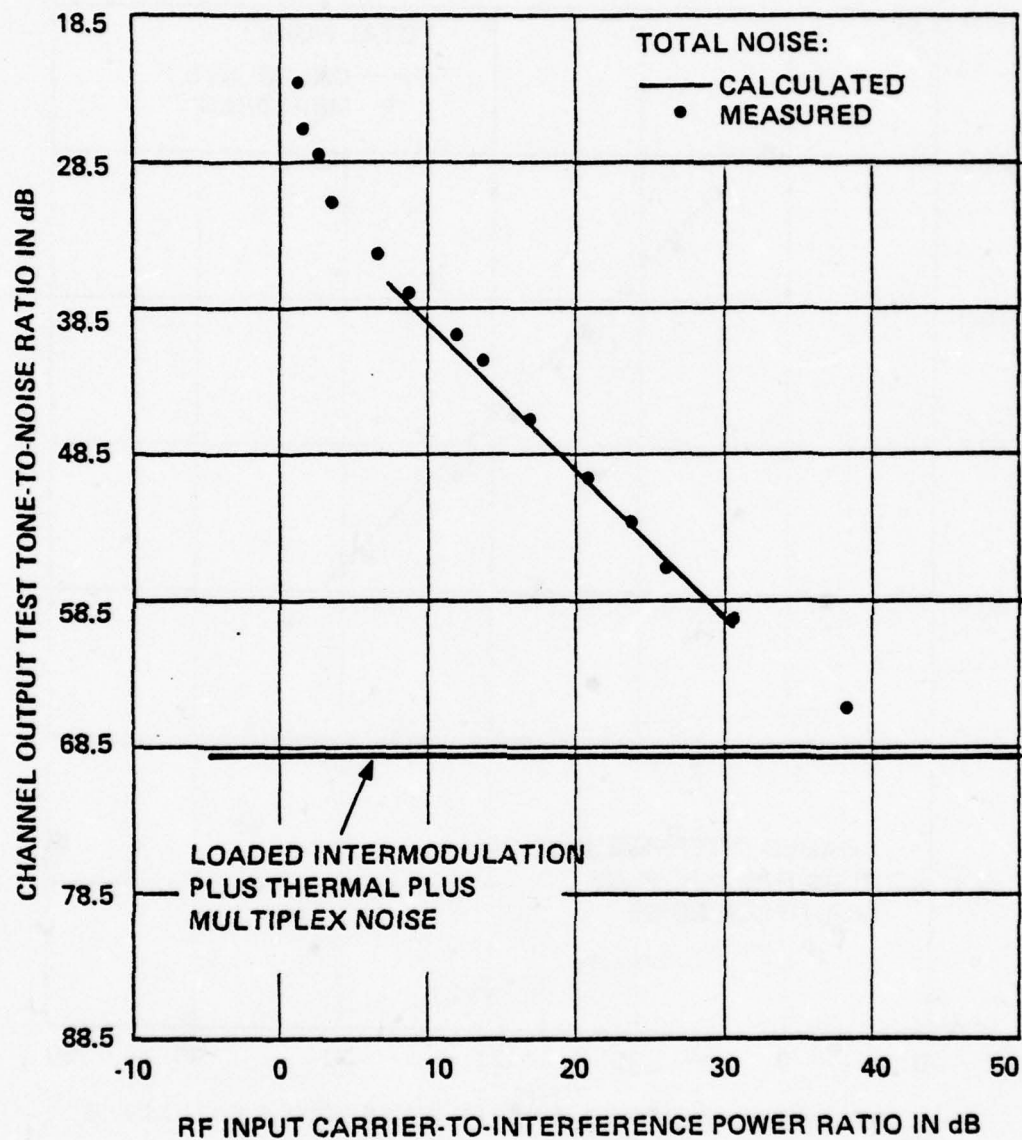


Figure 112. Transfer function for on-tune DSSS interference 180° biphase-modulated by a 5-Mbps code; low test channel (340-344 kHz).

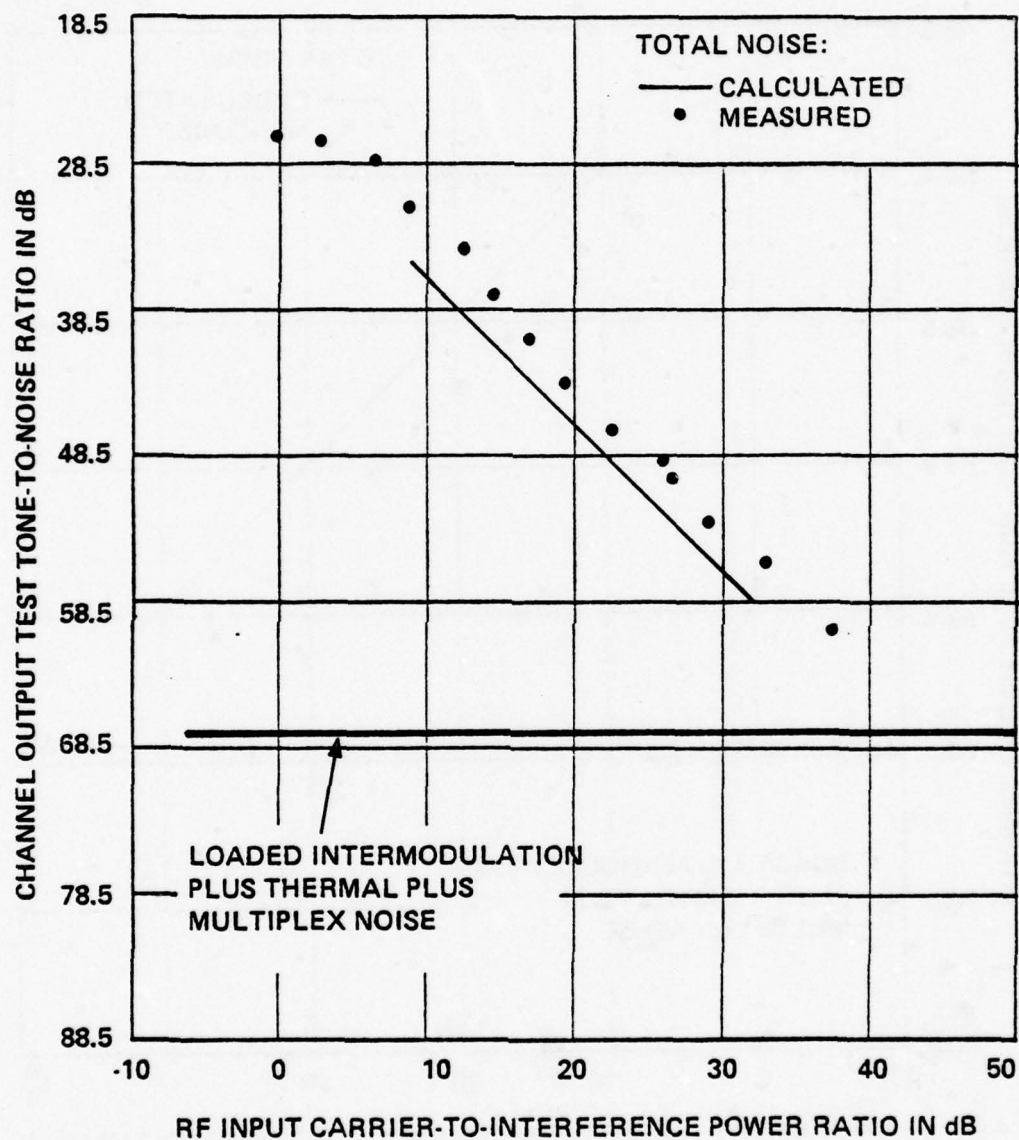


Figure 113. Transfer function for on-tune DSSS interference 180° biphas-modulated by a 125-kbps code; high test channel (2432-2436 kHz).

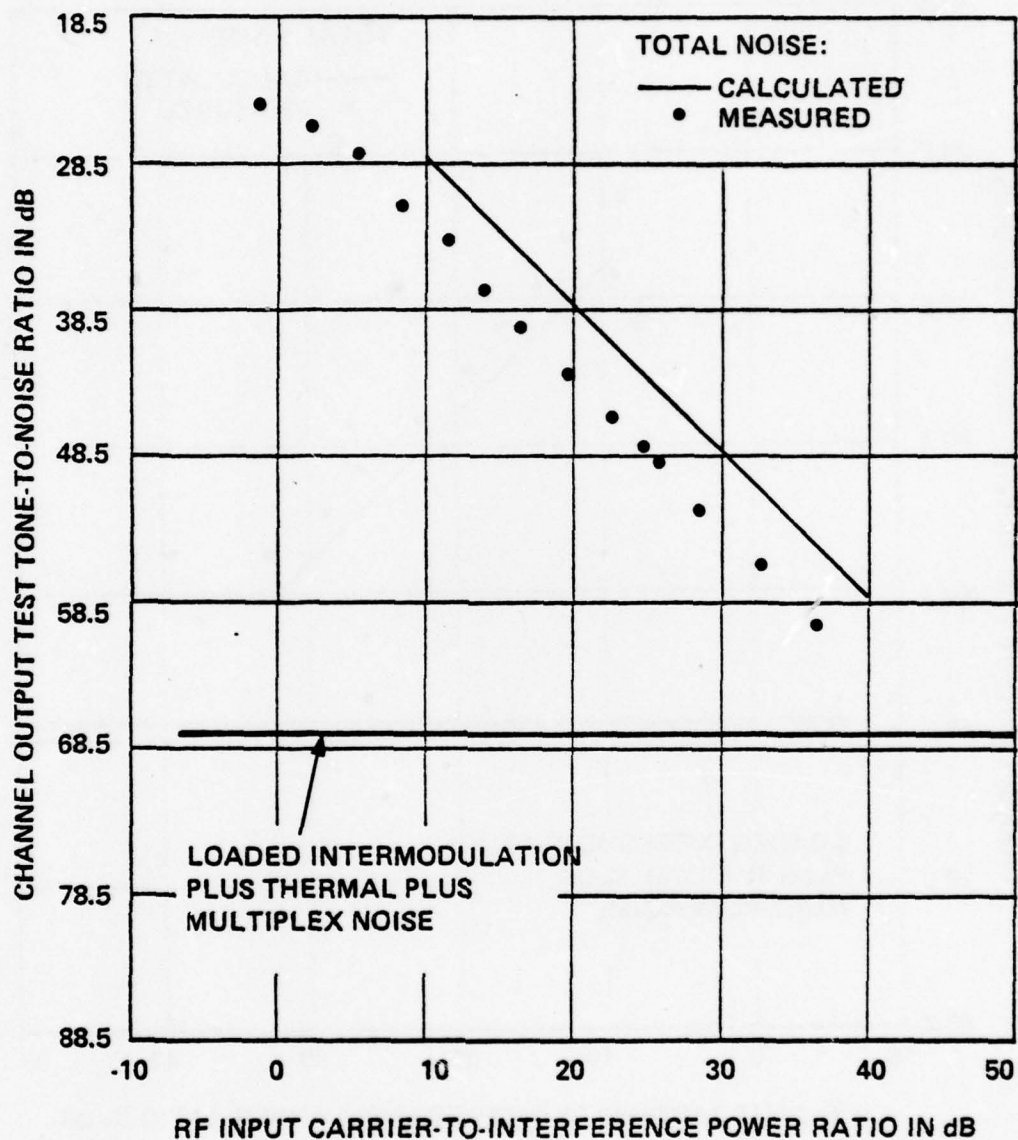


Figure 114. Transfer function for on-tune DSSS interference 180° biphase-modulated by a 2.5-Mbps code; high test channel (2432-2436 kHz).

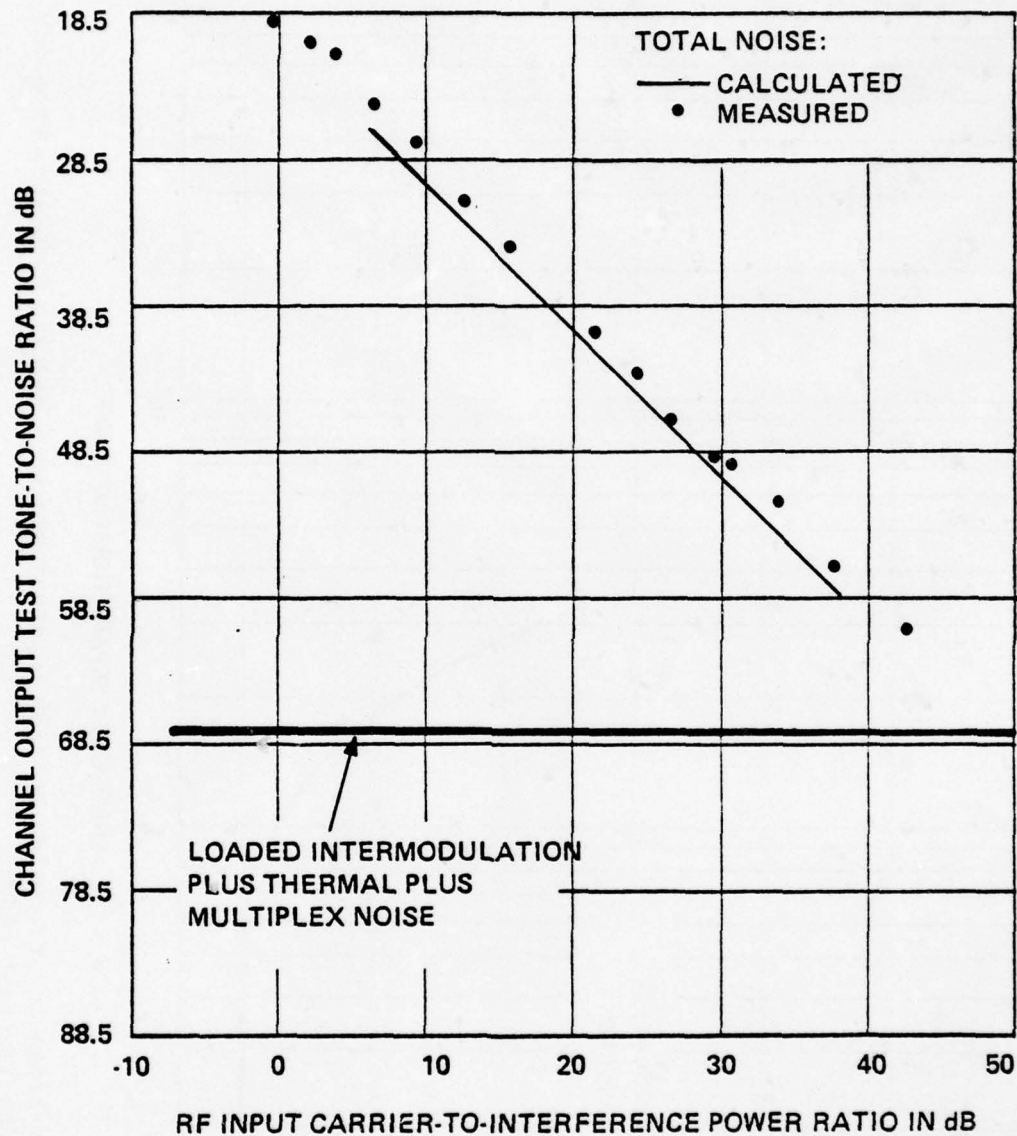


Figure 115. Transfer function for on-tune DSSS interference 180° biphas-modulated by a 5-Mbps code; high test channel (2432-2436 kHz).

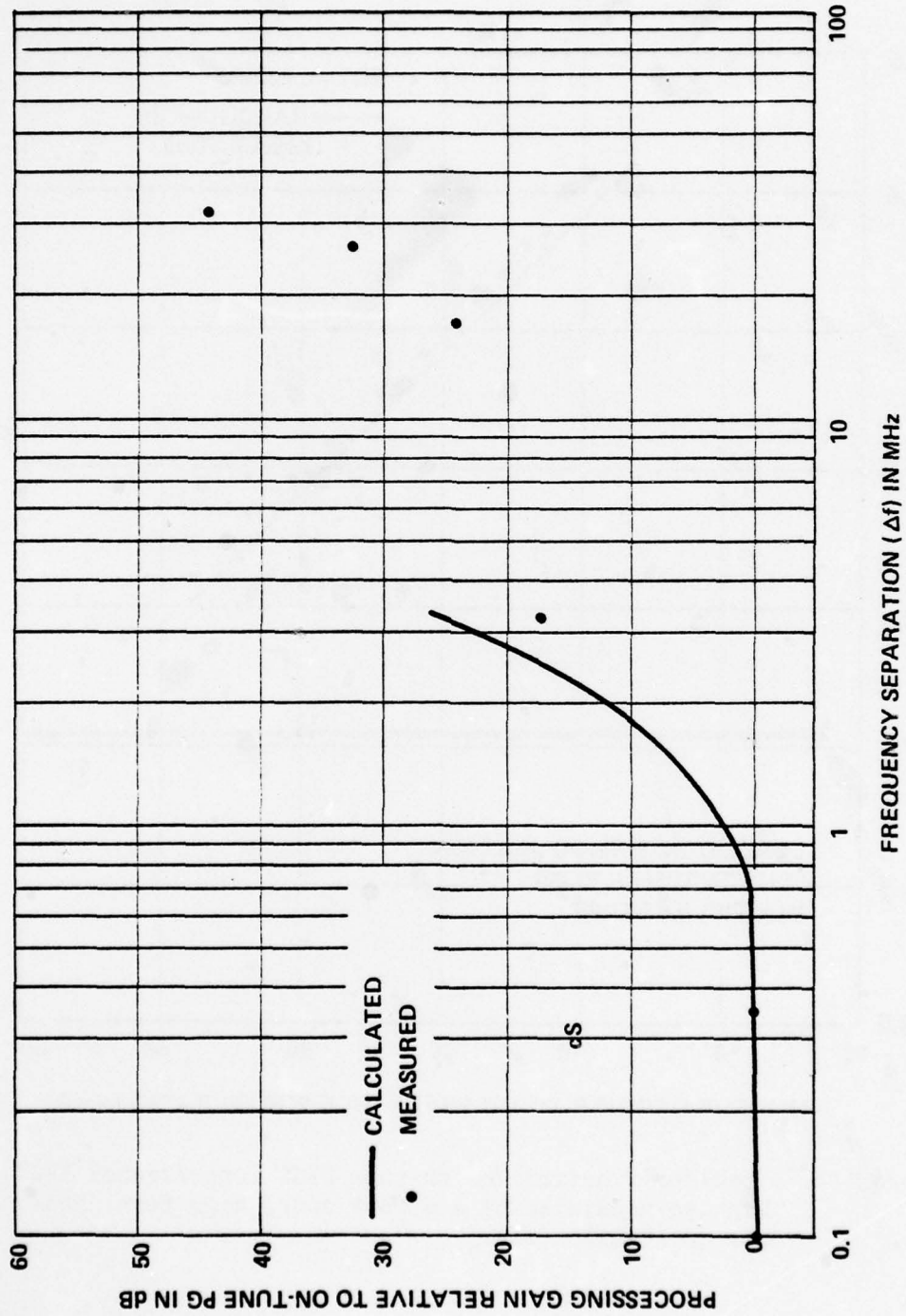


Figure 116. Off-frequency rejection to DSSS interference 180° biphas-modulated by a 125 kbps code; low test channel (340-344 kHz).

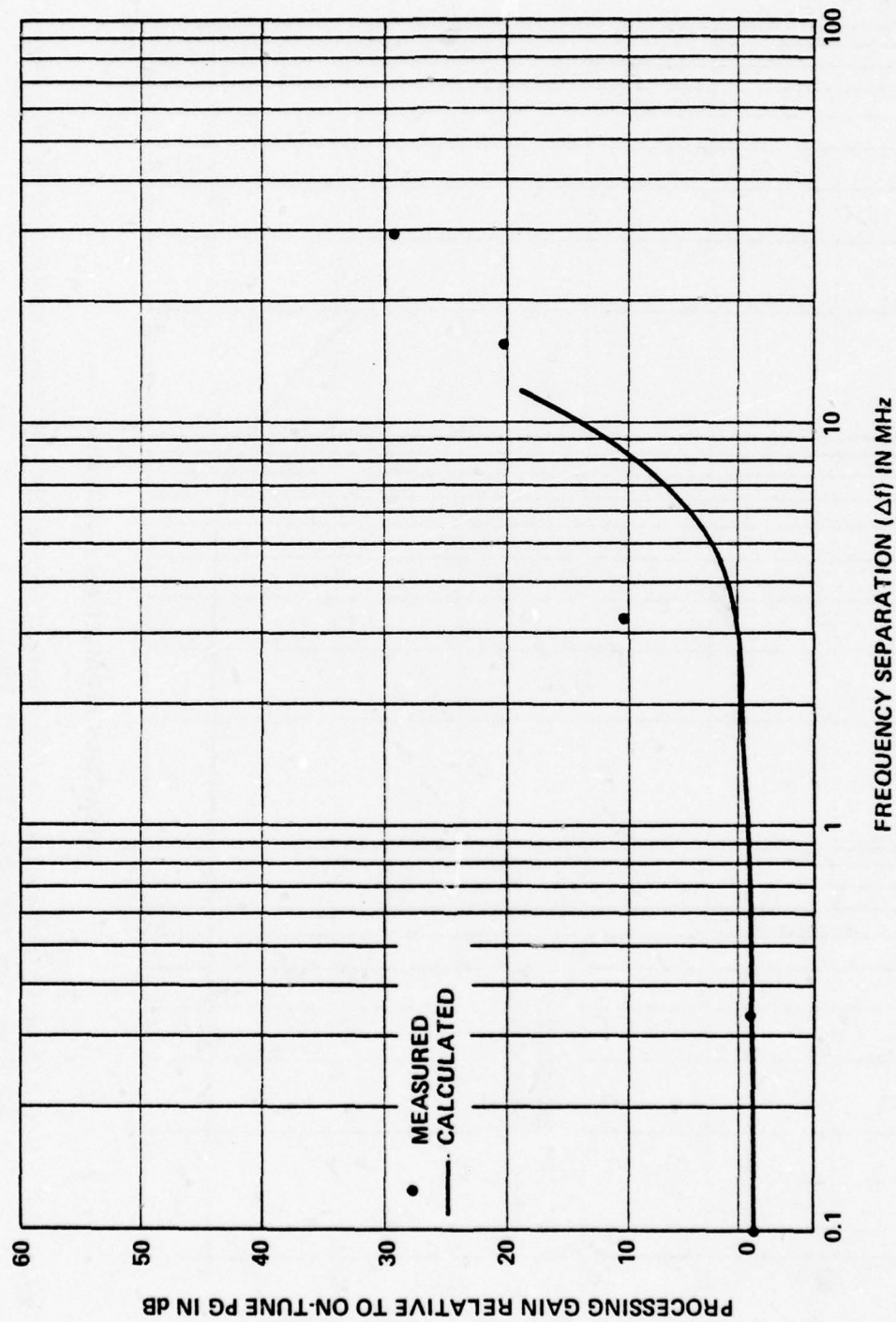


Figure 117. Off-frequency rejection to DSSS interference 180° biphase-modulated by a 2.5-Mbps code; low test channel (340-344 kHz).

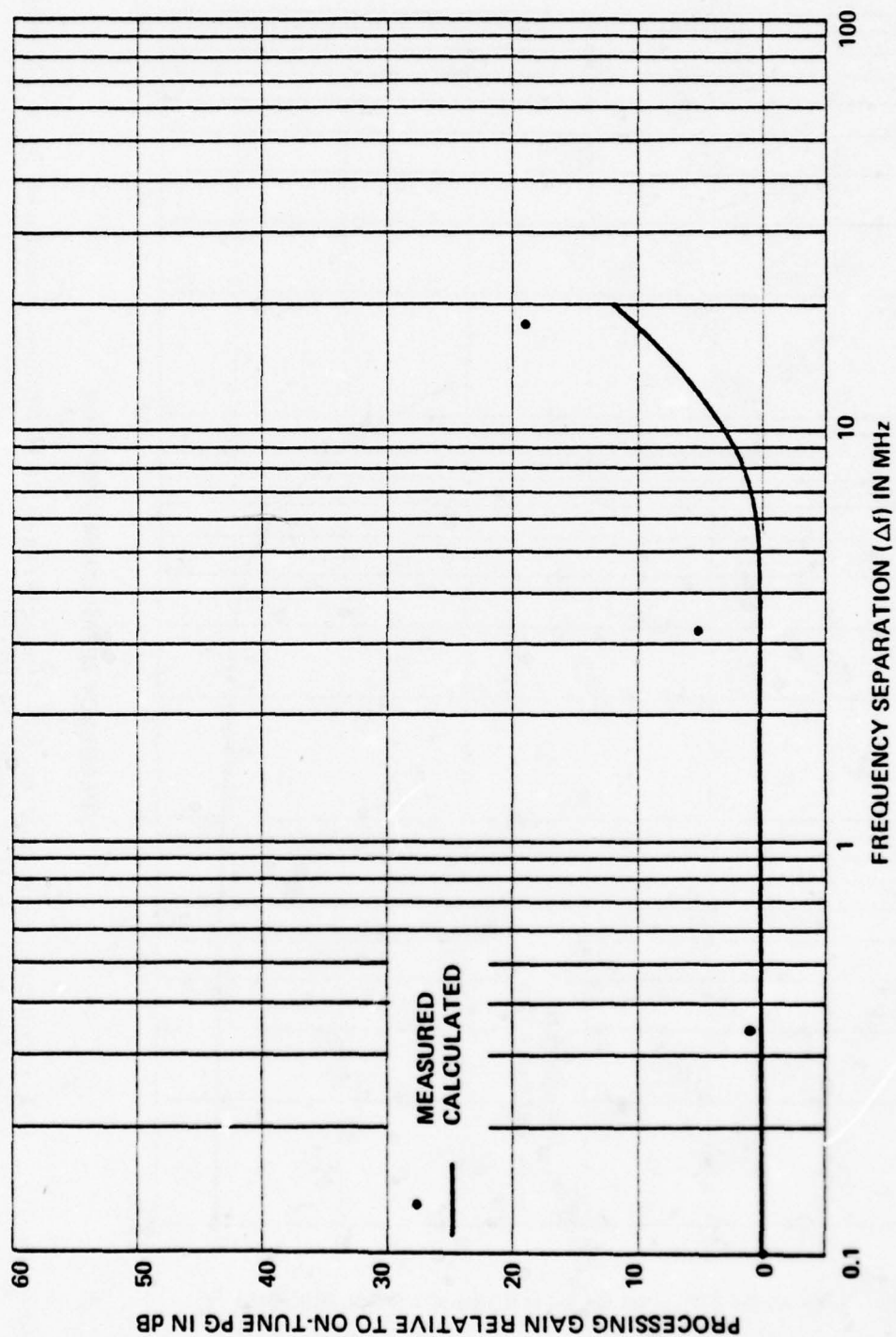


Figure 118. Off-frequency rejection to DSSS interference 180° biphas-modulated by a 5-Mbps code; low test channel (340-344 kHz).

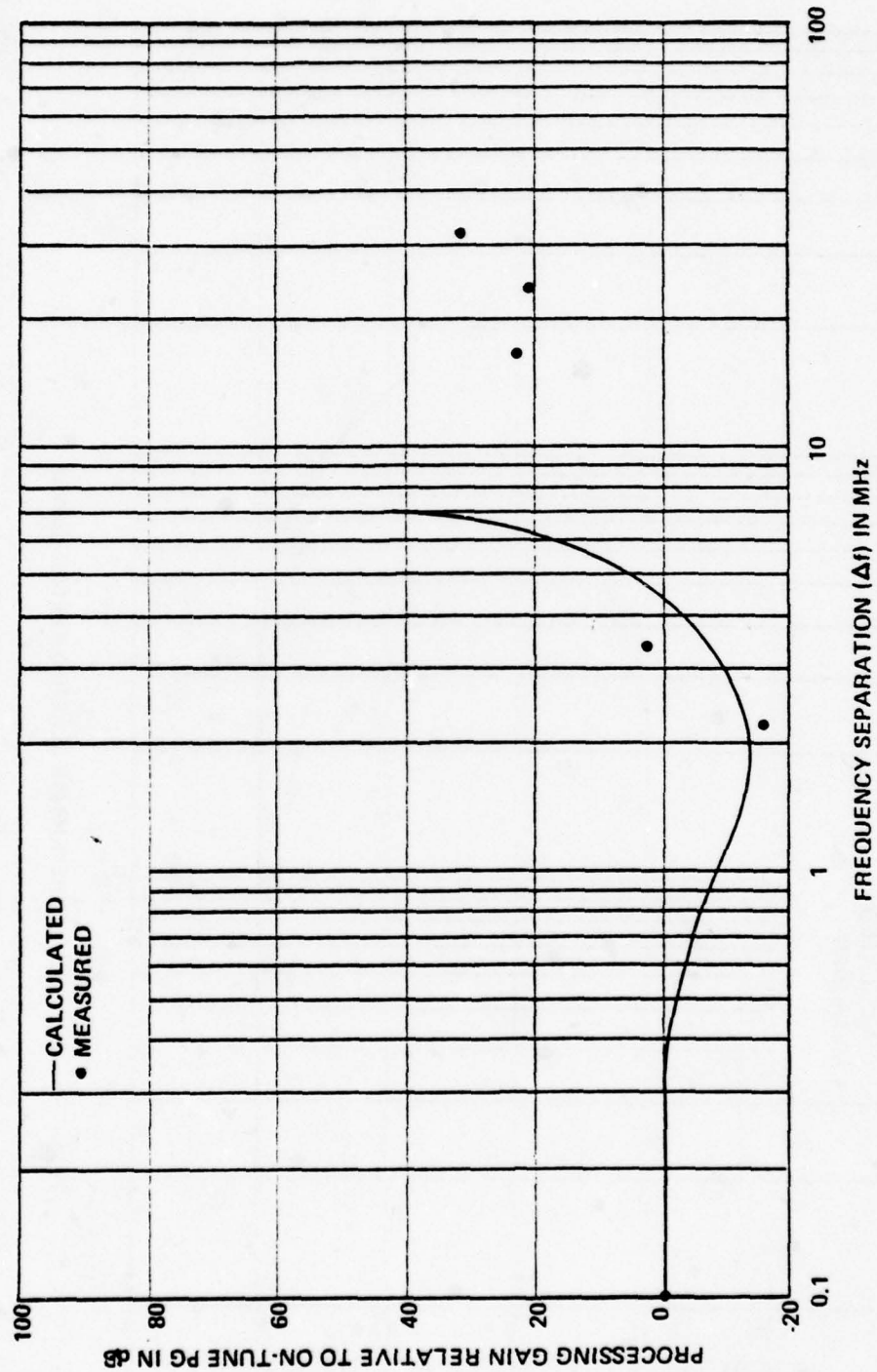


Figure 119. Off-frequency rejection to DSSS interference 180° biphas-modulated by a 125-kbps code; high test channel (2432-2436 kHz).

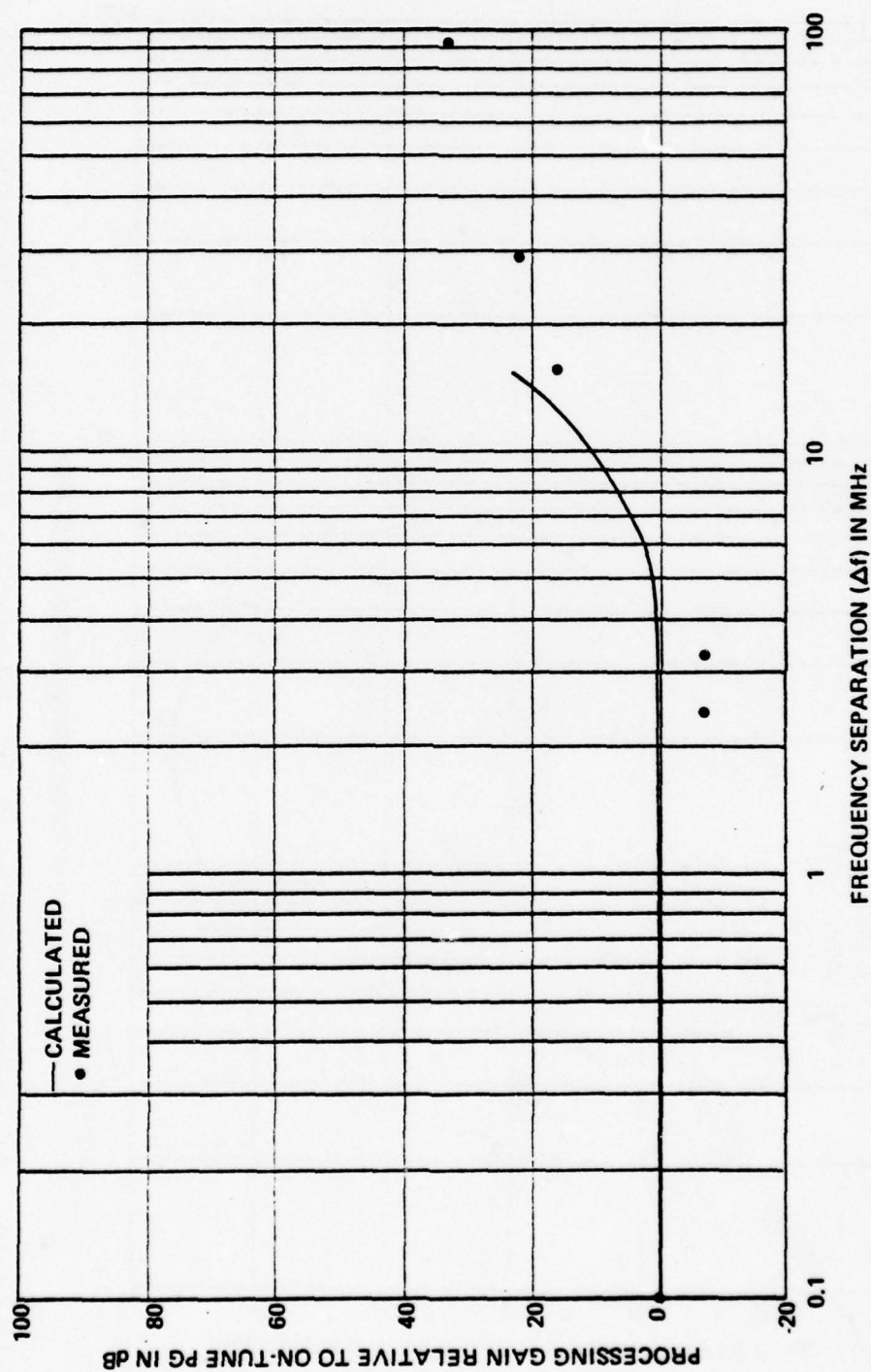


Figure 120. Off-frequency rejection to DSSS interference 180° biphase-modulated by a 2.5-Mbps code; high test channel (2432-2436 kHz).

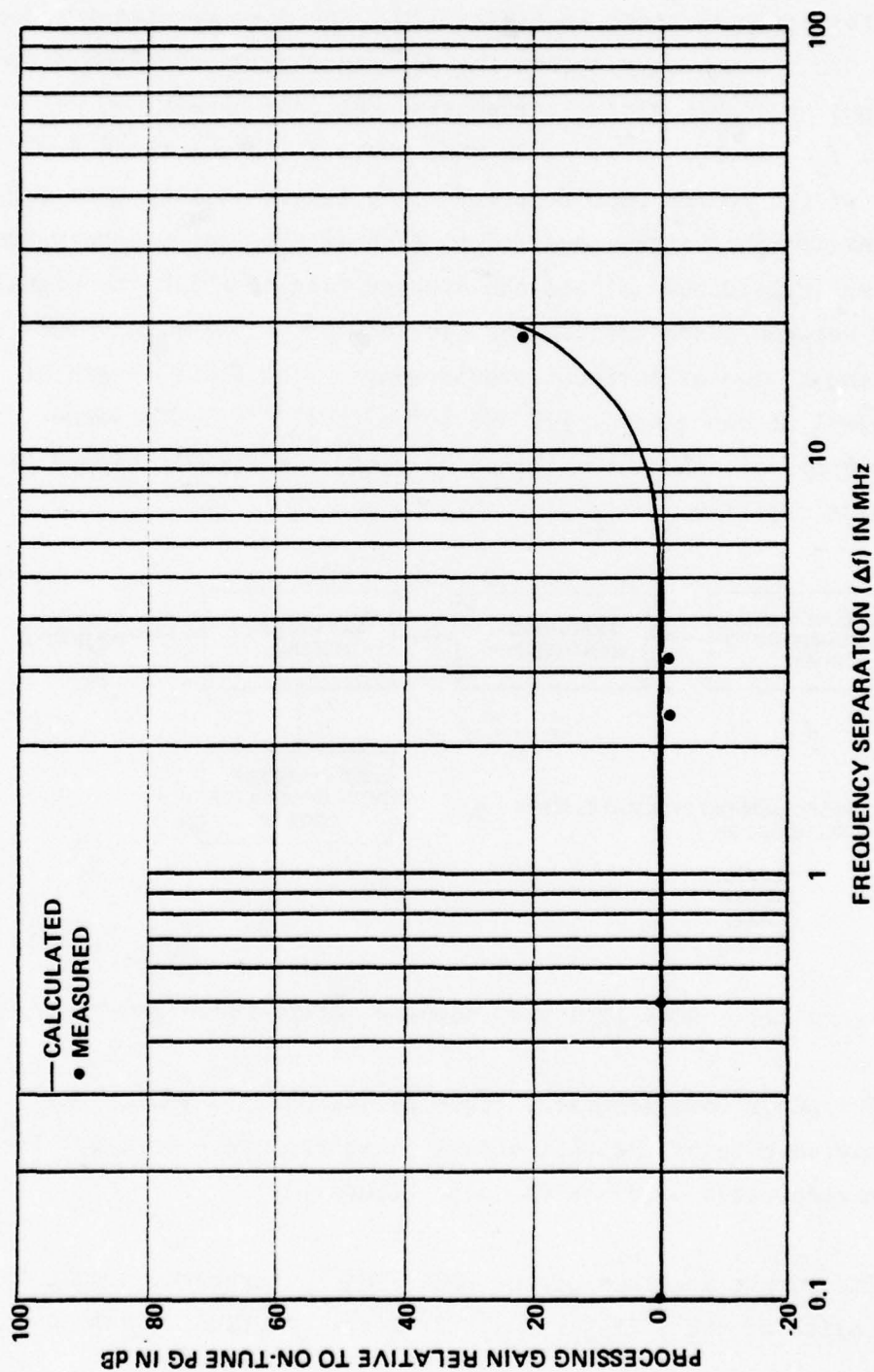


Figure 121. Off-frequency rejection to DSSS interference 180° biphase-modulated by a 5-Mbps code; high test channel (2432-2436 kHz).

from two code generators. A block diagram of the FHSS interference generator setup is shown in Figure 122. One code generator (code 1) was used to randomly select the RF frequency of the FHSS signal from four available discrete frequency choices, namely, f_0 , $f_0 + 14$ MHz, $f_0 - 14$ MHz and $f_0 + 25$ MHz, where f_0 is the tuned frequency of the FDM/FM test receiver. The length of time that the FHSS interference signal dwelled on each of the four discrete frequencies (0.1-10,000 μ s) and the average rate at which the signal hopped between these frequencies (10-10,000 hps) were adjusted according to the measurement requirements. The frame length of the code 1 sequence was 2,147,483,647 bits ($2^{31} - 1$, Mersenne prime generator) and was obtained by using a maximally tapped 31-bit shift register.

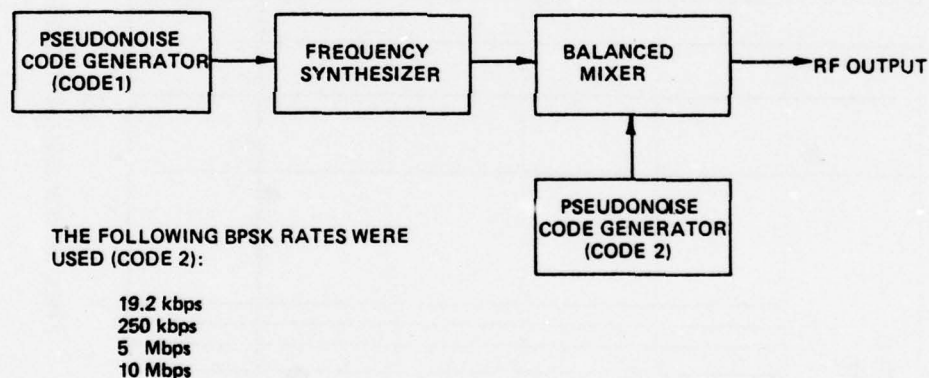


Figure 122. BPSK frequency-hopping interference generator.

The other code generator (code 2) was used to select the information rate of the BPSK signal being frequency hopped. The information rates used are shown in Figure 122.

The output spectrum of the BPSK FHSS interference signal is a composite of the BPSK $[(\sin x)/x]^2$ power spectrum, sidebands

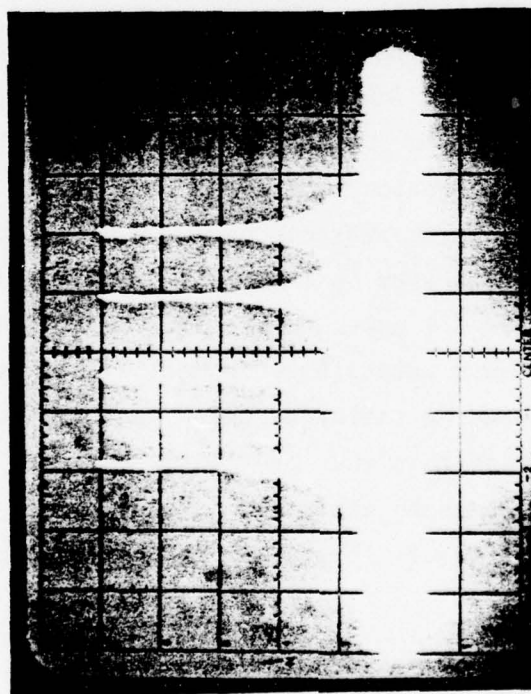
generated by hopping, and spurious frequencies generated as by-products. The measured spectral characteristics of four of the BPSK FHSS interference signals used in the measurements are shown in Figures 123 through 126.

Measurement Results

The results of the channel output noise measurements for BPSK FHSS interference are shown in Figures 127 through 153. From these measurements the following conclusions can be drawn:

1. The level of interference noise (for a constant C/I power ratio) in a multiplexer channel of a given FDM/FM system is primarily a function of the dwell time and the inband hop rate of the BPSK FHSS signal
2. The level of interference noise (for constant values of C/I, dwell time and inband average hop rate) in a multiplexer channel of a given FDM/FM system is only slightly dependent on the BPSK information code rate
3. The level of interference noise in a multiplexer channel of a given FDM/FM system is inversely proportional to the C/I power ratio. For C/I power ratios smaller than approximately 0 dB, the noise in a multiplexer channel will increase only slightly with decreasing ratios of C/I. Note further that this behavior is different than that previously observed for radar pulsed interference where the noise level remained practically constant for ratios of \hat{C}/\hat{I} smaller than approximately -2 dB.

The C/I power ratios for the BPSK FHSS interference were calculated from the measured \hat{C}/\hat{I} power ratios as follows:



Spectrum Analyzer:
Vertical Scale 10 dB/cm
Horizontal Scale 10 MHz/cm
Bandwidth 100 kHz
FHSS Signal:
Dwell Time 100 μ s
Average Hop Rate 1000 hps
BPSK Code 19.2 kbps

Figure 123. FHSS signal, 180° biphase-modulated by a 19.2-kbps code.

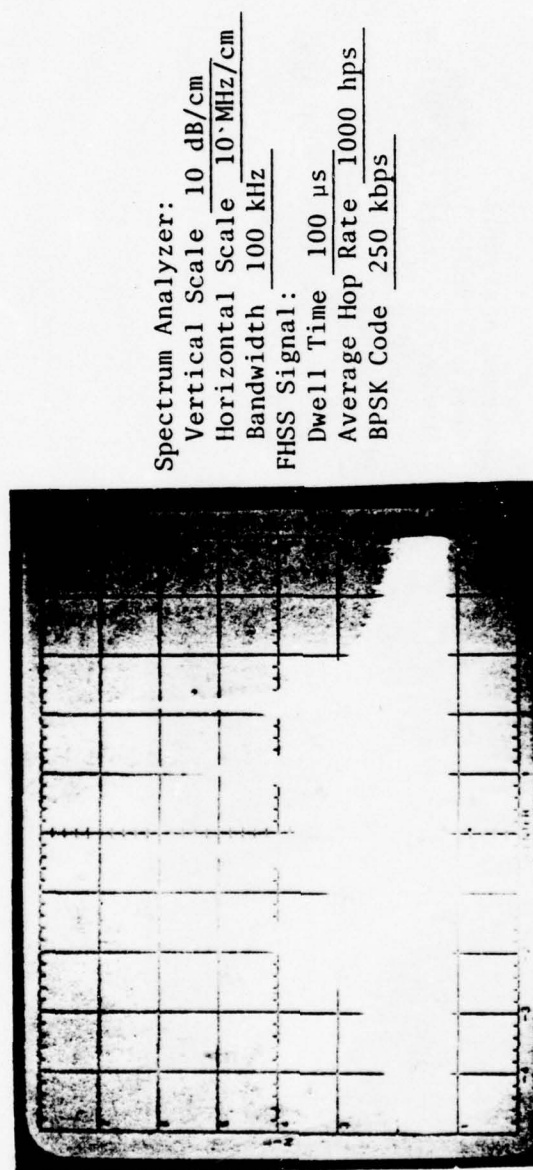


Figure 124. FHSS signal, 180° biphase-modulated by a 250-kbps code.

Spectrum Analyzer:
Vertical Scale 10 dB/cm
Horizontal Scale 20 MHz/cm
Bandwidth 300 kHz
FHSS Signal:
Dwell Time 100 μ s
Average Hop Time 1000 hps
BPSK Code 5 Mbps

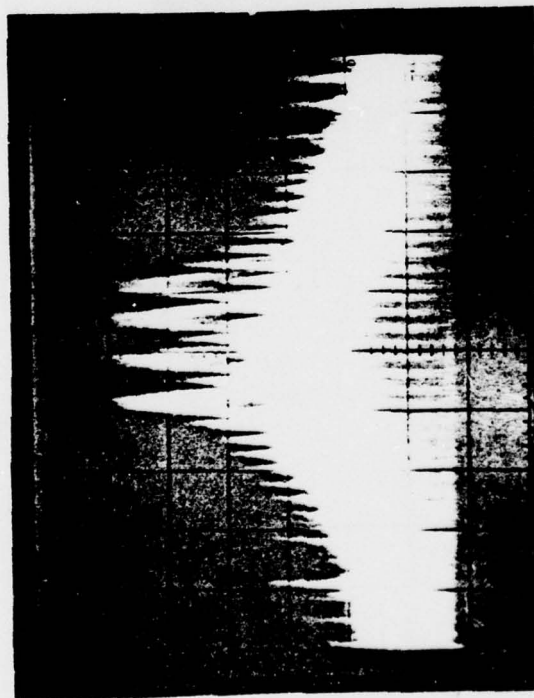


Figure 125. FHSS signal, 180° biphase-modulated by a 5-Mbps code.



Spectrum Analyzer:
Vertical Scale 10 dB/cm
Horizontal Scale 20 MHz/cm
Bandwidth 300 kHz
FHSS Signal:
Dwell Time 100 μ s
Average Hop Rate 100 hps
BPSK Code 10 Mbps

Figure 126. FHSS signal, 180° biphase-modulated by a 10 Mbps code.

$$C/I = (C/\hat{I}) - 10 \log \left[\begin{array}{l} \text{(dwell time)} \\ \text{(seconds)} \\ \text{(inband average hop rate)} \\ \text{(hops per second)} \end{array} \right]. \quad (95)$$

The data presented in Figures 127 through 153 can be used to predict the degradation in FDM/FM systems whose modulation characteristics and channel capacities differ from those of the system tested. For those cases, the processing gain corrections outlined in Section 7 should be applied to the data.

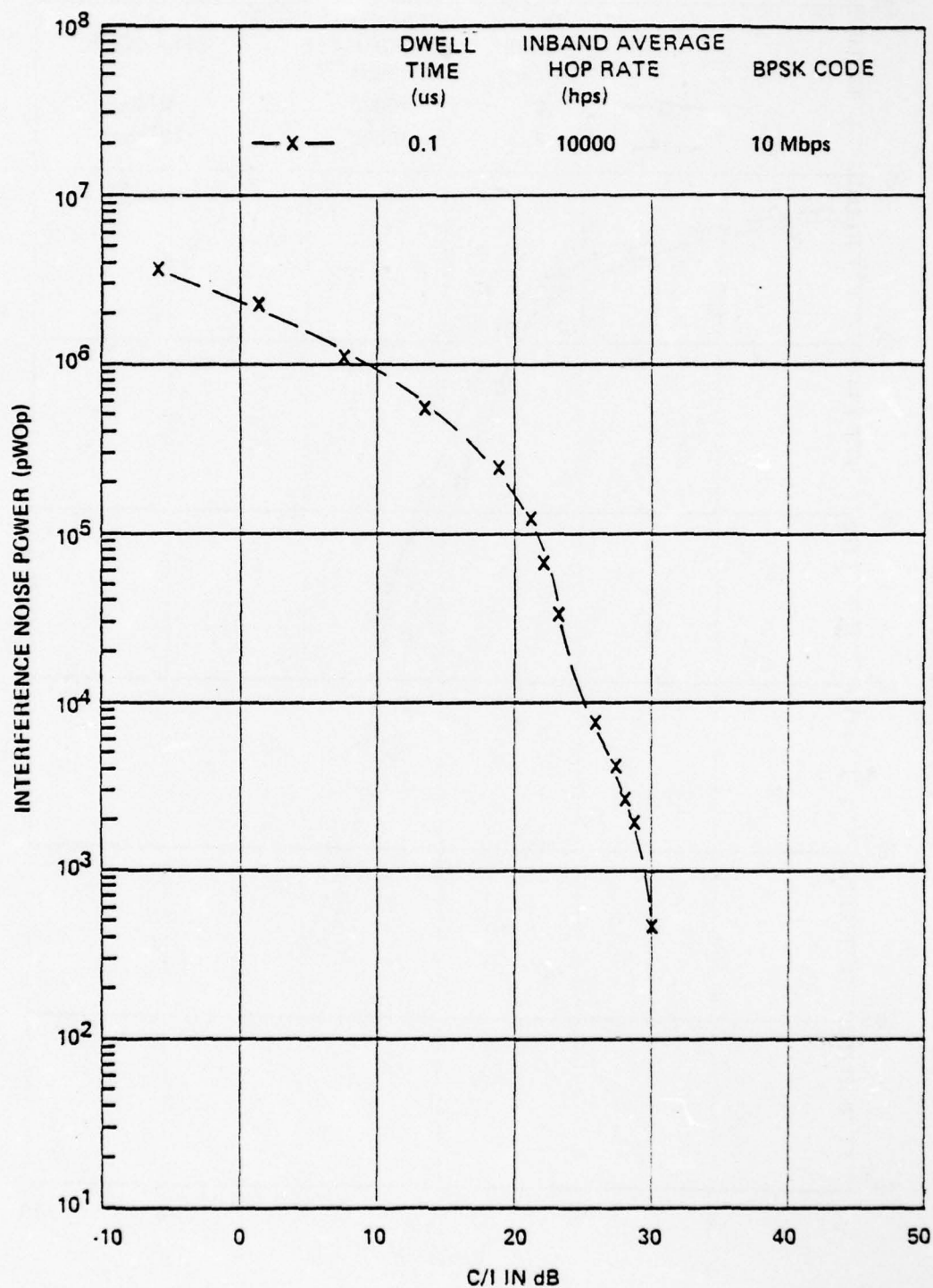


Figure 127. Measured interference noise power in a low baseband channel (340-344 kHz) for BPSK FHSS interference; dwell time = 0.1 μ s, inband average hop rate = 10,000 hps.

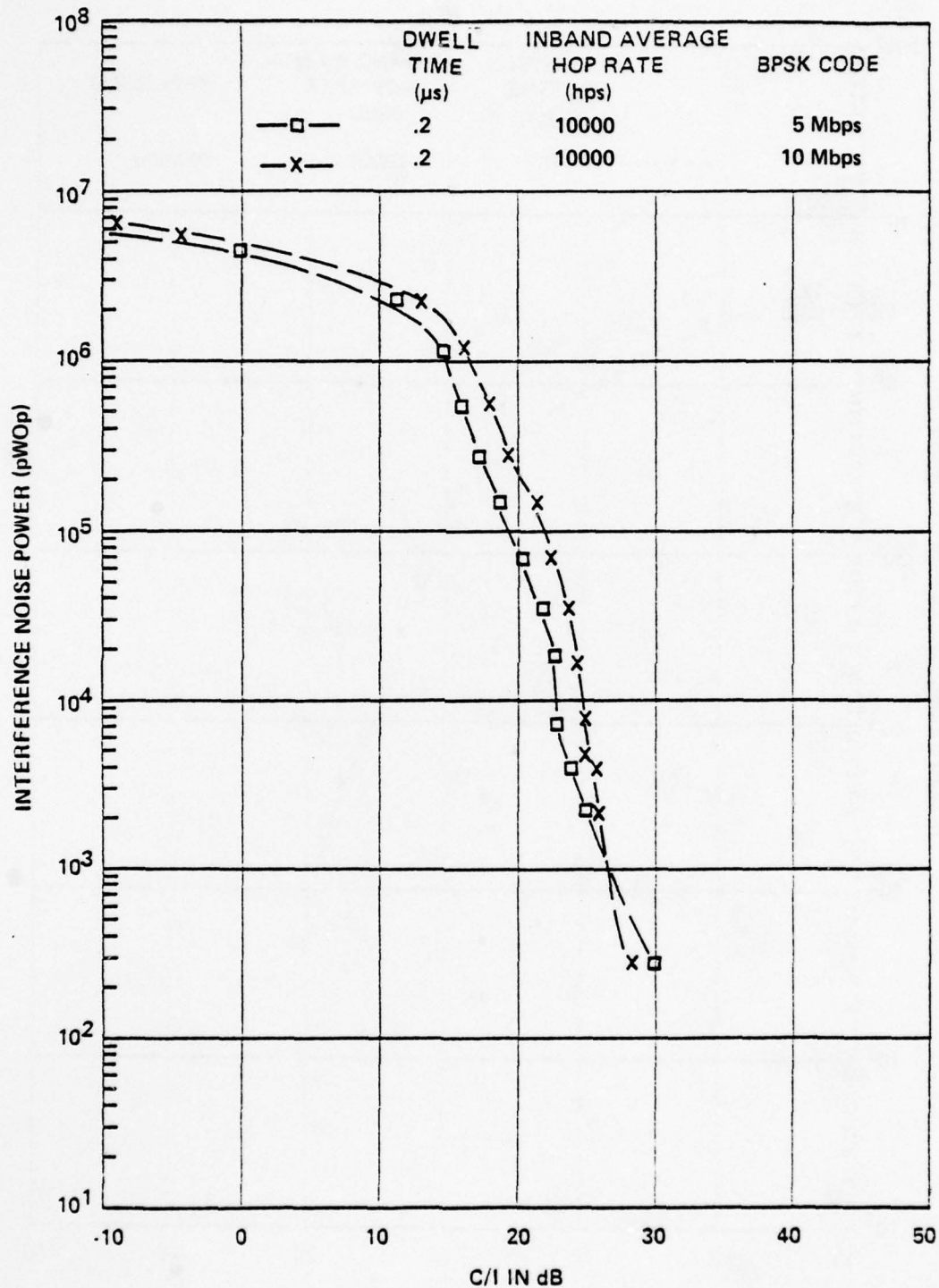


Figure 128. Measured interference noise power in a low baseband channel (340-344 kHz) for BPSK FHSS interference; dwell time = 0.2 μ s, inband average hop rate = 10,000 hps.

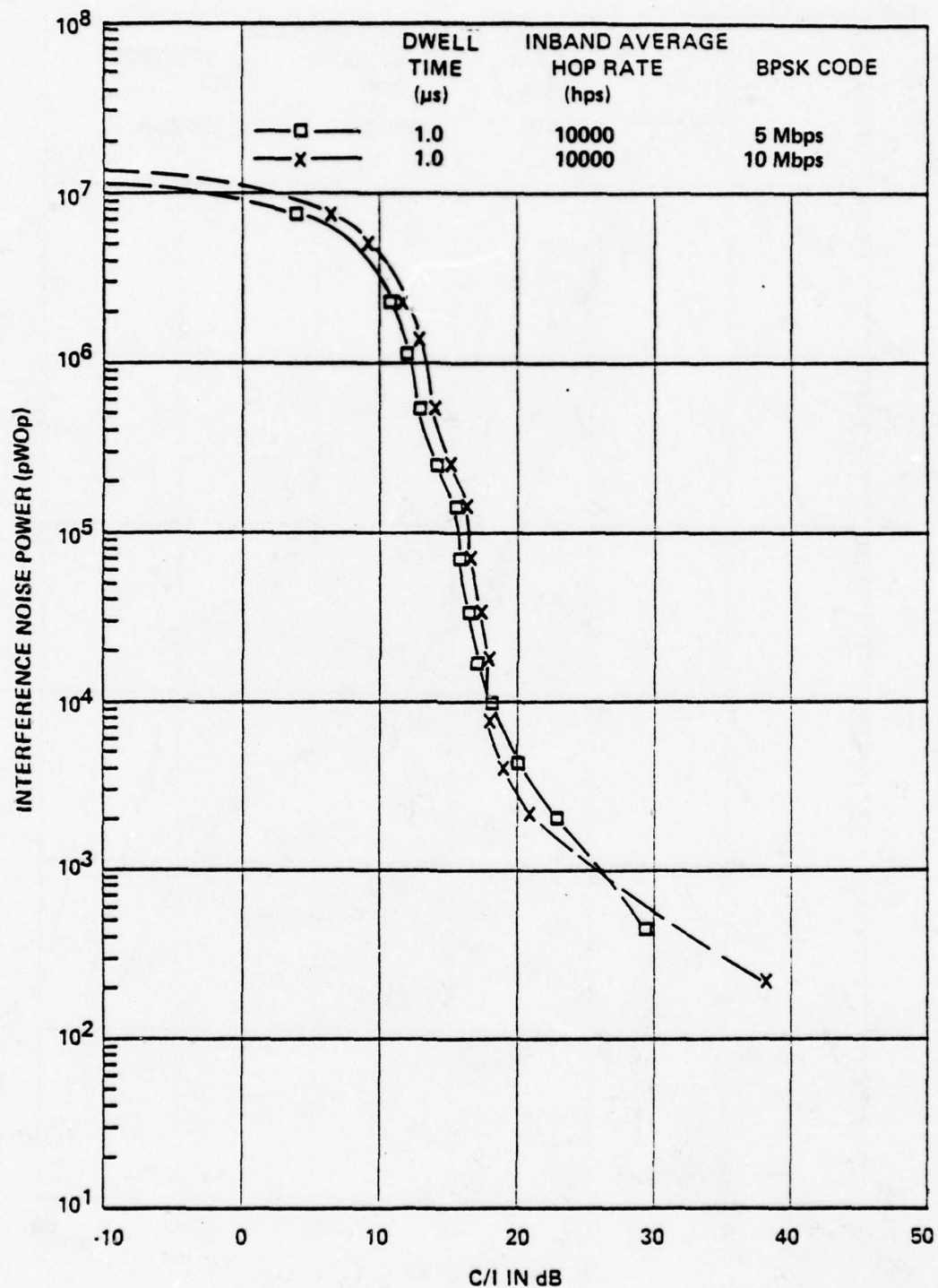


Figure 129. Measured interference noise power in a low baseband channel (340-344 kHz) for BPSK FHSS interference; dwell time = 1 μ s, inband average hop rate = 10,000 hps.

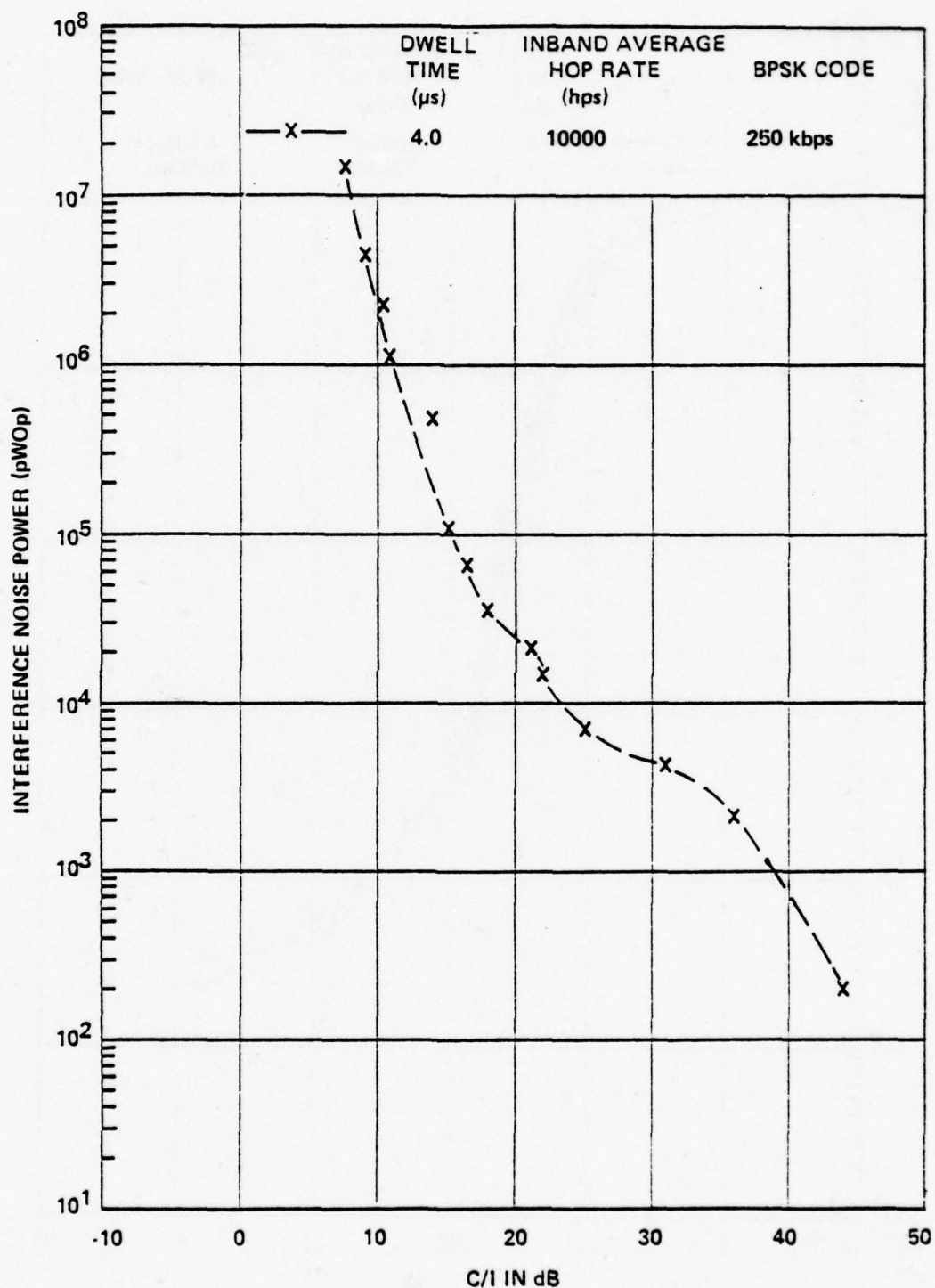


Figure 130. Measured interference noise power in a low baseband channel (340-344 kHz) for BPSK FHSS interference; dwell time = 4.0 μs, inband average hop rate = 10,000 hps.

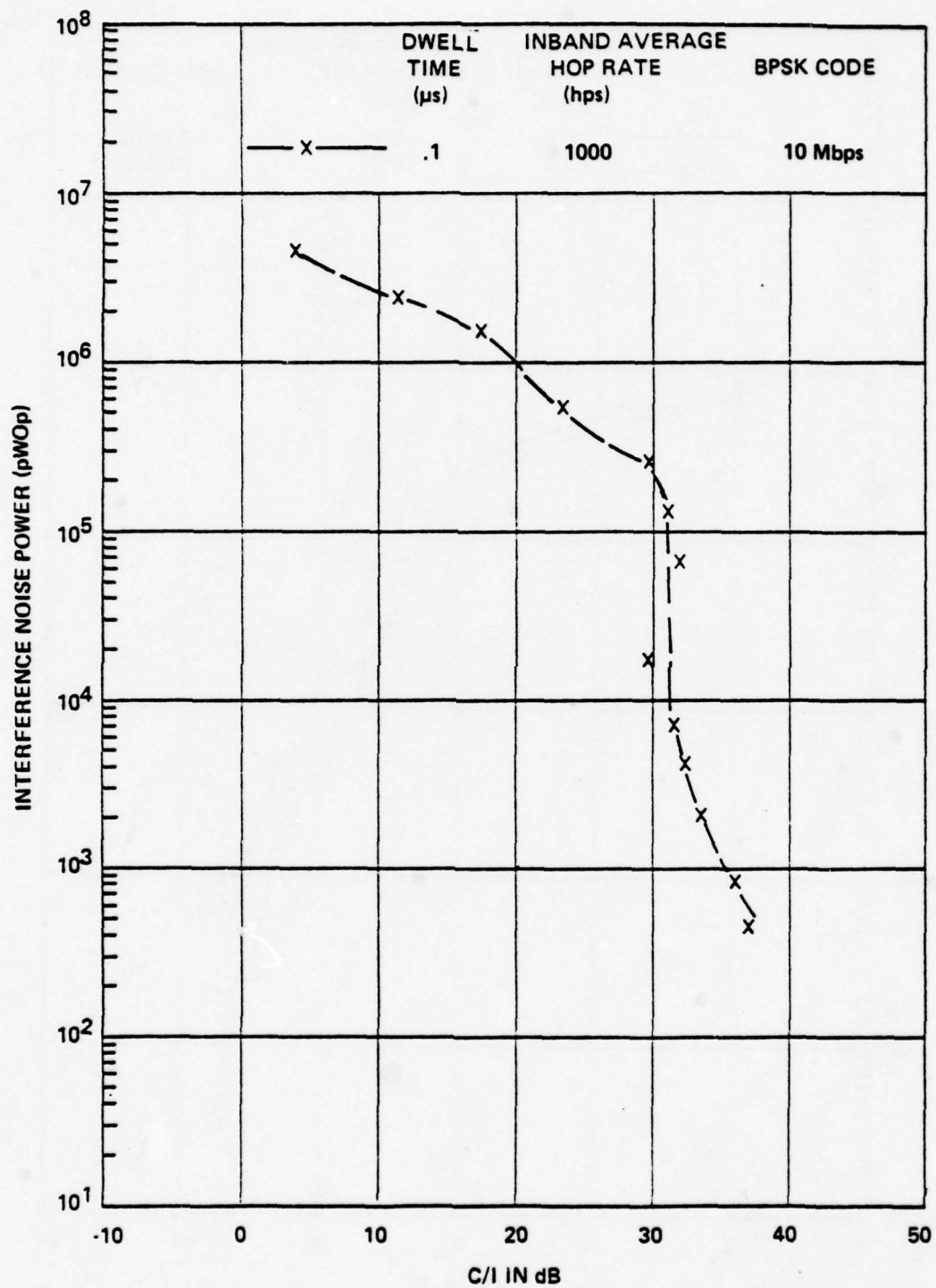


Figure 131. Measured interference noise power in a low baseband channel (340-344 kHz) for BPSK FHSS interference; dwell time = 0.1 μ s, inband average hop rate = 1000 hps.

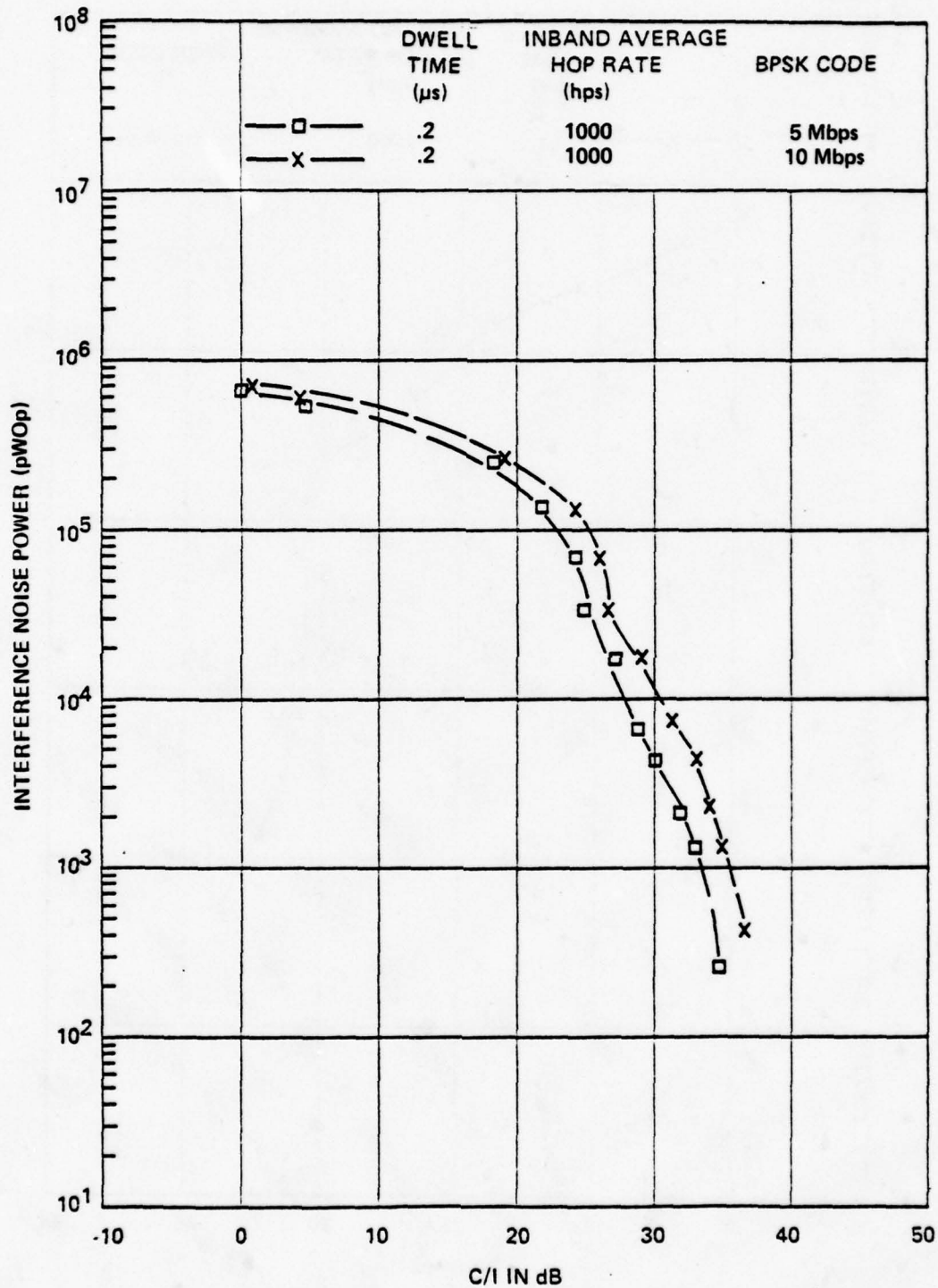


Figure 132. Measured interference noise power in a low baseband channel (340-344 kHz) for BPSK FHSS interference; dwell time = 0.2 μ s, inband average hop rate = 1000 hps.

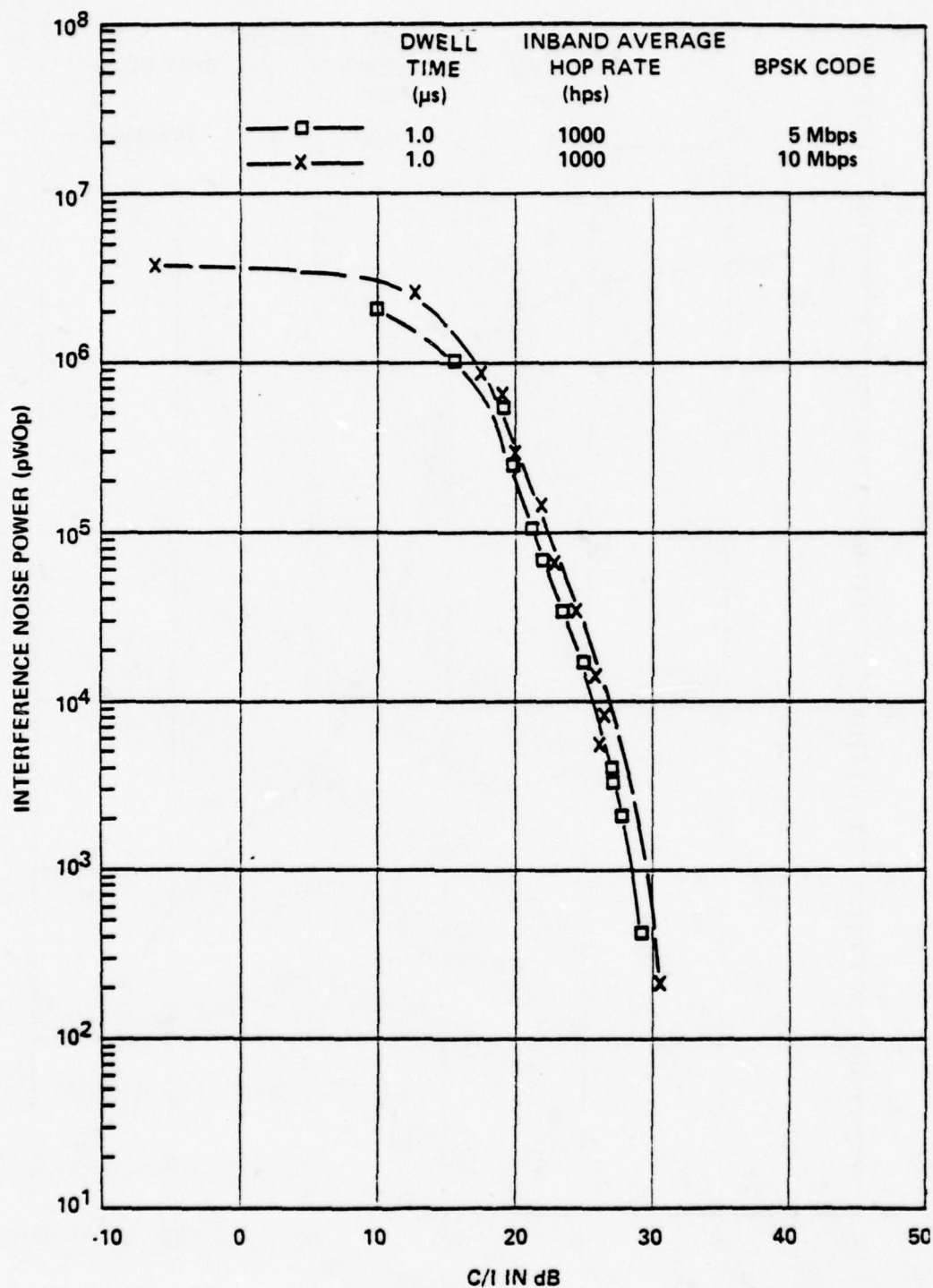


Figure 133. Measured interference noise power in a low baseband channel (340-344 kHz) for BPSK FHSS interference; dwell time = 1 μ s, inband average hop rate = 1000 hps.

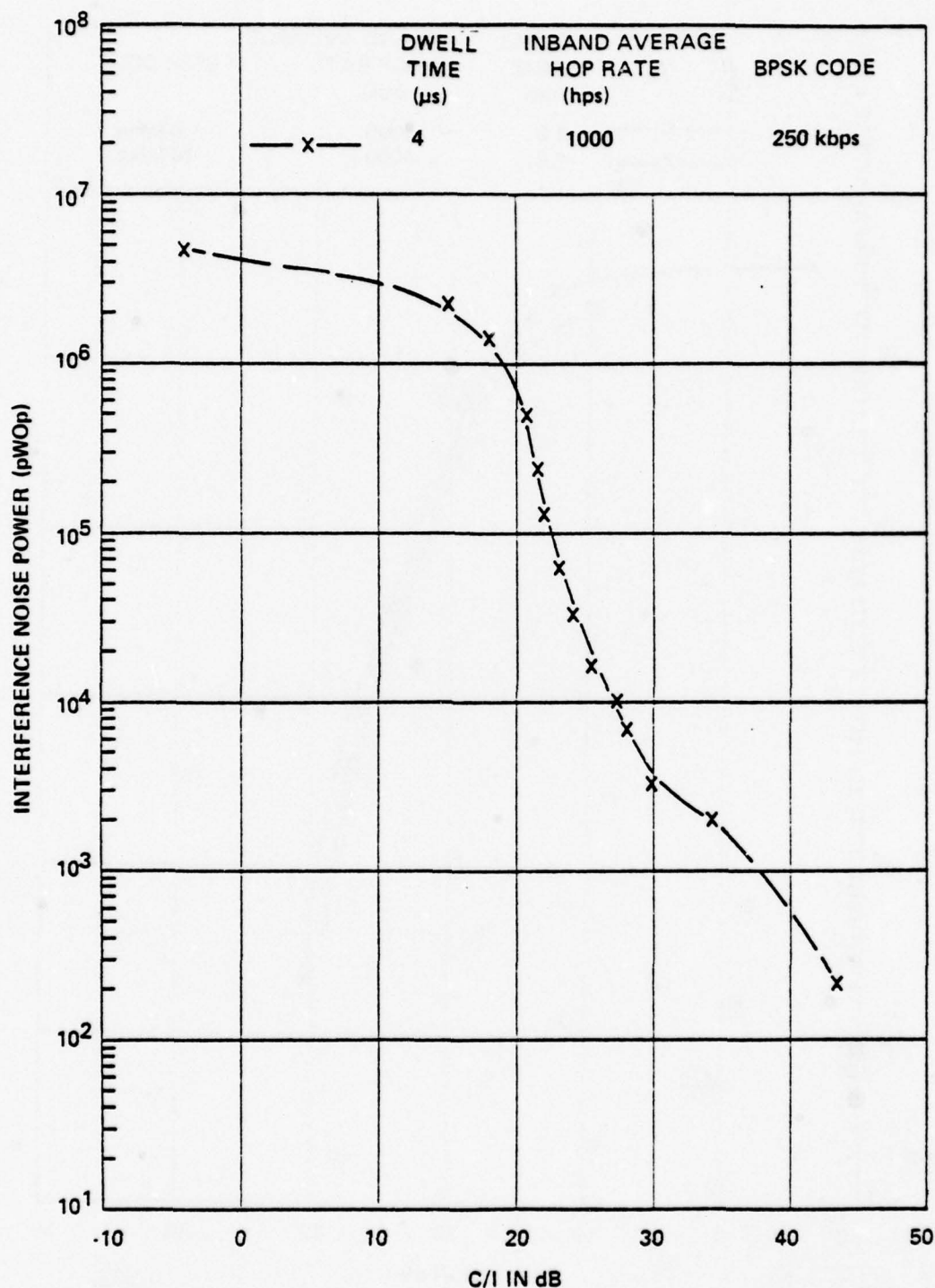


Figure 134. Measured interference noise power in a low baseband channel (340-344 kHz) for BPSK FHSS interference; dwell time = 4 μ s, inband average hop rate = 1000 hps.

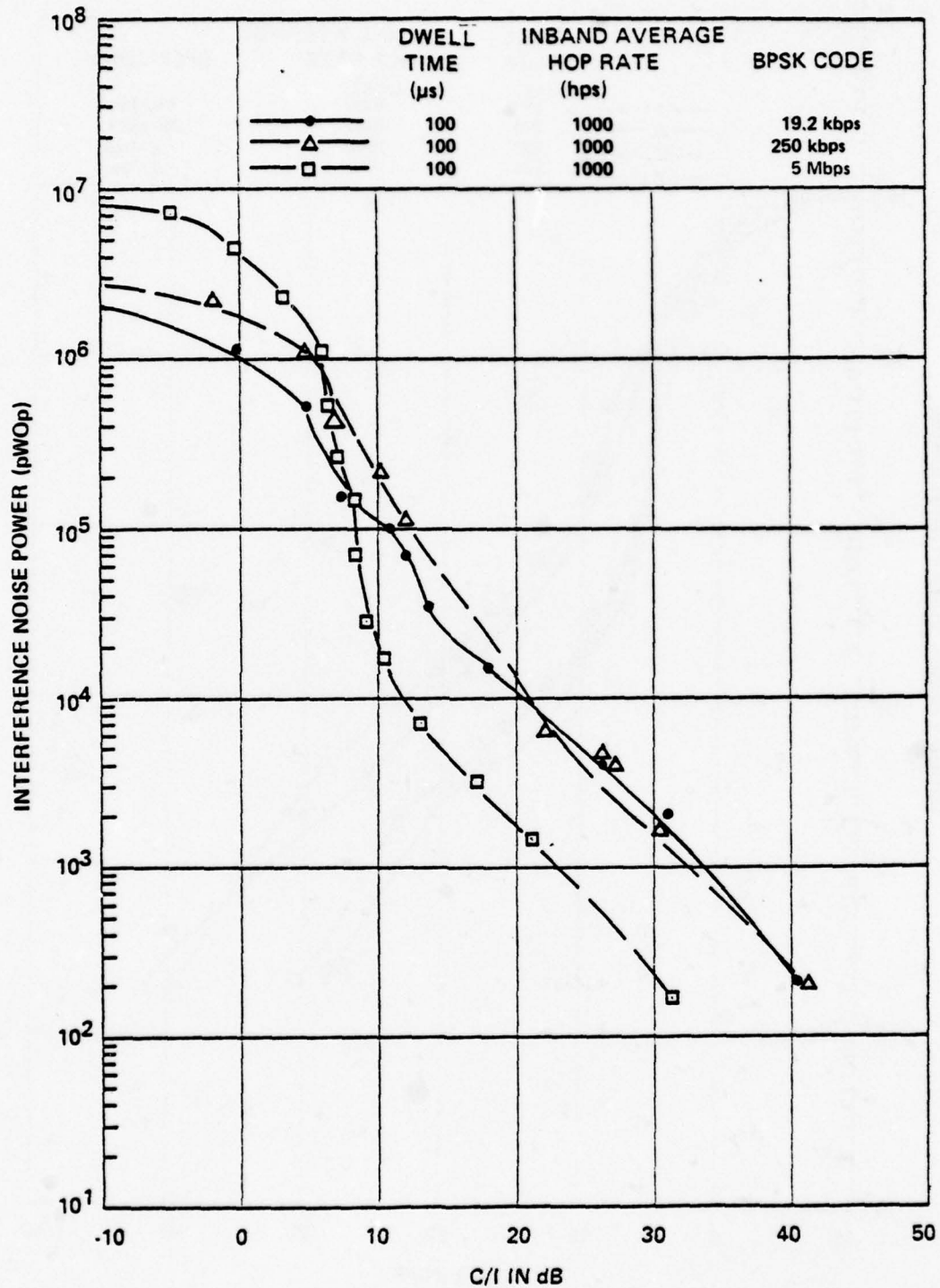


Figure 135. Measured interference noise power in a low baseband channel (340-344 kHz) for BPSK FHSS interference; dwell time = 100 μ s, inband average hop rate = 1000 hps.

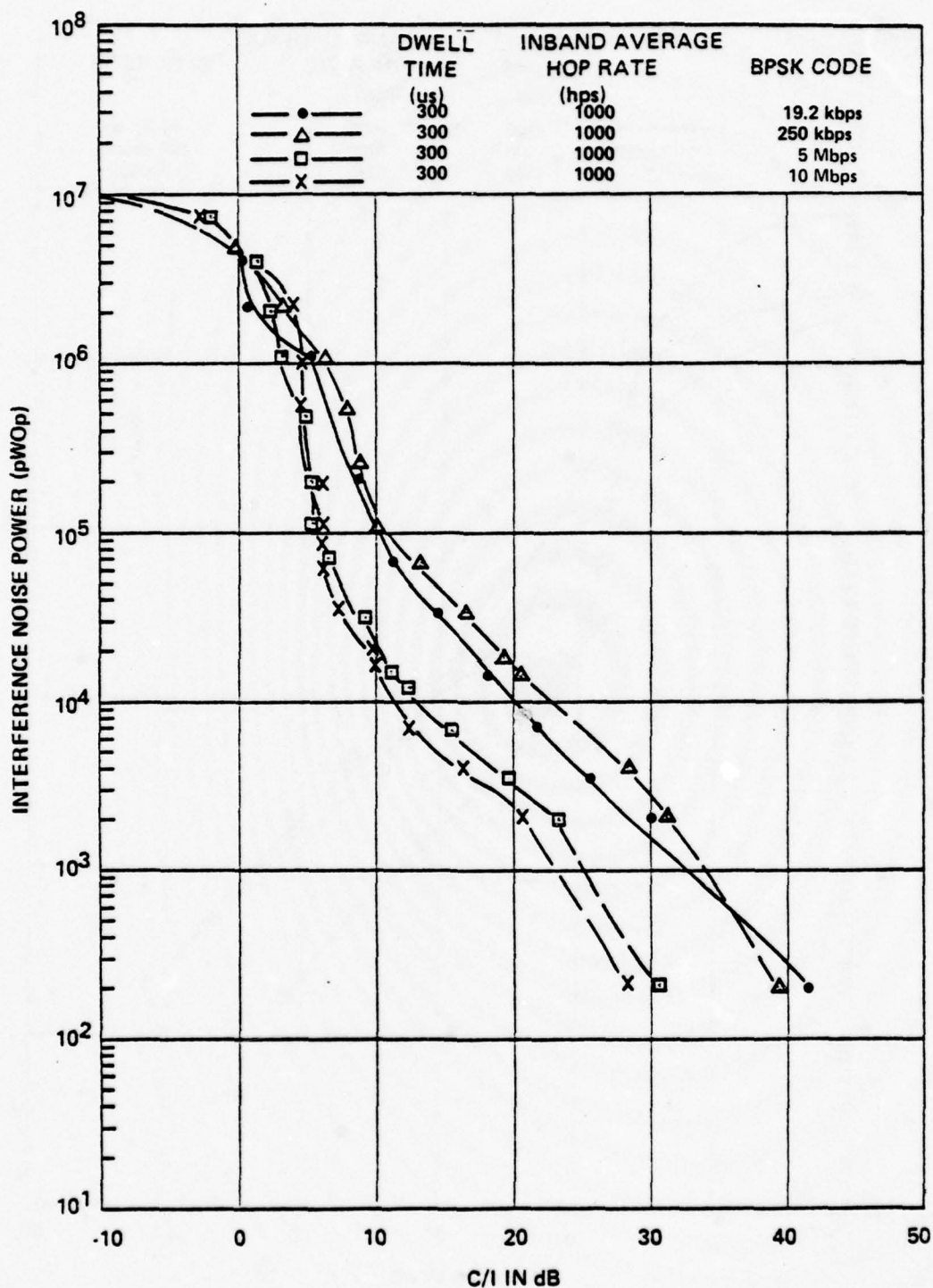


Figure 136. Measured interference noise power in a low baseband channel (340-344 kHz) for BPSK FHSS interference; dwell time = 300 μ s, inband average hop rate = 1000 hps.

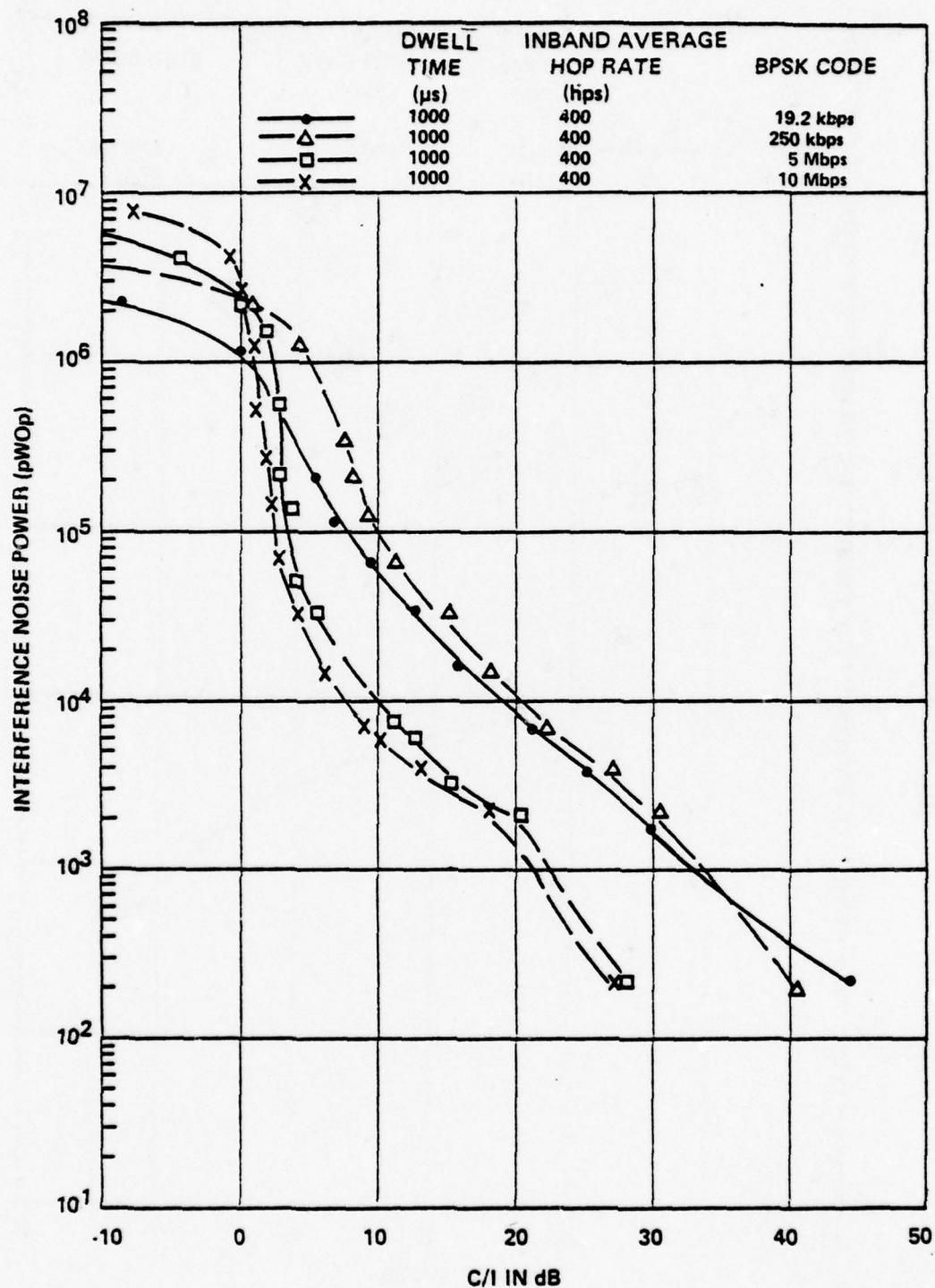


Figure 137. Measured interference noise power in a low baseband channel (340-344 kHz) for BPSK FHSS interference; dwell time = 1000 μ s, inband average hop rate = 400 hps.

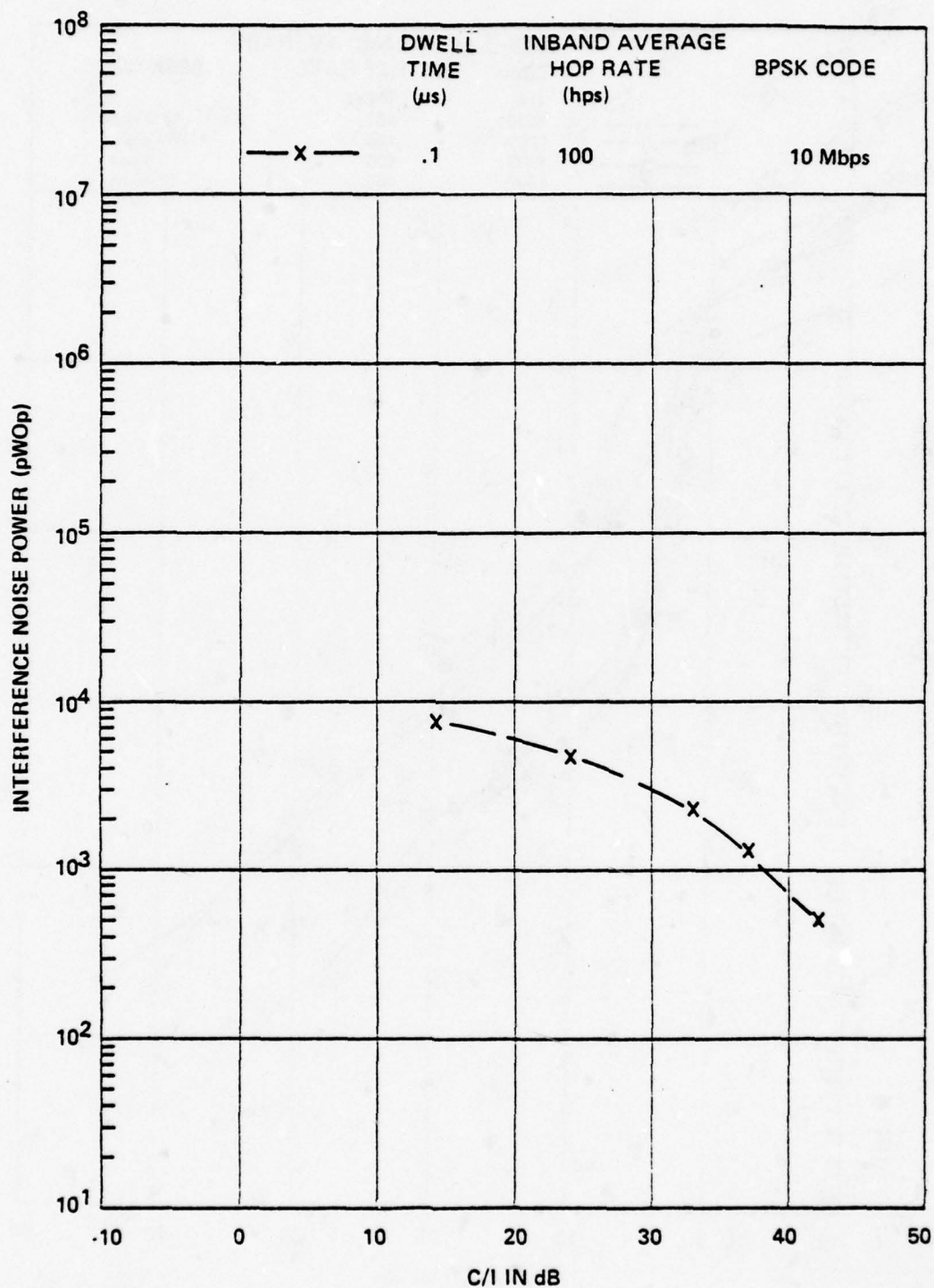


Figure 138. Measured interference noise power in a low baseband channel (340-344 kHz) for BPSK FHSS interference; dwell time = 0.1 μ s, inband average hop rate = 100 hps.

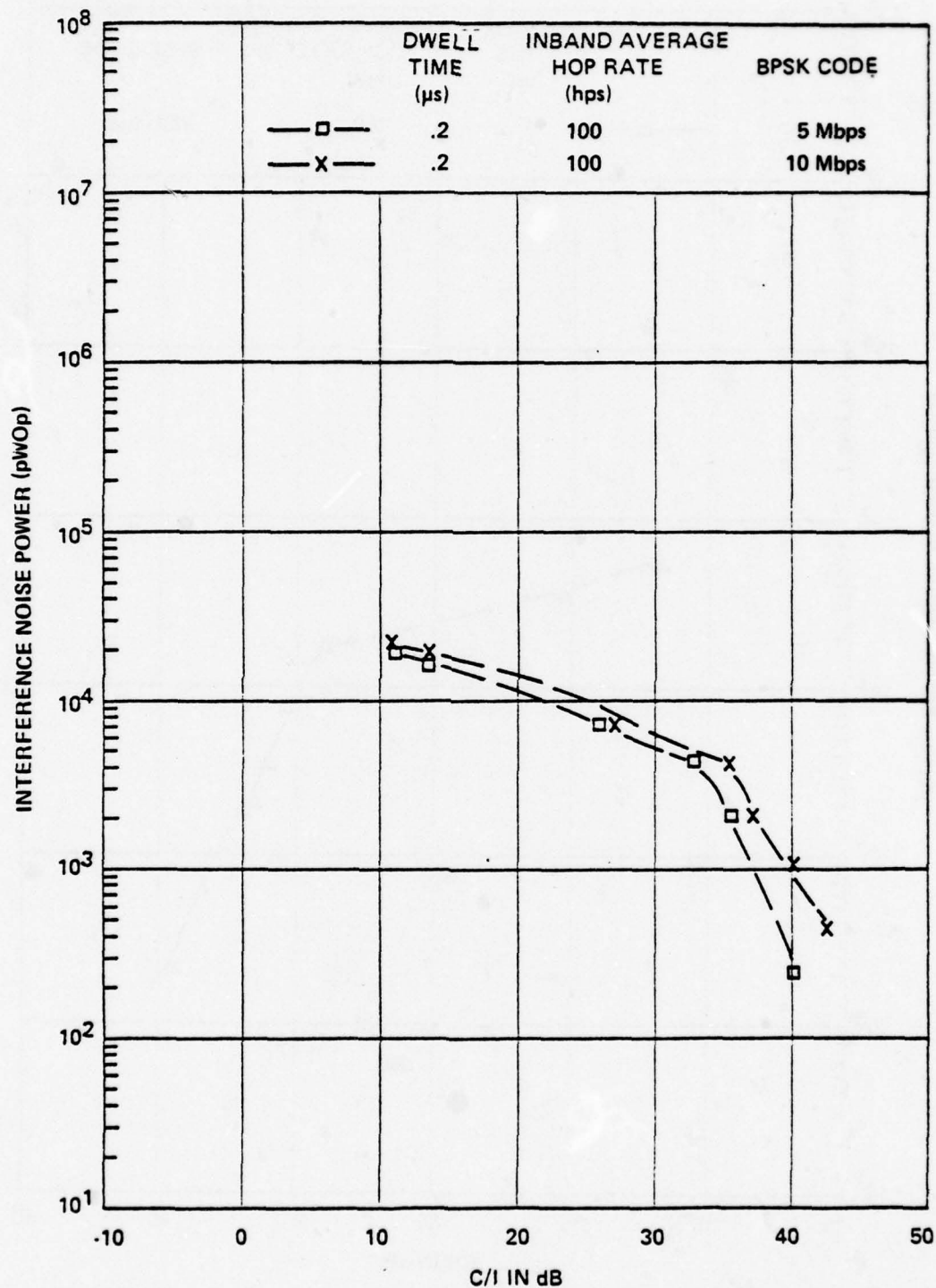


Figure 139. Measured interference noise power in a low baseband channel (340-344 kHz) for BPSK FHSS interference; dwell time = 0.2 μ s, inband average hop rate = 100 hps.

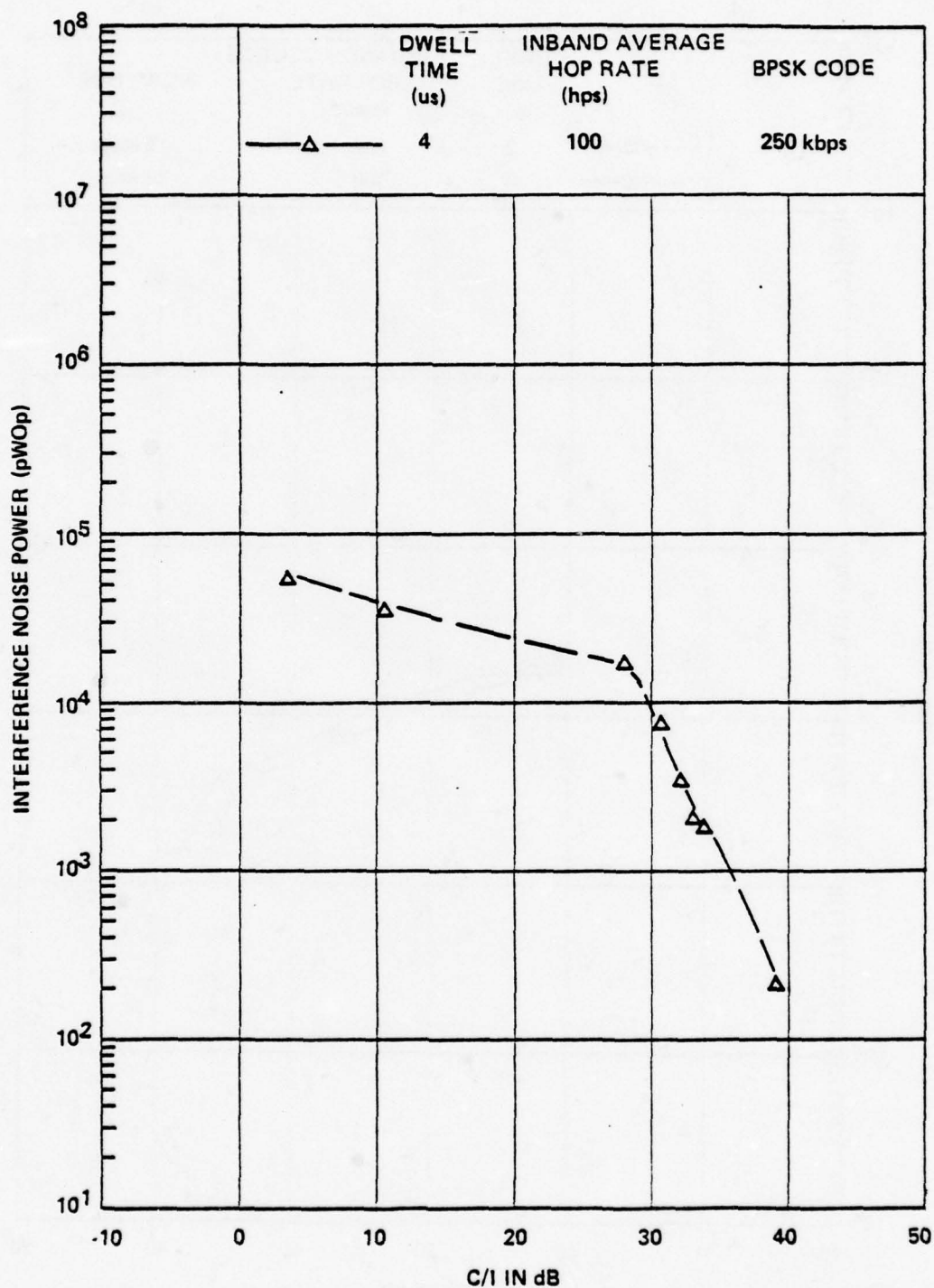


Figure 140. Measured interference noise power in a low baseband channel (340-344 kHz) for BPSK FHSS interference; dwell time = 4 μ s, inband average hop rate = 100 hps.

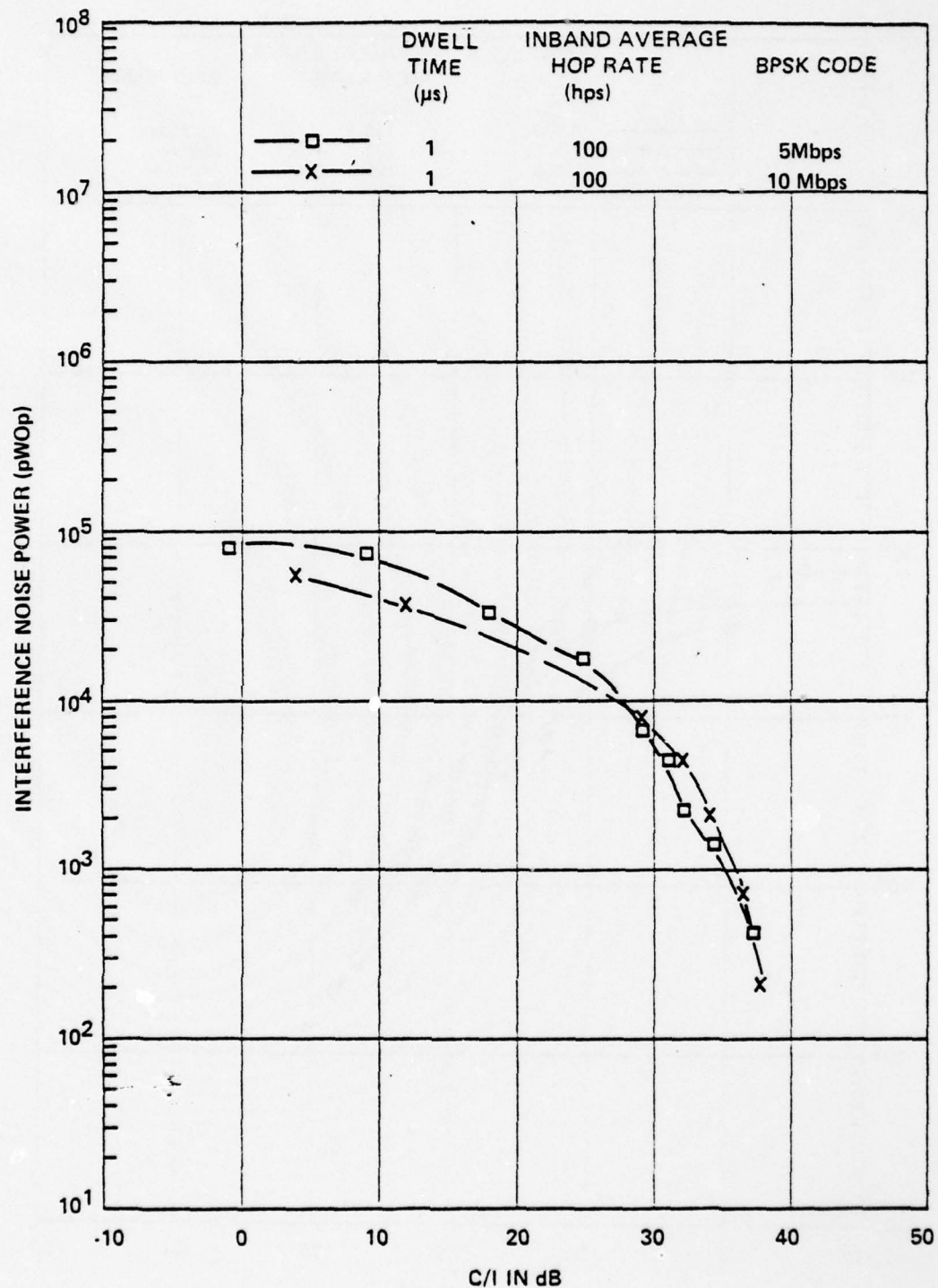


Figure 141. Measured interference noise power in a low baseband channel (340-344 kHz) for BPSK FHSS interference; dwell time = 1 μ s, inband average hop rate = 100 hps.

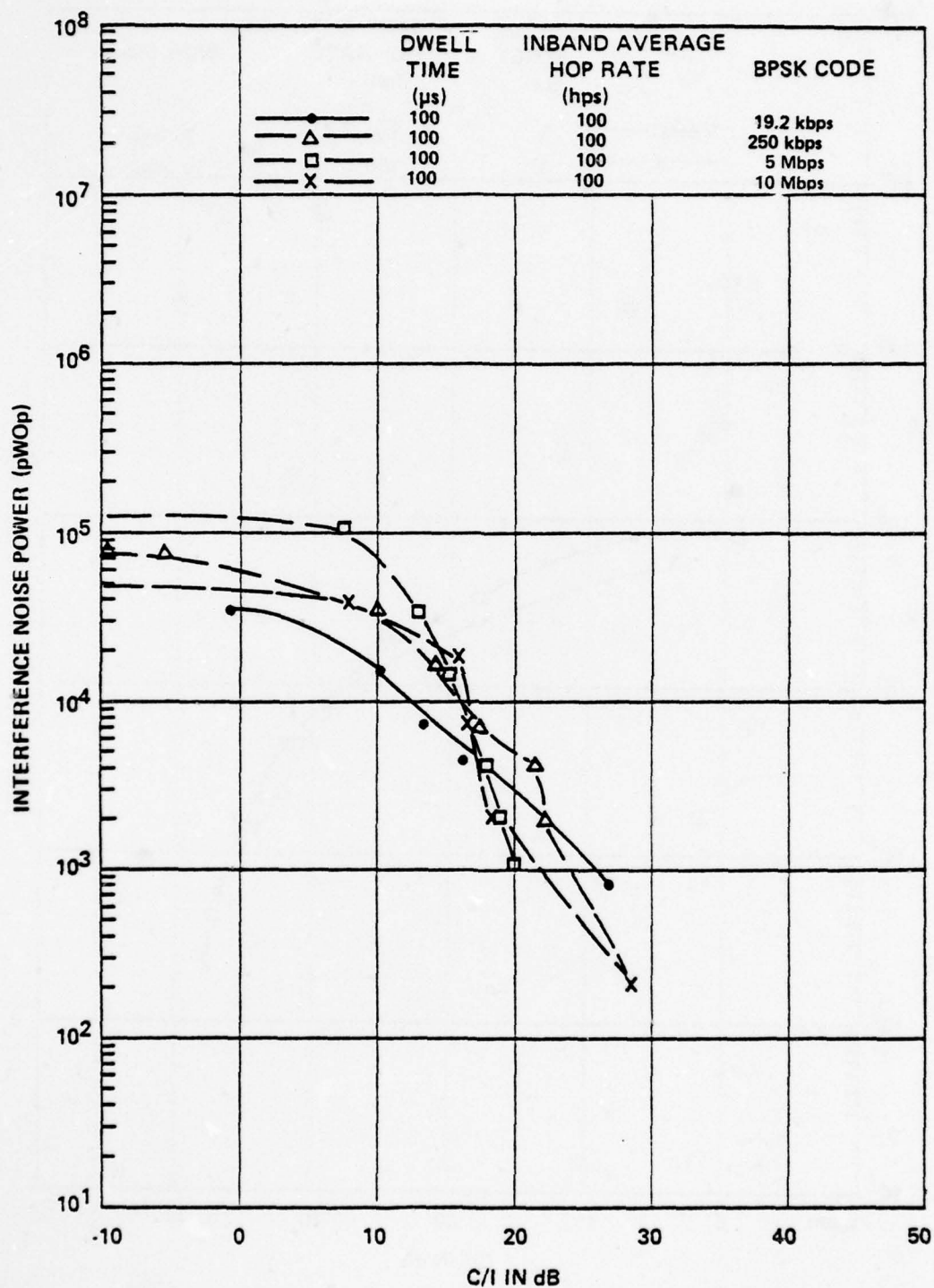


Figure 142. Measured interference noise power in a low baseband channel (340-344 kHz) for BPSK FHSS interference; dwell time = 100 μ s, inband average hop rate = 100 hps.

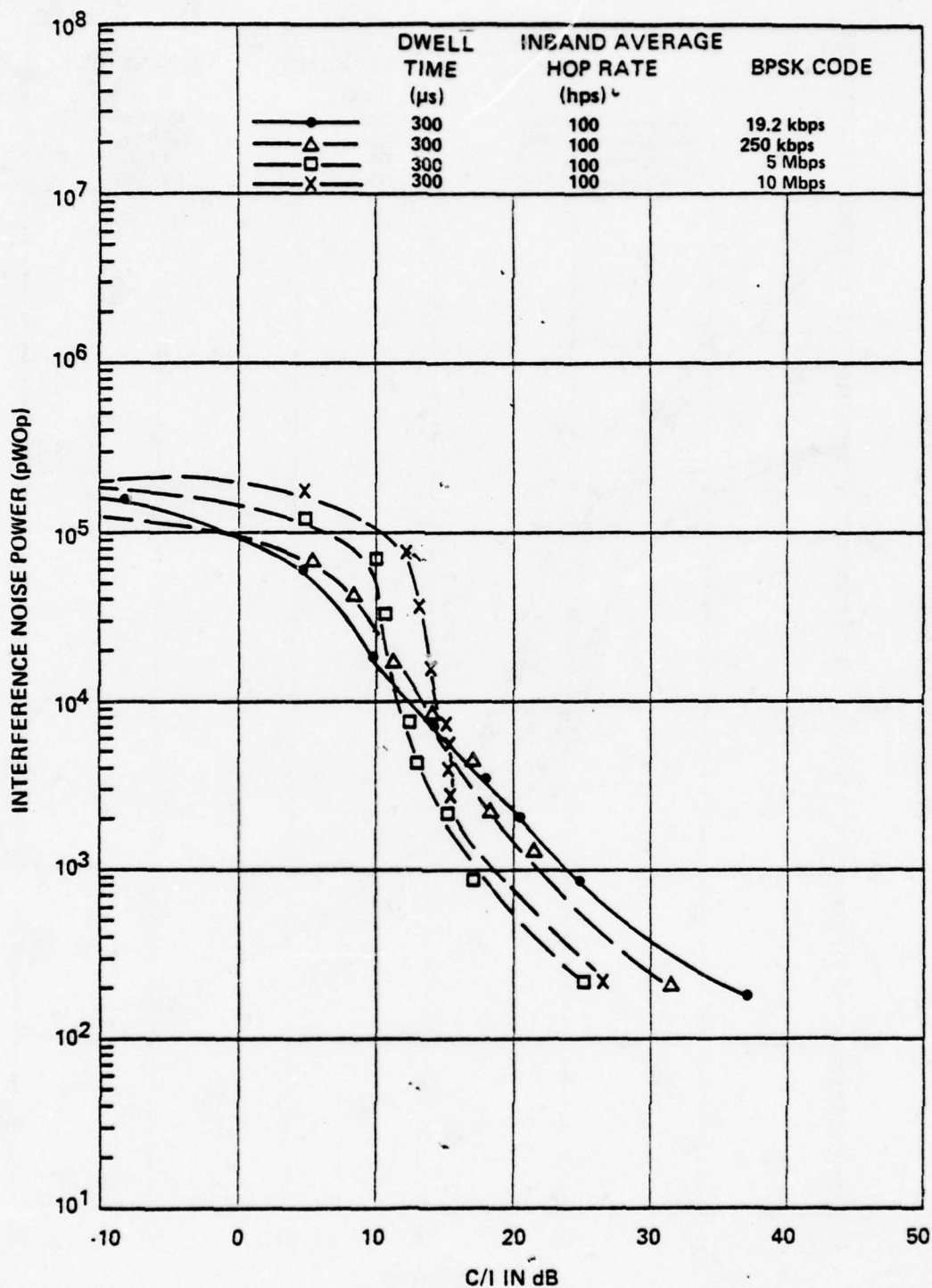


Figure 143. Measured interference noise power in a low baseband channel (340-344 kHz) for BPSK FHSS interference; dwell time = 300 μ s, inband average hop rate = 100 hps.

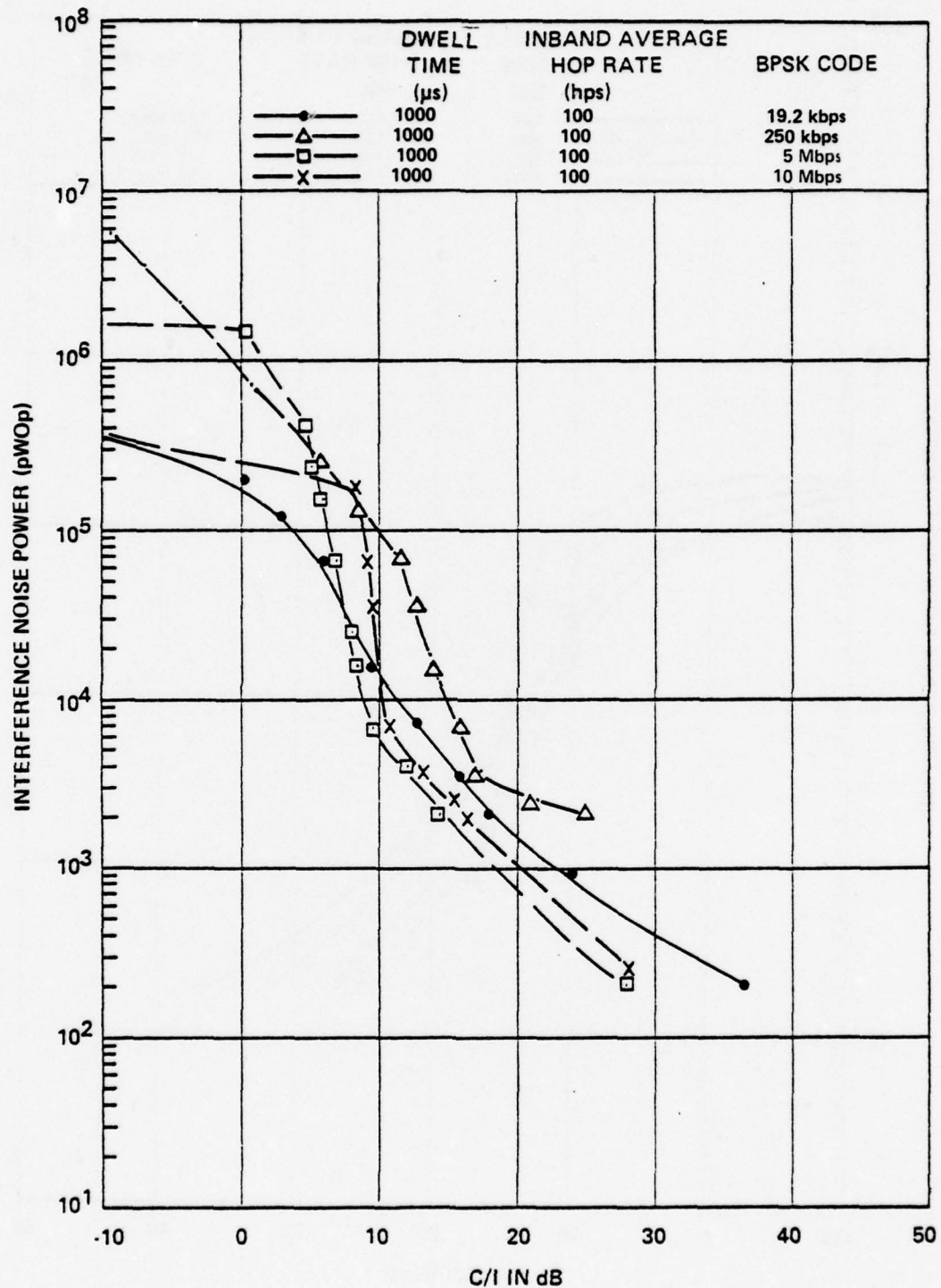


Figure 144. Measured interference noise power in a low baseband channel (340-344 kHz) for BPSK FHSS interference; dwell time = 1000 μ s, inband average hop rate = 100 hps.

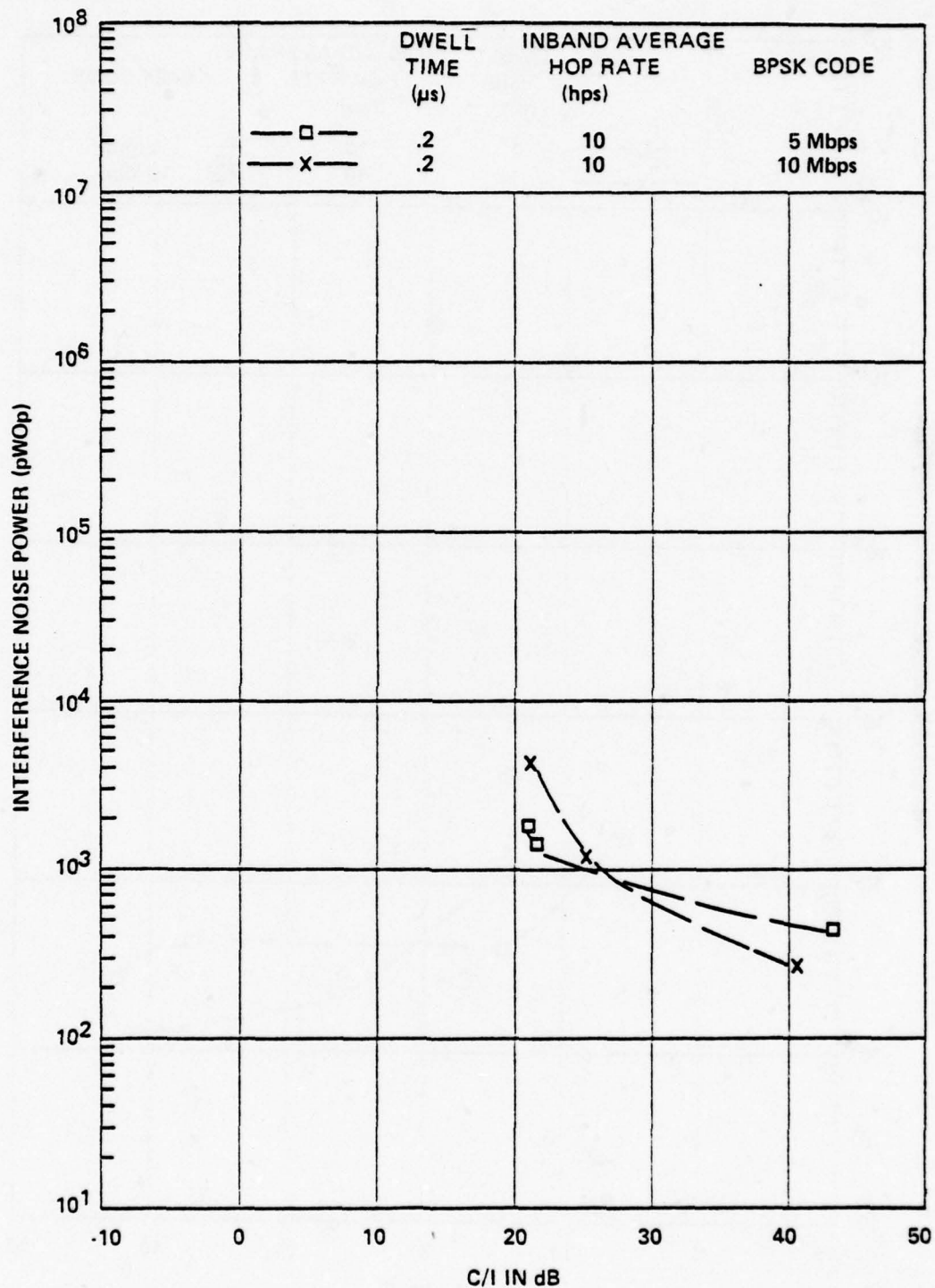


Figure 145. Measured interference noise power in a low baseband channel (340-344 kHz) for BPSK FHSS interference; dwell time = $0.2 \mu\text{s}$, inband average hop rate = 10 hps.

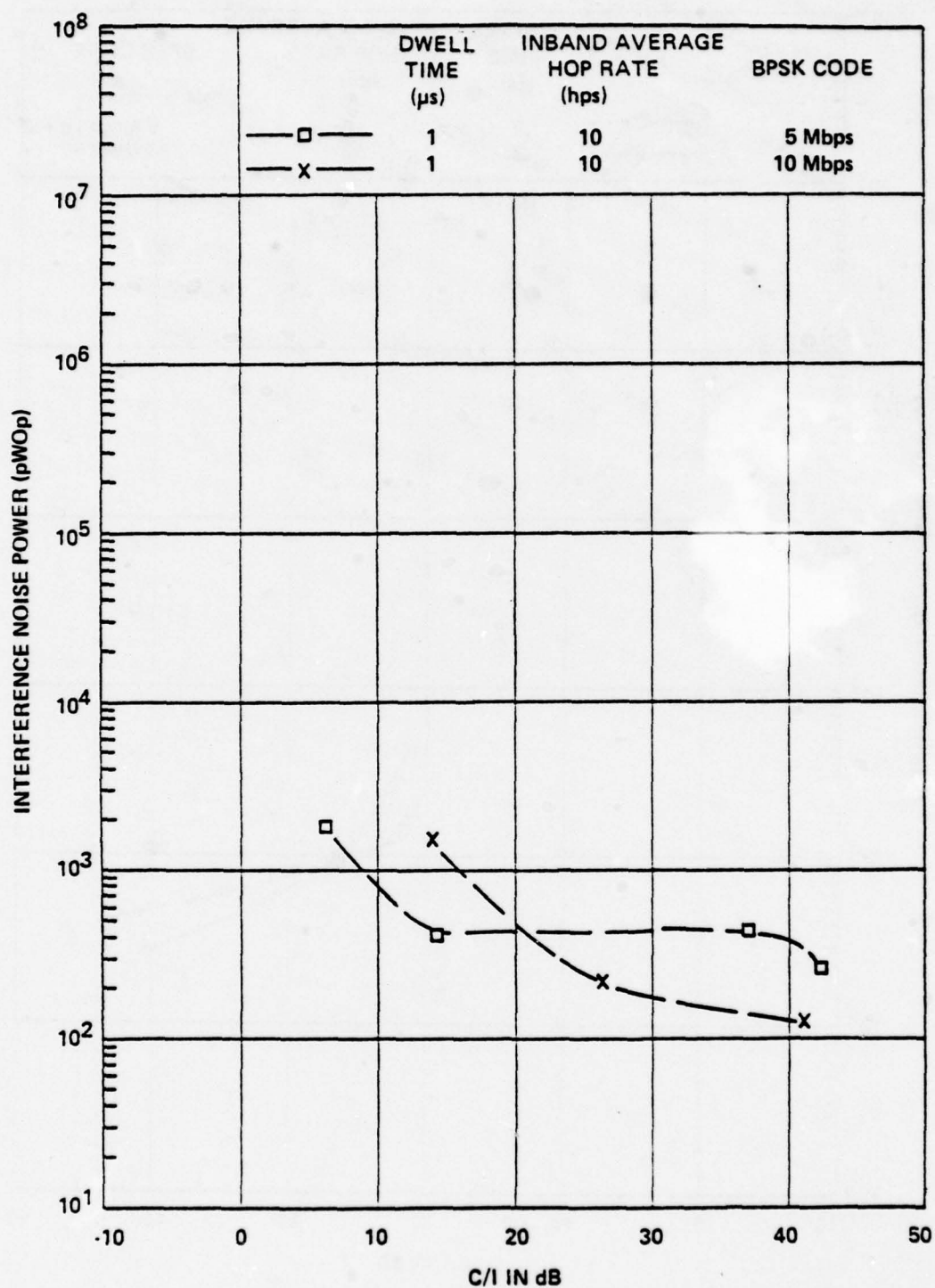


Figure 146. Measured interference noise power in a low baseband channel (340-344 kHz) for BPSK FHSS interference; dwell time = 1 μ s, inband average hop rate = 10 hps.

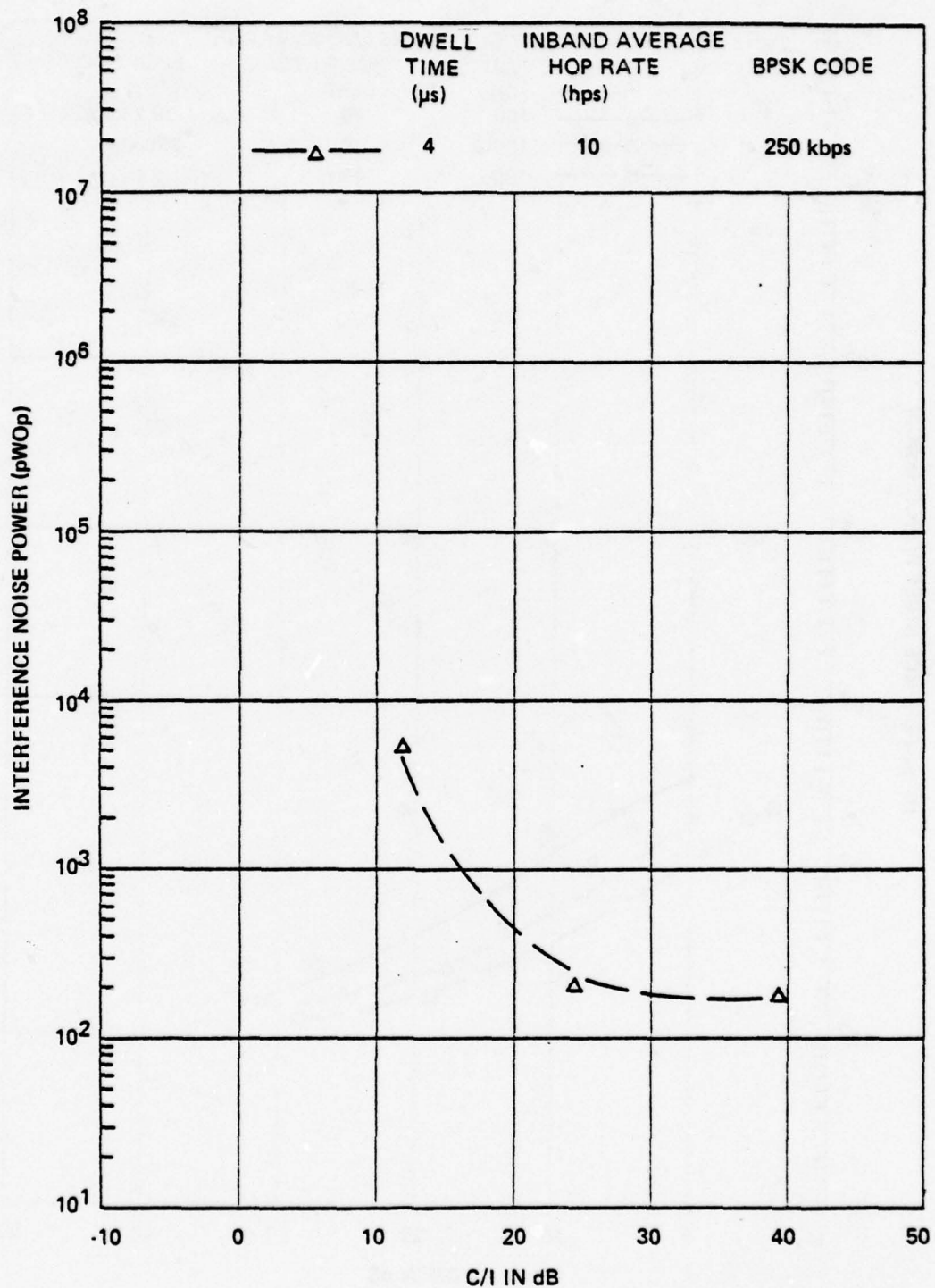


Figure 147. Measured interference noise power in a low baseband channel (340-344 kHz) for BPSK FHSS interference; dwell time = 4 μ s, inband average hop rate = 10 hps.

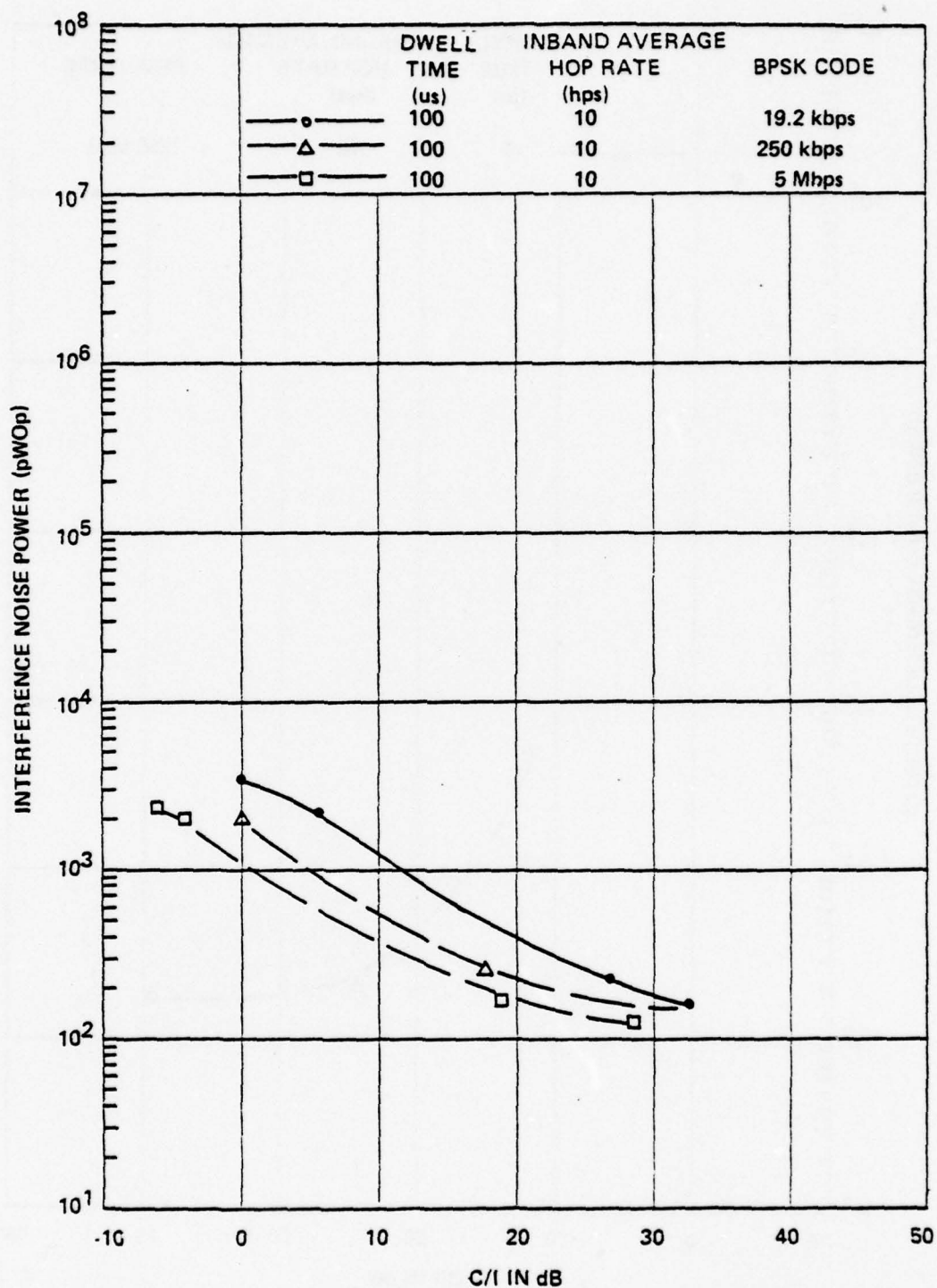


Figure 148. Measured interference noise power in a low baseband channel (340-344 kHz) for BPSK FHSS interference; dwell time = 100 μs, inband average hop rate = 10 hps.

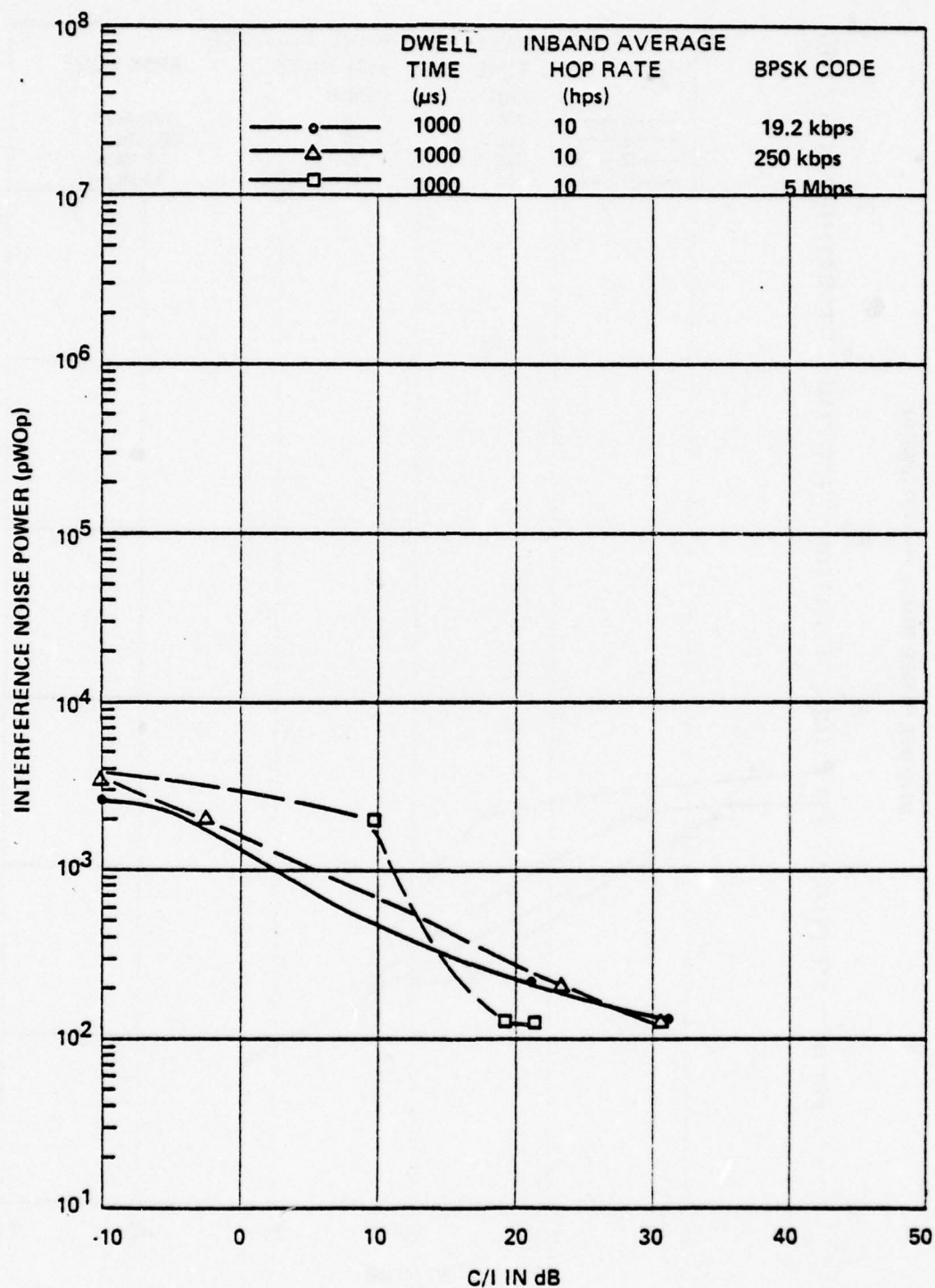


Figure 149. Measured interference noise power in a low baseband channel (340-344 kHz) for BPSK FHSS interference; dwell time = 1000 μ s, inband average hop rate = 10 hps.

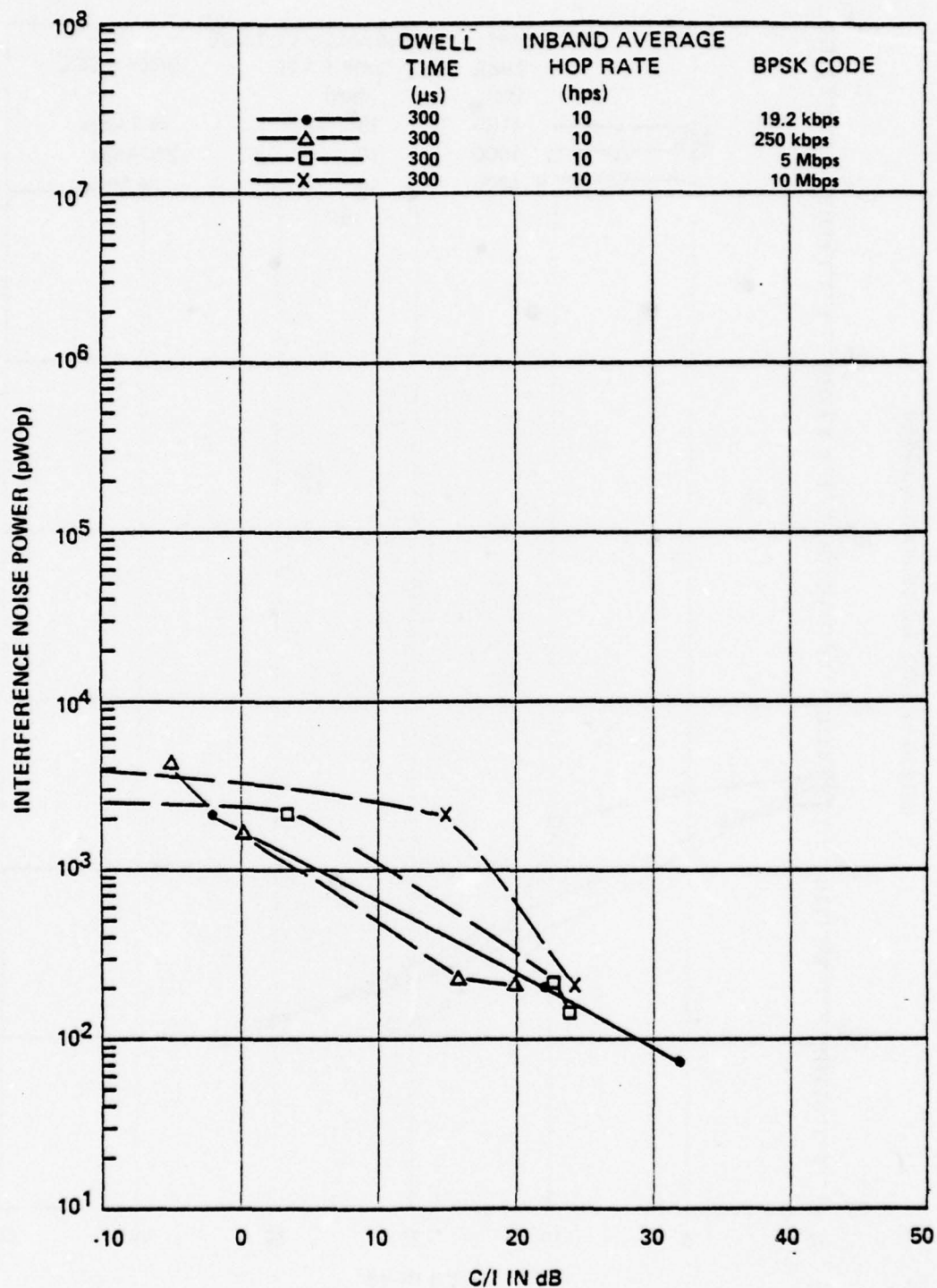


Figure 150. Measured interference noise power in a high baseband channel (2432-2436 kHz) for BPSK FHSS interference; dwell time = 300 μ s, inband average hop rate = 10 hps.

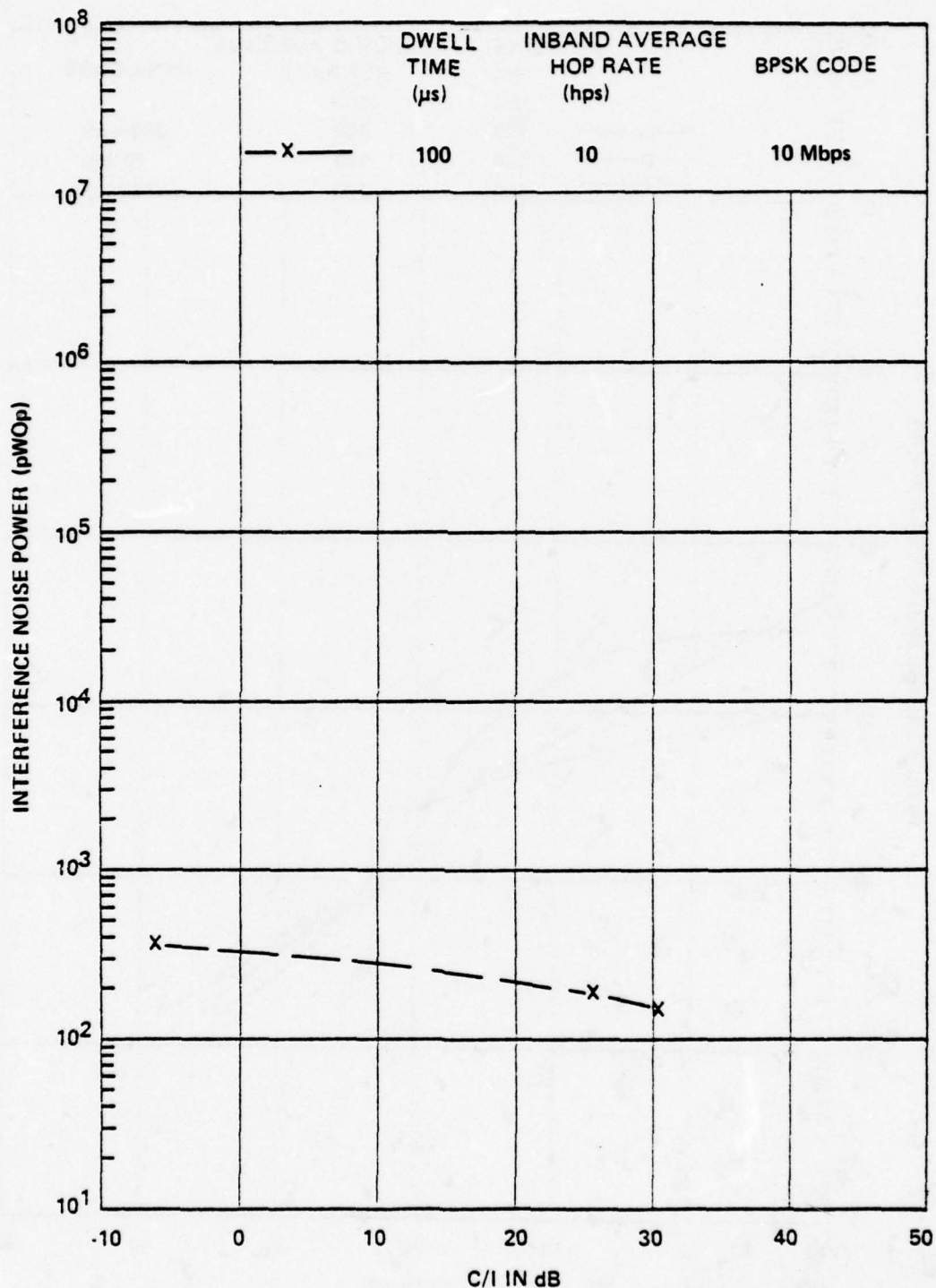


Figure 151. Measured interference noise power in a high baseband channel (2432-2436 kHz) for BPSK FHSS interference; dwell time = 100 μs , inband average hop rate = 10 hps.

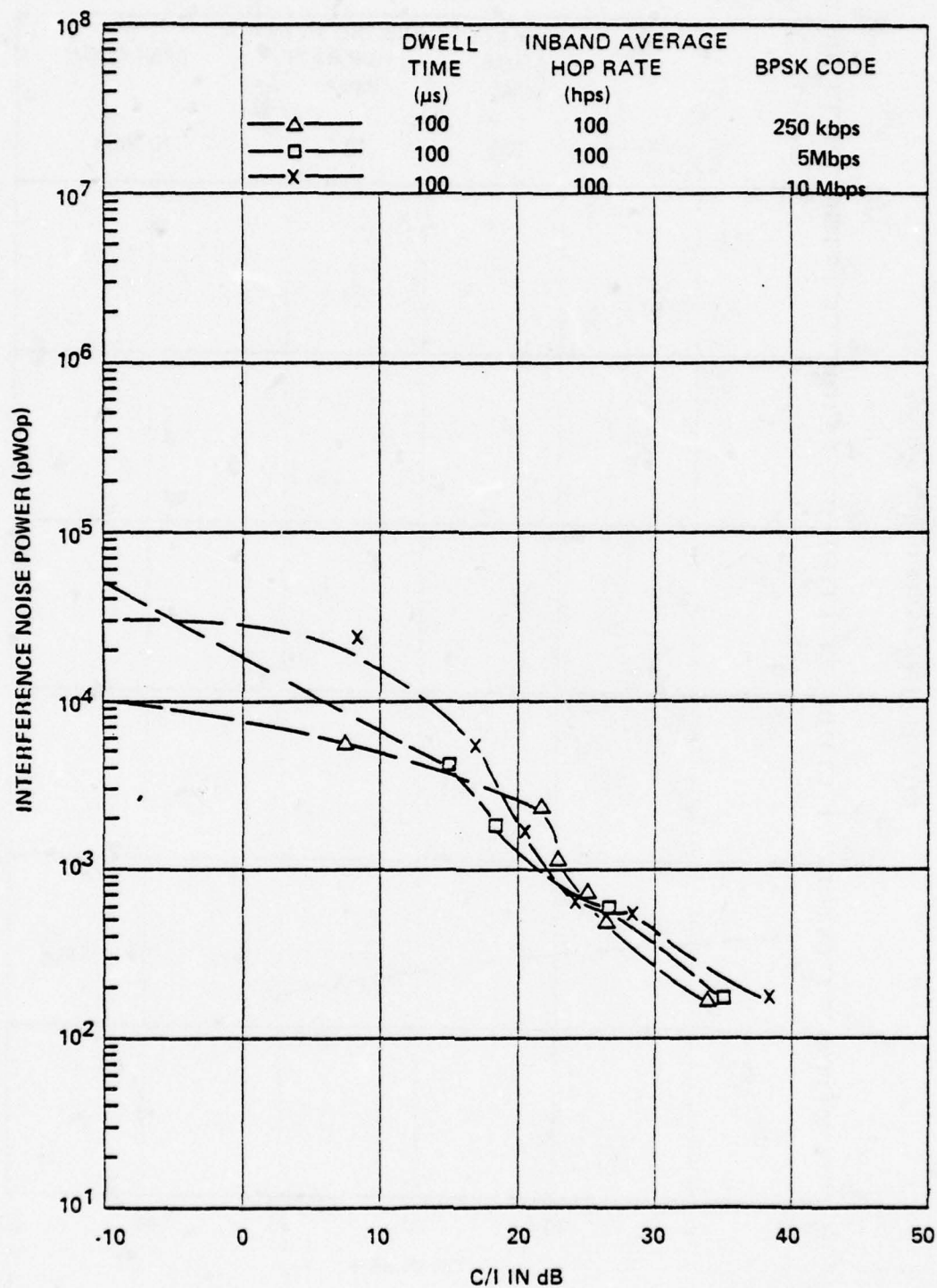


Figure 152. Measured interference noise power in a high baseband channel (2432-2436 kHz) for BPSK FHSS interference; dwell time = 100 μ s, inband average hop rate = 100 hps.

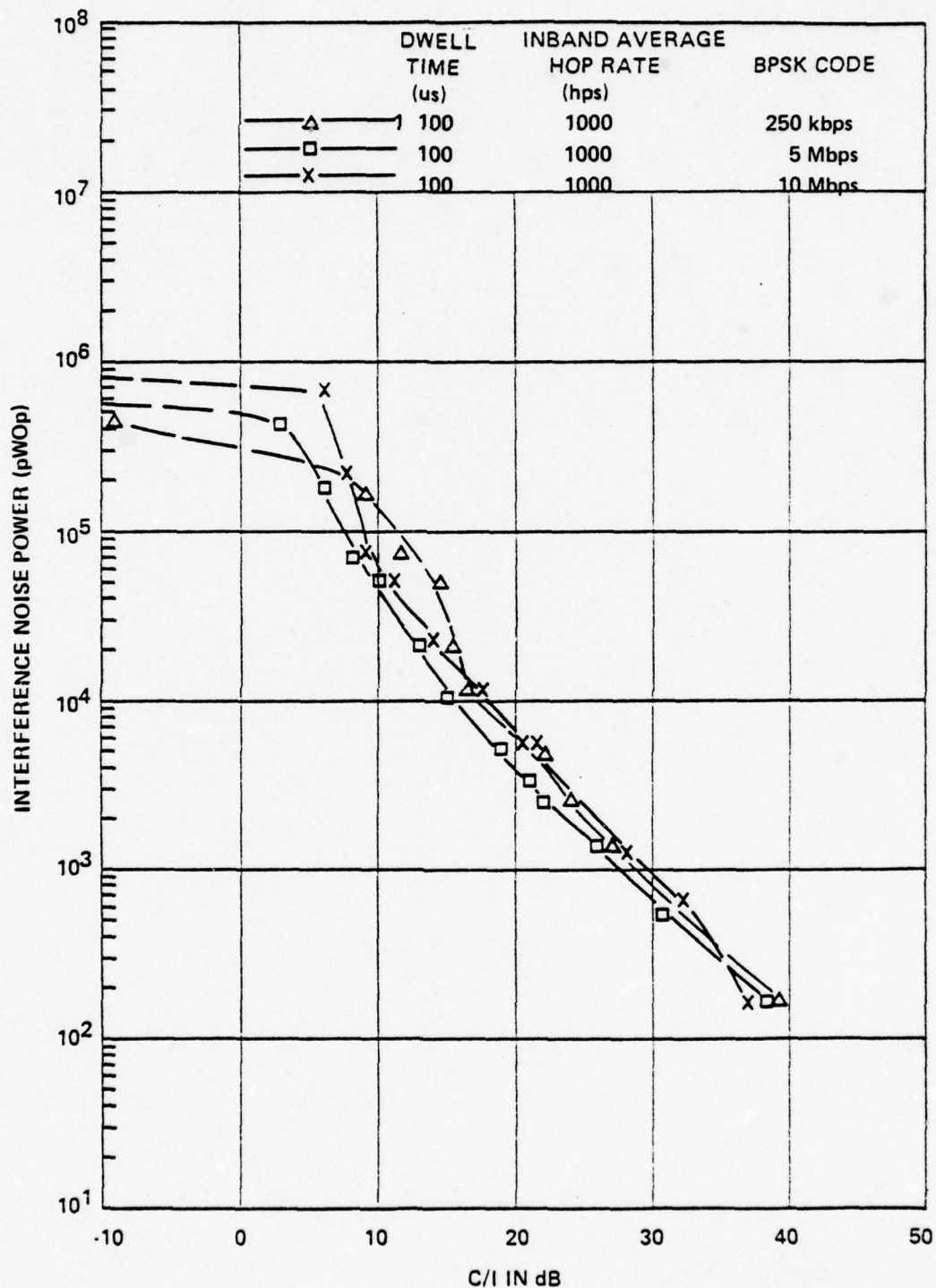


Figure 153. Measured interference noise power in a high baseband channel (2432-2436 kHz) for BPSK FHSS interference; dwell time = 100 μ s, inband average hop rate = 1000 hps.

SECTION 9

SUMMARY OF RESULTS

1. A computer simulation model was developed for determining the manner in which various types of undesired signals affect the performance of FDM/FM receivers. The theoretical details of the computer model, including the user-oriented documentation and model validation, were reported in ECAC-UM-78-018 (Reference 5).

2. A detailed, two-phase FDM/FM measurements program was successfully completed. The results of Phase I, which consisted of measuring the characteristics of a 600-channel and a 1200-channel FDM/FM system, are included herein as APPENDIX A. The results of Phase II, which consisted of measuring the performance degradation in a 600-channel FDM/FM receiver due to interference, are summarized in Sections 4 through 8. The methodologies used in the Phase II measurements together with the raw data were reported in ECAC-HDBK-77-041, Volumes 1 through 8 (References 9 and 10).

- Some of the measurement methodologies developed for the Phase I measurements are currently being used to update MIL-STD-449(D).

3. A large amount of information on FDM/FM systems (i.e., modulation characteristics, baseband noise-loading techniques, emission spectrum synthesis techniques, etc.) has been included in this report (Sections 2, 3 and 4 and APPENDIXES A, B and C) to facilitate performing degradation analyses for FDM/FM systems.

- Equations 1 through 5 are used to compute the baseband noise-loading levels.

- Equations 8 through 11 are used to compute the FDM modulation characteristics.
- TABLE 3 summarizes the transmission parameters specified by CCIR and DCA for FDM/FM systems of the type widely used by the terrestrial and satellite services.
- TABLE 6 summarizes the transmission parameters of FDM/FM systems used in Intelsat IV.
- Equation 15, which was derived from the Phase I measured data, extends the limits of the equations available in the literature for computing the power spectrum of FDM/FM systems with low values of RMS modulation indices.
- Figures C-1 and C-2, which were derived from the Phase I measured data, represent a graphical technique for obtaining the power spectrum of preemphasized FDM/FM systems with intermediate values of RMS modulation indices.

4. The FDM/FM receiver power transfer functions (i.e., the relationships between the audio output S/N power ratio and the RF input C/I and C/N power ratios) for various types of interference signals were developed. The power transfer functions, together with the methodology used to develop them, are presented in Sections 4 through 8 as follows:

- Figure 11 shows the receiver power transfer function model used throughout the report.
- The noise power transfer equations developed by Fagot and Magne, (Reference 27) are presented.

Section 5: Power Transfer Functions for ECM (i.e., barrage and spot noise, amplitude-modulated barrage noise, pulse-modulated barrage noise, swept-spot noise) Interference

- Techniques for simulating and generating ECM signals are presented.

Section 6: Power Transfer Functions for CW and noise-modulated FM (i.e., narrowband FM, FDM/FM) interference

- The noise power ratio equations developed by Hamer (Reference 19) are presented.

Section 7: Power Transfer Functions for Chirp and Nonchirp Radar Pulse Interference

- The concept of two degradation regions of FDM/FM communication systems subjected to pulse radar interference is demonstrated.
- For on-tune pulse interference, the envelope of the maximum observed interference in the worst performing voice channel can be calculated from Equations 92 and 93.
- Performance degradation will increase as the pulse interference is off-tuned slightly.

Section 8: Power Transfer Functions for Direct-Sequence (DS) and Frequency-Hopping Spread-Spectrum (FHSS) Interference

- DSSS interference behaves as noise-modulated FM interference whose RMS deviation corresponds to $1.6 R_c$, where R_c is the modulating code rate.

- The level of interference noise in a multiplexer channel of a given FDM/FM system is inversely proportional to the C/I power ratio. For C/I power ratios smaller than approximately 0 dB, the noise in a multiplexer channel will increase only slightly with decreasing ratios of C/I.
- FHSS interference behaves as a combination of pulse interference and noise interference.

5. The relationship between channel output S/N power ratio and voice intelligibility was investigated and the results are presented graphically in APPENDIX B.

- For all interference signals, the articulation index is dependent only on the S/N power ratio at the output of a voice channel and can be calculated from Equation B-6.
- The relationships between articulation index and articulation score are presented graphically in Figures B-5 through B-9.

APPENDIX A

PARAMETER MEASUREMENT DATA

This appendix documents the results of the MIL-STD-449(D) transmitter and receiver parameter measurements conducted on a 600-channel and a 1200-channel Lenkurt 78A2 FDM/FM microwave system. TABLES A-1 and A-2, respectively, summarize the transmitter and receiver parameter measurement results and the figure and table numbers corresponding to their location.

TABLE A-1
SUMMARY OF TRANSMITTER PARAMETER MEASUREMENT RESULTS AND LOCATION
(LENKURT 78A2 600- AND 1200-CHANNEL SYSTEMS)

Transmitter Measurements	System Capacity (Channels)	Table(s)	Figure(s)
Modulator Bandwidth	600 1200		A-1 A-2
Modulation Characteristics	600 1200		A-3, A-4 A-5, A-6
Power Output	600 1200	A-3	
Carrier Frequency Stability	600 1200	A-4 A-5	
Noise Calibration Photographs for Emission Spectrum Measurements	600 1200		A-7 to A-14
Emission Spectrum Characteristics (Narrowband)	600 1200		A-15 to A-21 A-22 to A-28
Emission Spectrum Characteristics (Wideband)	600 1200	A-6	
Transmitter Intermodulation	600 1200	A-7	

TABLE A-2
SUMMARY OF RECEIVER PARAMETER MEASUREMENT RESULTS AND LOCATION
(LENKURT 78A2 600- AND 1200-CHANNEL SYSTEMS)

Receiver Measurements	System Capacity (Channels)	Table(s)	Figure(s)
Sensitivity	600 1200	A-8 A-9	A-29 to A-34 A-35, A-36
Dynamic Range	600 1200		A-37
Audio Selectivity	600-Channel 46A2 Multiplex		A-38 A-39
AGC Characteristics	600 1200		A-40 A-41
RF Selectivity	600 1200		A-42 A-43
IF Selectivity	600 1200		
Spurious Response	600 1200	A-10	
Intermodulation	600 1200	A-11	
Oscillator Emission	600 1200	A-12	
Discriminator Bandwidth	600		A-44, A-45

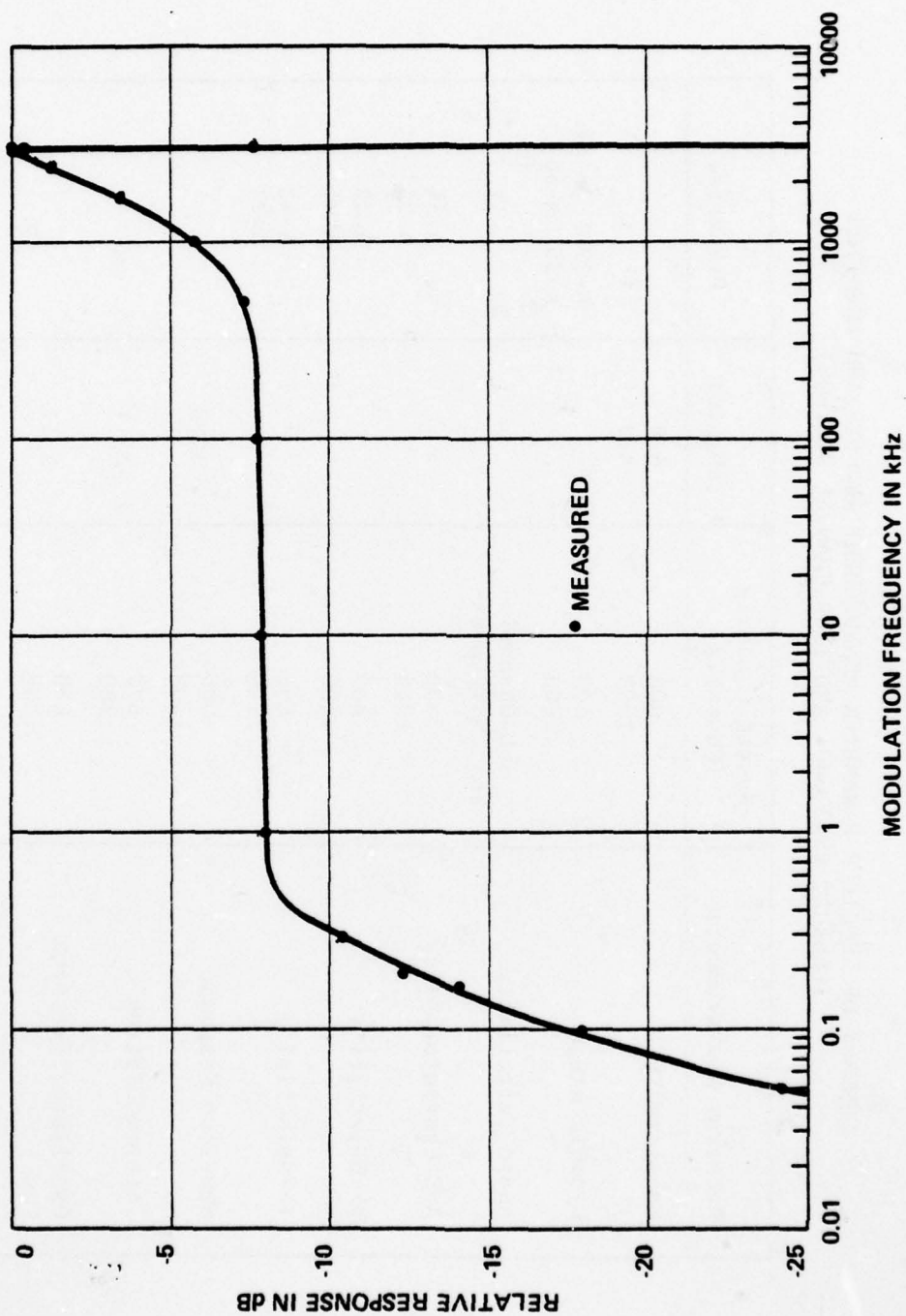


Figure A-1. Transmitter modulation bandwidth, 600-channel system.

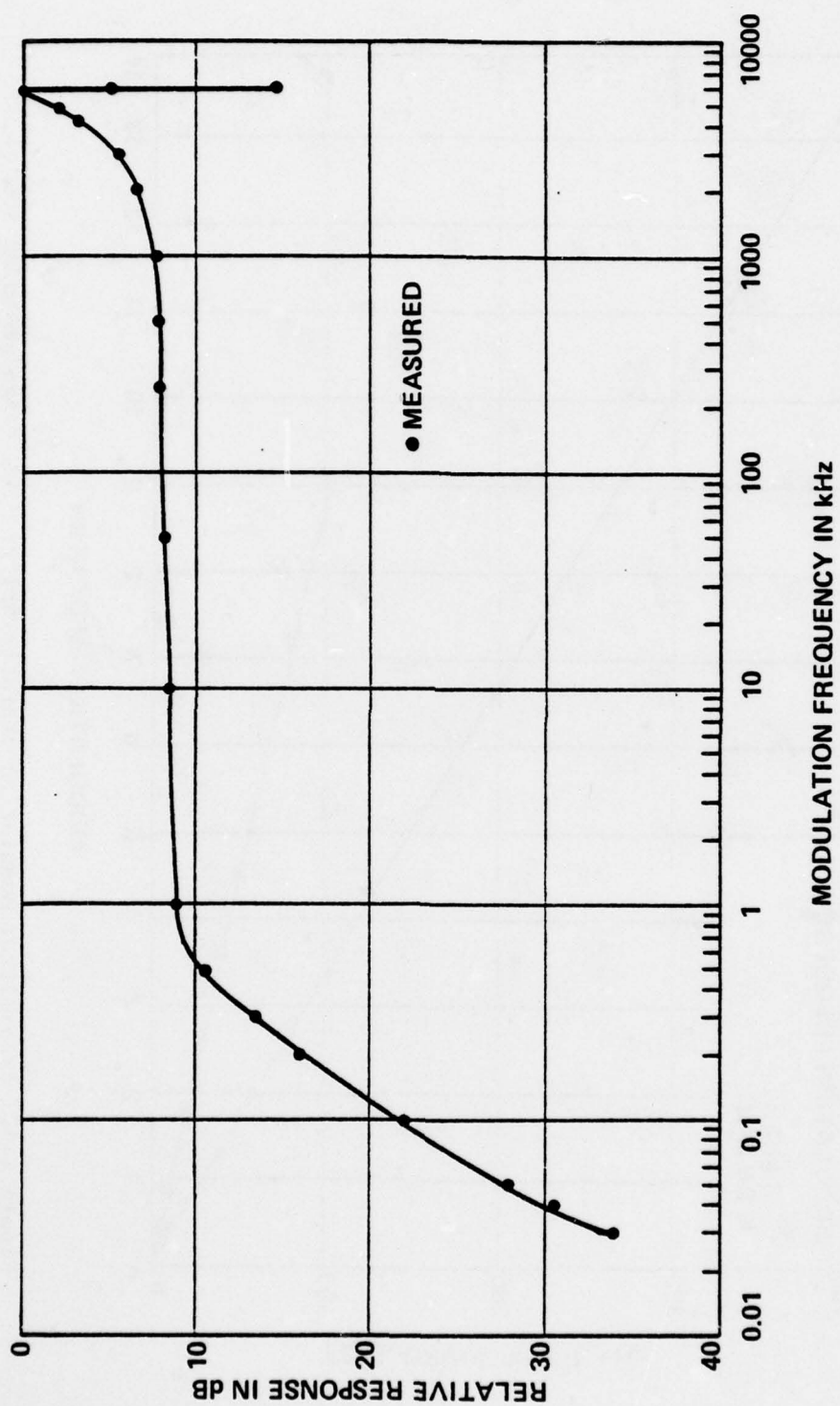


Figure A-2. Transmitter modulation bandwidth, 1200-channel system.

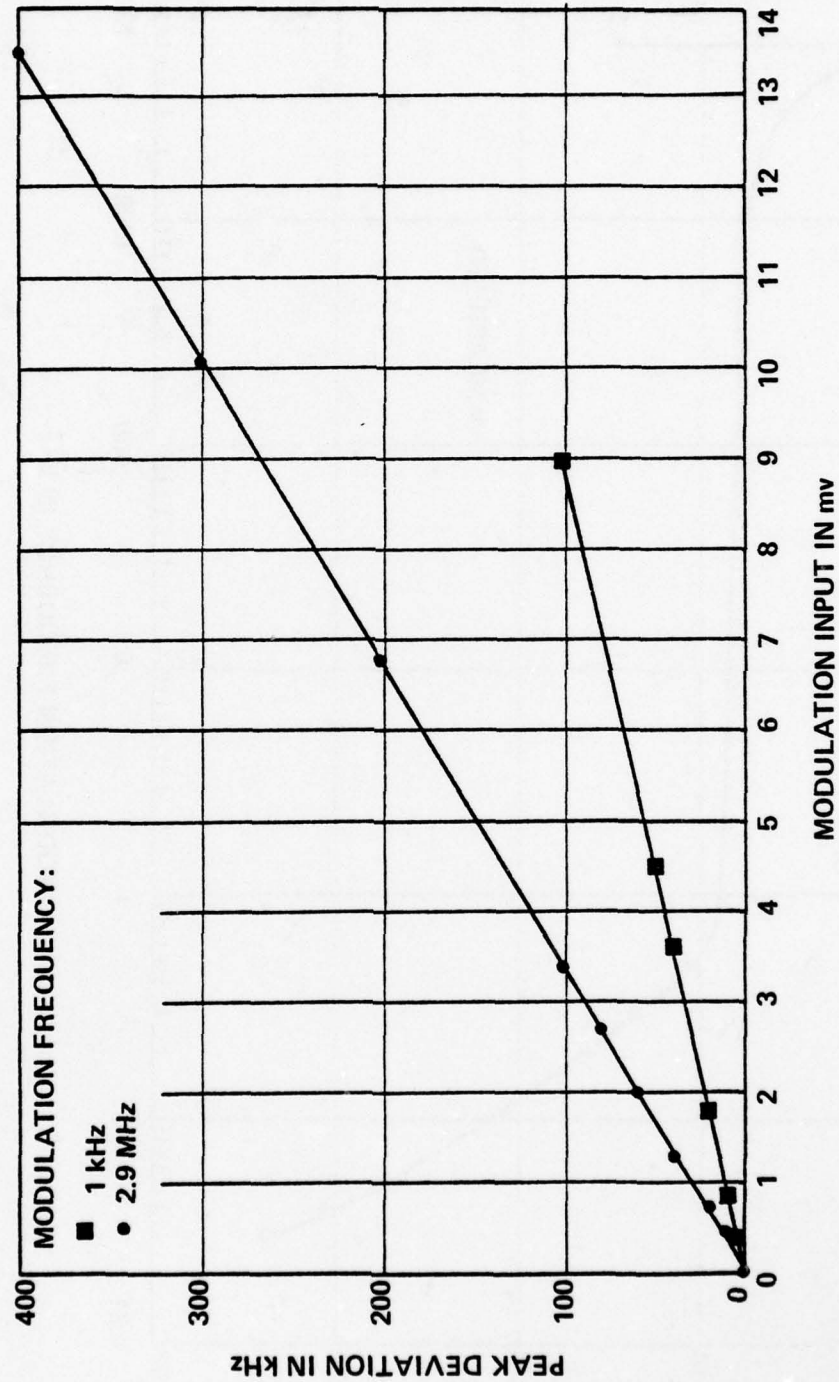


Figure A-3. Transmitter modulation characteristics (low range expanded scale), 600-channel system.

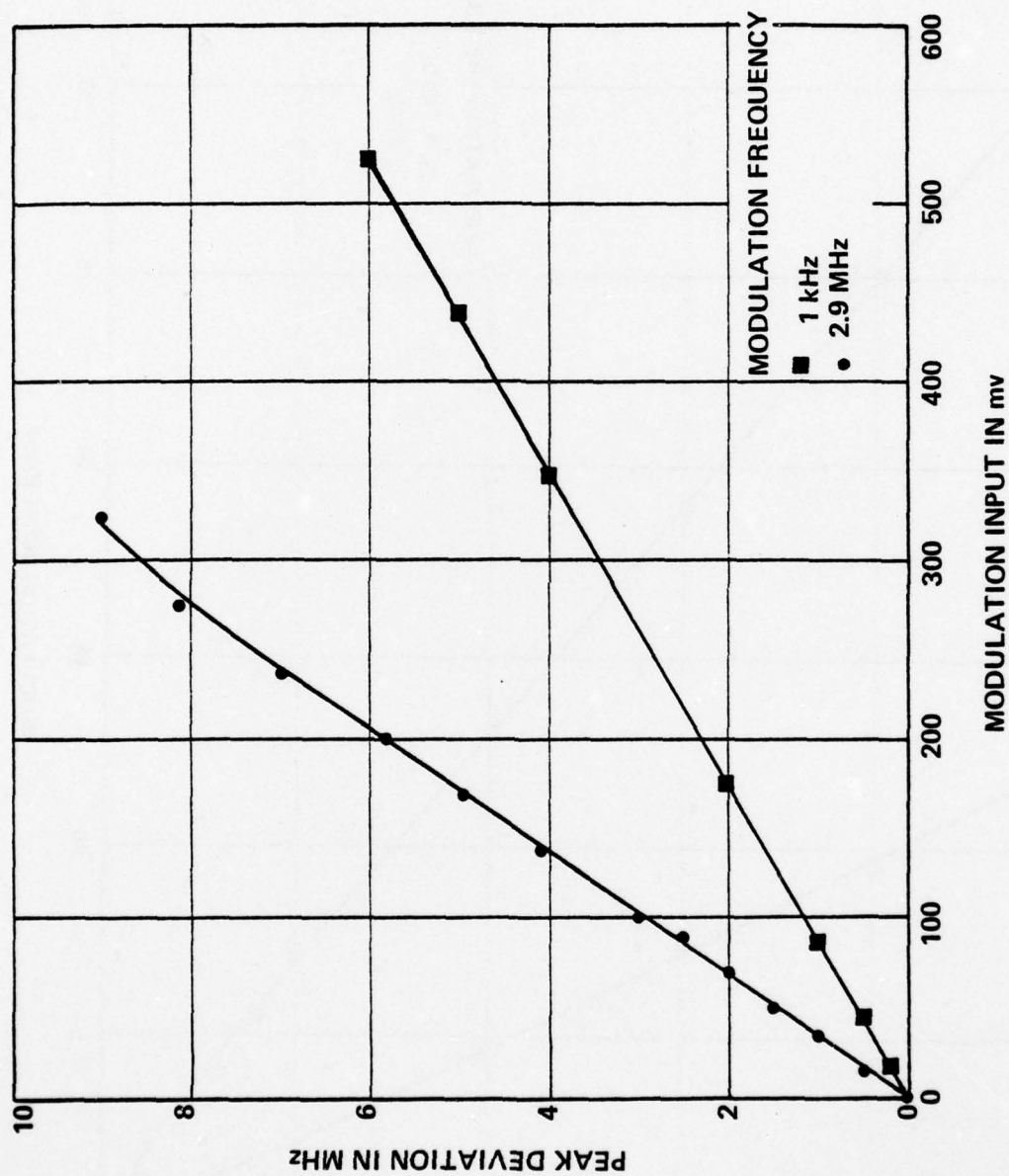


Figure A-4. Transmitter modulation characteristics (full range), 600-channel system.

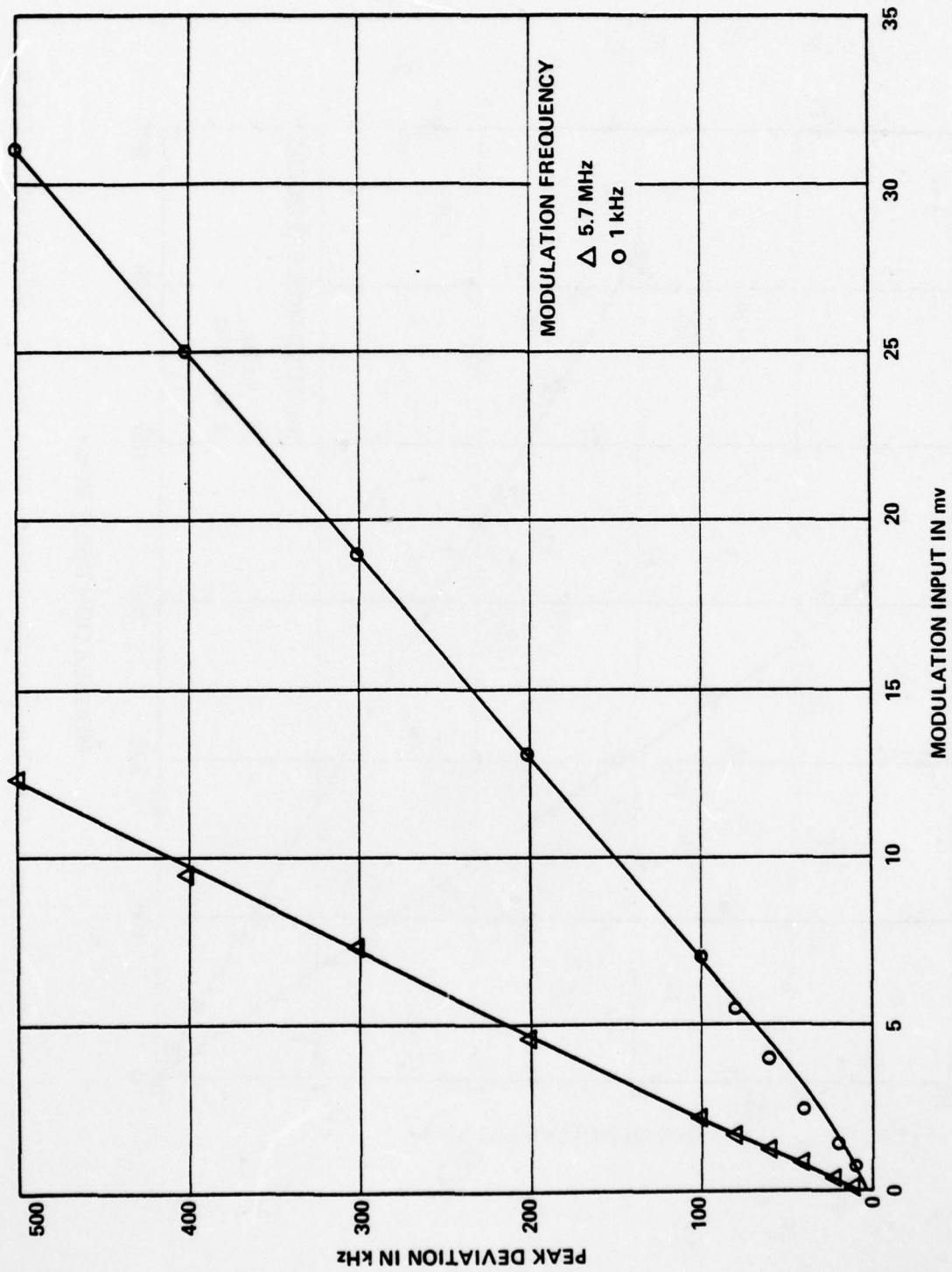


Figure A-5. Transmitter modulation characteristics (low range expanded scale), 1200-channel system.

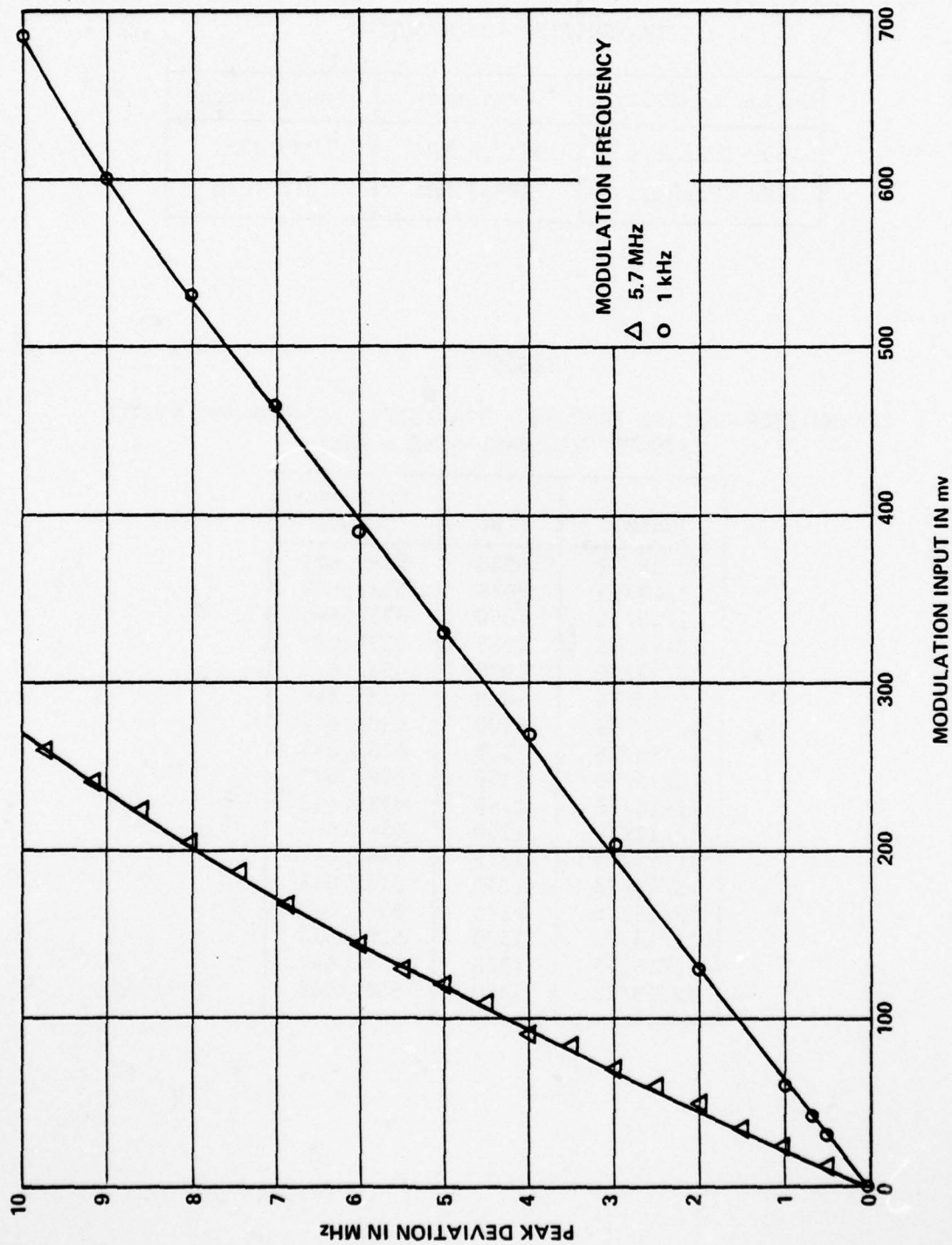


Figure A-6. Transmitter modulation characteristics (full range), 1200-channel system.

TABLE A-3

TRANSMITTER POWER OUTPUT

System Capacity	Frequency	Power Output
600 Channels	6382.6 MHz	30 dBm
1200 Channels	5982.3 MHz	31.2 dBm

TABLE A-4

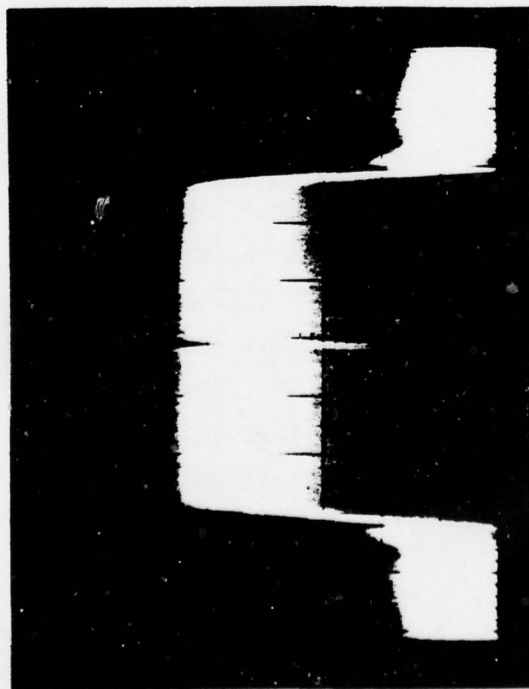
TRANSMITTER CARRIER FREQUENCY STABILITY, 600-CHANNEL SYSTEM
(TUNED FREQUENCY 6382.6 MHz)

Date	Time	Frequency (MHz)
12/18/75	0930	6382.643
12/18/75	0945	6382.642
12/18/75	1000	6382.643
12/18/75	1015	6382.643
12/18/75	1030	6382.642
12/18/75	1045	6382.644
12/18/75	1100	6382.643
12/18/75	1115	6382.643
12/18/75	1130	6382.643
12/18/75	1145	6382.642
12/18/75	1200	6382.644
12/18/75	1215	6382.642
12/18/75	1230	6382.643
12/18/75	1245	6382.643
12/18/75	1300	6382.643
12/18/75	1315	6382.642
12/18/75	1330	6382.642

TABLE A-5

TRANSMITTER CARRIER FREQUENCY STABILITY, 1200-CHANNEL SYSTEM
(TUNED FREQUENCY 5982.3 MHz)

Date	Time	Frequency (MHz)
8/4/76	0800	5982.274
8/4/76	0815	5982.272
8/4/76	0830	5982.271
8/4/76	0845	5982.271
8/4/76	0900	5982.270
8/4/76	0915	5982.270
8/4/76	0930	5982.269
8/4/76	0945	5982.269
8/4/76	1000	5982.269
8/4/76	1015	5982.269
8/4/76	1030	5982.268
8/4/76	1045	5982.268
8/4/76	1100	5982.268
8/4/76	1115	5982.268
8/4/76	1130	5982.268
8/4/76	1145	5982.269
8/7/76	1200	5982.268



Transmitter:

Tuned Frequency 6.0 GHz
Modulation 60-2660 kHz Bandwidth-Limited Noise
Modulation Level 12.8 dBm0
Power Density -20 dBm/MHz

Spectrum Analyzer Settings:

Input Attenuation 10 dB
Scanwidth 1 MHz/div.
Bandwidth 30 kHz
Sweep time 1 s/div.

Photograph:

Center Frequency 6.0 GHz

Figure A-7. Noise modulation signal used in spectrum analyzer noise calibration measurements.

AD-A068 757

IIT RESEARCH INST ANNAPOLIS MD

F/G 17/2.1

WIDEBAND FDM/FM MICROWAVE RADIO RELAY PERFORMANCE DEGRADATION I--ETC(U)

APR 79 A A HERNANDEZ

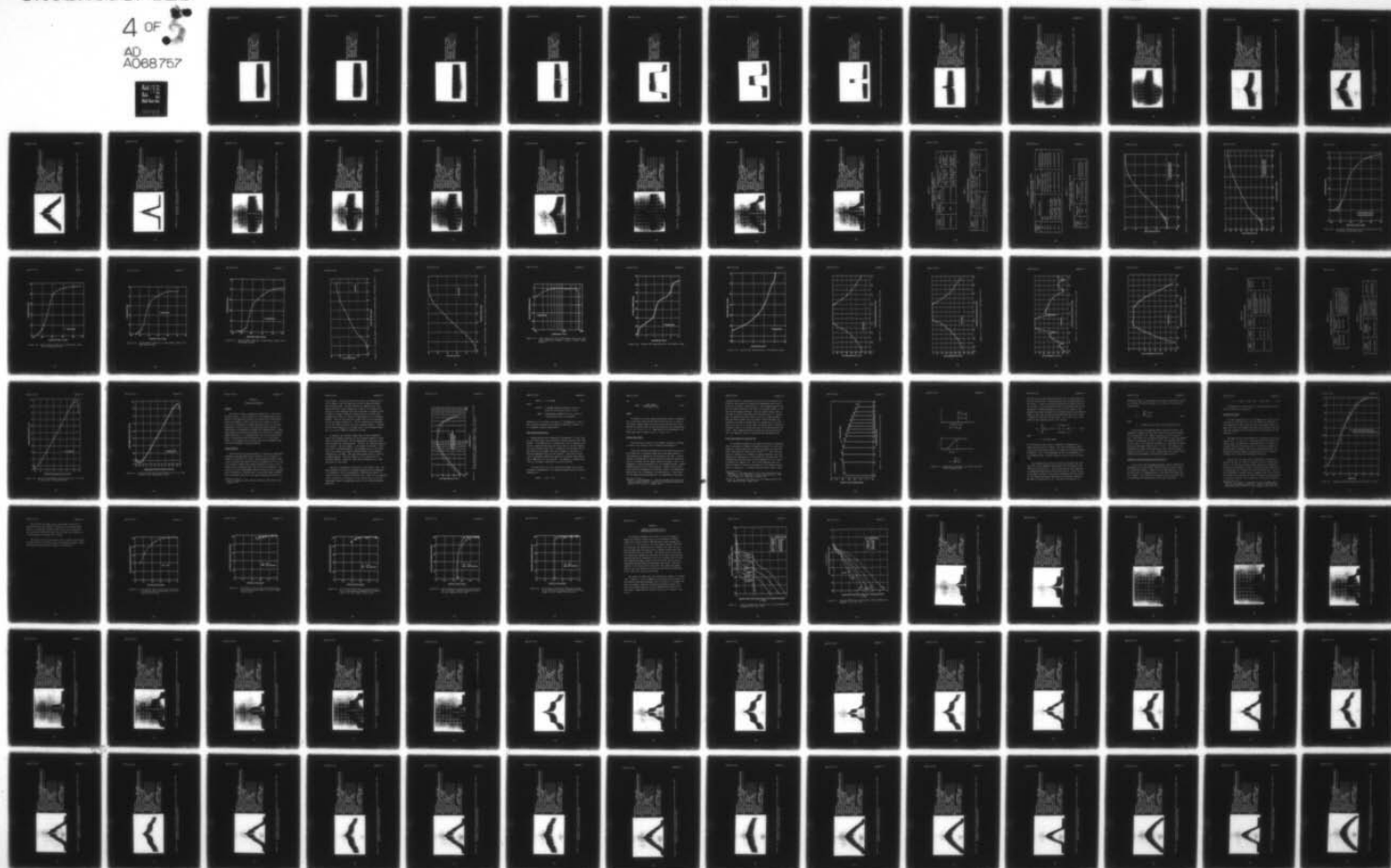
F19628-78-C-0006

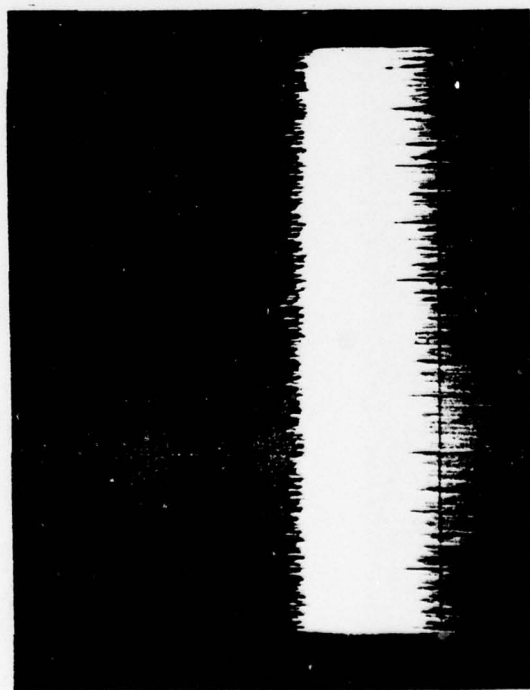
UNCLASSIFIED

ESD-TR-79-100

NL

4 OF 5
AD
A068757





Spectrum Analyzer Settings:

Input Attenuation	10 dB
Scanwidth	10 kHz/div.
Bandwidth	1 kHz
Sweptime	1 s/div.
Log Reference	0 dBm

Figure A-8. Spectrum analyzer noise calibration photograph, scanwidth = 10 kHz/division.

Spectrum Analyzer Settings:
Input Attenuation 10 dB
Scanwidth 50 kHz/div.
Bandwidth 1 kHz
Sweep time 1 s/div.
Log Reference 0 dBm

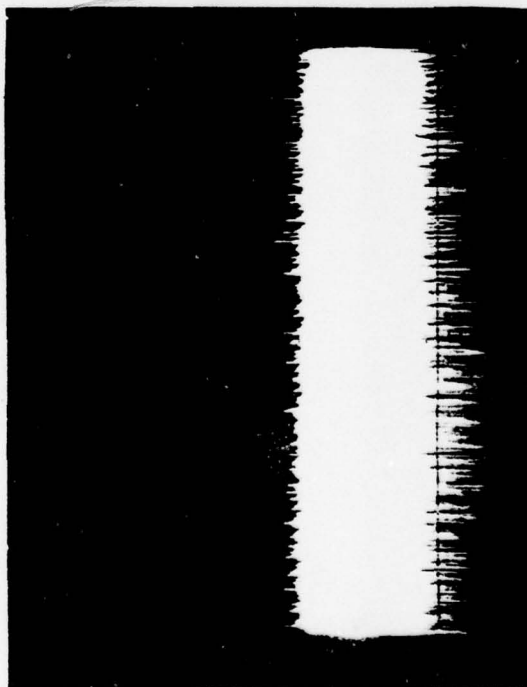


Figure A-9. Spectrum analyzer noise calibration photograph, scanwidth = 50 kHz/division.

Spectrum Analyzer Settings:

Input Attenuation	10 dB
Scanwidth	100 kHz/div.
Bandwidth	1 kHz
Sweep time	1 s/div.
Log Reference	0 dBm

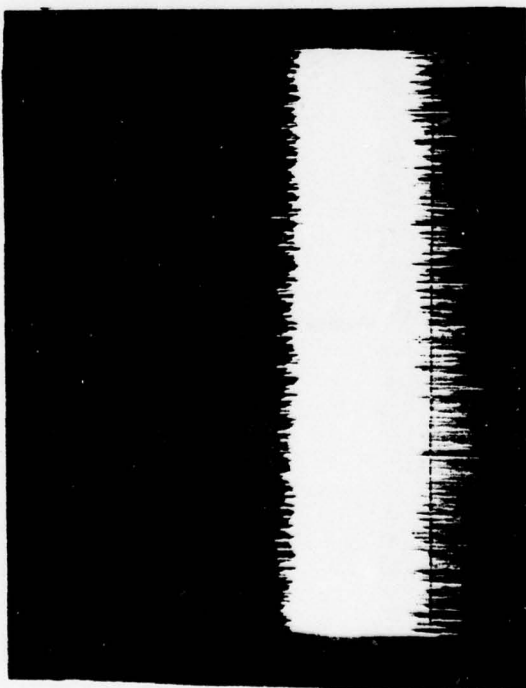


Figure A-10. Spectrum analyzer noise calibration photograph, scanwidth = 100 kHz/division.

Spectrum Analyzer Settings:

Input Attenuation	10 dB
Scanwidth	500 kHz/div.
Bandwidth	1 kHz
Sweptime	1 s/div.
Log Reference	0 dBm

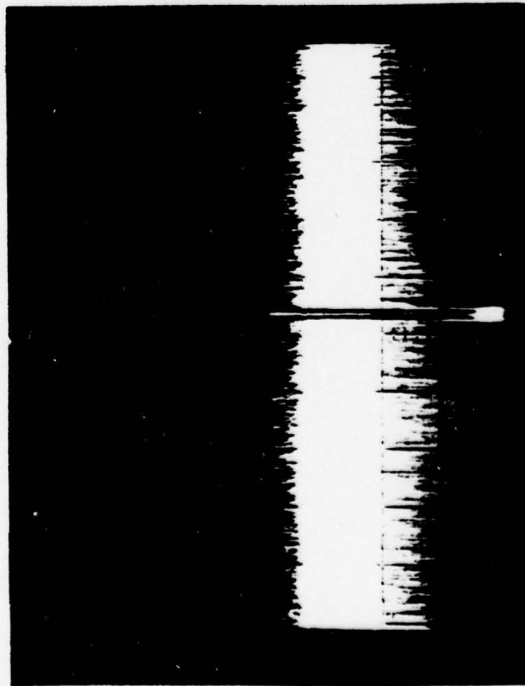
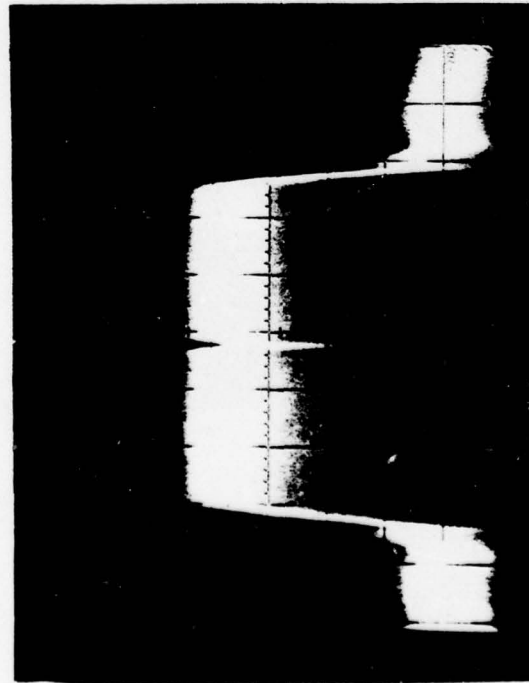


Figure A-11. Spectrum analyzer noise calibration photograph, scanwidth = 500 kHz/division.



Spectrum Analyzer Settings:

Input Attenuation	10 dB
Scanwidth	1 MHz/div.
Bandwidth	100 kHz
Sweep time	1 s/div.
Log Reference	0 dBm

Figure A-12. Spectrum analyzer noise calibration photograph, scanwidth = 1 MHz/division.

Spectrum Analyzer Settings:

Input Attenuation	10 dB
Scanwidth	2 MHz/div.
Bandwidth	100 kHz
Sweeptime	1 s/div.
Log Reference	0 dBm

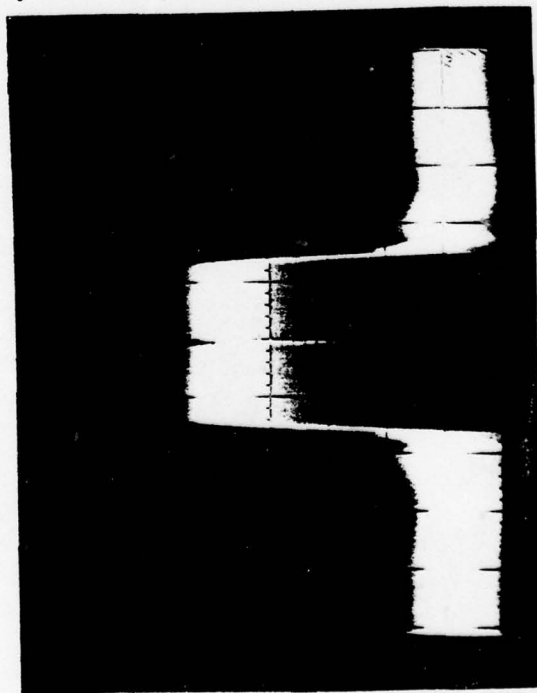
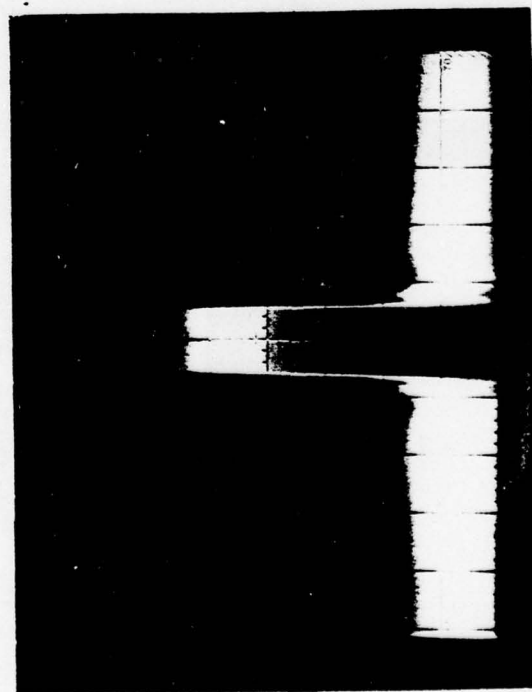


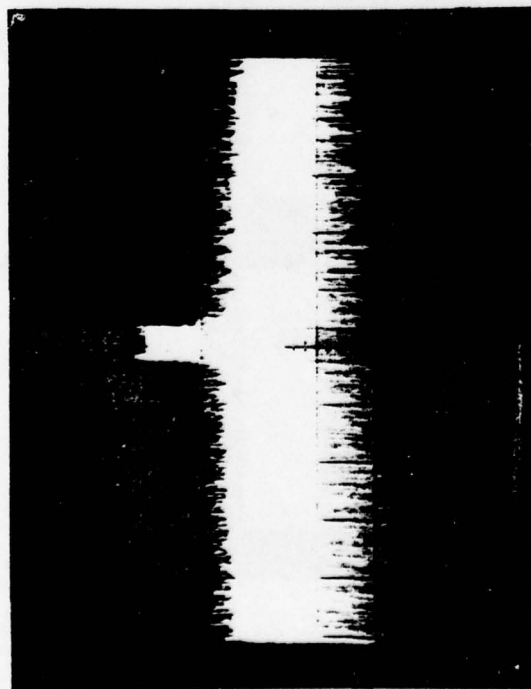
Figure A-13. Spectrum analyzer noise calibration photograph, scanwidth = 2 MHz/division.



Spectrum Analyzer Settings:

Input Attenuation	10 dB
Scanwidth	5 MHz/div.
Bandwidth	100 kHz
Sweep time	1 s/div.
Log Reference	0 dBm

Figure A-14. Spectrum analyzer noise calibration photograph, scanwidth = 5 MHz/division.

**Transmitter:**

Tuned Frequency 6382.6 MHz
 Modulation 60-2660 kHz Bandwidth-Limited Noise
 Modulation Level 12.8 dBm0

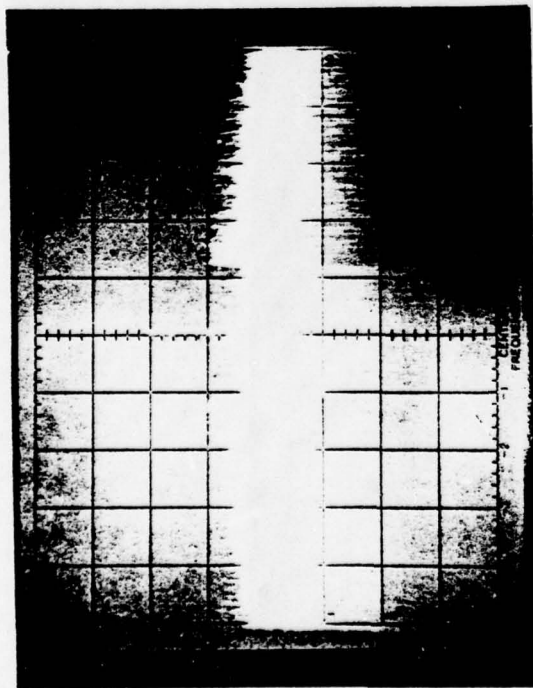
Spectrum Analyzer Settings:

Input Attenuation 10 dB
 Scanwidth 10 kHz/div.
 Bandwidth 1 kHz
 Sweeptime 1 s/div.
 Log Reference 0 dBm
 Line Attenuation 37 dB

Photograph:

Harmonic Fundamental
 Center Frequency 6382.6 MHz
 Top Line Reference 33 dBm

Figure A-15. Narrowband emission spectrum characteristics of 600-channel Lenkurt 778A2 transmitter, 10 kHz/division.

**Transmitter:**

Tuned Frequency 6382.6 MHz
 Modulation 60-2660 kHz Bandwidth-Limited Noise
 Modulation Level 12.8 dBm0

Spectrum Analyzer Settings:

Input Attenuation 10 dB
 Scanwidth 50 kHz/div.
 Bandwidth 1 kHz
 Swepttime 1 s/div.
 Log Reference 0 dBm
 Line Attenuation 37 dB

Photograph:

Harmonic Fundamental
 Center Frequency 6382.6 MHz
 Top Line Reference 33 dBm

Figure A-16. Narrowband emission spectrum characteristics of 600-channel Lenkurt 778A2 transmitter, 50 kHz/division.

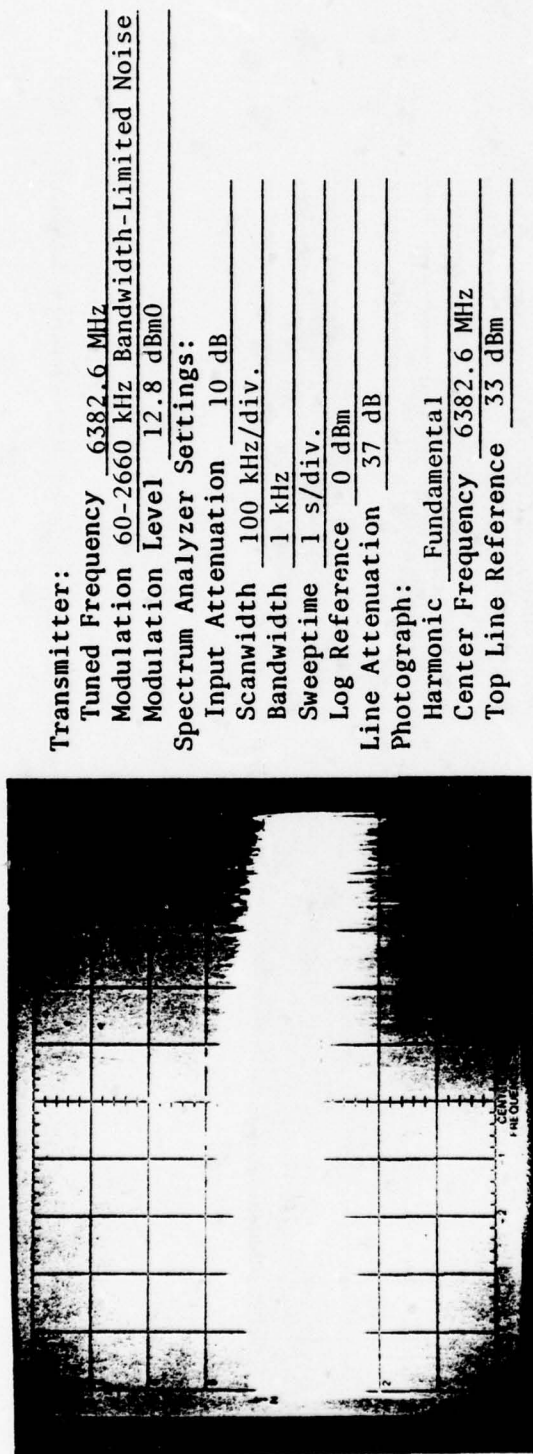


Figure A-17. Narrowband emission spectrum characteristics of 600-channel Lenkurt 778A2 transmitter, 100 kHz/division.



Transmitter:

Tuned Frequency 6382.6 MHz
 Modulation 60-2660 kHz Bandwidth-Limited Noise
 Modulation Level 12.8 dBm0

Spectrum Analyzer Settings:

Input Attenuation 10 dB
 Scanwidth 500 kHz/div.
 Bandwidth 1 kHz
 Sweptime 1 s/div.
 Log Reference 0 dBm
 Line Attenuation 37 dB

Photograph:

Harmonic Fundamental
 Center Frequency 6382.6 MHz
 Top Line Reference 33 dBm

Figure A-18. Narrowband emission spectrum characteristics of 600-channel Lenkrut 778A2 transmitter, 500 kHz/division.

**Transmitter:**

Tuned Frequency 6382.6 MHz
 Modulation 60-2660 kHz Bandwidth-Limited Noise
 Modulation Level 12.8 dBm0

Spectrum Analyzer Settings:

Input Attenuation 10 dB
 Scanwidth 1 MHz/div.
 Bandwidth 100 kHz
 Sweeptime 1 s/div.
 Log Reference 0 dBm
 Line Attenuation 37 dB

Photograph:

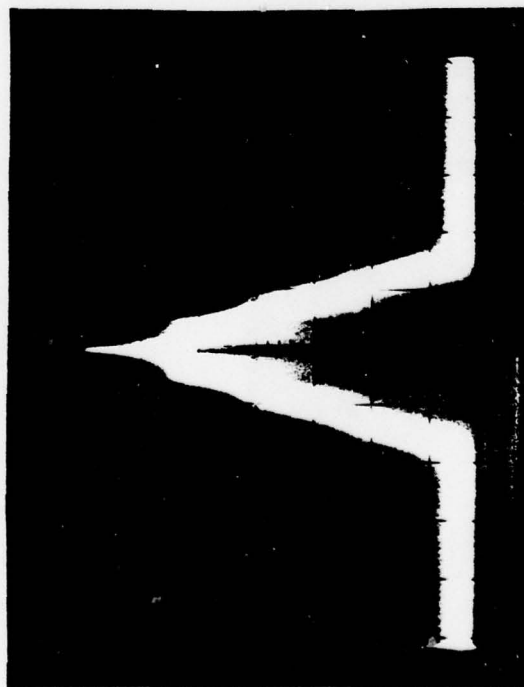
Harmonic Fundamental
 Center Frequency 6382.6 MHz
 Top Line Reference 33 dBm

Figure A-19. Narrowband emission spectrum characteristics of 600-channel Lenkurt 778A2 transmitter, 1 MHz/division.

Transmitter:
 Tuned Frequency 6382.6 MHz
 Modulation 60-2660 kHz Bandwidth-Limited Noise
 Modulation Level 12.8 dBm0
 Spectrum Analyzer Settings:
 Input Attenuation 10 dB
 Scanwidth 2 MHz/div.
 Bandwidth 100 kHz
 Swepttime 1 s/div.
 Log Reference 0 dBm
 Line Attenuation 37 dB
 Photograph:
 Harmonic Fundamental
 Center Frequency 6382.6 MHz
 Top Line Reference 33 dBm



Figure A-20. Narrowband emission spectrum characteristics of 600-channel Lenkurt 778A2 transmitter, 2 MHz/division.

**Transmitter:**

Tuned Frequency 6382.6 MHz
 Modulation 60-2660 kHz Bandwidth-Limited Noise
 Modulation Level 12.8 dBm0

Spectrum Analyzer Settings:

Input Attenuation 10 dB
 Scanwidth 5 MHz/div.
 Bandwidth 100 kHz
 Swepttime 1 s/div.
 Log Reference 0 dBm
 Line Attenuation 37 dB

Photograph:

Harmonic Fundamental
 Center Frequency 6382.6 MHz
 Top Line Reference 33 dBm

Figure A-21. Narrowband emission spectrum characteristics of 600-channel Lenkurt 778A2 transmitter, 5 MHz/division.

Transmitter:

Tuned Frequency 5982.3 MHz
 Modulation 60-5564 kHz Bandwidth-Limited Noise
 Modulation Level 15.8 dBm0

Spectrum Analyzer Settings:

Input Attenuation 10 dB
 Scanwidth 10 kHz/div.
 Bandwidth 1 kHz
 Sweeptime 1 s/div.
 Log Reference 0 dBm
 Line Attenuation 42 dB

Photograph:

Harmonic Fundamental
 Center Frequency 5982.3 MHz
 Top Line Reference 38 dBm

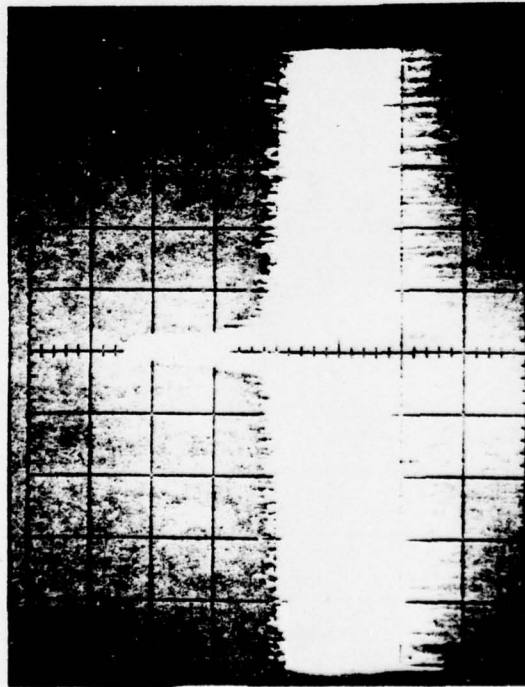
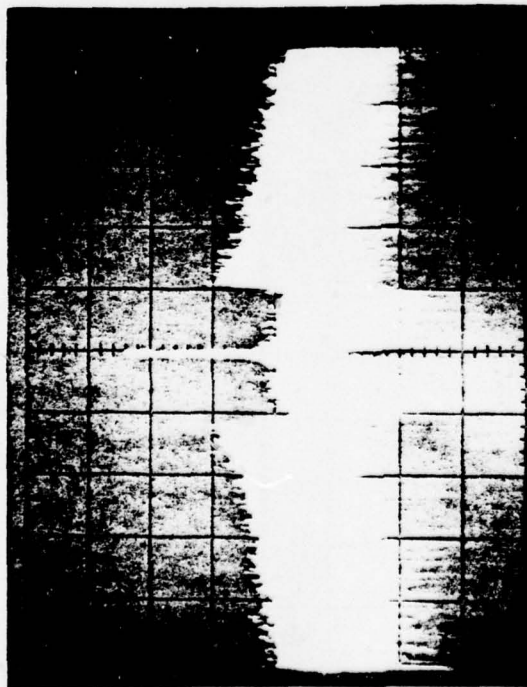


Figure A-22. Narrowband emission spectrum characteristics of 1200-channel Lenkurt 778A2 transmitter, 10 kHz/division.



Transmitter:

Tuned Frequency 5982.3 MHz
 Modulation 60-5664 kHz Bandwidth-Limited Noise
 Modulation Level 15.8 dBm0

Spectrum Analyzer Settings:

Input Attenuation 10 dB
 Scanwidth 50 kHz/div.
 Bandwidth 1 kHz
 Sweeptime 1 s/div.
 Log Reference 0 dBm
 Line Attenuation 42 dB

Photograph:

Harmonic Fundamental
 Center Frequency 5982.3 MHz
 Top Line Reference 38 dBm

Figure A-23. Narrowband emission spectrum characteristics of 1200-channel Lenkurt 778A2 transmitter, 50 kHz/division.

Transmitter:

Tuned Frequency	5982.3 MHz
Modulation	60-5564 kHz Bandwidth-Limited Noise
Modulation Level	15.8 dBm0

Spectrum Analyzer Settings:

Input Attenuation	10 dB
Scanwidth	100 kHz/div.
Bandwidth	1 kHz
Sweeptime	1 s/div.
Log Reference	0 dBm
Line Attenuation	42 dB

Photograph:

Harmonic	Fundamental
Center Frequency	5982.3 MHz
Top Line Reference	38 dBm

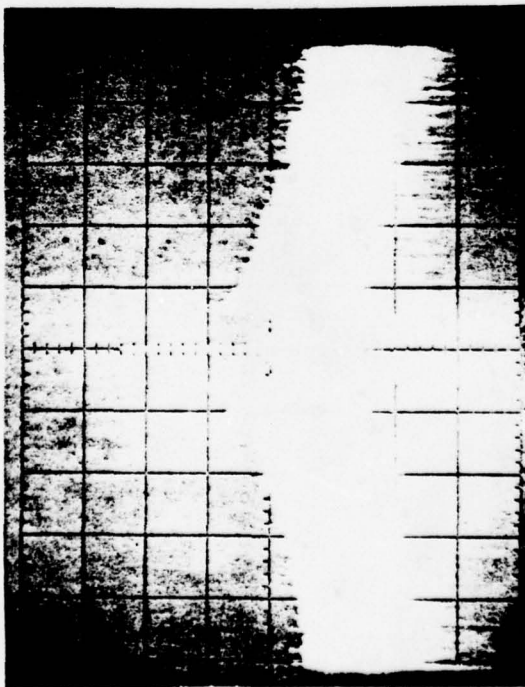


Figure A-24. Narrowband emission spectrum characteristics of 1200-channel Lenkurt 788A2 transmitter, 100 kHz/division.

Transmitter:
 Tuned Frequency 5982.3 MHz
 Modulation 60-5564 kHz Bandwidth-Limited Noise
 Modulation Level 15.8 dBm0

Spectrum Analyzer Settings:
 Input Attenuation 10 dB
 Scanwidth 500 kHz/div.
 Bandwidth 1 kHz
 Sweep time 1 s/div.
 Log Reference 0 dBm
 Line Attenuation 42 dB

Photograph:
 Harmonic Fundamental
 Center Frequency 5982.3 MHz
 Top Line Reference 38 dBm

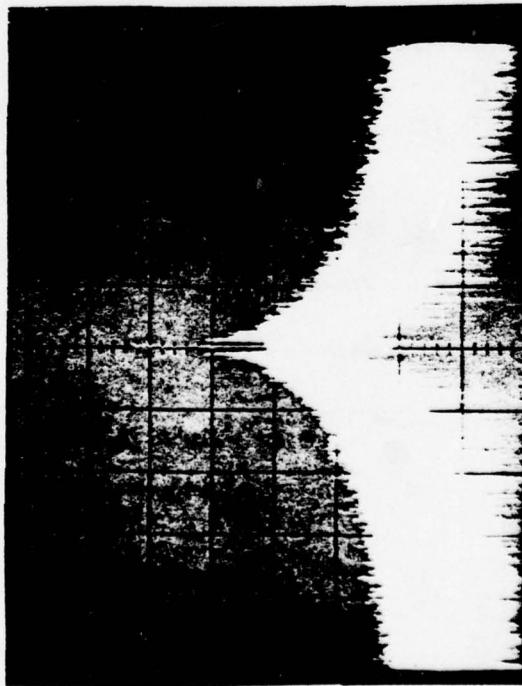
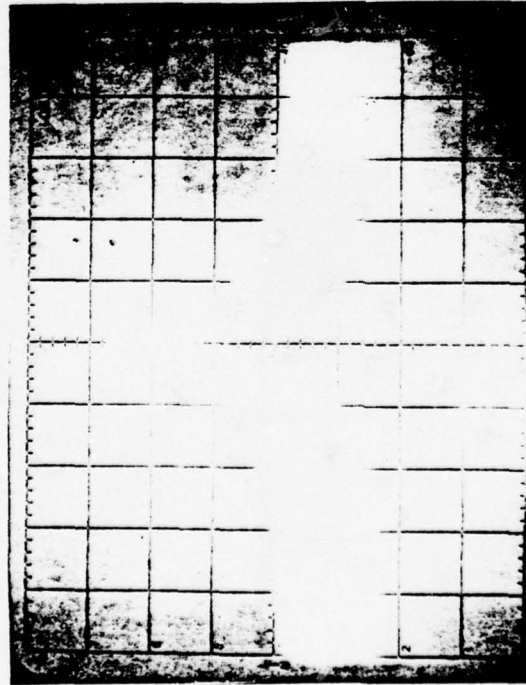


Figure A-25. Narrowband emission spectrum characteristics of 1200-channel Lenkurt 778A2 transmitter, 500 kHz/division.

**Transmitter:**

Tuned Frequency 5982.3 MHz
 Modulation 60-5664 kHz Bandwidth-Limited Noise
 Modulation Level 15.8 dBm0

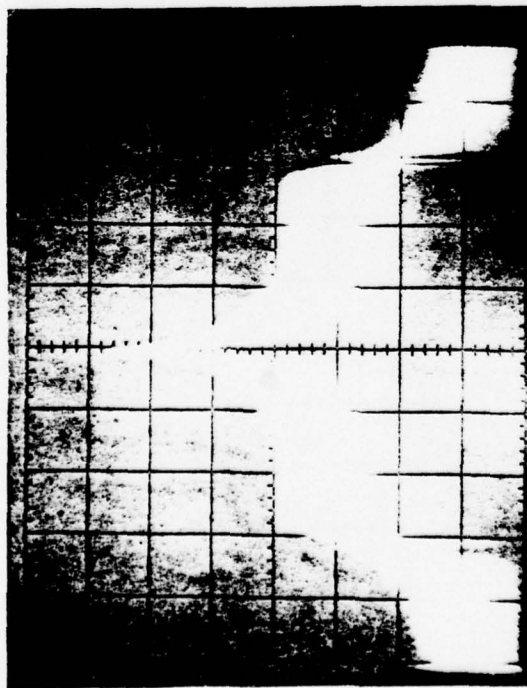
Spectrum Analyzer Settings:

Input Attenuation 10 dB
 Scanwidth 1 MHz/div.
 Bandwidth 100 kHz
 Sweeptime 1 s/div.
 Log Reference 0 dBm
 Line Attenuation 42 dB

Photograph:

Harmonic Fundamental
 Center Frequency 5982.3 MHz
 Top Line Reference 38 dBm

Figure A-26. Narrowband emission spectrum characteristics of 1200-channel Lenkurt 778A2 transmitter, 1 MHz/division.

**Transmitter:**

Tuned Frequency 5982.3 MHz
 Modulation 60-5564 kHz Bandwidth-Limited Noise
 Modulation Level 15.8 dBm0

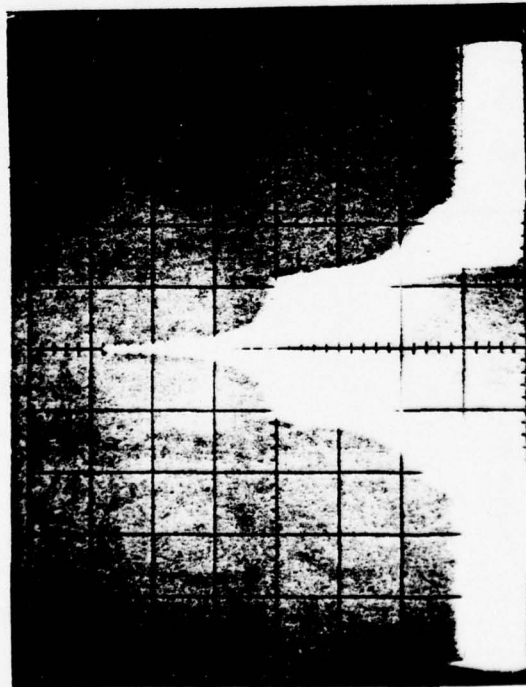
Spectrum Analyzer Settings:

Input Attenuation 10 dB
 Scanwidth 2 MHz/div.
 Bandwidth 100 kHz
 Sweeptime 1 s/div.
 Log Reference 0 dBm
 Line Attenuation 42 dB

Photograph:

Harmonic Fundamental
 Center Frequency 5982.3 MHz
 Top Line Reference 38 dBm

Figure A-27. Narrowband emission spectrum characteristics of 1200-channel Lenkurt 778A2 transmitter, 2 MHz/division.



Transmitter:

Tuned Frequency 5982.3 MHz
 Modulation 60-5564 kHz Bandwidth-Limited Noise
 Modulation Level 15.8 dBm0

Spectrum Analyzer Settings:

Input Attenuation 10 dB
 Scanwidth 5 MHz/div.
 Bandwidth 100 kHz
 Swepttime 1 s/div.
 Log Reference 0 dBm
 Line Attenuation 42 dB

Photograph:

Harmonic Fundamental
 Center Frequency 5982.3 MHz
 Top Line Reference 38 dBm

Figure A-28. Narrowband emission spectrum characteristics of 1200-channel Lenkurt 778A2 transmitter, 5 MHz/division.

TABLE A-6
WIDEBAND EMISSION SPECTRUM CHARACTERISTICS
(LENKURT 778A2 TRANSMITTER)

System Capacity	Measuring Instrument	Range of Observation	Measurement System Sensitivity	Emissions
600 Channels	FSVM	3.87 to 12.0 GHz	≥ -90 dBm to 8 GHz and ≥ -70 dBm from 8 GHz to 12 GHz	No wideband emissions were observed
1200 Channels	FSVM	3.87 to 12.0 GHz	≥ -90 dBm to 10 GHz and ≥ -70 dBm from 10 GHz to 12 GHz	No wideband emissions were observed

TABLE A-7
TRANSMITTER INTERMODULATION

System Capacity	Measured Intermodulation and Level	Interference Frequency (f_i) and Level	Transmitter Frequency (f_o) and Level
600 Channels	$2f_i - f_o = 6254.948$ MHz at a level of -70 dBm	$f_i = 6318.774$ MHz at a level of 10 dBm	$f_o = 6382.6$ MHz at a level of 30 dBm
1200 Channels	No intermodulation products were observed		

TABLE A-8
RECEIVER SENSITIVITY 600-CHANNEL SYSTEM
(TUNED FREQUENCY 6382.6 MHz)

Receiver Power (dBm)	Modulating Signal	Output Measurement Location	Standard Response
-70.6	None	124-ohm receiver output	20 dB CW quieting
-83.5	None	Receiver baseband output	20 dB CW quieting
-84.5	None	Low channel (340-344 kHz)	20 dB CW quieting
-89.0	1 kHz, 0 dBmO, low channel 12.8 dBmO noise, baseband	Low channel (340-344 kHz)	10 dB(S+N+D)/(N+D)
-86.0	1 kHz, -8 dBmO, low channel 12.8 dBmO noise, baseband	Low channel (340-344 kHz)	10 dB(S+N+D)/(N+D)
-84.0	1 kHz, -15 dBmO, low channel 12.8 dBmO noise, baseband	Low channel (340-344 kHz)	10 dB(S+N+D)/(N+D)

TABLE A-9
RECEIVER SENSITIVITY 1200-CHANNEL SYSTEM
(TUNED FREQUENCY 5982.3 MHz)

Receiver Power (dBm)	Modulating Signal	Output Measurement Location	Standard Response
-63.5	None	124-ohm receiver output	20 dB CW quieting
-77.6	None	Receiver baseband output	20 dB CW quieting

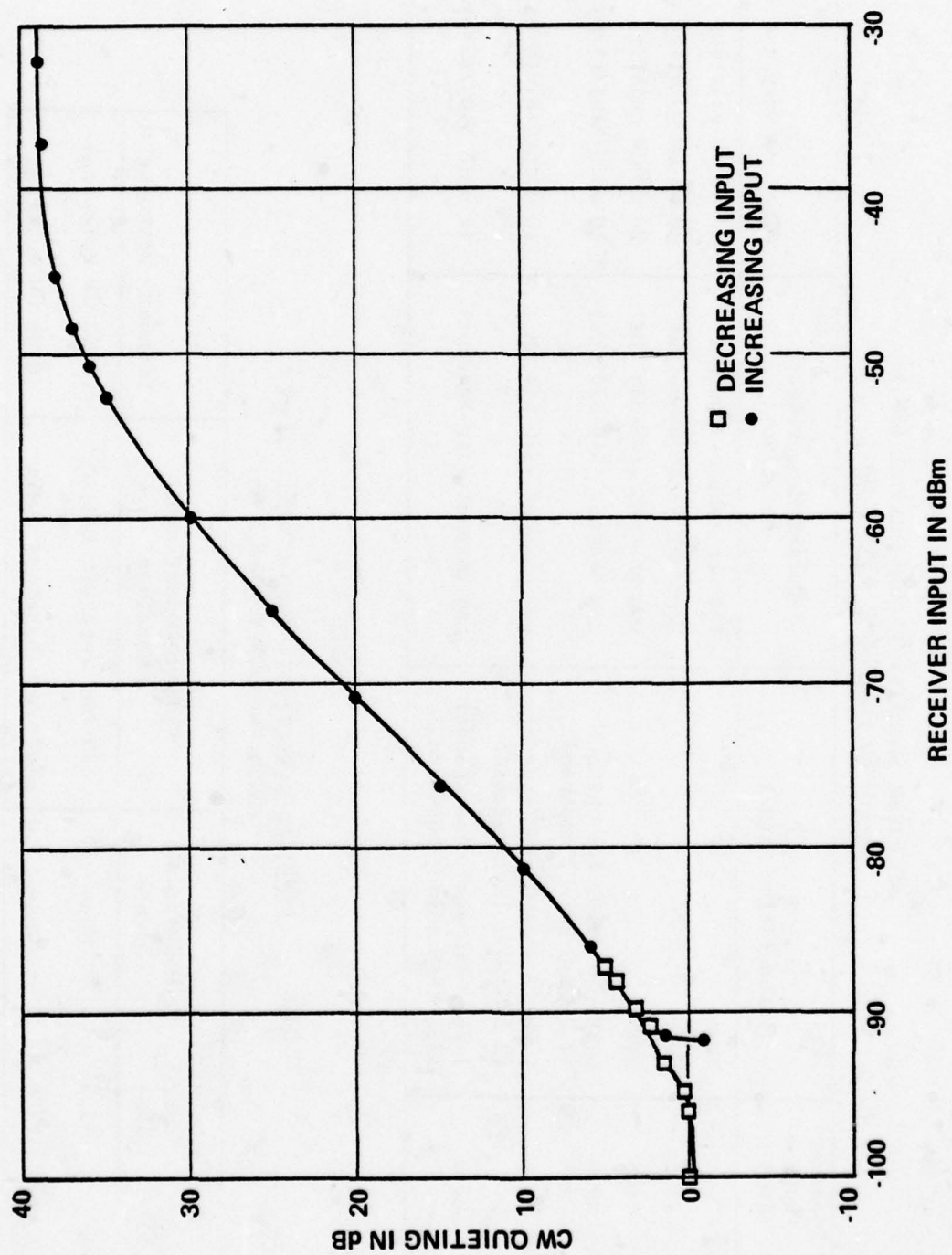


Figure A-29. CW quieting dynamic range at the receiver 124-ohm output, 600-channel system.

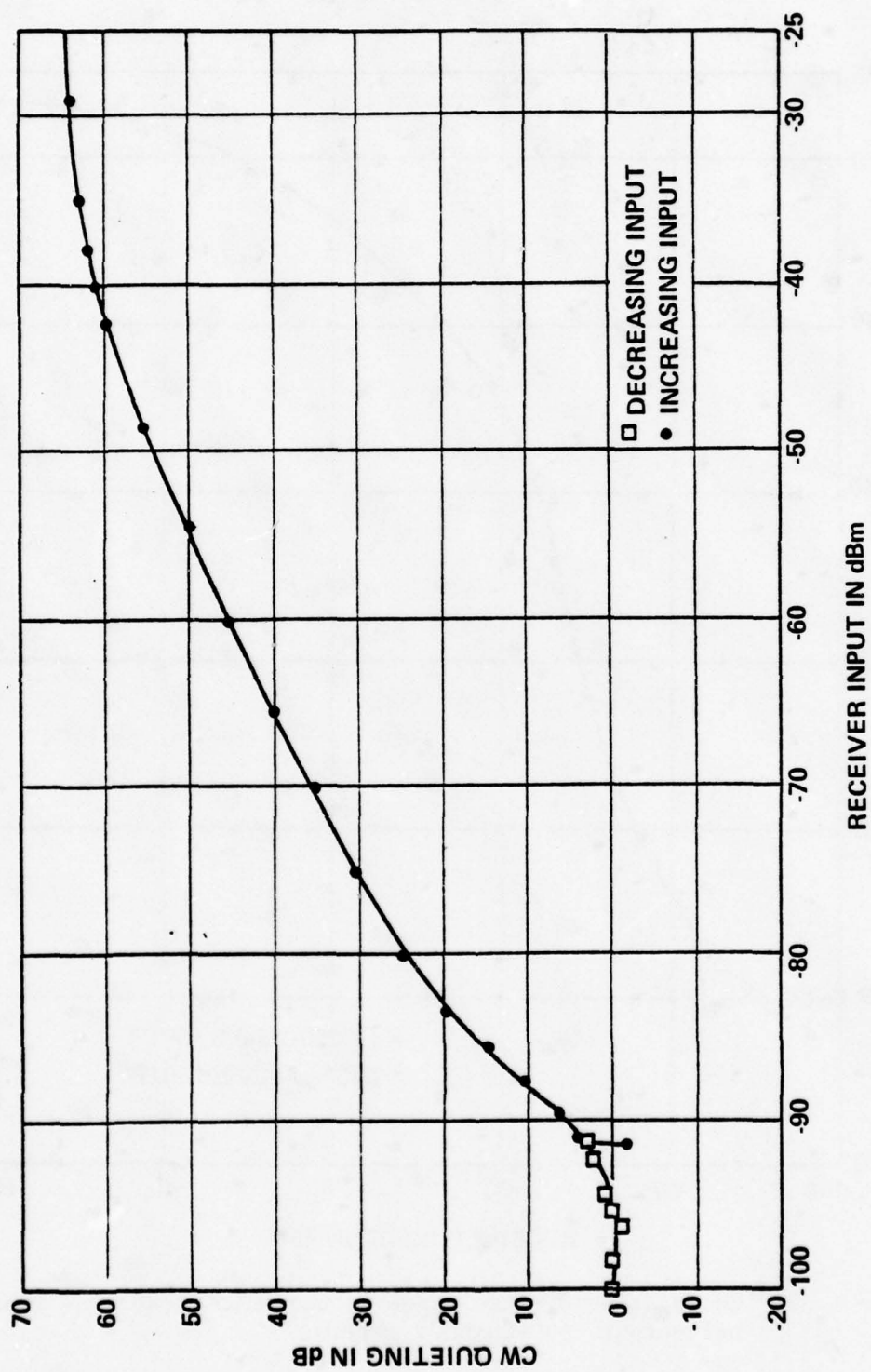


Figure A-30. CW quieting dynamic range at the receiver baseband output, 600-channel system.

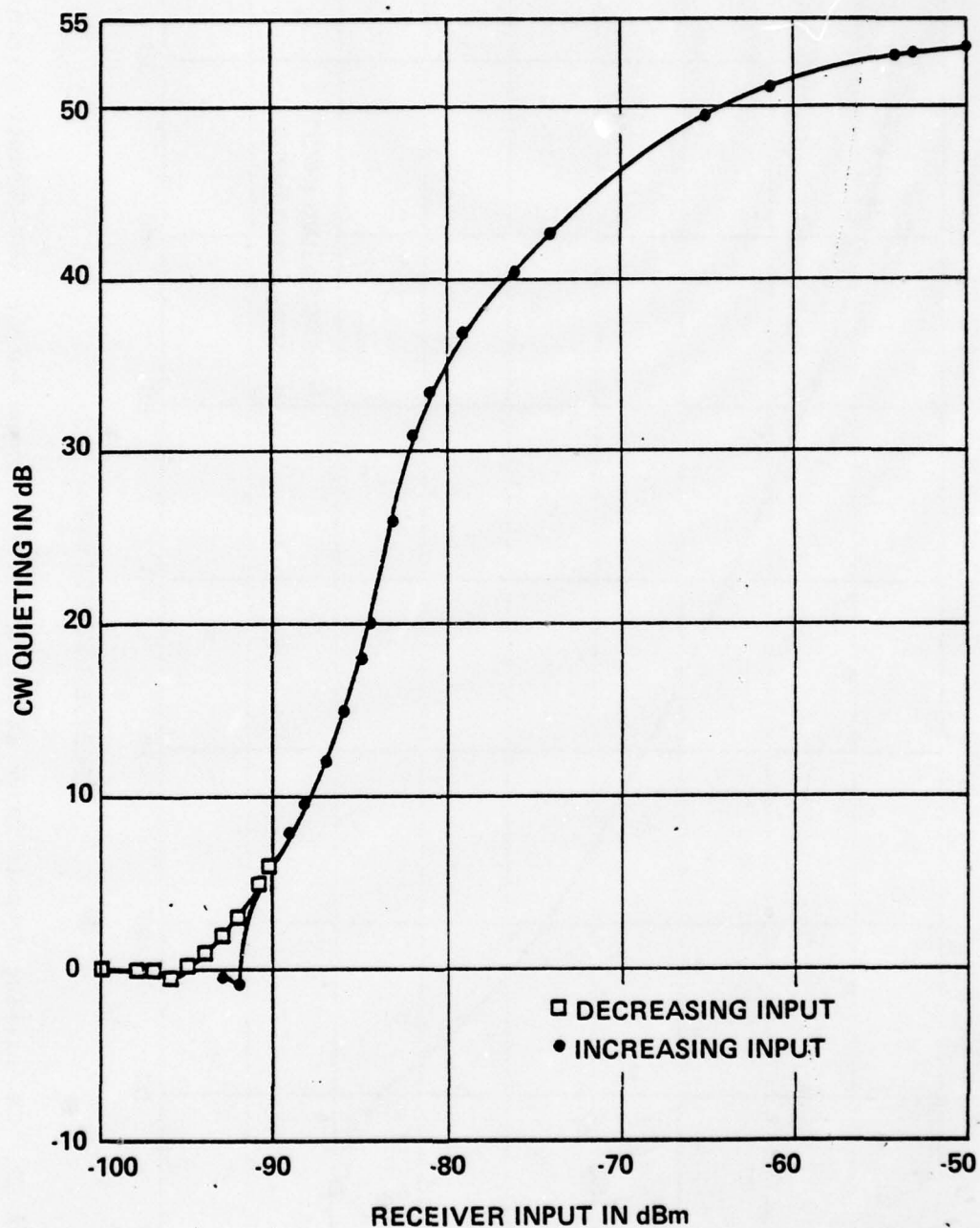


Figure A-31. CW quieting dynamic range at the multiplexer low channel output, 600-channel system.

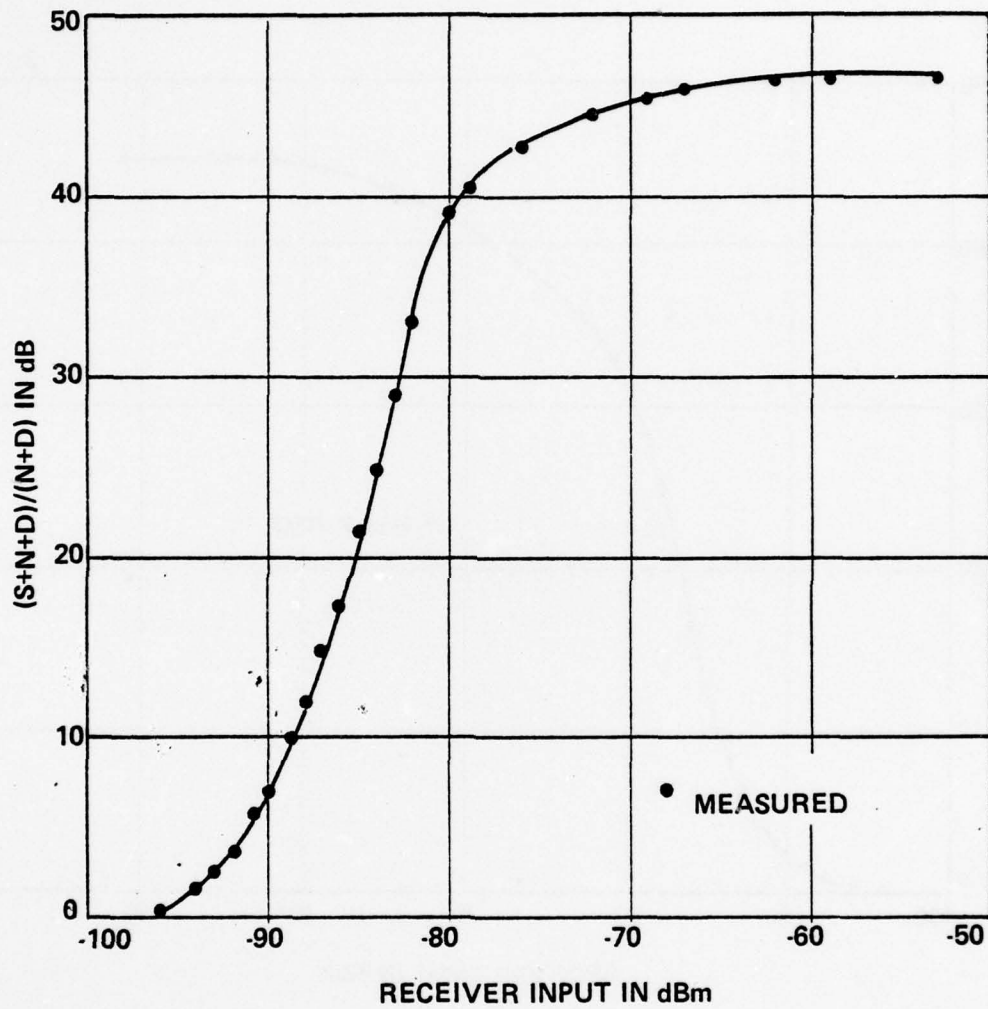


Figure A-32. System dynamic range for -16 dBm channel signal level, 600-channel system.

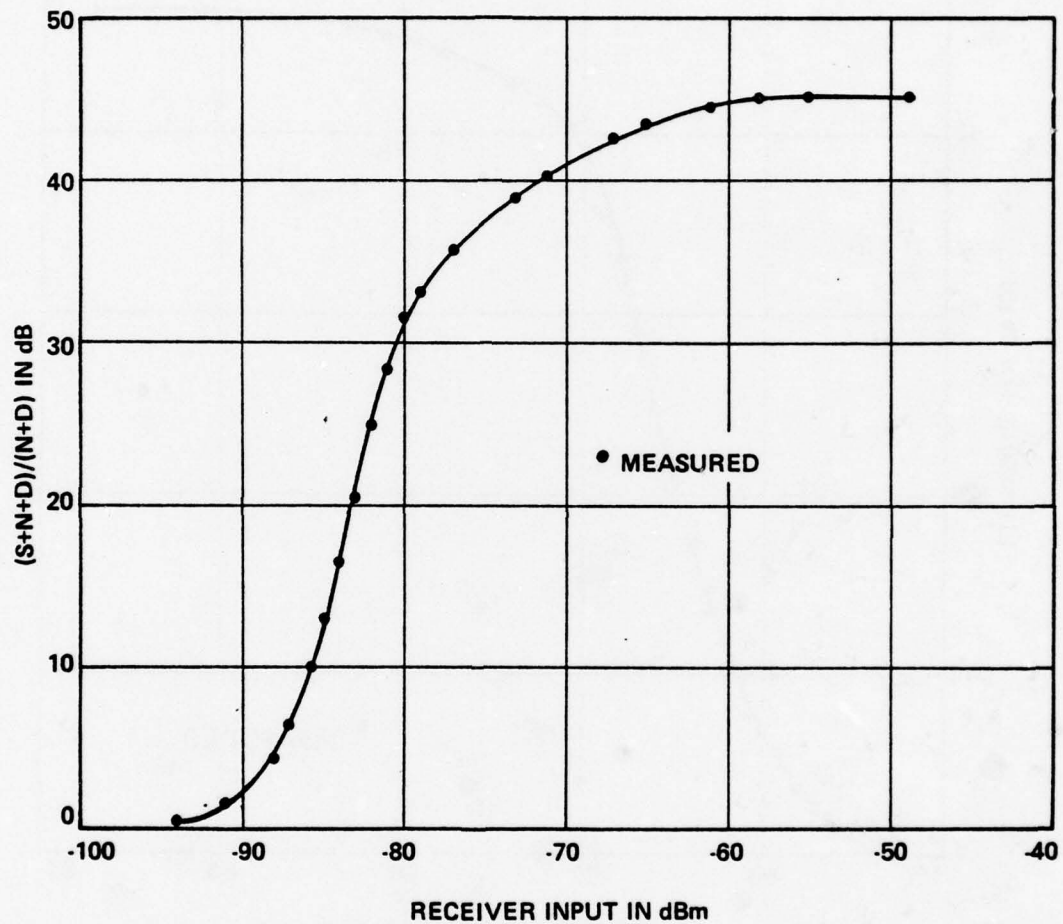


Figure A-33. System dynamic range for -24 dBm channel signal level, 600-channel system.

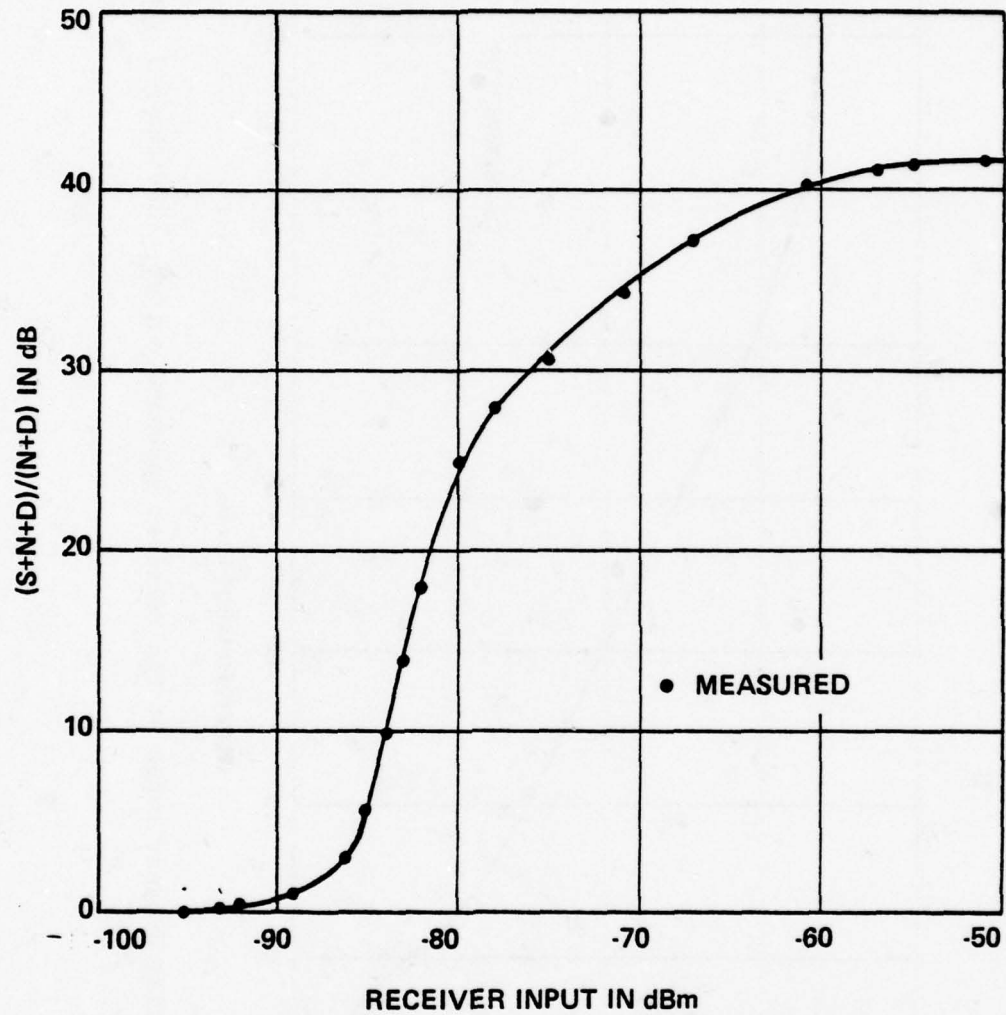


Figure A-34. System dynamic range for -31 dBm channel signal level, 600-channel system.

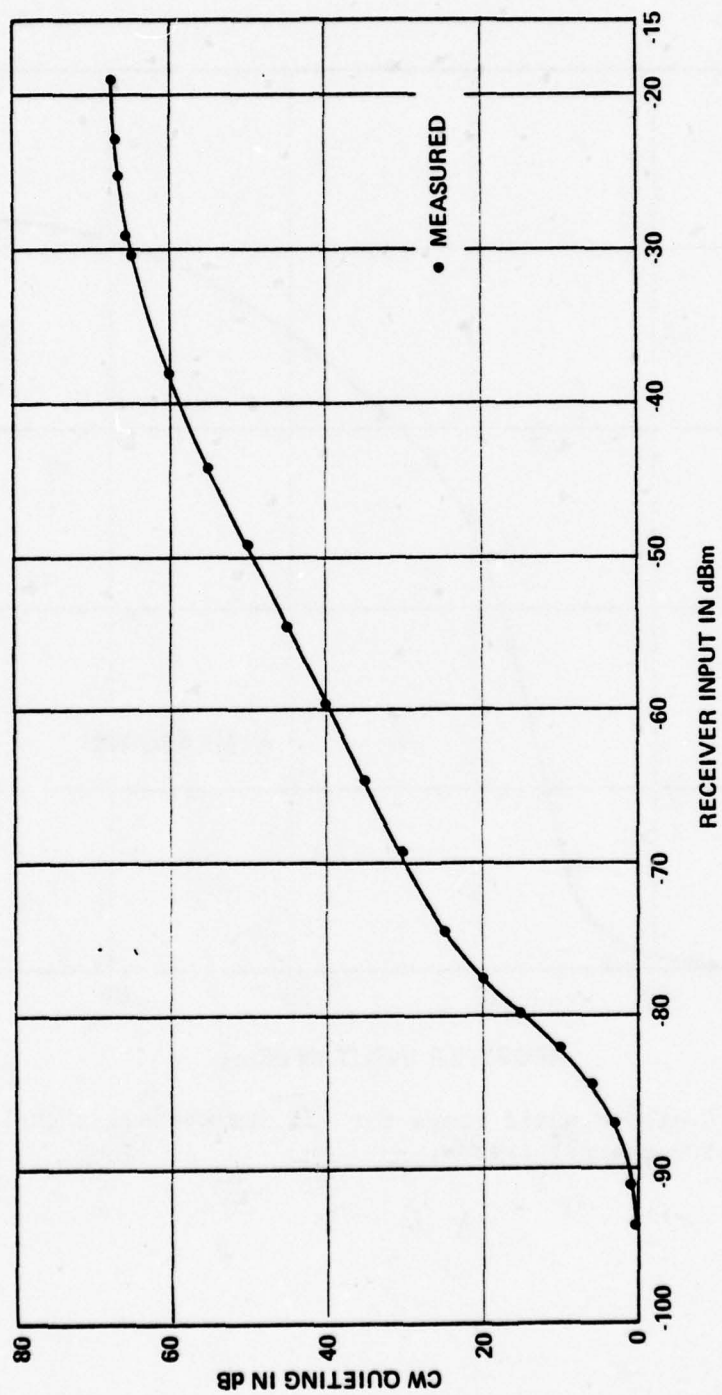


Figure A-35. CW quieting dynamic range at the receiver baseband output, 1200-channel system.

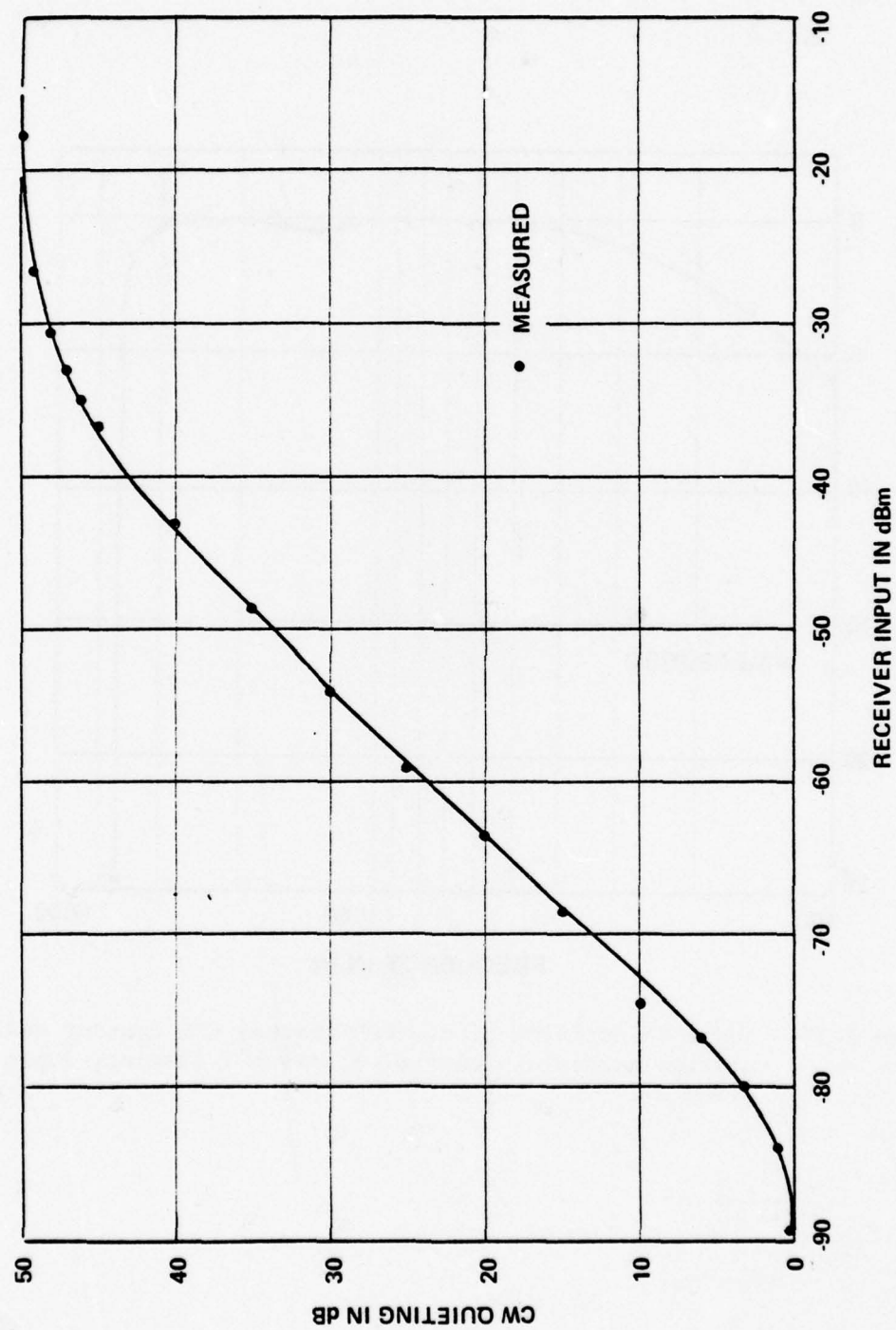


Figure A-36. CW quieting dynamic range at the receiver 124-ohm output, 1200-channel system.

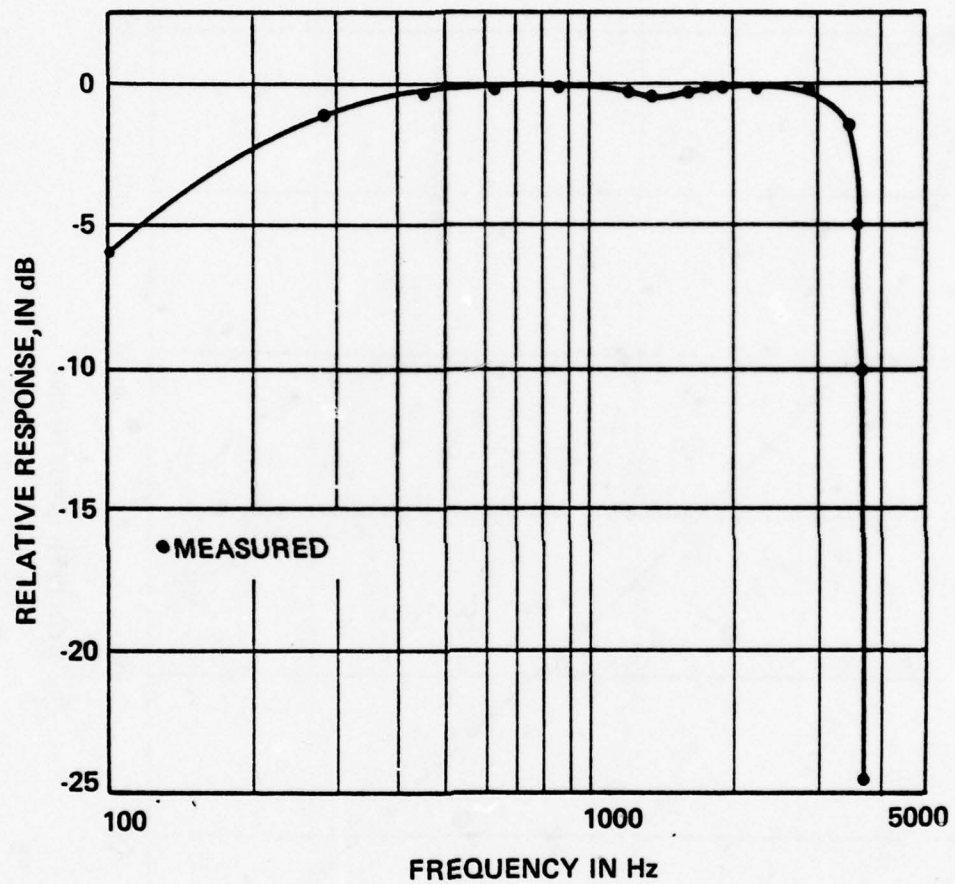


Figure A-37. Audio selectivity of the 600-channel GTE Lenkrut 46A2 carrier multiplex (channel 8, group 1 carrier, super group 2).

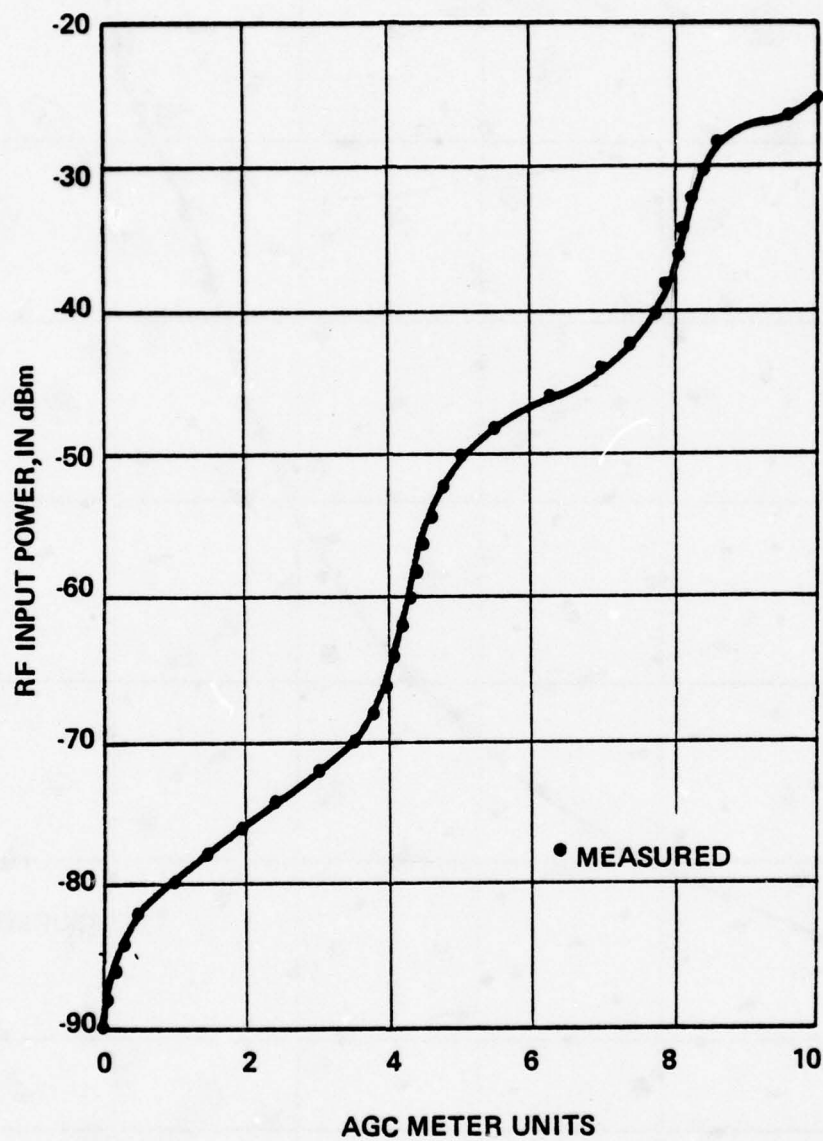


Figure A-38. Receiver AGC characteristics, 600-channel system.

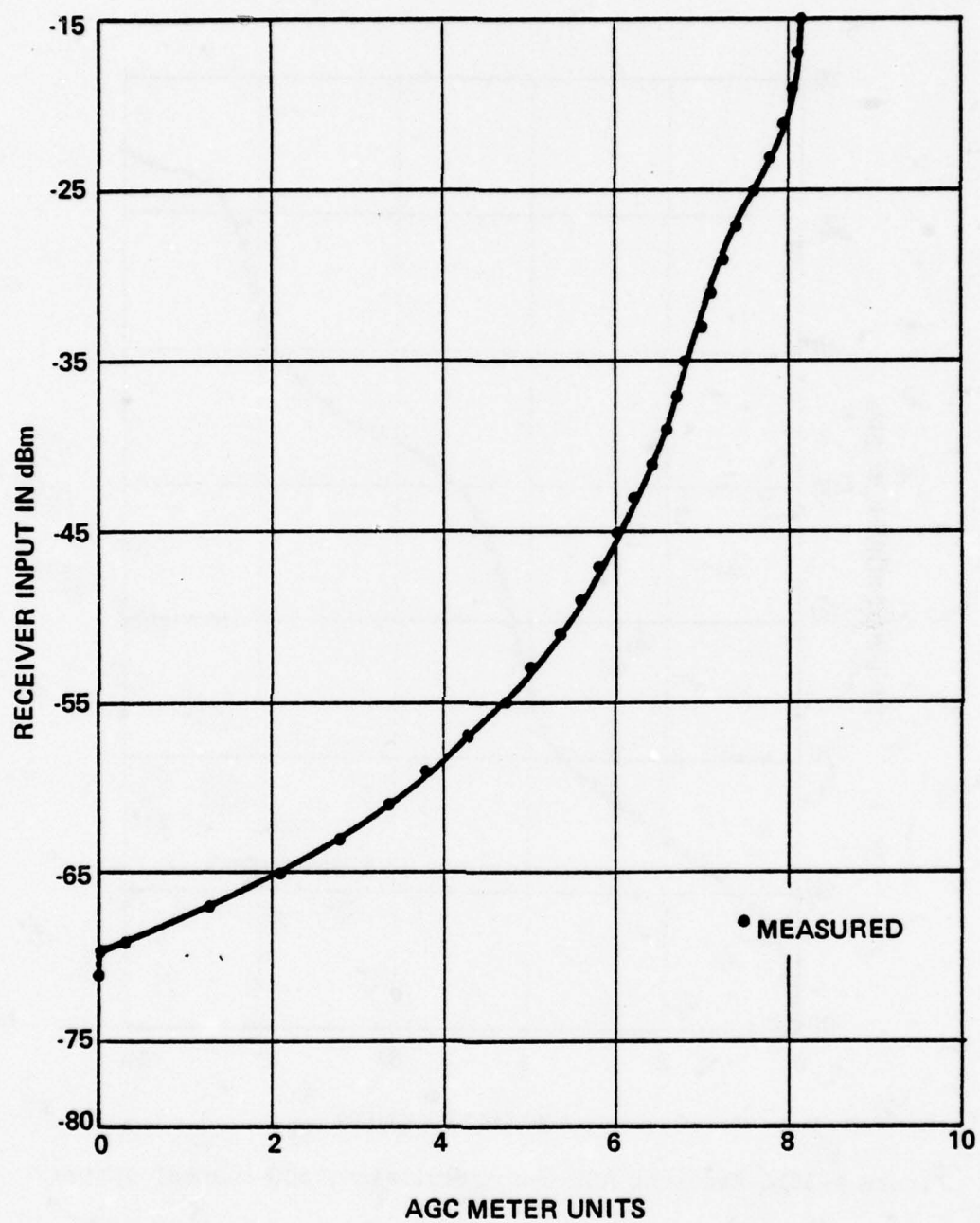


Figure A-39. Receiver AGC characteristics, 1200-channel system.

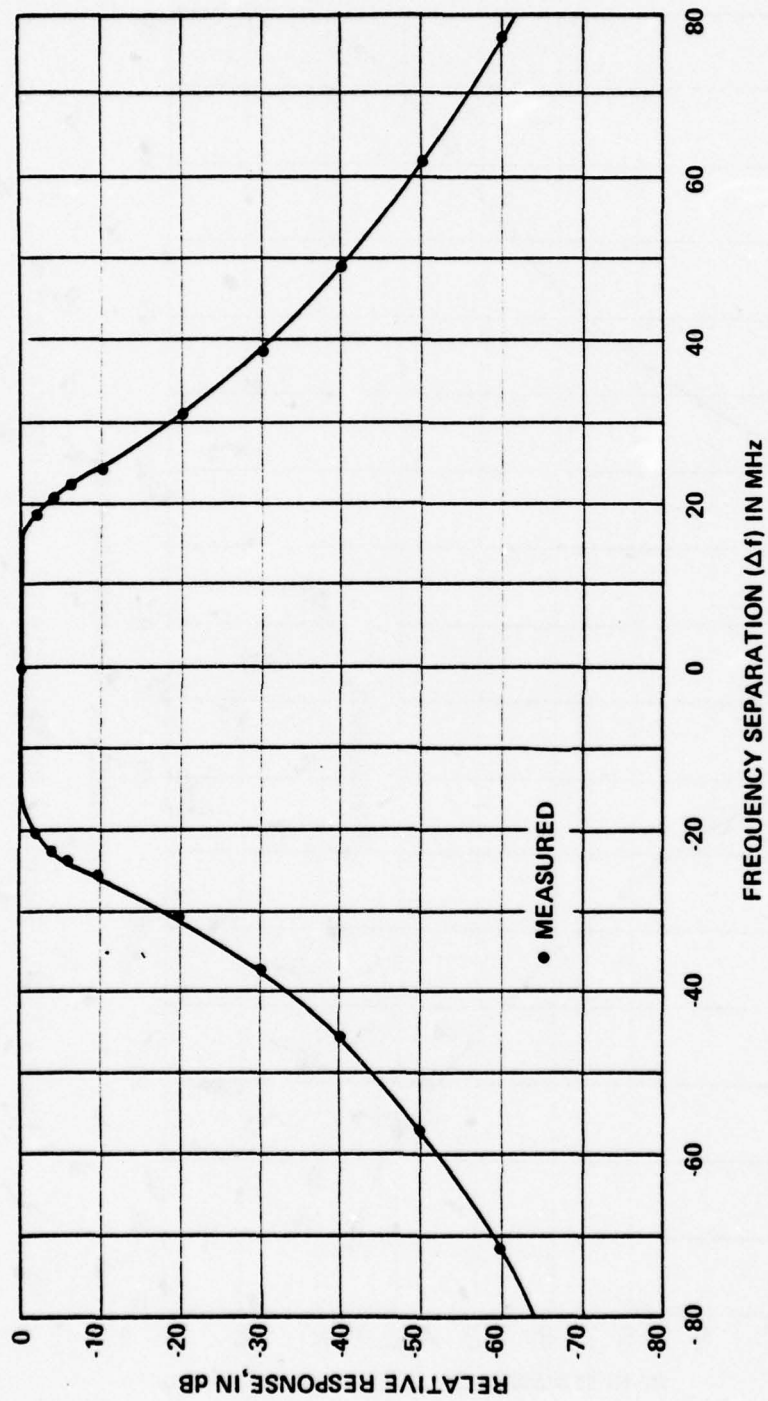


Figure A-40. Receiver RF selectivity, 600-channel system.

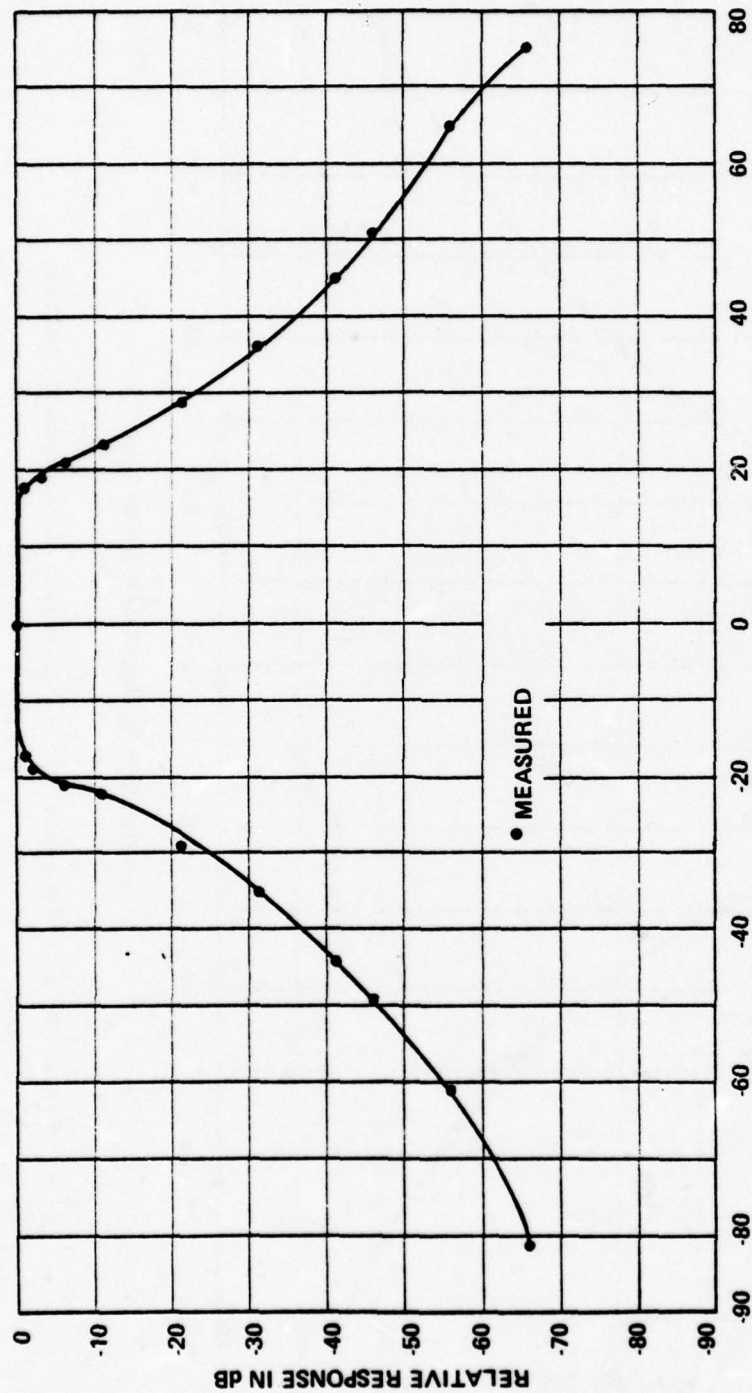


Figure A-41. Receiver RF selectivity, 1200-channel system.

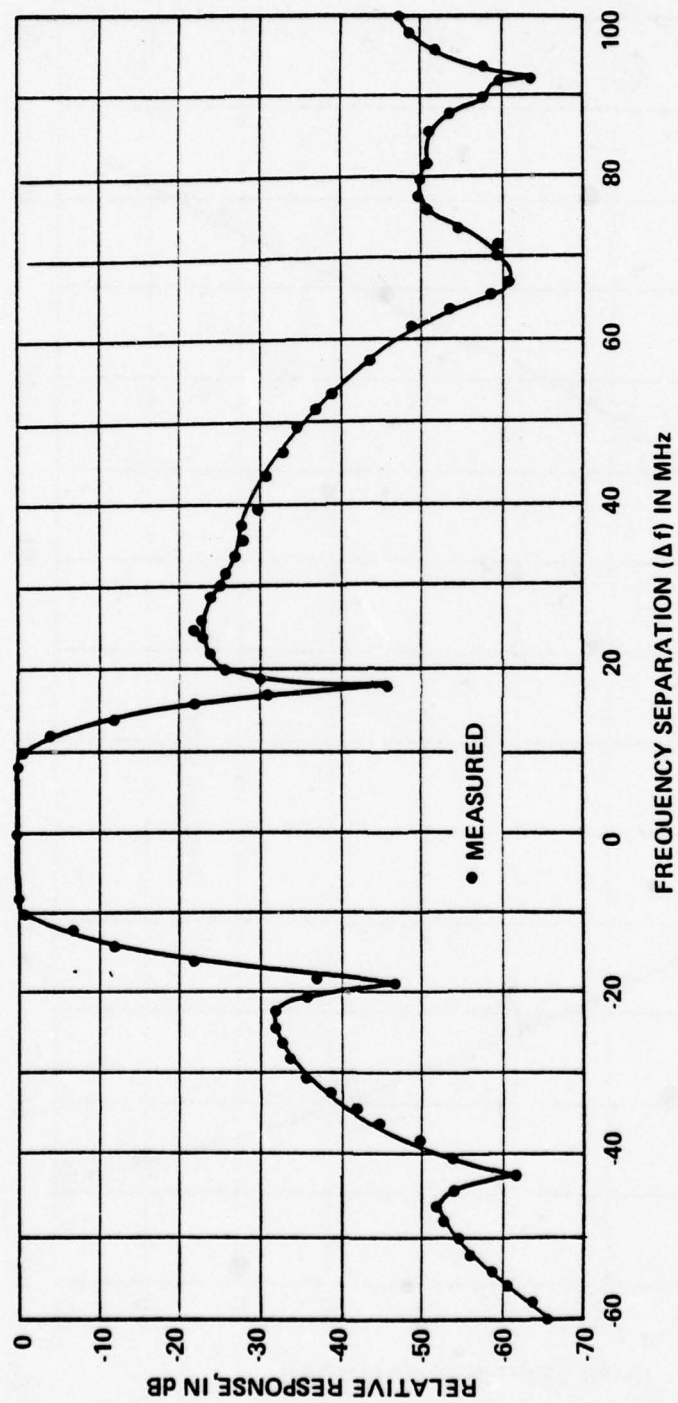


Figure A-42. Receiver IF selectivity, 600-channel system.

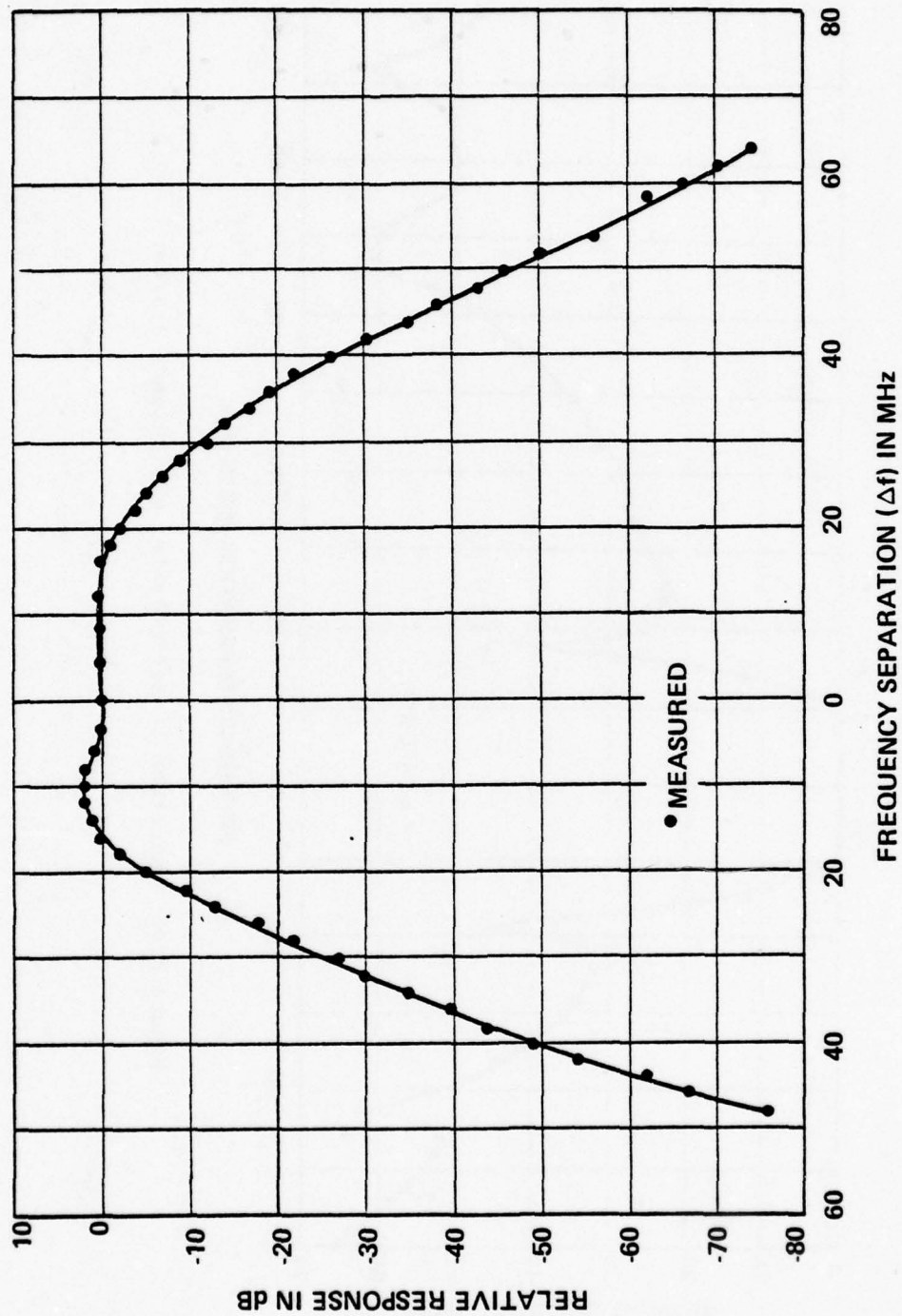


Figure A-43. Receiver IF selectivity, 1200-channel system.

TABLE A-10
RECEIVER SPURIOUS RESPONSE

System Capacity	Spurious Frequency	Spurious Response	RF Level Required for CW Quieting	Receiver Tuned Frequency
600 Channels	6529.0 MHz	(1, 1+) Image frequency	2.5 dBm for 20 dB CW quieting at receiver baseband output and 1.0 dBm for 20 dB CW quieting at multiplexer channel output	6382.6 MHz
	11760.4 MHz	(2, 1-)	-42 dBm for 20 dB CW quieting at receiver baseband output	
1200 Channels	11886.6 MHz	(2, 1+)	-28 dBm for 20 dB CW quieting at receiver baseband output	5982.3 MHz
	5893.1 MHz	(3, 3-)	10 dBm for 6 dB CW quieting at receiver baseband output	

TABLE A-11
RECEIVER INTERMODULATION CHARACTERISTICS

System Capacity	Receiver Tuned Frequency	Intermodulation Product
600 Channels	6382.6 MHz	Observation of the receiver IF auxiliary, baseband and multiplex channel outputs revealed an absence of intermodulation products
1200 Channels	5982.3 MHz	

TABLE A-12
RECEIVER OSCILLATOR EMISSION

System Capacity	Measuring Instrument	Range of Observation and Sensitivity	Emissions
600 Channels	FSVM	3.87 - 12.0 GHz with a sensitivity that exceeded -70 dBm over observation range	No emissions were observed
1200 Channels	Spectrum Analyzer		

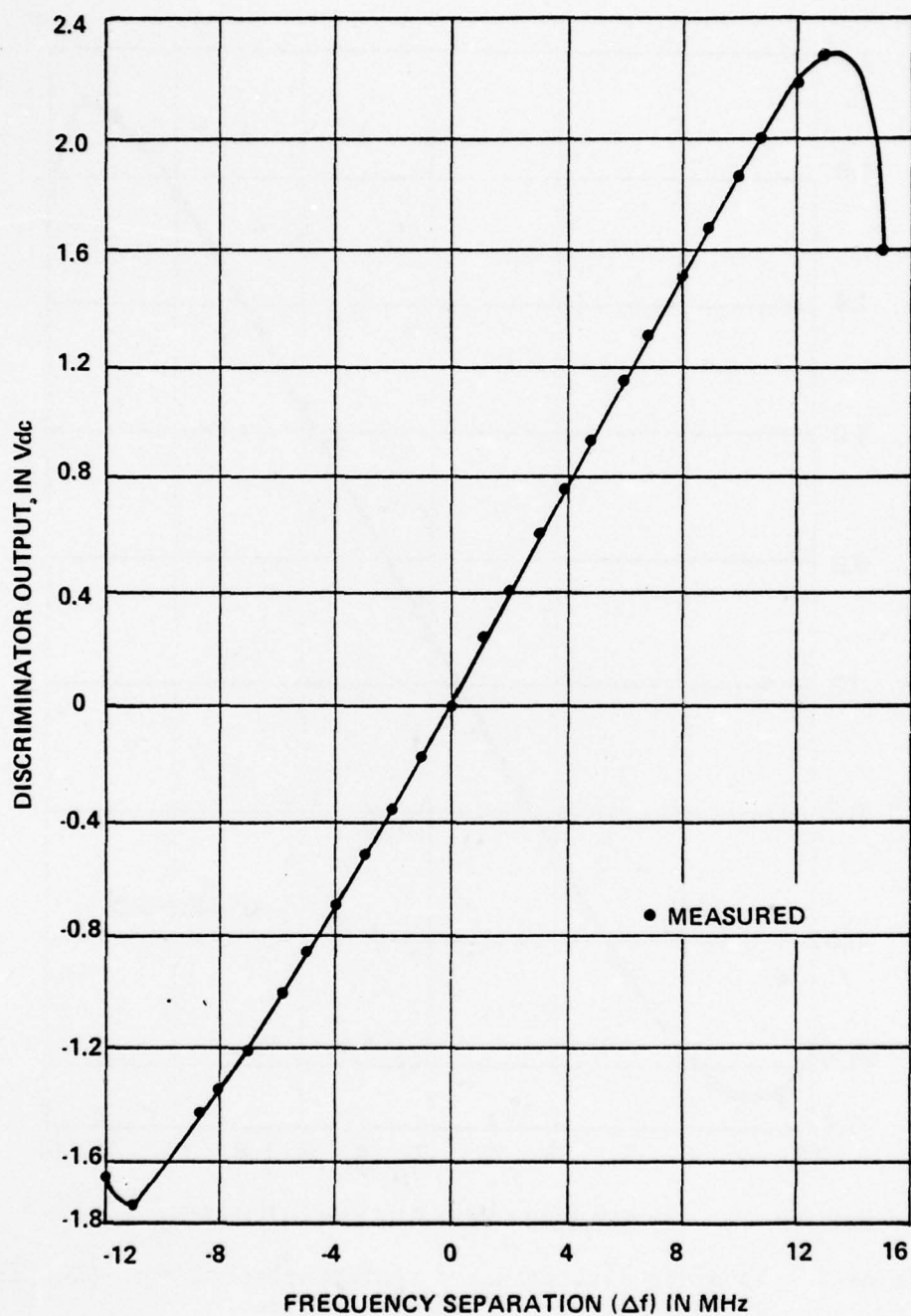


Figure A-44. Receiver discriminator characteristics for -70.6 dBm RF input level, 600-channel system.

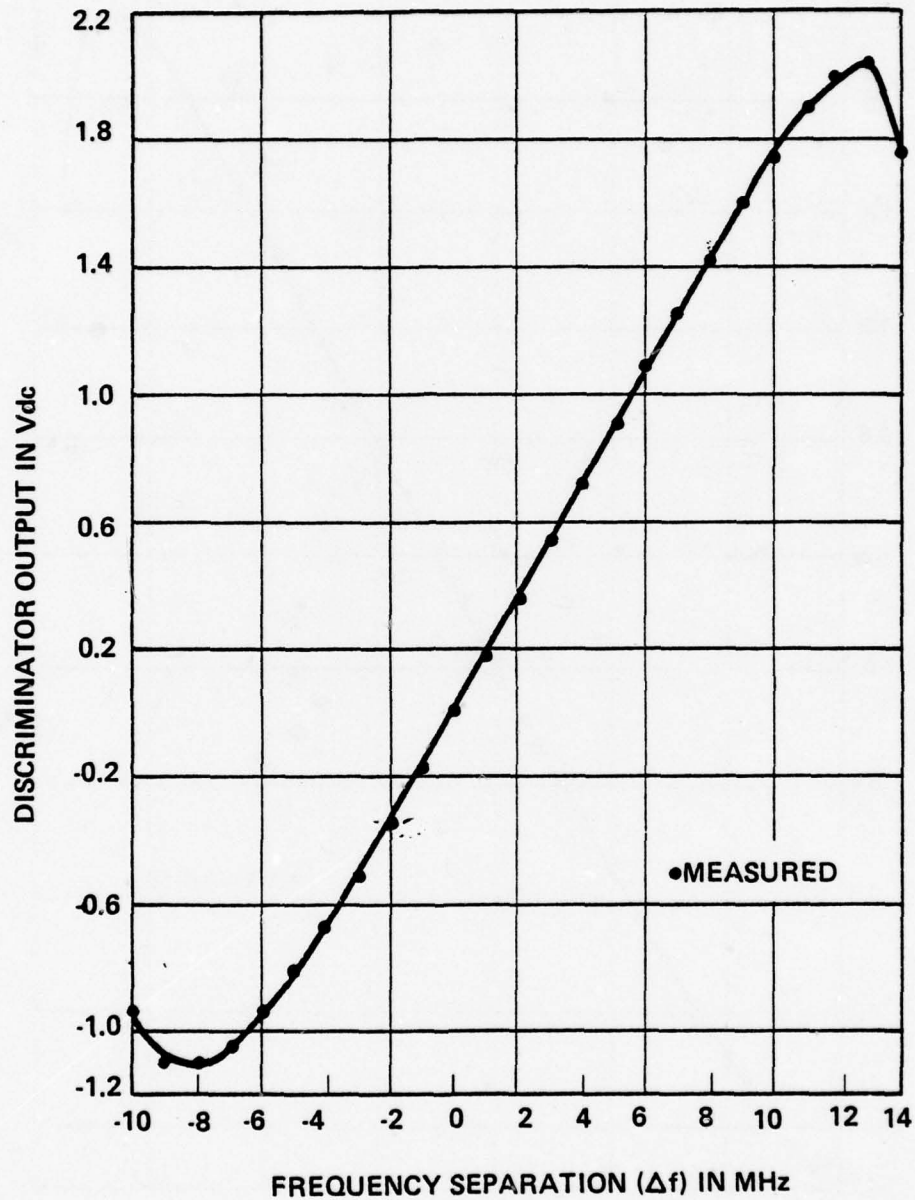


Figure A-45. Receiver discriminator characteristics for -83.5 dBm RF input level, 600-channel system.

APPENDIX B
RECEIVER PERFORMANCE

GENERAL

The ability of man to communicate effectively is one of his greatest assets. If one considers a system communicating information as including the listener, an evaluation of system performance can be made in terms of how well the listener is able to discern the information or signal being delivered by the system. Researchers, over the years, have developed several methods for evaluating the performance of analog voice communications systems. These methods can generally be grouped into one of two categories, namely objective (i.e., weighted noise, test tone-to-noise power ratio, Articulation Index) and subjective (i.e., Articulation Score). This appendix will consider some of the techniques used with both performance evaluation methods.

NOISE WEIGHTING

The term noise has been described as a mixture of undesirable frequencies and amplitudes which interfere with the signals intended to be received.³⁵ Earlier research geared towards finding a unit to measure the effects of noise interference in the 3.1-kHz voice channel revealed that certain frequencies of noise will interfere with conversation more than will other frequencies. The results of earlier measurements, made to develop a unit to measure noise interference, indicated that a 1-kHz noise signal produced more interference than any of the other frequencies of noise in a

³⁵*Units for Measuring Power, Levels and Noise*, GTE Lenkurt Incorporated, 1973.

voice channel. These tests took into account the hearing ability of the human ear and the efficiency of the telephone equipment that was being used. The data obtained by comparing the interfering effects of other frequencies of noise to the effects produced by a 1-kHz frequency were used to generate a weighting curve. A number of slightly different weighting curves have been used throughout the years as a result of improvements in the telephone handset. Plots of the three most recent types of noise-weighting curves are shown in Figure B-1. The F1A weighting was developed in the late 1930's using the 302 type telephone handset. Although the F1A noise weighting is no longer used in the telephone industry, it is still common to industrial systems.

At present, the two most common types of noise weighting used in the telephone industry are the C-message weighting, widely used in the United States, and the psophometric weighting, widely used in Europe and internationally. The unit of C-message weighting is the dBrnc. The term, dBrnc, is the number of dB above a reference noise, C-message weighted. The reference noise is the noise level that produces the same interfering effect using C-message weighting as a -90 dBm, 1-kHz tone would produce using a type 500 telephone handset. The term, dBrnc0, is also often used in C-message weighting. dBrnc0 is simply dBrnc referenced to a 0 dBm test point in the system.

The unit of psophometric weighting is the picowatt, pWp. The main difference between the C-message weighting and the psophometric weighting is that the psophometric weighting uses 800 Hz instead of 1-kHz as a standard reference tone. Since the two weighting curves (Figure B-1) are similar, we can convert units in the one measurement method to approximate values in the other measurement method by:

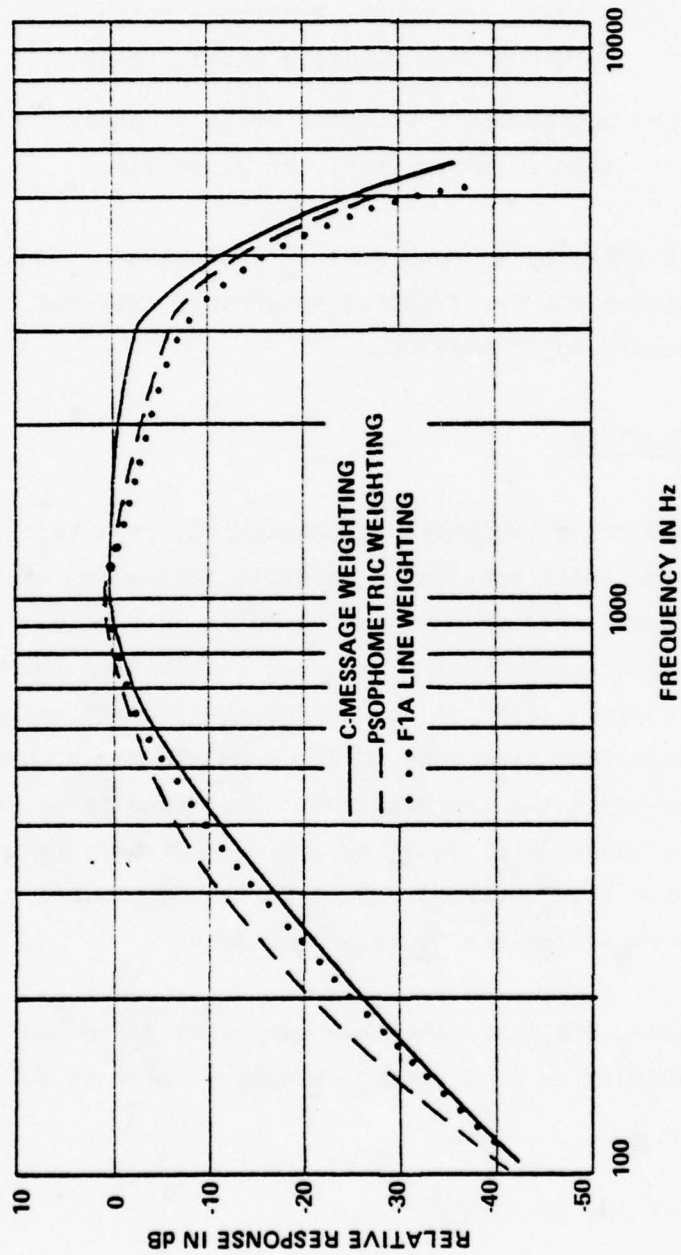


Figure B-1. Noise weighting for telephone message circuits. All curves are referred to 1000 Hz except psophometric, which is referred to 800 Hz.

$$dBrnc0 = 10 \log pWOp \quad (B-1)$$

where

$dBrnc0$ = C-message-weighted reference noise at a point of zero relative level, in dB

$pWOp$ = psophometric-weighted noise at a point of zero relative level, in picowatts.

Equation B-1 is in error by as much as 1 dB (Reference 7) due to the variations between the two types of weighting. However, it is a commonly accepted approximation.

TEST TONE-TO-NOISE RATIO

Specifying the noise (weighted or unweighted) in a test channel as a noise power ratio provides a relative indication of interference. An alternative is to express the noise in decibels relative to a specified absolute test tone level in the test channel. Test tone-to-noise ratio (S/N) is defined as the decibel ratio of the level of the standard test tone (0 dBm0) to the noise in a 3100-Hz bandwidth within the test channel. Test tone-to-noise ratio is therefore numerically equal to the channel noise expressed in dBm0 with the sign inverted. For example, a channel noise level of -40 dBm0 is equivalent to an S/N of 40 dB.

For white noise, the test tone-to-noise power ratio can be converted to psophometric- or C-message-weighted noise as follows (Reference 7):

$$dBrnc0 = 88.5 - S/N \quad (B-2)$$

and

$$pWOp = \frac{0.56 \times 10^9}{\text{antilog}_{10}(S/N)/10} \quad (B-3)$$

SINAD

The SINAD is an audio output power measure which is measured with a distortion analyzer and which yields the ratio, in dB, of the channel output signal plus noise plus distortion plus interference-to-channel output noise plus distortion plus interference, $(S + N + D + I)/(N + D + I)$. When there is no interference, the SINAD power ratio reduces to $(S + N + D)/(N + D)$.

ARTICULATION INDEX

The articulation index (AI) performance evaluation technique is based on the original work of French and Steinberg.³⁶

French and Steinberg determined that the speech spectrum can be divided into N contiguous bands which contribute equally to intelligibility as measured by articulation score (AS). Current methods of determining AI include empirically derived correction factors to account for the upward spread of masking. This is the phenomenon in which interference at a low frequency masks a higher frequency portion of the voice spectrum. Effects of noise and other factors (interference, distortion) prevent the N bands from making their full contribution to intelligibility. Since intensity of speech and interference may vary depending on the band, a

³⁶French, N. and Steinberg, J., "Factors Governing the Intelligibility of Speech Sounds," *Journal of the Acoustical Society of America*, Vol. 19, No. 1, January 1947.

weighting factor is determined for each band which reflects the fact that some bands do not make their maximum possible contribution to the speech intelligibility. The weighting factors vary for each band according to the ratio of the speech energy in the band to the hearing threshold. When the speech energy level in the band is 30 dB or more above the threshold level, it contributes its maximum value and, hence, has a unit weighting factor. When the speech energy level is between 0 and 30 dB above the threshold, the band's contribution is in proportion to its maximum as its level is to 30 dB. When the energy level is below the threshold, there is no contribution and the weighting factor vanishes. These weighting factors are additive and the sum can be used with empirical curves to determine the corresponding AS.

Voice Intelligibility Analysis Set

An instrument produced by the General Electronics Laboratory (GEL) to measure the effects of undesired signals on voice intelligibility without subjective listener evaluation is called the Voice Intelligibility Analysis Set (VIAS).^{37,38} This device divides the spectrum into a number of unequal bandwidths (14) and measures the contribution to intelligibility for each band. The contributions from the bands are then averaged over all 14 bands to produce the composite AI. The 14 VIAS frequency bands are shown in Figure B-2 and the calculation of AI is depicted graphically in Figure B-3. A synthetic desired speech signal, which

³⁷Thompson, A., *The Application of the Voice Interference Analysis System to the Prediction of Voice Intelligibility - Part 1*, Bell Report No. A70009-280, November 1967.

³⁸Fitts, R., *Electronic Evaluation of Voice Communications Systems*, RADC-TDR-63-355, August 1963.

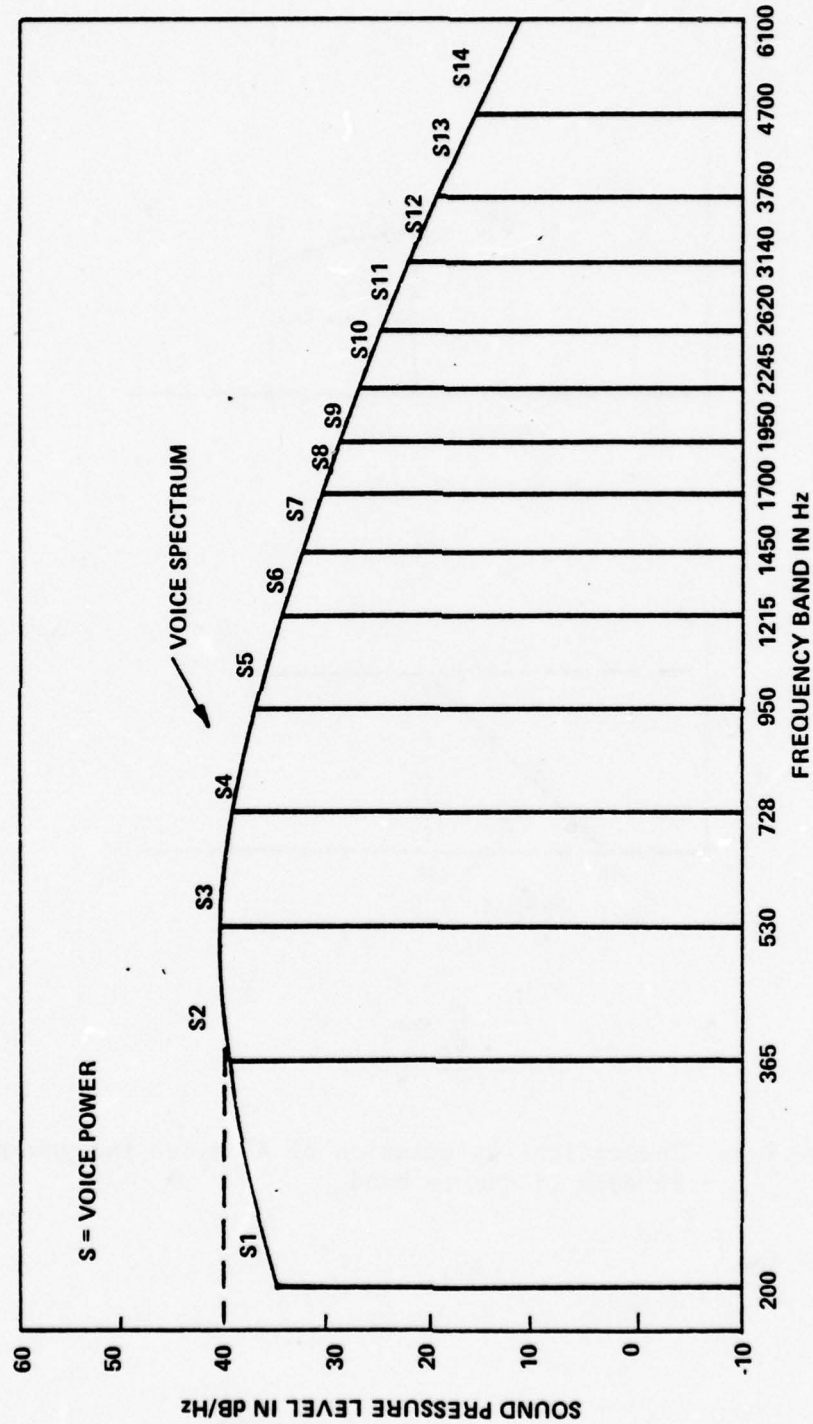


Figure B-2. Long-term speech spectrum and associated AI bands.

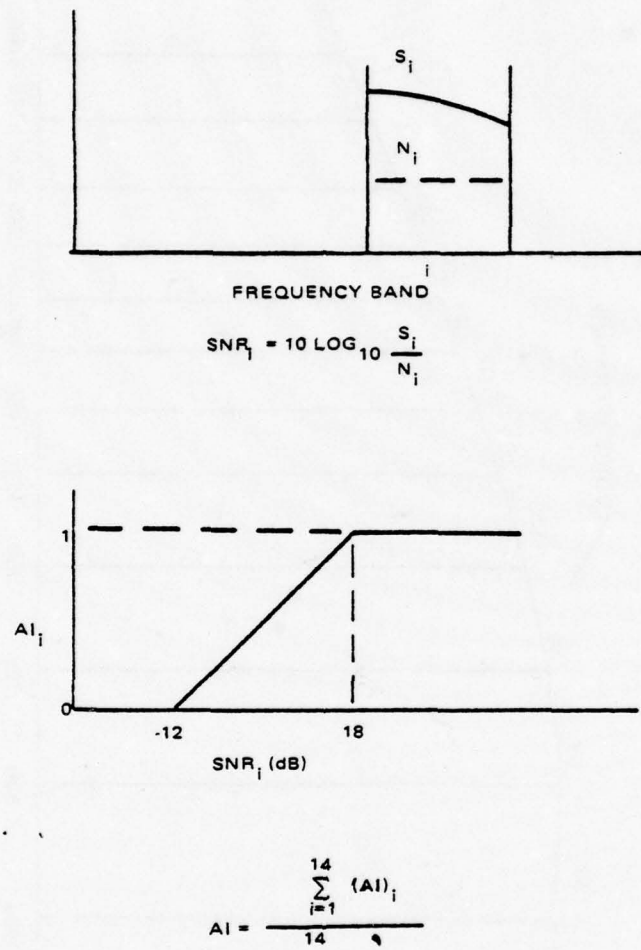


Figure B-3. Theoretical calculation of AI given the power in each frequency band.

consists of a triangle-modulated 950-Hz tone, is transmitted over the test channel and is then measured by the recording portion of the device, in order to establish representative speech levels in the 14 bands. The average power (over a 10-second period) of the components of undesired signal in each of the 14 bands is then measured and, from knowledge of the average portion of the desired signal in each band, the desired-to-undesired signal ratio, SNR_i , is computed in decibels for each band. An AI value (AI_i) is assigned to each frequency band by the relation:

$$AI_i = \begin{cases} 1 & \text{for } SNR_i \geq 18 \\ (SNR_i + 12)/30 & \text{for } -12 < SNR_i < 18 \\ 0 & \text{for } SNR_i \leq -12 \end{cases} \quad (B-4)$$

where

i = the band number.

The articulation index value is computed by averaging the AI_i values for each of the 14 bands. The VIAS incorporates empirically derived correction factors to account for the upward spread of masking. This is the phenomenon in which interference at a low frequency masks a higher frequency portion of the voice spectrum.

The characteristics of the system being evaluated may indicate that certain frequency bands should not be allowed to contribute to the overall AI. This arises when the audio spectrum is bandpass-filtered above 200 and below 6100 Hz. Since the desired-signal spectrum is artificially generated from 200 to 6100 Hz, the highest and lowest frequencies are actually attenuated and make no contribution to AI. The easiest solution is to

disregard certain AI_i contributions by using a contribution factor C_i (in VIAS, the switch settings). The total AI value is then calculated by:

$$AI = \frac{\sum_{i=1}^{14} C_i (AI_i)}{14} \quad (B-4)$$

where

C_i = depends on the audio filter characteristics.

In the case of the standard FDM 3.1-kHz voice channel, the uppermost two bands (in VIAS, the 13th and 14th switch settings) do not contribute to AI. Hence, C_{13} and C_{14} are set equal to zero. With these two contribution factors set to zero, the highest possible AI attainable is $12/14 = 0.857$. The accepted practice for this case is to normalize the measured or calculated AI values by multiplying these values by $14/12 = 1.167$. The range of the normalized AI values is now from zero to one, with the highest possible AI given by $AI = 1.000$. Normalizing the AI values allows comparing the performance of different systems directly.

Comparisons Between Measured and Predicted AI

AI was one of the performance measures used to evaluate the performance of the 600-channel FDM/FM system for various types of interference signals. Based on the AI data analyzed, it can be shown that AI is dependent only on the S/N at the output of a test channel. The relationship between S/N and AI for all types of interference was empirically derived and is given by:

$$AI = 0.5239 + 0.0241 (S/N) - 0.0003 (S/N)^2 \quad (B-6)$$

The measured AI values and the AI values predicted by Equation B-6 are shown in Figure B-4.

ARTICULATION SCORE

The basic requisite for a voice communication system is the retention of intelligibility, which is defined by Robertson as "the capability of that system to convey the speech sounds in a manner such that any thoughts which may have existed in the original vocal message will be retained and can be recovered by the recipient."³⁹

One measure of the intelligibility is provided by the articulation test. In this test, a preselected group of sounds, syllables, words, or sentences is presented orally to a panel of listeners who record what they hear. The results expressed in percent correct, commonly known as the Articulation Score (AS), provide the relative measure of intelligibility of a specific system or for a particular interference condition.

The AS tests were made using a prerecorded, phonetically balanced 50-word list (PB-50) to simulate the test channel modulation. The resultant channel output signal plus interference plus noise was recorded on tapes, and the tapes were submitted to a trained panel of listeners who record what they hear. The results expressed in percent correct, commonly known as the Articulation Score (AS), provide the relative measure of intelligibility of a specific system or for a particular interference condition.

³⁹Robertson, W. Douglas, *A Comparison of the Procedures and Results of Intelligibility Tests for a Number of Interference Conditions*, ECAC-TM-X-003-10, ECAC, Annapolis, MD, April 1962.

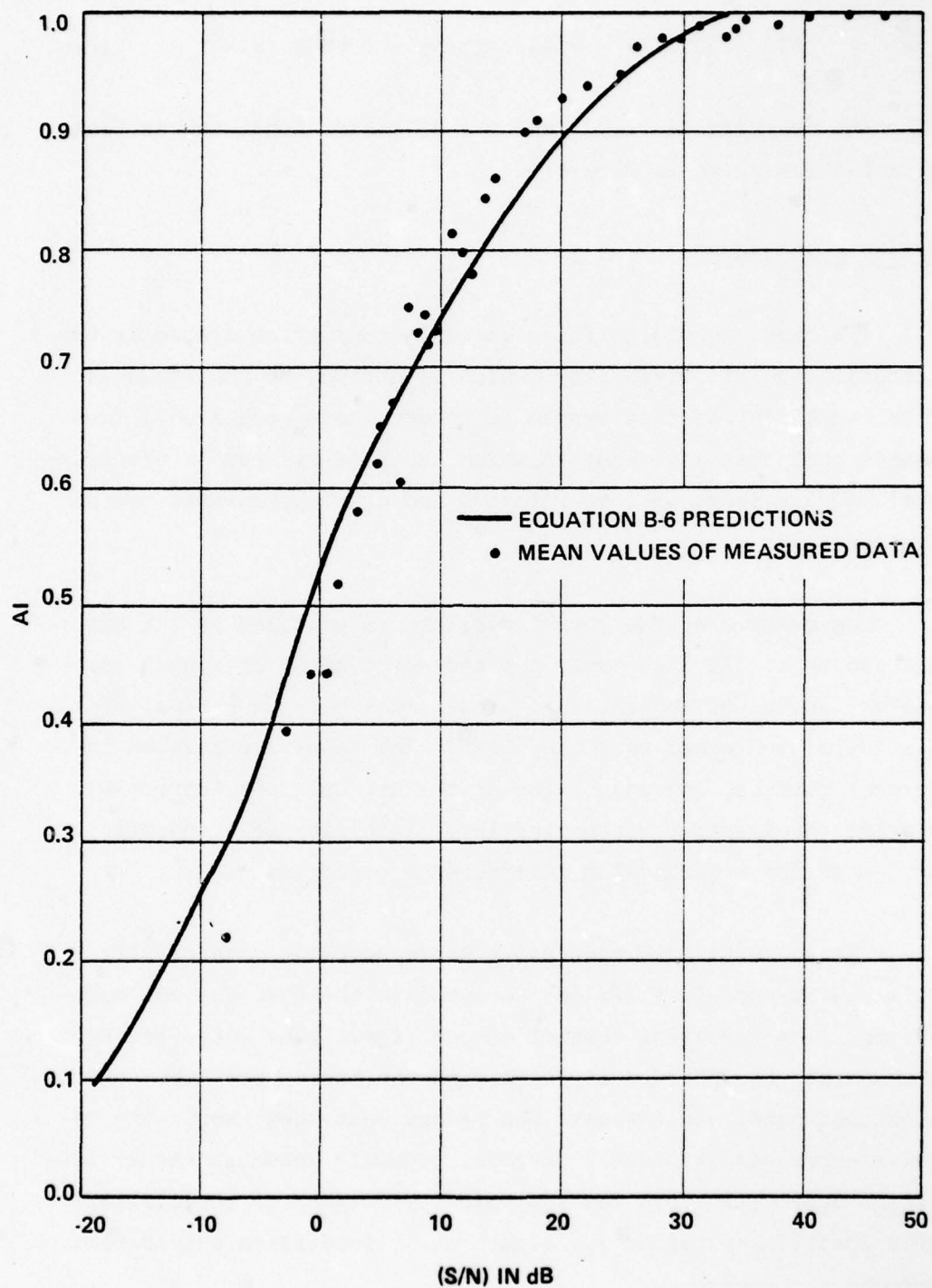


Figure B-4. Comparisons between measured and predicted AI scores.

The AS tests were made using a prerecorded, phonetically balanced 50-word list (PB-50) to simulate the test channel modulation. The resultant channel output signal plus interference plus noise was recorded on tapes, and the tapes were submitted to a trained panel of listeners for scoring.

The results of the AS tests were used to obtain relationships between AS and AI for various types of interfering signals. These relationships are depicted in Figures B-5 through B-9.

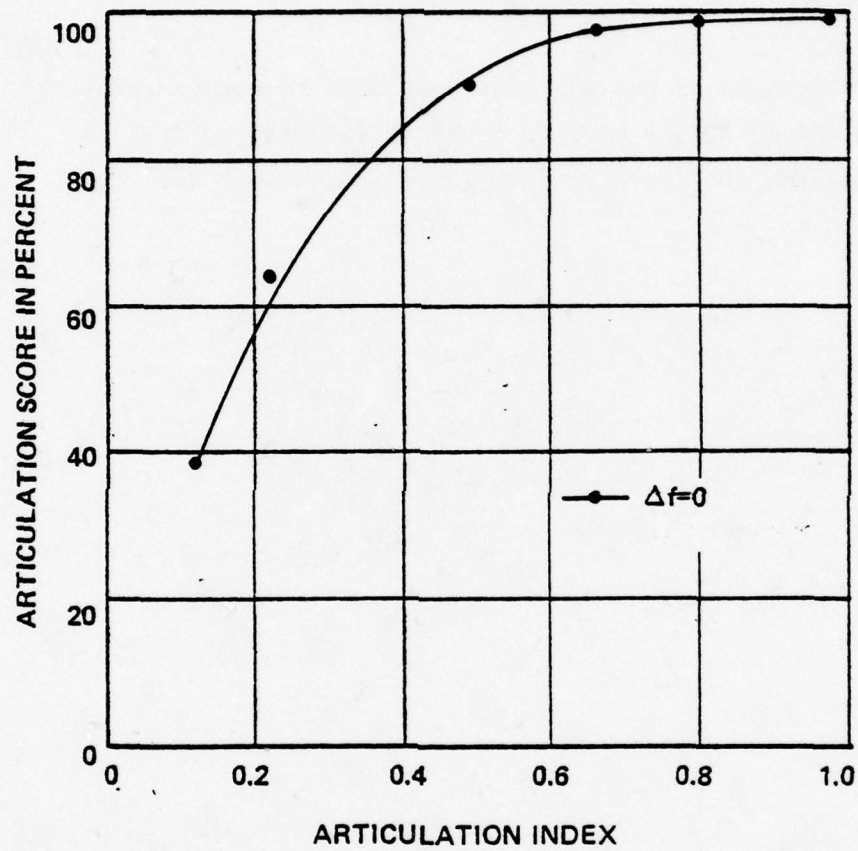


Figure B-5. Articulation score versus articulation index for Gaussian noise interference; low test channel (340-344 kHz).

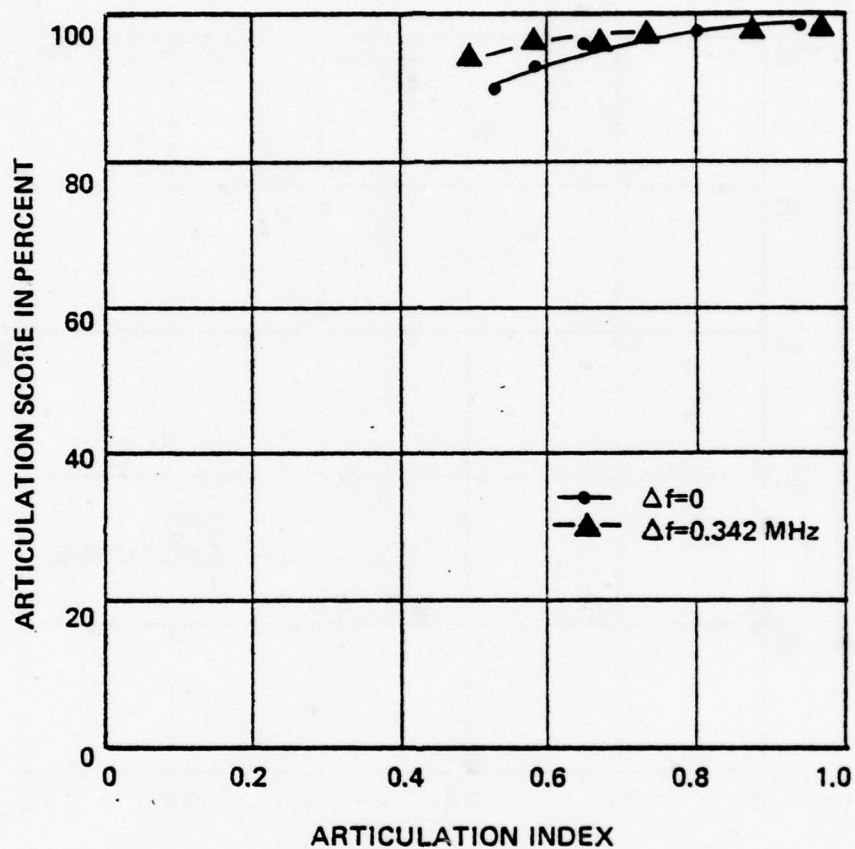


Figure B-6. Articulation score versus articulation index for a CW interfering signal; low test channel (340-344 kHz).

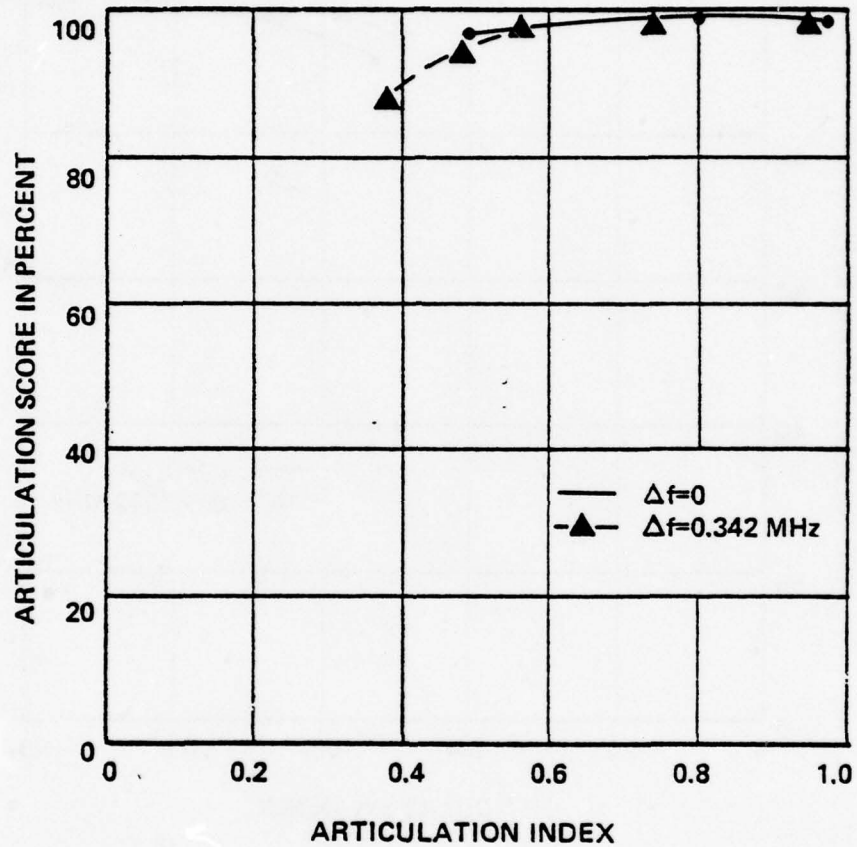


Figure B-7. Articulation score versus articulation index for a single channel narrowband FM interfering signal; low test channel (340-344 kHz).

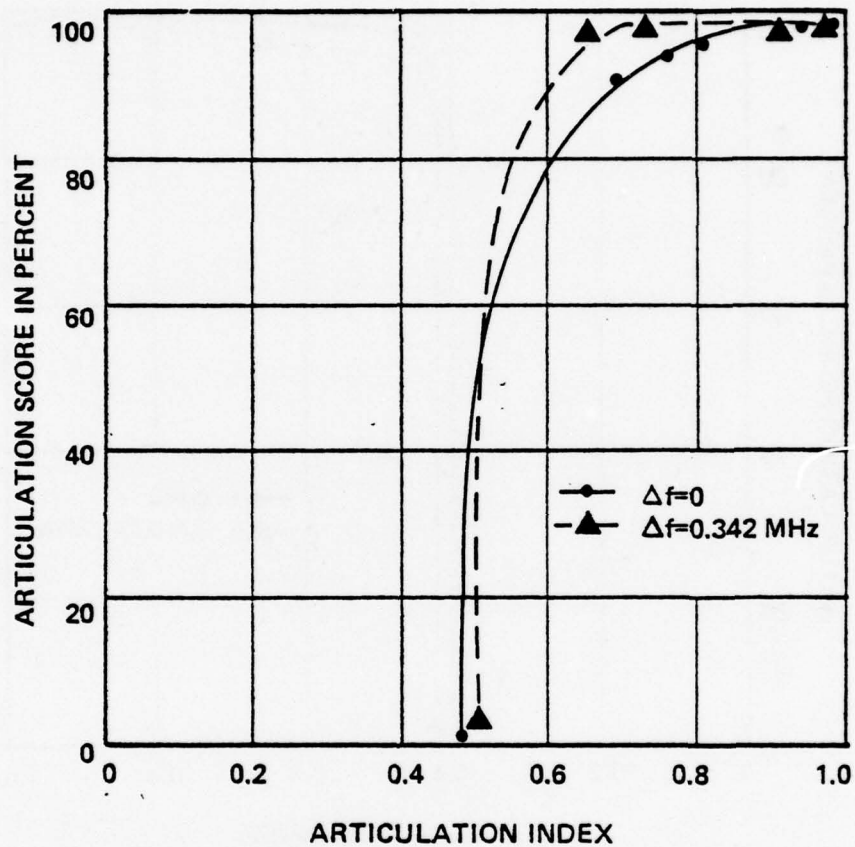


Figure B-8. Articulation score versus articulation index for a 12-channel FDM/FM interfering signal; low test channel (340-344 kHz).

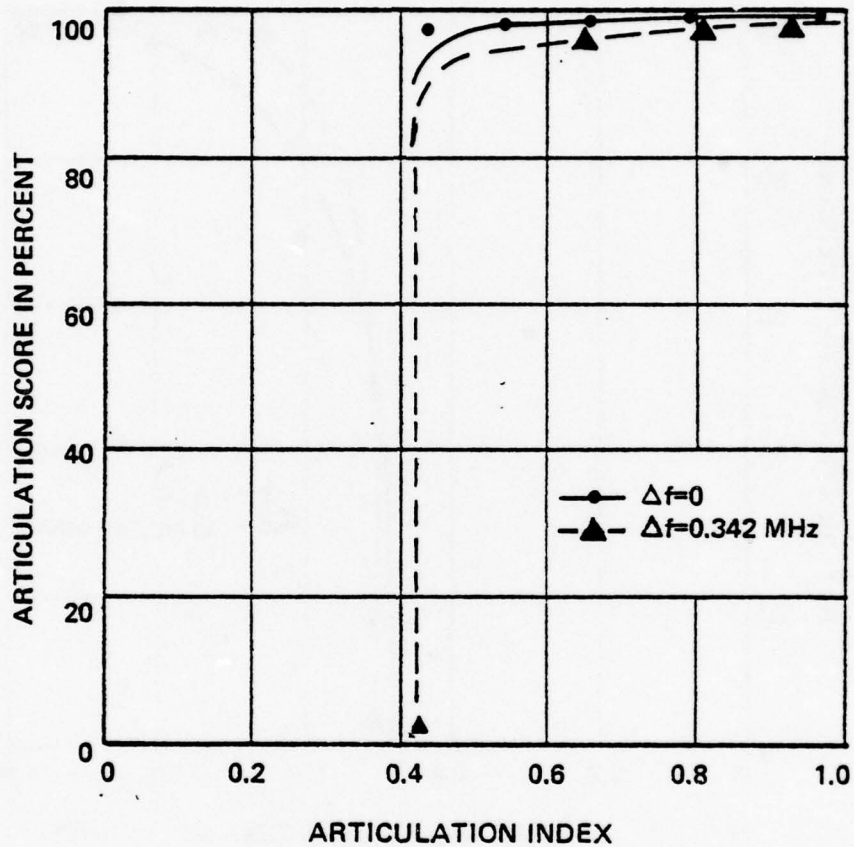


Figure B-9. Articulation score versus articulation index for an identical 600-channel FDM/FM interfering signal; low test channel (340-344 kHz).

APPENDIX C

SPECTRAL CHARACTERISTICS OF
PREEMPHASIZED FDM/FM SIGNALS

This appendix documents the results of a test designed to measure the spectral characteristics of preemphasized FDM/FM signals for various values of RMS modulation index ranging from 0.007 to 1.3. For this test, the 1200-channel Lenkurt 778A2 FDM/FM transmitter was modulated with a random noise signal having a Gaussian amplitude distribution and a uniform average power spectrum between 60 kHz and 5564 kHz. The method used to noise load the transmitter baseband was identical to the white noise testing procedure previously described in Section 2, except that the total noise modulating signal power was set to various levels and corresponding emission spectrum photographs were taken. Equation 9 (Section 3) was then used to relate the total modulating signal power to the total RMS carrier deviation from which the RMS modulation index can readily be calculated.

The results of these tests are presented in Figures C-1 through C-38. Figures C-1 and C-2 summarize the spectral data contained in the emission spectrum photographs shown in Figures C-3 through C-38. These two figures represent a generalized graphical method from which the emission spectrum of CCIR preemphasized FDM/FM can be calculated. Dimensionless variables are used as in Figure 9, Section 3.

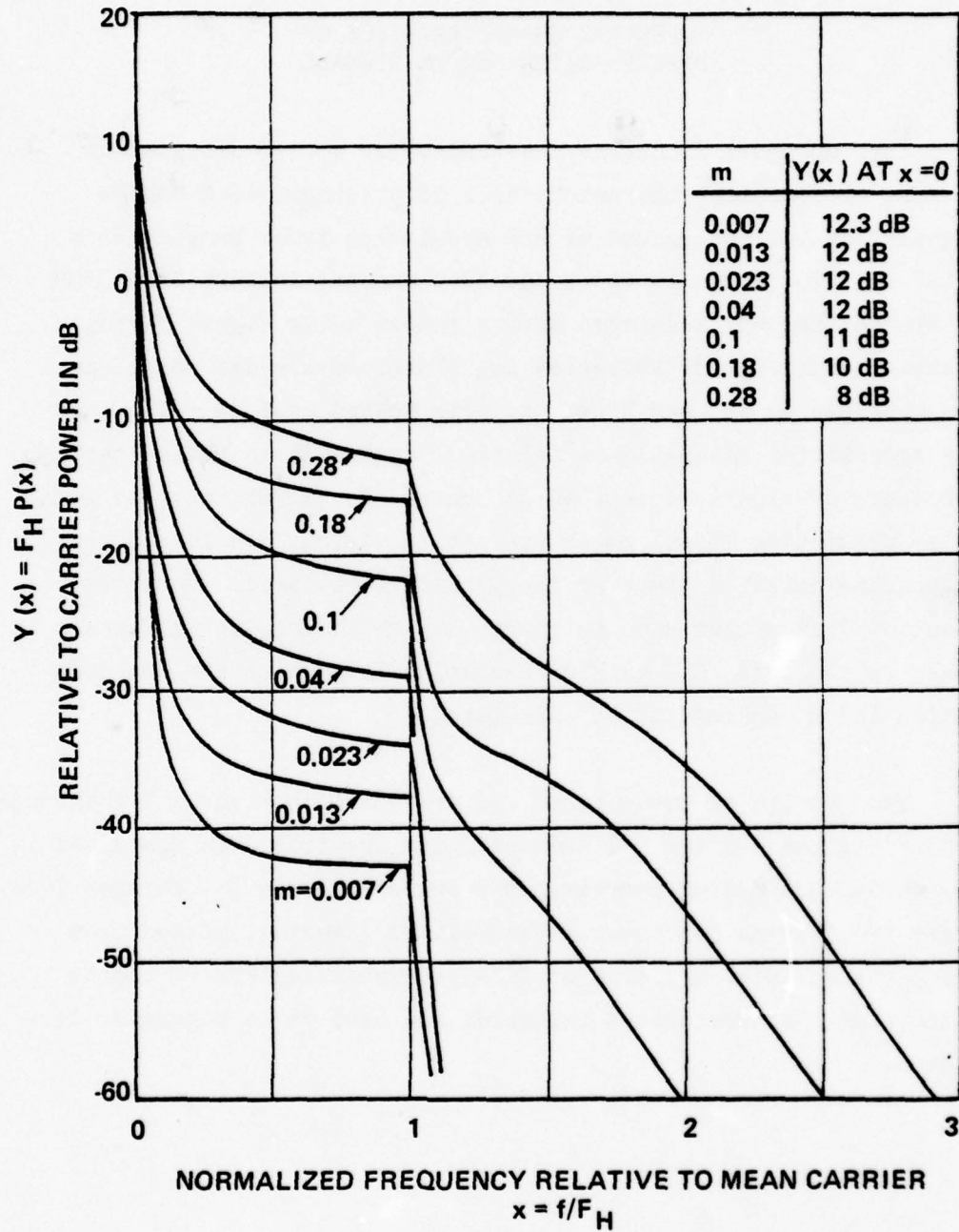


Figure C-1. Relative FDM/FM power spectra for a CCIR preemphasized baseband ($0.007 \leq m \leq 0.28$).

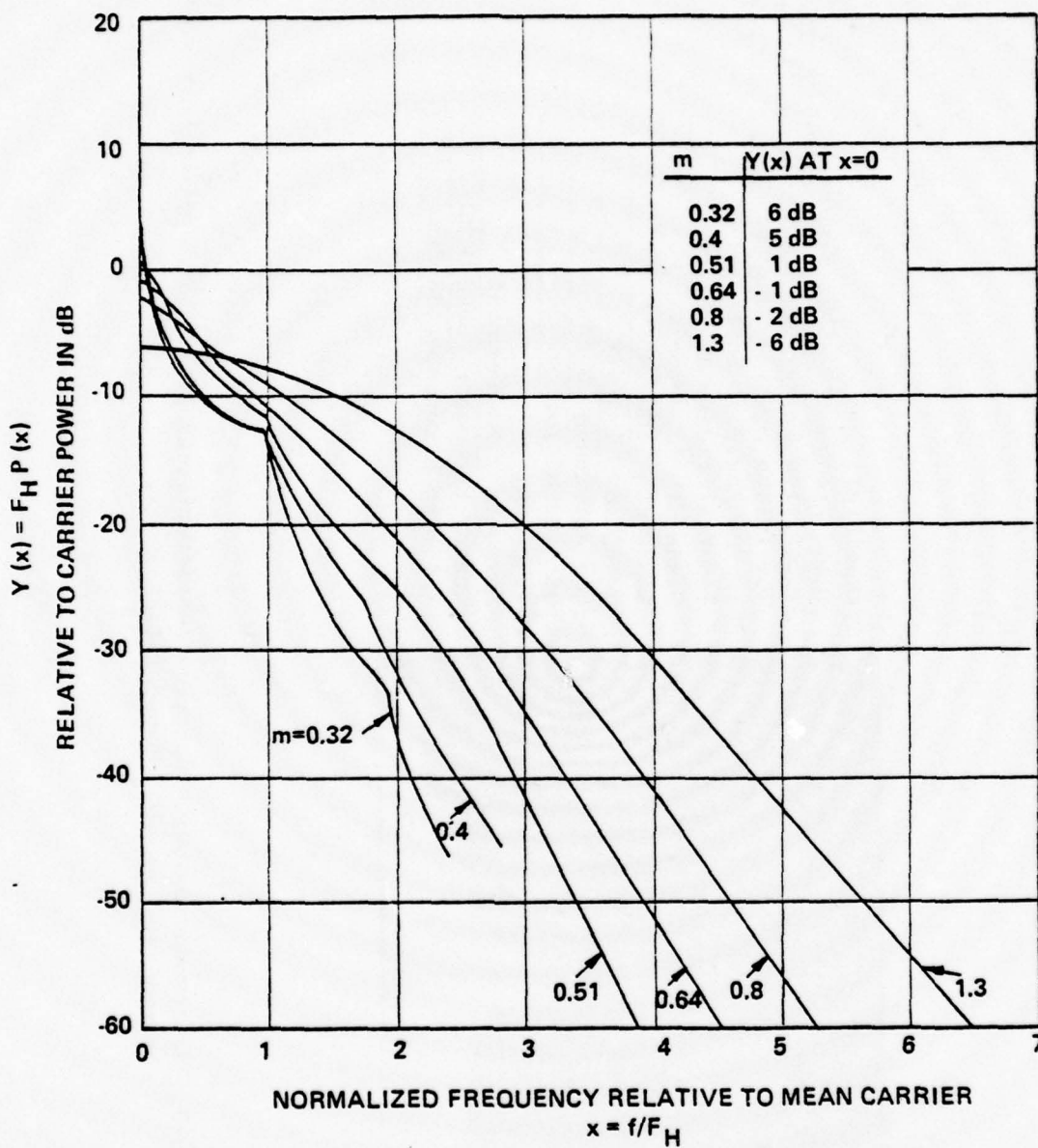


Figure C-2. Relative FDM/FM power spectra for a CCIR preemphasized baseband ($0.32 \leq m \leq 1.3$).

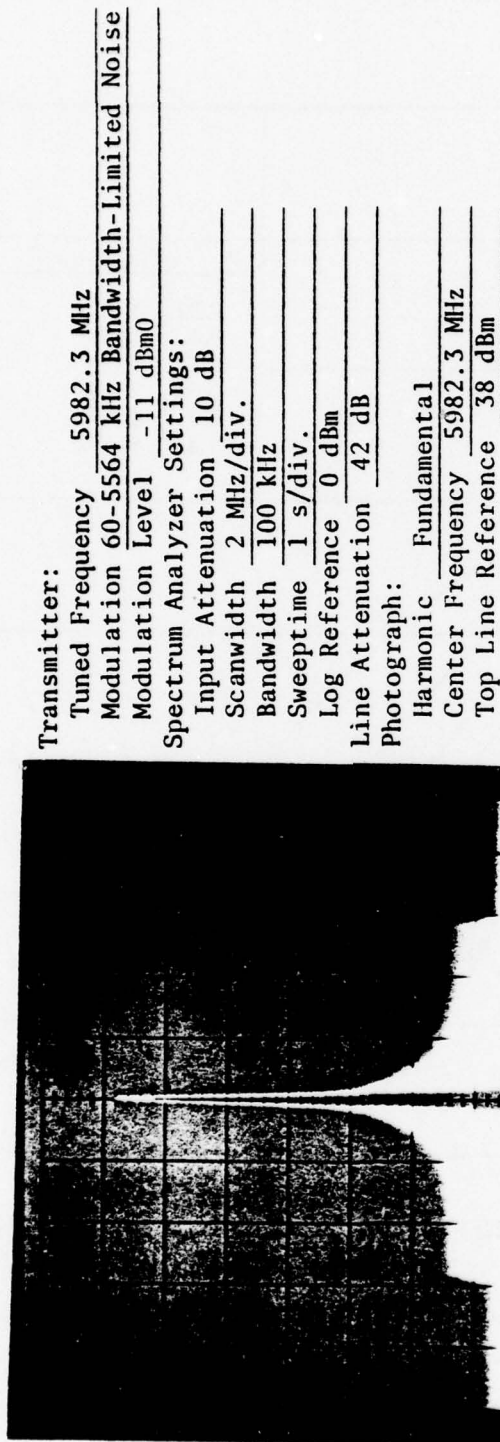


Figure C-3. Narrowband emission spectrum characteristics of 1200-channel Lenkurt 778A2 transmitter, 0.007 RMS modulation index.

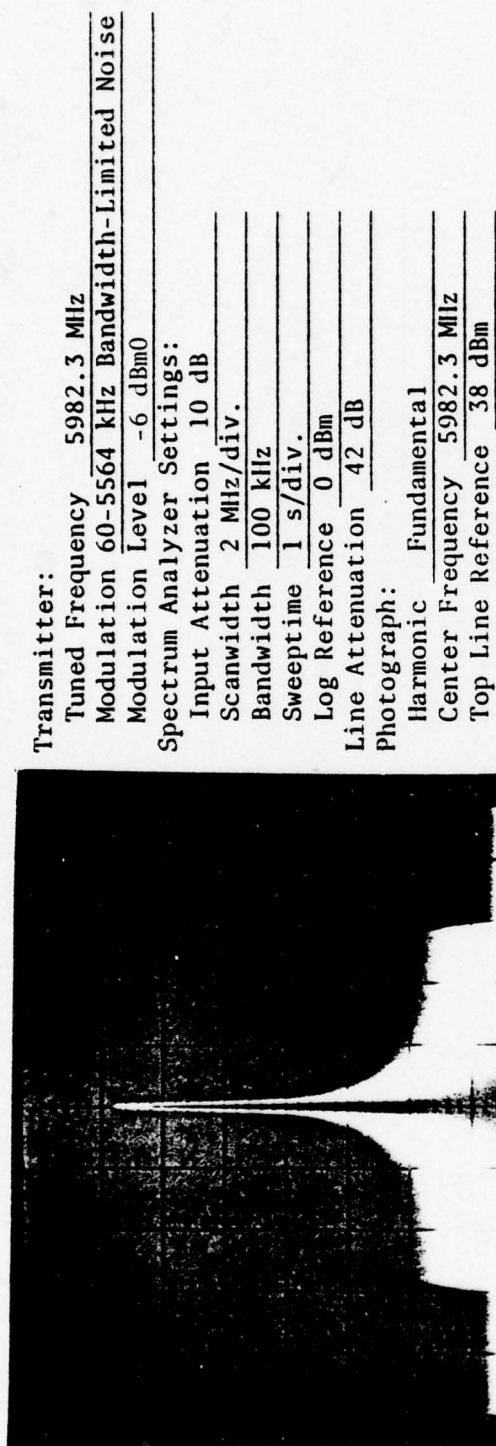


Figure C-4. Narrowband emission spectrum characteristics of 1200-channel Lenkurt 778A2 transmitter, 0.013 RMS modulation index.

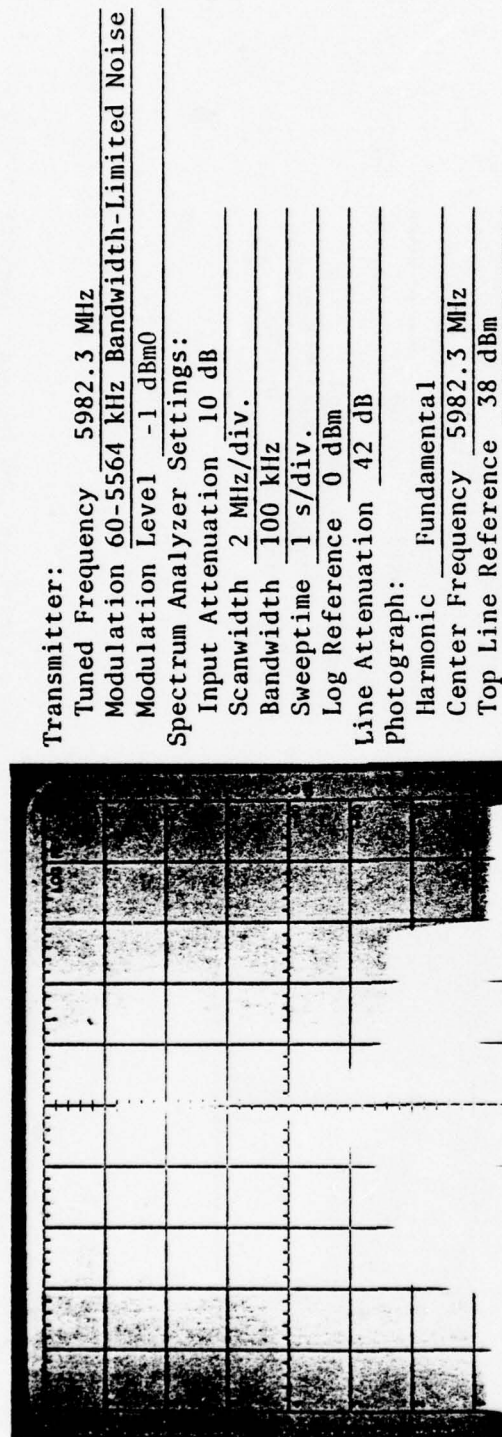


Figure C-5. Narrowband emission spectrum characteristics of 1200-channel Lenkurt 778A2 transmitter, 0.023 RMS modulation index.

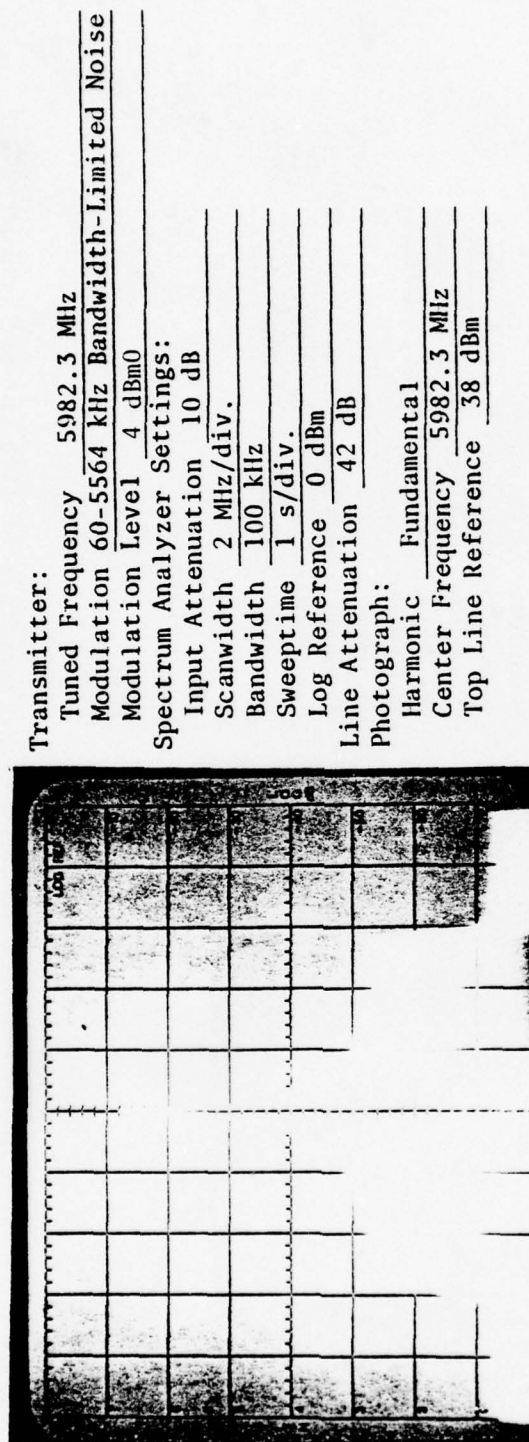


Figure C-6. Narrowband emission spectrum characteristics of 1200-channel Lenkurt 778A2 transmitter, 0.04 RMS modulation index.

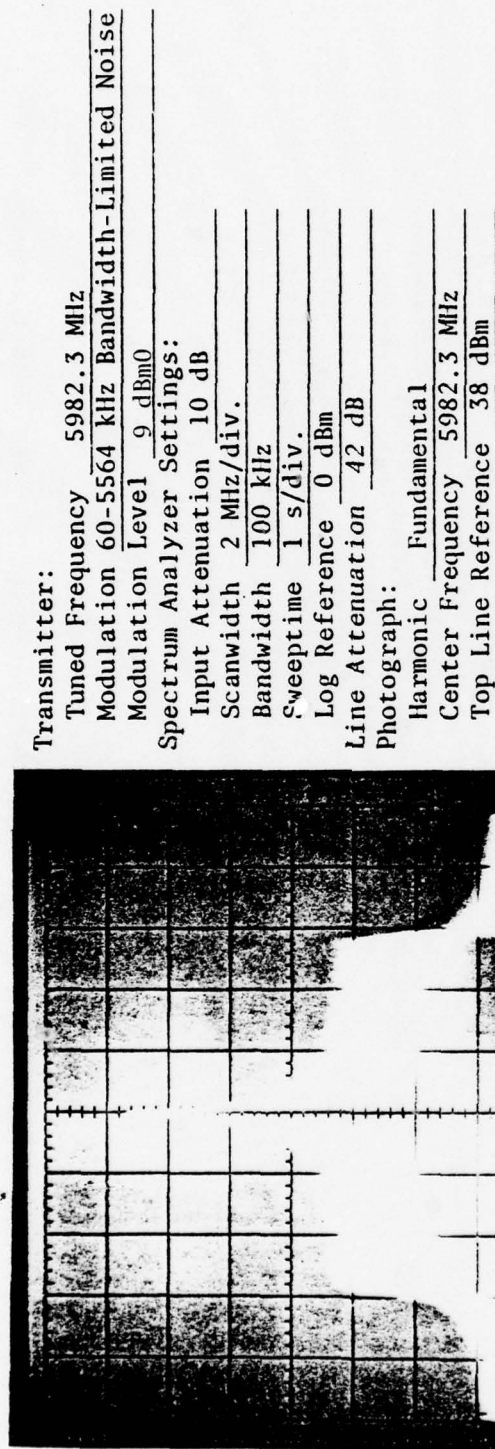


Figure C-7. Narrowband emission spectrum characteristics of 1200-channel Lenkurt 778A2 transmitter, 0.07 RMS modulation index.

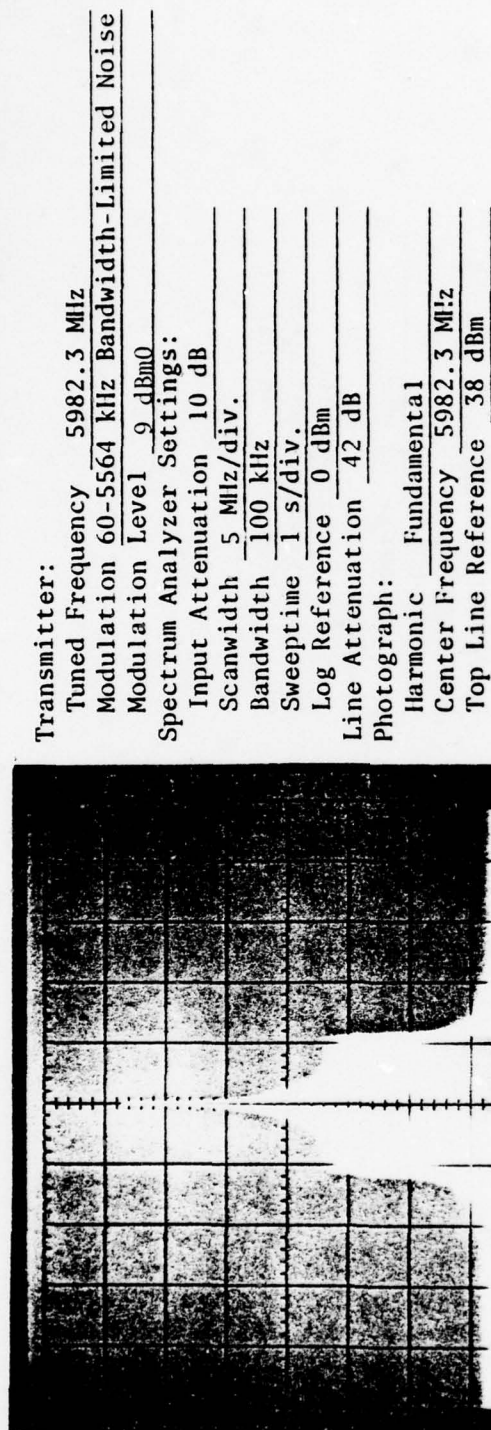


Figure C-8. Narrowband emission spectrum characteristics of 1200-channel Lenkurt 778A2 transmitter, 0.07 RMS modulation index.

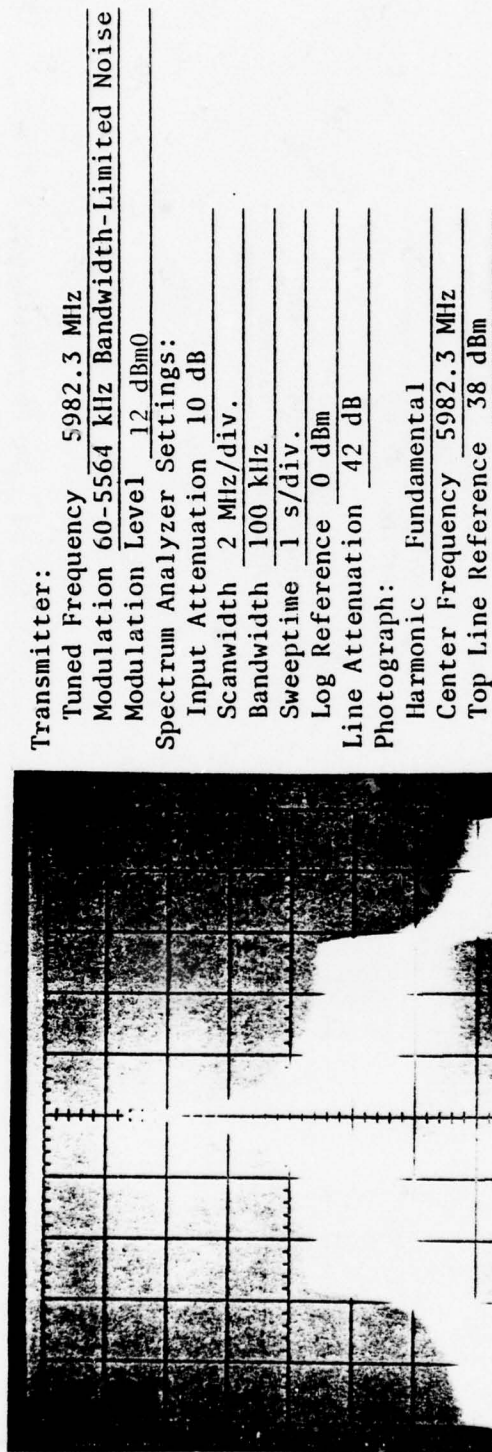
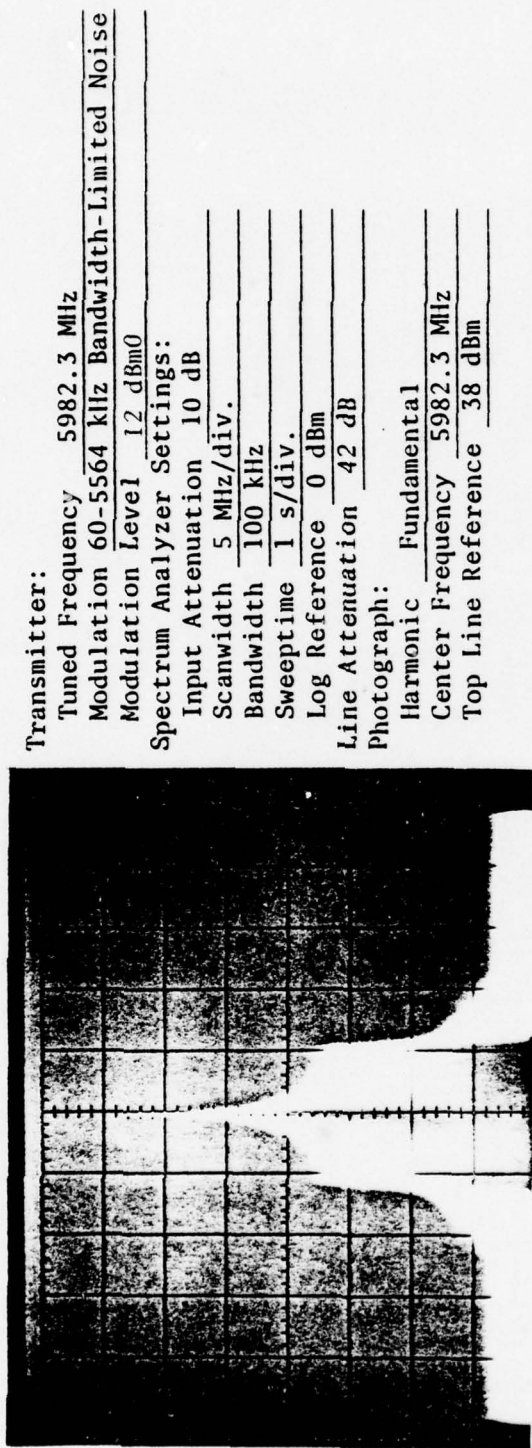


Figure C-9. Narrowband emission spectrum characteristics of 1200-channel Lenkurt 778A2 transmitter, 0.1 RMS modulation index.



Transmitter:
 Tuned Frequency 5982.3 MHz
 Modulation 60-5564 kHz Bandwidth-Limited Noise
 Modulation Level 12 dBm0
 Spectrum Analyzer Settings:
 Input Attenuation 10 dB
 Scanwidth 5 MHz/div.
 Bandwidth 100 kHz
 Sweeptime 1 s/div.
 Log Reference 0 dBm
 Line Attenuation 42 dB
 Photograph:
 Harmonic Fundamental
 Center Frequency 5982.3 MHz
 Top Line Reference 38 dBm

Figure C-10. Narrowband emission spectrum characteristics of 1200-channel Lenkurt 778A2 transmitter, 0.1 RMS modulation index.

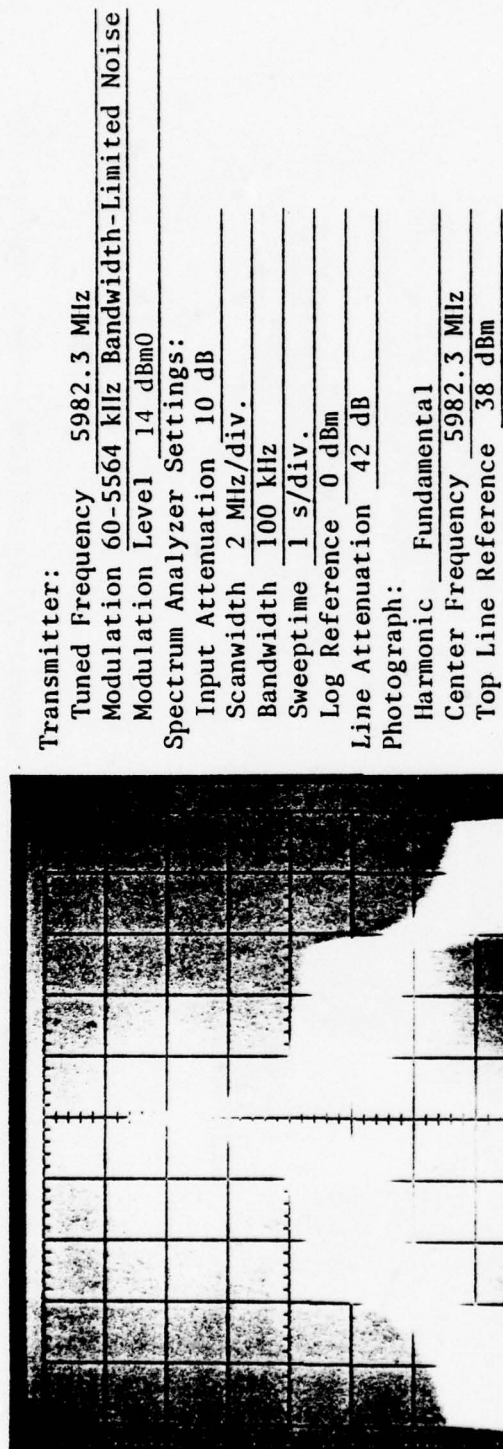


Figure C-11. Narrowband emission spectrum characteristics of 1200-channel Lenkurt 778A2 transmitter, 0.13 RMS modulation index.

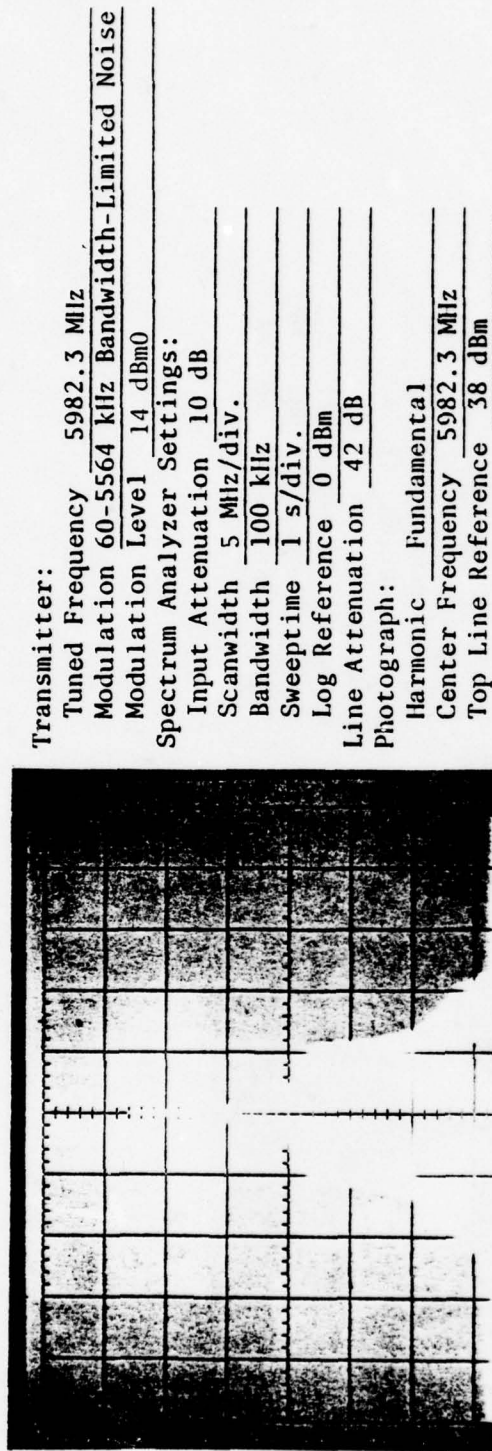


Figure C-12. Narrowband emission spectrum characteristics of 1200-channel Lenkurt 778A2 transmitter, 0.13 RMS modulation index.

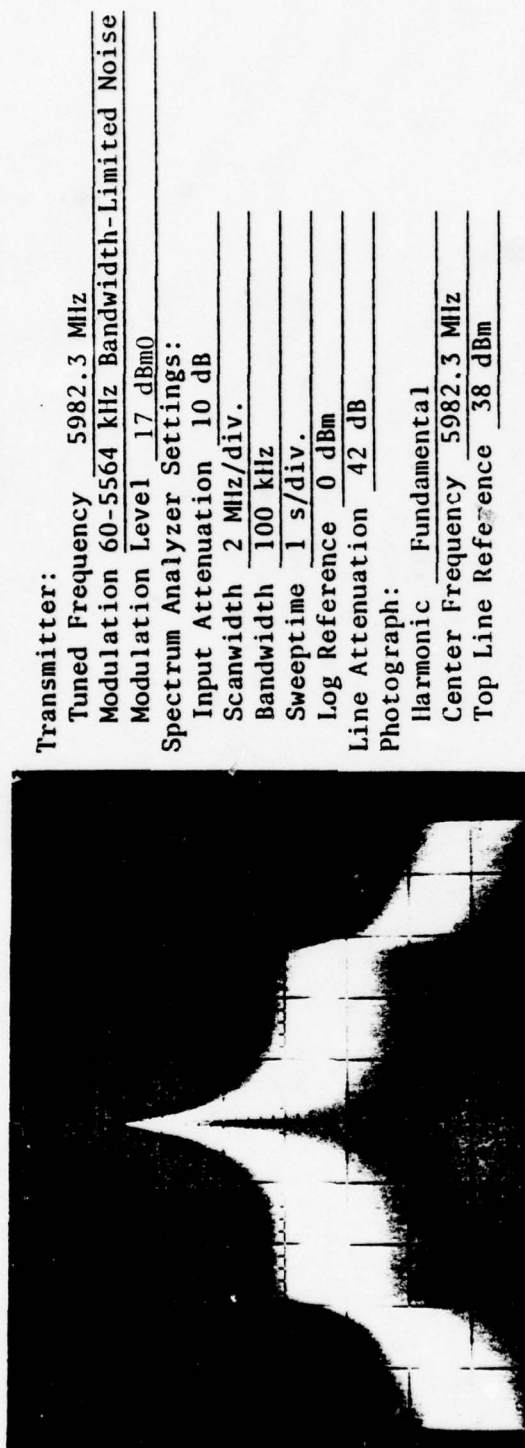


Figure C-13. Narrowband emission spectrum characteristics of 1200-channel Lenkurt 778A2 transmitter, 0.18 RMS modulation index.

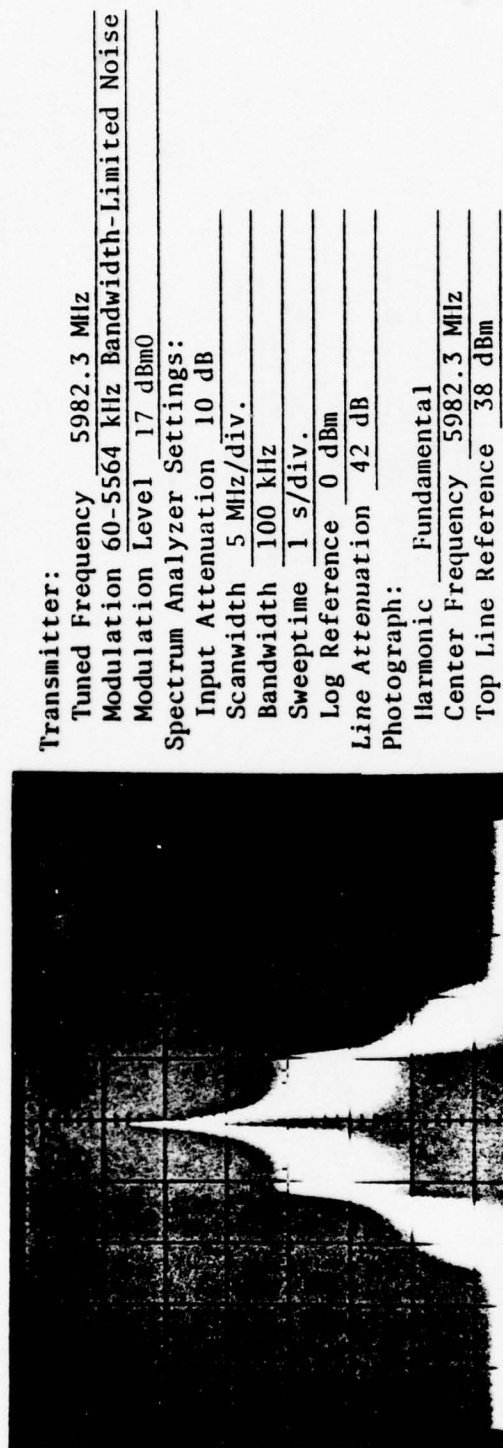


Figure C-14. Narrowband emission spectrum characteristics of 1200-channel Lenkurt 778A2 transmitter, 0.18 RMS modulation index.

Transmitter:
 Tuned Frequency 5982.3 MHz
 Modulation 60-5564 kHz Bandwidth-Limited Noise
 Modulation Level 19 dBm0
 Spectrum Analyzer Settings:
 Input Attenuation 10 dB
 Scanwidth 2 MHz/div.
 Bandwidth 100 kHz
 Sweeptime 1 s/div.
 Log Reference 0 dBm
 Line Attenuation 42 dB
 Photograph:
 Harmonic Fundamental
 Center Frequency 5982.3 MHz
 Top Line Reference 38 dBm



Figure C-15. Narrowband emission spectrum characteristics of 1200-channel Lenkurt 778A2 transmitter, 0.23 RMS modulation index.

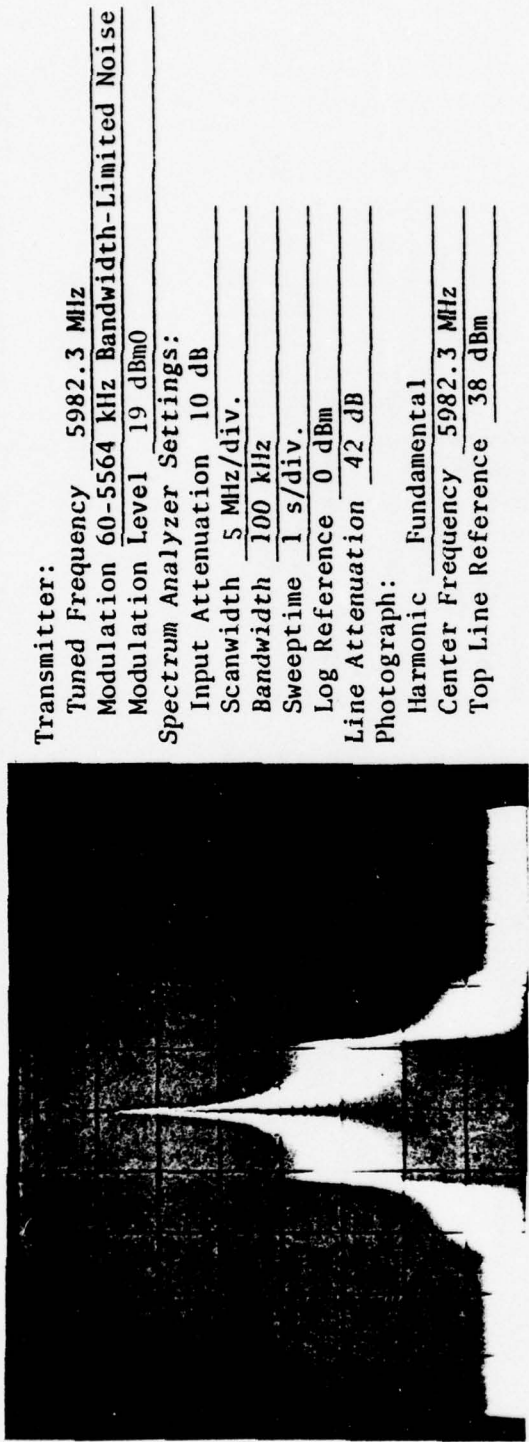


Figure C-16. Narrowband emission spectrum characteristics of 1200-channel Lenkurt 778A2 transmitter, 0.23 RMS modulation index.

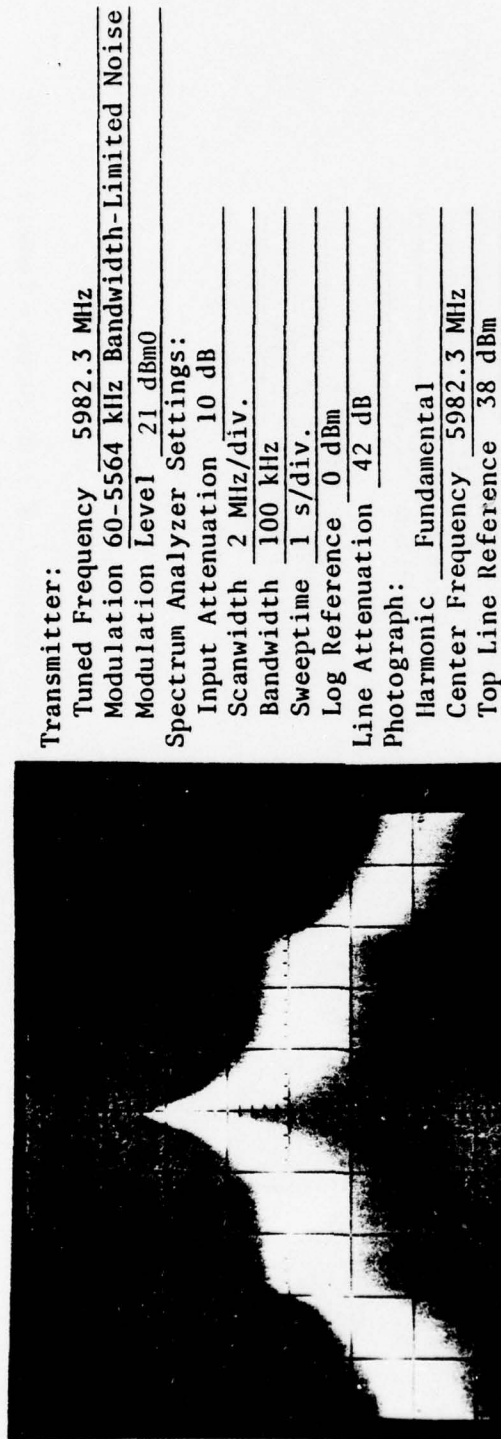


Figure C-17. Narrowband emission spectrum characteristics of 1200-channel Lenkurt 778A2 transmitter, 0.28 RMS modulation index.

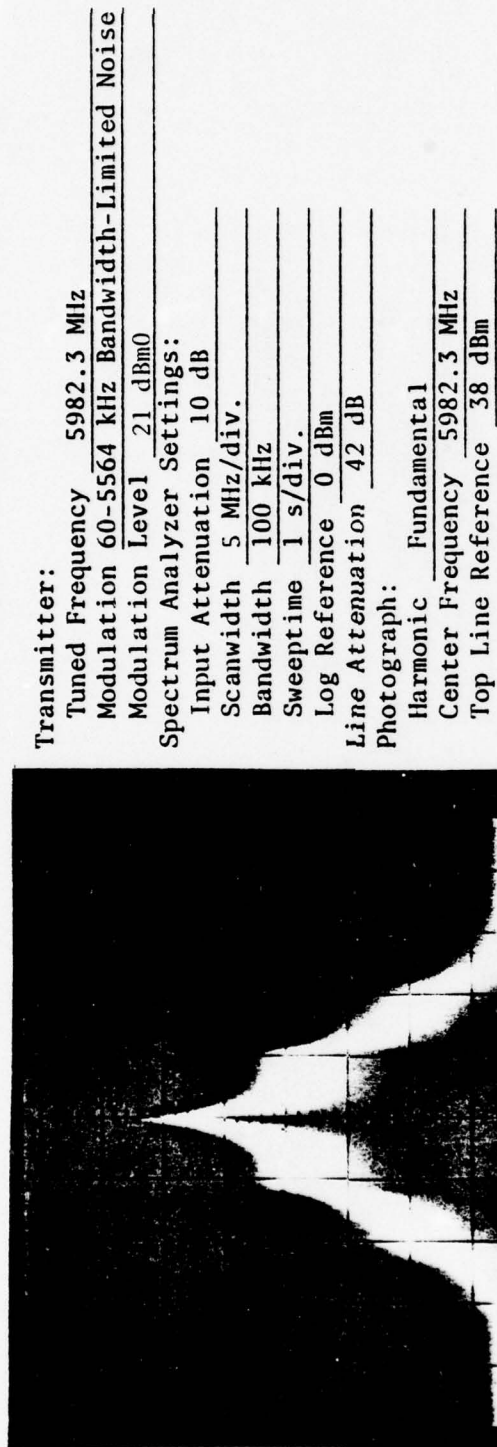


Figure C-18. Narrowband emission spectrum characteristics of 1200-channel Lenkurt 778A2 transmitter, 0.28 RMS modulation index.

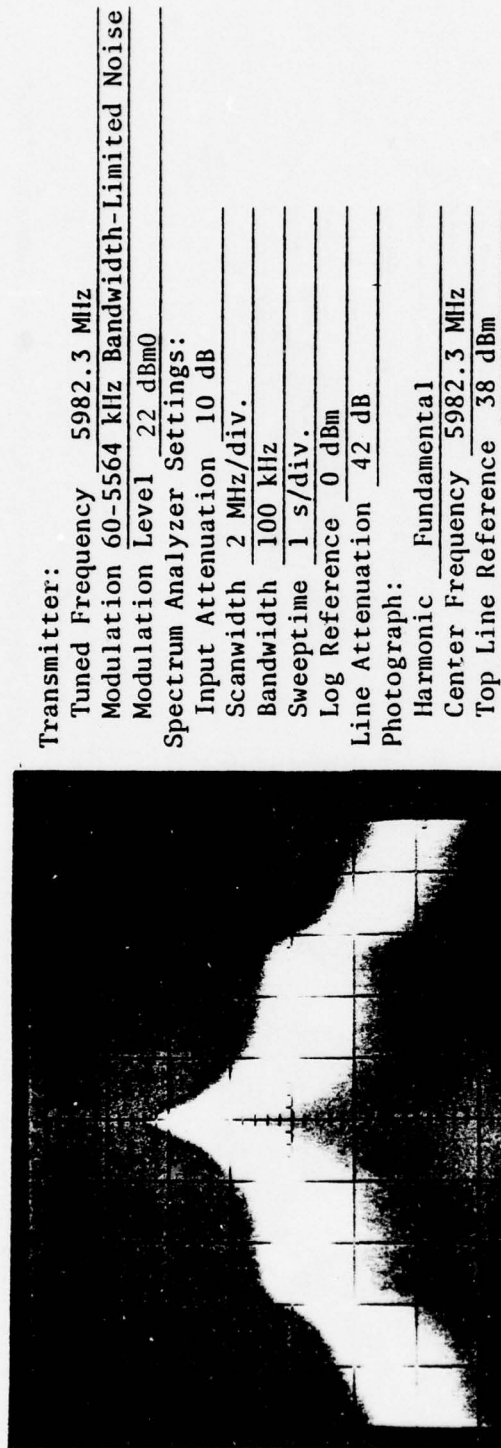


Figure C-19. Narrowband emission spectrum characteristics of 1200-channel Lenkurt 778A2 transmitter, 0.32 RMS modulation index.

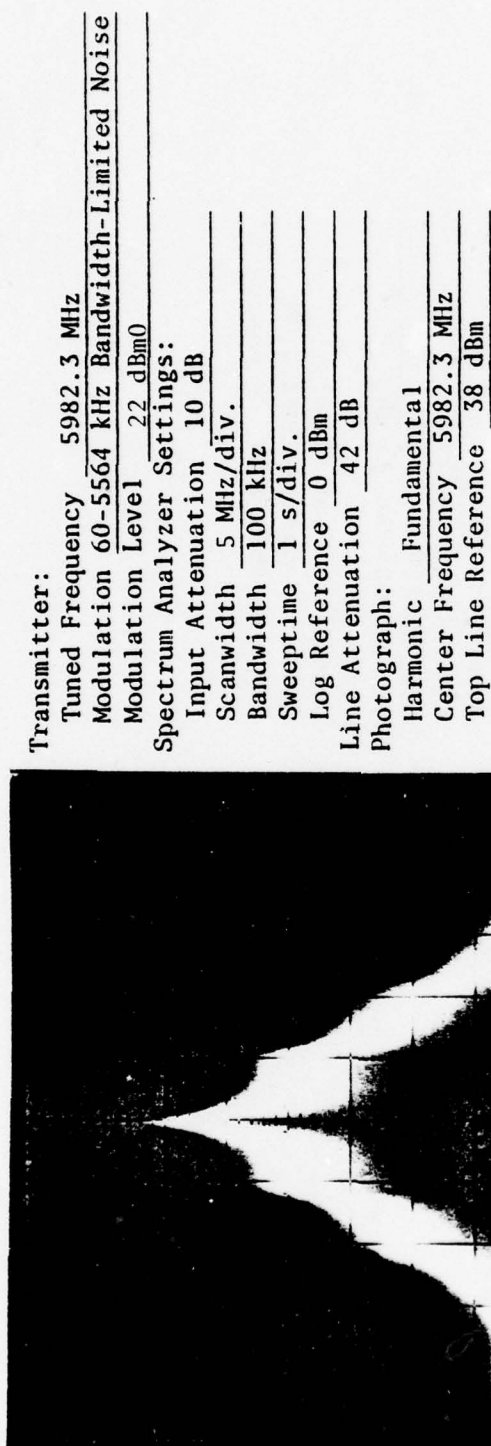


Figure C-20. Narrowband emission spectrum characteristics of 1200-channel Lenkurt 778A2 transmitter, 0.32 RMS modulation index.

Transmitter:
 Tuned Frequency 5982.3 MHz
 Modulation 60-5564 kHz Bandwidth-Limited Noise
 Modulation Level 23 dBm0

Spectrum Analyzer Settings:
 Input Attenuation 10 dB
 Scanwidth 2 MHz/div.
 Bandwidth 100 kHz
 Sweptime 1 s/div.
 Log Reference 0 dBm
 Line Attenuation 42 dB

Photograph:
 Harmonic Fundamental
 Center Frequency 5982.3 MHz
 Top Line Reference 38 dBm



Figure C-21. Narrowband emission spectrum characteristics of 1200-channel Lenkurt 778A2 transmitter, 0.36 RMS modulation index.

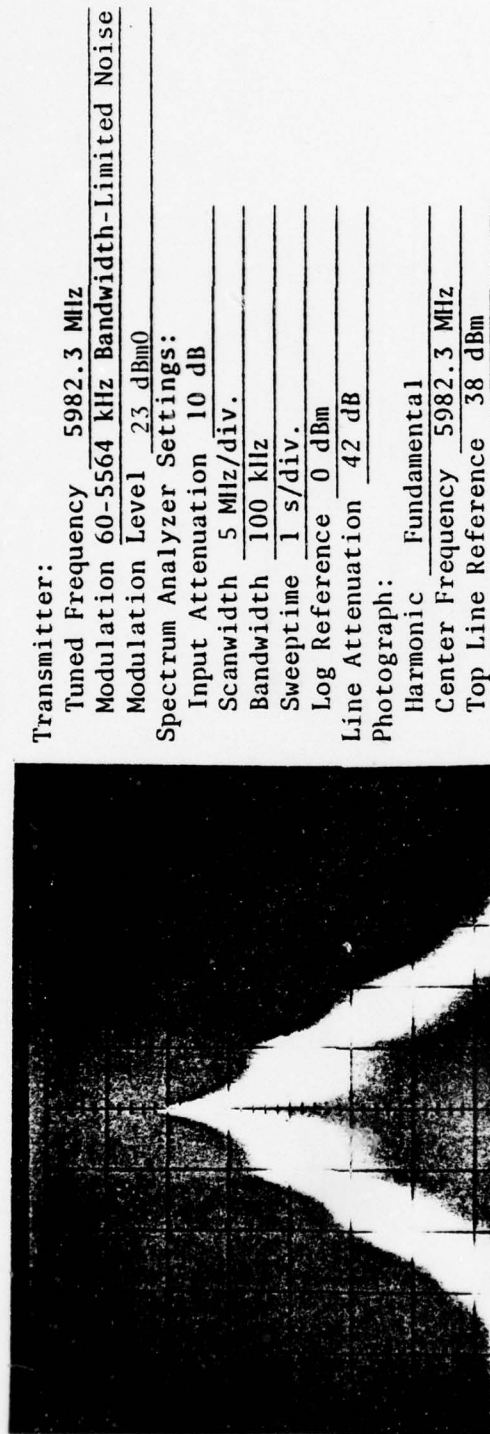


Figure C-22. Narrowband emission spectrum characteristics of 1200-channel Lenkurt 778A2 transmitter, 0.36 RMS modulation index.

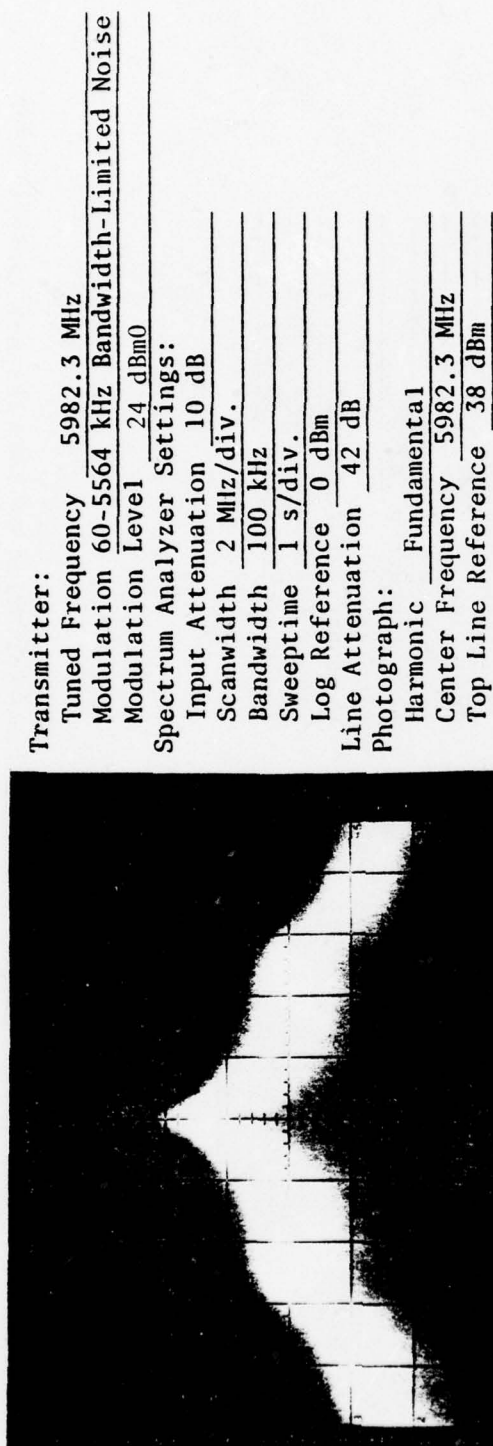


Figure C-23. Narrowband emission spectrum characteristics of 1200-channel Lenkurt 778A2 transmitter, 0.4 RMS modulation index.

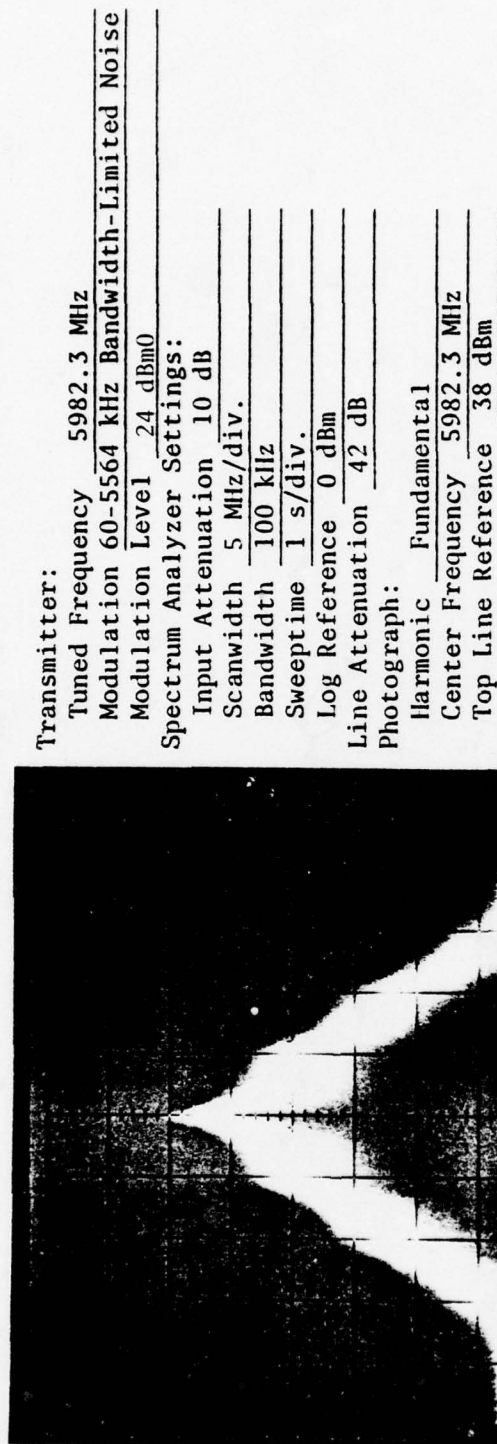


Figure C-24. Narrowband emission spectrum characteristics of 1200-channel Lenkurt 778A2 transmitter 0.4 RMS modulation index.

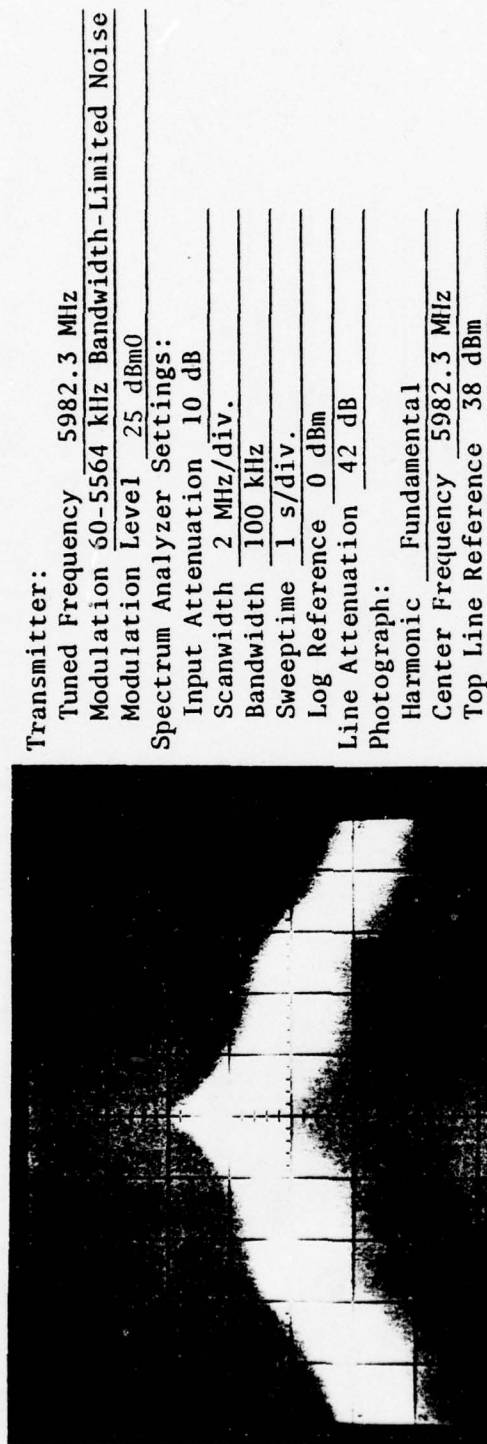


Figure C-25. Narrowband emission spectrum characteristics of 1200-channel Lenkurt 778A2 transmitter, 0.45 RMS modulation index.

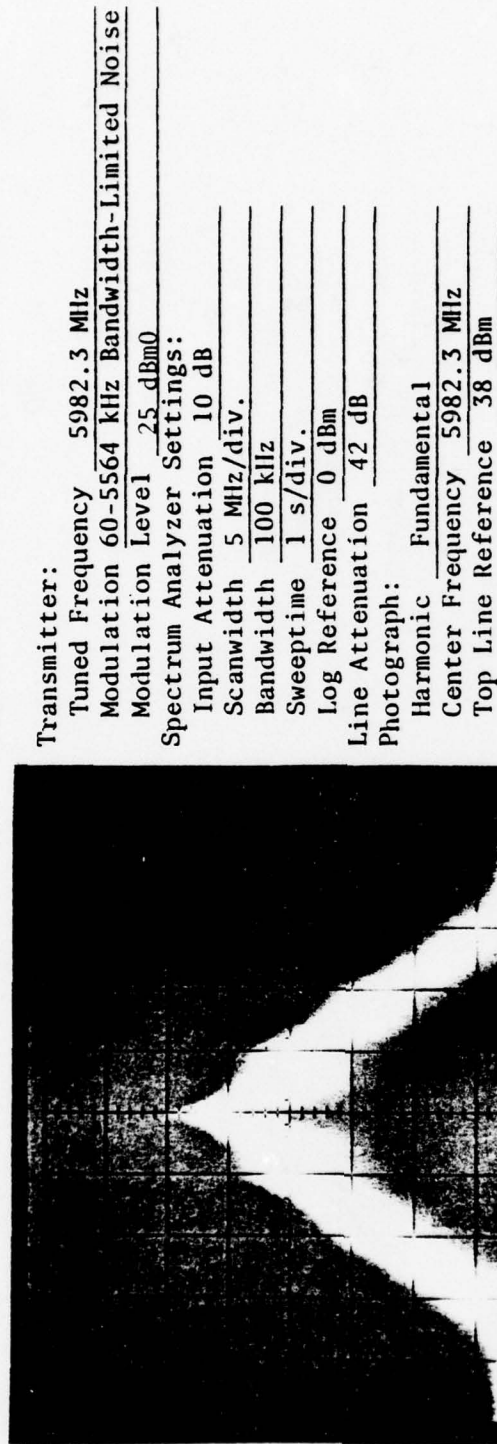


Figure C-26. Narrowband emission spectrum characteristics of 1200-channel Lenkurt 778A2 transmitter, 0.45 RMS modulation index.

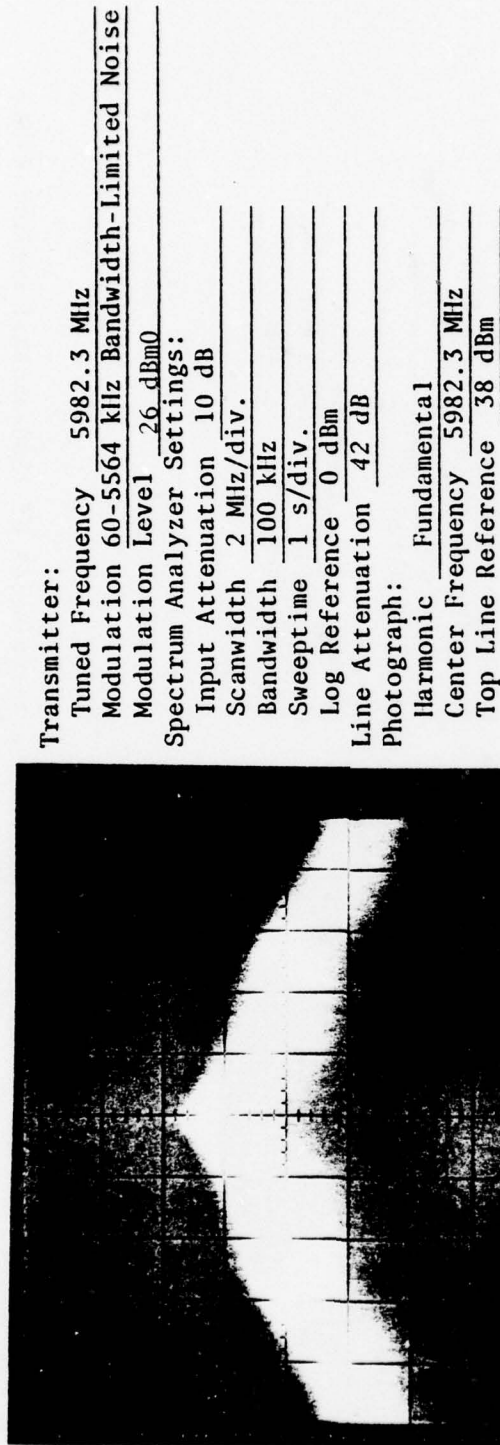


Figure C-27. Narrowband emission spectrum characteristics of 1200-channel Lenkurt 778A2 transmitter, 0.51 RMS modulation index.

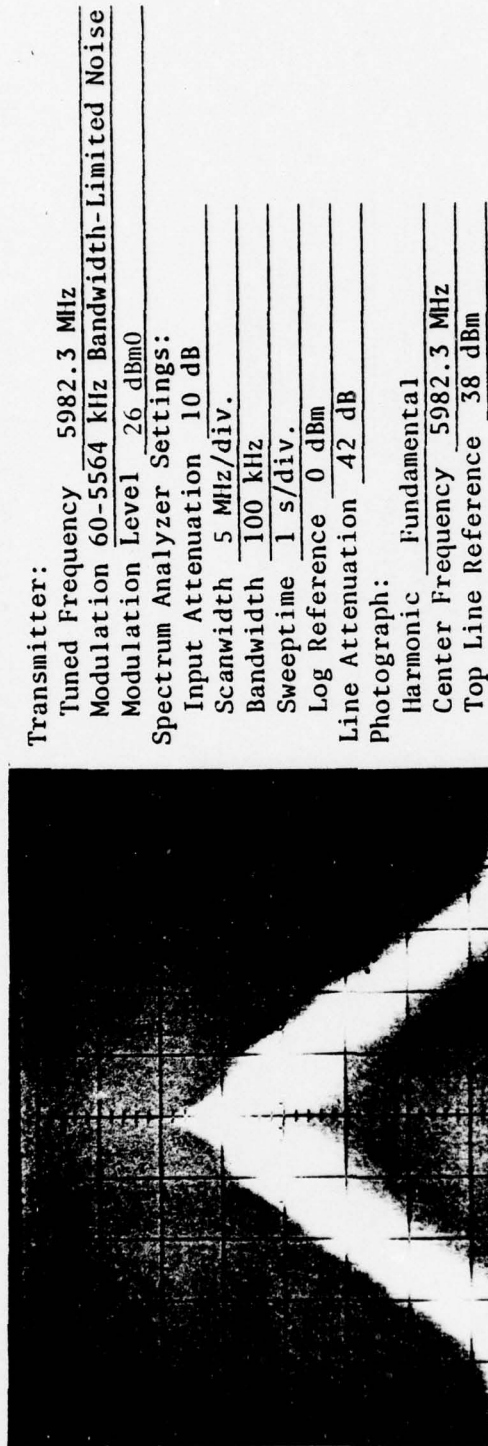


Figure C-28. Narrowband emission spectrum characteristics of 1200-channel Lenkurt 778A2 transmitter, 0.51 RMS modulation index.

Transmitter:
 Tuned Frequency 5982.3 MHz
 Modulation 60-5564 kHz Bandwidth-Limited Noise
 Modulation Level 28 dBm0

Spectrum Analyzer Settings:
 Input Attenuation 10 dB
 Scanwidth 2 MHz/div.
 Bandwidth 100 kHz
 Sweep time 1 s/div.
 Log Reference 0 dBm
 Line Attenuation 42 dB

Photograph:
 Harmonic Fundamental
 Center Frequency 5982.3 MHz
 Top Line Reference 38 dBm



Figure C-29. Narrowband emission spectrum characteristics of 1200-channel Lenkurt 778A2 transmitter, 0.64 RMS modulation index.

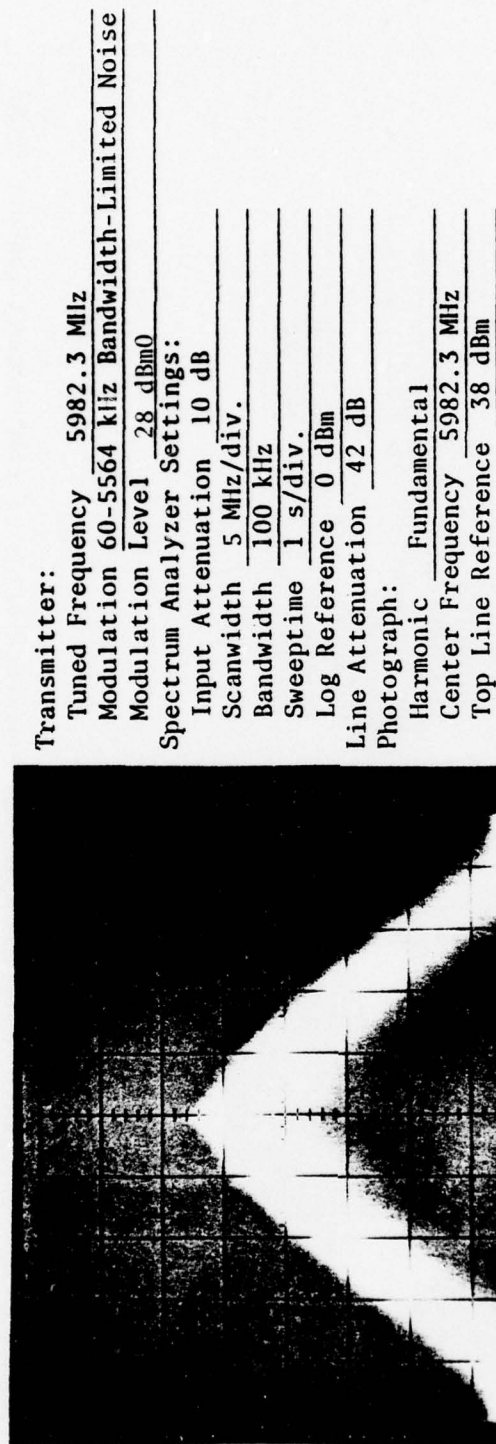


Figure C-30. Narrowband emission spectrum characteristics of 1200-channel Lenkurt 778A2 transmitter, 0.64 RMS modulation index.

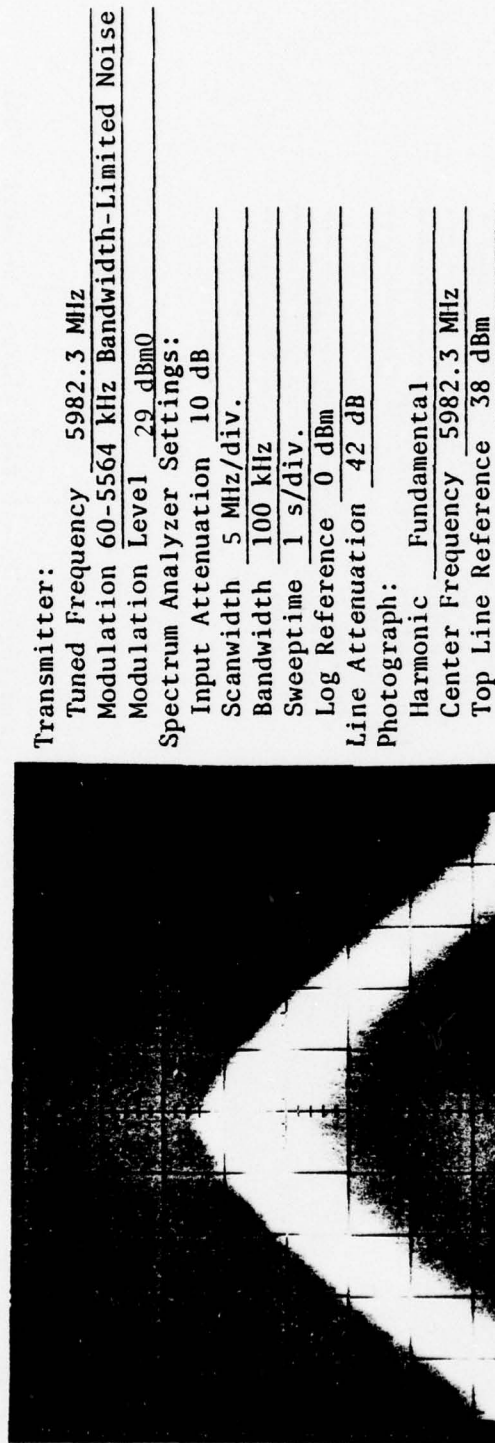


Figure C-31. Narrowband emission spectrum characteristics of 1200-channel Lenkurt 778A2 transmitter, 0.7 RMS modulation index.

Transmitter:

Tuned Frequency 5982.3 MHz
 Modulation 60-5564 kHz Bandwidth-Limited Noise
 Modulation Level 29 dBm0

Spectrum Analyzer Settings:

Input Attenuation 10 dB
 Scanwidth 10 MHz/div.
 Bandwidth 100 kHz
 Swepttime 1 s/div.
 Log Reference 0 dBm
 Line Attenuation 42 dB

Photograph:

Harmonic Fundamental
 Center Frequency 5982.3 MHz
 Top Line Reference 38 dBm

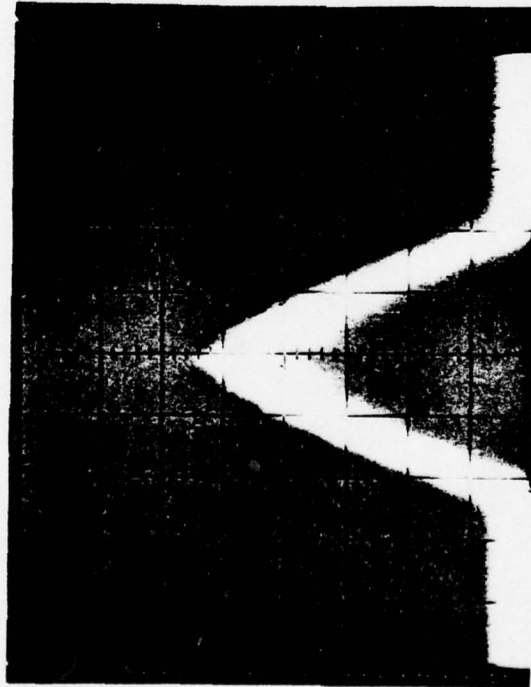


Figure C-32. Narrowband emission spectrum characteristics of 1200-channel Lenkurt 778A2 transmitter, 0.7 RMS modulation index.

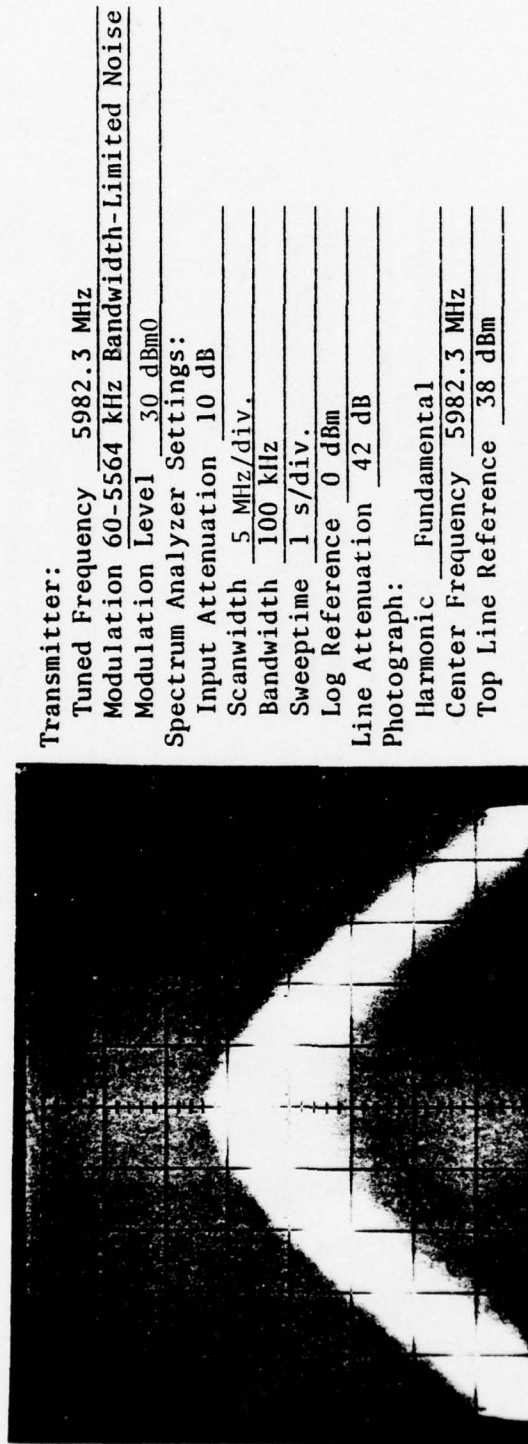


Figure C-33. Narrowband emission spectrum characteristics of 1200-channel Lenkurt 778A2 transmitter, 0.8 RMS modulation index.

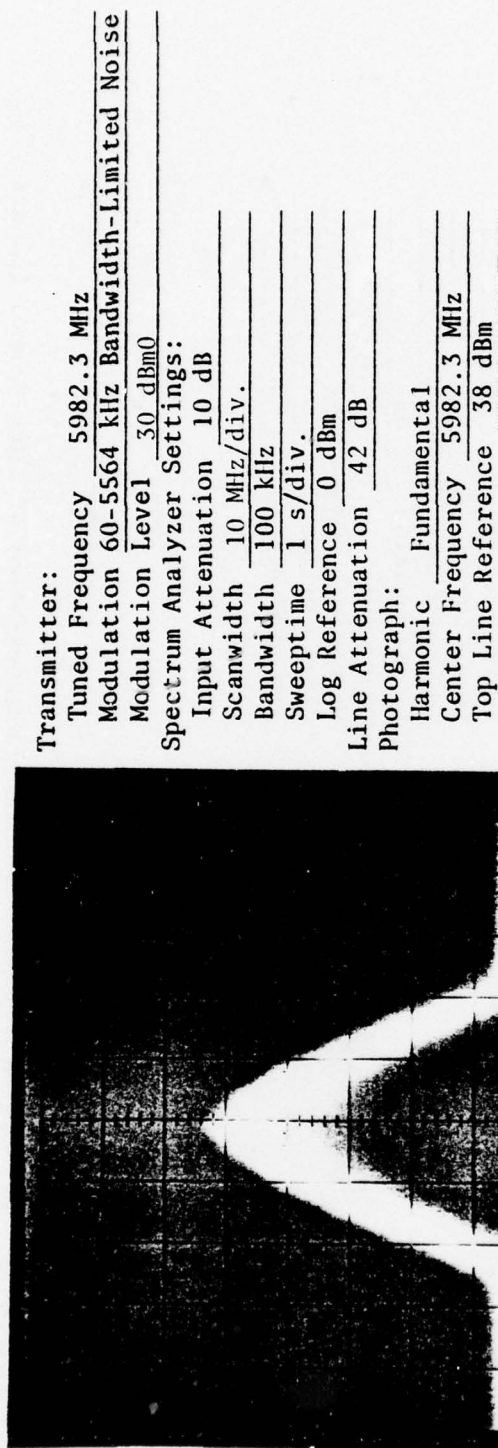


Figure C-34. Narrowband emission spectrum characteristics of 1200-channel Lenkurt 778A2 transmitter, 0.8 RMS modulation index.

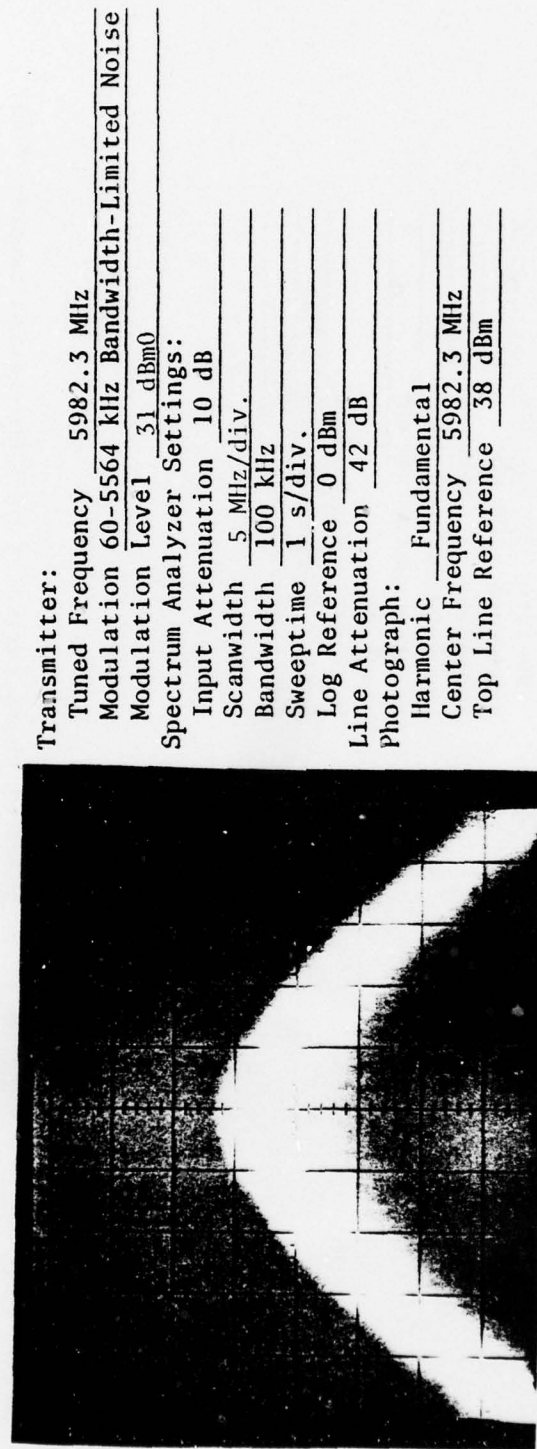


Figure C-35. Narrowband emission spectrum characteristics of 1200-channel Lenkurt 778A2 transmitter, 0.9 RMS modulation index.

AD-A068 757

IIT RESEARCH INST ANNAPOLIS MD
WIDEBAND FDM/FM MICROWAVE RADIO RELAY PERFORMANCE DEGRADATION I--ETC(U)
APR 79 A A HERNANDEZ

F/G 17/2.1

F19628-78-C-0006

UNCLASSIFIED

ESD-TR-79-100

NL

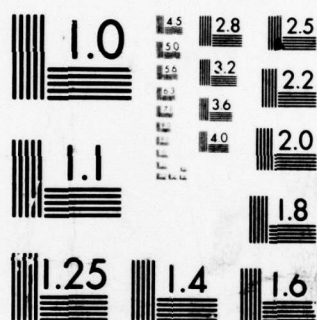
5 OF 5

AD
A068757



END
DATE
FILMED

6 --79
DDC



MICROCOPY RESOLUTION TEST CHART
NATIONAL BUREAU OF STANDARDS-1963-A

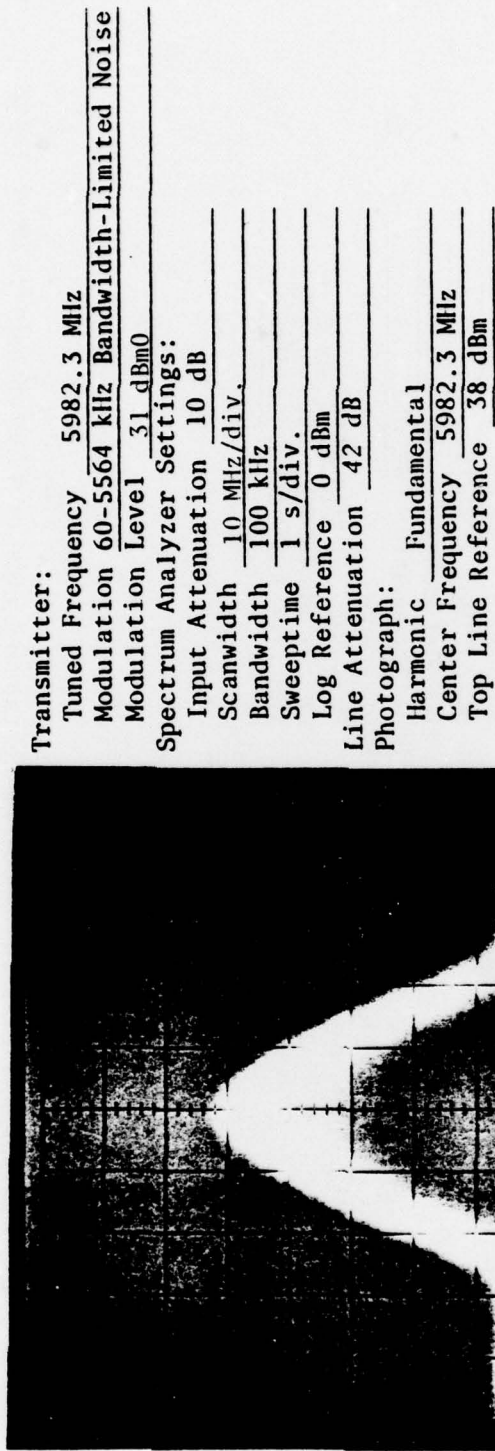


Figure C-36. Narrowband emission spectrum characteristics of 1200-channel Lenkurt 778A2 transmitter, 0.9 RMS modulation index.

Transmitter:
 Tuned Frequency 5982.3 MHz
 Modulation 60-5564 kHz Bandwidth-Limited Noise
 Modulation Level 34 dBm0
 Spectrum Analyzer Settings:
 Input Attenuation 10 dB
 Scanwidth 5 MHz/div.
 Bandwidth 100 kHz
 Swepttime 1 s/div.
 Log Reference 0 dBm
 Line Attenuation 42 dB
 Photograph:
 Harmonic Fundamental
 Center Frequency 5982.3 MHz
 Top Line Reference 38 dBm



Figure C-37. Narrowband emission spectrum characteristics of 1200-channel Lenkurt 778A2 transmitter, 1.3 RMS modulation index.

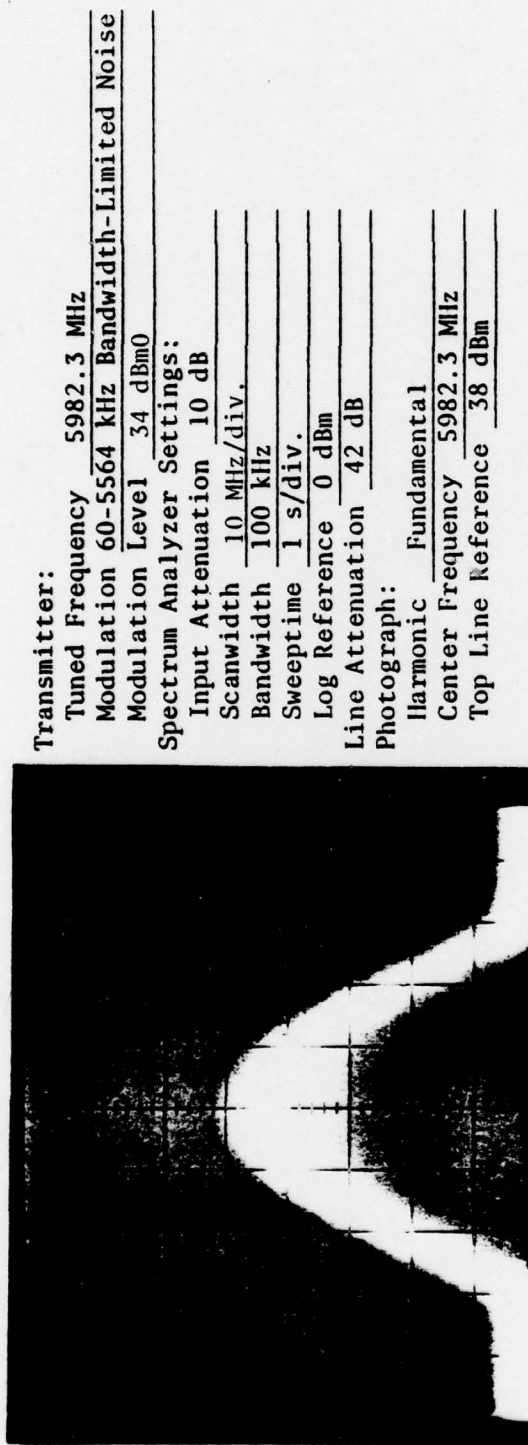


Figure C-38. Narrowband emission spectrum characteristics of 1200-channel Lenkurt 778A2 transmitter, 1.3 RMS modulation index.

ESD-TR-79-100

REFERENCES

1. Hatch, W., Hinkle, R., and Mayher, R., *Analysis of Pulsed Interference to Amplitude Modulated Receivers*, ESD-TR-70-207, ECAC, Annapolis, MD, December 1970.
2. Conklin, S., *Analysis of Pulsed Interference to Television Receivers*, ESD-TR-75-079, ECAC, Annapolis, MD, October 1974.
3. Hernandez, A., *Investigation of Pulsed Interference to Narrowband FM Receivers*, ESD-TR-75-023, ECAC, Annapolis, MD, January 1976.
4. Military Standard, *Radio Frequency Spectrum, Measurements of*, MIL-STD-449(D), February 1973.
5. Hernandez, A. A., Lewis, C. W., *A Model for Time Waveform Simulation of FDM/FM Receivers*, ECAC-UM-78-018, ECAC, Annapolis, MD, November 1978.
6. *All Solid-State Microwave Radio*, GTE Lenkurt, 78A2, Issue Two, August 1971.
7. Tant, M. J., *Multichannel Communication Systems and White Noise Testing*, Marconi Instruments, New Jersey, July 1974.
8. "GTE Lenkurt 78A2/B2 Solid State Microwave System (System Noise Measurements)," *GTE Practices*, Section 394-781-681, Issue Two, January 1975.
9. Hernandez, A., *Lenkurt Wideband FDM/FM Measurements Handbook (Volume 1)*, ECAC-HDBK-77-041-1, ECAC, Annapolis, MD, September 1977.
10. Hernandez, A., *Lenkurt Wideband FDM/FM Measurements Handbook (Volumes 2 through 8)*, ECAC-HDBK-77-041-2 through ECAC-HDBK-77-041-8, ECAC, Annapolis, MD, May 1978.
11. *Military Communication System Technical Standards*, MIL-STD-188 Series.
12. Holbrook, B. D., and Dixon, J. T., "Load Rating Theory for Multichannel Amplifiers," *Bell System Tech. J.*, Volume 18 (October 1939), pp. 624-644.
13. Middleton, D., "The Distribution of Energy in Randomly Modulated Waves," *Philosophical Magazine*, 42, 1951, p. 689.

REFERENCES (Continued)

14. Ferris, C. C., "Spectral Characteristics of FDM/FM Signals," *IEEE Trans. Commun. Technol.*, Vol. COM-16, April 1968, pp. 233-238.
15. Medhurst, R. G., "RF Bandwidth of Frequency-Division Multiplex Systems Using Frequency Modulation," *Proc. IRE*, Vol. 44, No. 2, February 1956.
16. Medhurst, R. G., "RF Spectra and Interfering Carrier Distortion in FM Trunk Radio Systems with Low Modulation Ratios," *IRE Trans. On Communication Systems*, Vol. CS-9, No. 2, June 1961.
17. Stewart, J., "The Power Spectrum of a Carrier Frequency Modulated by Noise," *Proc. IRE*, Vol. 42, October 1954.
18. Middleton, D., *An Introduction to Statistical Communication Theory*, New York, McGraw Hill, 1960.
19. Hamer, R., "Radio-Frequency Interference to Multichannel Telephony FM Radio Systems," *Inst., Elec. Eng.*, Paper 3326E, January 1961, pp. 75-89.
20. Cherry, E. C., and Rivlin, R. S., "Non-Linear Distortion, With Particular Reference to the Theory of Frequency Modulated Waves," *Philosophical Magazine*, 32, 1941, p. 265.
21. Hamer, R., and Acton, R. A., "Power Spectrum of a Carrier Modulated in Phase or Frequency by White Noise," *Electronic and Radio Engineer*, Vol. 34, 1957, p. 246.
22. Pontano, B. A., Fuenzalida, J. C., and Chitre, Nand Kishore, M., "Interference into Angle-Modulated Systems Carrying Multichannel Telephony Signals," *IEEE Trans. on Communication*, Vol. COM-21, No. 6, June 1973.
23. Abramson, N., "Bandwidth and Spectra of Phase-and-Frequency-Modulated Waves," *IEEE Trans. on Communication Systems*, Vol. CS-11, No. 4, December 1963.
24. *Spectra and Bandwidth of Frequency-Modulated Emissions*, CCIR Report No. 419, XIIth Plenary Assembly, New Delhi, 1970.
25. *Reference Data for Satellite Communications Earth Stations*, ITT Space Communications, Inc., Ramsey, NJ, Revised June 1973.

REFERENCES (Continued)

26. *GTE Lenkurt 46A Carrier System Engineering Considerations*, GTE Lenkurt Incorporated, San Carlos, CA, Issue 2, June 1971.
27. Fagot, J., and Magne, P., *Frequency Modulation Theory*, Pergamon Press, The MacMillan Company, New York, 1961.
28. MIL-STD-188-313, *Subsystem Design and Engineering Standards and Equipment Technical Design Standards for Long-Haul Communications Transversing Microwave LOS Radio and Tropospheric Scatter Radio*, 19 December 1973.
29. "Preemphasis Characteristics for Frequency-Modulation Systems," *CCIR Recommendation 275-2*, CCIR XIIth Plenary Assembly, Volume IV, Part 1, New Delhi, 1970.
30. International Radio Consultative Committee (CCIR), XIIth Plenary Assembly, New Delhi, Volume IV, Part 2, 1970, p. 203.
31. Ng, H.J.Y., *A Parametric Examination of the Processing Gain Relationship of a Frequency Division Multiplex Receiver Subject to Frequency Division Modulation Interference*, OT Report TN-79-1, U.S. Department of Commerce/Office of Telecommunications, March 1976.
32. Wachs, M. R., and Arroyo, B., *Technical Consideration of Frequency Sharing Between Satellite Communications and Radar*, International Conference on Communications (ICC '78), IEEE, 1978.
33. Hernandez, A. A., *Effects of Pulse Interference on FDM/FM Multichannel Telephony Transmissions of the Fixed Satellite Service*, ECAC-CR-78-075, ECAC, Annapolis, MD, August 1978.
34. Dixon, R. C., *Spread Spectrum Systems*, John Wiley and Sons, New York, 1976.
35. *Units for Measuring Power, Levels and Noise*, GTE Lenkurt Incorporated, 1973.
36. French, N., and Steinberg, J., "Factors Governing the Intelligibility of Speech Sounds," *Journal of the Acoustical Society of America*, Vol. 19, No. 1, January 1947.

REFERENCES (Continued)

37. Thompson, A., *The Application of the Voice Interference Analysis System to the Prediction of Voice Intelligibility - Part 1*, Bell Report No. A70009-280, November 1967.
38. Fitts, R., *Electronic Evaluation of Voice Communications Systems*, RADC-TDR-63-355, August 1963.
39. Robertson, W. Douglas, *A Comparison of the Procedures and Results of Intelligibility Tests for a Number of Interference Conditions*, ECAC-TM-X-003-10, ECAC, Annapolis, MD, April 1962.

DISTRIBUTION LIST FOR
ESD-TR-79-100
"WIDEBAND FDM/FM MICROWAVE RADIO RELAY
PERFORMANCE DEGRADATION INVESTIGATION"

ADDRESS	NO. COPIES	ADDRESS	NO. COPIES
ARMY		CDR, USA555	1
HQDA (DAMO-TCF)	1	ATTN: ATSM-CO (COL DAVIS)	
WASHINGTON, DC 20310		FORT GORDON, GA 30905	
USACC	1	USCINCEUR RAPLO 80NN	1
CH: C-E SERVICES DIVISION		BOX 345 (LTC G. CARNES)	
ATTN: CC-OPS-CE		US EMBASSY	
WASHINGTON, DC 20301		APU NY 09080	
CDR, USAERADCOM	1	CDR, 5TH SIGNAL COMMAND	1
ATTN: DRDCO-COM-RT-2 (P. SASS)		ATTN: CCE-PO-F	
FORT MONMOUTH, NJ 07703		APU NY 09056	
CDR, USACORADCOM	1	COMMANDER IN CHIEF	1
ATTN: DRSEL-RO-TS-F (R. TALLMAN)		US SOUTHERN COMMAND	
FORT MONMOUTH, NJ 07703		ATTN: SC-G/MR. HEISS	
CDR, USACORADCOM	1	APD NY 09826	
ATTN: DRDCO-COM-RT-3 (P. MAJOR)		COMMANDER	1
FORT MONMOUTH, NJ 07703		USARMY ALASKA	
CDR, USACORADCOM	1	ATTN: ARAGS	
ATTN: DRDCO-COM-RT-5 (W. KESSELMAN)		APD SEATTLE 98749	
FORT MONMOUTH, NJ 07703		HQ BERLIN BRIGADE	1
CDR, USACORADCOM	1	RADIO SYSTEM BRANCH	
ATTN: DRDCO-SEI-A (S. SEGNER)		C-E DIVISION	
FORT MONMOUTH, NJ 07703		APD NY 09205	
CDR, USAMIRCOM	1	CDR, 7TH SIGNAL COMMAND	1
ATTN: DRCPH-TN-E		ATTN: CGN-PO-OP	
REDSTONE ARSENAL, AL 35809		FORT RITCHIE, MD 21719	
CDR, USAMIRCOM	1	CDR, 11TH SIGNAL GROUP	1
ATTN: DRONI-TE (D. SMITH)		ATTN: CCE-PO	
REDSTONE ARSENAL, AL 35809		FORT HUACHUCA, AZ 85613	
CDR, USATECON	1	CORADCOM	1
ATTN: DRSTE-EL (L. DOUGHTY)		PHNSCS	
ABERDEEN PROVING GROUND, MD 21005		ATTN: DRCPH-MSC-TN-S3	
CDR, USACC	1	FY. MONMOUTH, NJ 07703	
ATTN: CC-OPS-G		CDR, USAEPG	1
FORT HUACHUCA, AZ 85613		ATTN: MR. R. SOUTHWICK	
CDR, USACSA	1	FORT HUACHUCA, AZ 85613	
ATTN: CCM-ICE		CDR, USACC	1
FORT MONMOUTH, NJ 07703		ATTN: CC-OPS-W (N. WILSON)	
CDR, USACEEIA	1	FORT HUACHUCA, AZ 85613	
ATTN: CCC-EMEO (MR. M. HERREL)		CDR, USACSA	1
FORT HUACHUCA, AZ 85613		ATTN: CCM-SG-(N)-TCN (BILL WRYE)	
OFFICE OF THE AREA FREQUENCY COORDINATOR	1	FORT HUACHUCA, AZ 85613	
ATTN: DDB APC ARIZONA (MR. M. BERGE)		CDR, USACEEIA	1
FORT HUACHUCA, AZ 85613		ATTN: CCC-EMEO-EC (MR. B. ALLEN)	
ARMY FREQUENCY COORDINATOR	1	FORT HUACHUCA, AZ 85613	
EASTERN US		CDR, USASC65	1
ATTN: CC-OPS-CE-SE (CHRIS WALL)		ATTN: CD-RSD (MR. SIEMEN)	
FORT GEORGE G. MEADE, MD 20755		FORT GORDON, GA 30905	
ARMY FREQUENCY COORDINATOR	1	AIR FORCE	
CENTRAL US		HQ USAF/FMO	1
ATTN: CC-OPS-CE-SC (G. CUNNINGHAM)		WASHINGTON, DC 20330	
FORT SAN HOUSTON, TX 78234		HQ ASD/ENAMA	1
ARMY FREQUENCY COORDINATOR	1	WRIGHT-PATTERSON AFB, OH 45433	
ATTN: CC-OPS-CE-SU (J. BARR)		HQ AFSC/SDOD	1
PRESIDIO OF SAN FRANCISCO		ANDREWS AFB	
SAN FRANCISCO, CA 94129		WASHINGTON, DC 20334	
DOD ARMY FREQUENCY COORDINATOR	1	HQ RADC/RBC	1
ATTN: MR. G. HUNGATE		GRIFFISS AFB, NY 13441	
USAR, MN 55002		1837TH E&I GROUP/EPE	1
CDR, OCEC	1	KEESLER AFB, MS 39034	
ATTN: CODE 430		HQ AFCS/DOYF	1
RESTON, VA 22090		SCOTT AFB, IL 62225	
CDR, USAFORSOM	1	HQ ADTC/DC	1
ATTN: AFCE (D. TOLLEY)		EGLIN AFB, FL 32542	
FORT MCPHERSON, GA 30330		HQ TANC/OA	1
CDR, USARMY SIGNAL SCHOOL	1	EGLIN AFB, FL 32542	
ATTN: ATSM-CTO (W. HANDEL)			
FORT GORDON, GA 30905			

ADDRESS	NO. COPIES	ADDRESS	NO. COPIES
HQ. RADC (AFSC)		COMMANDER (CODE 2011)	1
ATTN: MR. JOHN P. SHINNARD	1	NAVAL TELECOMMUNICATIONS COMMAND	
GRIFFISS AFB, NY 13441		4401 MASSACHUSETTS AVE., N.W.	
		WASHINGTON, DC 20360	
AIR UNIVERSITY LIBRARY	1	CHIEF OF NAVAL MATERIAL (MAT-0856/HUNEY)	1
MAXWELL AFB, AL 36112		NAVY DEPARTMENT	
AFGL (SULR)	2	WASHINGTON, DC 20360	
HANSCOM AFB, MA 01731		SUPERINTENDENT (DR. R. ADLER)	1
		NAVAL POSTGRADUATE SCHOOL	
		MONTREY, CA 93940	
MARINE CORPS		COMMANDER (EX-5103/R. PHIDE)	1
COMMANDANT OF THE MARINE CORPS	1	NAVAL ELECTRONIC SYSTEMS COMMAND	
(ATTN: LNC)		WASHINGTON, DC 20360	
HEADQUARTERS, U.S. MARINE CORPS		COMMANDING OFFICER	1
WASHINGTON, DC 20380		NAVAL ELECTRONIC SYSTEMS ENGINEERING	
DIRECTOR, DEVELOPMENT CENTER	1	ACTIVITY, ST. INIGUES	
MARINE CORPS DEVELOPMENT AND		ATTN: J. KNOEDEL	
EDUCATION COMMAND		ST. INIGUES, MD 20684	
(ATTN: CCC DIV. SYSTEMS DEFINITIONS BR.)			
QUANTICO, VA 22134		DDO & OTHERS	
DIRECTOR, DEVELOPMENT CENTER	1	DIRECTOR	1
MARINE CORPS DEVELOPMENT AND		DEFENSE COMMUNICATIONS AGENCY	
EDUCATION COMMAND		ATTN: CODE 404A	
(ATTN: CCC DIV. TELCOM BR.)		WASHINGTON, DC 20305	
QUANTICO, VA 22134		DIRECTOR	2
DIRECTOR, DEVELOPMENT CENTER	1	NATIONAL SECURITY AGENCY	
MARINE CORPS DEVELOPMENT AND		ATTN: W36/MR. V. MCCUNNELL	
EDUCATION COMMAND		PT. GEORGE G. MEADE, MD 20755	
(ATTN: CCC DIV. ELECTRONICS BR.)		COMMANDER IN CHIEF	1
QUANTICO, VA 22134		U.S. EUROPEAN COMMAND	
DIRECTOR, DEVELOPMENT CENTER	1	ATTN: ECJ6-PP	
MARINE CORPS DEVELOPMENT AND		APO NY 09128	
EDUCATION COMMAND		COMMANDER IN CHIEF, PACIFIC	1
(ATTN: COMMUNICATION OFFICERS SCHOOL)		ATTN: J611	
QUANTICO, VA 22134		BOX 29732A	
COMMANDING OFFICER	1	CP HM SMITH, HI 96861	
MARINE CORPS TACTICAL SYSTEMS		COMMANDER IN CHIEF	1
SUPPORT ACTIVITY		U.S. SOUTHERN COMMAND	
CAMP PENDLETON, CA 92055		ATTN: SC-G	
COMMANDER	1	APO NY 09824	
NAVAL OCEAN SYSTEMS CENTER		COMMANDER IN CHIEF, ATLANTIC	1
(MARINE CORPS LIAISON OFFICE)		ATTN: M612B	
SAN DIEGO, CA 92152		NORFOLK, VA 23511	
COMMANDER	1	COMMANDER IN CHIEF	1
NAVAL ELECTRONIC SYSTEMS COMMAND (CODE 540)		U.S. READINESS COMMAND	
WASHINGTON, DC 20380		ATTN: RCJ6-T	
NAVY		MACDILL AFB, FL 33608	
CHIEF OF NAVAL OPERATIONS (OP-941P)	1	CAPT. T. TRUE, USAF	1
NAVY DEPARTMENT		ASSISTANT U.S. MEMBER ARPA	
WASHINGTON, DC 20380		NATO/OTAN	
DIRECTOR	1	APO NY 09667	
NAVY ELECTROMAGNETIC SPECTRUM CENTER		NATIONAL TELECOMMUNICATIONS &	1
NAVAL COMMUNICATION UNIT WASHINGTON		INFORMATION ADMIN.	
WASHINGTON, DC 20390		ATTN: STAN COHN	
COMMANDER (EX-51024)	1	1325 G. ST., N.W.	
NAVAL ELECTRONIC SYSTEMS COMMAND		WASHINGTON, DC 20005	
WASHINGTON, DC 20360		DEFENSE DOCUMENTATION CENTER	12
COMMANDER (EX-51023)	1	CAMERON STATION	
NAVAL ELECTRONIC SYSTEMS COMMAND		ALEXANDRIA, VA 22314	
WASHINGTON, DC 20360		ESD/DR1	7
COMMANDER (EX-51032/COUNTS)	1	HANSCOM AFB, MA 01731	
NAVAL ELECTRONIC SYSTEMS COMMAND		DR MOTOWISA KANDA	1
WASHINGTON, DC 20360		ELECTROMAGNETIC FIELDS DIVISION	
COMMANDER (EX-304/CAUFFMAN)	1	NATIONAL BUREAU OF STANDARDS	
NAVAL ELECTRONIC SYSTEMS COMMAND		BOULDER, CO 80303	
WASHINGTON, DC 20360		MR. JOHN P. MURRAY	1
COMMANDER (CODE 8105/HOCKWAY)	1	INSTITUTE FOR TELECOMMUNICATIONS	
NAVAL OCEAN SYSTEMS CENTER		SCIENCES	
SAN DIEGO, CA 92152		NTIA	
		BOULDER, CO 80303	

DISTRIBUTION LIST

ADDRESS

NO. COPIES

ECAC INTERNAL DISTRIBUTION

XM	1
CAA	3
CAR	1
DOKAT	5
DOKC-M	5
DOKE-A	1
DOKC (MADISON)	1
DOKC (PORTASIK)	1
DOKC-A (WU)	1
DOKC-M (REILLY)	1
DOKC-R (HAUSER)	1
DOKE-A (HALL)	1
DOKE-A (HERNANDEZ)	2
DOKE-A (WACKERHAGEN)	1
DOKE-B (HARRISON)	1
DOKE-E (KOLESAR)	1
DOKE-E (SHALVI)	1
DOKE-S (PETSU)	1
DOKP-C (MORGAN)	1
P. NEWHOUSE	1